Molecules in diffuse interstellar clouds

Thesis

UNRESTRICTED

MOLECULES IN DIFFUSE INTERSTELLAR CLOUDS

BY

Colin Adrian Smith

BSc. CChem. MRSC

A thesis submitted to The Open University

for the degree of Master of Philosophy

June 1987

Department of Chemistry

The Open University

Milton Keynes

MK7 6AA

Date of Submission: 1st December 1987

Date of Award: 2nd March 1988

For Lyn.

INTERSTELLAR CHEMISTRY

The apparently unusual conditions under which chemistry occurs in space are really the ordinary conditions for chemical phenomena in nature. It is the general circumstances common to terrestrial chemistry that are rare and exotic; a strong tendency towards thermodynamic equilibrium; stable molecules; temperatures about 300K; pressures near atmospheric and liquid water.

Professor Harold C Urey, 1893-1981
University of California.

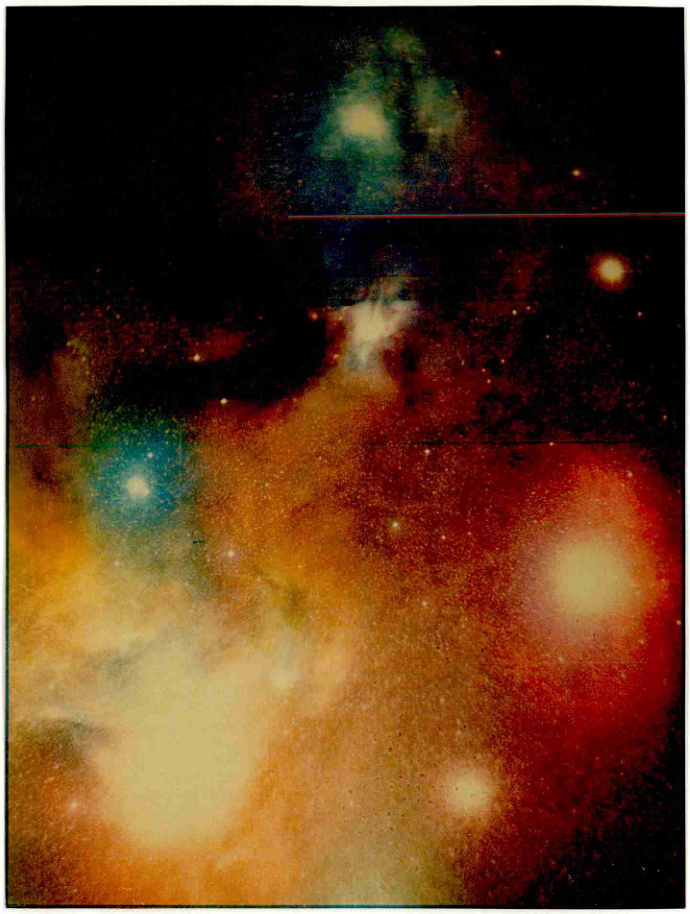

THE OPHIUCHUS CLOUD

This photograph shows the region around the star ρ Oph (top centre) on the border of the constellations Ophiuchus and Scorpio. Most of the colours are due to reflection nebulae. The one exception is the red HII region around σ Sco (lower right). Other stars in this photograph include HD 147889 (below ρ Oph), 22 Sco (to the left) and HD 148478, Antares, (bottom left.) Below σ Sco is the globular cluster M4. (See Pwa & Pottasch 1984 (544) for a review of this area.)

ABSTRACT

The existence of diatomic molecules in the diffuse interstellar gas has been known since the late thirties and from that time numerous observations have been made, at visible and ultraviolet wavelengths, of interstellar molecular absorption lines in the spectra of bright stars. The derivation of quantitative data on the column densities of the various molecules observed depends on a knowledge of certain molecular parameters, particularly the oscillator strength or f value of the transition being studied. Unfortunately the use of widely differing f values for each transition observed has led to confusion in calculating the true column densities of molecules along lines of sight.

This thesis attempts to overcome the problem by scaling the quantitative data available in the published literature using a common set of oscillator strengths. Lists of molecular oscillator strengths for the major transitions observed are included in a review of molecular spectroscopy. The result is a catalogue of lines of sight toward over two hundred stars detailing the column densities of CH, CH^+, $^{13}CH^+$, CO, ^{13}CO, CN, C_2, C_3, H, H_2, HD, OH, H_2O, HCl, NH, N_2, CS^+, CO^+ and H_2O^+. Tables of each stars characteristics, molecular radial velocities and references for each line of sight are also included.

Following a review of the current state of interstellar chemistry, the relationships between the molecules in the catalogue are examined using sample correlation coefficients, and correlation diagrams. The results of this large data set confirm modern chemical theories and show that ion molecule reactions are the dominant mechanism for the formation of molecules in diffuse interstellar clouds.

ACKNOWLEDGEMENTS

I would like to thank the following

1. Dr. W.B. Somerville, my external supervisor, of the Department of Physics and Astronomy, University College, London.

2. Dr. E.A. Moore and Dr. K. Bolton, my internal supervisors, of the Department of Chemistry at the Open University.

3. Dr. D. McNally, Assistant Director of the University of London Observatory, Mill Hill Park, London for his permission to use the observatory library.

CONTENTS

		Page No.
INTRODUCTION		15.
PART 1		18.
A REVIEW OF INTERSTELLAR CHEMISTRY AND PHYSICS		
1.	THE INTERSTELLAR MEDIUM	19.
1.1.	The large scale structure of the Galaxy.	22.
1.2.	Composition of the interstellar gas.	26.
1.3.	Classification of interstellar clouds.	31.
1.4.	Interstellar dust.	40.
2.	MOLECULAR SPECTROSCOPY	43.
2.1.	Optical spectroscopy.	44.
2.2.	Diatomic molecules.	45.
2.2.1.	Molecular quantum numbers.	45.
2.2.2.	Electron configurations.	53.
2.2.3.	Electronic transitions.	61.
2.2.4.	Transitions at microwave frequencies.	91.
2.3.	Symmetry and electronic spectra of triatomic molecules.	99.
2.4.	Transition probabilities and the oscillator strength.	108.
2.4.1.	Line intensities.	109.
2.4.2.	The oscillator strength.	112.
2.4.3.	Methods of determining transition probabilities.	115.
2.5.	Oscillator strengths used to determine column densities.	120.
2.6.	Calculation of column density.	151.
2.6.1.	The equivalent width.	151.
2.6.2.	The curve of growth.	153.

Page No.

3. INTERSTELLAR CHEMISTRY 163.

3.1. Tests of chemical models. 165.

3.2. Gas phase reactions. 167.

3.2.1. Ion molecule reactions. 167.

3.2.2. Photochemistry. 173.

3.3. Interstellar molecules. 174.

3.3.1. Hydrogen and Deuterium chemistry. 174.

3.3.2. Carbon chemistry. 179.

3.3.3. Water and Hydroxyl chemistry. 200.

3.3.4. Nitrogen chemistry. 203.

3.3.5. Chlorine chemistry. 206.

3.3.6. Sulphur chemistry. 208.

3.3.7. Silicon chemistry. 209.

3.4. The effect of a shock on a diffuse cloud. 212.

3.5. Isotopic abundances. 222.

3.6. Excited states. 226.

4. OBSERVATIONS OF THE INTERSTELLAR GAS 230.

4.1. Prior to 1950. 232.

4.2. Optical observations since 1950. 234.

4.3. Satellite observations. 247.

4.3.1. The satellites. 249.

4.3.2. Ultraviolet satellite observations. 253.

4.4. Observations at microwave frequencies. 261.

Page No.

PART 2 268.

TABLES OF OBSERVATIONS AND CORRELATIONS BETWEEN MOLECULES

1. TABLES OF OBSERVATIONS 269.

Table 26. A catalogue of the stars toward which observations of molecules have been made, 270.

Table 27. Molecular column densities. 287.

Table 28. Molecular radial velocities. 316.

Table 29. References for each line of sight. 327.

2. CORRELATION DIAGRAMS 353.

3. CORRELATIONS BETWEEN MOLECULES 404.

3.1. The sample correlation coefficient. 404.

3.2. Correlations with the average total hydrogen density 407.

3.3. The gradient of the slope of a correlation diagram. 409.

3.4. Conclusions. 411.

Page No.

APPENDICES 436.

1. Spectral type and luminosity class. 437.

2. Colour and colour excess. 442.

3. Radial velocity. 444.

REFERENCES AND BIBLIOGRAPHY 447.

Page No.

LIST OF FIGURES

1.	Spiral structure of the Galaxy.	23.
2.	Molecular cloud complex in Orion.	25.
3.	The structure of the interstellar gas showing the different cloud types.	32.
4.	Coupling and precession of the vectors in Hund's cases a and b.	49.
5.	Molecular orbital energy level diagram for homonuclear diatomic molecules.	55.
6.	Electronic transitions observed in the homonuclear diatomic molecule C_2.	57.
7.	Transitions between $^1\Sigma_g^+$ and $^1\Sigma_u^+$ states illustrating the various symmetry selection rules.	62.
8.	Energy levels involved in the rotational fine structure of an electronic transition for a diatomic molecule.	66.
9.	The $A^1\Pi - X^1\Sigma^+$ Spectrum of CH^+.	67.
10.	The $A^2\Delta - X^2\Pi$ Spectrum of CH.	69.
11.	The $B^2\Sigma^- - X^2\Pi$ Spectrum of CH.	70.
12.	The $B^2\Sigma^+ - X^2\Sigma^+$ Spectrum of CN.	72.
13.	The $A^2\Sigma^+ - X^2\Pi_{3/2}$ Spectrum of OH.	74.
14.	The $B^1\Sigma_u^+ - X^1\Sigma_g^+$ Spectrum of H_2.	75.
15.	Microwave transitions of CO and CN.	93.
16.	Microwave transitions of CH and OH showing Λ doubling.	96.
17.	Equivalent width of a spectral line.	152.
18.	The curve of growth.	152.
19.	Strömgren curves of growth for three stars in the Perseus 2 cloud.	160.
20.	Curves of growth for absorption lines in the direction of Zeta Ophiuchi and AE Aurigae.	161.
21.	Curves of growth for molecular hydrogen toward four stars.	162.

Page No.

22. Chemical reaction schemes for interstellar molecules. 199.

23. The interstellar spectral lines of CH^+ at 4232.5 Å and 3957.7 Å toward Zeta Ophiuchi. 223.

24. Interstellar spectral lines toward Chi Ophiuchi. 238.

25. Absorption spectra of CH and CH^+ toward three stars. 239.

26. The interstellar spectral line of CH at 4300.3 Å. 241.

27. Interstellar spectral lines of CN toward Chi Ophiuchi. 242.

28. The absorption spectrum of C_2 toward HD 154368. 244.

29. Spectrum of interstellar C_2 toward Zeta Persei. 245.

30. The International Ultraviolet Explorer Satellite (IUE). 250.

31. Copernicus spectra of ^{12}CO and ^{13}CO toward Zeta Ophiuchi. 254.

32. Copernicus spectra of CO toward Zeta Ophiuchi. 255.

33. Copernicus spectra of molecular hydrogen toward Zeta Ophiuchi and Phi 1 Orionis. 257.

34. Spectra of H_2 and HD toward Zeta Ophiuchi. 258.

35. IUE spectra of ^{12}CO and ^{13}CO toward HD 149404 and HD 152236. 260.

36. Emission spectra showing the 3335.5 MHz line of radio CH. 264.

37. Colour index and temperature. 443.

38. Radial velocity with respect to the Local Standard of Rest. 443.

Page No.

LIST OF TABLES

1.	Cosmic abundances in The Galaxy of the first twenty elements in the Periodic Table.	29.
2.	Interstellar abundances of diatomic molecules.	30.
3.	Properties of clouds and other regions in the interstellar medium.	33.
4.	Lowest electron configurations of diatomic molecules.	59.
5.	Excited electron configurations of diatomic molecules.	60.
6.	Allowed electronic transitions.	64.
7.	Table of important electronic transitions, wavelengths and oscillator strengths for interstellar molecules observed using optical and ultraviolet spectroscopy.	76.
8.	Microwave transitions of diatomic molecules.	98.
9.	A compilation of f values for the $A'\pi - X'\Sigma^+$ transition of CH^+.	122.
10.	A compilation of f values for the absorption line at 4232.5 Å used to determine CH^+ column densities.	124.
11.	A compilation of f(00) values for the (00) band of the CH $A^2\Delta - X^2\pi$ transition.	128.
12.	A compilation of f(00) values for the (00) band of the CH $B^2\Sigma^- - X^2\pi$ transition.	130.
13.	A compilation of f values for the absorption line at 4300.3 Å used to determine CH column densities.	131.
14.	A compilation of f values for the $B^2\Sigma^+ - X^2\Sigma^+$ transition of CN.	133.
15.	A compliation of f values for the absorption line at 3874.6 Å used to determine CN column densities.	135.
16.	A compilation of f(10) values for the (10) band of the CO $A'\pi - X'\Sigma^+$ transition.	137.
17.	A compilation of f(00) values for the (00) band of the OH $A^2\Sigma^+ - X^2\pi_{3/2}$ transition.	139.
18.	A compilation of f(00) values for the (00) band of the NH $A^3\pi_i - X^3\Sigma^-$ transition.	143.
19.	A compilation of f(v'v'') values for the $A'\pi_u - X'\Sigma_g^+$ transition of C_2 (Phillips band).	146.

		Page No.
20.	A compilation of f values for the absorption line at 8757.7 Å used to determine C_2 column densities.	148.
21.	Reaction rate coefficients (1)	171.
22.	Reaction rate coefficients (2)	172.
23.	Column densities in a diffuse interstellar cloud before and after a shock.	216.
24.	Relative abundances of isotopic species.	225.
25.	Equivalent widths of the R(2) line of CN at 3873.369Å toward ζ Oph.	229.
26.	A catalogue of the stars towards which observations of molecules have been made.	270.
27.	Molecular column densities.	287.
28.	Molecular radial velocities.	316.
29.	References for each line of sight.	327.
30.	Numbers of available pairs and sample correlation coefficients for molecules.	406.
31.	Correlations of atomic abundances with the average total hydrogen density	408.
32.	Correlations of molecular abundances with the average total hydrogen density	410.
33.	Spectral types.	438.
34.	Luminosity classes.	440.

INTRODUCTION

1. INTRODUCTION

It is now over eighty years since J. Hartmann published his results on the star δ Ori, in which the first observation of a diffuse gaseous component of the interstellar medium was reported. Thirty three years later P. Swings and L. Rosenfield correctly attributed the interstellar spectral lines discovered by P. Merrill to diatomic molecules. This was the first suggestion that molecules, as well as atoms, might be present in the interstellar gas. Previous observations had only been of atomic sodium and calcium. The list of molecules detected using visible and ultraviolet spectroscopy has since grown to include CH, CH^+, CN, CO C_2, H_2, HD and OH. Upper limits have also been derived for C_3, H_2O, HCl, NH, N_2, CS^+, CO^+ and H_2O^+.

To account for the observed abundances of these molecules theorists have formulated chemical reaction schemes based on purely gas phase reactions and on models that incorporate reactions on the surfaces of interstellar grains. So far neither approach has been totally successful in explaining the abundances of all the molecules observed. This thesis examines the chemistry of interstellar molecules and the molecular observations it attempts to explain. The objective is neatly summarised in the last sentence of a recent paper by A.P.C. Mann and D.A. Williams in the Monthly Notices of the Royal Astronomical Society (Mann & Williams 1985 (353)). The sentence reads "The most pressing need in these studies appears to be to broaden the observational data set to provide tighter constraints on models".

Mann and Williams have attempted to relate their observational data to various models of the chemistry inside a diffuse interstellar cloud. In this thesis the data set has been increased by collecting together all of the observational data on interstellar molecules available in the published literature. No new observations of interstellar molecules have been made. However, for the first time a complete set of data is now available in which molecular column densities have been scaled using a common set of oscillator strengths so that column densities of molecules are easily compared. This large data set will make it easier to test the validity of chemical models, which, unfortunately, abound with little observational evidence to support many of them.

The thesis is in two parts. The first section is a review of current research in the area of interstellar chemistry and physics. The second section consists of tables which contain the data on the molecules observed. An attempt to fit these observations to current theories of interstellar chemistry is made using correlation diagrams, and correlation coefficients calculated from the data in the tables.

PART 1

A REVIEW OF INTERSTELLAR CHEMISTRY AND PHYSICS

1. THE INTERSTELLAR MEDIUM

1. THE INTERSTELLAR MEDIUM

Matter in the Universe is distributed in a highly non-uniform manner, concentrated largely into galaxies which occupy only 10^{-7} of the total volume of the Universe. In addition to stars, the galaxies contain diffuse low density interstellar matter. This is also non-uniform in nature and contains irregular high density regions or clouds which extend from 2 to 200 parsecs in diameter.

The interstellar clouds occupy 5% of the galactic volume and possess gaseous densities in a range from 10^2 to over 10^6 atoms and molecules per cm^3. In addition to gas the clouds also contain dust, about 1% of the matter by mass, made up of grains $\lesssim 0.1\mu m$ in size. The Kinetic temperature of clouds, except for HII and other ionised regions, is of the order of 10 to 100K.

In our Galaxy, interstellar material accounts for about 10% of the known galactic mass. The dust and gas in the interstellar medium can be seen, along with O and B stars that have condensed out of the gas, in the spiral arms of the Galaxy where the interstellar material is concentrated into individual clouds.

Matter in the primeval universe consisted almost entirely of hydrogen and helium, but this has since been processed through many generations of stars. Stars return most of their mass to the interstellar medium so that there is a continual re-cycling with progressive enrichment of the heavy elements. These are synthesised by nuclear fusion in the interiors of stars and in supernova explosions. Some of the stellar material is lost in explosive outbursts, such as supernovae, but most mass loss occurs in less violent ways, for example in stellar winds from red giants and as planetary nebulae. The synthesis of the chemical elements in the interiors of stars and their expulsion into interstellar space provides the ingredients for the subsequent formation of molecules in the interstellar gas.

The stars exist in dynamic equilibrium with the interstellar medium and from observational data is is clear that the distribution of interstellar matter follows closely that of the youngest stars confirming their intimate relationship. However, although the stars in our Galaxy are concentrated into a thin flat disc about 500 to 600 pc thick and 40 kpc in diameter, interstellar matter is more closely confined to the galactic plane in a disc 250pc thick and 30 kpc in diameter.

1.1 LARGE SCALE STRUCTURE OF THE GALAXY

The average density of the interstellar gas is one hydrogen atom per cm^3, but on a local scale the density of the gas varies considerably. As well as being concentrated into interstellar clouds the gas also varies with galactic radius forming recognisable spiral arms (figure 1). In the region at the centre of our galaxy the gas is flowing outward, and is piling up in an expanding ring referred to as the 3kpc arm. Outside of this the spiral arms are the dominant feature. Most of our knowledge aboout the large scale distribution of the interstellar gas in the region of the spiral arms is based on radio observations of the hydrogen atom at a wavelength of 21cm.

Carbon monoxide has been used to study the distribution of molecular hydrogen. CO excited in collisions with H_2 is observed using the $J = 1 \rightarrow 0$ rotational transition at 2.6mm. Millimetre wave observations of the emission from CO have proved to be an important method for determining the physical and chemical properties of dense interstellar regions that are not observable using optical methods because of the opacity of the dust and gas. Interpretation of the CO data shows the interstellar medium to be dominated by very massive long lived cloud complexes often referred to as Giant Molecular Clouds, with a typical mass of $10^5 M_\odot$, where $M_\odot$ is one solar mass, and a typical density of 600 atoms per cm^3.

Figure 1

SPIRAL STRUCTURE of THE GALAXY

(From Simonson 1976)

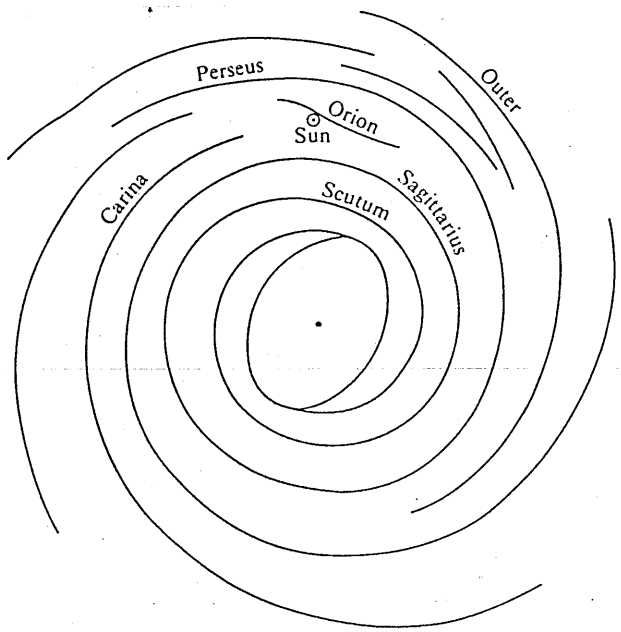

The Galaxy revealed by H 21 cm emission.

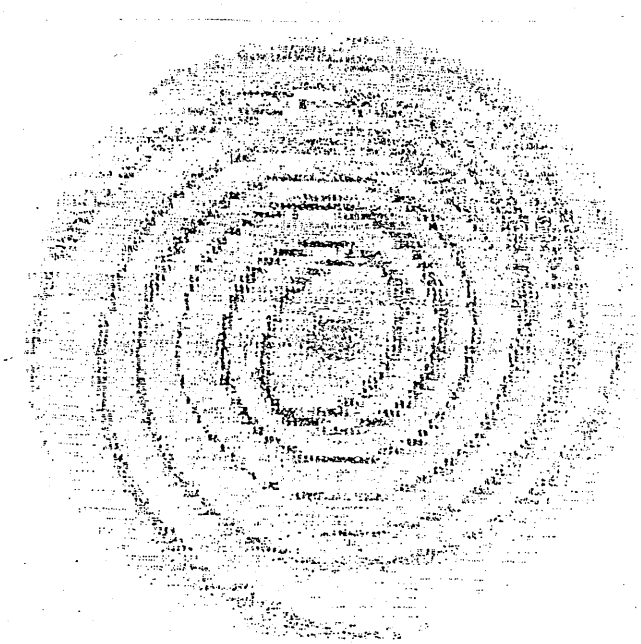

The Galaxy deduced from H 21 cm line mapping.

Although separated by wide gaps in space they are a major constituent of the galactic disc and a dominant component of the region between the Sun and the galactic centre. They are also some of the largest objects in our Galaxy having a diameter of 40 - 100 pc. Recent reviews based on millimetre observations have been given by Solomon and Sanders 1980 (304) Blitz 1982 (303) and Webster and Longair 1984 (306).

The best studied example of a molecular cloud is the nearest and is located in Orion. A map of the area made using the J = 1→0 transition of CO shows three large clouds plus a number of smaller clouds and filaments (figure 2). The fragmentary structure is a common feature of molecular clouds and the different components are said to make up a single molecular cloud complex. Numerous clumps or condensations are seen in the clouds where stellar formation is proceeding.

Smaller clouds exist with a continuous distribution of masses, but they are harder to detect. They are also sites of star formation but do not appear to contain the massive energetic stars that produce the infrared sources that have been detected in the cores of the giant molecular clouds.

Some of the 2.6mm CO features coincide with the 21cm atomic hydrogen data, such as the 3kpc arm, but there is some controversy over whether the CO data shows the spiral structure of the Galaxy. The data does show, however, that the interstellar gas is strongly concentrated into a disc in the plane of the Galaxy.

Figure 2

MOLECULAR CLOUD COMPLEX in ORION

(From Webster and Longair 1984)

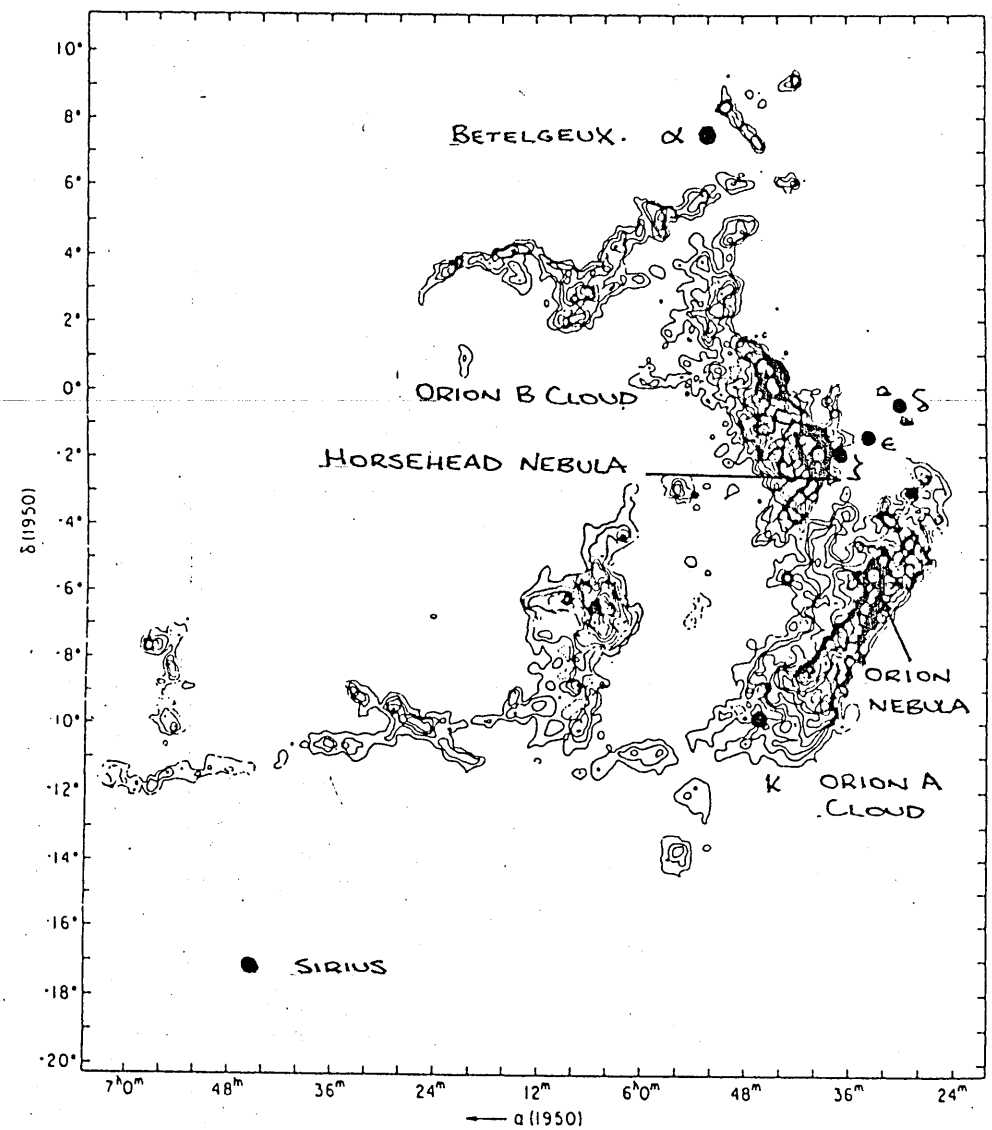

A map of the molecular cloud complex in Orion. This map shows contours of the distribution of the carbon monoxide molecule, as observed in the $J = 1 \rightarrow 0$ transition.

Many of the molecular clouds lie in a ring between 4 and 8 kpc from the galactic centre. A few lie further from the galactic centre than the Sun, and there is a dense concentration right at the centre of the Galaxy itself. The molecular cloud associated with the radio source Sgr. B2 is where many of the complex interstellar molecules have been found.

The atomic hydrogen is more uniformly spread than the molecular gas, it extends much farther out, and lies in a layer twice as thick as the molecular gas. Recent evidence of higher than expected rotation rates in outer parts of the galactic disk and dynamical considerations have also led to the inference of a huge corona enveloping the Galaxy. (de Boer & Savage 1982 (442), Hey 1983 (443)).

1.2. COMPOSITION OF THE INTERSTELLAR GAS

The total mass of interstellar matter in the Galaxy is about $5 \times 10^9 M_\odot$, where $M_\odot$ is one solar mass. 1% of this is in the form of dust whilst the other 99% is made up of a tenuous gas. The gaseous component of interstellar matter consists of essentially two components; the ionised and neutral forms. The ionised gas is the smaller component making up only 3% of the total mass. The other 97% is in the form of neutral clouds of atoms and molecules.

About 50% of the gas in interstellar clouds is in molecular form with molecular hydrogen being the most abundant molecule, about $2 \times 10^9 M_\odot$ in the Galaxy. Hydrogen makes up the vast bulk of matter in the Universe perhaps 73% by mass or 92% by number of atoms. The bulk of the interstellar

hydrogen occurs in atomic hydrogen or HI regions where the gas is almost completely neutral. Here there are large variations from place to place in the size, shape, density and temperature of the interstellar clouds. Molecular clouds are typically much colder and denser than atomic clouds. A high density corresponds to a low temperature because the heating of the gas by stellar radiation or by collision with fast cosmic ray particles depends on the density whereas the cooling of the gas by the emission of forbidden spectral lines excited by collisions depends on the square of the density. So as the density increases, the cooling rate increases faster than the heating rate and the temperature equilibrium is lower.

The largest clouds of molecular hydrogen are embedded in atomic hydrogen gas. The atomic component can be studied using the transition at 21cm (see Greisen & Liszt 1986(474)), but molecular hydrogen cannot be studied directly using radio astronomical techniques as it has no dipole moment. However, in diffuse regions it is seen in the ultraviolet absorption spectra of bright stars. Molecular hydrogen is widely distributed, but only in clouds, and although the energy threshold for direct photodissociation is above the Lyman limit, it can be destroyed in low density regions. In the denser clouds the bulk of the material is believed to be H_2 but it has to be studied by observing other species, particularly CO. The CO abundance is easily related to the H_2 abundance. The ratio of carbon monoxide to molecular hydrogen is deduced from the cosmic carbon abundance and the assumption that 10% of the carbon is in

the form of CO. This is partly confirmed by U.V. observations of both molecules.

The correlation between CO and H_2 is examined in greater depth in part 2 of this thesis.

Most of the rest of the matter in the Universe, about 25% by mass, is helium. Heavier atoms constitute less than 2% of the total mass. (Table 1). Carbon monoxide is the second most abundant molecule, about $2 \times 10^6 M_\odot$, as is evident from recent large scale surveys of the Galaxy at radio frequencies. All the molecules except CO are no more abundant than 10^{-6} relative to H_2 and the rarest molecules only 10^{-11} or 10^{-12} as common as H_2. The abundances are not universal and vary from cloud to cloud, and between different parts of the same cloud, (Table 2). Molecular abundances tend to reflect the abundances of their constituent elements. Molecules containing hydrogen, carbon, oxygen and nitrogen are quite common, silicon and sulphur compounds are rare, and other elements of still lower abundances have yet to be detected in molecules. Metals, such as magnesium, iron and aluminium have relatively high cosmic abundances, and if these elements are not preferentially depleted onto grains it is reasonable to expect to detect their oxides, carbides and hydrides in interstellar space. The fact that they are refractory is not a problem since refractory species such as SiO and SiS are observed.

Silicon compounds have been discussed by Turner & Dalgarno 1977 (225) and alkali metal hydrides by Kirby & Dalgarno 1978 (76).

TABLE 1

COSMIC ABUNDANCES IN THE GALAXY OF THE FIRST TWENTY ELEMENTS IN THE PERIODIC TABLE

From Allen 1973 (260)

ELEMENT	SYMBOL	LOG ABUNDANCE*	
		BY NUMBER	BY MASS
HYDROGEN	H	12·00	12.00
HELIUM	He	10.93	11.53
LITHIUM	Li	0.7	1.6
BERYLLIUM	Be	1.1	2.0
BORON	B	< 3	< 4
CARBON	C	8.52	9.60
NITROGEN	N	7.96	9.11
OXYGEN	O	8.82	10.02
FLUORINE	F	4.6	5.9
NEON	Ne	7.92	9.22
SODIUM	Na	6.25	7.61
MAGNESIUM	Mg	7.42	8.81
ALUMINIUM	Al	6.39	7.78
SILICON	Si	7.52	8.97
PHOSPHORUS	P	5.52	7.01
SULPHUR	S	7.20	8.71
CHLORINE	Cl	5.6	7.2
ARGON	Ar	6.8	8.4
POTASSIUM	K	4.95	6.54
CALCIUM	Ca	6.30	7.90

* Normalised so that Hydrogen = 12.00

TABLE 2

INTERSTELLAR ABUNDANCES OF DIATOMIC MOLECULES (Duley & Williams 1984 (351))

MOLECULE	CHEMICAL FORMULA	*FRACTIONAL ABUNDANCE	CLOUD TYPE	TRANSITION	ABS/ EMIS
MOLECULAR HYDROGEN	H_2	0.1	Diffuse	UV	ABS
MOLECULAR HYDROGEN	H_2	1.0	Dark	IR	EMIS
METHYLIDINE ION	CH^+	10^{-8}	Diffuse	V	ABS
METHYLIDINE	CH	10^{-8}	Diffuse	V	ABS
METHYLIDINE	CH	10^{-8}	Dark	R	EMIS
HYDROXYL	OH	10^{-7}	Diffuse	V/UV	ABS
HYDROXYL	OH	-	Dark	R	ABS/EMIS
DIATOMIC CARBON	C_2	10^{-8}	Diffuse	V	ABS
CYANOGEN	CN	10^{-8}	Diffuse	V	ABS
CYANOGEN	CN	10^{-9}	Dark	R	EMIS
CARBON MONOXIDE	CO	10^{-6}	Diffuse	UV	ABS
CARBON MONOXIDE	CO	10^{-5}	Dark	R	EMIS
CARBON MONOXIDE ION	CO^+	10^{-11}	Dark	R	EMIS
NITRIC OXIDE	NO	10^{-8}	Dark	R	EMIS
CARBON MONOSULPHIDE	CS	10^{-9}	Dark	R	EMIS
SILICON MONOXIDE	SiO	-	Circumstellar	R	EMIS
SULPHUR MONOXIDE	SO	10^{-10}	Dark	R	EMIS
NITROGEN SULPHIDE	NS	10^{-10}	Dark	R	EMIS
SILICON SULPHIDE	SiS	10^{-10}	Dark	R	EMIS

*NOTE: Typical fractional abundance relative to hydrogen e.g. n (molecule) / n H_{TOT} for that molecule observed in the type of cloud described in column four.

Small molecules are the most abundant and until recently all the large organic molecules detected have been aliphatic. Despite extensive searches no ring compounds had been found, although some such as benzene have no suitable spectral lines. Detection of the ring molecule cyclopropenylidene in our galaxy and in the radio galaxy Centaurus A has recently been reported by Thaddeus 1985 (497), Matthews 1985 (496) and Seaquist 1986 (472).
Free radicals and molecular ions are also present in the interstellar gas and play an important role in the cloud chemistry.

The molecules H_2, CO, OH, NH_3, CS and H_2CO are quite widely distributed. They are found in many directions in the Galaxy in contrast to the larger organic molecules which are restricted to the very high density clouds. Many of the molecules are found in the inner part of the rotating disc region of the Galaxy inferred from 21cm observations. Some are found only in the Orion molecular cloud and the source Sgr B2 at the centre of the Galaxy. Molecules have also been detected in extragalactic objects, for example the Magellanic clouds, (Bel et al 1986 (470)).

1.3. CLASSIFICATION OF INTERSTELLAR CLOUDS

The gaseous component of the interstellar medium may be classified into several distinct regions (Figure 3). These are summarised in Table 3, and some of the major categories are discussed below. (A recent review of the interstellar medium is given by McCray and Snow 1979 (389)).

TYPES OF INTERSTELLAR CLOUD

1. Diffuse Clouds

The diffuse interstellar clouds have an average density of

Figure 3

THE STRUCTURE OF THE INTERSTELLAR GAS SHOWING THE DIFFERENT CLOUD TYPES.

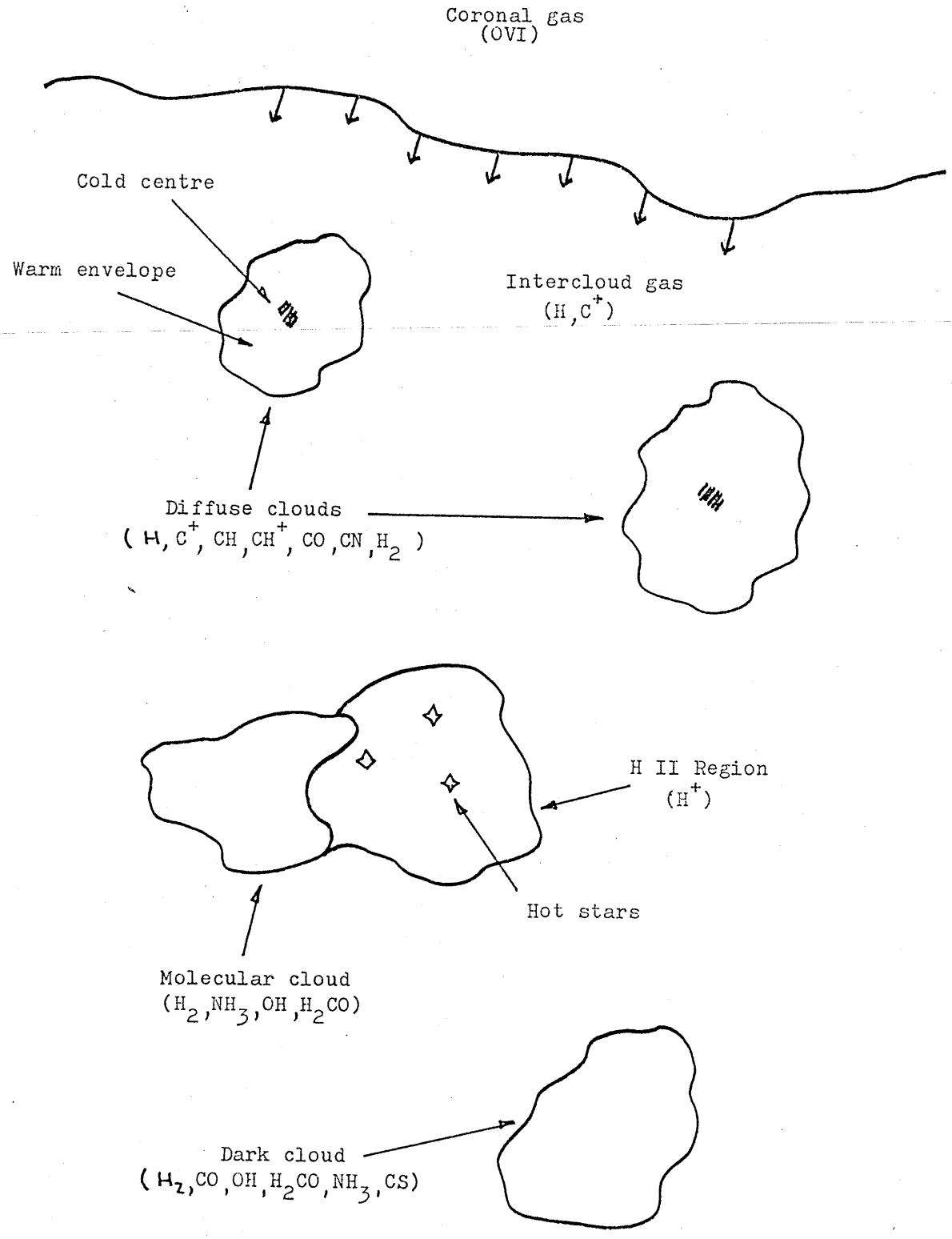

TABLE 3

PROPERTIES OF CLOUDS AND OTHER REGIONS IN THE INTERSTELLAR MEDIUM (Duley & Williams 1984 (351))

TYPE	DENSITY OF H ATOMS	MASS	KINETIC TEMPERATURE	RADIUS	SPECIES OBSERVED	OTHER
HII REGION	$10^2 - 10^3 cm^{-3}$	-	$10^4 K$	1 - 10pc	H^+, C^+ N^+, O^+	Line & Continuum Radiation
INTERCLOUD GAS	$0.1\ cm^{-3}$	-	$10^4 K$	-	H, C^+	No Molecules
DIFFUSE CLOUDS	$100 cm^{-3}$	50 M⊙	$10^2 K$	2pc	C^+ CH CH^+ CO CN H_2	Diatomic Molecules Observed
DARK CLOUDS	$10^4 cm^{-3}$	10^2-10^4 M⊙	10 - 20K	5pc	H_2, NH_3 H_2CO, OH	Many Large Molecules
MOLECULAR CLOUDS	$10^6 cm^{-3}$	$\lesssim 10^6$ M⊙	50K	$\lesssim$ 30pc	H_2, NH_3 OH, H_2CO	Emit IR Radiation
CIRCUMSTELLAR SHELLS	-	-	$10^2 - 10^3 K$	-	SiO, C_2H_2	Molecules & dust Observed
COMPACT HII REGIONS	$10^3 - 10^4 cm^{-3}$	-	$10^2 - 10^3 K$	-	SiO, H_2O OH	IR & radio Emission Maser Action
CORONAL GAS	$10^{-2}\ cm^{-3}$	-	$10^5 - 10^6 K$	-	O VI	Occupies 50% of ISM Highly Ionised gas
GIANT MOLECULAR CLOUDS	$600 cm^{-3}$	5×10^5 M⊙	10K	40 -100pc	H_2	Major Component of Galaxy

100 or less atoms and molecules per cm^3 and a temperature of $\leqslant$ 100K. Their diameters are of the order of several parsecs and they are found in all parts of the Galaxy. An example is the cloud in front of the star ζ Oph. The gas is distributed in clumps, the line of sight through the gas showing multiple components. For example Blades et al 1980 (293) have shown distinct clouds to exist along the line of sight to α Cyg using measurements of the Na I D lines. Simple molecular species such as CH, CH^+, CO, CN and H_2 are found in these regions. Ions like C^+ and Ca^+, produced by photo ionisation by starlight, are also present. The cold core of a diffuse cloud is often surrounded by much warmer, 8000K, envelopes of ionised and neutral gas formed by the heating effects of UV photons and soft X-ray photons respectively. This envelope may be swept away by a passing shock wave from a supernova explosion and will then form a separate cloud without a cold core. If this occurs the cold cloud will generally not have time to reform its warm envelope before the process is repeated (see Spitzer 1982 (257)).

2. Dark Clouds

The dark interstellar clouds are denser than the diffuse clouds and appear darker because they are more opaque to visible and ultraviolet radiation. They are not associated with star formation, young stars or H II regions. An example is TMC 1, in Taurus, which may be in the last stages of evolution before stars form. It is also possible that TMC 1 is a highly evolved quiescent object and that no stars will ever form. (see Hobbs 1983 (147) and Duvert 1986 (518).

They are optically extended regions having densities up to 10^4 atoms and molecules per cm^3 and temperatures from 10 to 20K. Their radii are of the order of 5 parsecs. More complex molecules are found in these regions, including CO, OH, H_2CO, NH_3 and CS.

3. Molecular Clouds

The black molecular clouds are much higher in density, up to 10^6 or more atoms and molecules per cm^3, and they are hotter, a temperature of 50K is typical. Their radii are of the order of 30 parsecs, and they are associated with H II regions and star formation. The most complex molecules are detected in these regions, examples are Sgr B2 and Sgr A which lie at the centre of the Galaxy.

4. Intercloud Gas

21 cm line studies of atomic hydrogen show the presence of a very diluted, $< 0{\cdot}1$ atoms per cm^3, but hot intercloud gas, in which the diffuse clouds are embedded. A temperature of 10^3K to 10^4K is comparable with that of radiatively excited regions. The gas is composed of mainly hot atomic hydrogen and some of the gas is ionised. The intercloud gas occupies most of the space between the spiral arms of the Galaxy as well as some space within the spiral arms. Thus most of the galactic disc is taken up by intercloud gas.

5. Coronal Gas

Recent observations of the soft X-ray background emission from the Galaxy and of ultraviolet interstellar absorption by the O^{5+} ion (O VI) have led to the identification of a further very hot ionised component of the intercloud gas at very low densities.

The temperature of this coronal gas is 10^5 to 10^6K and its density about 10^{-2} atoms per cm^3. It may occupy about 50% of the total interstellar volume. It is the result of the heating of low density gas by interstellar shock waves caused by supernovae explosions. The passage of a supernova remnant through the intercloud medium will tend to sweep away any low density material present replacing it with coronal gas. The swept material will be compressed into a denser thin sheet by the force of the exploding hot gases and will be cooled to a low temperature providing additional material for the cold clouds. As a result of this continual sweeping action much of the intercloud gas is assumed to be coronal gas.

6. H II Regions

Apart from interstellar gas and dust, space is also filled with photons and cosmic particles produced by a variety of mechanisims.

The ultraviolet radiation field at wavelengths $\geqslant 912$ Å, the ionisation limit for hydrogen, is the result of integrated starlight. At wavelengths <912 Å most photons are absorbed by the ionisation of hydrogen in the immediate vicinity of the stars from which they originate. However, if the surface temperature of a star is higher than about 10^4K it radiates a sufficient number of ultraviolet photons of wavelength shorter than the Lyman series limit at 912 Å to ionise the hydrogen atoms within a reasonable distance. This H II region around the star is called a Strömgren sphere, although it is usually very irregular in shape because of density irregularities in the gas. Between the H II region and the neutral H I region there is also an ionisation front.

Recombination in H II regions forms neutral atoms and is followed by a cascade of line emission in the H I spectrum with eventual re-ionisation. The red colour of emission nebulae is due to the strong Balmer line at 6562 Å ($n = 2 \leftarrow 3$). Other strong optical emission lines are due to oxygen and nitrogen.

The densities of H II regions are of the same order as those of the cold diffuse clouds about 100 atoms per cm^3, and the kinetic temperature about 10,000K. For the hottest stars the radius of an H II region can exceed 100pc, the area depending on the star's temperature and the density of the gas in space. In addition to the H II region there is a lower density higher temperature intercloud component of the ionised hydrogen gas which is not seen optically.

The ionised gas or plasma in the H II region radiates strong recombination lines in the microwave as well as the visible part of the spectrum and a strong Bremsstrahlung continuum spectrum in the radio frequency range. A good example of an H II region is the Orion nebula which is being produced by the radiation from an association of very young blue giant O and B stars, the dominant ones being the Trapezium stars θ^1 Ori A, B, C and D.

H II regions and molecular cloud complexes are intimately related. About 80% of all visible H II regions in the Galaxy are associated with molecular clouds. The short-lived O and B stars form inside the molecular clouds and the ultraviolet radiation they produce ionises the gas surrounding them resulting in an H II region.

The resultant expansion of an H II region can result in a shock, behind which lies the hot gas necessary to produce the CH^+ molecular ion, seen in diffuse clouds, in the quantities observed using optical spectroscopy.

7. Other Regions

Other regions in space toward which molecules have been found include planetary nebulae, clouds of hot high density gas that have been ejected from a central star and are expanding radially outwards. An example is the Ring nebula in Lyra. Other gaseous regions include the tenuous gas associated with supernova remnants and the gas around stars undergoing mass loss, such as T. Tauri stars. Observations of molecules toward supernova remnants have been made by Gondhalekar and Phillips 1980 (143) and Phillips and Gondhalekar 1983 (134). Clavel and Flower 1980 (295) have searched for CO in the spectrum of the planetary nebula IC 418.

CLASSIFICATION BY THE AMOUNT OF HYDROGEN PRESENT

It is useful to distinguish between the various types of interstellar cloud by using the amount of hydrogen present as a guide.

The diffuse clouds are transparent enough to be studied by means of the absorption lines they produce in the spectra of background stars, whereas the dark clouds are opaque at visible wavelengths. The difference may be stated in terms of the total column density of hydrogen through the cloud, N_H.

$$N_H = \int [n(H) + 2n(H_2)]\, dl.$$

Dalgarno & Black 1976 (18).

For diffuse clouds $N_H \lesssim 5 \times 10^{21}$ cm $^{-2}$ corresponding to a visual extinction $A_V \lesssim 3$ magnitudes. For the dark clouds $N_H \gtrsim 5 \times 10^{21}$ cm^{-2} corresponding to a visual extinction $A_V \gtrsim 3$ magnitudes.

The actual distinction between the two types of cloud though is not quite so clear. Federman and Willson 1982 (50) in a survey of radio emission from CH toward α Cam and K Cas conclude that diffuse clouds are the outer relatively transparent portions of dark clouds.

Interstellar clouds are truly interstellar and are not particularly associated with any individual stars. The distinction between the cloud and intercloud regions is in some ways more fundamental than that between H I and H II regions. The same cloud could appear dark or as an emission nebula according to where it is in relation to nearby stars. In some cases the nearby stars are being formed out of the cloud and the young hot stars will form an H II region in parts of the cloud as is happening in the Orion nebula. A review of the interstellar medium by Heiles 1974 (261) based on Ca II, NaI and H I observations outlines a picture of interstellar space containing a large number of very large aggregates with properties similar to those of cloud complexes. Low density clouds are separated by an intercloud region which is perhaps also cloudy.

This study is concerned primarily with the diffuse interstellar clouds in which the optical diatomic free radicals CH, CH^+ and CN and the ultraviolet molecules and radicals H_2, CO and OH are seen in the absorption spectra of background stars. Although more complex species are present in the dark and black molecular clouds they are so

opaque that starlight cannot penetrate them.

These clouds are related to the dark objects seen in projection against bright emission nebulae and are studied using microwave and infrared techniques.

1.4. INTERSTELLAR DUST

The second component of the interstellar medium is dust. This consists of small solid particles or grains and is well mixed with the gas. The total amount of matter in the grains is only a few per cent of the total mass of material in interstellar space, but they reflect starlight so effectively that they dominate this process. If a cloud of gas and dust is near to a star not hot enough to produce an H II region it can appear bright simply by reflection of the starlight. These reflection nebulae appear blue, an example being the Pleiades in Taurus. The composition of this material is still uncertain and it is the object of much discussion at present. Molecular ice (Jones and Williams 1984 (266)), silicates, iron and graphite have been suggested. An infrared absorption feature around 10μm wavelength is generally taken to be an indicator of silicate minerals and another absorption feature at 3μm is related to water ice. Composites of graphite and silicates are probably covered with an ice mantle in the denser clouds. Dust clouds are often detected by their obscuration of the stars behind them, for example the Coal Sack in the constellation of the Southern Cross. They can also appear as silhouettes in front of bright gas clouds to form dark nebulae. For example the Horsehead nebula in Orion.

Two hypotheses concerning the origin of interstellar dust have been advanced.

1. That the dust has condensed from the elements present in

interstellar space. However, this is unlikely under the conditions present although ice mantles may form this way.

2. That the dust is formed in the atmospheres of Red Giants and in new planetary systems.

The subject of the composition and formation of interstellar dust will not be discussed further (for a review see Whittet 1981 (525) and Greenberg 1984 (527)), but its presence in space is important for the formation of interstellar molecules. Dust grains both absorb and scatter starlight, the combined effect is called extinction, and this increases rapidly with decreasing wavelength. From optical observations it is easy to determine the relative extinction or colour excess along a line of sight. The variation of extinction with wavelength can be explained by assuming a mixture of grains with a wide range of sizes. Extinction in the visible region requires a grain size of about 0.1μm. Recent observations of the extinction in the UV require a second component of much smaller grains, about 0.01μm in size.

Interstellar dust plays an important role in protecting molecules from the dissociative effects of starlight and provides sites for surface reactions between atoms and molecules. Molecules are concentrated into clouds simply because in lower density regions they would form more slowly and be destroyed very rapidly. Most molecules are destroyed by photons from starlight with energies less than the Lyman limit $h\nu < 13.598$eV corresponding to a wavelength > 912 Å.

In low density neutral hydrogen clouds molecular lifetimes

are only 10 to 100 years, much shorter than the time required to form a molecule. In the dustier regions not only are reaction rates higher but the dust in the outer parts of the cloud absorbs the destructive photons. In the less dense regions the only molecules that can survive are diatomic species like CH, CH^+, CN, CO and H_2.
They are formed more readily and have a higher threshold towards photodestruction.

2. MOLECULAR SPECTROSCOPY

2. MOLECULAR SPECTROSCOPY

2.1. OPTICAL SPECTROSCOPY

Spectroscopy, the study of the interaction between radiation and matter is an important tool in unravelling the physics and chemistry of the interstellar medium. Radiation from space provides most of the information we receive on Earth about the Universe, and a detailed understanding of how this radiation was produced gives information on the emitting and absorbing materials along the line of sight. In addition, it also provides information on the density, temperature and velocity of the atoms, molecules and dust grains that are interacting with the radiation. A thorough survey of the radiative processes that operate in the interstellar medium has been given by Spitzer 1978 (292).

When light having a continuous spectrum is passed through a molecular gas, an absorption spectrum containing bands is produced. The bands usually have at one end a sharp edge called the band edge or band head, where the intensity falls suddenly to zero. On the other side the intensity falls off more or less slowly. Accordingly as this takes place towards shorter or longer wavelengths the bands are said to be shaded to the violet or to the red.

At greater resolution the bands can be seen to consist of large numbers of individual lines. In a simple case like CN, a band will consist of a series of lines which draw farther and farther apart from one another as the distance from the band head increases. The bands and their constituent lines make up the vibrational and rotational fine structure of electronic transitions between the ground and excited states of molecules. Such spectra usually occur at visible and ultraviolet wavelengths.

2.2. DIATOMIC MOLECULES

In order to interpret molecular spectra it is necessary to know something about the structure of the molecules giving rise to the absorption bands.

2.2.1. MOLECULAR QUANTUM NUMBERS

In some respects diatomic molecules behave like atoms and their energy distribution follows a similar pattern.

First consider the case of a single electron in an atom. The electron moving about the nucleus possesses orbital angular momentum a measure of which is given by the quantum number ℓ. The angular momentum is quantised and expressed in terms of the unit $h/2\pi$ where h = Planck's constant. Angular momentum $\underline{\ell}$ is a vector quantity and is given by

$$|\underline{\ell}| = \sqrt{\ell(\ell+1)} \qquad (2.1.)$$

ℓ and $\underline{\ell}$ are zero or positive.

The electron is also spinning about an axis, and its spin is designated by the quantum number S, which has a value of $\frac{1}{2}$. The spin angular momentum $\underline{S}$ is given by

$$|\underline{S}| = \sqrt{S(S+1)} \qquad (2.2.)$$

The total angular momentum $\underline{J}$ is given by the sum of the orbital and spin momenta.

$$\underline{J} = \underline{\ell} + \underline{S} \qquad (2.3.)$$

or in terms of the quantum number J

$$|\underline{J}| = \sqrt{J(J+1)} \qquad (2.4.)$$

where J is half integral.

This picture may now be expanded to atoms with more than one electron. In this case the total orbital angular momentum $\underline{L}$ is given by

$$\underline{L} = \Sigma \underline{l} \qquad (2.5.)$$

and the total spin angular momentum $\underline{S}$ by

$$\underline{S} = \Sigma \underline{s} \qquad (2.6.)$$

Likewise the total angular momentum for all the electrons is given by

$$\underline{J} = \underline{L} + \underline{S} \qquad (2.7.)$$

$\underline{L}$ and $\underline{S}$ may also be expressed in terms of the total orbital and total spin quantum numbers L and S, where

$$|\underline{L}| = \sqrt{L(L+1)} \qquad (2.8.)$$

and L = 0, 1, 2

$$|\underline{S}| = \sqrt{S(S+1)} \qquad (2.9.)$$

and S is integral or zero when the number of electrons is even, and half integral when the number of electrons is odd.

Likewise the total angular momentum $\underline{J}$ for all the electrons is given by

$$|\underline{J}| = \sqrt{J(J+1)} \qquad (2.10.)$$

Where J is integral if S is integral or half integral when S is half integral.

In terms of the quantum numbers

$$J = L + S, L + S - 1, \ldots |L-S| \qquad (2.11.)$$

In the case of a diatomic molecule the total orbital angular momentum is, as for atoms with several electrons, given by

$$|\underline{L}| = \sqrt{L(L+1)} \qquad (2.12.)$$

Where the quantum number $L = \Sigma l, \Sigma l - 1, \ldots$.

However the axial component of $\underline{l}$ the orbital angular momentum for each electron is more important in molecules than the angular momentum itself and is given the symbol λ. The axial component for several electrons is given by Λ. Since by definition all individual λ lie along the internuclear axis we can say,

$$\Lambda = \Sigma \lambda \qquad (2.13.)$$

The states corresponding to $\Lambda = 0, 1, 2, 3...$ are given the Greek letters $\Sigma, \Pi, \Delta, \Phi...$ Λ is necessarily positive but may point either way. Although orbital axial coupling is strong spin axial coupling can be weak. The total spin angular momentum is given by

$$|\underline{S}| = \sqrt{S(S+1)} \qquad (2.14.)$$

where the total spin quantum number S is given by

$$S = \Sigma s, \Sigma s-1... \qquad (2.15.)$$

The axial component (in the direction of positive Λ) of the total spin momentum is designated by Σ, which may be positive or negative. The multiplicity of the state is given by $2\Sigma + 1$.

There are other sources of angular momentum in a diatomic molecule apart from those due to orbital and spin angular momentum. They are rotation of the molecule as a whole and nuclear spin. The nuclear spin has very weak coupling so the other three may be considered without it. The ways in which these angular momenta may be coupled together are given by Hund's cases a to e. We shall only consider cases a and b.

HUND'S CASE a

Hunds case a applies to diatomic molecules where the internuclear distance is small enough for there to be a sufficiently strong electric field along the internuclear axis to prevent the total orbital and total spin angular momenta from directly coupling (Figure 4a). Magnetic interaction between $\Lambda\underline{k}$ and the total spin angular momentum though is strong where k is the unit vector along the internuclear axis. This results in the $\underline{S}$ vector being strongly coupled to the magnetic field along the internuclear axis so that its axial component Σ is quantised

$$\Sigma = \underline{S}.\underline{k} \qquad (2.16.)$$

and $$\Sigma = S, S-1, \ldots -S \qquad (2.17.)$$

Σ is the axial component in the direction of Λ and so may be positive or negative, and S is the total spin quantum number.

The total angular momentum along the internuclear axis is given by $\Omega.\underline{k}.$, where

$$\Omega = |\Lambda + \Sigma| \qquad (2.18.)$$

The nuclei in the rigid diatomic molecule may be regarded as rotating as a whole about an axis perpendicular to the internuclear axis and having an angular momentum $\underline{O}$. If the interaction between $\Omega\,\underline{k}$ and $\underline{O}$ is very weak then these two may be combined to form a resultant angular momentum $\underline{J}$ where

$$\underline{J} = \underline{O} + \Omega\underline{k} \qquad (2.19.)$$

and the quantum number J is given by

$$J = \Omega, \Omega + 1, \Omega + 2, \ldots \qquad (2.20.)$$

COUPLING AND PRECESSION OF THE VECTORS IN HUND'S CASES (a) AND (b).

Figure 4a

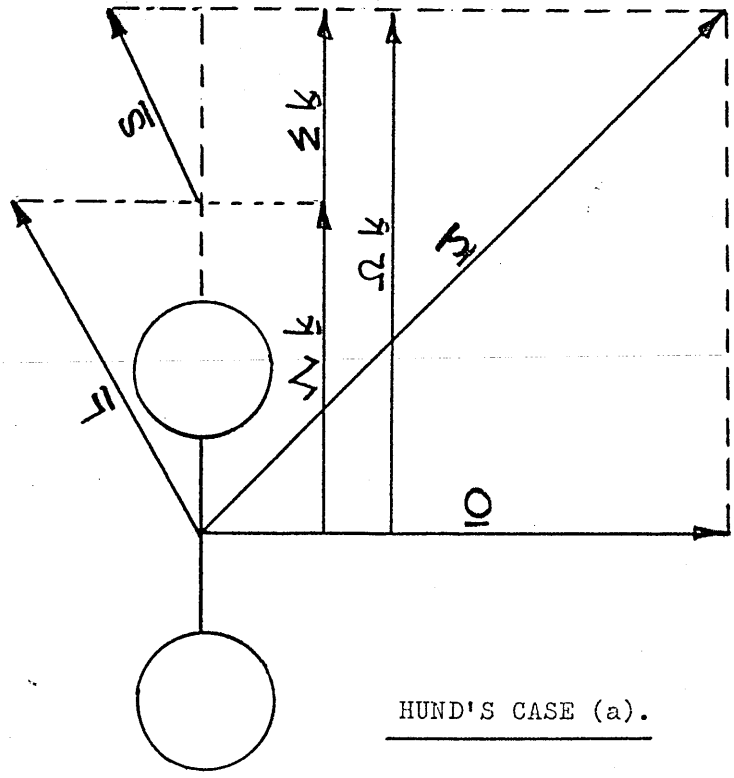

HUND'S CASE (a).

Figure 4b

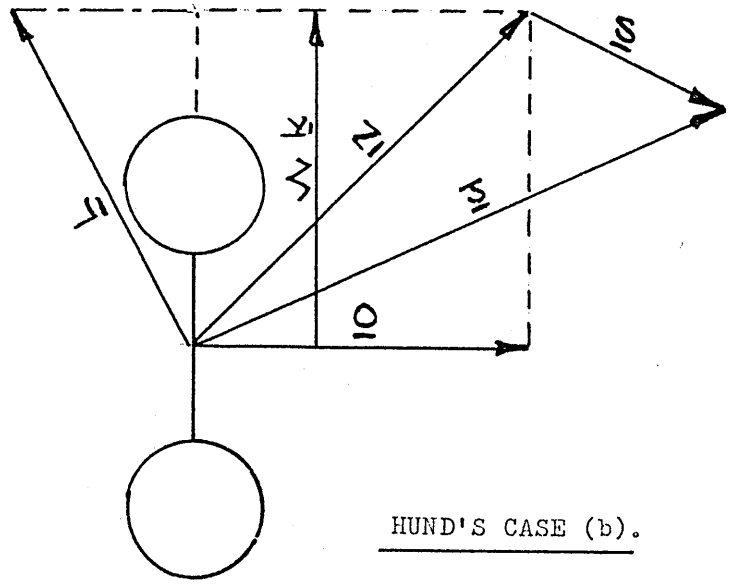

HUND'S CASE (b).

HUND'S CASE b

As with case a the internuclear distance is small enough for there to be a sufficiently strong electric field along the internuclear axis to prevent $\underline{L}$ and $\underline{S}$ from directly coupling (Figure 4b). Case b differs from case a in that the magnetic interaction between $\Lambda\underline{k}$ and $\underline{S}$ is negligible compared to that between the molecular rotation angular momentum $\underline{O}$ and $\Lambda\underline{k}$. $\Lambda\underline{k}$ combines with $\underline{O}$ to give a resultant angular momentum $\underline{N}$, where

$$\underline{N} = \underline{O} + \Lambda\underline{k} \qquad (2.21.)$$

and the quantum number N is given by

$$N = \Lambda, \Lambda + 1, \Lambda + 2 \qquad (2.22.)$$

$\underline{N}$ is called the total angular momentum apart from spin.

The spin angular momentum vector $\underline{S}$ couples with $\underline{N}$ to give a resultant $\underline{J}$ called the total angular momentum including spin.

$$\underline{J} = \underline{N} + \underline{S} \qquad (2.23.)$$

where the quantum number J is given by

$$J = N + S, N + S - 1, \ldots |N-S| \qquad (2.24.)$$

Since S may have integer or half integer values according to whether there is an even or odd number of electrons in the molecule it can be seen that J is integral when the number of electrons is even and half integral when the number of electrons is odd.

SYMMETRY

Information on the symmetry characteristics of the wavefunction of a molecular electronic state is given by a + or - sign. If the wave function of the electron eigenfunction does not change sign on reflection of the co-ordinates to the other side of a plane between the two nuclei then it is +. If the sign is changed it is -. This information is added as a right hand superscript to the term symbol. For example $^1\Sigma^+$. $^1\Pi$ and other non zero Λ terms have both + and - symmetry within them.

A subscript of g or u is given when the atoms joined by the bond are identical or isotopes of the same element. If the electron eigenfunction remains unaltered in sign after reflection through the centre of symmetry then the state is g. If it is altered then the state is u. For example $^1\Sigma_g$.

The information about the electronic structure of a molecular state is summed up in a term symbol of the general type

$$^{2\Sigma+1}\Lambda_{\Omega}^{+\text{ or }-}{}_{u\text{ or }g}$$

u or g symmetry characteristics are only applicable to homonuclear diatomic molecules like H_2 and C_2.

The ground state is labelled X and successive higher levels of the same spin multiplicity are identified by the letters A, B, C etc. Levels of different spin multiplicity are identified by the lower case letters a, b, c etc. For example $X\,^1\Sigma_g^+$ is the ground state of H_2.

SYMMETRY PROPERTIES OF ROTATIONAL LEVELS

The rotational levels of a diatomic molecule may also be classified as + or -. If the sign of the total eigenfunction remains unchanged after reflection of all the points in the molecule through the origin of the co-ordinates then the rotational level is +. If however the sign of the total eigenfunction changes it is -.

For homonuclear diatomic molecules, the rotational levels are also characterised by s (symmetric) and a (antisymmetric). When an exchange of the positions of the nuclei in the molecule leaves the total eigenfunction unchanged the rotational levels are said to be s, if, however, the total eigenfunction changes sign the levels are said to be a.

For a given electronic state of the molecule either the + rotational levels are all s and the - rotational levels all a or conversely these relations are reversed.

2.2.2. ELECTRON CONFIGURATIONS

The representation of the electronic structure of a molecule by its electron configuration is only an approximation. However, we begin by placing the electrons in the lowest possible orbitals as far as is allowed by the Pauli Exclusion Principle, thus obtaining the ground state. The order of the molecular orbitals depends on the internuclear distance and on the nuclear charge. If these are altered, that is in different molecules, considerable alterations in the order of the orbitals results. For unlike atoms, the relative positions of the orbitals at large internuclear distances depends greatly on the degree of dissimilarity of the atoms. For the H_2 molecule and the diatomic hydrides the internuclear distances are small and so it can be assumed that they approach fairly closely the united atom. The ground state of H_2 is the state in which both electrons are in the lowest orbital $(1s\sigma_g)^2$. This is the $X^1\Sigma_g^+$ state.

Most of the excited states result from one of the electrons going from the lowest orbital to one of the higher orbitals, $2s\sigma$, $2p\sigma$, $2p\pi$, etc. In each case for H_2, a singlet and a triplet state result.

For most of the diatomic hydride molecules only a few electronic states have been found. CH has seven electrons and the lowest electronic configuration is $(1s\sigma)^2(2s\sigma)^2(2p\sigma)^2(2p\pi)^1$ which gives the $X^2\Pi$ state as ground state in agreement with experiment. Since the energy difference between $2p\sigma$ and $2p\pi$ is small the lowest excited states are obtained not by bringing the $2p\pi$ electron to higher orbitals but by

transferring an electron from the $2p\sigma$ to the $2p\pi$ orbital. The resulting configuration $(1s\sigma)^2(2s\sigma)^2(2p\sigma)^1(2p\pi)^2$ gives rise to four states $A^2\Delta$, $B^2\Sigma^-$, $C^2\Sigma^+$ and $(^4\Sigma^-)$, only three of which have been observed. The unobserved fourth state is given in brackets.

The ground state electronic configuration of the CH^+ molecular ion is $(1s\sigma)^2(2s\sigma)^2(2p\sigma)^2$ which is the $X^1\Sigma^+$ state. Excitation of an electron from the $2p\sigma$ orbital to the $2p\pi$ orbital results in the electronic configuration $(1s\sigma)^2(2s\sigma)^2(2p\sigma)^1(2p\pi)^1$ giving rise to two states $A^1\pi$ and 3π.

In the case of a diatomic homonuclear molecule the order of the molecular orbitals may be altered slightly due to $S\sigma P\sigma$ interactions. This results in the $2p\pi_u$ orbital becoming lower in energy than the $2p\sigma_g$ orbital. (see figure 5 for the molecular orbital energy level diagram of homonuclear diatomic molecules). The extent of the energy shift will be greatest when the energy difference between the S and P orbitals is least, because then they can interact the most. The energy difference increases and the shift decreases with the atomic number of the atoms. So that in light molecules the $2p\pi_u$ orbital is lower in energy that the $2p\sigma_g$ orbital. This trend persists at least as far as N_2, after which, in heavy molecules, the $2p\sigma_g$ orbital becomes the lowest in energy.

For the C_2 molecule with 12 electrons two different electronic configurations have been suggested for the ground state. The first $(1s\sigma_g)^2(1s\sigma_u)^2(2s\sigma_g)^2(2s\sigma_u)^2(2p\pi_u)^4$ gives rise to the $X^1\Sigma_g^+$ state and

*

MOLECULAR ORBITAL ENERGY LEVEL DIAGRAM FOR HOMONUCLEAR DIATOMIC MOLECULES

Figure 5

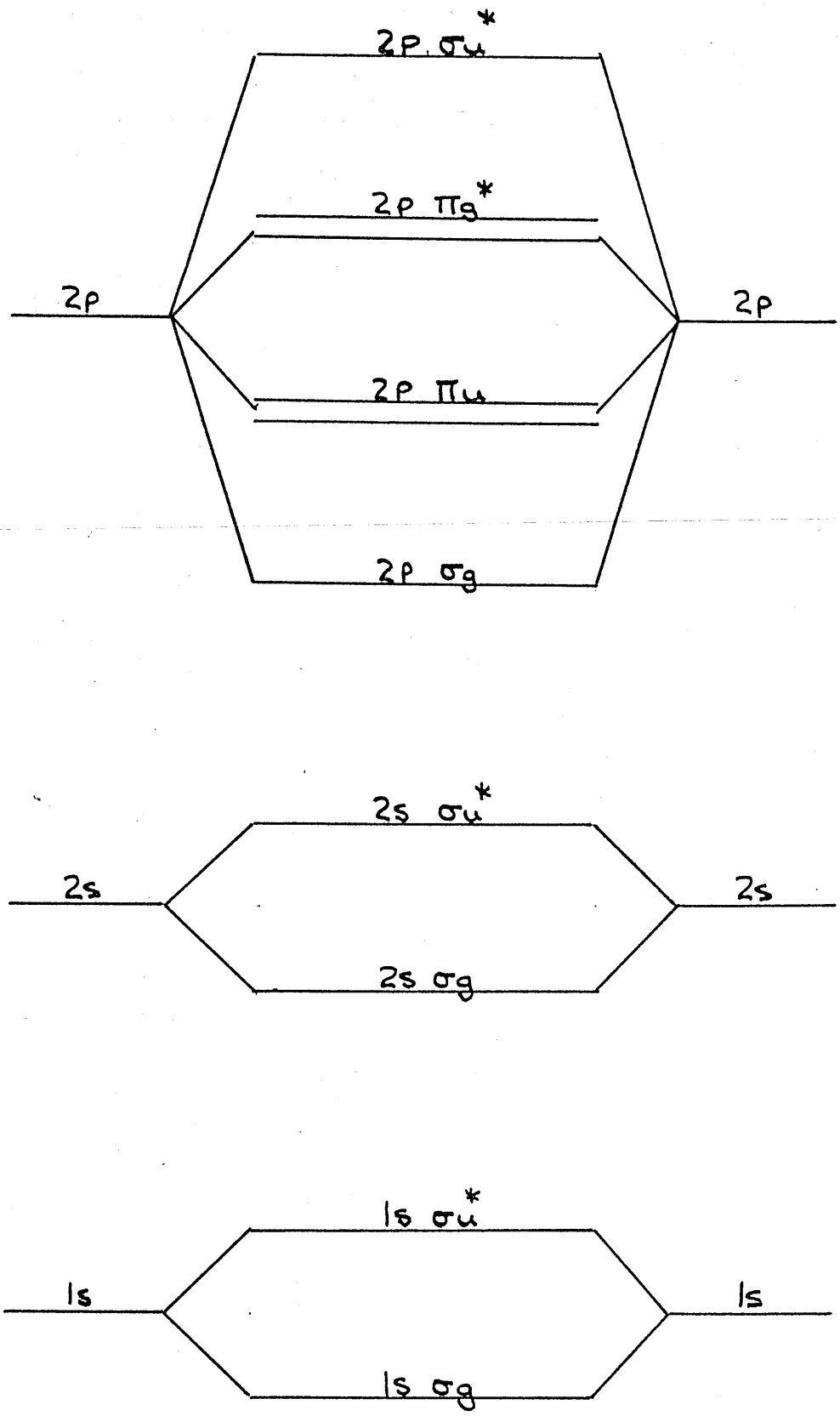

* Sσ-Pσ interactions have been ignored.

corresponds to the one that would be expected if the electrons are brought into the lowest possible orbitals. The second $(1s\sigma_g)^2(1s\sigma_u)^2(2s\sigma_g)^2(2s\sigma_u)^2(2p\pi_u)^3(2p\sigma_g)^1$ giving the $a^3\Pi_u$ state should correspond to an excited state. However experiments had shown (Herzberg 1950 (240)) that in the absorption spectrum of the C_2 molecule the Swan band's lower state is $a^3\Pi_u$. It was postulated this was due to the fact that the orbitals $2p\pi_u$ and $2p\sigma_g$ have not very different energies near the equilibrium internuclear distance so that when the interaction of the electrons is taken into account it may very well happen that the $a^3\Pi_u$ state resulting from $(2p\pi_u)^3(2p\sigma_g)^1$ lies lower than the $(2p\pi_u)^4$, $X^1\Sigma_g^+$ state. However later work (Ballik & Ramsey 1963 (466)) has shown that $X^1\Sigma_g^+$ is in fact the true ground state; with the $a^3\Pi_u$ state only $610cm^{-1}$ higher in energy. (See Figure 6). The same electron configuration that gives rise to the $a^3\Pi_u$ ground state also gives the $A^1\Pi_u$ state which has been observed as the lower state of the Deslandres-d'Azambuja bands. The upper states of these bands and the Swan bands $C^1\Pi_g$ and $d^3\Pi_g$ respectively belong to the configuration $(1s\sigma_g)^2(1s\sigma_u)^2(2s\sigma_g)^2(2s\sigma_u)^1(2p\pi_u)^3(2p\sigma_g)^2$. The $(2p\pi_u)^4$, $X^1\Sigma_g^+$ state has been observed as the lower state of the Mulliken bands at 2300Å. The upper state $D^1\Sigma u^+$ has the electron configuration $(1s\sigma_g)^2(1s\sigma_u)^2(2s\sigma_g)^2(2s\sigma_u)^1(2p\pi_u)^4(2p\sigma_g)^1$. A transition in emission from the $A^1\Pi_u$ state to the $(2p\pi_u)^4$, $X^1\Sigma_g^+$ state has also been found by Phillips. (See Figure 6).

Figure 6

ELECTRONIC TRANSITIONS OBSERVED IN THE HOMONUCLEAR DIATOMIC MOLECULE C_2

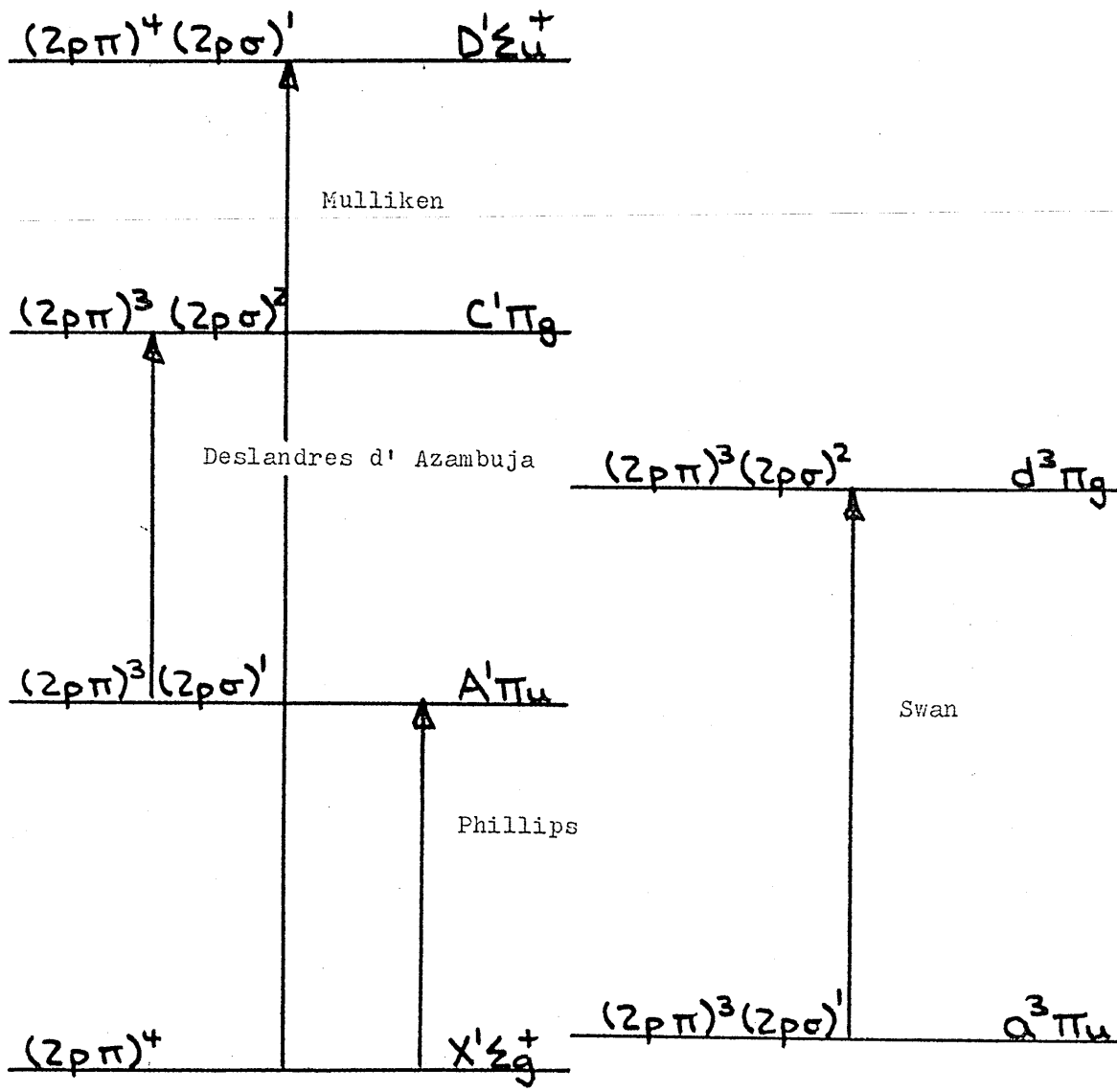

The CN radical and the molecular ions N_2^+ and CO^+ have 13 electrons and a ground state electron configuration of $(1s\sigma_g)^2(1s\sigma_u)^2(2s\sigma_g)^2(2s\sigma_u)^2(2p\pi_u)^4(2p\sigma_g)^1$. This is the $X^2\Sigma_g^+$ state. (In the case of CN and CO^+ the distinction between u and g disappears). The first two excited states are $A^2\Pi$ and $B^2\Sigma^+$, which result from the electron configurations $(1s\sigma_g)^2(1s\sigma_u)^2(2s\sigma_g)^2(2s\sigma_u)^2(2p\pi_u)^3(2p\sigma_g)^2$ and $(1s\sigma_g)^2(1s\sigma_u)^2(2s\sigma_g)^2(2s\sigma_u)^1(2p\pi_u)^4(2p\sigma_g)^2$ respectively, (See Larsson, Siegbahn & Ågren 1983 (228)).

The molecules CO and N_2 have 14 electrons giving a ground state configuration $(1s\sigma_g)^2(1s\sigma_u)^2(2s\sigma_g)^2(2s\sigma_u)^2(2p\pi_u)^4(2p\sigma_g)^2$ which is the $X^1\Sigma_g^+$ state. In the case of CO, as for CN, the nuclei of the molecule have unequal charges so that the distinction between g and u disappears. In consequence there is a slight alteration of the order of the orbitals when compared with N_2.

However the differences thereby introduced are small and the electron configurations of the ground and excited states for CO and N_2 are effectively the same.

TABLE 4

LOWEST ELECTRON CONFIGURATIONS OF DIATOMIC MOLECULES

MOLECULE	LOWEST ELECTRON CONFIGURATION	GROUND STATE
H_2	$(1s\sigma_g)^2$	$X^1\Sigma_g^+$
CH	$(1s\sigma)^2\ (2s\sigma)^2\ (2p\sigma)^2\ (2p\pi)^1$	$X^2\Pi$
CH^+	$(1s\sigma)^2\ (2s\sigma)^2\ (2p\sigma)^2$	$X^1\Sigma^+$
*N_2^+, CO^+, CN	$(1s\sigma_g)^2\ (1s\sigma_u)^2\ (2s\sigma_g)^2\ (2s\sigma_u)^2\ (2p\pi_u)^4\ (2p\sigma_g)^1$	$X^2\Sigma_g^+$
*CO, N_2	$(1s\sigma_g)^2\ (1s\sigma_u)^2\ (2s\sigma_g)^2\ (2s\sigma_u)^2\ (2p\pi_u)^4\ (2p\sigma_g)^2$	$X^1\Sigma_g^+$
C_2	$(1s\sigma_g)^2\ (1s\sigma_u)^2\ (2s\sigma_g)^2\ (2s\sigma_u)^2\ (2p\pi_u)^4$	$X^1\Sigma_g^+$
OH	$(1s\sigma)^2\ (2s\sigma)^2\ (2p\sigma)^2\ (2p\pi)^3$	$X^2\Pi$
NH	$(1s\sigma)^2\ (2s\sigma)^2\ (2p\sigma)^2\ (2p\pi)^2$	$X^3\Sigma^-, a^1\Delta, {}^1\Sigma^+$

* For heteronuclear diatomic molecules like CO^+, CN and CO the distinction between u and g disappears.

TABLE 5

EXCITED ELECTRON CONFIGURATIONS OF DIATOMIC MOLECULES

MOLECULE	EXCITED ELECTRON CONFIGURATIONS	EXCITED STATE
H_2	$(1s\sigma_g)^1\ (1s\sigma_u)^1$	$b^3\Sigma u^+$, $B^1\Sigma^+u$
CH	$(1s\sigma)^2\ (2s\sigma)^2\ (2p\sigma)^1\ (2p\pi)^2$	$A^2\Delta$, $c^2\Sigma^+$ $(^4\Sigma^-)$, $B^2\Sigma^-$
CH^+	$(1s\sigma)^2\ (2s\sigma)^2\ (2p\sigma)^1\ (2p\pi)^1$	$A^1\pi$, $a^3\pi$
*N_2^+, CO^+, CN	$(1s\sigma_g)^2\ (1s\sigma_u)^2\ (2s\sigma_g)^2\ (2s\sigma_u)^2\ (2p\pi_u)^3\ (2p\sigma_g)^2$ $(1s\sigma_g)^2\ (1s\sigma_u)^2\ (2s\sigma_g)^2\ (2s\sigma_u)^1\ (2p\pi_u)^4\ (2p\sigma_g)^2$	$A^2\pi$ $B^2\Sigma^+$
CO, N_2	$(1s\sigma_g)^2\ (1s\sigma_u)^2\ (2s\sigma_g)^2\ (2s\sigma_u)^2\ (2p\pi_u)^4\ (2p\sigma_g)^1\ (2p\pi_g)^1$ $(1s\sigma_g)^2\ (1s\sigma_u)^2\ (2s\sigma_g)^2\ (2s\sigma_u)^2\ (2p\pi_u)^3\ (2p\sigma_g)^2\ (2p\pi_g)^1$	$A^1\pi_g$, $a^3\pi_g$ $^3\Sigma u^+$
C_2	$(1s\sigma_g)^2\ (1s\sigma_u)^2\ (2s\sigma_g)^2\ (2s\sigma_u)^1\ (2p\pi_u)^4\ (2p\sigma_g)^1$ $(1s\sigma_g)^2\ (1s\sigma_u)^2\ (2s\sigma_g)^2\ (2s\sigma_u)^1\ (2p\pi_u)^3\ (2p\sigma_g)^2$ $(1s\sigma_g)2\ (1s\sigma_u)^2\ (2s\sigma_g)^2\ (2s\sigma_u)^2\ (2p\pi_u)^3\ (2p\sigma_g)^1$	$D^1\Sigma u^+$ $C^1\pi_g$, $d^3\pi_g$ $A^1\pi u$, $a^3\pi u$
OH	$(1s\sigma)^2\ (2s\sigma)^2\ (2p\sigma)^1\ (2p\pi)^4$	$A^2\Sigma^+$
NH	$(1s\sigma)^2\ (2s\sigma)^2\ (2p\sigma)^1\ (2p\pi)^3$	$A^3\pi$, $C^1\pi$

* For heteronuclear diatomic molecules like CO^+, CN and CO the distinction between u and g disappears.

2.2.3. ELECTRONIC TRANSITIONS

SELECTION RULES

The quantum numbers and symmetry properties of diatomic molecules affect their spectra through a set of selection rules.

In general for a diatomic molecule the following rules apply,

$$\Delta\Lambda = 0, \pm 1$$
$$\Delta S = 0$$
$$\Delta\Sigma = 0$$
$$\Delta\Omega = 0, \pm 1$$

For molecules of Hunds case a and b the first rule means that $\Sigma-\Sigma$, $\Sigma-\Pi$, $\Pi-\Pi$, $\Pi-\Delta$ transitions but not $\Sigma-\Delta$, $\Sigma-\Phi$ and $\Pi-\Phi$ transitions can occur.

Furthermore for transitions between Σ^+ and Σ^- states, $\Sigma^+-\Sigma^+$ and $\Sigma^--\Sigma^-$ are allowed but $\Sigma^+-\Sigma^-$ transitions are not allowed. However Σ^+ and Σ^- states can combine with Π states.

Symmetry selection rules (Figure 7) state that positive terms combine only with negative terms and vice versa. Therefore $+ \leftrightarrow -$ is allowed but $+ \leftrightarrow +$ and $- \leftrightarrow -$ are not,

For homonuclear molecules such as H_2 and C_2, symmetric terms combine only with symmetric terms and antisymmetric terms only with antisymmetric terms. Therefore $s \leftrightarrow s$ and $a \leftrightarrow a$ are allowed but $a \leftrightarrow s$ is not. In the case of a molecule with nuclei of equal charge even electronic states combine only with odd states. Therefore $g \leftrightarrow u$ is allowed, but $g \leftrightarrow g$ and $u \leftrightarrow u$ are not.

Figure 7

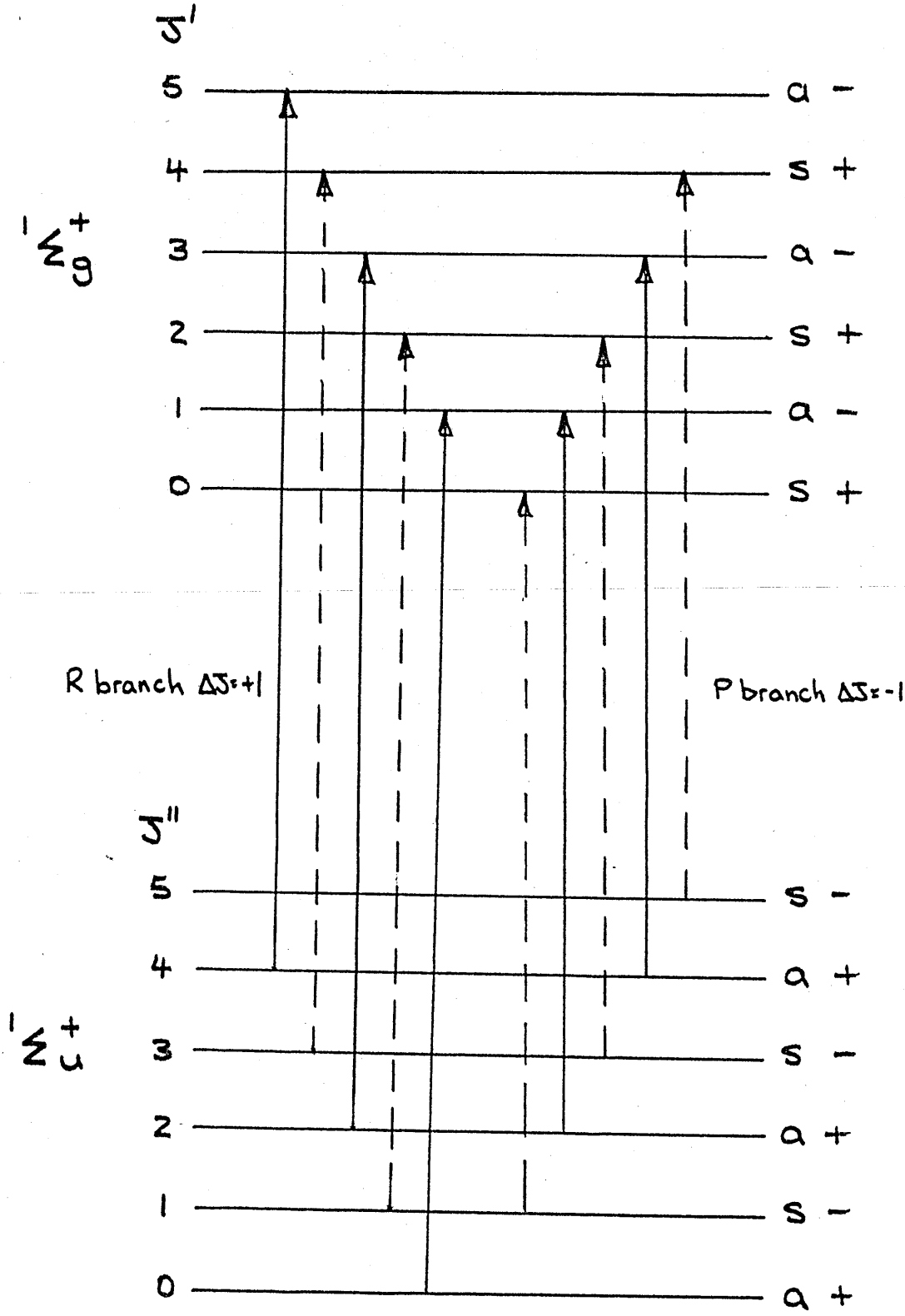

TRANSITIONS BETWEEN $^1\Sigma_g^+$ AND $^1\Sigma_u^+$ STATES ILLUSTRATING THE VARIOUS SYMMETRY SELECTION RULES.

For states that are Hunds case a the following applies

$$\Delta J = 0, \pm 1$$

but for transitions where

$\Omega = 0 \rightarrow \Omega = 0$, $\Delta J = 0$ is not allowed.

For states that are Hunds case b,

$$\Delta N = 0, \pm 1$$

but for a $\Sigma - \Sigma$ transition,

$\Delta N = 0$ is not allowed.

TABLE 6

ALLOWED ELECTRONIC TRANSITIONS

HETERONUCLEAR	HOMONUCLEAR
UNEQUAL NUCLEAR CHARGE	EQUAL NUCLEAR CHARGE
$\Sigma^+ - \Sigma^+$	$\Sigma_g^+ - \Sigma_u^+$
$\Sigma^- - \Sigma^-$	$\Sigma_g^- - \Sigma_u^-$
$\Pi - \Sigma^+$	$\Pi_g - \Sigma_u^+$ $\Pi_u - \Sigma_g^+$
$\Pi - \Sigma^-$	$\Pi_g - \Sigma_u^-$ $\Pi_u - \Sigma_g^-$
$\Pi - \Pi$	$\Pi_g - \Pi_u$
$\Pi - \Delta$	$\Pi_g - \Delta_u$ $\Pi_u - \Delta_g$
$\Delta - \Delta$	$\Delta_g - \Delta_u$

All the transitions in table 6 are possible as singlets, doublets and triplets, but intercombinations such as singlet - triplet are not allowed.

EXAMPLES OF ELECTRONIC TRANSITIONS AT OPTICAL AND ULTRAVIOLET WAVELENGTHS

An energy level diagram illustrating the vibrational and rotational fine structure that is shown in the electronic spectra of interstellar diatomic molecules is shown in figure 8. The change in vibrational energy is denoted by the letters V^{1} and V^{11}, in brackets, where V^{1} is the upper vibrational level and V^{11} is the lower vibrational level. Thus (10) indicates a transition from $V^{11}=0$ to $V^{1}=1$.

In the case of changes in rotational level, transitions where $\Delta J = +1$ are given the letter R, for $\Delta J = -1$ the letter P, and for $\Delta J = 0$ the letter Q. The number in brackets that follows the letter refers to the value of J from which the line originated. For example R(0) refers to a transition from $J^{11}=0$ to $J^{1}=1$, where J^{11} is the lower state and J^{1} is the upper state.

1. $^{1}\Pi - {}^{1}\Sigma^{+}$

This electronic transition is seen in the spectra of CH^{+} (Figure 9, Douglas & Herzberg 1942 (507), Douglas & Morton 1960 (501)) CO, HCl and C_2.

Transitions with $\Delta J=0$ as well as $\Delta J = \pm 1$ are possible and give rise to one P, one Q and one R branch. However in a $^{1}\Pi$ state the smallest J value is J=1. As a result the lines P(1) and Q(0) do not occur. Also for a homonuclear molecule like C_2 every second line in the branches is weak or missing. Note that the lines of the R and P branches have the upper Λ component as the upper state. The Q branch (not shown) has the lower Λ component as the upper state. Λ doubling only occurs in the $^{1}\Pi$ state. Doublets are not seen because of the selection rule that only $+ \leftrightarrow -$ transitions are allowed. Since in the upper state one of the two components of the Λ doublet is + and the other is -, a given lower state can only combine with one or the other.

Figure 8

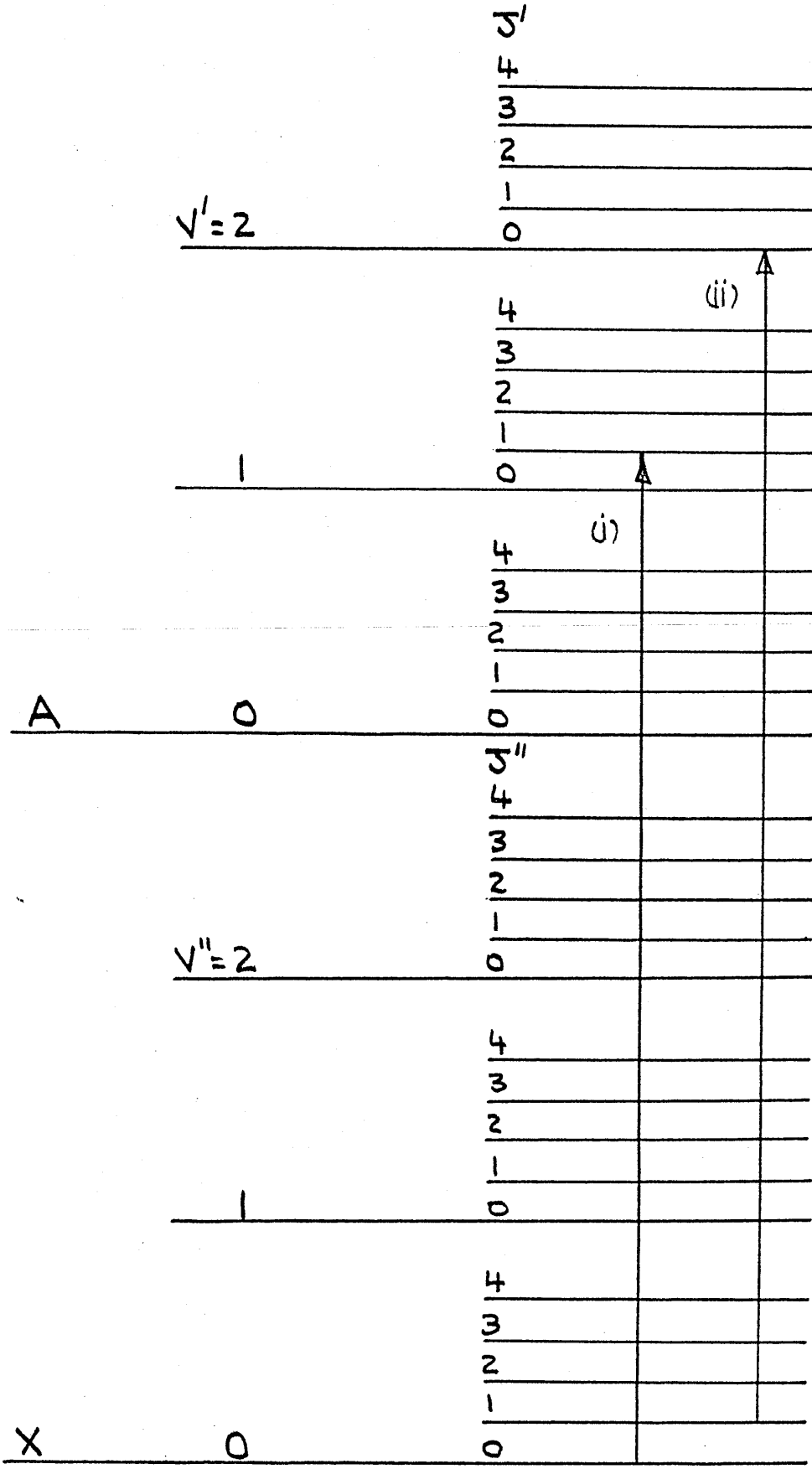

ENERGY LEVELS INVOLVED IN THE ROTATIONAL FINE STRUCTURE OF AN ELECTRONIC TRANSITION FOR A DIATOMIC MOLECULE.

Figure 9

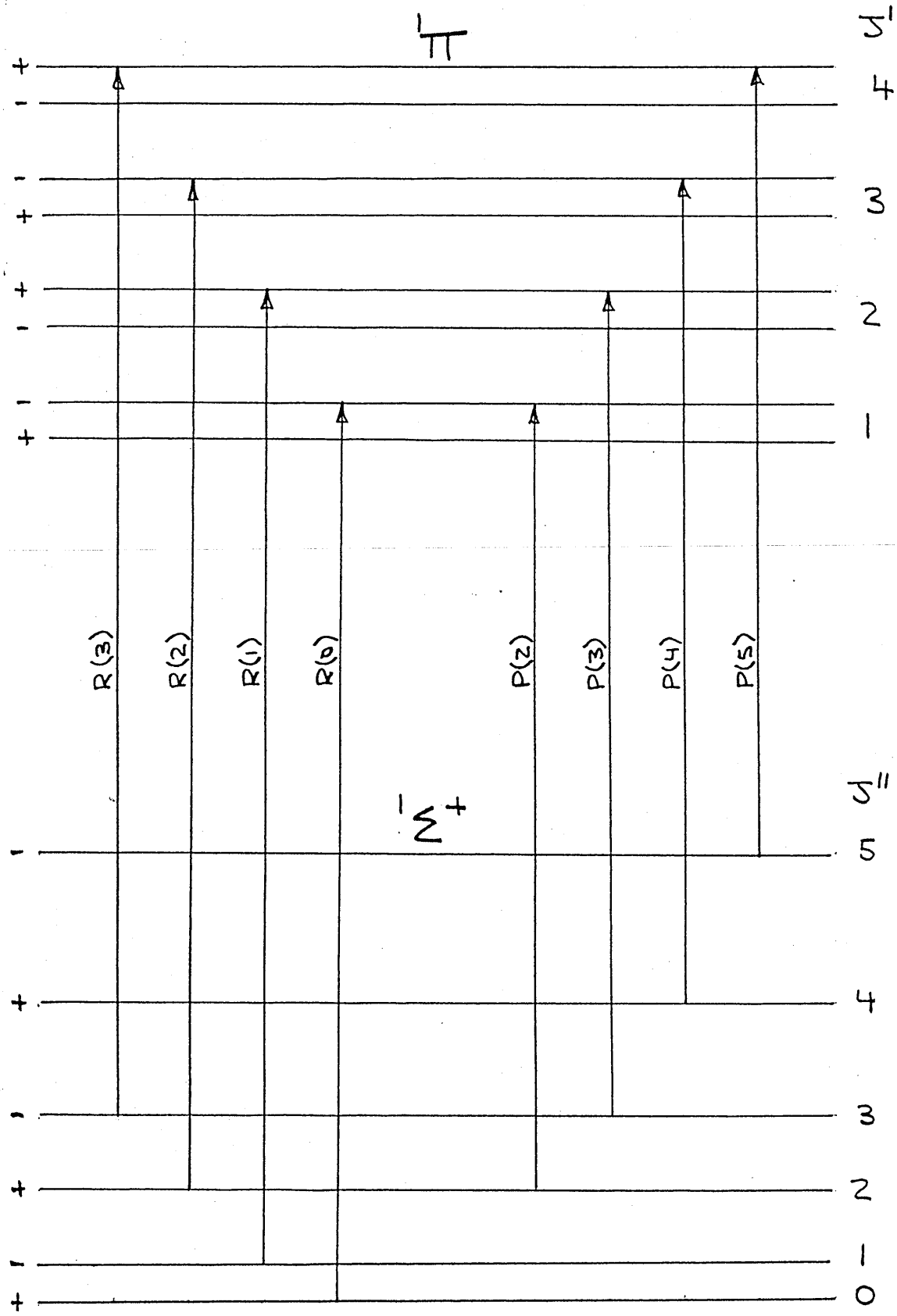

THE $A^1\Pi - X^1\Sigma^+$ SPECTRUM OF CH^+

2. $^2\Delta - ^2\Pi$

This particular electronic transition is seen in the spectrum of CH (Figure 10). $^2\Delta - ^2\Pi$ transitions are similar to $^2\Pi - ^2\Pi$ and $^3\Pi - ^3\Pi$ transitions, in which there are four main branches of each of the classes P, Q and R, except that the Q branches are very intense. The major line of importance for CH is an unresolved doublet at 4300.321Å the $R_2(1)$ line. The $^2\Pi$ state is a good case b for high J values. However the $^2\Pi$ energy levels for the lowest J values in the case of CH show a considerable departure from Hunds case b towards case a. The $^2\Delta$ energy levels are good case b for all J values.

3. $^2\Sigma^- - ^2\Pi$

This electronic transition is also seen in the CH molecule (Figure 11, Herzberg & Johns 1969 (244)). For $^2\Sigma - ^2\Pi$ transitions exactly the same branches occur as for $^2\Pi - ^2\Sigma$ transitions. The actual $F_2' - F_1'$ separations in the $^2\Sigma^-$ state are so small that it is not certain even that $F_2' > F_1'$. $^2\Sigma$ states are always Hunds case b. For a given value of N there are two sublevels with $J=N+\frac{1}{2}$ and $J=N-\frac{1}{2}$. These are called F_1 and F_2 respectively. The $^2\Pi$ state is also Hunds case b, but in this case the F_1 and F_2 levels are split into two by Λ doubling. On account of this all satellite lines except $^PQ_{12}(\frac{1}{2})$ should be superimposed on and add to the intensity of the corresponding main lines.

NOTE ON NOTATION

The existence of satellite series for which $\Delta J \neq \Delta N$ has forced the adoption of a notation for such series, for example the $^PQ_{12}(\frac{1}{2})$ line at λ3900Å of CH.

The large letter (Q in this case) denotes the value of ΔJ, a superscript P is added to denote in a similar manner ΔN, which is really more significant than ΔJ in determining the form of the branches. In cases where $\Delta J = \Delta N$ the superscript is usually omitted. The subscript 12 denotes in order the initial and final types of

Figure 10

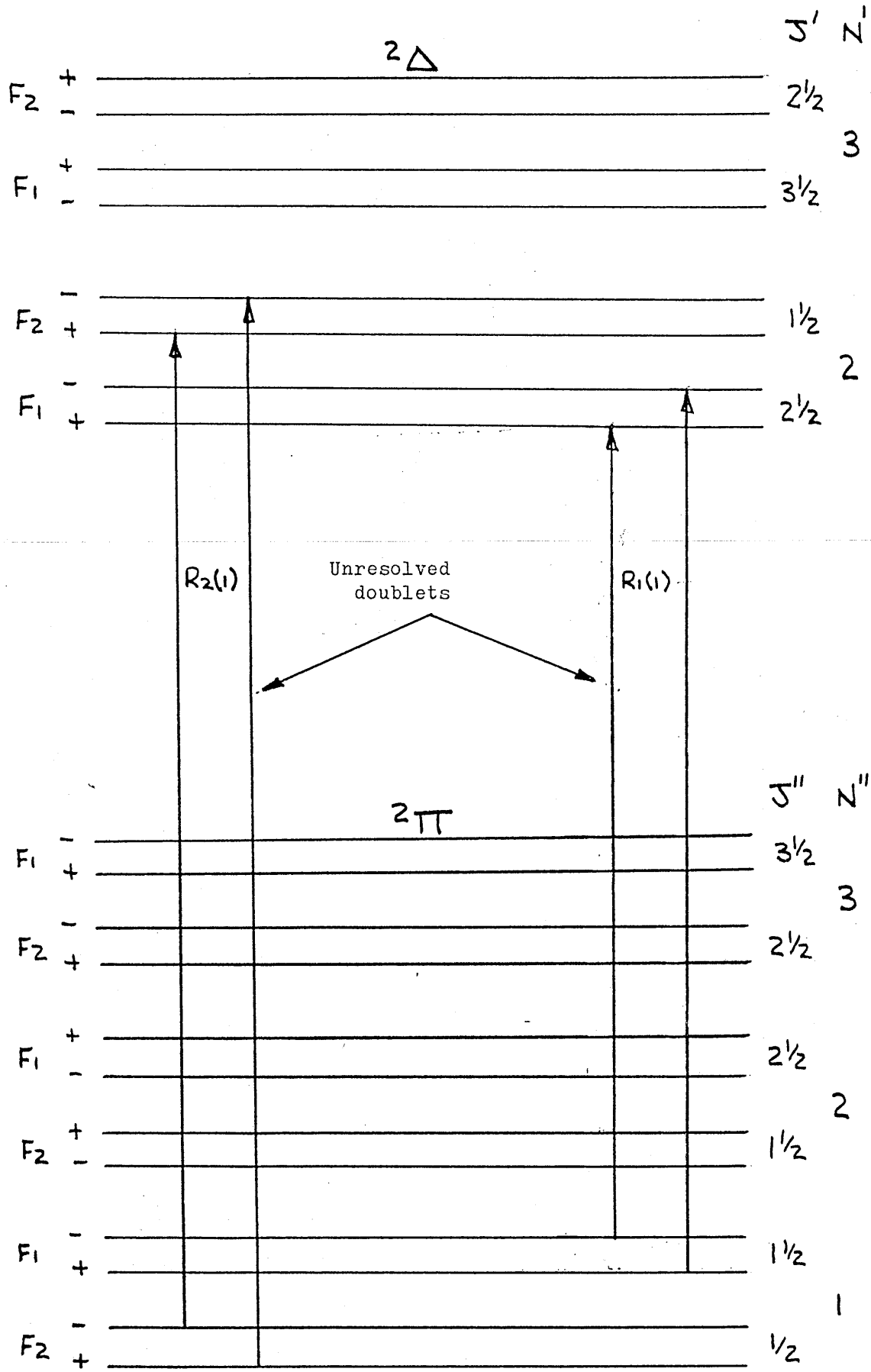

THE $A^2\Delta - X^2\Pi$ SPECTRUM OF CH

Figure 11

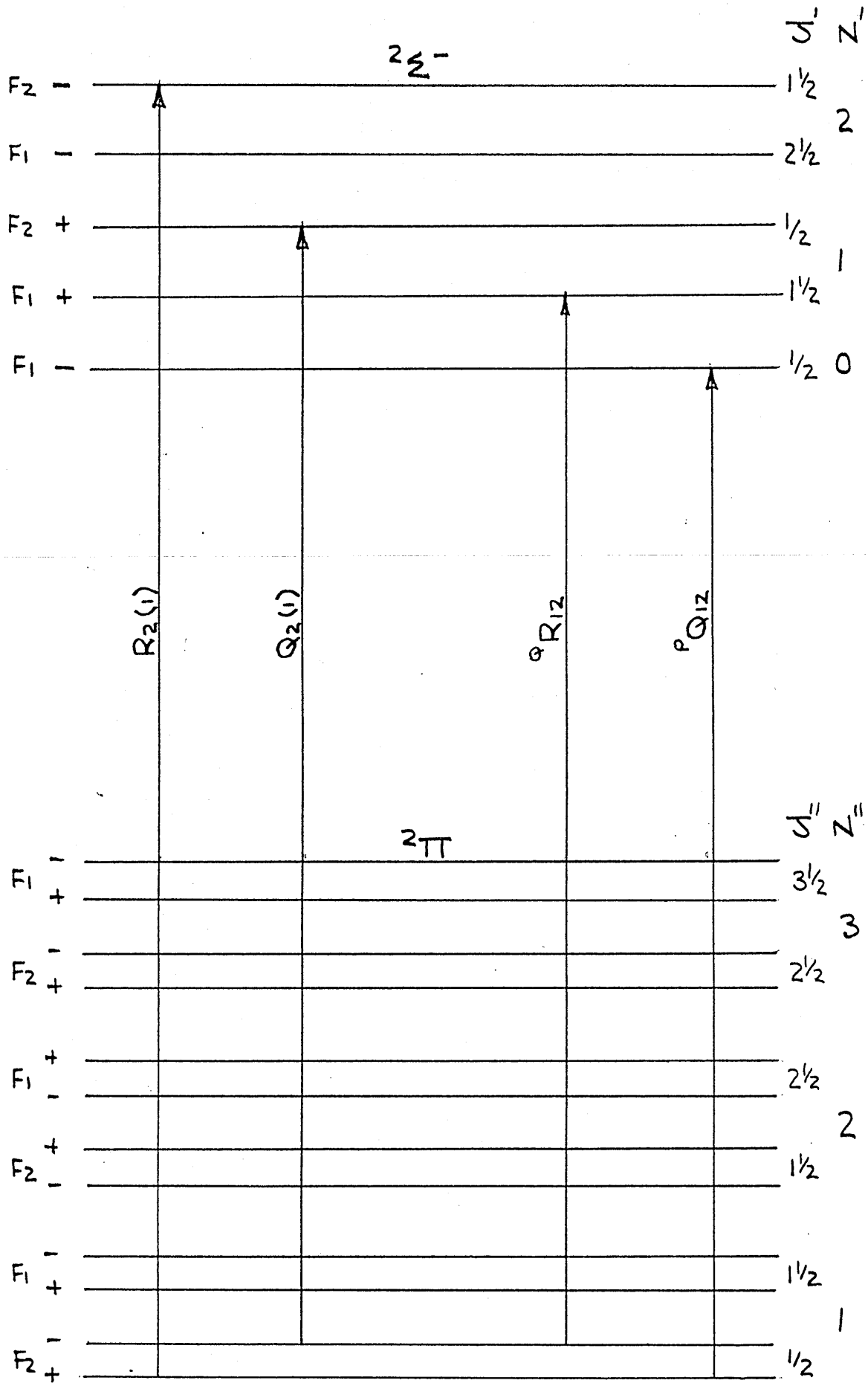

THE $B^2\Sigma^- - X^2\Pi$ SPECTRUM OF CH

rotational states. For example ${}^{P}Q_{12}$ denotes a transition from an F_1 to an F_2 state. If the initial and final states are identical, for example ${}^{P}Q_{11}$ then only a single subscript need be written i.e. ${}^{P}Q_1$. Likewise ${}^{P}R_{11}$ can be written R_1. Each individual line in a series is also denoted by a number in parenthesis giving the value of J'' (ground state) for the line. For example ${}^{P}Q_{12}(\frac{1}{2})$. In some cases (main lines) the number in parenthesis will be N'' (see Herbigs notation, 1968 (54)). For clarity this has been adopted in the energy level diagrams given here, except for the ${}^{P}Q_{12}(\frac{1}{2})$ satellite at λ3900 in CH where the number in parenthesis is J'' in order to distinguish it from the ${}^{P}Q_{12}(1\frac{1}{2})$ line which is too weak to be detected.

4. $^2\Sigma^+ - {}^2\Sigma^+$

This transition is seen in CN (Figure 12) and CO^+. For $^2\Sigma - {}^2\Sigma$ transitions the selection rule $\Delta N = \pm 1$ holds. Each line of the P and R branches according to the rule $\Delta J = 0, \pm 1$ is split into three components. The component (dashed line) for which $\Delta J = 0$ (ΔJ is unequal to ΔN) falls off in intensity with increasing N. Therefore except for very small values of N a splitting of the lines into two components of about equal intensity will occur. There will be a doublet P branch and a doublet R branch.. The best examples are provided by the violet bands of CN, and the ultraviolet bands of CO^+. The branches shown by a dashed line have $\Delta J = 0$ and are therefore Q branches. However the lines of these Q branches lie very close to the corresponding lines (with equal N and ΔN) of the P and R branches. In fact, they form satellite branches. These Q branches therefore have the form of an R and a P branch respectively and not that of a Q branch. Such branches are called R form Q branches ${}^{R}Q$, or P form Q branches ${}^{P}Q$. The subscripts 21 or 12 are to indicate that the transition takes place from a term of the series F_2 to one of the series F_1 or vice versa.

Figure 12

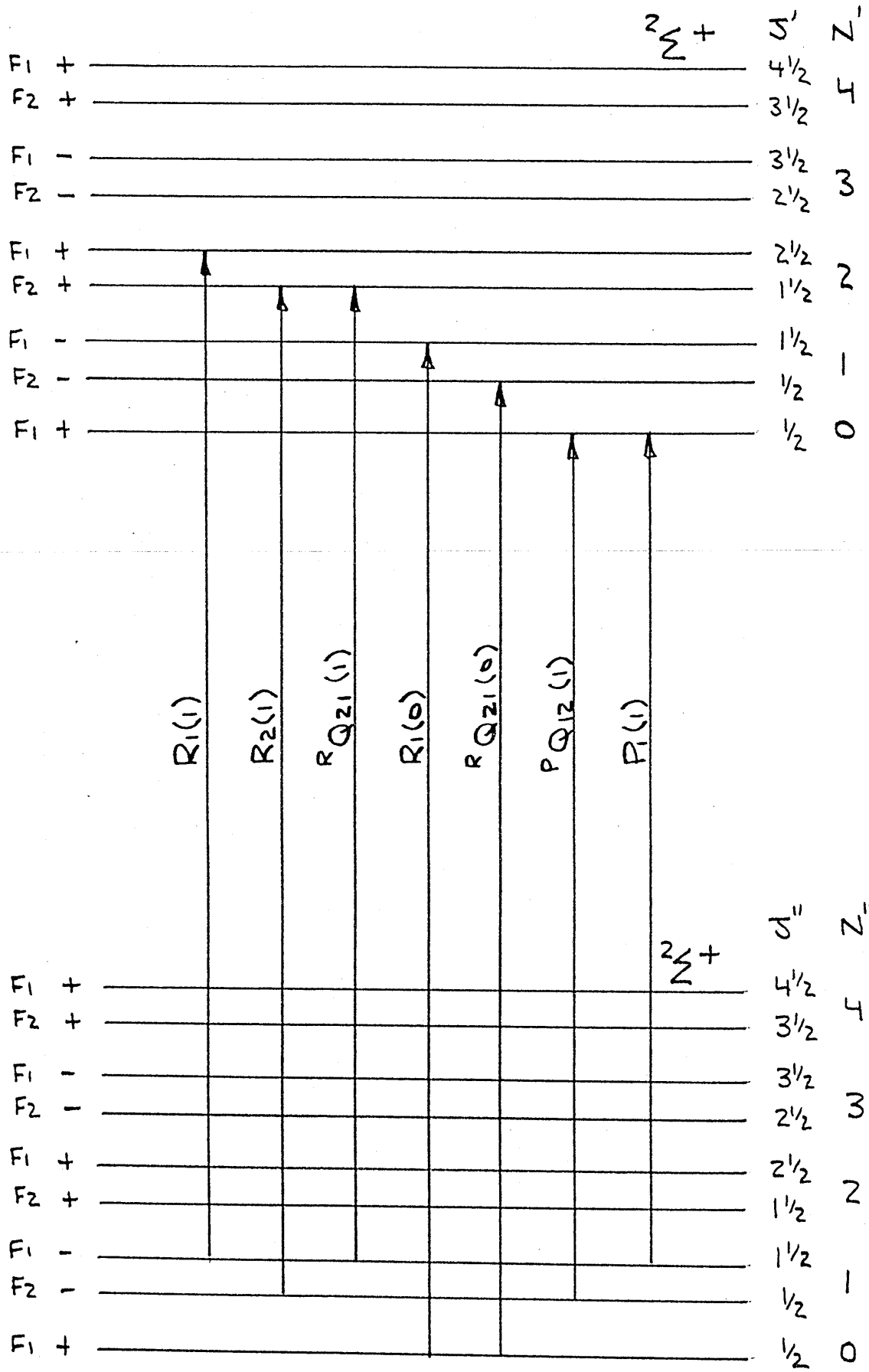

THE $B^2\Sigma^+ - X^2\Sigma^+$ SPECTRUM OF CN

5. $^2\Sigma^+ - {}^2\Pi_{3/2}$

This transition is seen in the spectrum of OH (Figure 13). The selection rules $\Delta J = 0, \pm 1$ and $+ \leftrightarrow -$ apply. The $^2\Sigma^+ - {}^2\Pi$ bands of OH have been described in detail by Dieke and Crosswhite 1962 (284).

6. $^1\Sigma^+ - {}^1\Sigma^+$

The $^1\Sigma^+ - {}^1\Sigma^+$ transition is seen in the spectra of H_2 (Figure 14), HD, CO and C_2. For this transition $\Delta N = 0$ is forbidden and since $N = J, \Delta J = 0$ is also forbidden. Thus only transitions with $\Delta J = \pm 1$ occur. A single P and a single R branch is obtained. For molecular hydrogen the Lyman bands which occur in absorption have P and R branches only, and are a $^1\Sigma_u^+ - {}^1\Sigma_g^+$ transition.

A list of molecules observed in the interstellar gas, their electronic transitions and wavelengths, is given in Table 7.

Figure 13

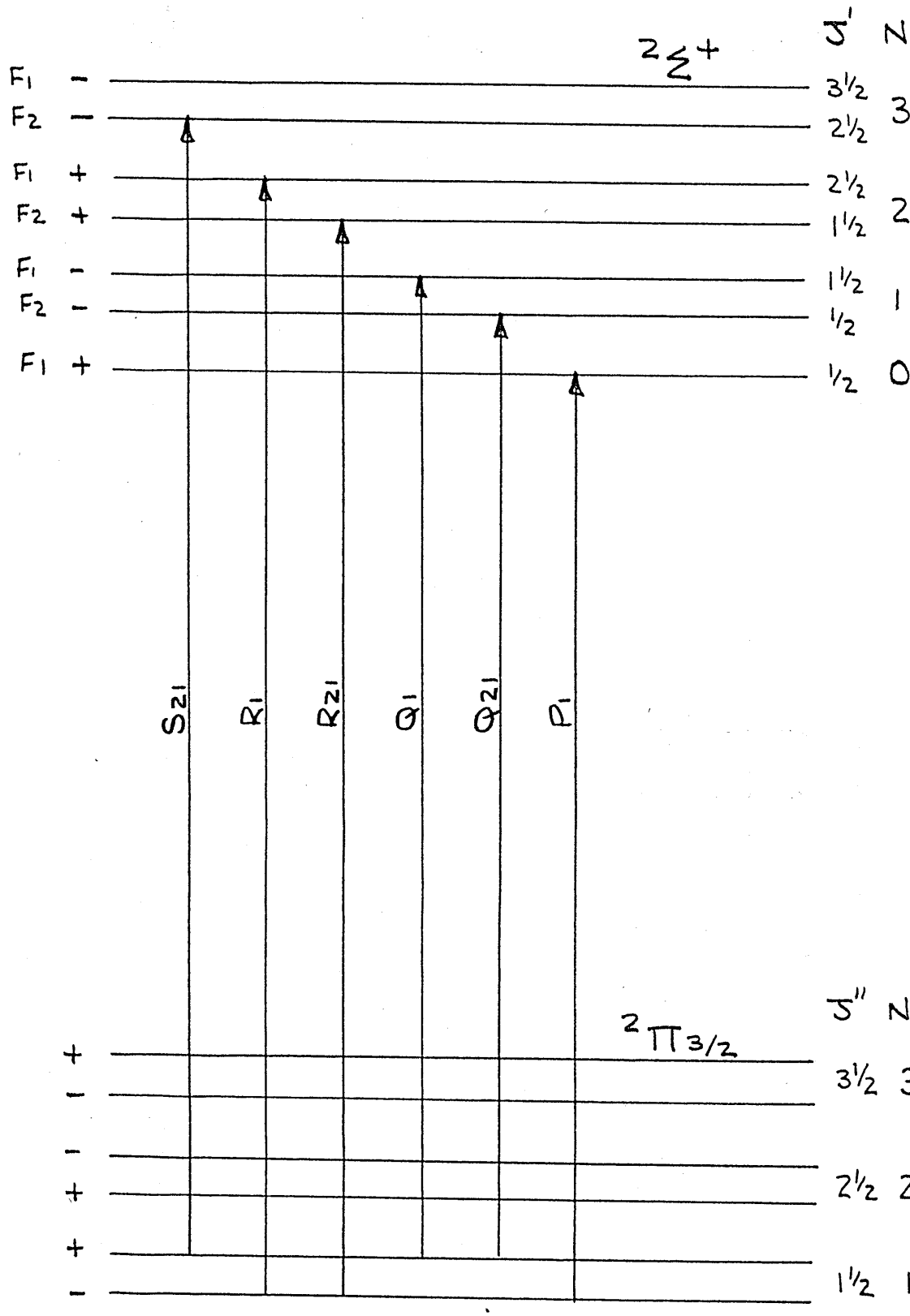

THE $A^2\Sigma^+ - X^2\Pi_{3/2}$ SPECTRUM OF OH

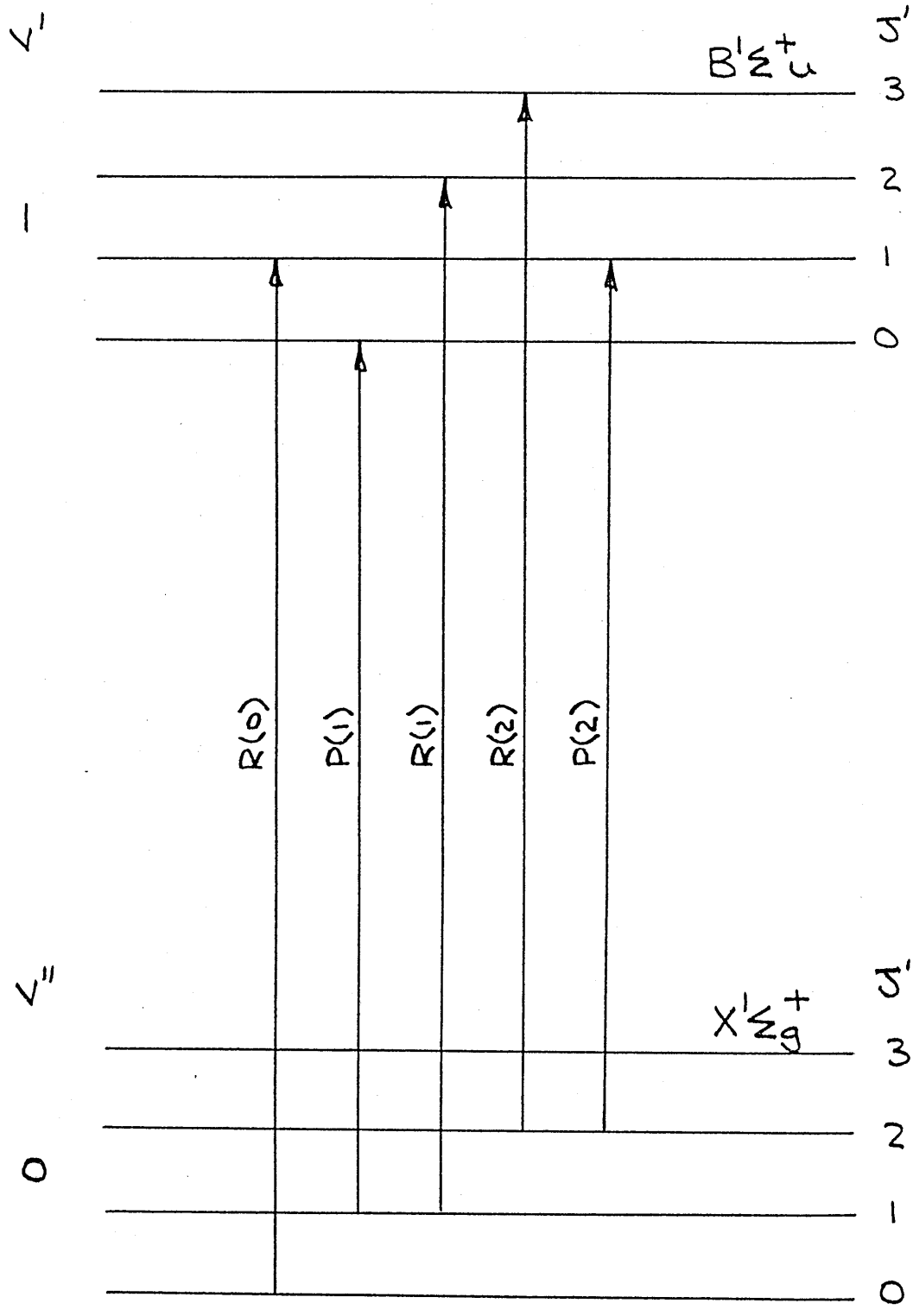

THE $B^1\Sigma_u^+ - X^1\Sigma_g^+$ SPECTRUM OF H_2

TABLE 7

TABLE OF IMPORTANT ELECTRONIC TRANSITIONS, WAVELENGTHS AND OSCILLATOR STRENGTHS FOR INTERSTELLAR MOLECULES OBSERVED USING OPTICAL AND ULTRAVIOLET SPECTROSCOPY

The Oscillator Strength of the strongest line was used to scale column densities in cases where more than one spectral line was present

MOLECULE	TRANSITION	Å WAVELENGTH	1) f el.	2) q(v'v'')	3) f(v'v'')	4) f TOTAL	REFERENCE
CH							1) Fink & 3) Welge 1967 (129)
	$A^2\Delta - X^2\Pi$ (00) $R_2(1)$	4300.321	5.2×10^{-3}	0.993	5.2×10^{-3}	5.2×10^{-3}	2) Liszt & Smith 1972 (272) 4) Herbig 1968 (54)
CH	$B^2\Sigma^- - X^2\Pi$ (00)		2.8×10^{-3}	1.0	2.8×10^{-3}	-	1) Fink & 3) Welge 1967 (129)
	$^pQ_{12}(1)$	3890.213				9.32×10^{-4}	2) Assumed to be 1.0
	$Q_2(1) + {}^QR_{12}(1)$	3886.410				1.40×10^{-3}	4) Herbig 1968 (54)
	$R_2(1)$	3878.768				7.68×10^{-4}	
CH	$C^2\Sigma^+ - X^2\Pi$ (00)		7.2×10^{-3}	0.999	7.2×10^{-3}	-	1) Chaffee 3) & Lutz 4) 1977 (46)
	$^pQ_{12}(1)$	3146.01				2.4×10^{-3}	2) Hinze Lie & Liu 1975 (278)
	$Q_2(1) + {}^QR_{12}(1)$	3143.15				3.6×10^{-3}	
	$R_2(1)$	3137.53				1.2×10^{-3}	

MOLECULE	TRANSITION	Å WAVELENGTH	1) f el.	2) q(v v'')	3) f(v'v'')	4) f TOTAL	REFERENCE
CH^+	$A^1\Pi - X^1\Sigma^+$ (00)R(0)	4232.548	-	-	5.57 x 10^{-3}	5.57 x 10^{-3}	3) Mahan & O'Keefe 1981 (62)
	(10)R(0)	3957.692	-	-	9.1 x 10^{-3}	9.1 x 10^{-3}	3) Brooks & Smith 1975 (49)
	(20)R(0)	3745.310	-	-	3.6 x 10^{-3}	3.6 x 10^{-3}	4)

MOLECULE	TRANSITION	Å WAVELENGTH	1) f el.	2) q(v'v'')	3) f(v'v'')	4) f TOTAL	REFERENCE
CO	$A^1\Pi - X^1\Sigma^+$ (00)	1544.45	-	-	2.0×10^{-2}	-	3) Lassettre & Skerbele 1971 (128)
	(10)	1509.75			3.8×10^{-2}		
	(20)	1477.57			4.29×10^{-2}		
	(30)	1447.36			3.60×10^{-2}		
	(40)	1419.04			2.51×10^{-2}		
	(50)	1392.53			1.55×10^{-2}		
	(60)	1367.62			8.48×10^{-3}		
	(70)	1344.18			4.37×10^{-3}		
	(80)	1322.15			2.17×10^{-3}		
	(90)	1301.40			1.08×10^{-3}		
	(100)	1281.87			5.00×10^{-4}		
	(110)	1263.43			2.50×10^{-4}		
	(120)	1246.06			1.00×10^{-4}		
CO	$B^1\Sigma^+ - X^1\Sigma^+$ (00)	1150.48	-	-	7.6×10^{-3}	-	3) Smith 1978 (127)
CO	$C^1\Sigma^+ - X^1\Sigma^+$ (00)	1087.867	-	-	8.9×10^{-2}	-	3) Smith 1978 (127)
CO	$E^1\Pi - X^1\Sigma^+$ (00)	1076.033	-	-	12×10^{-2}	-	3) Smith 1978 (127)

MOLECULE	TRANSITION	Å WAVELENGTH	1) f el.	2) q(v'v'')	3) f(v'v'')	4) f TOTAL	REFERENCE
CN	$B^2\Sigma^+ - X^2\Sigma^+$ (00)		3.42×10^{-2}	0.9	3.42×10^{-2}	-	1) Jackson 3) 1974 (298) /Lambert 1978 (172)
	$R_1(0)+{}^{R}Q_{21}(0)$	3874.608				3.42×10^{-2}	
	$R_1(1) + R_2(1) + {}^{R}Q_{21}(1)$	3873.998				2.28×10^{-2}	2) Halmann & Laulicht 1966 (262)
	$P_1(1) + {}^{P}Q_{12}(1)$	3875.763				1.14×10^{-2}	4) Federman et al 1984 (283)

MOLECULE	TRANSITION		Å WAVELENGTH	1) f el.	2) q(v'v'')	3) f(v'v'')	4) f TOTAL	REFERENCE
C_2	$A^1\Pi u - X^1\Sigma_g^+(10)$	R(0)	10143.744	-	-	1.38×10^{-3}	1.38×10^{-3}	3) Brault 4) et al 1982 (219)
C_2	$A^1\Pi u - X^1\Sigma_g^+(20)$			-	-	1.7×10^{-3}	-	3) Van Dishoeck 1983 (233)
		R(0)	8757.686				1.7×10^{-3}	
		R(2)	8753.949				6.8×10^{-4}	
		Q(2)	8761.194				8.5×10^{-4}	4) Van Dishoeck & de Zeeuw 1984 (212)
		P(2)	8766.031				1.7×10^{-4}	
		R(4)	8751.685				5.7×10^{-4}	
		Q(4)	8763.751				8.5×10^{-4}	
		P(4)	8773.430				2.8×10^{-4}	
C_2	$A^1\Pi u - X^1\Sigma_g^+(30)$	R(0)	7719.329			7.5×10^{-4}	7.5×10^{-4}	3) Van 4) Dishoeck 1983 (233)
C_2	$D^1\Sigma u^+ - X^1\Sigma_g^+(00)$				0.997	5.5×10^{-2}	-	2) Hsu & Smith 1977 (423)
		R(0)	2313.19				5.5×10^{-2}	3) Smith 1969 (196)
		R(2)	2312.74				3.3×10^{-2}	4) Snow 1978 (175)
C_2	$F^1\Pi u - X^1\Sigma_g^+(00)$	R(0)	1341.63	-	-	1×10^{-1}	1×10^{-1}	3) Chaffee 4) et al 1980 (165)

MOLECULE	TRANSITION	Å WAVELENGTH	1) f el.	2) q(v'v'')	3) f(v'v'')	4) f TOTAL	REFERENCE
C_3	$A^1\Pi u - X^1\Sigma_g^+(000)-(000)$	4050.	2.46×10^{-2}	0.741	18×10^{-3}	-	1) Becker et al 1979 (287) 2) Peric, Radic et al 1977 (315) 3) Clegg & Lambert 1982 (123)

MOLECULE	TRANSITION		Å WAVELENGTH	1) f el.	2) q(v'v'')	3) f(v'v'')	4) f TOTAL	REFERENCE
H_2	$B^1\Sigma_u^+ - X^1\Sigma_g^+$ (10)			-	-	5.79 x 10^{-3}	-	3) Allison & Dalgarno 1970 (121)
		R(0)	1092.194				5.79 x 10^{-3}	4) Savage et al 1977 (70)
		R(1)	1092.732				3.86 x 10^{-3}	
		P(1)	1094.052				1.93 x 10^{-3}	

MOLECULE	TRANSITION	Å WAVELENGTH	1) f el.	2) q(v'v'')	3) f(v'v'')	4) f TOTAL	REFERENCE
HD	$B^1\Sigma^+_u - X^1\Sigma^+_g$		-	-	-	-	3) Allison 4) & Dalgarno 1970 (121)
	(00) R(0)	1105.837			7.601×10^{-4}	7.601×10^{-4}	
	(30) R(0)	1066.271			1.138×10^{-2}	1.138×10^{-2}	
	(40) R(0)	1054.288			1.608×10^{-2}	1.608×10^{-2}	

MOLECULE	TRANSITION	Å WAVELENGTH	1) f el.	20 q(v'v'')	3) f(v'v'')	4) f TOTAL	REFERENCE
OH	$A^2\Sigma^+ - X^2\Pi_{3/2}(00)$		-	-	8.0 x 10^{-4}	-	3) Golden 1963 (130)
	$Q_1(1) + Q_{21}(1)$	3078.44, .47				3.8 x 10^{-4}	
	$S_{21}(1)$	3062.52				0.2 x 10^{-4}	4) Herbig 1968 (54)
	$P_1(1)$	3081.66				2.4 x 10^{-4}	
	$R_1(1) + R_{21}(1)$	3072.06, .01				1.6 x 10^{-4}	
OH	$D^2\Sigma^- - X^2\Pi$ (00)		-	-	3.64 x 10^{-3}	-	3) Ray & Kelly 1975 (193)
	$Q_1(3/2)$	1222.071				1.51 x 10^{-3}	
	$P_1(3/2)$	1222.524				1.19 x 10^{-3}	4) Snow 1976 (183)

MOLECULE	TRANSITION	Å WAVELENGTH	1) f el.	2) q(v'v'')	3) f(v'v'')	4) f TOTAL	REFERENCE
H_2O	$\tilde{C}^1B_1$-$\tilde{X}^1A_1$(000)-(000)		-	-	-	-	4) Smith et al 1981 (180)
	211 - 101	1239.382				4.3 x 10^{-3}	* Smith & Zweibel 1976 (192)
	110 - 000	1239.728				*1.8 x 10^{-2}	
	111 - 101	1240.153				5.7 x 10^{-3}	
H_2O	$\tilde{F}$ - $\tilde{X}$ (000)-(000)		-	-	-	-	
	111 - 000	1114.225	-	-	-	3.0 x 10^{-2}	

MOLECULE	TRANSITION		Å WAVELENGTH	1) f el.	2) q(v'v'')	3) f(v'v'')	4) f TOTAL	REFERENCE
HCl	$c^1\Pi - X^1\Sigma^+$ (00)			-	-	-	-	4) Smith et al 1980 (181)
		R(0)	1290.257				0.185	
		R(1)	1289.983				0.097	
		R(2)	1289.745				0.074	
	(10)	R(0)	1247.079				0.022	

MOLECULE	TRANSITION	Å WAVELENGTH	1) f el.	2) q(v'v'')	3) f(v'v'')	4) f TOTAL	REFERENCE
NH	$A^3\Pi_i - X^3\Sigma^-$ (00)		8.0×10^{-3}	0.999	8.0×10^{-3}	-	1) Bennett & Dalby 1960 (112)
	$R_1(0)$	3358.06				4.3×10^{-3}	2) Hsu & Smith 1977 (423)
	$R_{Q_{21}}(0)$	3353.92				2.5×10^{-3}	3)
	$R_{P_{31}}(0)$	3351.71				0.93×10^{-3}	4) Herbig 1968 (54)
	$S_{R_{21}}(0)$	3347.32				0.18×10^{-3}	
	$S_{Q_{31}}(0)$	3345.59				0.14×10^{-3}	
	$T_{R_{31}}(0)$	3335.53				0.02×10^{-3}	

MOLECULE	TRANSITION	Å WAVELENGTH	1) f el.	2) q(v'v'')	3) f(v'v'')	4) f TOTAL	REFERENCE
N_2	$a^1\Pi_g - X^1\Sigma_g^+$ (80)		-	-	-	-	4) Snow 1975 (8)
	R(0)	1226.84				1.0 x 10^{-2}	
	S(0)	1226.75				5.0 x 10^{-3}	
	(60)		-	-	-	-	
	R(0)	1273.30				1.0 x 10^{-2}	
	S(0)	1273.20				5.0 x 10^{-3}	
	$P^1\Sigma_u^+ - X^1\Sigma_g^+$ (00)	958.5	-	-	0.14	-	3) Lawrence et al 1968 (273)
	$l'\Pi_u - X^1\Sigma_g^+$ (00)	960.2	-	-	4.0 x 10^{-2}	-	

MOLECULE	TRANSITION	Å WAVELENGTH	1) f el.	2) q(v'v'')	3) f(v'v'')	4) f TOTAL	REFERENCE
CO^+	$A^2\Pi_i - X^2\Sigma^+$ (20)	4250.94	-	-	8.6×10^{-4}	-	3) Mahan & O'Keefe 1981 (62) Holland & Maier 1972 (419)
	$B^2\Sigma^+ - X^2\Sigma^+$ (00)	2191.21	-	-	7.0×10^{-4}	-	3) Jenkins et al 1973 (53)

MOLECULE	TRANSITION	Å WAVELENGTH	1) f el.	2) q(v'v'')	3) f(v'v'')	4) f TOTAL	REFERENCE
H_2O^+	$\tilde{A}^2A_1 - \tilde{X}^2B_1$ (080)-(000)						4) Smith 1984 (211)
	$1_{10} - 0_{00}$	6146.802	-	-	-	4.3×10^{-4}	
	(060)-(000)						
	$1_{10} - 0_{00}$	6973.720	-	-	-	4.3×10^{-4}	
CS^+	$A^2\Pi_i - X^2\Sigma^+$ (30)				7.56×10^{-4}	-	3) Larsson 1985 (540)
	$^RQ_{21}$	6701.57					
	Q_{11}	6840.37					

2.2.4. TRANSITIONS AT MICROWAVE FREQUENCIES

Transitions between rotational levels of diatomic molecules in their ground electronic and vibrational states occur at microwave frequencies. If the molecule is regarded as a rigid rotator then the various rotational energy levels are given by

$$E_{rot} = BJ(J+1) \qquad (2.25)$$

where $B = \frac{h^2}{8\pi^2 \mu r^2}$

μ = Reduced mass.

r = Internuclear distance.

In order to absorb microwave radiation the molecule must have a dipole moment. This means that homonuclear diatomic molecules like C_2 and H_2 have no dipole allowed rotational spectrum since they do not have a dipole moment. For a heteronuclear diatomic molecule the frequency ν of a transition between two rotational levels is given by

$$h\nu = \Delta E = BJ'(J'+1) - BJ''(J''+1) \qquad (2.26)$$

where J' = Excited level and J'' = the Ground level. For pure rotational spectra the following selection rule holds

$$\Delta J = \pm 1.$$

Thus $J' = J'' + 1$, and

$$\Delta E = 2BJ'$$

The allowed values of ΔE are therefore 2B, 4B, 6B etc, and the spectrum should consist of a series of equally spaced lines. The value of B depends on the moment of inertia I of the molecule and hence mainly on the reduced mass, since

$$I = \mu r^2 \qquad (2.27)$$

In practice the molecule is found to stretch at high J, whereby r increases. A more accurate value for the energy of the rotational levels is then given by

$$E_{rot} = BJ(J+1) - DJ^2(J+1)^2 \qquad (2.28)$$

where $D = \frac{4B^3}{W^2}$

and W = Angular velocity of rotation.

This results in the spectral lines slowly converging. Only four molecules observed in diffuse clouds at optical and ultraviolet wavelengths have also been observed in emission at microwave frequencies. They are CO, CN, CH and OH.

1. CO

The simplest case is CO for which the ground state term is $X\,^1\Sigma$. For $^1\Sigma$ states Λ and Σ are zero and Hunds cases a and b are identical. The rotation is described by the angular momentum J of magnitude $[J(J+1)]^{\frac{1}{2}}$ with quantum number J = 0, 1, 2... The transitions J = 2 → J = 1 and J = 1 → J = 0 occur at 1.3mm and 2.6mm respectively and are shown in figure 15a. Both transitions have been detected in emission in the interstellar medium.

2. CN

The ground state term for CN is $X^2\Sigma^+$ which is Hunds case b. For a Σ state, Λ = 0 and N = Λ, Λ + 1, Λ + 2... = 0, 1, 2. Since CN has an odd number of electrons S is half integral which means that J = $\frac{1}{2}$, when N = 0 and $\frac{1}{2}$ or $\frac{3}{2}$ when N = 1. Each rotational level is then split into hyperfine levels.

Figure 15a

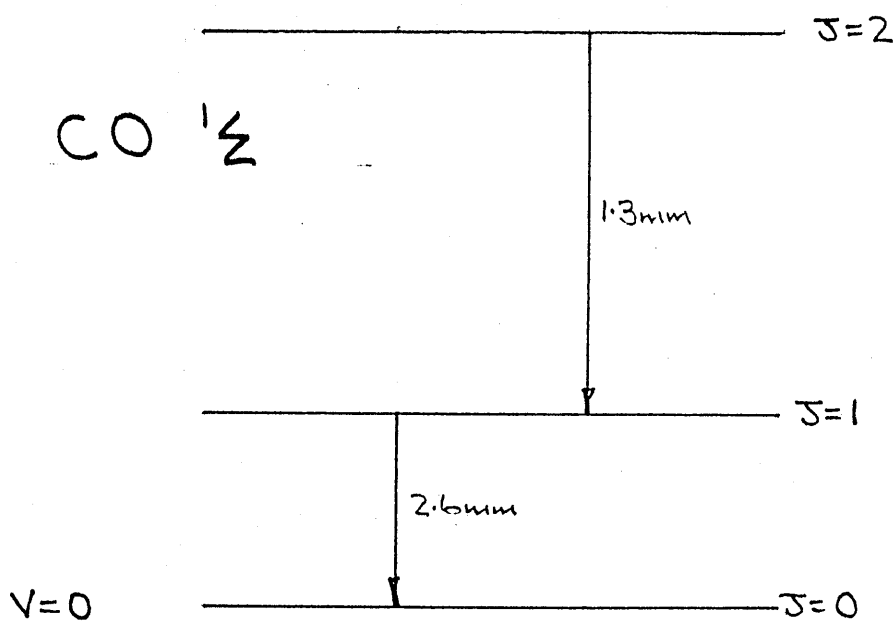

Figure 15b

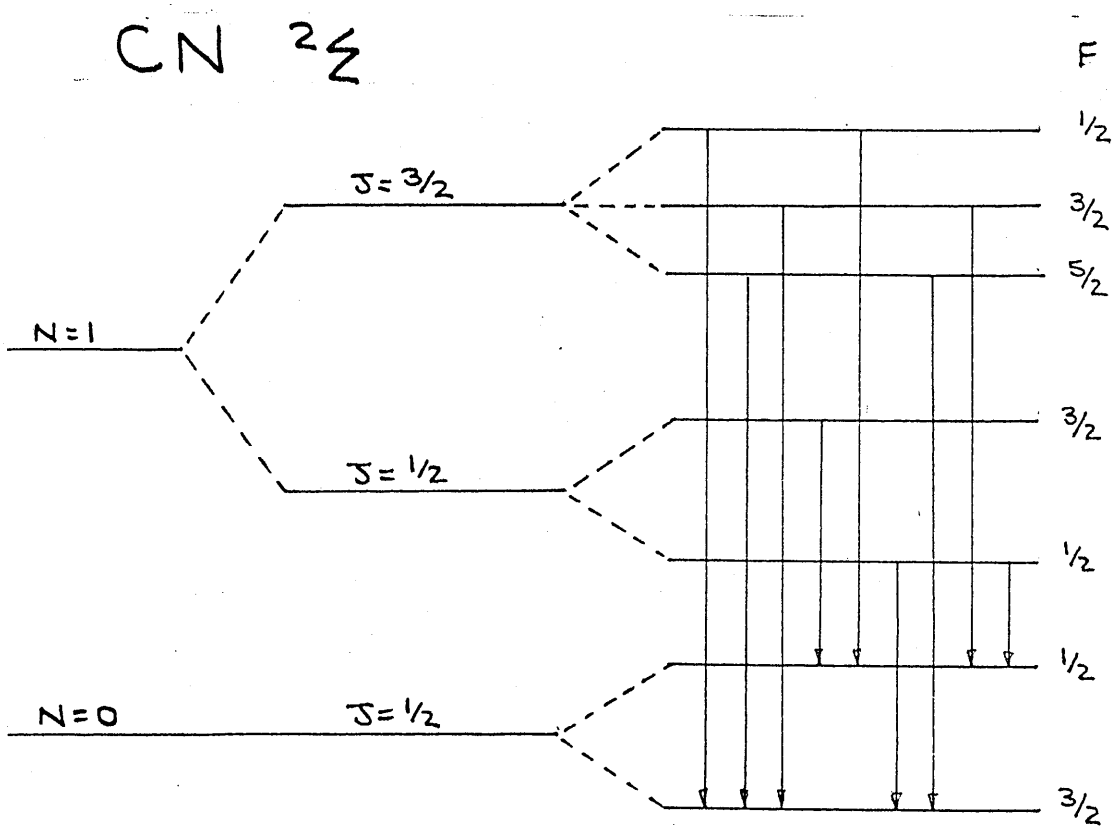

The observed interstellar hyperfine components of the N = 1 - 0 transition occur in two groups, the $J = \frac{1}{2} - \frac{1}{2}$ multiplet consists of four lines between 113.124 GHz and 113.191 GHz and the $J = \frac{3}{2} - \frac{1}{2}$ multiplet consists of five lines between 113.488 GHz and 113.520 GHz. The energy level diagram for CN is shown in figure 15b.

3. CH and OH

For a diatomic molecule in a Σ state the electronic wavefunction is symmetrical about the nuclear axis. The axis of molecular rotation is perpendicular to the nuclear axis and the moment of inertia and energy of rotation are the same about any such axis. When the quantum number Λ is not zero, as for Π and Δ states the electronic wavefunction is not symmetrical about the nuclear axis and there are two principal rotation axes at right angles to each other. Rotations about these axes have slightly different energies and so all the rotational energy levels are split into two. It is always a doubling for a non-zero value of Λ The Λ doubled levels are labelled using the +, - symmetry property. In addition the letters c and d are employed to distinguish the components resulting from Λ doubling of the rotational levels in electronic states with $\Lambda > 0$ which fall in or between Hunds cases a and b. The letters are alloted on the basis of transition properties as made from the observed band structure itself. Hyperfine structure from proton spin splits each of these levels into two again. The levels are labelled F, with

$$F = J \pm \frac{1}{2}.$$

For hyperfine transitions the selection rules are $\Delta F = 0, \pm 1$ and $F = 0 \rightarrow F = 0$ is forbidden, (see Lien 1984 (330)).

CH and OH both exhibit Λ doubling. Although Hunds case a notation is often used for CH (eg $^2\Pi_{1/2}$), the coupling of angular momenta is closer to Hunds case b for CH in its ground state $X^2\Pi$, (Ziurys et al 1983 (221), Brown & Evenson 1983 (220)). The pattern of rotational levels can be described in terms of the case b quantum number N. For a Π state $\Lambda = 1$ and $N = \Lambda, \Lambda + 1, \Lambda + 2..., = 1,2,3...$ N is split into two components by coupling with the spin vector, each having the quantum number J where $J = N + \frac{1}{2}$ (ie $\frac{3}{2}$ for $N = 1$) or $J = N - \frac{1}{2}$ (ie $\frac{1}{2}$ for $N = 1$). The $J = \frac{3}{2}$ and $J = \frac{1}{2}$ components are often referred to as the F_1 and F_2 components respectively. The lowest rotational level $J = \frac{1}{2}$ is split into two components by Λ doubling and each of these levels is then split into two by coupling with proton spin. This gives the four hyperfine levels shown in figure 16a. The three allowed hyperfine transitions have all been observed in the interstellar medium at microwave frequencies.

The ground state term of OH is also $X^2\Pi$ and is a good approximation to Hunds case a. For a Π state, $\Lambda = 1$ and $\Omega = \Lambda + \Sigma$ can be either $\frac{3}{2}$ or $\frac{1}{2}$. The ground state is $^2\Pi_{3/2}$ and J has values of $J = \Omega, \Omega + 1, \Omega + 2...$ $= \frac{3}{2}, \frac{5}{2}, \frac{7}{2}...$ The $J = \frac{3}{2}$ rotational level is split into two components by Λ doubling. Each of these levels is then split into two to give the four hyperfine levels shown

MICROWAVE TRANSITIONS of CH and OH showing ∿ DOUBLING

Figure 16a

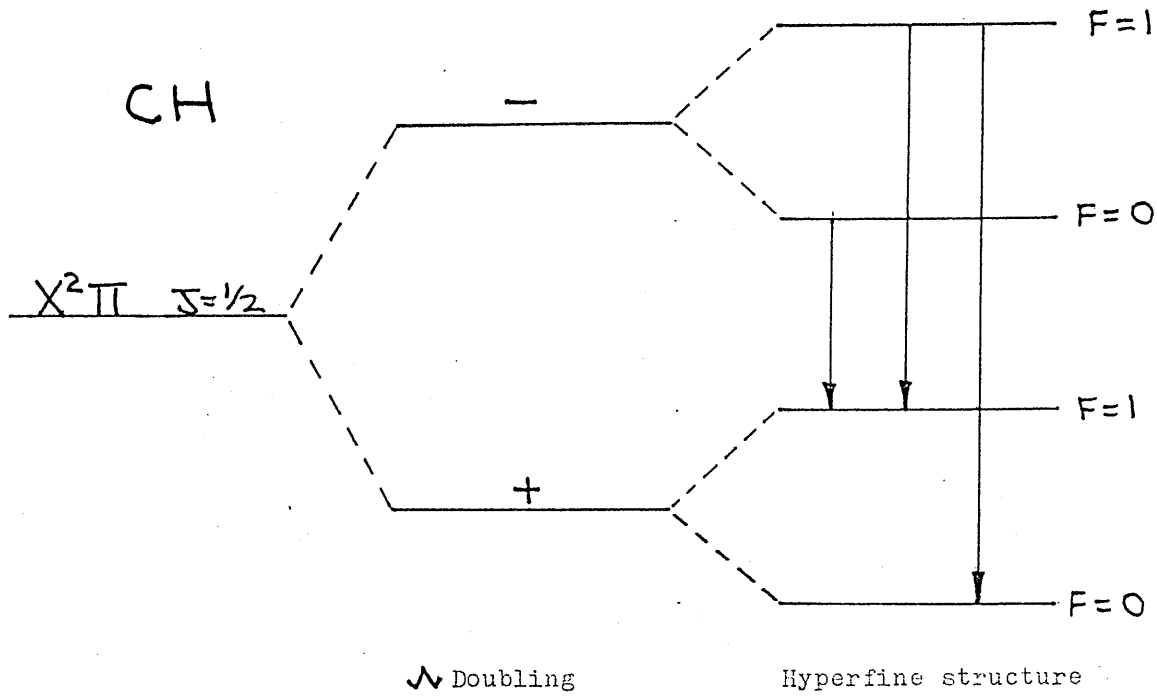

Figure 16b

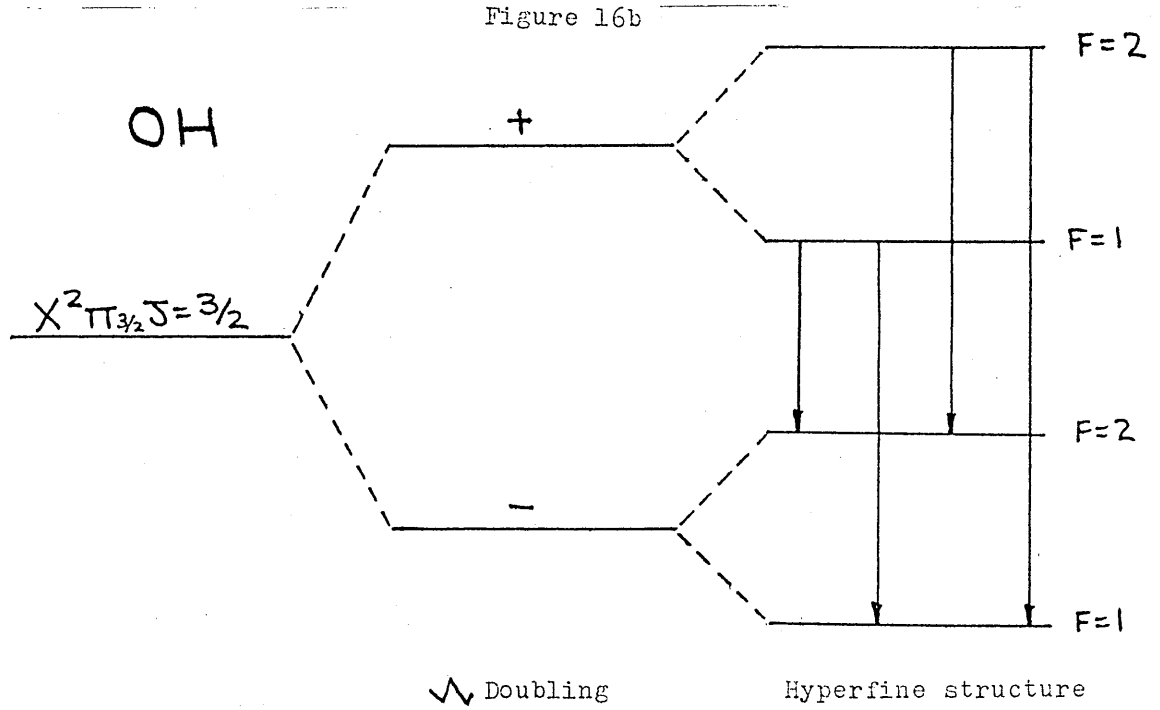

in figure 16b. The four allowed transitions between the hyperfine levels fall into two pairs. The strong lines at 1667 MH_Z and 1665 MH_Z and the weaker satellite lines at 1612 MH_Z and 1720 MH_Z.

Meerts and Dymanus 1975 (218) have made a study of the hyperfine Λ doubling spectrum of OH using molecular beam electric resonance to obtain a complete set of transitions. Coxon et al 1979 (253) have also observed the microwave spectrum of OH in the $X^2\Pi$ ground state and Brown et al 1986 (517) have made laboratory measurements of the far infrared spectrum. The frequencies and wavelengths for the observed interstellar microwave transitions of CO, CN, CH and OH are given in table 8.

TABLE 8

MICROWAVE TRANSITIONS OF DIATOMIC MOLECULES

MOLECULE	TRANSITION	FREQUENCY MHz	WAVELENGTH	REFERENCE
CH	$X^2\Pi_{\frac{1}{2}}$ $J = \frac{1}{2}$			
	$F = 0 - 1$	3263.794	9.19cm	Rydbeck
	$F = 1 - 1$	3335.481	8.99cm	1974 (186)
	$F = 1 - 0$	3349.193	8.95cm	
^{12}CO	$X^1\Sigma^+$ $V = 0$			
	$J = 1 - 0$	115,271.204	2.60mm	Knapp
	$J = 2 - 1$	230,537.974	1.30mm	& Jura
^{13}CO	$X^1\Sigma^+$ $V = 0$			1976 (3)
	$J = 1 - 0$	110,201.370	2.72mm	
	$J = 2 - 1$	220,398.714	1.36mm	
CN	$X^2\Sigma^+$ $N = 1 - 0$		2.64mm	Turner &
	$J = \frac{3}{2} - \frac{1}{2}$			Gammon
	$F = \frac{1}{2} - \frac{3}{2}$	113,520.34		1975 (2)
	$F = \frac{3}{2} - \frac{3}{2}$	113,509.06		
	$F = \frac{1}{2} - \frac{1}{2}$	113,499.72		
	$F = \frac{5}{2} - \frac{3}{2}$	113,491.15		
	$F = \frac{3}{2} - \frac{1}{2}$	113, 488.39		
	$J = \frac{1}{2} - \frac{1}{2}$			
	$F = \frac{3}{2} - \frac{3}{2}$	113,191.33		
	$F = \frac{3}{2} - \frac{1}{2}$	113,170.87		
	$F = \frac{1}{2} - \frac{3}{2}$	113,144.34		
	$F = \frac{1}{2} - \frac{1}{2}$	113,123.83		
OH	$X^2\Pi_{3/2}$ $J = \frac{3}{2}$			
	$F = 1 - 2$	1612.231	18.59cm	Somerville
	$F = 1 - 1$	1665.402	18.00cm	1978 (232)
	$F = 2 - 2$	1667.359	17.98cm	
	$F = 2 - 1$	1720.530	17.42cm	
	$J = \frac{5}{2}$			Winnewisser
	$F = 2 - 2$	6030.739		1974 (309)
	$F = 3 - 3$	6035.085		
	$J = \frac{7}{2}$			
	$F = 4 - 4$	13,441.371		
	$X^2\Pi_{\frac{1}{2}}$ $J = \frac{1}{2}$			Somerville
	$F = 0 - 1$	4660.242	6.43cm	1978 (232)
	$F = 1 - 1$	4750.656	6.31cm	
	$F = 1 - 0$	4765.562	6.29cm	

2.3. SYMMETRY AND ELECTRONIC SPECTRA OF TRIATOMIC MOLECULES

1. ELECTRONIC STATES AND GROUP THEORY

The water molecule H_2O is a simple case of a non-linear triatomic molecule of the type AB_2. The symmetry elements of this molecule are a two fold proper axis of rotation C_2, and two vertical planes of symmetry, one which bisects the molecule σv, and a second which is in the molecular plane $\sigma v'$. So on the basis of symmetry H_2O is easily distinguished from linear triatomic molecules like C_3 and HCN. Water is said to belong to the point group C_{2v}. A point group is labelled Cn if it contains no symmetry element other than a n fold proper axis of rotation. When in addition to the n fold axis there is also a set of n vertical planes which intersect in that axis the point is called Cnv. See, for example, Urch 1970 (440) and Cotton 1971 (441).

The next step is to consider the effect of the symmetry operators, characteristic of the shape of the molecule, on the orbitals that the molecule contains. A point group may be defined by a set of matrices where each matrix represents the action of an operator in the group. This set of matrices is called a representation of the group, and there may be more than one representation. These are called reducible representations since it may be possible to reduce the matrices, in which case smaller representations can be found within the larger one. If however, this is not possible the original representation is said to be irreducible. The irreducible representations of a group are given a symbol, dependent on their symmetry, first proposed by R.S. Mulliken.

All singlet representations are designated A or B, doubly degenerate representations are designated E and triply degenerate representations are designated T. Singly

degenerate representations which are symmetric with respect to rotation by $\frac{2\pi}{n}$ about the principle Cn axis are designated A, whilst those antisymmetric in this respect are designated B. Subscripts 1 and 2 are usually attached to A and B to designate those which are respectively symmetric and antisymmetric with respect to a C_2 perpendicular to the principal axis or to a vertical plane of symmetry. Primes and double primes are attached to indicate those representations which are respectively symmetric and antisymmetric with respect to a horizontal plane of symmetry σh. In groups with a centre of inversion the subscript g is attached to symbols for representations which are symmetric with respect to inversion and the subscript u is used for those which are antisymmetric to inversion.

Lower case letters are used for the symmetries of molecular orbitals and capital letters are used for the symmetries of molecular states. (See Mulliken 1933 (444) for a review). The coupling of the spin S with orbital motion may lead to a splitting of the electronic state into 2S + 1 components. This multiplicity is written as a superscript in front of the group theoretical symbol. For example, when S = 0 we may have $^1A_1$, $^1B_2$, ^1E... states and so on.

In the case of triatomic molecules it is not possible to designate levels of the same spin multiplicity as the ground state by the letters X, A, B, C..., as used for diatomic molecules, without confusion with the group theoretical species symbols A, B, E, T... Therefore a tilde is added to the letters that designate the level of a particular state, ie. $\tilde{X}$, $\tilde{A}$, $\tilde{B}$, $\tilde{C}$. Lower case letters, $\tilde{a}$, $\tilde{b}$, $\tilde{c}$ ane used for states of a different spin

multiplicity to the ground state. For example the ground state of water is $\tilde{X}^1A_1$. (see Douglas 1963 (493) who first used this notation for ammonia).

In general polyatomic molecules have a finite number of representations. However, this number increases with the number of symmetry elements, so that for linear molecules like HCN and C_3, which belong to the point groups $C_{\infty v}$ and $D_{\infty h}$ respectively, there are an infinite number of representations which are identical with the states of diatomic molecules.

For the point group $C_{\infty v}$ there are two non degenerate states Σ^+ and Σ^- and an infinite number of degenerate states, Π, Δ, Φ corresponding to the values, $\Lambda = 1, 2, 3\ldots$, where Λ is the electronic orbital angular momentum about the symmetry axis. Examples are the ground state of C_3 which is $\tilde{X}\,^1\Sigma_g^+$ and the ground state of HCN which is $\tilde{X}\,^1\Sigma^+$.

The probability that an electronic transition between two states $\Psi 1$ and $\Psi 2$ will occur is given by the transition moment R, where,

$$R = \int \Psi_2 \mu \Psi_1 \, d\tau \qquad (2.29)$$

μ is the electric dipole moment, and $d\tau$ the volume element.

This equation must balance in symmetry too, therefore

$$\Gamma(R) = \Gamma(\Psi_2)\Gamma\mu\,\Gamma(\Psi_1) \qquad (2.30)$$

where Γ is the representation.

The representation of the electronic eigen functions Ψ_2 and Ψ_1, may be found by considering the representations of the individual molecular orbitals. The representation of an electron in an orbital is the representation of that orbital, and the representation of the molecular state is the direct product of the representations of each electron that makes up that state.

Thus the configuration $\psi_1' \psi_2' \psi_3' \psi_4'$

has the representation $\Gamma(\psi_1)\,\Gamma(\psi_2)\,\Gamma(\psi_3)\,\Gamma(\psi_4)$

Whether or not a transition is allowed or forbidden is determined using the symmetry properties of the molecule.

2. VIBRATIONAL LEVELS

In the gas phase, the electronic spectra of molecules like water will show vibrational and rotational fine structure. Consider a polyatomic molecule having N atoms; the position of each atom is specified by three co-ordinates x, y and z. Thus the total number of co-ordinates required to describe the molecule is 3N, the molecule is said to have 3N degrees of freedom. For a non-linear molecule 3N-6 degrees of freedom are in the form of vibrational motion. For a linear molecule this is increased to 3N-5. Since a N atom molecule has N-1 bonds, N-1 of the vibrations are stretches and the other 2N-5 (in the non-linear case) or 2N-4 (in the linear case) are bending vibrations.

Water is a triatomic molecule and therefore has 3N-6, = 3 vibrational motions referred to as the normal modes of vibration. Further, each motion is labelled as either symmetric or antisymmetric by referring the molecular vibration to the C_2 symmetry axis.

If the vibrating molecule is rotated by 180° and the vibration is quite unchanged in character, then the vibration is said to be symmetric. This is the case for one of the stretching vibrations in water. The bending vibration in water is also symmetric. Rotation of the second stretching motion in water about the C_2 axis produces a motion that is antiphase with the original,

so the vibration is said to be antisymmetric. The three vibrational motions are labelled ν_1, ν_2 and ν_3 in decreasing frequency within their symmetry type, ν_1 having the highest fully symmetric frequency. The vibrational state of the molecule is described by three quantum numbers V_1, V_2 and V_3 corresponding to the vibrational modes ν_1, ν_2 and ν_3. Transitions from the various vibrational levels of one electronic state to those of another give rise to a band system. (000) - (000) indicates a transition from $V_1'' = 0$, $V_2'' = 0$, $V_3'' = 0$ in the lower electronic state to $V_1' = 0$, $V_2' = 0$, $V_3' = 0$ in the higher electronic state.

3. ROTATIONAL LEVELS

The rotational fine structure is dependent on the shape of the molecule. In fact, the rotation of a polyatomic molecule can be quite complex, and for clarity the rotation is resolved into three rotational components about three mutually perpendicular directions through the centre of gravity. These are called the principal axes of rotation. Therefore, the molecule has three principal moments of inertia , one about each axis labelled Ia, Ib and Ic. Polyatomic molecules are classified according to the relative values of these moments of inertia . In general molecules are said to be linear, symmetric top, spherical top or asymmetric top.

The case where two moments of inertia are equal is called a symmetric top. Linear molecules are a special case of the symmetric top since the two largest moments of inertia are equal and the third is zero. The case where all three moments of inertia are equal is called a spherical top and, the case in which all three moments of inertia are

different is called an asymmetric top. Water is an example of an asymmetric top molecule.

A. LINEAR MOLECULES

The simplest transitions for linear molecules are those, where the molecule is linear in both the upper and the lower state, and in which both states are singlets. For example the $^1\Pi_u - {}^1\Sigma_g^+$ transition of C_3 (Gausset et al 1965 (494)) in which both states are singlet and have $D\infty h$ symmetry. The rotational fine structure is governed by the selection rule,

$$\Delta J = 0, \pm 1 \text{ (except, } J = 0 \not\leftrightarrow J = 0)$$

where J is the total angular momentum quantum number. This gives rise to three branches P, Q and R.

In terms of the symmetry properties

$$+ \longleftrightarrow -, \quad + \not\leftrightarrow +, \quad - \not\leftrightarrow -$$

$$s \longleftrightarrow s, \quad a \longleftrightarrow a, \quad s \longleftrightarrow a$$

There are three types of singlet bands, those without a Q branch, those with only a weak Q branch and those with a strong Q branch. These three types correspond to $\Delta K = 0$, with $K = 0$, $\Delta K = 0$ with $K \neq 0$ and $\Delta K = \pm 1$ respectively. Where K is the quantum number of the angular momentum about the internuclear axis.

$$K = |\Lambda \pm l| \qquad (2.31)$$

That is the sum of the electronic and vibrational angular momenta.

B. SYMMETRIC TOP MOLECULES

In the case of the symmetric top the rotational energy levels are described by two quantum numbers J, and its projection K onto the axis of symmetry where K takes the 2(J + 1) values, -J, -J + 1, ...J. The quantum numbers are often written as J_K and the selection rules are

$\Delta K = 0, \quad \Delta J = 0, \pm 1 \qquad$ if $K \neq 0$

$\Delta K = 0, \quad \Delta J = \pm 1 \qquad$ if $K = 0$

when the transition moment of the electronic transition is parallel to the top axis, and

$\Delta K = \pm 1, \ \Delta J = 0, \pm 1$

when the transition moment is perpendicular to the top axis.

The symmetry rules are the same as for linear molecules,

$+ \longleftrightarrow -, \quad + \not\longleftrightarrow +, \quad - \not\longleftrightarrow -$

C. ASYMMETRIC TOP MOLECULES

For an asymmetric top molecule, J is usually written with two subscripts Ka and Kc, the quantum numbers of rotation about the a and c axes in the limiting cases of the corresponding prolate and oblate symmetric tops. Each level of the asymmetric top is completely described by J Ka Kc.

The selection rules depend on the axis in the molecule of the electric dipole moment.

$\Delta J = 0, \pm 1$ (except $J = 0 \not\longleftrightarrow J = 0$)

In addition for multiplet states with small

multiplet splitting,

$$\Delta N = 0, \pm 1$$

Where N is the total angular momentum apart from spin.

The symmetry properties of rotational levels are determined by their behaviour with respect to rotation by 180^{o} about the three axes, ie C_2^{a}, C_2^{b} and C_2^{c}. However it is only necessary to indicate this behaviour about the c and a axes, giving four possible types of rotational level ++, +-, -+, and --. The first sign refers to the C_2^{c} operation and the second sign refers to the C_2^{a} operation.

In terms of symmetry, if the transition moment is in the direction of the axis of the smallest moment of inertia (a axis) only, then

$$++ \leftrightarrow -+ \quad \text{and} \quad +- \leftrightarrow --$$

can occur. If the transition moment is in the direction of the b axis,

$$++ \leftrightarrow -- \quad \text{and} \quad +- \leftrightarrow -+$$

can occur, and if the transition moment is in the direction of the c axis,

$$++ \leftrightarrow +- \quad \text{and} \quad -+ \leftrightarrow --$$

can occur. Transitions between levels of the same symmetry are forbidden.

The selection rules may also be stated in terms of Ka and Kc. If the transition moment is in the direction of the a axis,

$$\Delta Ka = 0, \pm 2, \quad \Delta Kc = \pm 1, \pm 3$$

In the direction of the b axis,

$\Delta Ka = \pm 1, \pm 3, \Delta Kc = \pm 1, \pm 3$

In the direction of the c axis

$\Delta Ka = \pm 1, \pm 3, \Delta Kc = 0, \pm 2$

The branches that follow from the selection rules are designated in the usual way.

A left superscript gives the ΔK value where p means $\Delta K = -1$ and r means $\Delta K = +1$. The first subscript gives the Ka value of the lower state and the second subscript the Kc value. For example the three branches of the band with $K' = 0$ and $K'' = 1$ are ${}^{p}R_{1,J-1}(J)$, ${}^{p}Q_{1,J}(J)$ and ${}^{p}P_{1,J-1}(J)$. Alternatively the individual lines are described by the J Ka Kc values of the upper and lower state. For example ${}^{p}Q_{1,J}(3)$ would be $3_{03} - 3_{13}$.

2.4 TRANSITION PROBABILITIES AND THE OSCILLATOR STRENGTH

The accurate measurement of the concentration of free radicals and other molecular species in the interstellar medium, comets and flames depends upon our knowledge of the radiative lifetime of the excited state which is determined by the transition probability of the absorption band observed.

The relationships between radiative lifetimes, transition probabilities and oscillator strengths have been discussed in depth by Larsson 1983 (299).

Studies of the intensity of spectral lines allow the derivation of transition probability data and the physico chemical conditions in the light source or absorbing layer. Transition probability data include the Einstein A and B coefficients, oscillator strengths and absorption coefficients.

For astrophysicists the most important factor is the oscillator strength or f value. This has been determined by a variety of methods including emission and absorption, beam foil, molecular beam and shock tube spectroscopy, as well as by theoretical considerations of molecular models. The situation with regard to molecular f values is however not good. Molecular spectra are extremely complex showing many lines which depend in a very sensitive manner on the excitation conditions.

The wavelength of a molecular line is related to changes in electronic, vibrational and rotational energy by the equation,

$$\frac{hc}{\lambda} = h\nu$$
$$= \Delta E_{el} + \Delta E_{vib} + \Delta E_{rot} \qquad (2.32)$$

The change in electronic energy ΔE_{el} locates the whole band system in the spectrum. The change in vibrational energy ΔE_{vib} locates the position of the band in the band system and the change in rotational energy ΔE_{rot} locates the line in the band.

Most molecular transitions occur in band systems located between the vacuum ultraviolet and the near infrared. Vibrational - rotational spectra occur in the near infrared. Pure rotational spectra occur at microwave frequencies. Most electronic transitions in astronomical spectra occur in absorption from the ground vibrational level in the ground electronic state.

The existence of local thermodynamic equilibrium in astronomical objects means that they give rise to spectra similar to those of laboratory origin. Such spectra therefore offer a considerable amount of information if reliable transition probability data are available. Unfortunately not all of the lines in many spectra have been analysed or identified and some of those that have are of variable quality. There is also a lack of theoretical work on derived quantities such as Franck-Condon factors and Hönl-London factors.

In interstellar space the cold gas shows only absorption spectra. Identification can be made by comparison with laboratory spectra, however this should be done for several lines to be certain. This can be made more difficult when several atomic and molecular features are interlaced.

2.4.1. LINE INTENSITIES

The probabilities of electronic transitions under the influence of electro magnetic radiation are determined by the eigenfunctions of the states involved. Thus the intensities of the emitted or absorbed spectral lines can be obtained.

The interaction of an electromagnetic wave with an atomic system is the interaction of the electric vector of the wave with the electric dipole moment of the system.

The probability of a transition between two states E1 and E2 produced by the interaction is proportional to the square of the matrix element known as the transition moment R, whose components depend on the eigenfunctions of the two states Ψ_1 and Ψ_2.

If R is not zero the two states can combine with each other with a certain probability of emission or absorption of radiation. If R = 0 then the transition is forbidden. R is given by the equation

$$R = \int \Psi_2 \mu \Psi_1 \, d\tau \qquad (2.33)$$

where Ψ_2 and Ψ_1 are the eigenfunctions of the two states

μ = Electric dipole moment.

$d\tau$ = Volume element.

For a molecular system the total eigenfunction Ψ is to a first approximation the product of the electronic, vibrational and rotational eigenfunctions, and the reciprocal of the internuclear distance r.

$$\Psi = \Psi_{el} \frac{1}{r} \Psi_{vib} \Psi_{rot} \qquad (2.34)$$

For a molecular system bathed in radiation of energy density ρ of frequency ν_{12} corresponding to the transition $E_1 \longrightarrow E_2$ the rate of absorption of radiation via an electric dipole process is given by $n_1 B_{12} \rho$

Where B_{12} is Einsteins coefficient of Induced Absorption given by

$$B_{12} = \frac{8\pi^3}{3h^2} (R_{12})^2 = B_{21} \qquad (2.35)$$

R_{12} = Transition moment

n_1 = No. density of molecules in the lower state E_1

Decay from an excited state to a state of lower energy may occur by two radiative processes, spontaneous and

stimulated emission. Stimulated emission is analogous to the process described for absorption. The rate of emission is given by $n_2 \; B_{21} \rho$ where ρ is of frequency ν_{21}. B_{21} is called Einsteins coefficient of stimulated emission. Spontaneous emission occurs via a pathway that is independent of the power density of the radiation and occurs at a rate $n_2 \; A_{21}$ where A_{21} is Einsteins coefficient of spontaneous emission, given by

$$A_{21} = \frac{64\pi^4}{3hc^3}\nu_{21}^3 \; (R_{21})^2 \qquad (2.36)$$

n_2 = No. density of molecules in upper state E_2.

ν_{21} = Frequency of transition $E_2 \longrightarrow E_1$.

The absolute intensity of electronic transitions is usually determined from the absorption spectrum since for emission it is difficult to determine the number of molecules in the excited state. The primary experimental datum in absorption is the absorption coefficient $k\nu$ defined by

$$I\nu = I^o_\nu e^{-k\nu \Delta x} \qquad (2.37)$$

where $I\nu$ = Final intensity.

I^o_ν = Initial intensity.

after transmission through a column of gas of length Δx. The absorption coefficient varies across an absorption band, ie. with frequency.

(Note: The extinction coefficient $\epsilon = \frac{k\nu}{2.303}$).

For small values of Δx the light absorbed in a transition I abs, is given by

$$I \text{ abs} = \int (I^{o}_{\nu} - I_{\nu}) \, d\nu$$

$$= I^{o}_{\nu} \Delta x \int k_{\nu} \, d\nu \qquad (2.38)$$

where I^{o}_{ν} is assumed to be constant over the width of the band.

The intensity of absorption, that is the energy absorbed from the incident beam is given by

$$I \text{ abs} = B_{12} \rho h \bar{\nu} c \, n_1 \Delta x \qquad (2.39)$$

$\bar{\nu}$ is the wave number of the transition = $\frac{\nu}{c}$

If $I^{o} = c\rho$ is the intensity of the incident radiation

$$I \text{ abs} = I^{o} B_{12} h \bar{\nu} n_1 \Delta x \qquad (2.40)$$

Substituting (2.38) into (2.40) and taking $I^{o} = I^{o}_{\nu}$, we obtain for the integrated absorption coefficient, that is the sum of the absorption coefficients for all frequencies in the absorption band.

$$\int k_{\nu} \, d\nu = n_1 B_{12} h \bar{\nu}$$

$$= \frac{8\pi^3 \bar{\nu}}{3hc} n_1 |R_{12}|^2 \qquad (2.41)$$

2.4.2. THE OSCILLATOR STRENGTH

Frequently the experimental data are expressed in terms of the oscillator strength f, which is a dimensionless quantity.

$$f = \frac{m hc^2 \bar{\nu}}{\pi e^2} B_{12}$$

$$= \frac{8\pi^2 m c \bar{\nu}}{3he^2} (R_{12})^2$$

(Herzberg 1950 (240)) (2.42)

where m and e are the mass and charge of the electron. The integrated absorption coefficient is related to the oscillator strength by

$$\int k_{\nu} \, d\nu = \frac{\pi e^2}{mc} n_{\nu} f \qquad (2.43)$$

Where n_ν is the number of molecules capable of absorbing radiation of frequency ν.

The oscillator strength is used as a reference against which to compare spectral line intensities. Fully allowed transitions have f values close to unity. f values of forbidden lines, however, may be several orders of magnitude less.

The probability that an electron in its ground state will be excited to a higher energy level by a photon is different for different transitions. If not the absorption features in a spectrum would all have the same equivalent width. The rate at which a molecule absorbs electromagnetic radiation in a particular transition can be expressed as a fraction of the rate at which a classical electron oscillator would absorb. That is an electron in an idealised molecule that absorbs and emits radiation at the maximum rate. This fraction is called the oscillator strength and is a characteristic of a transition between two energy levels. The optical absorption lines in the visible and ultraviolet parts of the spectra of diffuse interstellar clouds arise from the transitions between rotational levels in molecules undergoing vibrational and electronic excitation also. As such the total oscillator strength will have three parts corresponding to the electronic, vibrational and rotational factors. The total oscillator strength has been defined by Herbig 1968 (54) as,

$$f\ TOTAL = \frac{\lambda(v'v'')}{\lambda(J'J'')}\ fel\left[\lambda(v'v'')\right] q(v'v'')\ \frac{SJ}{(2J''+1)} \qquad (2.44)$$

In most cases $\frac{\lambda(v'v'')}{\lambda(J'J'')}$ is close to unity,

$$\therefore f \text{ TOTAL} = fel\left[\lambda(v'v'')\right] \; q(v'v'') \; \frac{SJ}{(2J''+1)} \qquad (2.45)$$

Single primes denote upper states and double primes denote lower states.

The band oscillator strength is given by

$f(v'v'') = fel\left[\lambda(v'v'')\right] \; q\,(v'v'')$ (Schadee 1967(111))

1. $\lambda(v'v'')$ and $\lambda(J'J'')$ represent the wavelengths of the band origin and of the rotational line in question, (where J is the total angular momentum quantum number).

2. $\frac{SJ}{(2J''+1)}$ is the rotational factor. SJ is the Hönl London or intrinsic line strength factor normalised according to Schadee 1967 (see also Schadee 1971 (498)). It determines the relative intensity distribution line by line within a band.

3. $q(v'v'')$ is the Franck Condon factor. This determines the relative intensity in absorption or emission of vibrational bands in the electronic spectra of molecules. It is defined by,

$$q(v'v'') = \left| \int \Psi'(v') \; \Psi''(v'') \; dr \right|^2 \qquad (2.46)$$

Where $\Psi'(v')$ and $\Psi''(v'')$ are vibrational wave-functions of the levels v' and v'', r is the internuclear distance.

4. fel is the component of the total oscillator strength characteristic of the electronic transition. It has been noted by Frisch 1972 (4) that the rotational factor = 1 for the R(0) line of a singlet

transition, for example the $A^1\Pi - X^1\Sigma^+$ transition of CH^+. In this case f(v'v'') = f TOTAL. For all other cases f TOTAL should be used to calculate molecular column densities. In practice this is not always possible due to a lack of fundamental molecular data, so that approximations are often made.

2.4.3. METHODS OF DETERMINING TRANSITION PROBABILITIES

The oscillator strength is the most important quantity required for the determination of molecular abundances from optical data. Experimental methods to determine this factor include the following.

EMISSION SPECTROSCOPY

Emission spectra are richer than absorption spectra as they contain bands for many v'' progressions depending on the method of excitation. The intensity of emission is determined by the product of population and transition probability, however different emission sources maintain different relative population distributions. Thus while intensity distributions can easily be interpreted in relative terms, absolute information on population distribution is required before emission intensities can be interpreted in terms of absolute transition probabilities.

ABSORPTION SPECTROSCOPY

In absorption measurements the ratio of emergent to incident intensity is measured rather than intensity alone. Thus the response does not have to be known absolutely, provided that the detector has a linear response at each wavelength. Often a room temperature absorption cell is used in which only a few vibrational levels will be visible as bands in the resultant spectrum.

LIFETIME MEASUREMENTS

Lifetime measurements can be used to determine oscillator strengths provided that

a) Decay from the upper state is not compensated for in any way by cascading from higher states.

b) Decay from the upper state occurs solely by radiative channels.

c) One of the radiative channels is dominant, from which transition probability data can be inferred.

Examples of methods employed are,

1. ELECTRON BOMBARDMENT

Bennett and Dalby 1960 (112) have measured the oscillator strengths for the $A^3\Pi - X^3\Sigma$ transition of NH and the $A^2\Delta - X^2\Pi$ and $B^2\Sigma - X^2\Pi$ transitions of CH. They used the radiative lifetimes of excited states created by bombarding a suitable parent gas at low pressures with electrons. When the exciting source is removed the light output is measured as a function of time to yield the radiative lifetime for spontaneous emission from the upper state. This is then used to calculate the oscillator strength as the lifetime T is related to the oscillator strength of the electronic transition by,

$$fel = \frac{mc\lambda^2}{8\pi^2 e^2} \quad \frac{gm}{gn} \quad \frac{1}{T} \qquad (2.47)$$

where gm and gn are the degeneracy of the upper and lower electronic states respectively.

2. DELAYED COINCIDENCE

In this technique a pulsed beam of electrons (typically 20 - 100 ev at a repetition frequency

of some KHz) excites a target of free molecules. The excitation is viewed with a monochromator which selects the particular transition of interest, and a multichannel analyser displays the decay curve of the transition being studied.

3. HIGH FREQUENCY DEFLECTION

This is essentially an improved delayed coincidence technique. Brzozowski et al 1974 (145), 1976 (95) have used this technique to measure lifetimes for excited states in CH^+ and CH respectively. A strong electron current in the KeV range excites a gas at 1μm pressure and the excitation is repeated after some five lifetimes of the transition studied by high frequency deflection of the electron current.

Since it is difficult to pulse a high power electron gun at a 20MHz repetition frequency a continuous electron beam is swept in front of a slit using a high frequency applied to two deflection plates along the beam. After the slit the electron beam appears as a linear particle train which can excite a gas volume after which it can be collected by a plate and give a trigger pulse to a conventional multichannel coincidence system.

The high electron currents and the high duty cycle of the excitation process in this technique make possible lifetime measurements at much higher spectral resolution than other methods permit.

4. PHASE SHIFT

In the conventional coincidence technique with exciting electron pulses at KHz repetition

frequencies a lot of intensity is lost in the long dark intervals between the pulses if the lifetime of the transition is in the nano second range. In the phase shift technique an electron beam is continuously exciting a gas at low pressure but the beam is sinusoidally modulated at radio frequencies. The emitted light from an excited level will then also be modulated at the same frequency but shifted in phase relative to the excitation due to the finite lifetimes of the excited states. The phase shift is a function of the mean lifetime of the state and by measuring the shift at a number of modulation frequencies the decay curve can be calculated.

The lifetime T is derived from

$$\text{Tan } \phi = \omega T \qquad (2.48)$$

where ϕ = Absolute phase shift.

$\omega = 2\pi f$ = Circular modulation frequency.

T = Radiative lifetime.

Hesser 1968 (275) has given a detailed explanation of how the absolute transition probability, the electronic transition moment and the absolute oscillator strength can be calculated from the radiative lifetime of an excited vibrational level from the absolute phase shift vs frequency modulation curve.

Fink and Welge 1967 (129) have used the equation

$$fel = \frac{1}{T(v')} \frac{gm}{gn} \frac{mc}{8\pi^2 e^2} \frac{1}{\nu^2} \qquad (2.49)$$

where ν = Modulation frequency, to calculate electronic oscillator strengths for the $A^2\Delta - X^2\Pi$ and $B^2\Sigma^- - X^2\Pi$ transitions of CH using the Phase Shift method.

5. LASER INDUCED FLUORESCENCE

Mahan and O'Keefe 1981 (62) have obtained the laser induced fluorescence spectra of ions, created by electron impact ionisation of a selected background neutral gas, confined to a small spatial region within a three dimensional radio frequency quadrupole trap. This allows the storage of large numbers of ions for time periods limited only by collisions with background neutral gas molecules. Ions in the ground electronic state are excited with a brief laser pulse and the resulting fluorescence monitored as a function of time. The observed decay rate provides an unambiguous measurement of the upper levels radiative lifetime.

6. SHOCK HEATING

Reis 1965 (167) has determined the oscillator strength for CN by measuring the radiation from the shock layer about a hypervelocity projectile with a time of flight scanning spectrometer. Projectiles fired into a mixture of CO_2 and N_2 gases produce a shock heated gas whose spectrum shows the lines of the CN violet $B^2\Sigma^+ - X^2\Sigma^+$ system. The oscillator strength is then determined by fitting the measured power radiated from each band sequence to a synthetic spectrum.

Other methods of determining oscillator strengths are discussed by Ebster 1964 (505), Huber and Sandeman 1980 (503) and van Wijngaarden 1986 (508). Although these reviews deal with atomic oscillator strengths the methods discussed are equally applicable to molecules.

2.5 OSCILLATOR STRENGTHS USED TO DETERMINE COLUMN DENSITIES

1. CH^+

The $A^1\Pi - X^1\Sigma^+$ electronic transition has been used to study the abundance of the CH^+ molecular ion in interstellar space. However, for some time a large uncertainty has existed in the radiative lifetime of the $A^1\Pi$ state and this has resulted in a large uncertainty in the oscillator strength. Consequently estimates of the interstellar abundance of this important molecule vary considerably depending on which oscillator strength is used to calculate the column density. CH^+ is an important interstellar molecule and it is necessary to determine its correct abundance so that it can be used to test present theories of interstellar chemistry.

The two major absorption lines in the CH^+ spectrum occur at 4232.548 Å and 3957.692Å.. These are due to the (00)R(0) and (10) R(0) lines of the $A^1\Pi - X^1\Sigma^+$ electronic transition respectively. Since both lines are the R(0) line of a singlet transition f TOTAL = f(00) for the line at 4232.5Å and f(10) for the line at 3957.7Å. The line at 4232.5Å is invariably the strongest line and sometimes the only line present.

Blades 1975 (58) has presented a compilation of oscillator strengths for the 4232.5Å line in CH^+ up to 1975. A compilation of all f(00) values up to 1986 is given in table 9. Both tables clearly show the variation in oscillator strength determined using a variety of theoretical and experimental methods. The band oscillator strength f(00) has been determined by Erman 1977 (63) for the $A^1\Pi - X^1\Sigma^+$ transition and his value of $f(00) = 7.2 \times 10^{-3}$ was used by Federman 1982 (30) in a recent survey of CH^+ in diffuse interstellar clouds.

Federman notes however, that a more recent value of f(00) = 5.57×10^{-3} determined by Mahan and O'Keefe 1981 (62) using laser induced fluorescence spectroscopy is more reliable since it is independent of electrostatic repulsion. Therefore this value has been used here to scale the column densities of CH^+ calculated using other f(00) values, from the equivalent width of the line at 4232.5Å.

Other researchers have used a variety of f(00) values to calculate CH^+ column densities. For example Frisch 1972(4) used f(00) = 1.18×10^{-2}, Ohen 1973 (13) used f(00) = 1.46×10^{-2}, Chaffee 1974 (7) used f(00) = 6.45×10^{-3} and Hobbs 1973 (51) used f(00) = 4.0×10^{-2}. A complete list is given in table 10.

TABLE 9

A COMPILATION OF f VALUES FOR THE $A^1\Pi - X^1\Sigma^+$ TRANSITION OF CH^+

f (el)	f (00)	EXPERIMENTAL METHOD	REFERENCE
-	4×10^{-3}	Estimated from dipole strength	Bates & Spitzer 1951 (38)
-	6.8×10^{-2}	Electron beam phase shift method	Smith 1971 (168)
-	1.2×10^{-3}	Solar spectrum	Grevesse & Sauval 1971 (502)
2.2×10^{-2}	-	Estimated from data on CH.	Solomon & Klemperer 1972 (65)
2.2×10^{-2}	† 1.18×10^{-2}	Theoretical calculation	Frisch 1972 (4)
-	4.0×10^{-2}	Estimated from current data	Hobbs 1973a 1973b (51 & 140)
2.2×10^{-2}	* 1.46×10^{-2}	Theoretical calculation	Cohen 1973 (13)
-	6.45×10^{-3}	Ab initio calculation	Yoshimine et al 1973 (61)
-	1.15×10^{-2}	High frequency deflection technique	Brzozowski 1974 (145)
-	1.36×10^{-2}	Electron beam phase shift	Brooks & Smith 1975 (49)
-	7.2×10^{-3}	High frequency deflection technique	Erman 1977 (63)
-	7.43×10^{-3}	Theoretical calculation	Elander et al 1977 (453)
-	4.48×10^{-3}	Theoretical calculation	Saxon, Kirby & Liu 1980 (425)

continued...

TABLE 9 (continued)

f (el)	f (00)	EXPERIMENTAL METHOD	REFERENCE
-	5.57×10^{-3}	Laser induced fluorescence Spectra	Mahan & O'Keefe 1981 (62)
-	5.45×10^{-3}	Theoretical calculation	Larsson & Siegbahn 1983 (410)

† q(00) = 0.538 (Herbig 1968 (54))

* q(00) = 0.665 (Green, Hornstein & Bender 1973 (122))

TABLE 10

A COMPILATION OF f VALUES FOR THE ABSORPTION LINE AT 4232.5Å USED TO DETERMINE CH^+ COLUMN DENSITIES

f VALUE	USED BY
7.2×10^{-3}	Federman 1982 (30)
4.0×10^{-2}	Hobbs 1973 (51) Hobbs 1973 (140)
1.36×10^{-2}	Peimbert 1968 (59) Blades 1978 (25) Blades 1975 (58)
1.46×10^{-2}	Cohen 1973 (13)
6.45×10^{-3}	Chaffee 1974 (7) Chaffee 1979 (1) Chaffee 1975 (47) Frisch 1979 (23)
1.18×10^{-2}	Frisch 1972 (4)
1.40×10^{-2}	Vanden Bout 1980 (149) Jura & Smith 1977 (106)
5.57×10^{-3}	Crutcher 1985 (326) White 1984 (392) Hawkins 1985 (362) This study Crutcher & Chu 1985(348) Cardelli & Wallerstein 1986 (446)
5.50×10^{-3}	Lambert & Danks 1986 (405)

2. CH

The position with regard to oscillator strengths for the CH molecule is much clearer than it is for CH^+. The band oscillator strengths for the (00) bands of the $A^2\Delta - X^2\Pi$ and $B^2\Sigma^- - X^2\Pi$ electronic transitions have been determined by Fink and Welge, 1967 (129). They found fel = 5.2×10^{-3} for the $A^2\Delta - X^2\Pi$ transition and fel = 2.8×10^{-3} for the $B^2\Sigma^- - X^2\Pi$ transition. Assuming q(00) is close to unity for both bands, fel = f(00). The value of f(00) = 5.2×10^{-3} for the $A^2\Delta - X^2\Pi$ band agrees with the f(00) value of 5.3×10^{-3} used by Federman 1982 (30) in a study of CH in diffuse clouds. This is based upon lifetime measurements carried out by Brzouzowski et al 1976 (95). Interestingly Lambert 1978 (172) gives f(00) = 4.9×10^{-3} based upon the same lifetime measurements. This is in agreement with the value calculated by Bennett and Dalby 1960 (112) from the radiative lifetimes of excited states. Danks, Federman and Lambert 1984 (152) have used f(00) = 5.1×10^{-3} to calculate CH column densities in diffuse clouds. Again this oscillator strength is based upon the work of Brzouzowski. Herbig 1968 (54) in his study on ζ Oph used f(00) = 5.2×10^{-3} to calculate an f TOTAL value for the single line of the (00) band of the $A^2\Delta - X^2\Pi$ transition, and f(00) = 2.8×10^{-3} to calculate f TOTAL values for the three lines of the (00) band of the $B^2\Sigma^- - X^2\Pi$ transition. These values have been adopted in this study and the f TOTAL value of 5.2×10^{-3} for the $A^2\Delta - X^2\Pi$ (00) $R_2(1)$ line at 4300.321Å has been used to scale column densities calculated using other f values, from theequivalent width of this line. It is the strongest line in the CH spectrum, the $B^2\Sigma^- - X^2\Pi$ and $C^2\Sigma^+ - X^2\Pi$ transitions are rarely observed.

The majority of observers have used the f TOTAL values given by Herbig to calculate CH column densities (see table 13). However, Chaffee and Lutz 1977 (46) in their paper on CH toward ζ Per have used $f(00) = 5.9 \times 10^{-3}$ for the (00) band of the $A^2\Delta - X^2\Pi$ transition. This is based upon Smith's lifetime measurements of the $A^2\Delta$ state of CH (Smith 1971 (168)). They have also used $f(00) = 3.6 \times 10^{-3}$ for the (00) band of the $B^2\Sigma^- - X^2\Pi$ transition determined by Brooks and Smith 1974 (157). This gives a f TOTAL value of 1.8×10^{-3} for the line at 3886.4 Å. These values have been used by them to scale their previous results for CH toward ζ Per, (Chaffee 1974 (7)), the column densities having been determined from the $A^2\Delta - X^2\Pi$ and $B^2\Sigma^- - X^2\Pi$ transitions using the f TOTAL values given by Herbig.

The scaled results compare well with those determined using the $C^2\Sigma^+ - X^2\Pi$ transition and given in the 1977 paper.

Using the ratios,

$$\frac{f(C - X,00)}{f(B - X,00)} = 2.0$$

and

$$\frac{f(C - X,00)}{f(A - X,00)} = 1.2$$

determined by Linevsky 1967 (297) they find a band oscillator strength $f(00) = 7.2 \times 10^{-3}$ for the (00) band of the $C^2\Sigma^+ - X^2\Pi$ transition. Using this value f TOTAL = 1.2×10^{-3}, 3.6×10^{-3} and 2.4×10^{-3} for the lines at 3137 Å, 3143 Å and 3146 Å respectively.

Herbig 1968 (54) has used the column density of CH toward ζ Oph to calculate the electronic oscillator strength for the $C^2\Sigma^+ - X^2\Pi$ transition. Possibly this is the first estimate of a molecular f value from interstellar spectra. However, Chaffee and Lutz point out an error in his calculation and give a revised value of fel = 6.2×10^{-3}.

Hinze, Lie and Liu 1975 (278) have made theoretical calculations on the transition probabilities between low lying states of CH using accurate ab initio electronic wave functions, which have yielded radiative lifetimes for the v = o vibrational levels of the $A^2\Delta$, $B^2\Sigma^-$ and $C^2\Sigma^+$ states. For the $C^2\Sigma^+ - X^2\Pi$ transition they find a higher value of fel = 7.95×10^{-3}.

A compilation of f(00) values for the $A^2\Delta - X^2\Pi$ and $B^2\Sigma^- - X^2\Pi$ transitions is given in tables 11 and 12.

3. CN

Although one of the first interstellar molecules discovered the CN radical is not as widely distributed as CH and CH^+ and recent optical observations have been few. The important transition is the $B^2\Sigma^+ - X^2\Sigma^+$ violet band system, with lines at 3874.608Å, 3873.998Å and 3875.763Å. Some recent theoretical work on this system and the red $A^2\Pi - X^2\Sigma^+$ system has been carried out by Cartwright and Hay 1982 (222) and Larsson et al 1983 (228) with a view to a better understanding of the radiative and spectral properties of CN, (see Douglas & Routly 1955 (495) for other band systems of CN).

No observations of the $A^2\Pi - X^2\Sigma^+$ or the $B^2\Sigma^+ - A^2\Pi$ system have been made. CN is important as the radical appears in the atmospheres of red giants, and comets as well as in the interstellar gas.

The majority of observers have used the f TOTAL values given by Herbig for the three lines of the $B^2\Sigma^+ - X^2\Sigma^+$ transition, to calculate CN column densities. Herbig used the value fel = 1.9×10^{-2} determined by Reis 1965 (167) and the Franck Condon factor q(00) = 0.909 given by Halmann and Laulicht 1966 (262) to calculate f(00) = 1.73×10^{-2}.

TABLE 11

A COMPILATION OF f(00) VALUES FOR THE (00) BAND OF THE CH $A^2\Delta - X^2\Pi$ TRANSITION

f(00)	EXPERIMENTAL METHOD	REFERENCE
0.45×10^{-3}	Theoretical calculation	Lyddane et al 1941 (489)
8.0×10^{-3}	Theoretical calculation	Stephenson 1951 (492)
$10 - 14 \times 10^{-3}$	Theoretical calculation	Hurley 1959 (490)
4.9×10^{-3}	Electron bombardment	Bennett & Dalby 1960 (112)
9.4×10^{-3}	Electron collision	Jeunehomme & Duncan 1964 (207)
5.2×10^{-3}	Phase shift	Fink & Welge 1967 (129)
3.6×10^{-3}	Theoretical calculations	Huo 1968 (462)
3.5×10^{-3}	Pulsed radiolysis	Le Calvé 1969 (491)
6.0×10^{-3}	Phase shift	Hesser & Lutz 1970 (154)
5.9×10^{-3}	Phase shift	Smith 1971 (168)
5.0×10^{-3}	Lifetime of excited state	Grevesse & Sauval 1973 (452)
5.3×10^{-3}	Solar photospheric spectrum	Grevesse & Sauval 1973 (452)
6.78×10^{-3}	Theoretical calculation	Hinze Lie & Liu 1975 (278)
4.9×10^{-3}	High frequency deflection	Brzouzowski 1976 (95) Lambert 1978 (172)
5.3×10^{-3}	High frequency deflection	Brzouzowski 1976 (95) Federman 1982 (30)

continued...

TABLE 11 (continued)

f(00)	EXPERIMENTAL METHOD	REFERENCE
5.5×10^{-3}	Pulsed r.f. discharge	Carozza & Anderson 1977 (334) Lien 1984 (330)
5.06×10^{-3}	Radiative lifetimes	Larsson & Siegbahn 1983 (416) See also Brzouzowski et al 1976 (95) and Becker et al 1980 (426)
5.1×10^{-3}	Laser induced fluorescence	Garland & Crosley 1985 (409)

TABLE 12

A COMPILATION OF f(00) VALUES FOR THE (00) BAND OF THE CH $B^2\Sigma^- - X^2\Pi$ TRANSITION

f(00)	EXPERIMENTAL METHOD	REFERENCE
$8 - 18 \times 10^{-3}$	Theoretical calculation	Hurley 1959 (490)
1.2×10^{-3}	Electron bombardment	Bennett & Dalby 1960 (112)
3.0×10^{-3}	Graphite furnace	Linevsky 1967 (297)
2.8×10^{-3}	Phase shift	Fink & Welge 1967 (129)
2.5×10^{-3}	Theoretical calculations	Huo 1968 (462)
3.2×10^{-3}	Phase shift	Hesser & Lutz 1970 (154)
1.9×10^{-3}	Solar photospheric spectrum	Grevesse & Sauval 1973 (452)
2.5×10^{-3}	Life time of excited state	Grevesse & Sauval 1973 (452)
3.6×10^{-3}	Phase shift	Brooks & Smith 1974 (157)
4.16×10^{-3}	Theoretical calculation	Hinze, Lie & Liu 1975 (278)
3.1×10^{-3}	High frequency deflection	Brzozowski 1976 (95) Smith 1985 (394)
3.3×10^{-3}	Radiative lifetime & ab initio calculation	Lambert 1978 (172)
3.2×10^{-3}	Laser induced fluorescence	Garland & Crosley 1985 (409)

TABLE 13

A COMPILATION OF f VALUES FOR THE ABSORPTION LINE AT 4300.3 Å USED TO DETERMINE CH COLUMN DENSITIES

f VALUE	USED BY
5.1×10^{-3}	Danks 1983 (152)
5.2×10^{-3}	Herbig 1968 (54) Cohen 1973 (13) Chaffee 1974 (7) Chaffee 1975 (47) Chaffee 1979 (1) White 1984 (392) This study. Crutcher 1985 (326) Crutcher & Chu 1985 (348) Blades 1975 (58) Blades 1978 (25)
5.22×10^{-3}	Frisch 1972 (4)
5.3×10^{-3}	Cardelli & Wallerstein 1986 (446) Federman 1982 (30) Lien 1984 (330)
6.78×10^{-3}	Frisch 1979 (23)
5.9×10^{-3}	Chaffee & Lutz 1977 (46)

However, Federman, Danks and Lambert 1984 (283) in a recent survey on CN in diffuse clouds have used f(00) = 3.42×10^{-2}. This is based upon the lifetime studies of Jackson 1974 (298) and is given by Lambert 1978 (172). Federman et al cite the work of Duric, Erman and Larsson 1978 (288) whose experimental radiative lifetime for the $B^2\Sigma^+$ V = 0 state of 66.7ns agrees with Jackson's value of 65.6ns, and the theoretical lifetimes of Cartwright and Hay (62.05ns) and Larsson et al (66.60ns) as proof of the accuracy of this f value.

Jackson/Lambert's f(00) value has therefore been adopted in this study. The f TOTAL values for the R(0), R(1) and P(1) lines are given by Federman et al as 3.42×10^{-2}, 2.28×10^{-2} and 1.14×10^{-2} respectively. The f TOTAL value of 3.42×10^{-2} for the R(0) line of the (00) band of the $B^2\Sigma^+ - X^2\Sigma^+$ transition at 3874.608Å has been used to scale CN column densities calculated using other f TOTAL values.

A recent f(00) value has been determined by Danylewych and Nicholls 1978 (274) from photoelectric intensity measurements in emission, at medium and high intensity resolution, on the CN violet system. The CN radical was excited in the active nitrogen-carbon tetrachloride afterglow; a chemi luminescent reaction. By detailed comparison with computer synthesised spectra they deduced f(00) = 3.2×10^{-2}. This value agrees with that determined from Jackson's lifetime studies. A compilation of CN f values is given in table 14 and a list of f values used by workers to calculate CN column densities in table 15.

TABLE 14

A COMPILATION OF f VALUES FOR THE $B^2\Sigma^+ - X^2\Sigma^+$ TRANSITION OF CN

f el	f(00)	EXPERIMENTAL METHOD	REFERENCE
2.6×10^{-2}	-	Electric discharge/ Absorption spectra	White 1940 (479)
10.0×10^{-2}	-	Absorption spectrum in furnace	White 1940 (478)
2.7×10^{-2}	$^{*}2.48 \times 10^{-2}$	Electron bombardment	Bennett & Dalby 1962 (316)
1.3×10^{-2}	-	Shock wave heating	Tsang et al 1962 (312)
-	1.3×10^{-2}	Emission from shock heated gas.	Fairbairn 1964 (475)
1.9×10^{-2}	$^{\dagger}1.73 \times 10^{-2}$	Shock layer around projectile	Reis 1965 (167)
2.8×10^{-2}	-	Phase shift method	Moore & Robinson 1968 (317)
2.7×10^{-2}	-	Emission from shock tube	Levitt & Parsons 1969 (323)
3.9×10^{-2}	$^{o}3.64 \times 10^{-2}$	Phase shift	Liszt & Hesser 1970 (319)
6.56×10^{-2}	-	Chemiluminescence reaction	Cook & Levy 1972 (313)
3.5×10^{-2}	-	Shock tube	Arnold & Nicholls 1973 (310)
3.71×10^{-2}	-	Dissociation by vacuum UV flashlamp	Luk & Bersohn 1973 (318)
-	2.7×10^{-2}	Lifetime of excited state	Grevesse & Sauval 1973 (452)
-	1.05×10^{-2}	Solar photospheric spectrum	Grevesse & Sauval 1973 (452)

TABLE 14 (continued)

f el	f(00)	EXPERIMENTAL METHOD	REFERENCE
-	3.42×10^{-2}	Tunable dye laser	Jackson 1974 (298) Lambert 1978 (172)
-	3.2×10^{-2}	Nitrogen, Carbon tetrachloride afterglow	Danylewych & Nicholls 1978 (274) Davis 1986 (473)
-	Δ 3.11×10^{-2}	High frequency deflection	Duric et al 1978 (288)
-	3.4×10^{-2}	Theoretical calculation	Larsson et al 1983 (228) Smith 1985 (394)

NOTES: * q(00) = 0.9168 Dwivedi 1978 (322)
† q(00) = 0.909 Halmann & Laulicht 1966 (262)
Δ q(00) = 0.92 Duric et al 1978 (288)
o q(00) = 0.9179 Spindler 1965 (339)

TABLE 15

A COMPILATION OF f VALUES FOR THE ABSORPTION LINE AT 3874.6 Å USED TO DETERMINE CN COLUMN DENSITIES

f VALUE	USED BY
1.73×10^{-2}	Peimbert 1968 (59) Frisch 1972 (4) Chaffee 1974 (7) Chaffee 1979 (1) Frisch 1979 (23) Herbig 1968 (54) Blades 1975 (58) Blades 1978 (25)
2.48×10^{-2}	Meyer & Jura 1984 (281)
3.2×10^{-2}	White 1984 (392)
3.28×10^{-2}	Crutcher & Chu 1985 (348)
3.42×10^{-2}	Federman 1984 (283) Meyer & Jura 1985 (381) Crutcher 1985 (326) This study. Cardelli & Wallerstein 1986 (446)

4. CO

Two important electronic transitions of CO are observed in the ultraviolet part of the spectrum. The $A^1\Pi - X^1\Sigma^+$ electronic transition has several vibrational bands from the (00) band at 1544.45Å to the (12,0) band at 1246.06Å. This transition has been observed using the International Ultraviolet Explorer Satellite toward several stars. However as the resolution of modern spectrometers such as that on I.U.E. is only of the order of rotational splitting, only the vibrational bands can be resolved and the column density is calculated from an equivalent width derived from the entire vibrational line shape. The band most often used is the (1,0) band at 1509.75Å. Lassettre and Skerbele 1971 (128) have derived an f (10) value of 3.8×10^{-2} for this band and this has been used to scale column densities calculated using other f(10) values from the equivalent width of the (10) band. Usually several bands of the $A^1\Pi - X^1\Sigma^+$ transition are observed and it is possible to determine the column density by plotting a curve of growth. This may then be scaled using the f (10) value of Lassettre and Skerbele. This and other f (10) values are given in Table 16.

TABLE 16

A COMPILATION OF f (10) VALUES FOR THE (10) BAND OF THE CO $A^1\Pi - X^1\Sigma^+$ TRANSITION

f (10)	EXPERIMENTAL METHOD	REFERENCE
4.44×10^{-2}	Electron impact	Meyer, Skerbele & Lassettre 1965 (338)
2.7×10^{-2}	Shock tube	Rich 1968 (294)
1.95×10^{-2}	Phase shift	Hesser 1968 (275)
3.8×10^{-2}	Electron impact	Lassetre & Skerbele 1971 (128)
1.7×10^{-2}	Theoretical calculation	Kurucz 1976 (395) Smith 1985 (394)

NOTE: f (v'v'') values for other bands of the $A^1\Pi - X^1\Sigma^+$ transition are given in the references above, and in

1. Mumma, Stone & Zipf 1971 (314)
2. Pilling, Bass & Braun 1971 (311)
3. Field et al 1983 (412)

The $C^1\Sigma^+ - X^1\Sigma^+$ transition is also observed, notably by Federman 1980 (27) using the spectrometer on board the Copernicus satellite. The (00) band is at 1087.867 Å, and Federman has used the value f (00) = 8.9×10^{-2} given by Smith 1978 (127) to calculate the CO column density. The weaker $E^1\Pi - X^1\Sigma^+$ transition is also observed, and was used by Federman to confirm his CO results using the $C^1\Sigma^+ - X^1\Sigma^+$ transition. Smith gives a f (00) value of 12×10^{-2} for the (00) band of the $E^1\Pi - X^1\Sigma^+$ transition. The $B^1\Sigma^+ - X^1\Sigma^+$ transition is not observed as often as the previous band systems, the (00) band is at 1150.48 Å. The f (00) value given by Smith is f (00) = 7.6×10^{-3}. Smith's oscillator strengths were used to scale column densities calculated from bands in the $B^1\Sigma^+ - X^1\Sigma^+$, $C^1\Sigma^+ - X^1\Sigma^+$ and $E^1\Pi - X^1\Sigma^+$ transitions. (see also the work done by Cooper & Langhoff 1981 (413); from this Smith 1985 (394) in his list of band oscillator strengths quotes a value of f (00) = 1.0×10^{-2} for the (00) band of the $B^1\Sigma^+ - X^1\Sigma^+$ transition).

A recent paper by Krishnakumar & Srivastava 1986 (519) on the radiative lifetimes of the $B^1\Sigma^+$ and $C^1\Sigma^+$ states of CO includes lists of lifetime and oscillator strength measurements for the $B^1\Sigma^+ - X^1\Sigma^+$ transition at 1151 Å and the $C^1\Sigma^+ - X^1\Sigma^+$ transition at 1088 Å.

5. OH

The Hydroxyl radical has spectral lines in the visible and ultra-violet parts of the spectrum. The $A^2\Sigma^+ - X^2\Pi_{3/2}$ transition occurs at visible wavelengths and has been searched for by several workers and detected by Chaffee & Lutz 1977 (46) and Crutcher & Watson 1976 (113). Golden et al 1963 (130) using absorption spectroscopy found f (00) = 8.0×10^{-4}, for the (00) band. Using Golden's value Herbig 1968 (54) has calculated f TOTAL values for the four major rotational lines in the (00) band, and these are used in this study. Other values of f (00) are given in Table 17.

TABLE 17

A COMPILATION OF f (00) VALUES FOR THE (00) BAND OF THE OH $A^2\Sigma^+ - X^2\Pi_{3/2}$ TRANSITION

f (00)	EXPERIMENTAL METHOD	REFERENCE
50×10^{-4}	Theoretical calculation	Mulliken 1940 (477)
2.8×10^{-4}	Absorption spectrum	Dwyer & Oldenberg 1944 (476)
6.4×10^{-4}	Thermal dissociation	Dyne 1958 (482)
$18 - 1500 \times 10^{-4}$	Theoretical calculation	Hurley 1959 (490)
10.6×10^{-4}	Flame spectroscopy	Carrington 1959 (480)
9×10^{-4}	Shock tube emission	Lapp 1961 (486)
8.0×10^{-4}	Absorption spectroscopy	Golden et al 1963 (130)
8.0×10^{-4}	Electron bombardment	Bennett & Dalby 1964 (481)
35×10^{-4}	Shock tube emission	Watson & Ferguson 1965 (487)
12.8×10^{-4}	Pulsed discharge	Bird & Schott 1965 (488)
14.8×10^{-4}	Roschdestwensky hook technique	Anketell & Pery-Thorne 1967 (464)
9.3×10^{-4}	Optical radio frequency double resonance	German & Zare 1969 (458)
7.7×10^{-4}	Phase shift	Smith 1970 (341)
20.6×10^{-4}	Theoretical calculation	Henneker & Popkie 1971 (461)

TABLE 17 (continued)

f (00)	EXPERIMENTAL METHOD	REFERENCE
10.4×10^{-4}	Lifetime measurement	de Zafra et al 1971 (460)
8.39×10^{-4}	Electron beam phase shift	Elmergreen & Smith 1972 (454)
8.0×10^{-4}	Lifetime of excited state	Grevesse & Sauval 1973 (452)
7.0×10^{-4}	Solar photospheric spectrum	Grevesse & Sauval 1973 (452)
11.0×10^{-4}	Delayed coincidence	Dimpfl & Kinsey 1979 (424)
10.9×10^{-4}	Absorption measurements	Wang & Huang 1980 (418)
11.0×10^{-4}	Laser induced fluorescence	Smith & Crosley 1981 (420)
12.0×10^{-4}	Theoretical calculation	Van Dishoeck & Dalgarno 1983 (170)

The $D^2\Sigma^- - X^2\Pi$ transition occurs in the ultraviolet and has been observed using the spectrometer on the Copernicus satellite. The oscillator strength for the (00) band has been determined by Ray and Kelly 1975 (193) who found f (00) = 3.6×10^{-3}. This agrees with the value f (00) = 4×10^{-3} determined by Crutcher and Watson 1976 from the equivalent width of 5.8mÅ for the 1222.07Åline of OH toward o Per determined by Snow 1975 (8) and the equivalent width of the visible line at 3078 Å. The appropriate oscillator strength for the ultraviolet $D^2\Sigma^- - X^2\Pi$ transition has been discussed by Chaffee and Lutz 1977 (46) in some detail. They argue that the calculations used by Ray and Kelly are not correct. However to avoid confusion, Ray and Kelly's oscillator strength has been adopted in this study in line with the majority of observers. The f TOTAL values are given by Snow 1976 (183). A recent theoretical paper, Van Dishoeck & Dalgarno 1983 (170), gives fel = 1.0×10^{-2} for the D - X transition and f (00) = 1.2×10^{-2} for the (00) band.

6. H_2O

The spectrum of water vapour at high resolution in the vacuum ultraviolet wavelength region 1220 Å - 1240 Å was first analysed by Johns 1963 (199). The absorption spectrum shows sharp rotational structure below 1240 Å corresponding to the $\tilde{C}^1B_1 - \tilde{X}^1A_1$ band. More recently Connerade et al 1980 (202) have analysed the spectrum below 1200 Å in more detail.

The $\tilde{C}^1B_1 - \tilde{X}^1A_1$ electronic transition of H_2O has been examined by Smith and Zweibel 1976 (192) who estimate a f value of 1.8×10^{-2} for the line at 1239.7 Å. Recent work by Smith and Parkinson 1978 (182) is consistant with this value. They give f = $< 2.3 \times 10^{-2}$. They give oscillator strengths for five lines of the $\tilde{C}^1B_1 - \tilde{X}^1A_1$ transition.

Smith et al 1981 (180) have examined the $\tilde{F} - \tilde{X}$ band of H_2O at 1115 Å, and revised the results given by Smith and Parkinson for

the $\tilde{C} - \tilde{X}$ band.

Snow 1976 (183) and Smith and Snow 1979 (5) have used $f = 1.8 \times 10^{-2}$ determined by Smith and Zweibel to calculate upper limits to the column density of H_2O toward several stars. They observed the $\tilde{C} - \tilde{X}$ band system at 1239.7 Å. The $\tilde{F} - \tilde{X}$ band has been observed by Snow and Smith 1981 (120). They determined a H_2O column density of $5.3 \times 10^{12} cm^{-2}$ from the line at 1114.2 Å and Smith et al's f value of 3×10^{-2}. No attempt has been made here to scale H_2O results as they all use the same oscillator strength, except for an early result for H_2O toward o Per by Snow 1975 (8), who used an estimated f value for the 1239.7 Å line.

7. NH and N_2

The $A^3\Pi_i - X^3\Sigma^-$ transition of NH (see Dixon 1959 (367)) occurs in the visible part of the spectrum and has been the subject of many unsuccessful searches. Bennett and Dalby 1960 (112) have determined the electronic oscillator strength for the $A^3\Pi_i - X^3\Sigma^-$ transition from the radiative lifetime of the excited state. They found $fel = 8.0 \times 10^{-3}$, and since for the (00) band q(00) = 1, f(00) = 8.0×10^{-3}. This agrees with a recently determined value of f(00) = 7.7×10^{-3}, using laser induced fluorescence, by Fairchild et al 1984 (415). A list of f(00) values for NH is given in table 18. The f TOTAL values are given by Herbig 1968 (54).

The oscillator strengths for bands of the $a^1\Pi_g - X^1\Sigma_g^+$ transition of N_2 (see Vanderslice 1965 (455)) have been estimated by Snow 1975 (8). Lutz, Owen and Snow 1979 (119) have searched for the $P^1\,{}^1\Sigma_u^+ - X^1\Sigma_g^+$ and $^1\Pi_u - X^1\Sigma_g^+$ transitions of N_2 towards δ Sco and ϵ Per. They used the f(00) values of Lawrence et al 1968 (273) to calculate upper limits from the (00) bands of these two electronic transitions.

TABLE 18

A COMPILATION OF f (00) VALUES FOR THE (00) BAND OF THE NH $A^3\Pi_i - X^3\Sigma^-$ TRANSITION

f (00)	EXPERIMENTAL METHOD	REFERENCE
0.72×10^{-3}	Theoretical calculation	Lyddane 1941 (489)
$9.1 - 20 \times 10^{-3}$	Theoretical calculation	Hurley 1959 (490)
8.0×10^{-3}	Lifetime of excited state	Bennett & Dalby 1960 (112)
8.34×10^{-3}	Shock wave emission	Harrington 1966 (485)
1.6 to 7.9×10^{-3}	Theoretical calculations	Huo 1968 (462)
7.45×10^{-3}	Phase shift	Smith 1969 (463)
8.3×10^{-3}	Electron bombardment	Sawada & Kamada 1970 (483)
7.45×10^{-3}	Radiative lifetimes	Smith & Liszt 1971 (484)
9.2×10^{-3}	Solar photospheric spectrum	Grevesse & Sauval 1973 (452)
8.0×10^{-3}	Lifetime of excited state	Grevesse & Sauval 1973 (452)
7.7×10^{-3}	Laser induced fluorescence	Fairchild et al 1984 (415)

8. HCl

Morton 1975 (11) and Jura and York 1978 (117) have both used f TOTAL = 5×10^{-2} for the $C^1\Pi - X^1\Sigma^+(00)$ R(0) line of HCl at 1290.2Å, to calculate column densities. The value f TOTAL = 18.5×10^{-2} given by Smith et al 1980 (181) for the R(0) line has been used to scale column densities. This is slightly larger than the theoretical value of f (00) = 15×10^{-2} given by Van Dishoeck et al 1982 (417)

9. C_2 AND C_3

The C_2 molecule has several electronic transitions that are observed in interstellar spectra. The $A^1\Pi_u - X^1\Sigma_g^+$, Phillips transition has been observed by several observers. The most important band is the (20) band, the R(0) line of which is at 8757.686 Å, (See Chauville, Maillard & Mantz 1977 429)).

The question of which f (20) value to use to calculate C_2 column densities is rather akin to that of CH^+. The f (00) value for the (00) band of the $A^1\Pi_u - X^1\Sigma_g^+$ transition determined by Roux, Cerny and D'Incan 1976 (177) from emission lines in an oxyacetylene flame, $f(00) = 2.5 \times 10^{-3}$ was scaled by Hobbs 1979 (164) to give $f(20) = 1.3 \times 10^{-3}$.

$$f(20) = f(00) \left[\frac{\nu\,(20) q\,(20)}{\nu\,(00) q\,(00)} \right] \qquad (2.50)$$

where $\nu(\nu^1\text{-}0)$ and $q(\nu^1\text{-}0)$ are the band origins and Franck Condon factors respectively.

In a later paper, Hobbs et al 1983 (147), this was revised to f(20) = 1.7×10^{-3} based upon recent ab initio theoretical calculations by Van Dishoeck 1983 (233). The rotational factors for lines in the (20) band are given by Van Dishoeck and de Zeeuw 1984 (212) from which f TOTAL values may be calculated. The f TOTAL value for the R(0) line of the (20) band of the $A^1\Pi_u - X^1\Sigma_g^+$ transition, f TOTAL = 1.7×10^{-3} has been used to scale C_2 column densities calculated using other oscillator strengths.

A compilation of f (20), f (10) and f (00) values is given in table 19. A further list of oscillator strengths used by observers to calculate C_2 column densities is given in table 20. The (10) band of the $A^1\Pi_u - X^1\Sigma_g^+$ transition has been observed in interstellar spectra, in the near infrared. Lutz and Souza 1977 (178) and Souza and Lutz 1977 (176) scaled the f (00) value of Roux Cerny and D'Incan to give f (10) = 2.4×10^{-3}. Brault et al 1982 (219) have derived f (v'v'') values for the (00), (10) and (01) bands of the $A^1\Pi_u - X^1\Sigma_g^+$ transition of C_2 from a model atmosphere analysis of C_2 derived from a high quality solar spectrum. Their value of f (10) = 1.38×10^{-3} is adopted here. Recently Van Dishoeck and Black 1986 (448) have observed the (30) band of the $A^1\Pi_u - X^1\Sigma_g^+$ Phillips system at 7720 Å toward ζ Oph. Using an oscillator strength of f (30) = 7.5×10^{-4} from Dishoeck 1983 (233) they obtained a total C_2 column density of $N(C_2) = 1.5 \times 10^{13} cm^{-2}$. This is in good agreement with the value obtained by Danks & Lambert 1983 (195), from the (20) Phillips band and scaled using f (20) = 1.7×10^{-3} to give $N(C_2) = 1.3 \times 10^{13} cm^{-2}$. The $D^1\Sigma_u^+ - X^1\Sigma_g^+$ Mulliken electronic transition at 2312Å has been observed by Snow 1978 (175) using the Copernicus spectrometer. The f (00) value for the (00) band has been given by Smith 1969 (196), f (00) = 5.5×10^{-2}.

Several estimates have been made as to the f TOTAL value for the R(0) line of the $F^1\Pi_u - X^1\Sigma_g$ (00) band of C_2 at 1341.63Å. Chaffee et al 1980 (165) estimate f (00) $\simeq$ 0.1 which agrees with the results of Danks & Lambert 1983 (195), f (00) $\leq$ 0.14, ($f_{TOTAL} = f(00)$). Curtis et al 1976 (209) in a study on C_2 have made lifetime measurements for the upper states of the $d^3\Pi_g - a^3\Pi_u$ (Swan) $C^1\Pi_g - A^1\Pi u$ (Deslandres - d'Azambuja) and $D^1\Sigma^+ u - X^1\Pi_g$ (Mulliken) transitions, but only calculated oscillator strengths for the Swan bands.

TABLE 19

A COMPILATION OF f (v'v'') VALUES FOR THE $A^1\Pi_u - X^1\Sigma_g^+$ TRANSITION OF C_2 (PHILLIPS BAND)

f(00)	f(10)	f(20)	EXPERIMENTAL METHOD	REFERENCE
-	1.1×10^{-3}	-	Theoretical calculation	Clementi 1960 (384)
-	2.2×10^{-3}	-	Solar photospheric spectrum	Lambert & Mallia 1974 (383)
3.7×10^{-3}	-	2.2×10^{-3}	Shock tube emission	Cooper & Nicholls 1975 (200)
2.5×10^{-3}	-	-	Oxyacetylene flame	Roux, Cerny & D'Incan 1976 (177)
8.9×10^{-1}	-	-	Discharge	Suchard & Melzer 1976 (369)
-	2.4×10^{-3}	-	Scaled from (00) band	Lutz & Souza 1977 (178)
-	-	1.4×10^{-3}	Scaled from (00) band	Chaffee & Lutz 1978 (104)
-	-	1.3×10^{-3}	Scaled from (00) band	Hobbs 1979 (164)
-	-	1.35×10^{-3}	Scaled from (00) band	Chaffee et al 1980 (165)
1.41×10^{-3}	1.38×10^{-3}	-	Solar disc spectrum	Brault et al 1982 (219)
2.3×10^{-3}	1.8×10^{-3}	8.8×10^{-4}	High frequency deflection	Erman 1982 (162)
2.70×10^{-3}	2.84×10^{-3}	1.67×10^{-3}	Ab initio calculation	Van Dishoeck 1983 (233)
2.5×10^{-3}	-	-	Ab initio calculation	Pouilly 1983 (169)

TABLE 19 (continued)

f(00)	f(10)	f(20)	EXPERIMENTAL METHOD	REFERENCE
1.5×10^{-3}	-	1×10^{-3}	Calculated from Swan bands	Danks & Lambert 1983 (195)
2.7×10^{-3}	-	-	Ab initio calculation	Chabalowski et al 1983 (359)
1.38×10^{-3}	1.56×10^{-3}	1.00×10^{-3}	Emission after laser photolysis	Bauer et al 1985 (372)
1.38×10^{-3}	1.70×10^{-3}	-	Absorption spectra	Davis et al 1985 (344)

TABLE 20

A COMPILATION OF f VALUES FOR THE ABSORPTION LINE AT 8757.7 Å USED TO DETERMINE C_2 COLUMN DENSITIES

f VALUE	USED BY
1.35×10^{-3}	Hobbs 1981 (97) Hobbs 1979 (164) Chaffee et al 1980 (165) Hobbs & Campbell 1982 (166) Cosmovici 1981 (163)
1.7×10^{-3}	Hobbs et al 1983 (147) This study Van Dishoeck 1984 (212) Gredel & Munch 1986 (408)
8.8×10^{-4}	Lutz & Crutcher 1983 (146)
1.0×10^{-3}	Danks & Lambert 1983 (195)
1.4×10^{-3}	Chaffee & Lutz 1978 (104)

Clegg and Lambert 1982 (123) have searched for the $\tilde{A}^1\Pi_u - \tilde{X}^1\Sigma_g^+$ transition of C_3 near 4050 Å. They have calculated upper limits toward several stars using $f(000) = 1.8 \times 10^{-2}$. This is derived from the electronic oscillator strength $fel = 2.46 \times 10^{-2}$ of Becker at al 1979 (287) using laser induced fluorescence, and the Frank Condon factor $q(000) = 0.741$ from Perić - Radić et al 1977 (315).

10. H_2 and HD

The resonance lines of the electronic spectrum of the H_2 molecule lie in the extreme ultraviolet, near to those of atomic hydrogen. They may only be observed from above the atmosphere using satellite born ultraviolet spectrometers. Spectral lines observed by the Copernicus satellite were from an allowed electronic transition from the ground state, the $B^1\Sigma_u^+ - X^1\Sigma_g^+$ Lyman transition near 1092 Å. The f (v'v'') values for several bands have been tabulated by Allison and Dalgarno 1970 (121). The (10) band observed by the Copernicus satellite has an oscillator strength $f(10) = 5.79 \times 10^{-3}$. The f TOTAL values for the R(0), R(1) and P(1) lines have been given by Savage et al 1977 (70).

The spectrum of deuterated molecular hydrogen is very different from that of H_2. The rotational and vibrational energy levels are different and so are the transition probabilities. The $B^1\Sigma_u^+ - X^1\Sigma_g^+$ Lyman transition has been used to observe HD in the interstellar gas. The R(0) line of the (00), (30) and (40) bands has been detected by the Copernicus satellite. The f (v'v'') values are given by Allison and Dalgarno, and since the R(0) lines come from a singlet - singlet transition f (v'v'') = f TOTAL for the R(0) line.

11. CO^+, H_2O^+ AND CS^+

The CO^+ molecular ion has not yet been detected in diffuse clouds. However Herbig 1968 (54) and Crutcher 1985 (326) have both determined

equivalent width upper limits for the (20) band at 4250.94 Å and other bands of the $A^2\Pi_i - X^2\Sigma^+$ transition.

Herbig used a f (20) value of 5.6×10^{-4} to calculate a CO^+ column density toward ζ Oph. A modern value of f (20) = 8.6×10^{-4} has been used to scale this result. This is based on work by Mahan & O'Keefe 1981 (62) and Holland & Maier 1972 (419) and given in the table of f values by Smith 1985 (394).

A single measurement of the (00) band of the $B^2\Sigma^+ - X^2\Sigma^+$ transition of CO^+ at 2191.21 Å has been made by Jenkins et al 1973 (53). They determined an upper limit for CO^+ toward χ Per of $< 1.3 \times 10^{15} cm^{-2}$ using f (00) = 7×10^{-4}.

Two lines of the $\tilde{A}^2A_1 - \tilde{X}^2B_1$ transition of H_2O^+ have been searched for by Smith et al 1984 (211). They give f TOTAL = 4.3×10^{-4} for the $1_{10} - 0_{00}$ transitions in the (080)-(000) and (060)-(000) bands at 6147 Å and 6974 Å respectively. This is based on lifetime measurements made by Curtis & Erman 1977 (422). Upper limits for H_2O^+ were determined for four lines of sight, and have not been scaled. The electronic spectrum of H_2O^+ has been discussed by Lew & Heiber 1973 (428) and in detail by Lew 1976 (427).

The possibility that there may be significant concentrations of the CS^+ ion in diffuse clouds has been discussed by Quarta & Singh 1981 (159). Ferlet et al 1983 (148) and Ferlet et al 1986 (532) have searched for the $A^2\Pi_i - X^2\Sigma^+$ transition of CS^+ toward several stars. The 1986 paper gives upper limits for CS^+ toward ζ Oph and ζ Per of $< 1.9 \times 10^{11} cm^{-2}$ and $< 1.2 \times 10^{12} cm^{-2}$ respectively. These are calculated from observations of the (30) band, using f (30) = 7.56×10^{-4}. The oscillator strength is based on the theoretical calculations of Larsson 1985 (540). The $A^2\Pi_i - X^2\Sigma^+$ transition of CS^+ has been analysed in detail by Gauyacq & Horani 1978 (541).

A compilation of the oscillator strengths used to scale the column densities, given in table 27 at the rear of the thesis, is given in table 7.

2.6 CALCULATION OF COLUMN DENSITY

2.6.1. THE EQUIVALENT WIDTH

It is often not possible to gain precise details about the shape of the profile of a spectral line. The instrumentation may not be able to resolve it or the signal to noise ratio may be too low. The total strength of the line may then be estimated by measuring the area contained within the spectral line. The equivalent width $W\lambda$, the width of an equivalent area rectangle is defined as,

$$W\lambda = \int \frac{I\lambda^{(o)} - I\lambda}{I\lambda^{(o)}} \, d\lambda \qquad (2.51)$$

$$= n x \int \alpha\lambda \, d\lambda$$

$$= \frac{n \lambda_o^2}{c} \int \alpha\nu \, d\nu$$

$$= \frac{W\nu \, \lambda_o^2}{c}$$

$$= n x \lambda_o^2 \, r_o f \qquad (2.52)$$

in wavelength terms (Nicholls 1977 (45)).

Here $I\lambda^{(o)}$ is the intensity of a vanishing absorption line, in practice the stellar continuum intensity. $I\lambda$ is the observed intensity at wavelength λ of the absorption line. The integral is over the total absorption line. r_o is the classical radius of the electron, n the number density, x the path length, $\alpha\nu$ the molecular absorption cross section and f the oscillator strength.

We may also write,

$$W\nu = \int \frac{I\nu^{(o)} - I\nu}{I\nu^{(o)}} \, d\nu \qquad (2.53)$$

$$= n x \int \alpha\nu \, d\nu$$

$$= n x \pi c \, r_o f \qquad (2.54)$$

to give the equivalent width in frequency terms. In the

Figure 17

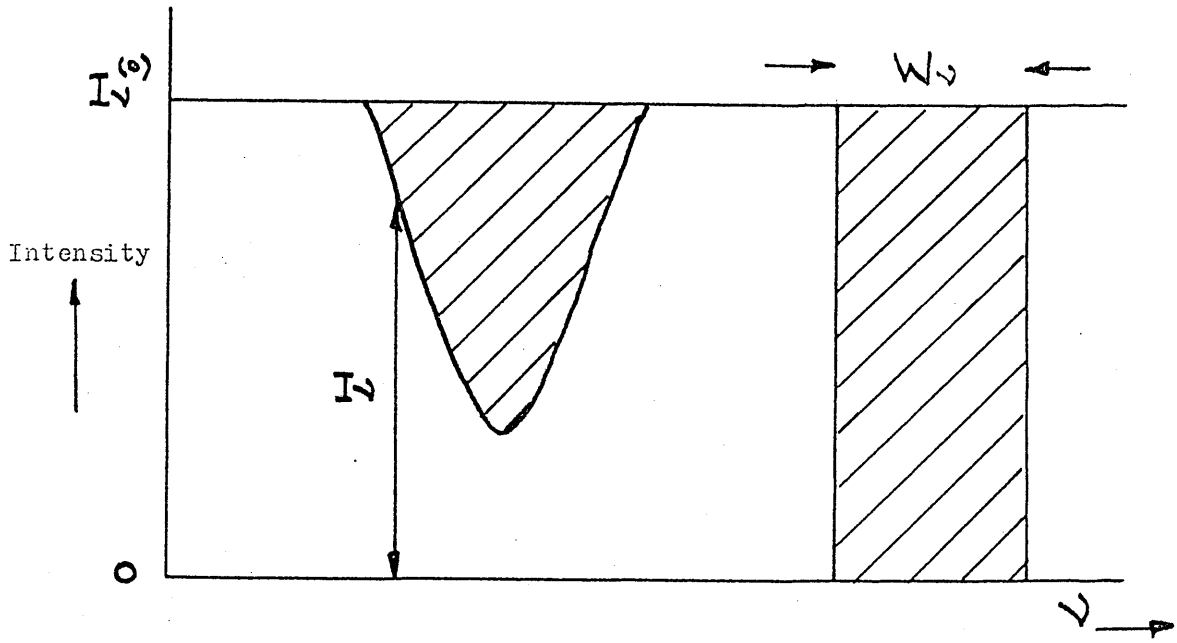

$$W_\nu = \int \frac{I_\nu^{(o)} - I_\nu \, d\nu}{I_\nu^{(o)}}$$

EQUIVALENT WIDTH OF A SPECTRAL LINE

Figure 18

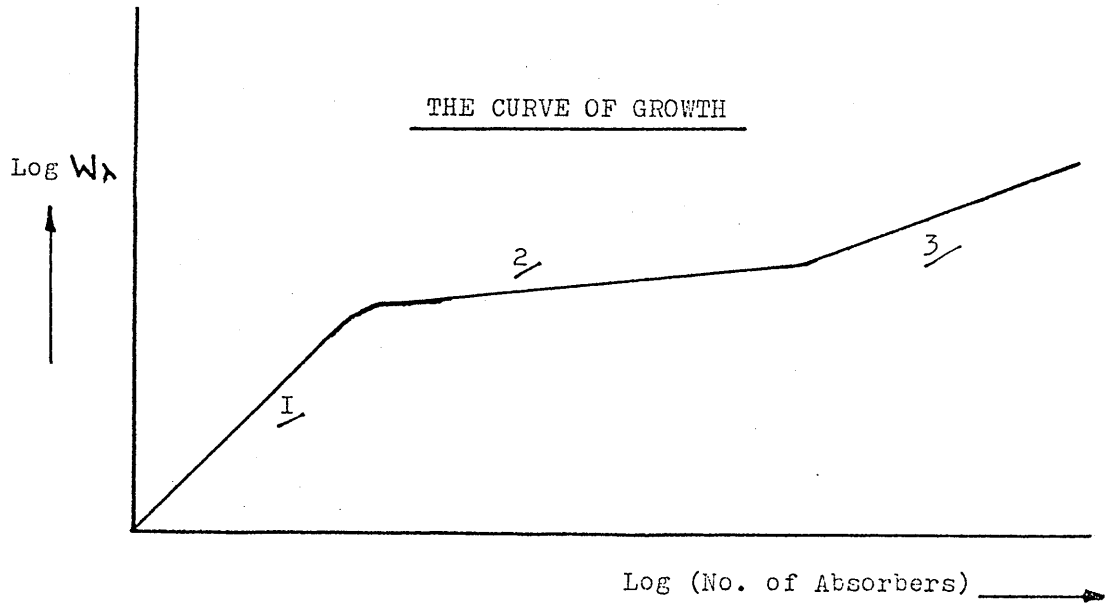

I. Linear.
2. Saturated.
3. Wings

optically thin case the equivalent width of a band is the sum of the equivalent widths of all its lines.

Depending upon the strength of the absorption line one of two techniques can be used for measuring the area contained within the line. For weak lines where $W\lambda \leq 200$ mÅ the method of triangles has been used in the past. The profile is approximated to a triangle whose area is given by the product of the full width at half maximum and the central normalised intensity. Heights above the photographic plate fog of maximum absorption Dp and continuum Dc are taken from the density tracing and converted via a calibration graph to intensities Ip and Ic. The half intensity value $(Ic - I_p)/2$ allows measurement of the full width at half maximum, and the equivalent width is then obtained from

$$W\lambda = FWHM \times \frac{Ic - Ip}{Ic} \qquad (2.55)$$

Detectors other than photographic plates often give intensities directly.

The profile is assumed to be Gaussian and the equivalent width is multiplied by 1.06 to give the final value. The factor 1.06 is the ratio of Gaussian to triangular areas. For strong lines it is better to determine the intensity profile and estimate the area under the curve rather than to rely on triangles. With saturation coming into the profile it becomes very different from a Gaussian curve. With the advent of modern computers this method is more likely to be used than the triangle technique.

2.6.2. THE CURVE OF GROWTH

Following the procedure outlined by Stromgren 1948 (110), let the total number of absorbing molecules in a column

of unit cross section between a star and the observer be N. (The number of species per cm^2 in the line of sight is called the column density). Also, let the line absorption coefficient at a wavelength λ be denoted by α_λ. Then the optical thickness τ_λ of the column at wavelength λ is given by,

$$\tau_\lambda = N\alpha_\lambda. \tag{2.56}$$

Incident radiation of intensity $I_\lambda^{(o)}$ emerging from the column will be reduced according to,

$$I_\lambda = I_\lambda^{(o)} e^{-\tau_\lambda/\lambda} \tag{2.57}$$

The equivalent width W_λ of an interstellar absorption line in wavelngth units is defined as,

$$W_\lambda = \int \frac{I_\lambda^{(o)} - I_\lambda}{I_\lambda^{(o)}} \, d\lambda \tag{2.58}$$

or,

$$W_\lambda = \int (1 - e^{-\tau_\lambda}) \, d\lambda \tag{2.59}$$

in terms of the optical thickness τ_λ. (The integral is extended over the entire line).

Suppose that there is only one interstellar cloud between the observer and the star and that the distribution of radial velocities can be sufficiently accurately described by a Gaussian distribution.

If there is no internal turbulent motion in the cloud, but only thermal motion of the molecules corresponding to a kinetic temperature T then the doppler constant b (in velocity units) is given by,

$$b = \sqrt{\frac{2kT}{Amo}} \tag{2.60}$$

where A is the molecular weight in units mo and k is the Boltzmann constant.

In the general case, b describes the velocity distribution

within the cloud produced by both thermal and turbulent motion. An equivalent temperature is then defined by equation (2.60).

In wavelength units,

$$b\lambda = \frac{b\,\lambda_o}{C}$$

$$= \sqrt{\frac{2kT}{Amo}} \quad \frac{\lambda_o}{C} \qquad (2.61)$$

The value of b determines by how much the spectral line is broadened and is important in constructing a curve of growth.

Writing equation (2.59) in units of $b\lambda$ the following is obtained,

$$\frac{W\lambda}{b\lambda} = \int (1 - e^{-(a\lambda/ao)\tau_o})\, d\nu \qquad (2.62)$$

Where τ_o the optical thickness at line centre corresponding to α_o the absorption coefficient at line centre has been introduced. $\alpha\lambda$ is the absorption coefficient of a stationery undisturbed molecule at wavelength λ.

The graphical relationship between τ_o and $W\lambda/b\lambda$ corresponds to a theoretical curve of growth for interstellar lines corresponding to the case of absorption by one cloud with a Gaussian radial velocity distribution.

When τ_o approaches zero, then equation 2.62 reduces to,

$$\frac{W\lambda}{b\lambda} = \sqrt{\pi}\ \tau_o$$

$$W\lambda = \sqrt{\pi}\ \tau_o\, b\lambda \qquad (2.63)$$

The column density N (defined as the product of the gaseous density and the cloud depth) is related to the optical depth at line centre τ_o by the equation,

$$\tau_o = \frac{N\sqrt{\pi}\ e^2}{mc^2}\ f\ \frac{\lambda^2}{b\lambda} \qquad (2.64)$$

where f = Total oscillator strength

λ = Wavelength of the transition

Therefore

$$W_\lambda = \sqrt{\pi}\ \frac{N\sqrt{\pi}\ e^2}{mc^2}\ f\ \frac{\lambda^2}{b_\lambda}\ b_\lambda$$

$$= \frac{N\ \pi\ e^2}{mc^2}\ f\ \lambda^2$$

or

$$N = \frac{mc^2}{\pi e^2}\ \frac{W_\lambda}{f\lambda^2} \qquad (2.65)$$

Therefore

$$N = 1.13 \times 10^{20}\ \frac{W_\lambda}{f\lambda^2} \qquad (2.66)$$

where W_λ is in $\mathring{A}$.

This equation is only valid for weak unsaturated absorption lines that lie on the linear part of the curve of growth. Note that N is independent of the doppler constant b. If the line is unsaturated the interstellar gas is said to be optically thin, τ_o is $\ll 1$.

A curve of growth, the way in which the equivalent width varies as a function of the number of absorbing species in the line of sight has three distinct stages, (figure 18).

1. The linear portion for which equation 2.66 is valid. Here only the Doppler core contributes to the absorption and the equivalent width increases linearly with the number of absorbing molecules. The column density may be calculated directly from equation 2.66, as W_λ depends very little on the line width. One advantage of the linear portion is that high spectroscopic resolution is not required to obtain useful results. Even if the different components of a spectral line are unresolved the same proportional relationship between W_λ and N holds provided each component is relatively weak.

2. The second part of the curve of growth is almost flat but still rises slowly. Here W_λ is close to its limiting value. The centre of the core is saturated, but the wings of the spectral line are still weak. W_λ scarcely varies at all with the number of absorbers. The value of W_λ now gives information on the line width but very little precise information on N (only a lower limit for N can be determined). The line is said to be saturated and the interstellar gas is optically thick, $\tau_o > 1$.

3. In the third section of the curve the core is saturated and there is now such strong absorption in the wings that adding more absorbers does make a difference to the total absorption. The equivalent width increases as the square root of the number of absorbers, $\tau_o \gg 1$. In a log-log plot the slope is half that in the linear portion of the curve of growth. The line profile is determined by the radiation damping wings and is called the damping part of the curve. Pressure damping is negligible in the case of interstellar spectral lines, but would dominate in the case of lines produced in stellar atmospheres.

It is possible for a molecule to absorb weakly a photon whose wavelength λ is appreciably different from λ_o the central wavelength of the absorption feature. For most interstellar molecules this absorption is too weak to notice, however for hydrogen the column density is so large that absorption can be seen at wavelengths several

Angstroms away from λ_o. An absorption feature broadened in this way is said to possess wings. Absorption features strong enough to show wings offer the advantage that they yield accurate values of the column density. A theoretical curve of growth is fitted to the observed wings to determine the column density, (see Savage et al 1977 (70)). So far the curve of growth has been defined as the graphical relationship between τ_o and W_λ / b_λ for a particular spectral line. If W_λ / b_λ and τ_o are multiplied by $1/\lambda$, we can plot $W_\lambda / b_\lambda . \lambda$. against $\frac{\sqrt{\pi}\ e^2}{mc^2} \quad \frac{N f \lambda}{b_\lambda}$

since, $\tau_o = \frac{\sqrt{\pi}\ e^2}{mc^2} \quad N \quad \frac{f \lambda^2}{b_\lambda}$

So for any value of b_λ we can plot a graph of W_λ / λ against $Nf\lambda$. For such a plot, theory predicts that different spectral lines should lie on the same curve. This gives a theoretical curve which we can use to calculate N from actual observations of W_λ. When the absorption lines in the spectrum of a star are observed we know λ, and f the oscillator strength of the transition, and can measure W_λ. An empirical curve of growth is plotted of Log W_λ / λ against Log $f\lambda$. A comparison of the two curves then determines N. This is done by relating the horizontal scales to give the best fit of the theoretical curve to the empirical points. Several examples of curves of growth are given in figures 19, 20 and 21. Figures 19 and 20 show points for different atoms and molecules fitted

to the theoretical curve. Figure 21 is similar but in this case all the points are molecular hydrogen, in different rotational states.

Figure 19

STRÖMGREN CURVES OF GROWTH for THREE STARS in the PERSEUS 2 CLOUD

(From Chaffee 1974)

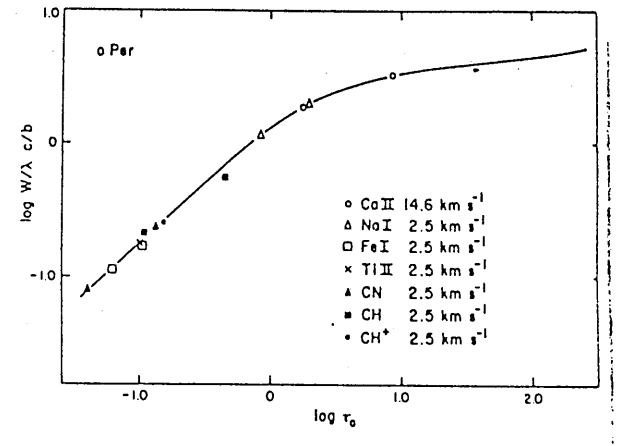

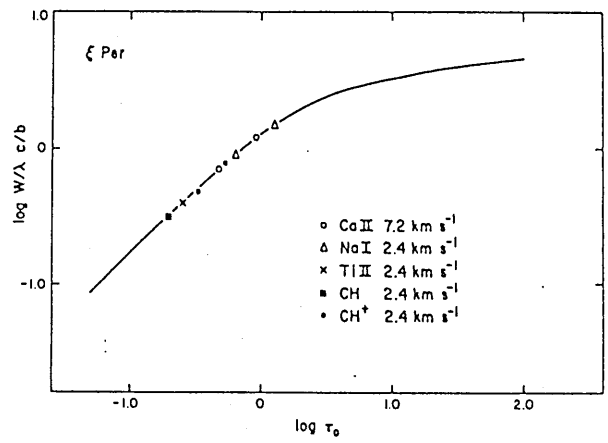

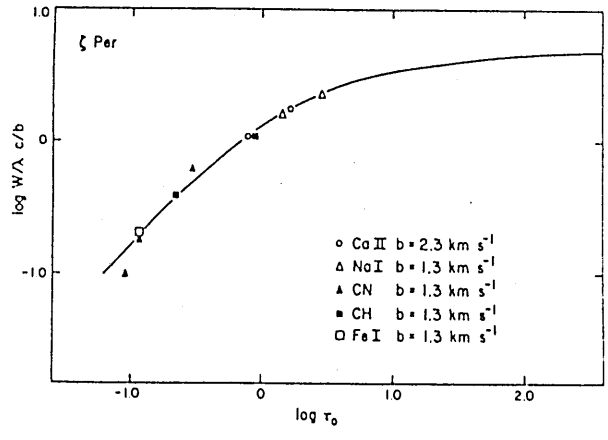

Figure 20

CURVES OF GROWTH for ABSORPTION LINES in the DIRECTION of ZETA OPHIUCHI and AE AURIGAE

(From Herbig 1968 and McLachlan and Nandy 1984)

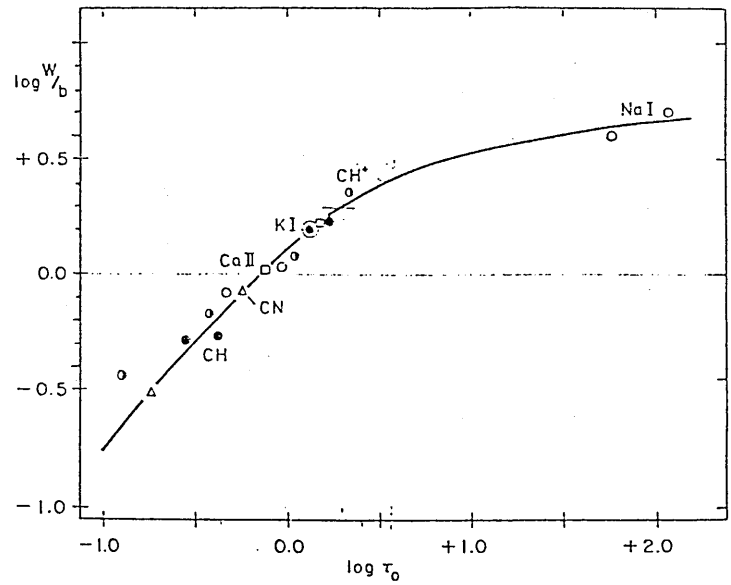

The solid line is the theoretical interstellar curve of growth for zero damping calculated by STRÖMGREN (1948). W is the equivalent width, b is the appropriate Doppler width, and τ_0 is the optical depth at the line center. The points represent individual lines in the −15 km/sec interstellar spectrum at ζ Ophiuchi, fitted to the curve

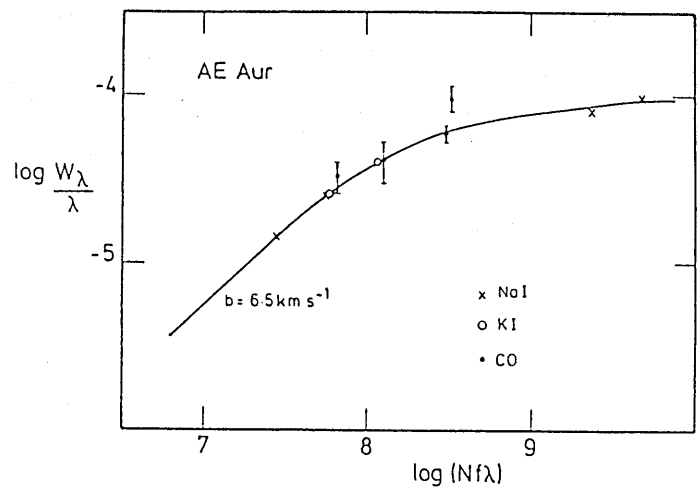

Empirical curve of growth for NaI, KI and CO in the direction of AE Aur.

Figure 21

CURVES OF GROWTH for MOLECULAR HYDROGEN TOWARD FOUR STARS

(From Spitzer, Cochran, and Hirshfeld 1974)

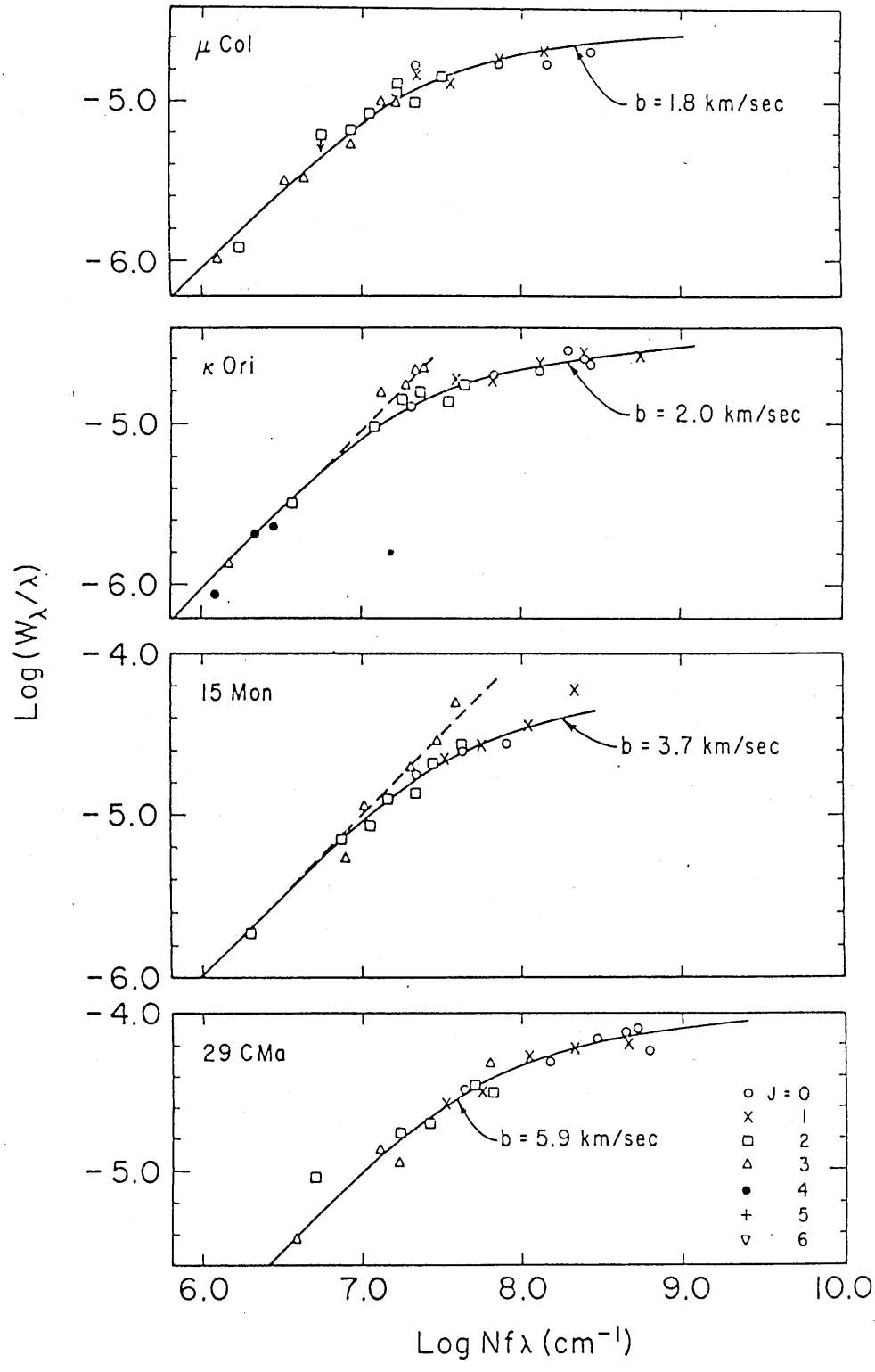

3. INTERSTELLAR CHEMISTRY

3. INTERSTELLAR CHEMISTRY

Interstellar chemistry is very different from the chemistry observed in terrestrial laboratories. Interstellar space is characterised by extremely low densities and consequently large deviations from thermodynamic equilibrium, a mixture of the elements in the ratio of their cosmic abundances, in many regions a relatively high ultraviolet flux and temperatures between 5 and 200K. Interstellar molecules have very short lifetimes in the interstellar radiation field and so cannot travel far from their place of origin before being destroyed unless protected. Hence molecules are formed in the regions in which they are observed. For diffuse regions such as the cloud in front of ζ Oph, times between collisions of hydrogen atoms with each other are 10^8 seconds. For hydrogen collisions with other species this becomes much greater. For the denser clouds these times become much shorter. Small energy barriers can seriously inhibit reactions if the temperature is sufficiently low. Even strongly exothermic reactions may have appreciable energy barriers to reaction. The reactions important to gas phase interstellar chemistry are difficult to study experimentally since the activation energy is too small to measure. The application of terrestrial data to interstellar conditions is also hampered by the non equilibrium conditions of interstellar molecules. The usual treatment of reaction rates assumes thermodynamic equilibrium and a Boltzmann energy distribution for each degree of freedom associated with the molecule.

Molecules form readily in the high density circumstellar shells immediately associated with newly formed stars or in the cool outer envelopes of evolved red giant stars. New stars could supply molecules to some nearby clouds but red giants are not

found near interstellar clouds or molecular sources and so cannot contribute significantly. Solid grains also form readily in circumstellar shells and are stable in interstellar space. Evaporation from grains when they approach hot stars could be a possible source of molecules. However it is more likely that the major formation processes take place within the interstellar clouds themselves.

Two types of process have been considered. The formation of molecules on grain surfaces and the formation of molecules by reactions between free atoms, molecules and ions in the interstellar gas. Both types are important and both must be invoked to explain the observations. For the diffuse clouds in which molecules are observed optically gas phase ion molecule reactions are by far the most important process in explaining interstellar molecular abundances.

3.1. TESTS OF CHEMICAL MODELS

Mumma and Donn 1973 (289) have suggested an ingenious method of determining the importance of a particular chemical reaction. This relies on the molecule being in an excited state after the reaction. The particular state depends on the nature of the reaction and is detected by the infrared emission emitted as the molecule returns to its ground state by cascading. Unfortunately this emission is too weak to be detected by present day equipment and we must still rely on measurements of chemical abundances.

In the diffuse clouds it appears that most species, except H_2, are formed through gas phase sequences initiated by cosmic ray or ultraviolet ionisation followed by charge exchange and ion molecule reactions. Evidence that favours this picture comes in two forms.

1. Recent detections are at about the predicted level of species expected to be abundant under this hypothesis. This includes OH, C_2 and CH.

2. Failure to detect species expected to be produced efficiently by grain surface reactions, but not by gas phase reactions. This includes NH and NaH.

Important tests which have been attempted include searches for N_2, HCl, and H_2O, all three of which are predicted to have substantial abundances in diffuse clouds if gas phase reactions dominate. The search for N_2 is hampered by the fact that the most favourable lines are below 1000 Å, where it has been feasible to observe only stars of low reddening. In the case of HCl, the current upper limit (Wright and Morton 1979 (194)) is well below the predicted level. The molecule H_2O has only been marginally seen yielding a column density larger than that predicted by current theories.

Recent work by Mann and Williams 1984 (267) has shown that uncertainties in the observations of CH and CN are currently so great that model chemistries with and without a contribution from reactions on the surface of grains provide a satisfactory fit to the observations. CO and OH appear not to be useful indicators of the chemical activity of grains in diffuse clouds, whereas a positive detection of NH at a column density of $1 \times 10^{11} cm^{-2}$ would very strongly imply grain surface catalysis of at least some simple molecules. At present gas phase ion molecule reactions are the favoured mechanism for the majority of small interstellar molecules.

3.2. GAS PHASE REACTIONS

3.2.1. ION MOLECULE REACTIONS

The low temperatures and low density encountered in the interstellar medium restrict the possible gas phase chemical reactions to binary collisions between species in their ground electronic and vibrational energy states. The time between reactive collisions is so long as to permit most ordinarily forbidden radiative emission processes to occur. Reactions must also be exothermic. The rate constant k for a bimolecular reaction is given by

$$k = Ae^{-Ea/KT} \qquad (3.1)$$

where A = Constant.

Ea = Activation energy.

K = Boltzmann Constant = R/N

N = Avogadro's Number

R = Gas Constant

T = Absolute Temperature

The activation energy is the minimum energy barrier that must be overcome to form products. The rate constant k is a product of the reaction cross section σ and the velocity v averaged over a Maxwellian distribution. Therefore

$$k = \sigma . v . \qquad (3.2)$$

In the interstellar medium most reactions between neutral species, even if they are exothermic, require an activation energy much greater than KT. Exceptions are reactions between atoms and reactive molecules. Exothermic ion molecule reactions of the type,

$$A^+ + B \longrightarrow C^+ + D \qquad (1)$$

dominate interstellar chemistry as they hardly ever require activation energy. These reactionspossess rate constants often totally independent of temperature. Of the possible two body processes only radiative association is effective if both A and B are neutral or both positively ionised atoms or molecules.

$$A + B \longrightarrow AB + h\nu \qquad (2)$$

Radiative association tends to be slow. When the two atoms collide the probability that a molecule will be formed is quite low. The atoms enter the collision with a total energy that is positive and will simply dissociate unless the energy is lost. Emission of the energy as radiation during the collision is important in astrophysical conditions but rarely seen in the laboratory. The photon emitted comes from an electronic dipole transition between two electronic energy states. An important radiative association reaction is

$$C^+ + H_2 \longrightarrow CH_2^+ + h\nu \qquad (3)$$

which initiates the formation of CH and CH^+ (See Barlow 1984 (236) for some new results on radiative association reaction rates).

Dissociative electron recombination reactions of the type,

$$AB^+ + e^- \longrightarrow AB^* \longrightarrow A + B \qquad (4)$$

also play a key role in the chemistry of molecular ions as they compete with chemical reactions and result in the removal of ions to form neutral species.

Dissociative recombination involves capture of an electron to form the neutral molecule in an excited

electronic state that can dissociate. In most cases this takes place immediately forming two atomic species. Recombination can also occur with the emission of a photon. This is called radiative recombination.

$$AB^+ + e^- \longrightarrow AB + h\nu \qquad (5)$$

This is much slower than dissociative recombination. Radiative attachment to form a negative ion is possible.

$$A + e^- \longrightarrow A^- + h\nu \qquad (6)$$

This is followed by associative detachment to form a molecule.

$$A^- + B \longrightarrow AB + e^- \qquad (7)$$

Dalgarno and McCray 1973 (206) point out that this sequence is unlikely to be important under astrophysical conditions though.

Charge transfer between atoms and molecules can also occur,

$$A^+ + B \longrightarrow B^+ + A \qquad (8)$$

Reaction between O and H^+ is the initial step in producing OH and H_2O.

Chemical exchange is another possibility where A and BC represent atoms or radicals that can be neutral or ionised.

$$A + BC \longrightarrow AB + C \qquad (9)$$

This reaction depletes certain neutral species. Reaction between neutral species is usually inhibited at low temperature by the existence of a repulsive barrier. If one of the reactants is charged there occurs a long range polarisation attraction which enhances the collision frequency and which suppresses the barrier.

Thus charge exchange and ion molecule reaction rates are much faster

$$AB^+ + C \longrightarrow AC^+ + B \qquad (10)$$

Hydrogen abstraction or transfer reactions are important in interstellar chemistry because of the abundance of hydrogen.

$$HnA^+ + H_2 \longrightarrow H\,n+1\,A^+ + H \qquad (11)$$

Abstraction reactions determine the history of positive ions, the reaction sequence terminating when the reaction becomes endothermic. The complex ion $Hn+1\,A^+$ is usually removed by dissociative recombination.

$$Hn+1\;A^+ + e^- \longrightarrow Hn\,A + H \qquad (12)$$

$$\longrightarrow Hn-1\;A + H_2 \qquad (13)$$

Molecules can also be destroyed by photodissociation. This however is a highly specific process. The chief contribution to the photodissociation of H_2 arises from excitations to the $^1\Sigma_u$ state followed by radiative decay into a state in the vibrational continuum of the $^1\Sigma_g$ ground state

$$AB + h\nu \longrightarrow A + B \qquad (14)$$

Photo ionisation can also occur.

$$AB + h\nu \longrightarrow AB^+ + e^- \qquad (15)$$

Molecules with ionisation potentials less than that of atomic hydrogen are photo-ionised in times of the order of hundreds of years. Molecular lifetimes increase with depth from the edge of an interstellar cloud.

Typical rate coefficients are given in table 21. These are taken from Mitchell Ginsburg and Kuntz 1978 (215), whilst more recent work by Viggiano et al 1980 (300) gives the rate coefficient for all possible product channels for several reactions. Examples are given in table 22.

TABLE 21

REACTION RATE COEFFICIENTS (1)

REACTION	TYPE	RATE ($cm^3 sec^{-1}$) COEFFICIENT
$C^+ + H_2 \longrightarrow CH_2^+ + h\nu$	Radiative Association	1.0×10^{-15}
$CH^+ + e^- \longrightarrow C + H$	Dissociative Recombination	1.0×10^{-7}
$CH_3^+ + e^- \longrightarrow CH_3 + h\nu$	Radiative Recombination	3.0×10^{-10}
$CH + O \longrightarrow CO + H$	Neutral Neutral	4.0×10^{-11}
$CO^+ + H \longrightarrow CO + H^+$	Charge Transfer	1.0×10^{-9}
$CH^+ + H_2 \longrightarrow CH_2^+ + H$	Hydrogen Abstraction	1.0×10^{-9}
$CH + h\nu \longrightarrow C + H$	Photodissociation	$\alpha = 1.4 \times 10^{-10}$ *
$CH + h\nu \longrightarrow CH^+ + e^-$	Photoionisation	$\alpha = 2.89 \times 10^{-10}$ *
$H_2 + p \longrightarrow H_2^+ + e^- + p$	Cosmic Ray Ionisation	2.3×10^{-17}

* The rate of these photodestruction processes has the form $k = a \exp(-b A_V) sec^{-1}$ where a is the rate coefficient in the unattenuated radiation field and A_V is the visual absorption in magnitudes. b is a constant taken from Black & Dalgarno 1977 (78)

TABLE 22

REACTION RATE COEFFICIENTS (2)

REACTION	RATE COEFFICIENT ($cm^3 sec^{-1}$)
1. $CH^+ + N \longrightarrow CN^+ + H$ $\longrightarrow H^+ + CN$	1.9×10^{-10}
2. $C_2^+ + N \longrightarrow C^+ + CN$	$< 4 \times 10^{-11}$
3. $CH^+ + O \longrightarrow CO^+ + H$ $\longrightarrow H^+ + CO$	3.5×10^{-10}
4. $C_2^+ + O \longrightarrow C^+ + CO$ $\longrightarrow CO^+ + C$	3.1×10^{-10}

3.2.2. PHOTOCHEMISTRY

Lifetimes of interstellar molecules are affected to a great extent by the radiation field that pervades the interstellar medium. The lifetime against photodestruction depends on 3 factors

1) The absorption cross section

2) The quantum yield or probability of dissociation

3) The interstellar radiation field

Lifetimes are orders of magnitude longer in clouds where there is high obscuration of interstellar radiation. In clear interstellar regions most molecules have lifetimes against photodissociation of the order of 100 years or less. Thus polyatomic molecules cannot exist in the diffuse clouds. Furthermore as they can only exist in dense clouds they can never have been exposed to the unobscured radiation from the time of their formation until protected by the dense clouds. They can only have been formed in the dense clouds, which imposes a restriction on possible mechanisms of formation. Polyatomic molecules are formed in the clouds where they now occur.

Diatomic molecules are more resistant to the interstellar radiation field, and can exist in larger less dense clouds.

In addition to photodissociation, molecules can also be destroyed by photoionisation, although the process is less important due to attenuation of short wavelength radiation in clouds, and interaction with X-rays and energetic particles.

Many general reviews on interstellar chemistry have been published. Notably Dalgarno and Black 1976 (18), Watson 1976 (201), Watson 1978 (197) Herbst and Klemperer 1976 (205) and Duley and Williams 1984 (351)

3.3 INTERSTELLAR MOLECULES

3.3.1. HYDROGEN AND DEUTERIUM CHEMISTRY

The formation of molecular hydrogen in interstellar clouds was discussed as long ago as 1960 by McCrea and McNally 1960 (156). They examined the possiblity of H_2 formation by surface reactions on interstellar dust grains, and indeed H_2 is one of the few interstellar molecules for which such chemical reactions are important, since radiative association of atomic hydrogen to form H_2 is strongly forbidden.

$$H + H \not\longrightarrow H_2 + h\nu \qquad (16)$$

Formation of molecular hydrogen on dust grains has been reviewed more recently by Barlow and Silk 1976 (160). They concluded that hydrogen atoms will be chemisorbed onto interstellar graphite grains with H_2 formation proceeding efficiently for grain temperatures less than 70K.

Grains are argued to be the principal sites for H_2 formation and that hydrogen recombination on grains to form H_2 provides the largest heat source in diffuse clouds if the albedo of interstellar dust in the 912Å - 1200Å region is high.

In general it is supposed that on striking the surface of an interstellar grain a hydrogen atom is physically absorbed through the Van der Waals interaction or chemisorbed and remains on the surface long enough to collide with another hydrogen atom and form a stable molecule. The hydrogen atoms move about on the grain by quantum mechanical tunnelling and tend to congregate preferentially at defects in the lattice which form sites of enhanced binding. Hydrogen has a very low absorption

energy which ensures that the release of the binding energy of a newly formed hydrogen molecule is adequate to liberate it from the grain surface. The grain temperature should be $<$ 20K to ensure that the hydrogen atoms reside on the surface long enough to react with one another. The large amount of molecular hydrogen observed in diffuse clouds confirms that the process of surface recombination is extremely efficient and is orders of magnitude more so for hydrogen than any other grain surface process in producing gaseous molecules.

$$H + H + \text{Grain} \longrightarrow H_2 + \text{Grain} \qquad (17)$$

Associative detachment of H^- is also possible, although not as efficient as grain catalysis.

$$H^- + H \longrightarrow H_2 + e^- \qquad (18)$$

The negative ion H^- is formed by radiative attachment.

$$H + e^- \longrightarrow H^- + h\nu \qquad (19)$$

Competing reactions that destroy H^- are

$$H^- + C^+ \longrightarrow H + C$$

and

$$H^- + H^+ \longrightarrow H + H \qquad (21)$$

So is photodetachment by starlight

$$H^- + h\nu \longrightarrow H + e^- \qquad (22)$$

Another possible sequence is

$$H + H^+ \longrightarrow H_2^+ + h\nu \qquad (23)$$

$$H_2^+ + H \longrightarrow H_2 + H^+ \qquad (24)$$

although it is unimportant at low temperatures.

The amount of H_2 in interstellar clouds is governed by the balance between the various formation and destruction mechanisms. The threshold for direct photodissociation of H_2 in the ground state corresponds to photons with a wavelength less than 845Å. These are normally excluded

by dust and are confined to the regions around hot stars from which they originate. H_2 in vibrationally excited states can be dissociated by photons with a wavelength longer than the Lyman limit at 912Å (Radiation with a wavelength less than 912Å is absorbed by hydrogen atoms). There are few such molecules however for this to be important.

In regions that are not opaque to ultraviolet photons of wavelengths between 912Å and 1108Å the dominant destruction process is the absorption of a photon followed by spontaneous radiative emission, resulting in two separate hydrogen atoms.

$$H_2 + h\nu \longrightarrow H_2^* \longrightarrow H + H + h\nu' \qquad (25)$$

Direct radiative dissociation is unlikely since the only dissociative transition stimulated by radiation longward of 912Å is $X^1\Sigma g^+ - b^3\Sigma u^+$ which is forbidden by the change in spin multiplicity. Radiative dissociation proceeds in two steps, a transition from the ground state to the $B^1\Sigma u^+$ or $C^1\Pi u$ states followed by a spontaneous decay to the vibrational continuum of the ground electronic state.

Photodissociation is here caused by line rather than continuum radiation. The consequence of this process is that after penetrating a certain H_2 column density the radiation field becomes too weak at the required frequencies to support H_2 line photodissociation. H_2 is then said to be self shielded. Thus cloud interiors are molecular while the surface is mostly composed of atomic hydrogen.

H_2 may be destroyed by X-ray photo ionisation, and dissociative photoionisation

$$H_2 + h\nu \longrightarrow H_2^+ + e^- \quad (26)$$

$$H_2 + h\nu \longrightarrow H + H^+ + e^- \quad (27)$$

(See Kirchner 1984 (237) for details of the H_2^+ spectrum and Shuter 1986 (521) who attempted to detect H_2^+ using radio techniques).

Cosmic rays (principally protons) are also effective in destroying H_2.

$$H_2 + P \longrightarrow H_2^+ + e^- + P \quad (28)$$

$$H_2 + P \longrightarrow H + H^+ + e^- + P \quad (29)$$

The presence of deuterated hydrogen HD in space was established by Spitzer et al 1973 (87). In sharp contrast to H_2, HD is produced by gas phase reactions. Watson 1973 (88) has argued that the ion molecule reaction

$$D^+ + H_2 \longrightarrow HD + H^+ \quad (30)$$

is an important source of HD (see also Smith, Adams & Alge 1982 (355)). The ionisation of deuterium is caused by direct ionisation or by charge exchange with H^+ formed by cosmic ray ionisation of atomic hydrogen.

$$D + H^+ \longrightarrow D^+ + H \quad (31)$$

Ionised deuterium is lost mainly by the reverse reaction

$$D^+ + H \longrightarrow H^+ + D \quad (32)$$

and by

$$D^+ + H_2 \longrightarrow HD + H^+ \quad (33)$$

$$D^+ + e^- \longrightarrow D + h\nu \quad (34)$$

$$D^+ + O \longrightarrow D + O^+ \quad (35)$$

The HD molecule is removed by

$$HD + H^+ \longrightarrow D^+ + H_2 \qquad (36)$$

and

$$HD + h\nu \longrightarrow HD^* \rightarrow H + D + h\nu' \qquad (37)$$

The rate of dissociation in diffuse clouds will exceed the rate for H_2 because deuterium is less abundant. Thus HD is destroyed more rapidly than H_2. Conversly a deuterium atom collides with an H_2 molecule in the gas much more frequently than it hits a dust grain. Replacement of H with D is energetically favourable because of the higher mass of D. The direct reaction,

$$H_2 + D \longrightarrow H + HD \qquad (38)$$

has a large activation energy which probably causes it to be negligible. However, the reaction

$$H_2 + D^+ \longrightarrow H^+ + HD \qquad (39)$$

is exothermic and will occur at rapid rates even at low temperatures. Hence HD is also formed rapidly in diffuse clouds.

Protons H^+, result from the direct ionisation of atomic and molecular hydrogen by cosmic rays and penetrating X-rays. They initiate many ion molecule reactions, and are indicative of a universal X-ray and cosmic ray flux. Other minor sources of protons are the chemical reactions,

$$C^+ + OH \longrightarrow CO + H^+ \qquad (40)$$

$$CH^+ + O \longrightarrow CO + H^+ \qquad (41)$$

$$He^+ + H_2 \longrightarrow He + H^+ + H \qquad (42)$$

They are removed by radiative recombination

$$H^+ + e^- \longrightarrow H + h\nu \qquad (43)$$

and by charge transfer reactions with molecular species.

$$H^+ + OH \longrightarrow OH^+ + H \quad (44)$$

$$H^+ + O_2 \longrightarrow O_2^+ + H \quad (45)$$

$$H^+ + H_2O \longrightarrow H_2O^+ + H \quad (46)$$

$$H^+ + NH_3 \longrightarrow NH_3^+ + H \quad (47)$$

$$H^+ + H_2CO \longrightarrow H_2CO^+ + H \quad (48)$$

$$H^+ + HCl \longrightarrow HCI^+ + H \quad (49)$$

Also reaction with atomic oxygen,

$$H^+ + O \longrightarrow H + O^+ \quad (50)$$

Ionised atomic hydrogen only occurs as an appreciable fraction in clouds close to hot stars. The boundary between HII and HI regions where atomic hydrogen predominates is sharp. Outside of the HII region there is little radiation of wavelength less than 912Å to support ionisation of HI.

3.3.2. CARBON CHEMISTRY

Carbon is an important constituent of interstellar space. Its cosmic abundance is comparable to that of nitrogen and oxygen, with hydrogen and helium the only elements whose abundance is significantly larger. In atomic hydrogen regions of moderate density ultraviolet starlight causes most gas phase carbon to be singly ionised. In fact, carbon provides most of the free electrons in these regions since it is the most abundant element with an ionisation potential below the Lyman limit. Carbon ions also provide a cooling mechanism for low temperature HI regions. Unfortunately C^+ is difficult to detect as its resonance lines at 1036Å and 1335Å are usually saturated. Measurements of CI are relatively easy though since its strongest lines are only mildly saturated. Surveys of carbon in the interstellar gas have been made by Jenkins and Shaya 1979 (301) and Jenkins, Jura and Loewenstein

1983 (302).

The principal initiating reactions in the synthesis of molecules with the general formulae CHn and C_2Hn appear to be,

$$C^+ + H_2 \longrightarrow CH_2^+ + h\nu \quad \text{(Figure 22a)} \qquad (51)$$

and

$$H_3^+ + C \longrightarrow CH^+ + H_2 \qquad (52)$$

The reactive oxygen atom also plays an important role in determining the concentration of CH, CH_2, CH_3 and CH_3^+.

The reactions of C^+ ions with CH_n molecules initiate C - C bond formation and the synthesis of C_2Hn and C_2Hn^+ molecules. Further reactions of C_2 Hn with C^+ and CH_3^+ and reactions of C_2 Hn^+ with C leads to species containing three carbon atoms.

1. CH and CH^+

The first attempt to explain the abundance of CH indicated by Adams' surveys was made by Bates and Spitzer 1951 (38). They examined the formation of CH by radiative association

$$C + H \longrightarrow CH + h\nu \qquad (53)$$

However because the carbon in diffuse clouds is mostly in the form of C^+ this reaction is not likely to be a large source of interstellar CH.

In a modified version (Solomon & Klemperer 1972 (65)) ionised carbon reacts with atomic hydrogen to form CH^+ by radiative association.

$$C^+ + H \longrightarrow CH^+ + h\nu \qquad (54)$$

This reaction is faster than the reaction involving only neutral atoms and could form the initial step in the formation of several interstellar species, for example CN and CO as well as CH. CH is formed by radiative

recombination.

$$CH^+ + e^- \longrightarrow CH + h\nu \qquad (55)$$

The CH^+ ion may also undergo dissociative recombination

$$CH^+ + e^- \longrightarrow C + H \qquad (56)$$

or reaction with other atoms,

$$CH^+ + O \longrightarrow CO + H^+ \qquad (57)$$

$$CH^+ + H \longrightarrow C^+ + H_2 \qquad (58)$$

CH is destroyed by photodissociation and photoionisation.

$$CH + h\nu \longrightarrow C + H \qquad (59)$$

$$CH + h\nu \longrightarrow CH^+ + e^- \qquad (60)$$

and by atomic reactions such as,

$$CH + H \longrightarrow C + H_2 \qquad (61)$$

$$CH + O \longrightarrow CO + H \qquad (62)$$

The conversion of CH into CO may occur more readily by the sequence of associative ionisation.

$$O + CH \longrightarrow HCO^+ + e^- \qquad (63)$$

Followed by dissociative recombination

$$HCO^+ + e^- \longrightarrow CO + H \qquad (64)$$

Other atomic reactions are,

$$CH + N \longrightarrow CN + H \qquad (65)$$

$$CH + C^+ \longrightarrow C_2^+ + H \qquad (66)$$

The reaction with C^+ to give CH^+

$$CH + C^+ \longrightarrow CH^+ + C \qquad (67)$$

is exothermic. If its rate coefficient is comparable to that of its competing channel it will be an effective means of transforming CH into CH^+.

A further atomic reaction is,

$$CH + C \longrightarrow C_2 + H \qquad (68)$$

Black and Dalgarno 1973 (29) have proposed a modification to the radiative association of C^+ and H, based on the assumption that the interstellar clouds in which CH has been detected contain significant amounts of H_2. CH is produced by the sequence

$$C^+ + H_2 \longrightarrow CH_2^+ + h\nu \quad \text{(see figure 22a)} \qquad (69)$$

$$CH_2^+ + e^- \longrightarrow CH + H \qquad (70)$$

A competing reaction is

$$C^+ + H_2^* \longrightarrow CH + H^+, \text{ where } H_2^* \text{ is vibrationally excited hydrogen.} \qquad (71)$$

Another source of CH_2^+ is,

$$CH^+ + H_2 \longrightarrow CH_2^+ + H \qquad (72)$$

This is complicated by the reactions,

$$CH_2^+ + H_2 \longrightarrow CH_3^+ + H \qquad (73)$$

$$CH_3^+ + e^- \longrightarrow CH_2 + H \qquad (74)$$

or

$$CH_3^+ + e^- \longrightarrow CH + H_2 \qquad (75)$$

Minor reactions with atoms like O also take place. The reaction of CH_3^+ with H_2 is endothermic causing the sequence to terminate at CH_3^+. Whether or not dissociative recombination reactions occur more rapidly than hydrogen abstraction depends on the fractional ionisation $\frac{n(e)}{n(H_2)}$ and on the relative efficiencies of the reactions. In diffuse clouds dissociative recombination is more efficient and the sequence will often terminate with the reaction

$$CH_2^+ + e^- \longrightarrow CH + H \qquad (76)$$

The CH_2 molecule will also undergo photodissociation

$$CH_2 + h\nu \longrightarrow CH + H \qquad (77)$$

and photoionisation

$$CH_2 + h\nu \longrightarrow CH_2^+ + e^- \qquad (78)$$

CH_3 is formed in dense clouds by

$$CH_2 + H_2 \longrightarrow CH_3 + H \qquad (79)$$

Which can be dissociated to give CH or CH_2

$$CH_3 + h\nu \longrightarrow CH_2 + H \qquad (80)$$

or

$$CH_3 + h\nu \longrightarrow CH + H_2 \qquad (81)$$

Watson 1974 (98) has examined the two exothermic reactions,

$$CH^+ + H_2 \longrightarrow CH_2^+ + H \qquad (82)$$

$$CH_2^+ + H_2 \longrightarrow CH_3^+ + H \qquad (83)$$

from which the dissociative recombination reactions,

$$CH_2^+ + e^- \longrightarrow C + H_2 \qquad (84)$$

$$CH_2^+ + e^- \longrightarrow CH + H \qquad (85)$$

$$CH_3^+ + e^- \longrightarrow CH + H_2 \qquad (86)$$

$$CH_3^+ + e^- \longrightarrow CH_2 + H \qquad (87)$$

are possible. CH is produced from the last reaction by the photodissociation of CH_2

$$CH_2 + h\nu \longrightarrow CH + H \qquad (88)$$

In the presence of H_2 the destruction of CH is also modified. Thus for the reaction

$$CH + C^+ \longrightarrow C_2^+ + H \qquad (89)$$

$$C_2^+ + H_2 \longrightarrow C_2H^+ + H \qquad (90)$$

$$C_2H^+ + e^- \longrightarrow CH + H \qquad (91)$$

which reforms CH.

Many of the gas phase reactions involve a partially closed cycle involving CH, CH_2 and CH_3 and their ions. The abundances of the observed species thus depend on the relative efficiencies of the various reactions and upon the number of cycles completed before an exit channel is encountered that interrupts the cycle. The initiating reaction,

$$C^+ + H_2 \longrightarrow CH_2^+ + h\nu \qquad (92)$$

must have a relatively high rate coefficient if the observed quantities of CH are to be reproduced. A critical test of the gas phase chemistry of hydrocarbon radicals would be the observation of CH_2 in diffuse clouds. Snow 1975 (8) has determined an upper limit of $N(CH_2) \leqslant 4 \times 10^{13}$ cm^{-2}.

A further model first proposed by Bates and Spitzer and further discussed by Stecher and Williams 1974 (36) is the formation of CH by the evaporation of grain mantles. Mantles are unlikely to accrete on grains in the unshielded interstellar medium but surface reactions may occur on grains in clouds where the radiation density is low. Under such conditions the temperature is low and mantle growth is possible leading to depletion of the surrounding gas. If a hot star then passes through the cloud the increased temperature will result in the evaporation of the grain mantles and the release of molecular species into space. If the composition of the dirty ice that constitutes a grain mantle is in the form of methane then the result of any reaction sequence will be CH where CH^+ is then formed by photoionisation.

The chemistry of CH^+ was also examined by Bates and Spitzer and then expanded by Solomon and Klemperer, who proposed the radiative association reaction

$$C^+ + H \longrightarrow CH^+ + h\nu \qquad (93)$$

Prasad and Huntress 1980 (125) however point out that this reaction is only important when $n(H_2) \ll n(H)$. The major source of CH^+ is the reaction,

$$C^+ + CH \longrightarrow C + CH^+ \quad (94)$$

A competing reaction is

$$C^+ + CH \longrightarrow C_2^+ + H \quad (95)$$

CH^+ is destroyed by the following reactions,

$$CH^+ + O \longrightarrow CO^+ + H \quad (96)$$

$$CH^+ + O \longrightarrow CO + H^+ \quad (97)$$

$$CH^+ + N \longrightarrow CN^+ + H \quad (98)$$

$$CH^+ + N \longrightarrow CN + H^+ \quad (99)$$

$$CH^+ + H \longrightarrow C^+ + H_2 \quad (100)$$

$$CH^+ + C \longrightarrow C_2^+ + H \quad (101)$$

The last reaction is not very important as most carbon is in the form C^+. The radiative recombination,

$$CH^+ + e^- \longrightarrow CH + h\nu \quad (102)$$

is a major loss process.

Other reactions are dissociative recombination

$$CH^+ + e^- \longrightarrow C + H \quad (103)$$

and relatively inefficient photodissociation.

$$CH^+ + h\nu \longrightarrow C^+ + H \quad (104)$$

Stecher and Williams 1972 (85) 1974 (35) have examined the endothermic reaction.

$$C^+ + H_2^* \longrightarrow CH^+ + H \quad (105)$$

in which the H_2 molecule is vibrationally excited by ultraviolet pumping of the ground state. However Dalgarno and Black 1976 (18) point out that this mechanism is unlikely to contribute significantly under typical conditions because the self shielding against ultraviolet photons that allows H_2 to survive also prevents the existence of any substantial concentration of H_2^* in equilibrium. It may only be important in non equilibrium circumstances. Recent work by Frisch and Jura 1980 (96) appears to confirm this.

Their observations of H_2 and CH^+ toward four stars using the Copernicus satellite do not agree with the abundance predictions of Stecher and Williams. The results appear to indicate a correlation between CH^+ and rotationally excited H_2. They do not advance an obvious explanation for this but suggest that CH^+ may be produced behind shock fronts or that a high mean density in the ultraviolet is important for producing CH^+. For example the evaporation of grain mantles should occur preferentially in regions of high radiation fields.

CH^+ is also formed by the photoionisation of CH, a major source in diffuse clouds.

$$CH + h\nu \longrightarrow CH^+ + e^- \qquad (106)$$

and by the reactions,

$$CH_2^+ + h\nu \longrightarrow CH^+ + H \qquad (107)$$

$$CH_3^+ + h\nu \longrightarrow CH^+ + H \qquad (108)$$

The importance of the reactions

$$CH^+ + H_2 \longrightarrow CH_2^+ + H \qquad (109)$$

$$CH^+ + e^- \longrightarrow C + H \qquad (110)$$

severely limit the abundance of CH^+ even in diffuse clouds. The first reaction ultimately leads to the formation of CH.

$$CH_2^+ + H_2 \longrightarrow CH_3^+ + H \qquad (111)$$

$$CH_3^+ + e^- \longrightarrow CH + H_2 \qquad (112)$$

Alternatively,

$$CH_2^+ + e^- \longrightarrow CH + H \qquad (113)$$

or

$$CH_2^+ + H_2 \longrightarrow CH_3^+ + H \qquad (114)$$

$$CH_3^+ + e^- \longrightarrow CH_2 + H \qquad (115)$$

$$CH_2 + h\nu \longrightarrow CH + H \qquad (116)$$

This appears to indicate that CH^+ and appreciable densities of H_2 cannot co-exist in an interstellar cloud. It has been suggested that when CH, CH^+ and H_2 are observed in the same line of sight that the CH^+ is located either in the outer lower density portion of the cloud or in a separate lower density cloud.

Elitzur and Watson 1978 (115) 1980 (60) have suggested that CH^+ is formed in the hot gas produced by a shock resulting from the expansion of a HII region around a parent star. The observed high CH^+ abundances can be explained by equilibrium gas phase chemical reactions only if the rate coefficient of dissociative recombination is unexpectedly low.

The reaction $CH^+ + e^- \longrightarrow C + H$ (117)

will lead to the rapid removal of CH^+. The hydrogen abstraction

$$CH^+ + H_2 \longrightarrow CH_2^+ + H \qquad (118)$$

is also rapid in which CH^+ is removed by reaction with molecular hydrogen.

The rate coefficient problem is overcome by the non equilibrium process proposed by Elitzur and Watson. Shock waves in interstellar clouds may be common because of the tendency for bulk motions in the interstellar medium to exceed the sound speed in the neutral gas. Examples of shock forming phenomena other than the expansion of HII regions include super novae, cloud-cloud collisions, galactic density waves, stellar winds and the expansion of gas around an association of stars.

At the temperatures produced in the small hot region just behind the shock front CH^+ is produced by the

endothermic reaction

$$C^+ + H_2 \longrightarrow CH^+ + H \qquad (119)$$

proceeding with little hindrance from the energy barrier. Evidence for shocks has come from the detection of radiative transitions between vibrational states in molecular hydrogen. After the shock has passed the primary mechanism of cooling for T > 300K in the post shock gas is by the radiative emission of rotationally excited H_2 molecules. Other mechanisms are radiative emission from low lying atomic states, particularly C^+ and O, vibrationally excited H_2 and kinetic energy loss due to the dissociation of H_2. Below 300 K, H_2O is a primary coolant with CO making a modest contribution. Other evidence for shocks is that the lines of sight in which CH^+ is observed are normally toward hot O and B stars which produce HII regions that generate shocks by their expansion.

In cooler regions CH^+ is produced by the reactions

$$C^+ + CH \longrightarrow CH^+ + C \qquad (120)$$

$$HCO^+ + C \longrightarrow CH^+ + CO \qquad (121)$$

$$H_3^+ + C \longrightarrow CH^+ + H_2 \qquad (122)$$

The last reaction is the principal pathway for producing CH^+ according to Prasad and Huntress 1980 (125). Mitchell Ginsburg and Kuntz 1977 (26) 1978 (215) have used a chemical system involving carbon and hydrogen to obtain steady state abundances of a number of molecules. The calculated CH abundance agrees well with the astronomical observations, however the computed CH^+ column densities are too low by a factor of 100.

Attempts to alter the reaction rates in order to increase the computed column density of CH^+ result in the abundance of CH being increased so that it far exceeds the observed amounts. A high radiation field might be the answer in that it decreases the amount of CH at the same time as increasing the abundance of CH^+

$$CH + h\nu \longrightarrow CH^+ + e^- \quad (123)$$

$$CH_2^+ + h\nu \longrightarrow CH^+ + H \quad (124)$$

An increase in the formation rate of H_2 will also favour CH^+ as,

$$C^+ + H_2 \longrightarrow CH_2^+ + h\nu \quad (125)$$

$$CH_2^+ + e^- \longrightarrow CH + H \quad (126)$$

$$CH + h\nu \longrightarrow CH^+ + e^- \quad (127)$$

and $$CH_2^+ + h\nu \longrightarrow CH^+ + H \quad (128)$$

However the results of Mitchell et al indicate that the radiation field has little effect on the abundance of CH^+. The shock theory appears to be the best at present for explaining the abundance of CH^+.

In the rest of Mitchell et al scheme it is assumed that H_2 is formed by surface catalysis on interstellar grains since no other process seems capable of explaining the large amount of H_2 observed by the Copernicus satellite. 55 reactions involving 18 species are used, including ion-neutral, neutral neutral and ion electron recombination reactions, cosmic ray and ultraviolet initiated ionisation and dissociation. This is later extended in the 1978 paper to 100 species and 455 reactions over a larger density range.

The radiative association reaction

$$C^+ + H_2 \longrightarrow CH_2^+ + h\nu \text{ (Figure 22a)} \quad (129)$$

plays an important part in the scheme.

This leads to CH and CH^+ through the reactions,

$$CH_2^+ + e^- \longrightarrow CH + H \qquad (130)$$

$$CH + h\nu \longrightarrow CH^+ + e^- \qquad (131)$$

At higher densities the bulk of carbon present will be in the form of CO, the reaction

$$CO + H^+ \longrightarrow C^+ + O + H \qquad (132)$$

sustaining a supply of the ion C^+, the dominant form of atomic carbon in interstellar space. The increase in the formation of neutral species such as C_2, CH, C_2H and CH_2 toward higher densities is somewhat suppressed by the formation of CO.

An interesting model to explain the abundance of CH^+ towards the Pleiades Cluster has been proposed by White 1984 (331). In this theory photoelectron emission from dust grains in the intense ultraviolet radiation field near the cluster stars provides the heating required for the endothermic reaction of C^+ with H_2. Two variations of the scheme are presented, the first in which the dust and gas remain well mixed, and the second in which radiation pressure separates the gas and dust. White notes that this model relies on the particular circumstances that occur in the Pleiades Cluster and that for the majority of lines of sight Elitzur and Watson correctly identify shocks as the heating agent necessary for CH^+ formation.

2. CO, CN and C_2

The dominant processes for diatomic molecules containing two heavy atoms, such as CO, CN and C_2, are probably gas phase reactions of the hydrides, CH, OH with atoms. For example exchange reactions of the form

$$AH + B \longrightarrow AB + H \qquad (133)$$

Either reactants or products may be ionised. For example the OH radical leads to CO via reactions with C^+

$$OH + C^+ \longrightarrow CO + H^+ \qquad (134)$$

To CO_2 via reaction with CO and to O_2 via reaction with O

In diffuse clouds CO is formed by the reactions

$$CO^+ + H \longrightarrow CO + H^+ \qquad (135)$$

$$HCO^+ + e^- \longrightarrow CO + H \qquad (136)$$

$$CH_2 + O \longrightarrow CO + H_2 \qquad (137)$$

and $$CH_2 + O \longrightarrow HCO + H \qquad (138)$$

$$HCO + h\nu \longrightarrow CO + H \qquad (139)$$

The CO^+ ion is formed by

$$C^+ + OH \longrightarrow CO^+ + H \qquad (140)$$

$$CH^+ + O \longrightarrow CO^+ + H \qquad (141)$$

The HCO^+ ion is formed by

$$CH + O \longrightarrow HCO^+ + e^- \qquad (142)$$

$$CH_3^+ + O \longrightarrow HCO^+ + H_2 \qquad (143)$$

$$CO^+ + H_2 \longrightarrow HCO^+ + H \qquad (144)$$

$$C^+ + H_2O \longrightarrow HCO^+ + O \qquad (145)$$

$$CH_2^+ + O \longrightarrow HCO^+ + H \qquad (146)$$

$$C + H_3O^+ \longrightarrow HCO^+ + H_2 \qquad (147)$$

The amount of HCO^+ is limited by dissociative recombination,

$$HCO^+ + e^- \longrightarrow CO + H \qquad (148)$$

CO is also formed by

$$CH^+ + O \longrightarrow CO + H^+ \quad (149)$$

$$CH + O \longrightarrow CO + H \quad (150)$$

$$C_2^+ + O \longrightarrow CO + C^+ \quad (151)$$

$$CN + O \longrightarrow CO + N \quad (152)$$

$$NO + C \longrightarrow CO + N \quad (153)$$

$$C_2 + O \longrightarrow CO + C \quad (154)$$

$$C_2H + O \longrightarrow CO + CH \quad (155)$$

Exchange collisions of hydrides with heavy atoms such as the first two reactions in this series are energetically favourable.

CO is also formed by the photodissociation of formaldehyde.

$$H_2CO + h\nu \longrightarrow CO + H_2 \quad (156)$$

$$H_2CO + h\nu \longrightarrow CO + H + H \quad (157)$$

CO is destroyed by photodissociation

$$CO + h\nu \longrightarrow C + O \quad (158)$$

and by reaction with He^+.

$$CO + He^+ \longrightarrow C^+ + O + He \quad (159)$$

The high observed abundance of CO is understood in terms of the abundances of the reactants leading to CO, its slow dissociation rate and its insensitivity to destruction through exchange reactions.

The cyanogen radical, like carbon monoxide, is produced through exchange reactions.

$$C_2^+ + N \longrightarrow CN + C^+ \quad (160)$$

$$C_2 + N \longrightarrow CN + C \quad (161)$$

$$CH + N \longrightarrow CN + H \quad (162)$$

$$C + NH \longrightarrow CN + H \quad (163)$$

$$CH^+ + N \longrightarrow CN + H^+ \quad (164)$$

$$C^+ + NH \longrightarrow CN + H^+ \quad (165)$$

by dissociative recombination

$$H_2CN^+ + e^- \longrightarrow CN + H_2 \quad (166)$$

$$HCN^+ + e^- \longrightarrow CN + H \quad (167)$$

$$C_2N^+ + e^- \longrightarrow CN + C \quad (168)$$

and by photodissociation

$$HCN + h\nu \longrightarrow CN + H \quad (169)$$

Federman et al 1984 (283) have examined the chemistry of CN. Initiating channels include the ion molecule reactions,

$$C^+ + NH \longrightarrow CN^+ + H \quad (170)$$

$$CH^+ + N \longrightarrow CN^+ + H \quad (171)$$

CN^+ then proceeds via hydrogen abstraction to CN.

$$CN^+ + H_2 \longrightarrow HCN^+ + H \quad (172)$$

$$HCN^+ + H_2 \longrightarrow H_2CN^+ + H \quad (173)$$

Electron dissociative recombination of HCN^+ and H_2CN^+ leads to CN.

$$HCN^+ + e^- \longrightarrow CN + H \quad (174)$$

$$H_2CN^+ + e^- \longrightarrow CN + H_2 \quad (175)$$

Since the branching ratios for the neutral products are generally not known each dissociative branch is assumed to have equal probability. A major problem in the ion molecule scheme is that at a kinetic temperature of $< 70K$ very little NH or CH^+ forms in a diffuse cloud. The formation of NH is inhibited by the small amount of ionised nitrogen present in neutral diffuse clouds.
In the gas phase NH is produced by hydrogen abstraction reactions such as

$$N^+ + H_2 \longrightarrow NH^+ + H \quad (176)$$

and electron dissociative recombination of

$$NH_2^+ + e^- \longrightarrow NH + H \quad (177)$$

and $NH_3^+ + e^- \longrightarrow NH + H_2$ (178)

The production of NH in the gas phase is thus limited by the amount of N^+ present. Production of CH^+ is low because of the endothermic nature of the reaction

$$C^+ + H_2 \longrightarrow CH^+ + H \quad (179)$$

Rate constants for the ion molecule reactions participating in the production of CN are known to be small (Viggiano 1980 (300)). The production of CN through solely neutral-neutral reactions would be ten times faster than through ion molecule reactions alone (like the one giving CH^+). The observed abundance of CH^+ though exceeds that predicted, an explanation for which is that the CH^+ is thought to reside in hot shocked gas. However the high CH^+ abundance does not lead to higher abundances of CN. The CH^+ ion often lies at a different radial velocity to the other diatomic molecules CH, CO and CN. A low density of CN in a shocked gas is expected because

1. The shock is optically thin and photodissociation is a major destruction mechanism for CN.
2. The shocked gas is low density anyway.
3. Molecular hydrogen with which CN is correlated is a minor constituent.

Federman 1984 (283) estimate that < 10% of the total interstellar CN is formed in the shocked gas.
The efficiency of the ion molecule scheme is enhanced if NH is formed by reactions on the surface of grains. However few observations of NH exist to clarify this point further. CN formation may also proceed via the neutral-neutral reactions,

$$CH + N \longrightarrow CN + H \quad (180)$$

$$C_2 + N \longrightarrow CN + C \quad (181)$$

Observational and theoretical evidence (see part 2) suggests that the second reaction is particularly important.

CN is the first carbon bearing diatomic molecule to be recognised as being formed through neutral-neutral reactions. The other molecules CH, CH^+ and CO are produced predominantly by ion molecule reaction schemes. The ion molecule reaction only scheme is thought to be relatively unimportant for CN.

The overall reaction scheme for the production of CN is,

$$C^+ + H_2 \longrightarrow CH_2^+ + h\nu \quad (182)$$

$$CH_2^+ + H \longrightarrow CH_3^+ + H \quad (183)$$

$$CH_3^+ + e^- \longrightarrow CH + H_2 \quad (184)$$

$$CH + C^+ \longrightarrow C_2^+ + H \quad (185)$$

$$C_2^+ + H_2 \longrightarrow C_2H^+ + H \quad (186)$$

$$C_2H^+ + H_2 \longrightarrow C_2H_2^+ + H \quad (187)$$

$$C_2H_2^+ + e^- \longrightarrow C_2H + H \quad (188)$$

$$C_2H + h\nu \longrightarrow C_2 + H \quad (189)$$

$$C_2 + N \longrightarrow CN + C \quad (190)$$

CN is therefore a third generation neutral molecule

$$CH \longrightarrow C_2 \longrightarrow CN \quad (191)$$

Removal of CN is dominated by photodissociation

$$CN + h\nu \longrightarrow C + N \quad (192)$$

exchange with oxygen

$$CN + O \longrightarrow CO + N \quad (193)$$

and reaction with He^+

$$CN + He^+ \longrightarrow C^+ + N + He \qquad (194)$$

Three photodestruction terms enter into the rate equation for CN, one term each for CH, C_2 and CN. Thus the attenuation factor that accompanies the photodestruction includes the sum of three optical depths indicating a strong exponential dependance for the column density of CN on the UV optical depth of the cloud. In dark clouds gas phase reactions may compete with photodissociation for removal of CN. Federman et al scheme predicts CN column densities that match the observed column densities to within a factor of two. This suggests that the reaction

$$C_2 + N \longrightarrow CN + C \qquad (195)$$

dominates the formation of CN in diffuse clouds. If CN formation is restricted to the alternative route.

$$CH + N \longrightarrow CN + H \qquad (196)$$

the predicted CN column densities are too small.

The molecule C_2 is produced by the reactions,

$$C + CH \longrightarrow C_2 + H \qquad (197)$$

$$C_2H_2^+ + e^- \longrightarrow C_2 + H_2 \qquad (198$$

$$C_2H^+ + e^- \longrightarrow C_2 + H \qquad (199)$$

The $C_2H_2^+$ and C_2H^+ ions are produced in a chain of reactions that occur when C^+, H_2 and CH_n species are present. For example,

$$CH + C^+ \longrightarrow C_2^+ + H \qquad (200)$$

$$C_2^+ + H_2 \longrightarrow C_2H^+ + H \qquad (201)$$

$$C^+ + CH_2 \longrightarrow C_2H^+ + H \qquad (202)$$

$C_2H_2^+$ is then produced by the reactions,

$$C_2H^+ + H_2 \longrightarrow C_2H_2^+ + H \quad (203)$$

$$C^+ + CH_3 \longrightarrow C_2H_2^+ + H \quad (204)$$

Electron recombination with $C_2H_2^+$ yields C_2H.

$$C_2H_2^+ + e^- \longrightarrow C_2H + H \quad (205)$$

The reaction

$$C_2H_2^+ + H_2 \longrightarrow C_2H_3^+ + H \quad (206)$$

is slow, so the sequence usually terminates before this at $C_2H_2^+$.

All of these species are destroyed by photodissociation and reactions with He^+.

The exchange reactions,

$$C_2 + N \longrightarrow CN + C \quad (207)$$

$$C_2H + O \longrightarrow CO + CH \quad (208)$$

are exothermic and may have no activation energy barrier. They will therefore affect the population of C_2 and C_2H.

3. FORMALDEHYDE

Formaldehyde H_2CO poses a critical test of molecule formation theories. Radiative association, followed by dissociative recombination

$$HCO^+ + H_2 \longrightarrow H_2HCO^+ + h\nu \quad (209)$$

$$H_2HCO^+ + e^- \longrightarrow H_2CO + H \quad (210)$$

is one possible mechanism. H_2CO is also a by-product of the reactions,

$$CH_3 + O \longrightarrow H_2CO + H \quad (211)$$

$$CH_3^+ + O \longrightarrow H_2CO^+ + H \quad (212)$$

$$H_2CO^+ + \text{Metal} \rightarrow H_2CO + \text{Metal}^+$$

Another source is,

$$H_3O^+ + CH_2 \longrightarrow H_3CO^+ + H_2 \quad (213)$$

$$H_3CO^+ + e^- \longrightarrow H_2CO + H \quad (214)$$

and so is

$$C_2H_2^+ + OH \longrightarrow H_2C_2O^+ + H \quad (215)$$

$$H_2C_2O^+ + OH \longrightarrow H_2CO + HCO^+ \quad (216)$$

$$H_2C_2O^+ + e^- \longrightarrow H_2CO + C \quad (217)$$

A minor source is,

$$H^- + HCO \longrightarrow H_2CO + e^- \quad (218)$$

H_2CO is destroyed in diffuse regions by photodissociation.

$$H_2CO + h\nu \longrightarrow CO + H_2 \quad (219)$$

$$H_2CO + h\nu \longrightarrow CO + H + H \quad (220)$$

$$H_2CO + h\nu \longrightarrow HCO + H \quad (221)$$

Photoionisation also occurs,

$$H_2CO + h\nu \longrightarrow H_2CO^+ + e^- \quad (222)$$

$$H_2CO + h\nu \longrightarrow HCO^+ + H + e^- \quad (223)$$

Neutral-neutral reactions such as

$$H_2CO + O \longrightarrow HCO + OH \quad (224)$$

are slower than ion molecule reactions in removing H_2CO.

$$H_2CO + C^+ \longrightarrow HC_2O^+ + H \quad (225)$$

$$H_2CO + C^+ \longrightarrow CH_2^+ + CO \quad (226)$$

$$H_2CO + C^+ \longrightarrow HCO^+ + CH \quad (227)$$

$$H_2CO + C^+ \longrightarrow H_2CO^+ + C \quad (228)$$

$$H_2CO + H_3^+ \longrightarrow H_3CO^+ + H_2 \quad (229)$$

$$H_2CO + HCO^+ \longrightarrow H_3CO^+ + CO \quad (230)$$

The last two reactions are hindered by

$$H_3CO^+ + e^- \longrightarrow H_2CO + H \quad (231)$$

reforming H_2CO.

(From Dalgarno 1975)

Figure 22a

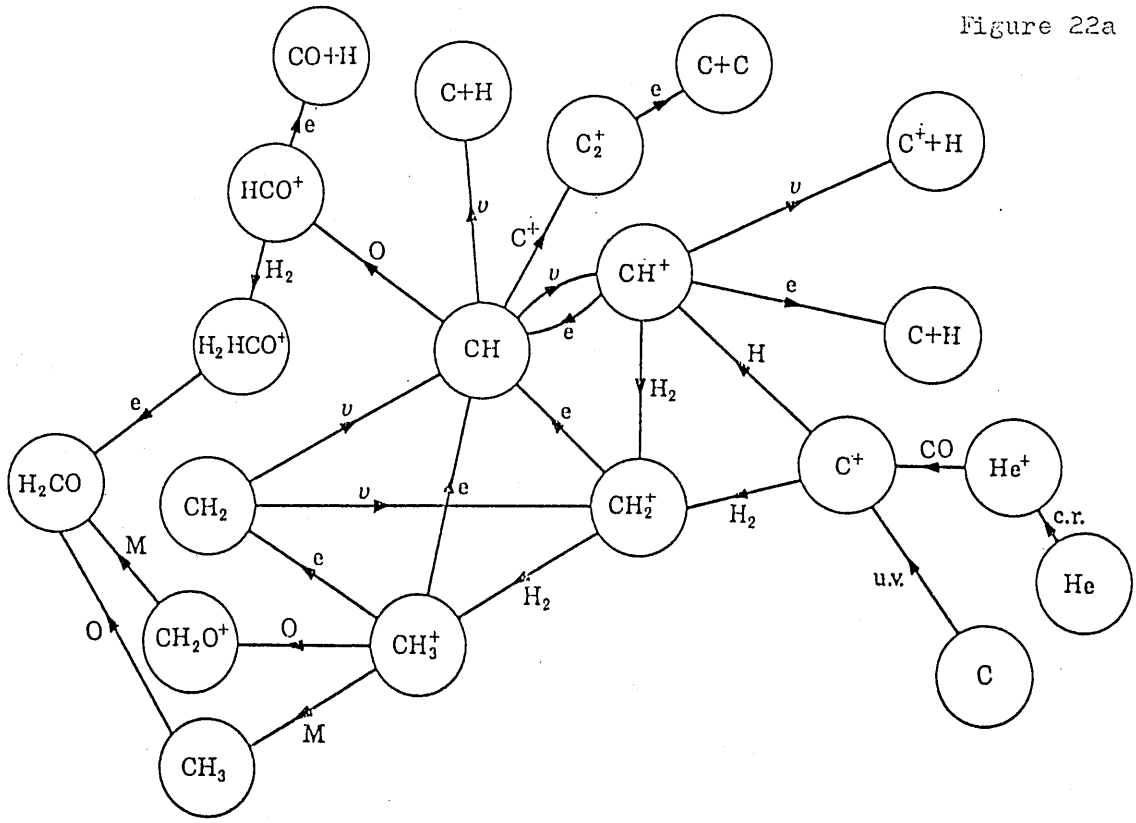

Chemical scheme initiated by $C^+ + H_2 \rightarrow CH_2^+ + h\nu$.

Figure 22b

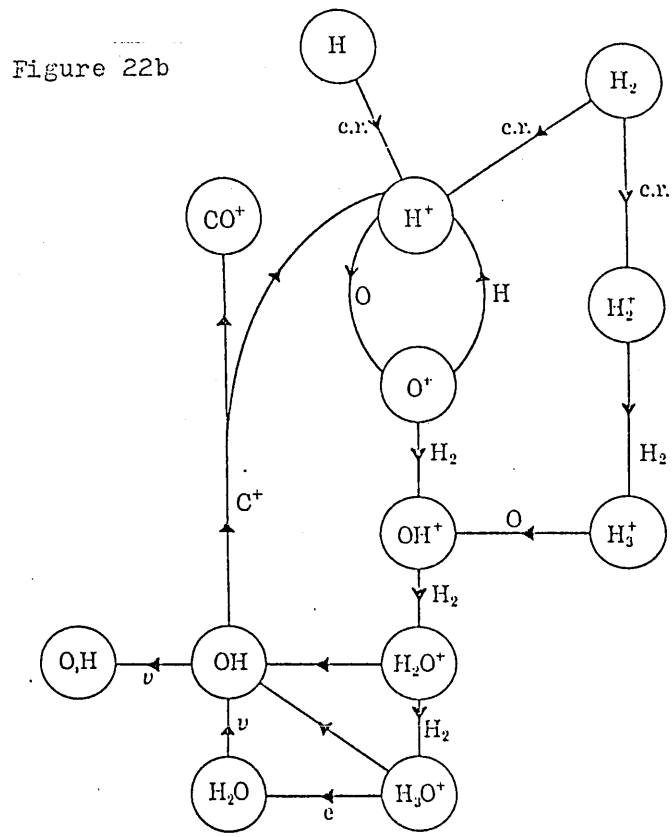

Chemical scheme initiated by $H^+ + O \rightarrow H + O^+$.

3.3.3. WATER AND HYDROXYL CHEMISTRY

The reactions that initiate OH bond formation are,

$$H^+ + O \longrightarrow O^+ + H \qquad \text{Figure 22b)} \qquad (232)$$

$$H_3^+ + O \longrightarrow OH^+ + H_2 \qquad (233)$$

The O^+ and OH^+ ions react with H_2 leading to H_2O^+ and H_3O^+. Dissociative recombination then yields OH.

$$H_2O^+ + e^- \longrightarrow OH + H \qquad (234)$$

$$H_3O^+ + e^- \longrightarrow OH + H_2 \qquad (235)$$

The last reaction competes with

$$H_3O^+ + e^- \longrightarrow H_2O + H \qquad (236)$$

$$H_2O + h\nu \longrightarrow OH + H \qquad (237)$$

The source of H_3^+ is cosmic ray ionisation followed by reaction with H_2.

$$H_2 + p \longrightarrow H_2^+ + e^- + p \qquad (238)$$

$$H_2^+ + H_2 \longrightarrow H_3^+ + H \qquad (239)$$

The amount of H_2^+ present is limited by the reactions,

$$H_2^+ + h\nu \longrightarrow H^+ + H \qquad (240)$$

$$H_2^+ + e^- \longrightarrow H + H \qquad (241)$$

$$H_2^+ + H \longrightarrow H^+ + H_2 \qquad (242)$$

and H_3^+ is removed by

$$H_3^+ + e^- \longrightarrow H_2 + H \qquad (243)$$

$$H_3^+ + e^- \longrightarrow H + H + H \qquad (244)$$

Recent laboratory work suggests that the latter reaction is the dominant channel over the energy range 0.01 to 0.05 ev. (Mitchell et al 1983 (238)).

A large fraction of OH in diffuse clouds is synthesised by

$$O^- + H \longrightarrow OH + e^- \qquad (245)$$

as well as dissociative recombination of H_2O^+ and H_3O^+.

The H_2O^+ and H_3O^+ ions are synthesised by a series of reactions involving molecular hydrogen.

$$O^+ + H_2 \longrightarrow OH^+ + H \quad (246)$$

$$OH^+ + H_2 \longrightarrow H_2O^+ + H \quad (247)$$

$$H_2O^+ + H_2 \longrightarrow H_3O^+ + H \quad (248)$$

This sequence can be interrupted by dissociative recombinations.

$$OH^+ + e^- \longrightarrow O + H \quad (249)$$

$$H_2O^+ + e^- \longrightarrow OH + H \quad (250)$$

and terminate in,

$$H_3O^+ + e^- \longrightarrow H_2O + H \quad (251)$$

$$H_3O^+ + e^- \longrightarrow OH + H_2 \quad (252)$$

Photodissociation of H_2O is also a source of OH

$$H_2O + h\nu \longrightarrow OH + H \quad (253)$$

but only when the abundance of H_2O is high. OH is lost by reaction with C^+

$$C^+ + OH \longrightarrow CO + H^+ \quad (254)$$

$$CO + H^+ \longrightarrow CO^+ + H \quad (255)$$

Reaction with H^+ and H_3^+ give

$$OH + H^+ \longrightarrow OH^+ + H \quad (256)$$

$$OH + H_3^+ \longrightarrow H_2O^+ + H_2 \quad (257)$$

and where the level of ionisation is low the following are important

$$OH + O \longrightarrow O_2 + H \quad (258)$$

$$OH + N \longrightarrow NO + H \quad (259)$$

$$OH + C \longrightarrow CO + H \quad (260)$$

Photodissociation and photoionisation also destroy OH.

$$OH + h\nu \longrightarrow O + H \quad (261)$$

$$OH + h\nu \longrightarrow OH^+ + e^- \quad (262)$$

Water is almost exclusively formed by dissociative recombination of H_3O^+.

$$H_3O^+ + e^- \longrightarrow H_2O + H \quad (263)$$

Also possible is the reaction

$$H_3O^+ + e^- \longrightarrow OH + H_2 \quad (264)$$

Uncertainty in the branching ratio ranges from one to ten in favour of OH. Recent work by Snow and Smith 1981 (120) indicates that Herbst's 1978 (190) branching ratio of 10 is correct. The first reaction may also terminate in

$$H_2O + H \longrightarrow OH + H_2 \quad (265)$$

Water may also be formed by associative detachment

$$O^- + H_2 \longrightarrow H_2O + e^- \quad (266)$$

Water may be destroyed by photodissociation and photoionisation.

$$H_2O + h\nu \longrightarrow OH + H \quad (267)$$

$$H_2O + h\nu \longrightarrow H_2O^+ + e^- \quad (268)$$

An as yet undetected molecule OD has been discussed by Croswell and Dalgarno 1985 (327). Because of the lack of self shielding of HD in diffuse clouds most of the deuterium is in atomic form. Reaction of O^+ with HD only produces small amounts of OD.

$$O^+ + HD \longrightarrow OD^+ + H \quad (269)$$

but must compete with

$$O^+ + HD \longrightarrow OH^+ + D \quad (270)$$

Other reactions are

$$OD^+ + H_2 \longrightarrow HDO^+ + H \quad (271)$$

$$HDO^+ + H_2 \longrightarrow H_2DO^+ + H \quad (272)$$

Production of OD occurs rapidly by the exchange reaction

$$D + OH \longrightarrow H + OD \qquad (273)$$

OD is destroyed by reaction with C^+

$$C^+ + OD \longrightarrow CO + D^+ \qquad (274)$$

$$C^+ + OD \longrightarrow CO^+ + D \qquad (275)$$

and by photodissociation

$$OD + h\nu \longrightarrow O + D \qquad (276)$$

3.3.4. NITROGEN CHEMISTRY

Neutral and ion molecule reactions play a significant role in the formation of N-N and N-O bonds. NO, so far found only in dense interstellar clouds (Liszt & Turner 1978 (320)) is formed by

$$OH + N \longrightarrow NO + H \qquad (277)$$

$$NH + O \longrightarrow NO + H \qquad (278)$$

$$NH_2^+ + O \longrightarrow NO + H_2^+ \qquad (279)$$

$$NH_3^+ + O \longrightarrow NO + H_3^+ \qquad (280)$$

$$N + H_2O^+ \longrightarrow NO + H_2^+ \qquad (281)$$

$$HNO^+ + e^- \longrightarrow H + NO \qquad (282)$$

$$HNO^+ + CO \longrightarrow HCO^+ + NO \qquad (283)$$

$$HNO^+ + N_2 \longrightarrow N_2H^+ + NO \qquad (284)$$

Reaction with nitrogen atoms initiates N-N bond formation.

$$NH^+ + N \longrightarrow N_2 + H^+ \qquad (285)$$

$$NH_2^+ + N \longrightarrow N_2 + H_2^+ \qquad (286)$$

$$NH + N \longrightarrow N_2 + H \qquad (287)$$

$$NO + N \longrightarrow N_2 + O \qquad (288)$$

Molecular nitrogen is destroyed by reaction with He^+, H_3^+ and H_2.

$$N_2 + He^+ \longrightarrow N + N^+ + He \quad (289)$$

$$N_2 + He^+ \longrightarrow N_2^+ + He \quad (290)$$

$$N_2 + H_3^+ \longrightarrow HN_2^+ + H_2 \quad (291)$$

$$N_2 + H_2 \longrightarrow N_2H + H \quad (292)$$

HN_2^+ reacts with CO to form N_2 again and HCO^+

$$HN_2^+ + CO \longrightarrow N_2 + HCO^+ \quad (293)$$

The reactions,

$$NH^+ + N \longrightarrow N_2^+ + H \quad (294)$$

$$N_2^+ + H_2 \longrightarrow N_2H^+ + H \quad (295)$$

$$N_2H^+ + e^- \longrightarrow N_2 + H \quad (296)$$

are also important, although suppressed by loss of NH^+ by reaction with H_2. Interstellar N_2 has not yet been detected in diffuse clouds.

However Lutz et al 1979 (119) have obtained upper limits toward ζ Sco and ϵ Per using the Copernicus satellite. Reactions between hydrogen and nitrogen lead to N-H bond formation.

$$H + H_3^+ \longrightarrow NH_2^+ + H \quad (297)$$

Also cosmic ray ionisation,

$$N + P \longrightarrow N^+ + e^- + P \quad (298)$$

followed by

$$N^+ + H_2 \longrightarrow NH^+ + H \quad (299)$$

Whilst dissociative recombination of N_2^+ and NO^+

$$N_2^+ + e^- \longrightarrow N + N \quad (300)$$

$$NO^+ + e^- \longrightarrow N + O \quad (301)$$

as well as dissociative charge transfer between He^+ and NO, and He^+ and N_2 re-cycles free nitrogen atoms.

$$He^+ + NO \longrightarrow He + N + O^+ \quad (302)$$

$$He^+ + N_2 \longrightarrow He + N + N^+ \quad (303)$$

There are strong links between the chemistry of CH, CN and NH. Atomic nitrogen plays an important role in the formation of C-N bonds at each step of the rapid

$$C^+ + CH_3^+ \longrightarrow CH_2, CH_3 \text{ chain.}$$

NH and NH_2 radicals are important in CN bond formation via reaction with C^+ ions.

$$C^+ + NH \longrightarrow CN + H^+ \quad (304)$$

$$C^+ + NH_2 \longrightarrow CN + H_2^+ \quad (305)$$

NH production mechanisms are analogous to those for OH. A major formation mechanism is

$$H^- + N \longrightarrow NH + e^- \quad (306)$$

Reactions of O^+ and N^+ ions also initiate the production of NH and OH. O^+ ions can be produced by charge transfer

$$O + H^+ \longrightarrow O^+ + H \quad (307)$$

or cosmic ray ionisation at lower temperatures

$$O + P \longrightarrow O^+ + P + e^- \quad (308)$$

Depending on the intensity of starlight the photodissociation of NH_2 can also make an appreciable contribution

$$NH_2 + h\nu \longrightarrow NH + H \quad (309)$$

The recombinations

$$NH_2^+ + e^- \longrightarrow NH + H \quad (310)$$

$$NH_3^+ + e^- \longrightarrow NH + H_2 \quad (311)$$

are also important mechanisms near chemical equilibrium. Reactions in the gas phase that are known to produce NH are significantly slower than the rate for surface reactions. This causes the NH abundance to be of special interest as an indicator for the role of surface reactions in producing molecules other than H_2, which is easily

returned to the gas by thermal evaporation.

Gas phase reactions leading to NH include,

$$N + H \longrightarrow NH + h\nu \quad (312)$$

$$H_3^+ + N \longrightarrow NH_2^+ + H \quad (313)$$

$$He^+ + N \longrightarrow N^+ + H \quad (314)$$

$$H_2 + N^+ \longrightarrow NH^+ + H \quad (315)$$

In diffuse clouds the H_3^+ abundance is low making reaction 313 uncompetitive. Reaction 314 with He^+ is also unlikely and the rate constant for radiative association between hydrogen and nitrogen atoms is small. If the observed abundance of OH is due to grain surface reactions then since their chemistry is similar, a similar abundance for NH should be evident. This is not the case, indicating that OH is produced in gas phase reactions whilst the lack of NH indicates the unimportance of surface reactions. The NH molecule is destroyed by photodissociation and photoionisation in diffuse clouds.

$$NH + h\nu \longrightarrow N + H \quad (316)$$

$$NH + h\nu \longrightarrow NH^+ + e^- \quad (317)$$

NH has proved evasive in optical spectra.

Upper limits have been obtained towards o Per by Crutcher & Watson 1976 (74) and ζ Oph by Herbig 1968 (54). Blades 1975 (58) could not detect NH toward several radio sources.

3.3.5. CHLORINE CHEMISTRY

Chlorine in diffuse clouds exists primarily in the ionised state and reacts effectively with molecular hydrogen. This reaction is exothermic by 0.17ev (Jura 1974 (116)) and is an important source of molecules.

$$Cl^+ + H_2 \longrightarrow HCl^+ + H \quad (318)$$

$$HCl^+ + H_2 \longrightarrow H_2Cl^+ + H \quad (319)$$

$$H_2Cl^+ + e^- \longrightarrow HCl + H \qquad (320)$$

The series of reactions leading to HCl may by broken by

$$HCl^+ + e^- \longrightarrow H + Cl \qquad (321)$$

$$HCl^+ + h\nu \longrightarrow H^+ + Cl \qquad (322)$$

$$H_2Cl^+ + h\nu \longrightarrow HCl^+ + H \qquad (323)$$

HCl is removed by photodissociation

$$HCl + h\nu \longrightarrow H + Cl \qquad (324)$$

and by reaction with C^+

$$HCl + C^+ \longrightarrow CCl^+ + H \qquad (325)$$

Jura has suggested that HCl^+ may be detected near 3600Å ($A^2\Sigma^+ - X^2\Pi$) and that HCl may be detected near 1291Å ($C^1\Pi - X^1\Sigma$). Jura and York 1978 (117) have subsequently obtained upper limits for HCl at 1290.257Å toward 10 stars. Smith et al 1980 (181) have examined the column densities of HCl along several lines of sight and conclude that to bring the ζ Oph theoretical model of Black and Dalgarno 1977 (78) into line with observation, the abundance of Cl^+ must be increased at the expense of HCl The reason is the high $N(Cl^+)/N(HCl)$ ratio toward ζ Oph. The reaction, (Black & Smith 1980 (335))

$$Cl^+ + H_2 \longrightarrow HCl^+ + H \qquad (326)$$

which leads to the formation of HCl should also remove Cl^+ in regions containing H_2. However, although the reaction is exothermic by 0.22 ev, a small energy barrier may exist in which case the predicted concentration of HCl would decrease. This would lead to an increase in Cl^+. The reaction,

$$HCl^+ + H_2 \longrightarrow H_2Cl^+ + H \qquad (327)$$

which is only slightly exothermic may also be inhibited by an energy barrier at low temperature. Hence the concentration of HCl^+ will be enhanced at the expense of HCl. The Cl+ abundance is not affected.

3.3.6. SULPHUR CHEMISTRY

In diffuse interstellar clouds sulphur is mainly singly ionised, and although it is chemically analogous to oxygen (i.e. below oxygen in the periodic table) its interstellar chemistry is different. The difference in the gas phase chemistry of sulphur and oxygen provides a ready explanation for the observed relative abundances of CS and CO. (CO is much higher). The molecular ion CS^+ is formed by reaction of S^+ with other abundant neutral molecules containing carbon.

$$S^+ + C_2 \longrightarrow CS^+ + C \qquad (328)$$

$$S^+ + CH \longrightarrow CS^+ + H \qquad (329)$$

Photoionisation of CS (as yet undetected in diffuse clouds) may be important

$$CS + h\nu \longrightarrow CS^+ + e^- \qquad (330)$$

A similar reaction involving SH is also possible

$$SH + C^+ \longrightarrow CS^+ + H \qquad (331)$$

An upper limit for CS has been derived using the Copernicus satellite, by Snow 1976 (183) toward ζ Oph. A similar position exists for SH, an upper limit toward o Per has also been reported by Snow 1975 (8).

In places where sulphur is not ionised CS^+ may be formed by the ion molecule reaction.

$$CH^+ + S \longrightarrow CS^+ + H \qquad (332)$$

CS^+ has been searched for toward δ Sco and ζ Oph by Ferlet et al 1983 (148), Ferlet et al 1986 (532). δ Sco has lines due to CH and CH^+ in its absorption spectrum whilst ζ Oph also has C_2 lines in its spectrum. Simple exothermic reactions of carbon bearing molecules with atomic sulphur could lead to CS^+ in diffuse clouds.

The most efficient destruction process for CS^+ will be dissociative recombination

$$CS^+ + e^- \longrightarrow C + S \qquad (333)$$

Reaction of CS^+ with H_2 gives

$$CS^+ + H_2 \longrightarrow HCS^+ + H \qquad (334)$$

$$HCS^+ + e^- \longrightarrow H + CS \qquad (335)$$

$$CS + h\nu \longrightarrow CS^+ + e^- \qquad (336)$$

which leads back to CS^+.

The chemistry of CS^+ has recently been reviewed by Quarta & Singh 1981 (159).

A further diatomic species S_2 has recently been discovered in emission in Comet IRAS Araki Alcock 1983d. CS is observed in most comets as a daughter product of CS_2 which is also thought to produce the S_2. (A'Hearn et al 1983 (227)).

3.3.7. SILICON CHEMISTRY

Although silicon compounds have been observed in the solar photosphere (Grevesse & Sauval 1970 (499), 1971 (500)), there have not been any detections in the diffuse interstellar medium. Yet silicon is chemically similar to carbon indicating that silicon compounds should exist in observable quantities. (Lovas 1974 (363) Turner & Dalgarno 1977 (225)).

Silicon ions can react with atomic hydrogen

$$Si^+ + H \longrightarrow SiH^+ + h\nu \qquad (337)$$

to form SiH^+, the analogue of CH^+. SiH^+ is then removed by dissociative recombination,

$$SiH^+ + e^- \longrightarrow Si + H \qquad (338)$$

or photodissociation,

$$SiH^+ + h\nu \longrightarrow Si^+ + H \qquad (339)$$

Other destructive reactions include,

$$SiH^+ + H \longrightarrow Si^+ + H_2 \quad (340)$$

$$SiH^+ + O \longrightarrow SiO^+ + H \quad (341)$$

Reaction with molecular hydrogen must be important to silicon chemistry, although it is not certain that the reaction is endothermic.

$$SiH^+ + H_2 \longrightarrow SiH_2^+ + H \quad (342)$$

The SiH^+ molecular ion has absorption bands near 3670Å in the optical region of the spectrum due to the $A'\pi - X'\Sigma^+$ transition.

Herbig 1968 (54) has derived an upper limit for SiH of $5.6 \times 10^{12} cm^{-2}$ toward ζ Oph from the $A^2\Delta - X^2\pi$ lines. More recently a value for the equivalent width of SiH at 4119.48Å of $< 8 m\text{Å}$ has been given by Crutcher 1985 (326). Transitions at microwave and far infrared frequencies, have been calculated by Brown et al 1985 (356). SiH^+ may react with oxygen, nitrogen and sulphur compounds to give SiO^+, SiO, SiS and SiN. SiO^+ may react with O to form O_2.

$$SiO^+ + O \longrightarrow Si^+ + O_2 \quad (343)$$

and with N to form NO and NO^+

$$SiO^+ + N \longrightarrow Si^+ + NO \quad (344)$$

$$Si^+ + NO \longrightarrow Si + NO^+ \quad (345)$$

Further reactions of SiO^+ and Si^+ with H_2 and H_2O give,

$$SiO^+ + H_2 \longrightarrow HSiO^+ + H \quad (346)$$

$$Si^+ + H_2O \longrightarrow HSiO^+ + H \quad (347)$$

Also reaction of SiO with H_3^+.

$$SiO + H_3^+ \longrightarrow HSiO^+ + H_2 \quad (348)$$

$HSiO^+$ is removed by dissociative recombination

$$HSiO^+ + e^- \longrightarrow SiO + H \qquad (349)$$

and reaction with CO

$$HSiO^+ + CO \longrightarrow HCO^+ + SiO \qquad (350)$$

Because the last two reactions are rapid, the abundance of $HSiO^+$ will be small.

A source of SiO^+ in warm clouds is the reaction

$$Si^+ + OH \longrightarrow SiO^+ + H \qquad (351)$$

and of SiO,

$$Si + OH \longrightarrow SiO + H \qquad (352)$$

In diffuse clouds silicon monoxide is destroyed by photodissociation.

$$SiO + h\nu \longrightarrow Si + O \qquad (353)$$

SiN is produced by reactions involving SiH, SiH^+ and SiH_2^+ with nitrogen. SiN is however rapidly destroyed by photodissociation.

In diffuse clouds a considerable fraction of sulphur is in the ionised form S^+ which reacts with SiH to form SiS

$$S^+ + SiH \longrightarrow H^+ + SiS \qquad (354)$$

or by

$$S^+ + SiH \longrightarrow SiS^+ + H \qquad (355)$$

$$SiS^+ + H_2 \longrightarrow SiSH^+ + H \qquad (356)$$

$$SiSH^+ + e^- \longrightarrow SiS + H \qquad (357)$$

SiS is destroyed by reaction with carbon,

$$SiS + C^+ \longrightarrow Si^+ + CS \qquad (358)$$

$$SiS + C^+ \longrightarrow Si + CS^+ \qquad (359)$$

Morton 1975 (11) has derived an upper limit for SiO toward ζ Oph of 7×10^{12} cm^{-2}, whilst the column density for SiS is computed to be 2×10^{11} cm^{-2}.

3.4 THE EFFECT OF A SHOCK ON A DIFFUSE CLOUD

The shock model has been proposed to explain the difference between the calculated and observed column densities of CH^+ in diffuse clouds. Observable radial velocity differences should arise between the gas in the hot post shock, the cool compressed post shock and the pre shock regions. If the shock is produced by the star under observation then the cool compressed gas will be moving towards the Sun at a velocity of $\sim 3 Kms^{-1}$ relative to the hot post shock gas where CH^+ is formed (Elitzur and Watson 1978 (115)). The pre shock gas will be moving away at $\sim 9 Kms^{-1}$ relative to CH^+. The velocity difference between CH^+ and the other molecules may be positive or negative if the shock is not of local origin and proceeds at any angle relative to the line of sight. If this scenario is correct then the various molecular species should occur in different locations, the geometry of the pre shock cloud strongly influencing the direction of the shock velocity. Elitzur and Watson 1980 (60) have extended their results on CH and CH^+ to include the effect of a shock on OH and H_2O. CH^+ is less sensitive than the other molecules to parameters such as density and the radiation field. The CH^+ abundance is roughly proportional only to the H_2 fractional abundance $X(H_2)$ at a given temperature, where,

$$X(H_2) = \frac{n(H_2)}{n(H)}$$

At large values of $X(H_2)$ the value of $N(CH^+)$ decreases due to the contribution from

$$CH^+ + H_2 \longrightarrow CH_2^+ + H \qquad (360)$$

to the destruction of CH^+.

For shock velocities exceeding $12 Kms^{-1}$ a decrease in the molecular column densities could also occur as the result of collisional dissociation of H_2 at the higher post shock temperatures since the major source of CH^+ is through the reaction

$$C^+ + H_2 \longrightarrow CH^+ + H \qquad (361)$$

The ζ Oph clouds are cited as an example of a shocked region. The main cloud at $-0.5 Kms^{-1}$ (LSR) in which most of the molecules are located is associated with the cold compressed gas that is expected behind a shock front after the gas has cooled. The CH^+ lines are centred at $1.4 Kms^{-1}$ and therefore arise in a different spatial location. This component is identified with the hot post shock gas. Elitzur and Watson 1978 (115) have suggested that thermal Doppler broadening will make an observable contribution to the absorption line profile of CH^+, if the molecule does occur in a hot post shock gas. In fact the breadth of the line profile toward ζ Oph corresponds to an effective temperature of $4.5 \times 10^3 K$ which is compatible with a hot post shock gas behind a shock front with a velocity of $12 Kms^{-1}$.

A third component at $5.5 Kms^{-1}$ has also been detected in OH at radio wavelengths (Crutcher 1979 (191)). This seems to represent the gas in front of ζ Oph which would be the pre shock gas for a shock moving into it from the star.

Unfortunately the radial velocity data obtained by optical measurements is not always good enough to detect a velocity shift of a few Kms^{-1}, between the lines of CH^+ and those of other molecules. A comprehensive set of data does not exist for more than a few lines of sight. The pre shock gas will usually be more difficult to detect because of its low density, than the cold compressed gas in the post shock region. This certainly appears to be the case for the ζ Oph clouds.

CH and most of the other molecules present in the cold post shock gas are produced by normal gas phase processes. Shocks will produce negligible abundances of molecules other than the hydrides CH, OH

NH and H_2O. Molecular hydrogen in the pre shock gas provides the source of hydrogen.

There are no stars toward which CH^+ has been detected (and by implication in which ashock is present) for which the fractional column density of H_2 is below the necessary value. There is also no observational evidence to conflict with the proposition that much less CH and H_2O, than CH^+ is produced by shocks entering a region of low fractional H_2 abundance. The same is true for OH. In contrast a shock entering a region of high fractional H_2 abundance will generate more H_2O than is compatible with the data in the few cases available. Clearly there is a need for more observational work on H_2O.

Mitchell and Deveau 1983 (161) (Table 23) have extended the work on shocks to include other molecules. They have examined a 10 Kms^{-1} shock and its effect on a cloud of initial density $100cm^{-3}$. A shock can transform a low density gas into a cloud of moderate density reaching a final value of $10^4 cm^{-3}$. Since the new cloud will be better shielded from ultraviolet radiation, the chemical composition of the cloud formed by the shock may persist for a long time, as radiative dissociation processes are inhibited. Some abundance enhancements occur in the hot post shock gas, but do not persist in the cooler post shock phase. CH^+, HCO^+, NH and CH_3 will be abundant only near the shock front whilst other species such as H_2O, CH_4 and NH_3 may remain abundant long after the shock has passed.

In a diffuse cloud C^+ is initially the most abundant carbon species. The endothermic reaction

$$C^+ + H_2 \longrightarrow CH^+ + H \qquad (362)$$

is fast at the high temperatures produced in a shock and leads to a reduction in C^+. The neutral atom however increases if the

molecule is sufficiently shielded from UV radiation. The C^+ abundance is also decreased by the exothermic reaction,

$$C^+ + H_2O \longrightarrow HCO^+ + H \quad (363)$$

which is important even after cooling is complete. In a shielded cloud C^+ is formed by

$$He^+ + CO \longrightarrow C^+ + O + He \quad (364)$$

and neutral carbon by

$$CH^+ + e^- \longrightarrow C + H \quad (365)$$

$$CH + H \longrightarrow C + H_2 \quad (366)$$

However in an unshielded region C will be photo ionised leading to C^+.

The CO molecule increases in abundance in the shock due to

$$C^+ + OH \longrightarrow H^+ + CO \quad (367)$$

$$CS + O \longrightarrow CO + S \quad (368)$$

$$HCO^+ + e^- \longrightarrow CO + H \quad (369)$$

$$C + OH \longrightarrow CO + H \quad (370)$$

$$CN + O \longrightarrow CO + N \quad (371)$$

These all occur in the hot post shock phase

At lower temperatures CO is formed by,

$$HCO^+ + e^- \longrightarrow CO + H \quad (372)$$

$$CH + O \longrightarrow CO + H \quad (373)$$

In point CO owes its enhanced production to an increase in OH, H_2O, HCO^+ and CN. None of these reactions is known to be strongly sensitive to temperature.

TABLE 23

COLUMN DENSITIES IN A DIFFUSE INTERSTELLAR CLOUD BEFORE AND AFTER A SHOCK

(From Mitchell & Deveau 1983 (161)

SPECIES	PRESHOCK	POST SHOCK $^{(2)}_{AV = \infty}$	POST SHOCK $^{(3)}_{AV = 1}$
CO	3.3×10^{14}	5.3×10^{15}	1.7×10^{16}
OH	1.4×10^{12}	2.7×10^{13}	4.4×10^{14}
H_2O	1.3×10^{11}	2.0×10^{16}	1.2×10^{15}
CH^+	1.6×10^{9}	2.4×10^{11}	2.4×10^{11}
CN	9.8×10^{10}	5.5×10^{13}	1.1×10^{14}
NH	1.8×10^{8}	3.0×10^{11}	3.4×10^{11}
C^+	1.9×10^{16}	7.2×10^{12}	1.4×10^{13}
N_2	6.9×10^{7}	6.9×10^{12}	4.3×10^{13}

NOTES (1) Column densities in cm^{-2}.

(2) Av = ∞ Complete shielding from ultraviolet radiation.

(3) Av = 1, Ultraviolet radiation only slightly attenuated.

OH and H_2O, originally discussed by Elitzur and Watson, have also been examined by Mitchell and Deveau. OH increases in the case of an unshielded cloud, but declines in the shielded case, whilst H_2O is high in the shielded case and declines in the unshielded cloud. During the initial hot phase the chemistry of both molecules is dominated by the reactions

$$O + H_2 \longrightarrow OH + H \quad (374)$$

$$OH + H_2 \longrightarrow H_2O + H \quad (375)$$

$$OH + H \longrightarrow O + H_2 \quad (376)$$

When the gas cools, in the unshielded case from 100 to several thousand years, the chemistry of OH is controlled by

$$C + OH \longrightarrow CO + H \quad (377)$$

$$OH + O \longrightarrow O_2 + H \quad (378)$$

$$CH + O \longrightarrow CH + OH \quad (379)$$

For moderate densities (Av = 1), the most important reactions are the first and

$$H_2O + h\nu \longrightarrow OH + H \quad (380)$$

$$OH + N \longrightarrow NO + H \quad (381)$$

while at later times in shielded regions

$$H_3O^+ + e^- \longrightarrow OH + 2H \quad (382)$$

$$H_2CO + O \longrightarrow HCO + OH \quad (383)$$

and $$C + OH \longrightarrow CO + H \quad (384)$$

become important. In the unshielded cloud at this time,

$$H_3O^+ + e^- \longrightarrow OH + 2H \quad (385)$$

$$O + H \longrightarrow OH + h\nu \quad (386)$$

$$CH_2 + O \longrightarrow CH + OH \quad (387)$$

and $$C^+ + OH \longrightarrow \text{Products}$$

become dominant.

Water, H_2O is formed in the cool postshock gas by

$$H_3O^+ + e^- \longrightarrow H_2O + H \quad (388)$$

and removed by

$$H_2O + h\nu \longrightarrow OH + H \quad (389)$$

$$H_2O + C^+ \longrightarrow HCO^+ + H \quad \text{in the unshielded regions} \quad (390)$$

In the shielded cloud the major destruction processes are

$$HCO^+ + H_2O \longrightarrow H_3O^+ + CO \quad (399)$$

$$HCS^+ + H_2O \longrightarrow H_3O^+ + CS \quad (392)$$

$$H^+ + H_2O \longrightarrow H_2O^+ + H \quad (393)$$

$$H_3^+ + H_2O \longrightarrow H_3O^+ + H_2 \quad (394)$$

The molecule CO^+ initially increases after the shock but decreases quickly. It is formed by

$$CH^+ + O \longrightarrow CO^+ + H \quad (395)$$

$$C^+ + OH \longrightarrow CO^+ + H \quad (396)$$

and destroyed by

$$CO^+ + H_2 \longrightarrow HCO^+ + H \quad (397)$$

In the cooler gas the reactions

$$He^+ + H_2CO \longrightarrow CO^+ + H_2 + He \quad (398)$$

$$CO + P \longrightarrow CO^+ + e^- + P \quad (399)$$

dominate. CO^+ reaches a high abundance due to the high post shock abundance of CH^+ and OH. Jenkins et al 1973 (53), and more recently Crutcher 1985 (326) have searched for CO^+, but give only upper limits to its abundance.

Cyanogen attains a very high abundance behind the shock. In the shielded regions it remains high for longer than in the unshielded parts of the cloud. CN is produced by the reactions,

$$C^+ + NH \longrightarrow CN^+ + H \quad (400)$$

$$CH^+ + N \longrightarrow CN^+ + H \quad (401)$$

CN^+ then reacts with, atomic hydrogen,

$$CN^+ + H \longrightarrow H^+ + CN \quad (402)$$

Reaction with H_2, leads to

$$CN^+ + H_2 \longrightarrow HCN^+ + H \quad (403)$$

HCN^+ is also formed by,

$$CH_2^+ + N \longrightarrow HCN^+ + H \quad (404)$$

$$CH_3^+ + N \longrightarrow HCN^+ + H_2 \quad (405)$$

then

$$HCN^+ + H_2 \longrightarrow H_2CN^+ + H \quad (406)$$

and

$$H_2CN^+ + e^- \longrightarrow CN + H_2 \quad (407)$$

CN is also formed by

$$C + NH \longrightarrow CN + H \quad (408)$$

NH is another molecule that will reach a high abundance in the hot post shock gas.

$$N + H_2 \longrightarrow NH + H \quad (409)$$

CS increases 100 fold and remains high, although it does decrease in an unshielded cloud.

$$HCS^+ + e^- \longrightarrow CS + H \quad (410)$$

$$CS^+ + H \longrightarrow H^+ + CS \quad (411)$$

$$HCS^+ + H_2O \longrightarrow H_3O^+ + CS \quad (412)$$

$$CH + S \longrightarrow CS + H \quad (413)$$

The ions CS^+ and HCS^+ are the products of reactions involving CH, CH_2 and C_2.

$$CH + S^+ \longrightarrow CS^+ + H \quad (414)$$

$$C_2 + S^+ \longrightarrow CS^+ + C \quad (415)$$

then $$CS^+ + H_2 \longrightarrow HCS^+ + H \quad (416)$$

and $$S^+ + CH_2 \longrightarrow HCS^+ + H \quad (417)$$

The increase in CS is directly accreditable to the high post shock abundance of CH, CH_2 and C_2.

Many of the carbon and oxygen bearing molecules such as CN, HCN, CH_4, C_2H_2, H_2CO, HCO^+ and CO^+ owe their abundance to an appreciable amount of C^+. The formation of NH, NH_2 , NH_3 , NO, N_2, OH, H_2O and O_2 is however independent of carbon and these molecules should be enhanced in a wider variety of shocked clouds.

In a shielded region (Av = ∞) CO^+, HCO^+, O_2, OH, CH^+, CH_2^+, CH_3^+, CH, CH_2, CH_3, NH, and NO reach a high abundance but decline after the shock has passed, whilst C, CH_4, C_2H_2, H_2O, CO_2, H_2CO, HCN, CN, NH_3, CS and H_2CS will remain high. CO and SO_2 also increase in abundance and density.

In unshielded regions (Av = 1), CH^+, CH_2^+, CH_3^+, HCO^+, OH, CO^+, O_2, H_2O, H_2CO, NH, NH_2, NH_3, NO and SO_2 are enhanced in the hot post shock gas, but decline as the gas cools. CO and HCN also increase in density.

Meyers et al 1985 (325) have examined the effect of a weak shock on interstellar gas toward the ρ Oph cloud, and how this enhances grain growth. Observations of CH and CH^+ indicate a shock with a velocity of 10 Kms^{-1} expanding away from the Sun into the ρ Oph cloud. There are two distinct regions along the line of sight. A low density, less depleted, atomic region associated with the pre shock gas and a predominantly molecular region associated with the post shock gas, which is highly depleted. The increased density resulting from the weak shock obviously has the effect of enhancing grain growth by increasing the rate of accretion of interstellar matter.

Recently Mitchell and Watt 1985 (377) have extended the work of Mitchell and Deveau to shocks with a range of speeds from 5 to 20 Kms^{-1} passing through diffuse clouds with gas densities in the range 5 to 50cm^{-3} and for several values of the molecular hydrogen concentration. The abundances of 112 species are followed in an

investigation of the chemical processes in the hot gas behind the shock, although they only specifically discuss 27 species whose post shock column densities reach a value of $10^{10} cm^{-2}$ for at least part of the range of parameters explored.

All of the species increase in abundance during the hot post shock phase, for the case of a 20 Kms^{-1} shock encountering a cloud of density $10cm^{-3}$ and a molecular hydrogen fraction of $\frac{n H_2}{n H} = 0.1$. At this density the gas requires several thousand years to cool to its preshock value. After 1000 years the abundance of most species falls due to photolytic reactions and the termination of high temperature reactions.

The majority of neutral species are found to increase in abundance as the total gas density increases whilst all ions remain very nearly constant over a range of densities. Abundances increase steeply with increasing shock speed up to $10Kms^{-1}$. Above this the increase is slower, and for some species, OH, H_2O, CO_2 and all ions, the abundance remains constant. A number of species CH, CH_2, C_3, H_2O increase as the abundance of H_2 increases, whilst others OH, N_2, NO, NH, CH^+ and CN are virtually independent of the H_2 abundance.

Mitchell and Watt have attempted to fit observational data from the literature to their model for CH^+, CH, CN, CO, C_2, OH, H_2O, NH, CH_2, C_3 and CO^+. For the majority of CH^+ sources they find that the observed CH^+ column density exceeds the predicted post shock column density. For two sources the model column densities are too low by a factor of ten. Since shocks with speeds greater than 20 Kms^{-1} will remain non dissociative the radial velocity difference between CH and CH^+ may exceed 5 Kms^{-1}. Observed differences are $< 3Kms^{-1}$. The model also predicts that CO should be more

abundant than CH by a factor of 10^2 - 10^3. In some sources the CO abundance is only greater than that of CH by a factor of 2 - 3. The CN abundance is consistent with predicted abundances for cold post shock gas. Several sources though have high CH abundances with a low CN abundance in conflict with the model. Predicted abundances of H_2O, NH and CH_2 are very close to observed upper limits. Predicted abundances of C_3 in some cases exceed the observed upper limits toward ζ Oph and ζ Per whilst the model predictions for C_2 fall short of the observed abundance. Considerably more work needs to be done to devise a model that will satisfy the observed abundances of all the molecular species present in diffuse clouds.

In another recent paper (Draine & Katz 1986 (520)) detailed results are given for a 10 Kms^{-1} shock propagating into a diffuse cloud with a hydrogen density of 50 cm^{-3}. It was found that magnetohydrodynamic shocks are capable of producing significant column densities of CH^+, OH, CH, HCO^+ and rotationally excited H_2. Miller et al 1986 (523) argue that the presence of a magnetic field may be deduced by the presence or absence of SH^+ in regions where CH^+ is observed and that this may be used to determine the type of shock that drives the chemistry.

3.5 ISOTOPIC ABUNDANCES

If different isotopic species of a molecule can be detected such as ^{12}CO and ^{13}CO, $^{12}CH^+$ and $^{13}CH^+$, and most recently ^{12}CN and ^{13}CN, (for example see figure 23), it is in principle possible to deduce from the line intensities the relative abundance

$$\frac{N(^{12}C)}{N(^{13}C)}$$

of the two carbon isotopes. The absolute abundance of either isotope cannot be deduced from molecular observations for it depends on the whole complex of processes of molecular formation

Figure 23

THE INTERSTELLAR SPECTRAL LINES of CH^+ at 4232.5 Å and 3957.7 Å TOWARD ZETA OPHIUCHI

(From Vanden Bout and Snell 1980)

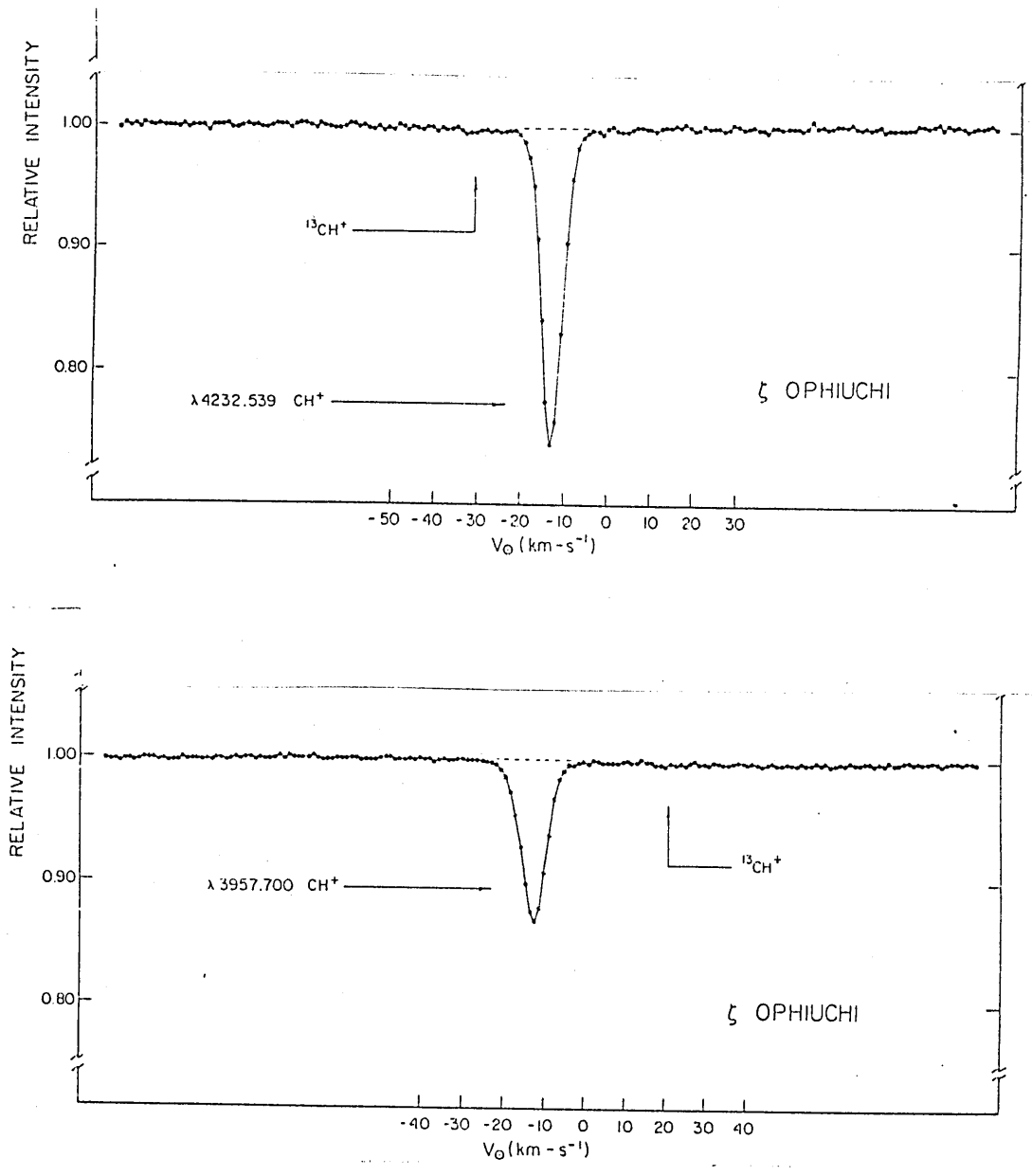

and destruction. The isotope abundance ratio may be compared with the solar system value and examined for variations from place to place in the Galaxy. The results relate to the history of the material in its processing by nucleosynthesis.

Hobbs 1972 (141) has determined the value of $\frac{^{12}C}{^{13}C}$ from CH^+ measurements toward six stars and found lower limits from $\frac{^{12}C}{^{13}C} > 20$ to $\frac{^{12}C}{^{13}C} > 77$. $^{13}CH^+$ was not detected toward any of the stars observed. The terrestrial value of $\frac{^{12}C}{^{13}C} = 89$. Other results found in the literature are given in table 24. The method is fraught with difficulty as different optical thickness's in the lines mean that relative intensities do not directly give abundances. Lines of the more abundant $^{12}CH^+$, ^{12}CO and ^{12}CN molecules will have greater optical depths. Observing these molecules in the wings of the line profile where the line is optically thin is one approach used to circumvent this problem although the line profile is produced by velocity effects so that different parts of it relate to different parts of the cloud. It may be presumed that the isotope ratio will be the same in different molecules containing the same atom in question. So that the ratio for a minor constituent where the lines are optically thin may be applied to a more abundant molecule. In general terms the abundance ratios for various isotopes of carbon, oxygen, nitrogen and sulphur are not greatly different from solar system ratios. The $^{12}C/^{13}C$ ratio is important in that it is sensitive to the detailed history of nuclear processing. In stars consuming hydrogen by the CNO cycle to form helium the equilibrium value of this ratio is 4. In hotter stars where helium is being consumed virtually all the ^{13}C is destroyed. Thus variations are to be expected with samples having different mixtures of material ejected from different stars.

TABLE 24

RELATIVE ABUNDANCES OF ISOTOPIC SPECIES

MOLECULE	STAR	ISOTOPIC RATIO	REFERENCE
CH^+	ζ Oph	$\frac{^{12}C}{^{13}C} = 30$	Augason & Herbig 1967 (364)
CH^+	ζ Oph	$\frac{^{12}C}{^{13}C} = 82\ (+55 - 15)$	Bortolot & Thaddeus 1969 (24)
CH^+	ζ Oph	$\frac{^{12}C}{^{13}C} = 75\ (+25, -15)$	Vanden Bout 1972 (22)
CH^+	ζ Oph	$\frac{^{12}CH^+}{^{13}CH^+} = 47\ (+12, -8)$	Vanden Bout & Snell 1980 (149) (Re analysis of Ref.24)
CH^+	20 Tau	$\frac{^{12}CH^+}{^{13}CH^+} = 49\ (+12, -8)$	Vanden Bout & Snell 1980 (149)
CH^+	ξ Per	$\frac{^{12}CH^+}{^{13}CH^+} = 59\ (+24, -13)$	Vanden Bout & Snell 1980 (149)
CH^+	ζ Oph	$\frac{^{12}CH^+}{^{13}CH^+} = 77\ (+17, -12)$	Vanden Bout & Snell 1980 (149)
CH^+	ζ Oph	$\frac{^{12}C}{^{13}C} = 43 \pm 6$	Hawkins et al 1985 (362)
CO	ζ Oph	$\frac{^{12}CO}{^{13}CO} = 50$	Crutcher & Watson 1981 (280)
CO	ζ Oph	$\frac{^{12}CO}{^{13}CO} = 55\ (+11, -11)$	Wannier et al 1982 (179)
CN	ζ Oph	$\frac{^{12}C}{^{13}C} = 50\ (+13, -10)$	Crane 1987 (555)

NOTE: $\frac{^{12}CH^+}{^{13}CH^+}$, $\frac{^{12}CO}{^{13}CO}$ and $\frac{^{12}CN}{^{13}CN}$ do not necessarily reflect the atomic abundance ratio $\frac{^{12}C}{^{13}C}$ because of fractionation.

Isotope fractionation can mean that the isotope abundance ratio in some molecules may not be the true isotope ratio of the material in the cloud. Certain chemical processes may proceed at different rates for different isotopes and molecules containing rare isotopes may be less shielded from destructive radiation in the clouds because the optical thickness in their resonance lines will be lower.

For example, consider the case of molecular hydrogen. Spitzer et al 1973 (87) using observations from the Copernicus satellite found a ratio of HD to H_2 equal to 10^{-6}. The true $\frac{N(D)}{N(H)}$ ratio is 1.8×10^{-5}. Corrections for the lack of effective shielding for HD means that one HD molecule is formed and destroyed for every 200 H_2 molecules.

3.6 EXCITED STATES

If ordinary inelastic collisions with other molecules are the dominant excitation process in the interstellar medium, then the excitation will be thermal and given by the equation

$$\frac{N_1}{No} = \frac{g_1}{go} \; e^{-(E_1 - Eo)/kT} \qquad (3.3)$$

where No and N_1 are the populations in the ground and excited states respectively, g_o and g_1 are statistical weights, Eo and E_1 are the energies in the ground and excited states and T is the kinetic temperature of the gas. This appears to be the case for CO molecules in collision with H_2.

Anomalous populations can also be produced, through chemical reactions, through interaction with an external radiation field and through collisional excitation followed by radiative cascade. Ultraviolet observations of H_2 using the Copernicus satellite (Savage et al 1977 (70)) show an excess population in states of higher rotational quantum number J. This has been explained

by the lower J states being populated in thermal equilibrium at a kinetic temperature typically about 80K and the higher J states, being less affected by collisions, being populated dominantly by radiative processes. The ultraviolet absorption is followed by downward cascade through various vibrational and rotational excited states. These levels therefore have excitation temperatures of 300K or more.

Among the interstellar molecules it seems that thermal equilibrium is rare. CO is an exception because its rotational lines have a relatively low radiative transition probability. Many molecules CH, OH, H_2O, HCN and H_2CO have population anomalies and show some maser action. Maser amplification will occur when there is a population inversion and has been discussed in detail by Cook 1977 (308), and by Norris 1986 (430).

One interesting aspect of the CN lines most commonly observed is that two of them R(1) and P(1) originate in the first excited level N = 1 and not in the ground state N = 0, which is 2.6mm lower in energy. From the intensity ratio of the lines originating from N = 0 (the R(0) line) and N = 1 (the R(1) line) a rotational temperature of 2.3K follows, a figure first derived by McKellar 1940 (69). The degree of excitation corresponding to 2.3K means that about a quarter of the CN molecules in the interstellar medium are in the N = 1 rotational state. This is rather too high to be explained by collisional excitation by hydrogen or starlight and is in fact due to the 3K microwave background radiation, a relic from the Big Bang. The CN molecules are bathed in this radiation which excites them into the higher rotational state. That the excitation is not due to local effects such as UV radiation from a nearby star is shown by the same excitation

temperature being calculated for CN in the spectra of different stars, in different directions in space. The significance of this to Cosmology has been discussed by Sciama 1975 (333). Interest also attaches to the possibility of observing absorption from the second rotational level of CN. Molecules in this state are excited by radiation of 1.3mm very close to the peak of the 3K black body spectrum of the microwave background radiation. Equivalent widths obtained for the R(2) line of CN toward ζ Oph are given in table 25.

Meyer and Jura 1985 (381) give W_λ = 0.08mÅ and 0.04mÅ for the R(2) line of CN toward ζ Per and o Per respectively. Crutcher 1985 (326) gives a much larger value of $W_\lambda = 6 \pm 2$mÅ for the R(2) line toward HD 29647.

He also gives a value of $W_\lambda = 5 \pm 2$mÅ for the P(2) line of CN. Munch 1964 (57) has also reported observing the P(2) line at 3876.30Å and the P(3) line at 3876.84Å of CN toward BD +66° 1674. Bortolot et al 1969 (144) also report upper limits for the CH $R_1(1)$ line at 4303.947Å ($W_\lambda < 0.44$) and the CH^+ R(1) line at 4229.337 ($W < 0.59$) both of which originate in higher rotational levels than the ground state.

TABLE 25

EQUIVALENT WIDTHS OF THE R(2) LINE OF CN AT 3873.369Å TOWARD ζ Oph

W_λ (mÅ)	REFERENCE
0.43	Bortolot et al 1969 (144)
0.17	Thaddeus 1972 (131)
0.077	Hegyi et al 1972 (296)
0.07	Meyer & Jura 1984 (281)
0.06	Meyer & Jura 1985 (381)
0.072	Crane et al 1986 (511)

4. OBSERVATIONS OF THE INTERSTELLAR GAS

4. OBSERVATIONS OF THE INTERSTELLAR GAS

The spectrum of a heavily reddened star contains absorption lines from atoms and molecules present in the interstellar gas between Earth and the star. The lines are identified as non stellar in origin (not produced in the stars atmosphere) for several reasons.

They are absorptions from the ground state of the molecular species concerned and therefore characteristic of a cold gas and not a hot stellar atmosphere. They are also much sharper than stellar lines because of the low density of the interstellar gas. Stars which are otherwise identical may or may not show these lines and the strengths of the lines tend to increase with distance. They also appear to be correlated with each other and with the interstellar reddening. The Doppler shift of the lines is completely unrelated to that of the stellar lines as discovered by Hartmann in 1904. Sometimes several Doppler components are seen corresponding to different gas velocities along the line of sight in several distinct clouds.

To study interstellar absorption lines it is necessary to look at stars with few absorption lines in their intrinsic stellar spectrum. The spectrum of a star like the Sun contains many thousands of absorption lines in the visible region and is therefore unsuitable as these make the task of identifying interstellar lines extremely difficult. Cooler stars give rise to spectra containing strong molecular bands that originate in the stellar atmosphere. The hottest stars have the simplest spectra and it is the spectra of the O and B stars found in HII regions that are most often studied. They also have the advantage of being very bright so they can be studied at large distances where the interstellar effects are larger. Unfortunately they are not very numerous.

4.1. PRIOR TO 1950

The first observation of the cold gaseous component of interstellar space was made by Hartmann 1904 (138). He observed the spectroscopic binary star δ Orionis and noticed that the calcium II K line at 3933.68Å exhibited a very peculiar behaviour. It appeared very weak, but almost perfectly sharp, and did not share in the periodic displacements of the lines caused by the orbital motion of the star. He argued that it could not have originated in the Earths atmosphere or from the second component of the binary system, but that at some point in space in the line of sight between the Sun and δ Orionis there is a cloud of gas which produces the absorption lines. This reasoning was supported by a similar phenomenon exhibited by the spectrum of nova Persei in 1901, in which the calcium II H and K, and the sodium I D lines were present.

As these lines remained relatively fixed in position and did not share in the orbital velocity oscillations of the hydrogen and helium lines arising in the stellar atmosphere they became known as stationary lines. Miss Heger 1919 (139) continued this work and observed the stars β Sco and δ Ori to determine if any peculiarity existed in the behaviour of the D lines of sodium I. The lines were found to be sharp and narrow and they behaved in the same manner as the calcium II lines observed previously confirming their status as stationary lines. Their radial velocities, in the case of δ Ori, also agreed with thosedetermined by Hartmann for the calcium II K line, indicating a common position in space. Miss Heger 1921 (150) continued her work on sodium I lines in B stars and found similar results for o Per.

The development of optical spectroscopy at two major astrophysical observatories, at Mount Wilson (Hale Observatories) in Pasadena, California, USA and the Dominion Astrophysical Observatory,

Victoria, BC in Canada led to further advances in interstellar astronomy.

Plaskett and Pearce 1933 (158) at the Dominion Astrophysical Observatory measured the radial velocities and intensities of interstellar lines in 314 stars, concluding that the diffuse matter in space must be uniformly distributed. However, this view was proved untenable by Beals 1936 (137) who, amongst others, showed the existence of multiple distinct interstellar clouds. Beals also measured the equivalent widths of the spectral lines rather than relying on qualitative estimates of line intensity. Further studies of the H and K lines of calcium II were made by Adams 1943 (109) and 1949 (10) at Mount Wilson who found the spectra of many stars very complex, and used measurements of radial velocities to distinguish individual interstellar clouds. The existence of molecules in space was first proposed by Russell 1935 (153) on the basis of unidentified lines discovered by Merrill 1934 (174). Dunham 1937 (73) in a search for atomic species other than CaII and NaI discovered unknown interstellar lines at 4300Å, 4232Å and reported a third line discovered by Adams at 3957Å. The true nature of the line at 4300Å was first realised by Swings and Rosenfeld 1937 (108) who correctly identified it as being due to the $A^2\Delta - X^2\Pi\,(00)\ R_2(1)$ transition of CH. McKellar 1940 (69) also identified the 4300Å line with CH from the available laboratory data. However, he made the point that more than one line is necessary for a positive identification. Some weaker lines of CH were later observed by Adams 1949 (10). He detected the four lines of CH at 4300Å, 3890Å, 3886Å and 3879Å in many of the 300 O and B stars observed. The lines at 4232Å and 3957Å were identified with CH^+ from laboratory work by Douglas and Herzberg 1941 (42), who also identified a further weak line at 3745Å, later observed by Adams

1949 (10). Further lines were identified with CN by McKellar 1940 (69).

Thus the basis for the observation of interstellar molecules at visible wavelengths using optical spectroscopy was established. The late thirties and early forties saw a flourish of work on optical molecules culminating in the work of W.S. Adams at Mount Wilson. He was able to benefit from the dark skies and lack of demand for telescope time during World War II, by completing the largest survey of CH, CH^+ and CN observations to this day. Adams 1941 (99) first observed the bright star ζ Oph and found lines due to CH, CN and CH^+ (although the latter was unidentified at the time). In his second paper, Adams 1943 (109) he reports observations of 50 stars for the H and K lines of CaII, he also found lines due to CH, CH^+ and CN in many of them. His most comprehensive survey, Adams 1949 (10), of 300 O and B stars indicated that about one star in four shows one or more of the interstellar lines of CN, CH, CH^+, Ca or Fe. In fact, many more stellar spectra showed lines of Ca than molecules. Radial velocity measurements suggested a common place of origin for the H and K lines of CaII and the molecular lines. Unfortunately Adams only made qualitative estimates of the intensity of the spectral lines, a point later corrected by Frisch 1972 (4) who re-measured some of Adams' plates and calculated column densities for CH and CH^+ in 30 stars using the curve of growth method devised by Stromgren 1948 (110).

4.2 OPTICAL OBSERVATIONS SINCE 1950

After the work by Adams there was a lull in optical observations. Routly and Spitzer 1952 (265) confirmed the distinct nature of interstellar clouds from observations of interstellar sodium and calcium. They measured the equivalent width and radial velocities for the D lines of NaI and the H and K lines of CaII toward several stars.

Rogerson, Spitzer and Bahng 1959 (44) used a high dispersion photoelectric spectrophotometer to obtain the equivalent widths of CH^+, at 4232Å, toward nine stars. Observational work on CN has been even less intensive in recent years when compared with the work on CH and CH^+. Munch 1964 (57) observed CN in a group of stars embedded in an emission nebula near the cluster NGC 7822, and Peimbert 1968 (59) has observed CN in stars toward the galactic plane. Herbig 1968 (54) in his paper on the bright star ζ Oph detected Na, CaII K, CH, CH^+ and CN. He also obtained upper limits for OH, NH and CO^+. Since Herbig's work the ζ Oph clouds have become the most intensively studied region of the diffuse interstellar medium using optical and ultraviolet spectroscopy. He analysed the strongest component at -1 Km sec^{-1} (LSR) to obtain the first complete set of data on the atomic and molecular composition of a specific interstellar cloud. ζ Oph exhibits a strong interstellar absorption spectrum which makes high resolution spectroscopy easy, the area surrounding the star being strewn with irregular patches and lanes of dark material. Black and Dalgarno 1977 (78) have suggested a model for the ζ Oph cloud based on gas phase chemical reactions. This model reproduces the abundances of CH, HD, OH, CO and CN but seriously under estimates the abundance of CH^+.

Frisch 1972 (4) re-measured 30 spectrograms taken by W.S. Adams for the equivalent widths of the CH and CH^+ lines. Her catalogue and subsequent correlations between molecular species was the first attempt since the work of Adams to examine a large body of data from which a chemical scheme could be derived. The next piece of optical work was carried out by Hobbs 1973 (51).

The 4232Å line of CH^+ was detected toward 28 stars using the Photoelectric Pressure Scanned Interference Optical Spectrometer or PEPSIOS of Yerkes Observatory at the coudé focus of the 107

inch telescope of McDonald Observatory. The PEPSIOS spectrometer is a versatile easily portable purely interferometric high resolution short range scanning instrument consisting of an interference filter and several simultaneously pressure swept Fabry Perot etalons in series. (Mack et al 1963 (305)).

The survey of Hobbs was unusual at the time in two respects,

1. He made photoelectric measurements of the intensity of the spectral lines, instead of using the photographic techniques (although photoelectric measures are now common) and

2. The CH^+ column densities were calculated from the fundamental relationship

$$\frac{N\pi e^2}{mc} f = N\int_0^\infty \alpha_\nu \, d\nu$$

$$= \int_0^\infty (-\log_e r_\nu) \, d\nu \qquad (4.1)$$

where α_ν = Absorption coefficient

r_ν = Residual intensity

Cohen 1973 (13) has made measurements of CaII, Na, CH and CH^+ in 30 stars. This survey which includes information on radial velocities has been used as the basis for a radio survey by Zuckerman and Turner 1975 (188). Cohen was unable to detect CN in any of the stars observed. However in a separate survey Blades and Bennewith 1973 (6) and Blades 1978 (25) have observed CN in the direction of the O type super giant HD 154368.

Chaffee 1974 (7), 1975 (47) has observed optical interstellar lines in the Perseus 2 cloud and in Ophiuchus. In the Perseus cloud CH, CH^+ and CN were detected, although the molecular and atomic constitution of the cloud was found to be rather heterogeneous varying by up to a factor of 10 from place to place. In the second study radial velocity differences of the order of 1km sec^{-1} were found to exist between CH and CH^+ toward four

stars in Ophiuchus. This is indicative of CH and CH^+ formation under different physical and chemical conditions. In a further survey Chaffee and Dunham 1979 (1) looked at four stars in the Cepheus OB2 association. CH and CH^+ column densities were found to be typical of diffuse clouds. CN was observed toward 3 stars, consistant with CN formation through exchange reactions involving CH and CH^+. Frisch 1979 (23) (Figure 24) examined the interstellar material in front of χOph in a piece of work similar to the work by Herbig on ζ Oph. She found both CH and CH^+, but with radial velocities that differed by 2 Km sec^{-1}. No CN was detected. Two more recent studies on particular lines of sight are those by Crutcher 1985 (326) toward HD 29647 and by Crutcher and Chu 1985 (348) toward HD 147889.

A survey by Federman 1980 (105) of molecules in the lines of sight toward ζ Per, o Per and ξ Per revealed a shift in velocity between CH and CH^+ (Figure 25). The observations confirm the predictions of the chemical model formulated by Elitzur and Watson 1978 (115), 1980 (60) which requires the presence of an interstellar shock to reproduce the observed amount of CH^+. Further work by Federman 1982a (126) on the diffuse interstellar gas near the Pleiades also shows evidence for a moderately strong shock of velocity 10-15 Km sec^{-1} for the line of sight toward 20 Tau where the CH line is blue shifted by 3-4 Km sec^{-1} with respect to the CH^+ line.

Federman 1982b (30) in a larger survey has observed CH and CH^+ in directions with known amounts of atomic and molecular hydrogen. Both radicals were detected only in directions with substantial amounts of interstellar molecular hydrogen. The CH line is shifted typically 2 to 3 Km sec^{-1} from the CH^+ line in 50% of the cases observed favouring a model that incorporates the presence of a shock, where CH^+ is formed in the hot post shock gas and CH is

Figure 24

INTERSTELLAR SPECTRAL LINES TOWARD CHI OPHIUCHI

(From Frisch 1979)

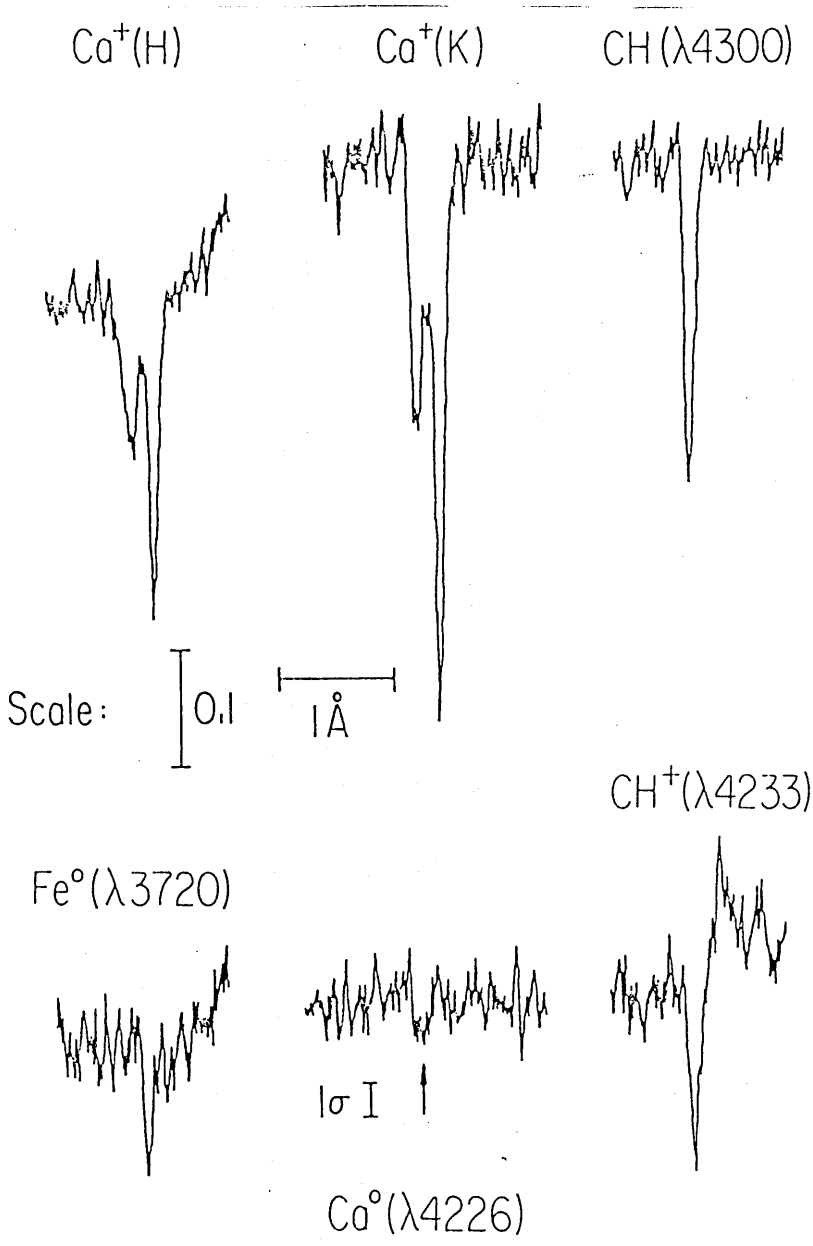

Figure 25

ABSORPTION SPECTRA of CH and CH^+ TOWARD THREE STARS

(From Federman 1980 and 1982a)

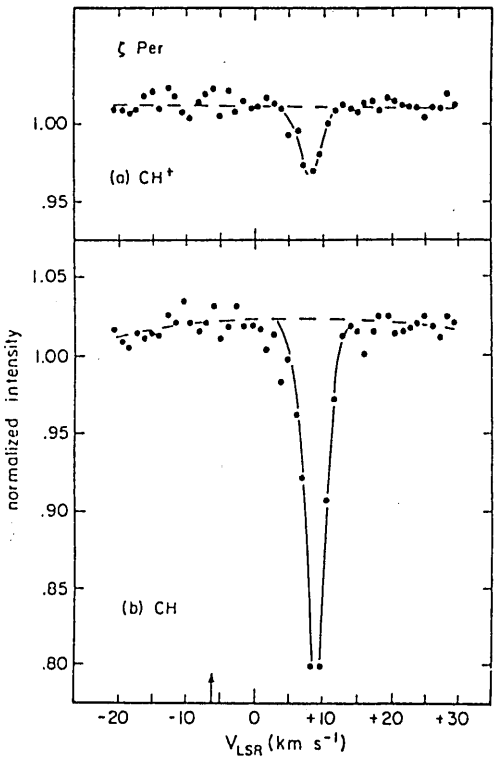

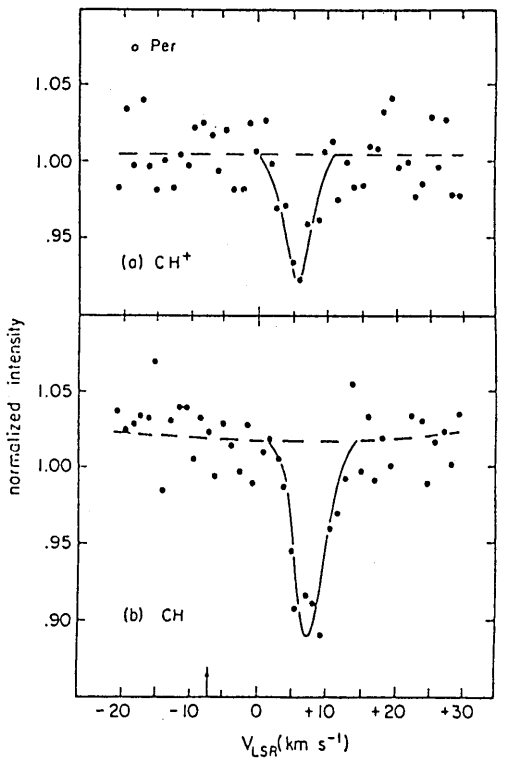

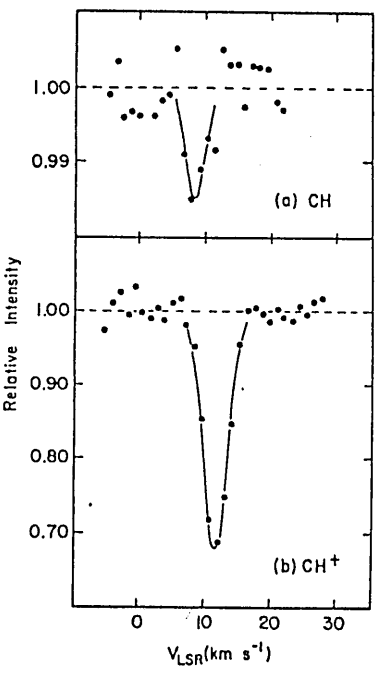

formed in the compressed cooled post shock gas. The observed correlation between CH and H_2 is consistent with their occupying the same volume in space. Protection from the interstellar ultraviolet radiation field is necessary for both molecules. Danks, Federman and Lambert 1984 (152) have made a further survey of CH at 4300 Å for 29 lines of sight in the galactic plane (Figure 26). A comparison of CH and H_2 column densities shows that they are proportional to one another. This would seem to confirm the reaction sequence

$$C^+ + H_2 \longrightarrow CH_2^+ + h\nu \qquad (1)$$

$$CH_2^+ + e^- \longrightarrow CH + H \qquad (2)$$

for the formation of CH. (See Black and Dalgarno 1973 (29), and the results from this study, which confirm this result). Federman, Danks and Lambert 1984 (283) have made a further survey of the $B^2\Sigma^+ - X^2\Sigma^+$ lines of CN toward 15 stars. (Figure 27). From this they have determined the relationship.

$$\text{Log N (CN)} \propto m \text{ Log N } (H_2) \qquad (4.2)$$

where $m = 3$.

This result is reproduced by a reaction network in which CN is produced primarily from C_2 by the neutral-neutral reaction

$$C_2 + N \longrightarrow CN + C \qquad (3)$$

(see the results at the end of this thesis).

and photodissociation is the main destruction pathway for the neutral molecules CH, C_2 and CN. Their survey is the first substantial work published on CN for some time. Other observations of CN have been carried out in order to determine the cosmic microwave background temperature. A list of these is given in section 3.6, table 25. The most recent observations are those of Meyer & Jura 1984 (281) and 1985 (381) who observed CN toward ζ Oph, ζ Per and o Per, and Crane 1986 (511).

Further work on stars in the Pleiades cluster has been carried out

Figure 26

THE INTERSTELLAR SPECTRAL LINE of CH at 4300.3Å

(From Danks et al 1984)

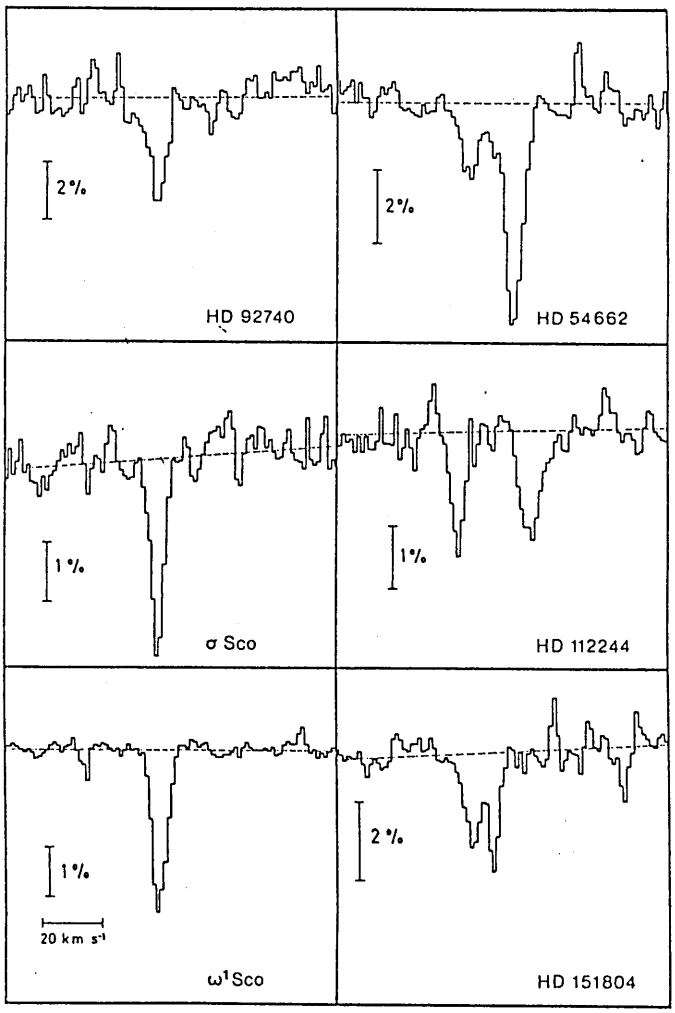

Figure 27

INTERSTELLAR SPECTRAL LINES of CN TOWARD CHI OPHIUCHI

(From Federman, Danks and Lambert 1984)

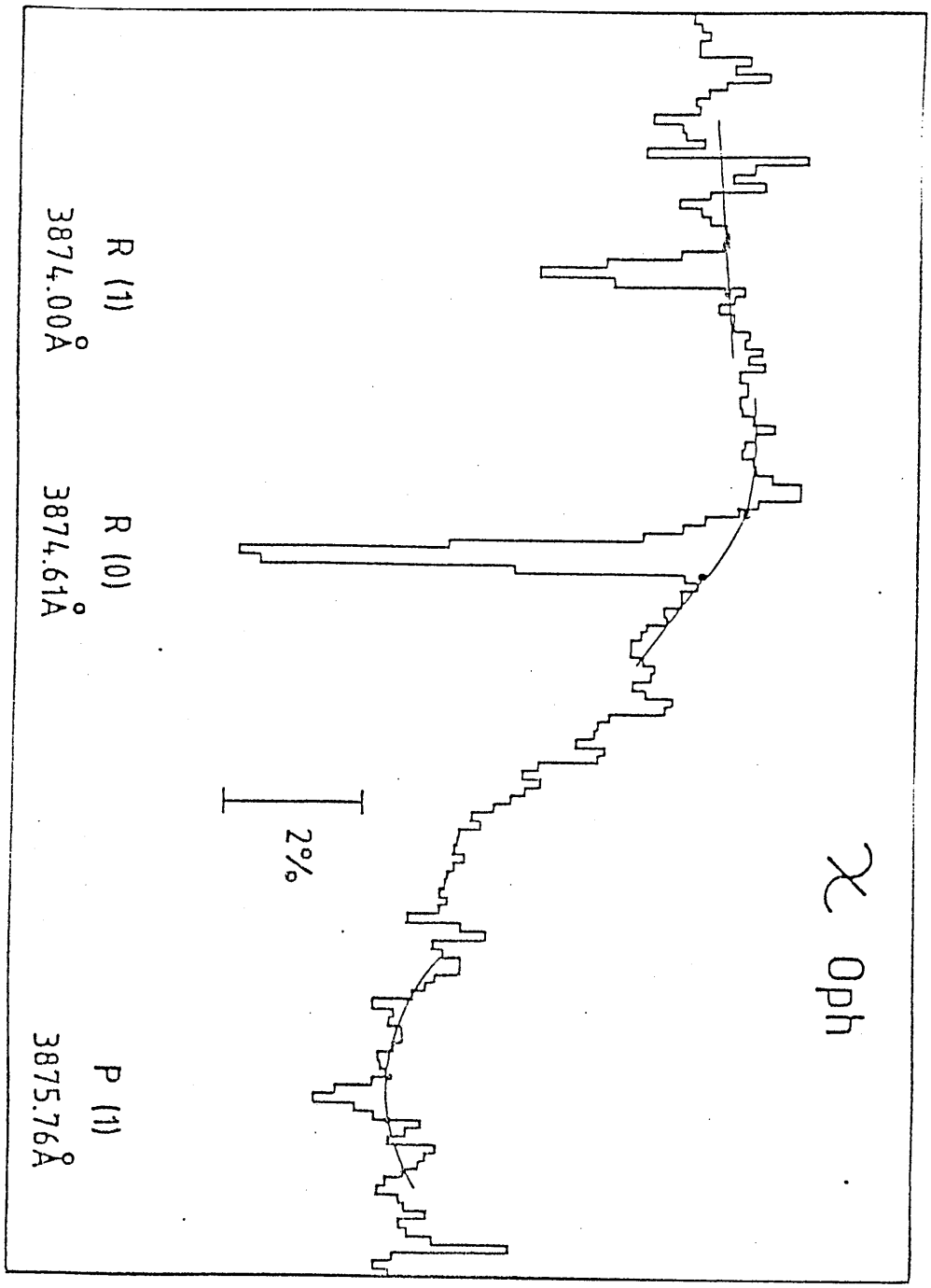

by White 1984 (392). From observations of Ca^+ and CH^+, it is concluded that the Ca^+ absorption occurs in the atomic gas at +7 Kms^{-1}(LSR) and that the CH^+ absorption occurs in the molecular gas within the cluster, at +10Kms^{-1} (LSR). Measurements have been made for 15 stars, column densities are given for CH^+ and upper limits given for CH and CN.

Other recent measurements on CH^+ are given by Lambert and Danks 1986 (405) who surveyed 65 lines of sight in the southern milky way, yielding 30 detections. The CH^+ column density is well correlated with rotationally excited H_2 detected by surveys with the Copernicus satellite. This is strong evidence that CH^+ is formed in warm gas where the reaction $C^+ + H_2 \longrightarrow CH^+ + H$ is effective. Shocks probably provide the necessary heating.

Further work by Cardelli & Wallerstein 1986 (446) on four stars embedded in the ρ Oph dark cloud complex has shown that $N(CH) \propto N(H_2)$ and for two lines of sight the relationship $N(CN) \propto N(H_2)^3$ is extended to reddenings as high as E(B-V) = 0.7. This does not extend to higher values of E(B-V) though, where CN is found to be under abundant by a factor of at least 10. Observations of CH, CH^+ and CN were made.

Another molecule observed using optical techniques is C_2. In some examples of recent surveys, Danks and Lambert 1983 (195) observed C_2 toward stars in the Ophiuchus cloud, van Dishoeck and de Zeeuw 1984 (212) searched for lines of the (2.0) Phillips band at 8750Å in the spectra of several southern stars (figure 28), Hobbs, Black and van Dishoeck 1983 (147) found C_2 in the spectrum of HD 29647 a star lying behind a substantial part of the Taurus molecular cloud complex, Chaffee et al 1980 (165) detected C_2 toward ζ Per (Figure 29), and Gredel & Munch 1986 (408) found C_2 lines in the spectra of southern reddened supergiants. The column densities determined for C_2 vary widely, mainly because of the lack

Figure 28

THE ABSORPTION SPECTRUM of C_2 TOWARD HD 154368

(From van Dishoeck and de Zeeuw 1984)

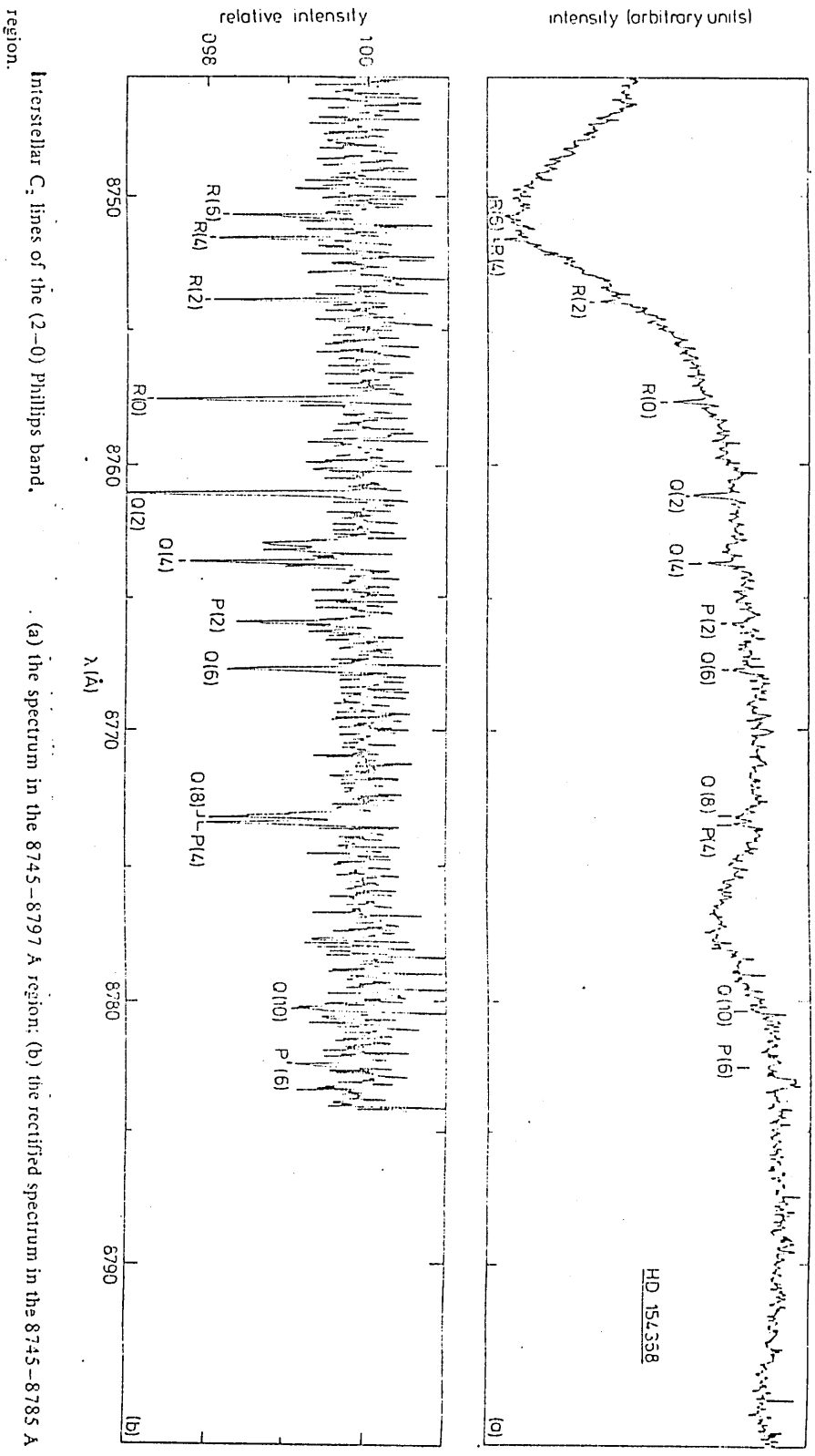

Interstellar C_2 lines of the (2–0) Phillips band. (a) the spectrum in the 8745–8797 Å region; (b) the rectified spectrum in the 8745–8785 Å region.

Figure 29

SPECTRUM of INTERSTELLAR C_2 TOWARD ZETA PERSEI

(From Chaffee et al 1980)

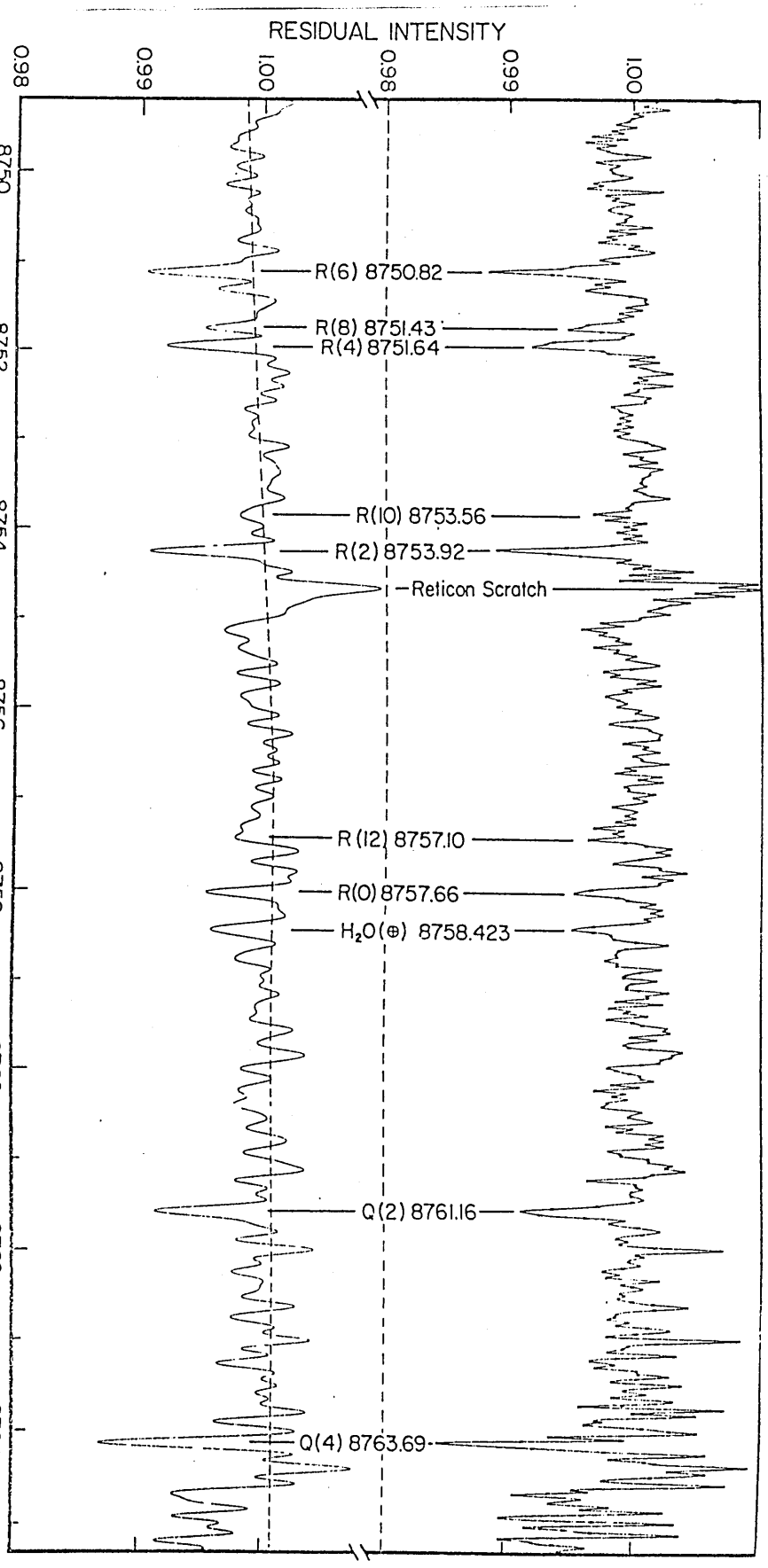

Raw data (*upper curve*) and smoothed spectrum (*lower curve*) for interstellar lines of the 2-0 Phillips band of C_2 toward ζ Per. Laboratory wavelengths are given on the abscissa.

of an agreed oscillator strength for the Phillips band at 8750Å which is the molecular band most often observed.

A search for the C_3 molecule by Clegg and Lambert 1982 (123) was unsuccessful. The molecular band at 4050Å (Gausset et al 1965 (494)) was not detected. A catalogue of carbon bearing diatomic molecules, that includes many of the CH, CH^+ and CN observations listed here has been given by Dickman, Somerville et al 1983(151).

There have been few observations of other molecular species at optical wavelengths as most molecules have their strongest absorption bands in the ultraviolet. A notable exception is the work by Crutcher and Watson 1976 (113) who observed the 3078Å line of OH toward o Per and ζ Oph. In a further paper (Crutcher and Watson 1976a (74)), they obtained an upper limit for the NH molecule toward o Per using the line at 3358Å. The absence of any appreciable amount of NH in a direction towards which OH has been detected is evidence in favour of a purely gas phase reaction scheme for molecules other than H_2, since NH would be expected to be as abundant as OH if reactions on grain surfaces dominate. Blades 1975 (58) in an earlier search for OH and NH was unable to detect either species.

Molecular ions are not as abundant as free radicals in the interstellar medium. Ferlet et al 1983 (148) claimed a tentative detection of CS^+ toward ζ Oph and δ Sco, however more recent work by Ferlet et al 1986 (532) does not confirm this result. Upper limits for CS^+ toward ζ Oph and ζ Per are given in the later paper. A search for H_2O^+ toward four stars by Smith, Schempp and Federman 1984 (211) gave significant upper limits for testing existing chemical models. Upper limits for the visible wavelength lines of CO^+ have been measured by Herbig 1968 (54) toward ζ Oph and by Crutcher 1985 (326) toward HD 29647.

Two other rich sources of optical molecules, are Comets (Arpigny 1965(380), Whipple & Huebner 1976 (379)) and the Night glow (Ingham 1962 (404)), the spectra of which show the molecules CO^+, N_2^+, H_2O^+ and OH.

4.3 SATELLITE OBSERVATIONS

The number of atoms and molecules that can be studied using optical techniques in the visible region of the spectrum is few as most species have their spectral lines in the ultraviolet which is cut off by absorption by ozone and other molecules in the Earth's atmosphere. So many transitions are in the ultraviolet because of the low temperature in the interstellar medium; this means that all interstellar electronic transitions are from the ground state. Only two atoms produce sufficiently strong absorption to permit intensive study. One is neutral sodium NaI and the other is singly ionised calcium CaII. Both produce strong interstellar absorption features in the spectra of hot stars. The interstellar lines are easy to distinguish from stellar lines, since sodium and calcium are highly ionised in the atmospheres of hot stars, so there is little absorption by NaI or CaII there. Each atom gives rise to a doublet, the sodium D lines at 5890Å and 5896Å, and the H and K lines of CaII in the violet at 3968Å and 3934Å respectively.

As these lines lie in the region that is accessible to ground based optical telescopes these two atoms have been used to study the interstellar medium since Hartmann first observed CaII in interstellar space at the turn of the century. Magnesium and iron also have visible absorption lines produced by neutral atoms in their ground state. Unfortunately both elements are easily ionised so that detection of these transitions is extremely rare. This is the case for most atoms except for NaI and CaII.

A similar picture is true for the observation of molecules. Only CH, CH^+, CN, C_2, OH and NH are observable at ground based optical wavelengths. The important spectral lines for these molecules all lie within the range 3000Å to 9000Å.With theexception of C_2, they all lie toward the blue end of the visible range. The OH radical also has lines in the ultraviolet, particularly the line at 1222Å. Other molecules of interest whose strongest lines lie in the ultraviolet part of the spectrum include H_2, HD, H_2O, HCl, N_2 and CO.

A great many atoms and molecules absorb radiation at wavelengths too short to permit passage through the ozone layer in our atmosphere because in the ground state the energy gap to the first excited level is too large for a visible photon. However ultraviolet photons with wavelengths between 920Å and 3000Å will excite most molecules.

Early observations in the ultraviolet were made with the aid of sounding rockets. Carruthers 1970 (72) used an Aerobee 150 rocket to fly a spectrograph that detected H_2 toward ϵ Per and ξ Per. Later Smith and Stecher 1971 (43) and Smith 1973 (100) detected CO towards ζ Oph and δ Sco using rocket borne instruments.

4.3.1. THE SATELLITES

The next step was to have a permanent orbiting observatory. Copernicus, the fourth Orbiting Astronomical Observatory (OAO 4) was launched by NASA on 21st August 1972 using an Altas Centaur rocket into a circular orbit 750 Km above the Earth. The satellite carried a 32 inch telescope-spectrometer for accurate measurements of the absorption of starlight by atoms and molecules in interstellar space. The instrument was designed by Princeton University and operated through the NASA Goddard Space Flight Center. Once on each orbit around the Earth the satellite established radio contact with one of several ground stations, transmitted all the data recorded, and received any commands for the next orbit. The Copernicus satellite performed perfectly apart from unexpectedly high noise levels in the phototubes used for the wavelength range 1600 to 3200Å. Satellite operations were finally terminated on 15th February 1981. By this time the sensitivity of the instrument at wavelengths between 1000Å and 1600Å had seriously declined making useful measurements difficult except for very bright stars. During its 8 year life however, Copernicus made an important contribution to ultraviolet astronomy and to our knowledge of the interstellar medium in particular. The OAO programme has been reviewed by Spitzer 1982 (257).

Copernicus was followed by another ultraviolet satellite, the International Ultraviolet Explorer (IUE) (Figure 30). This satellite is a joint NASA - ESA - UK project and consists of a 45 cm telescope and echelle spectrograph combination to measure the ultraviolet spectra of stellar objects.

Figure 30

THE INTERNATIONAL ULTRAVIOLET EXPLORER SATELLITE (IUE)

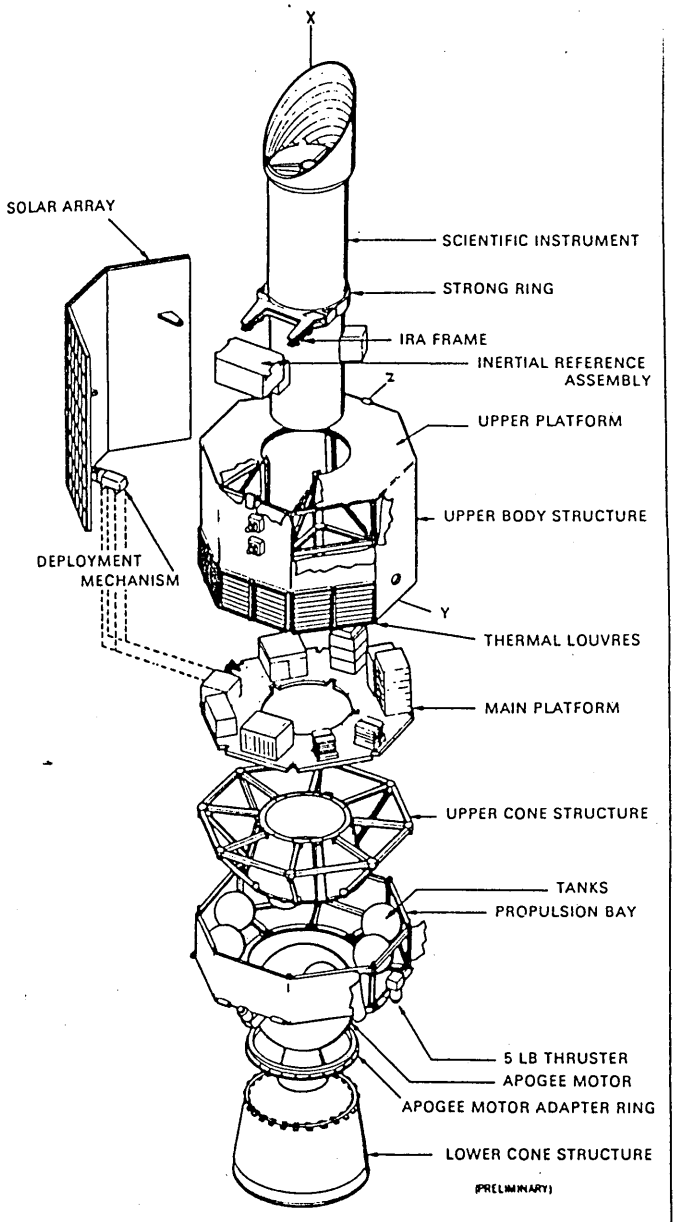

The satellite was launched on 26th January 1978 from Cape Canaveral in Florida USA using a Delta launch vehicle, into a geosynchronous orbit with a mean position over South America. This meant that the satellite was visible at all times from either ESAs ground station at Villafranca near Madrid, Spain or NASAs Goddard Space Flight Center. The orbit was also chosen because the Earth subtends an angle of 17^{o} as seen by the telescope and the area of sky available at any given time is much greater than from lower orbits or from the ground. A geosynchronous orbit also has the advantage that as the satellite moves along the ecliptic at the diurnal rate, the occurence of occulations is infrequent. Consequently over large portions of the sky neither long exposures nor the observation of variable phenomena need be interrupted. The penalty is that the observations are made in full sunlight so the telescope must be baffled to ensure adequate rejection of stray sunlight and earthlight. Astronomers working at the two ground stations are able to record and study ultraviolet spectra in near real time, allowing decisions to be made about the observing programme as it develops. The scientific aims of IUE call for high resolution spectra (0.1Å) of bright objects and low resolution spectra (6Å) of fainter objects. In order to measure the equivalent widths of molecular lines a resolution of 0.2Å is required. Due to the design of the imaging system in order to achieve adequate resolution the total spectrum is split into two ranges from 1165Å to 2126Å and 1845Å to 3230Å for high dispersion and from 1150Å to 2000Å and 1825Å to 3300Å for low dispersion, (see reference 342), so that two cameras are required to record the full spectrum.

The telescope is of Ritchey Chrétien design and focuses light onto either the shortwave or longwave spectrograph which produces a raster like echelle spectrum. A spectrograph with echelle optics gives a compact spectral format with high dispersion. Since the echelle image consists of many adjacent spectral orders displayed in a closely spaced array it makes efficient use of the field of view of a television camera onto which the final image is then focused. The camera consists of a S.E.C. vidicon tube preceded by an ultraviolet to visible converter and associated electronics. The spacecraft, its instrumentation and in flight performance has been reviewed by Macchetto and Penston 1978 (234), Boggess et al 1978a (249) and Boggess et al 1978b (250), and the image processing by Golton and Dunford 1979 (239).

4.3.2. ULTRAVIOLET SATELLITE OBSERVATIONS

1. COPERNICUS (OAO4)

The ultraviolet survey by Morton 1975 (11) of atoms and molecules in the line of sight toward ζ Oph was the first study on a particular cloud since the ground based optical work of Herbig. Only the molecules H_2, HD and CO were detected, but useful upper limits for several other molecular species were obtained. Jenkins et at 1973 (53) also failed to find any other molecules except CO, in a survey of four stars for molecules other than H_2 and HD using the Copernicus satellite. Other observations, in the direction of the Ophiuchus clouds, are those by Frisch 1980 (55) who observed the $C^1\Sigma^+ - X^1\Sigma^+$ band of CO at 1087Å as well as lines due to H_2. Also Wannier, Penzias and Jenkins 1982 (179) who detected the $A^1\Pi - X^1\Sigma^+$, $B^1\Sigma^+ - X^1\Sigma^+$ and $C^1\Sigma^+ - X^1\Sigma^+$ transitions of ^{12}CO and the $A^1\Pi - X^1\Sigma^+$ transition of ^{13}CO toward ζ Oph. These are shown in figure 31. Snow and Jenkins 1980 (48) found CO toward six stars in the ρ Ophiuchi cloud complex, whilst Snow 1975 (8) in an earlier survey of the line of sight to o Per, which is embedded in the near edge of a dense molecular cloud found lines due to CO, H_2, HD and possibly OH. Another survey by Snow 1977 (56) of the line of sight to ζ Per which lies in the Perseus II complex found absorption lines of the same molecules. Smith, Krishna Swamy and Stecher 1978 (21) have detected CO in the spectrum of ζ Oph and suggest that the strongest interstellar component is part of a supernova remnant (Figure 32). Perhaps the most comprehensive survey on CO using Copernicus has been the work done on CO in diffuse clouds by Federman et al 1980 (27). They detected the

Figure 31

COPERNICUS SPECTRA of ^{12}CO and ^{13}CO TOWARD ZETA OPHIUCHI

(From Wannier, Penzias, and Jenkins 1982)

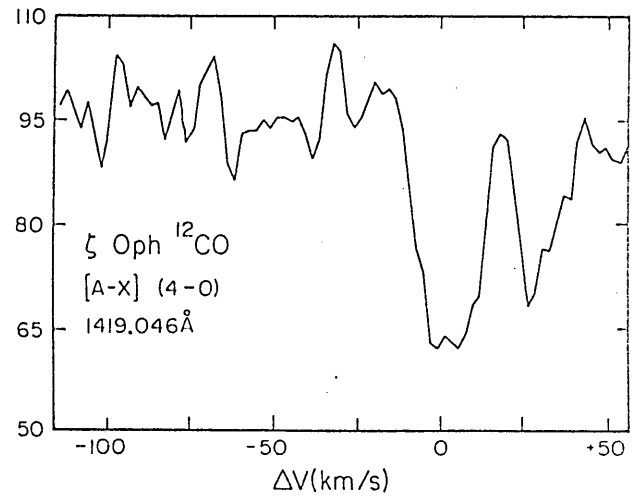

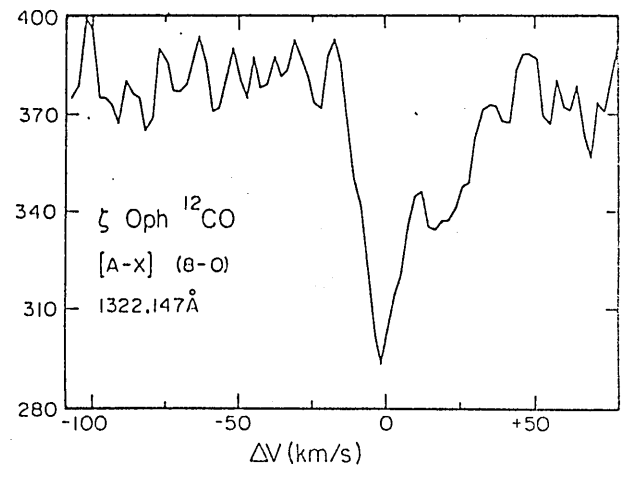

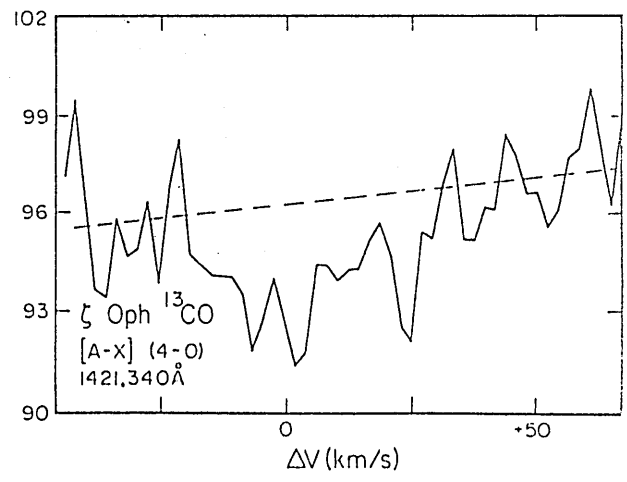

Figure 32

COPERNICUS SPECTRA of CO TOWARD ZETA OPHIUCHI

(From Smith, Krishna Swamy, and Stecher 1978)

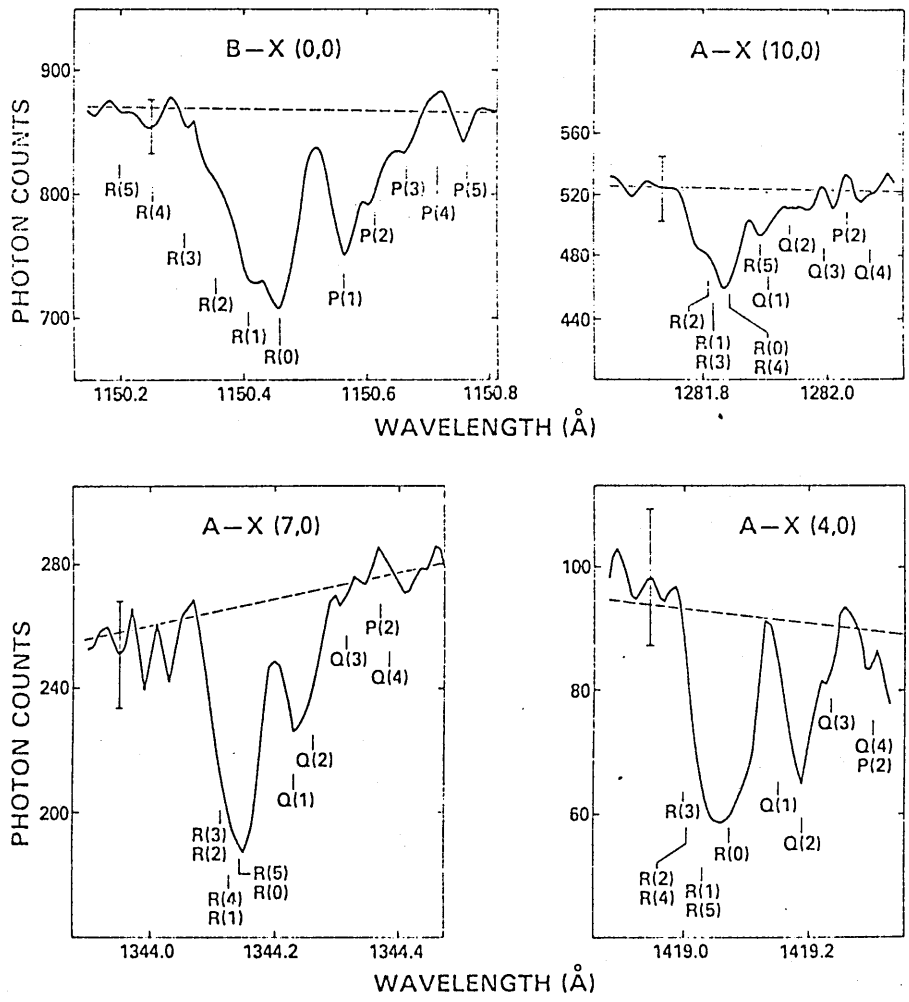

$C^1\Sigma^+ - X^1\Sigma^+$ band at 1087Å and the $E^1\Pi - X^1\Sigma^+$ band at 1076Å toward 17 of the 48 bright stars studied and obtained upper limits for a further 21. The CO column densities were in the range 10^{12} to 10^{15} cm^{-2} and correlated well with those of CI and H_2, the overall trend of the ultraviolet observations being in accord with gas phase chemistry.

A primary objective of the ultraviolet spectrometer on the Copernicus satellite was the detection of interstellar molecular hydrogen. Early work by Spitzer et al 1973 (87) detected H_2 and HD in several stars, and this was followed by a larger survey of 28 stars showing the (00) to (50) Lyman bands of H_2, (Spitzer, Cochran & Hirshfeld 1974 (107)). The survey by Savage et al 1977 (70) detected H_2 in the J = 0 and J = 1 rotational levels of the V^{11} = 0 vibrational state (Figure 33). In most cases the H_2 spectral lines exhibited strong damping wings and the column densities were derived by fitting damping profiles to the observed spectra. For stars with strong H_2 lines N(J = 0) + N(J = 1) is a good measure of $N(H_2)$ the total H_2 column density. A complementary survey of atomic hydrogen using the Lyman alpha line at 1216Å has been reported by Bohlin et al 1978 (71). This has allowed the total hydrogen column density to be calculated toward over 100 stars using the formula,

$$\begin{aligned} N \text{ total} &= N \text{ atomic} + N \text{ molecular} \\ N(H + H_2) &= N(H) + 2\,N(H_2) \end{aligned} \qquad (4.3)$$

The observational work has been continued by Bohlin et al 1983 (135) who give values for H and H_2 column densities toward 29 stars not previously observed.

Figure 33

COPERNICUS SPECTRA of MOLECULAR HYDROGEN TOWARD ZETA OPHIUCHI and PHI 1 ORIONIS

(From Savage, Bohlin, Drake, and Budich 1977)

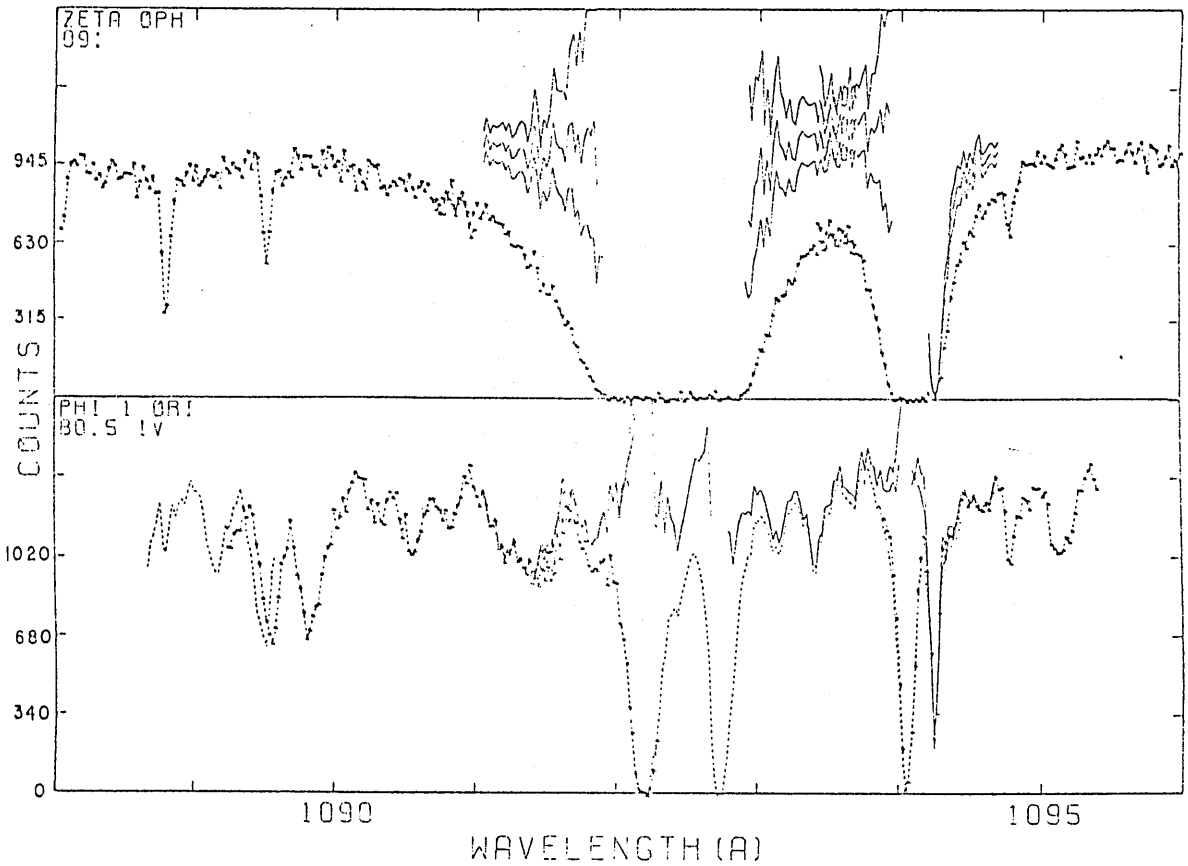

High-resolution (U1) scans of the H_2 (1, 0) Lyman lines for ζ Oph and ϕ^1 Ori corrected for stray and scattered light.

Figure 34

SPECTRA of H_2 and HD TOWARD ZETA OPHIUCHI

(From Wright and Morton 1979)

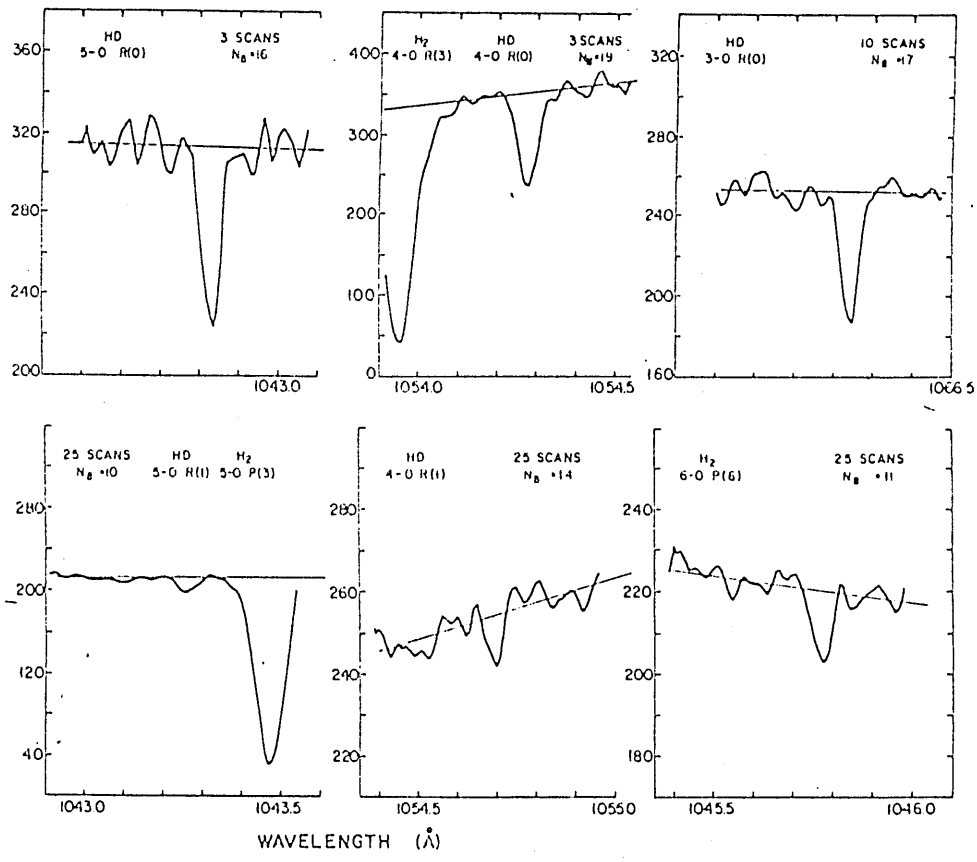

Other molecules observed using Copernicus include HCl, upper limits of which were obtained toward 10 stars by Jura & York 1978 (117) and toward ζ Oph by Wright and Morton 1979 (194). Wright and Morton also detected H_2 and HD, the spectra of which are shown in figure 34. Upper limits for N_2 toward ζ Sco and ϵ Per are given by Lutz, Owen & Snow 1979 (119). Searches for the UV lines of OH have been carried out by Snow 1976 (183), for OH and H_2O by Smith and Snow 1979 (5) and for H_2O by Snow and Smith 1981 (120). Jenkins et al 1973 (53) give an upper limit for the ultraviolet line of CO^+ in the line of sight to X_1 Persei.

2. INTERNATIONAL ULTRAVIOLET EXPLORER (IUE)

Unfortunately molecular hydrogen is not observable using the IUE satellite, because its spectral range does not reach to the major lines of H_2 below 1100Å. However, an important observable molecule is CO. The Tata Institute of Fundamental Research in India has published four papers on the observation of CO in celestial objects using IUE, Paper I (Tarafdar, Krishna Swamy and Vardya 1980 (41)) discusses the possibility that the CO detected toward 9Cep is circumstellar, the first observation of a molecule around a B star. Paper II by Tarafdar & Krishna Swamy 1981 (269) comes to a similar conclusion for CO toward ψ Per. A large study of CO in diffuse clouds is given in paper III, Tarafdar & Krishna Swamy 1982 (34) (See figure 35), whilst paper IV examines CO lines toward stars with low reddening, Tarafdar 1983 (268).
Other stars toward which CO has been detected are HD 102567 (de Loore et al 1981 (132)) and AE Aur

Figure 35

I.U.E. SPECTRA of ^{12}CO and ^{13}CO TOWARD HD 149404 and HD 152236

(From Tarafdar and Krishna Swamy 1982)

HD 149404

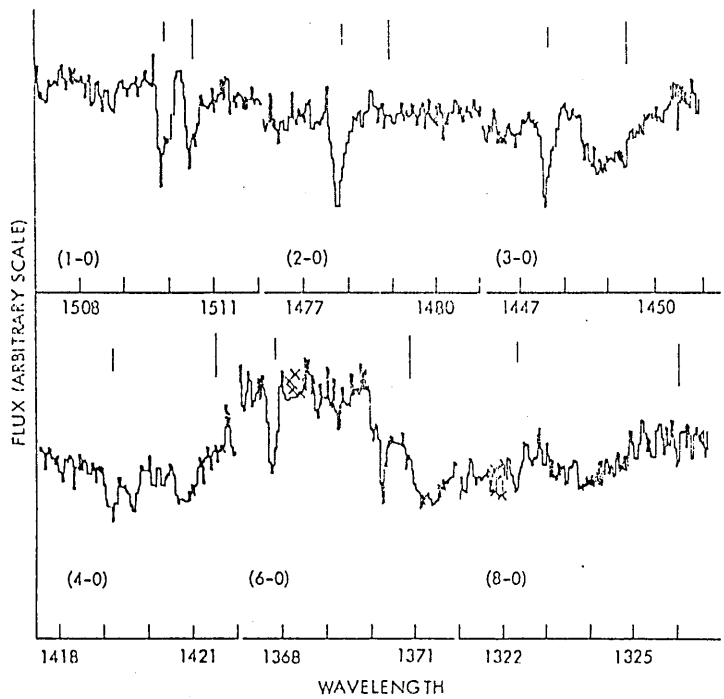

HD 152236

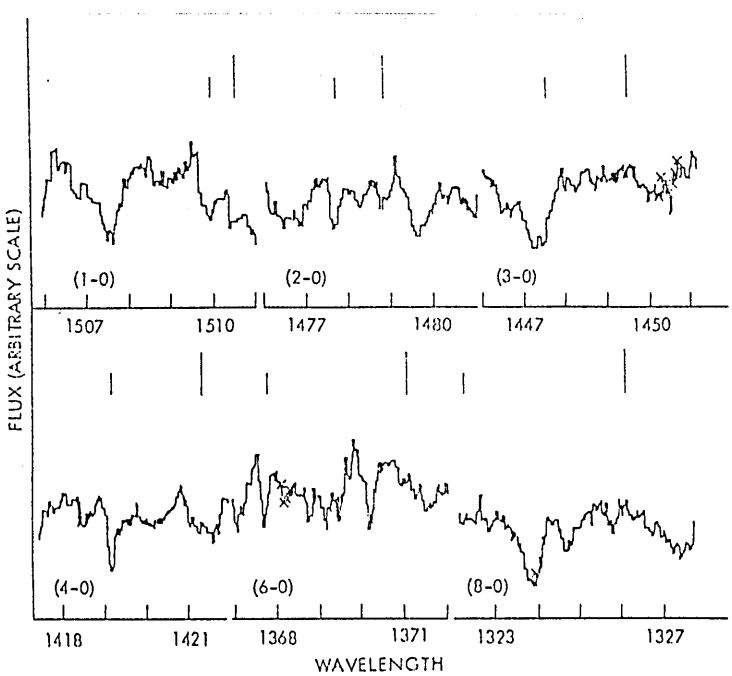

(McLachlan & Nandy 1984 (214)). Somerville et al 1982 (17) have observed CO in 16 of the 31 lines of sight examined in a study of diffuse clouds. This has since been expanded to 60 stars, with more than 30 detections of ^{12}CO and 10 of ^{13}CO (Somerville 1987 (387)). Black 1980 (14) in a similar survey detected CO in 12 of the 25 stars observed. However a search for lines due to CH, C_2, CH_2, OH, HCl and H_2O in one of these stars, HD 46223, proved negative except for a possible ultraviolet line of CH. At the time of writing, Pwa & Pottasch 1986 (515) have just published new observations of ^{12}CO and ^{13}CO toward ζ Oph and 9 Sgr. They give log N(^{12}CO) = 15.42 and Log N(^{13}CO) = 13.40 toward ζ Oph and Log N(^{12}CO) = 13.86 and Log N(^{13}CO) $<$ 13.3 toward 9 Sgr. Other molecules identified toward ζ Oph include OH, C_2, NO^+, HCl, SiO and a positive identification of NO, Log N(NO) = 13.42 in the -0.5 Km sec^{-1} (LSR) cloud.

In all of these studies lines of the fourth positive series of CO, the $A^1\Pi - X^1\Sigma^+$ band, have been observed. The spectrometer on the IUE satellite is unable to record the shorter wavelength lines of the $B^1\Sigma^+ - X^1\Sigma^+$, $C^1\Sigma^+ - X^1\Sigma^+$ and $E^1\Pi - X^1\Sigma^+$ bands also observable with Copernicus.

IUE has also been used to study molecules in comets. For example emission by OH in Halley's comet (Festou 1986 (436)).

4.4. OBSERVATIONS AT MICROWAVE FREQUENCIES

1. OH

The lambda doubling transition of OH was first detected in absorption by Weinreb et al 1963 (286) in dense cool clouds of dust and gas toward the radio source Cas A.

Two years later emission from OH radicals was observed in sources close to H II regions by Weaver et al 1965 (285). However the properties of the radiation were inconsistent with spontaneous emission from a gas in thermal equilibrium and it was soon appreciated that amplification by stimulated emission was taking place. For a comprehensive review of maser action in the OH molecule see Cook 1977 (308).

Despite its widespread occurrence in the interstellar medium few observations have been made of OH at radio frequencies in the diffuse clouds where OH is also observed at optical and ultraviolet wavelengths. Crutcher 1979 (191) has detected the 1667 MHz line of OH toward ζ Oph giving a column density of 8×10^{13} cm^{-2}, if the excitation temperature is 8K. This compares well with the optical result of 3×10^{13} cm^{-2} obtained by Crutcher and Watson 1976 (113). The OH radical has two velocity components at -0.6 Km sec^{-1} and 5.5 Km sec^{-1} (both LSR) in the line of sight to ζ Oph. The component at - 0.6 Km sec^{-1} corresponds to the most intense component of the ζ Oph clouds. Crutcher 1976 (40) has measured the 1667 MHz line of OH toward o Per, and Sancisi et al 1974 (223) have mapped the 1667 MHz line in the region of the Perseus OB2 dust cloud.

Observations of OH at submillimetre and far infrared frequencies towards the Orion nebula (M42) have been reported by Viscuso et al 1985 (376) and Viscuso et al 1985 (375).

2. <u>CH</u>

The three hyperfine components of the $X^2\Pi$ $J = \frac{1}{2}$ ground state Λ doublet of CH have been observed at radio

frequencies. Turner and Zuckerman 1974 (187) first observed one of the hyperfine components in emission toward Cas A at 3349.185 MHz. Later detection of all three lines (see Table 8) was made by Rydbeck et al 1974 (186) and Zuckerman and Turner 1975 (188). Rydbeck was unable to detect CH in directions in which it has been observed optically, for example χ Oph, ζ Oph, and 23 Tau. However, Zuckerman and Turner were able to detect lines toward three stars in the optical survey of Cohen 1973 (13); ζ Per, BD + 31° 643 and HD 147889. Most of the radio work has been directed toward extended sources in dense clouds, Mattila 1986 (471), Hjalmarson et al 1977 (189). Notable exceptions are the surveys by Lang and Willson 1978 (52) and Willson 1981 (64). They looked for CH emission (Figure 36) in the direction of bright stars which are associated with diffuse interstellar clouds and whose optical spectra show molecular lines. Federman and Willson 1982 (50) have measured the CH emission at 9cm toward the bright stars α Cam and κ Cas and from dark clouds near the stars reveal an association between diffuse clouds and dark clouds. For most lines of sight, diffuse clouds are the outer relatively transparent portions of dark clouds. Liszt 1979 (185) has detected radio CH toward ζOph, and Black et al 1974 (226) have detected 9cm emission due to CH in comet Kohoutek.

A mechanism for the excitation of CH has been given by Bouloy et al 1984 (231) in which collisions with atomic hydrogen are responsible for the overall inversion of the ground state Λ doublet.

Figure 36

EMISSION SPECTRA SHOWING THE 3335.5MHz LINE of RADIO CH

(From Willson 1981)

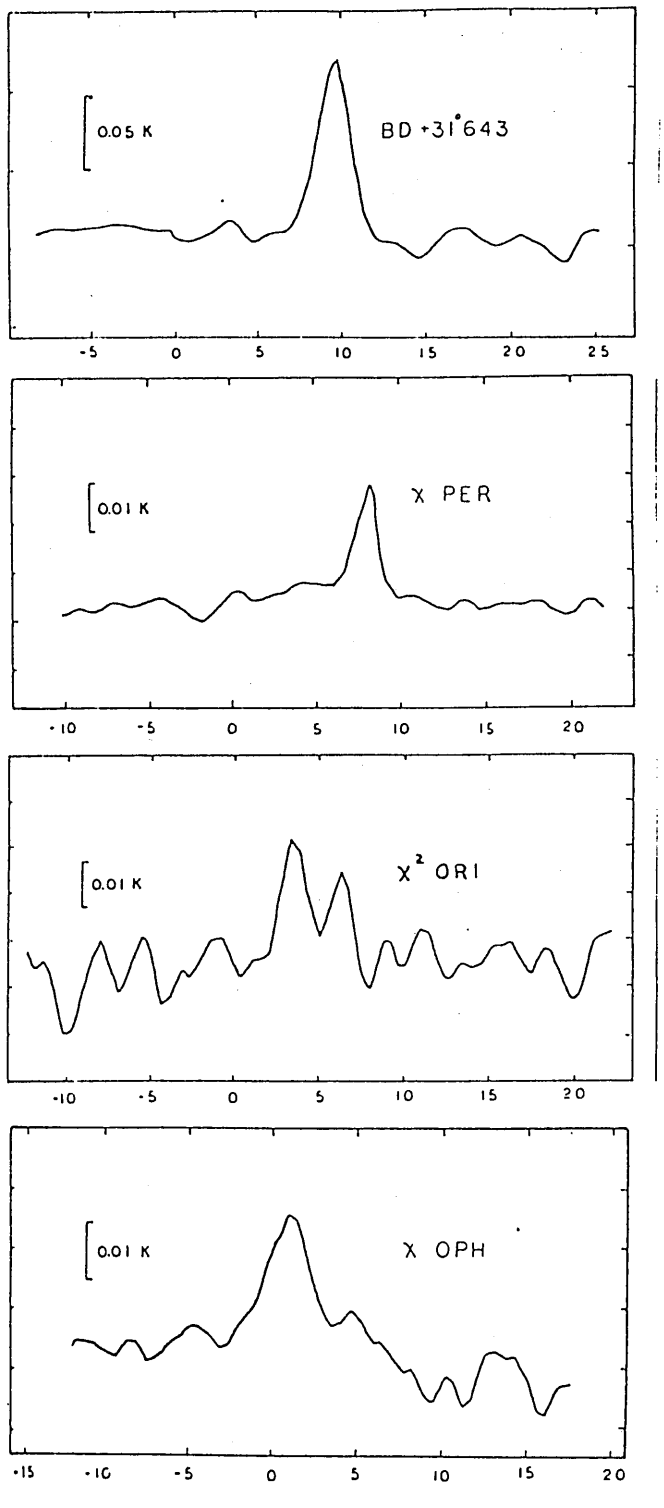

Work on transition frequencies for higher J values is continuing and may lead to radio observations of CH at frequencies in the far infrared as well as the microwave regions of the spectrum, Evenson et al 1971 (235) Brazier and Brown 1983 (171), Bogey et al 1983 (204), Brown and Evenson 1983 (220).

Ziurys et al 1983 (221) made a preliminary search for the $X^2\pi$ $J = {}^3/_2$ F_1 (first excited state) Λ doubling transition of CH at 700 MHz, based on the work of Brown and Evenson, who used laser magnetic resonance spectroscopy in a laboratory study on CH to yield transition frequencies with an accuracy of a few MHz. Although the results were negative, upper limits to the column densities for CH were of the same order of magnitude as those calculated from measurements of the ground state Λ doublet if the excitation temperature is $<$ 100- 700K. In a later paper (Ziurys & Turner 1985 (357)) Ziurys has reported the successful detection of the two main hyperfine components of the first excited state of CH toward W51 using the Arecibo 1000 ft radio telescope.

See also the submillimetre observations of CH in M42 made by Viscuso et al 1985 (376).

3. CO

The $J = 1 \longrightarrow 0$ radio frequency line of CO at 115,271.2 MHz was discovered in the direction of Orion by Wilson et al 1970 (102). Since then this line has been used to extensively map the extent of molecular clouds in the Galaxy. Few observations along optical lines of sight have been made. Crutcher 1976 (40) made radio observations of CO toward σ Per and ζ Oph. He found

that toward o Per the CO radio column density was an order of magnitude greater than the optical value. Toward ζ Oph the optical and radio measurements were in good agreement. Knapp and Jura 1976 (3) made radio measurements of CO in interstellar clouds that had previously been studied using optical spectral lines. Their results were consistent with a model in which CO is produced in gas phase reactions. Liszt 1979 (185) also detected CO emission toward ζ Oph and suggested that the conditions inside the ζ Oph cloud may be more rarified than is usually assumed. Further observations toward ζ Oph were made by Crutcher and Watson 1981 (280). They studied the $J = 1 \rightarrow 0$ transitions of ^{12}CO and ^{13}CO in order to derive the abundance ratio of the two carbon isotopes. ^{13}C is detected only in molecules and numerous observational studies have been performed mainly at radio frequencies in order to assess the Galactic $^{12}C/^{13}C$ ratio. The most recent survey of CO in diffuse clouds was carried out by Dickman et al 1983 (151). This study combined radio, optical and ultraviolet observations of carbon bearing diatomic molecules to produce the most comprehensive set of data available at the time. The column density of CO derived from the $J = 1 \rightarrow 0$ line agreed reasonably well with values for the same lines of sight calculated using the $J = 2 \rightarrow 1$ line and ultraviolet results from the IUE satellite.

4. CN

The radio frequency lines of the CN radical were first detected toward the Orion nebula and W51 by Jefferts et al 1970 (103) using the 11 metre radio telescope

of the National Radio Astronomy Observatory (NRAO) at Kitt Peak, Arizona, USA. Surveys of the diffuse interstellar medium for radio CN have been few. Turner and Gammon 1975 (2) detected CN in the direction of HD 21483 and possibly HD 154368 but were unable to detect CN along other lines of sight in which CN has been observed optically. Allen and Knapp 1978 (184) have observed several clouds with varying degrees of extinction but were unable to confirm Turner and Gammons detection of CN toward HD 21483. Other surveys (Churchwell 1980 (307), Crutcher et al 1984 (332)) have concentrated on dark clouds and molecular clouds associated with H II regions. The hyperfine components of the N = 1 - 0 transition are separated by more than typical line widths, but are close enough together that they can all be observed simultaneously in a single spectrum. Therefore their relative intensities can be obtained independent of calibration uncertainties. The hyperfine structure intensity ratios permit one to calculate the column density of CN in the N = 0 state. Since most CN is in the lowest rotational state, the total CN column density can be reliably estimated from the observed N = 1 - 0 transition. Recent reviews of the radio lines from interstellar molecules have been given by Zuckerman and Palmer 1974 (216), Somerville 1977 (33) and Somerville 1978 (232).

PART 2

TABLES OF OBSERVATIONS

AND CORRELATIONS BETWEEN MOLECULES

1. TABLES OF OBSERVATIONS

TABLE 26 DETAILS OF STARS

STAR	HD	RA (2000)	DEC (2000)	Sp	V	B-V	E(B-V)	M_V	d(pc)
		h m s	o ' "						
88 γ Peg	886	0 13 14.1	+15 11 01	B2 IV	2.83	-0.23	0.01	-3.0	150
15 κ Cas	2905	0 32 59.9	+62 55 55	B1 Ia	4.16	0.14	0.33	-6.6	930
22 o Cas	4180	0 44 43.4	+48 17 04	B2 V	4.54	-0.07	0.17	-2.5	210
27 γ Cas	5394	0 56 42.4	+60 43 00	B0 IVe	2.47	-0.15	0.15	-4.6	240
α Eri	10144	1 37 42.9	-57 14 12	B5 IV	0.46	-0.16	0.00	-1.6	26
φ Per	10516	1 43 39.6	+50 41 20	B1 IVpe	4.07	-0.04	0.22	-3.9	350
-	12953	2 08 40.4	+58 25 26	A1 Ia	5.67	0.61	0.58	-7.3	1900
φ Eri	14228	2 16 30.6	-51 30 44	B8 V	3.56	-0.12	0.00	-0.2	37
9 Per	14489	2 22 21.3	+55 50 45	A2 Ia	5.17	0.37	0.32	-7.5	2400
-	14633	2 22 54.2	+41 28 49	O8-9V	7.46	-0.21	0.10	-4.9	2570
-	20041	3 15 47.9	+57 08 27	A0 Ia	5.79	0.73	0.71	-7.1	1500
-	21278	3 28 03.0	+49 03 46	B3 V	4.98	-0.10	0.10	-1.7	200
-	21291	3 29 04.1	+59 56 25	B9 Ia	4.21	0.41	0.41	-7.1	1100
-	21389	3 29 54.8	+58 52 44	A0 Ia	4.54	0.56	0.54	-7.1	1100
-	21483	3 28 46.5	+30 22 32	B3 III	7.06	0.36	0.56	-2.9	460

STAR	HD	RA (2000)	DEC (2000)	Sp	V	B-V	E(B-V)	M_V	d(pc)
		h m s	o ' "						
-	21856	3 32 39.9	+35 27 42	B1 V	5.90	-0.06	0.20	-3.5	640
37 ψ Per	22192	3 36 29.3	+48 11 34	B5 Ve	4.23	-0.06	0.10	-0.9	92
39 δ Per	22928	3 42 55.4	+47 47 15	B5 III	3.01	-0.13	0.03	-2.2	100
40 Per	22951	3 42 22.5	+33 57 54	B0.5 V	4.97	-0.01	0.27	-4.0	424
38 o Per	23180	3 44 19.1	+32 17 18	B1 III	3.83	0.05	0.31	-4.4	310
16 Tau	23288	3 44 48.1	+24 17 22	B7 IV	5.45	-0.05	0.08	-1.0	180
17 Tau	23302	3 44 52.5	+24 06 48	B6 III	3.70	-0.11	0.03	-1.9	120
18 Tau	23324	3 45 09.7	+24 50 21	B8 V	5.65	-0.08	0.03	-0.2	150
19 Tau	23338	3 45 12.4	+24 28 02	B6 V	4.30	-0.11	0.03	-0.9	110
20 Tau	23408	3 45 49.5	+24 22 04	B7 III	3.88	-0.07	0.05	-1.6	120
21 Tau	23432	3 45 54.3	+24 33 17	B8 V	5.76	-0.04	0.07	-0.2	150
22 Tau	23441	3 46 02.8	+24 31 40	B9 V	6.42	-0.02	0.05	0.2	180
23 Tau	23480	3 46 19.5	+23 56 54	B6 IV	4.18	-0.06	0.08	-1.3	120
-	23512	3 46 34.6	+24 03 05	A0 V	8.11	0.36	0.37	0.8	171
-	23552	3 48 18.2	+50 44 12	B7 V	6.14	0.06	0.19	-0.6	180
-	23568	3 46 59.3	+24 31 13	B9.5 V	6.81	0.02	0.06	0.4	180
25 η Tau	23630	3 47 29.0	+24 06 18	B7 III	2.87	-0.09	0.03	-1.6	73
- Tau	23753	3 48 20.8	+23 25 16	B8 V	5.44	-0.07	0.04	-0.2	130
27 Tau	23850	3 49 09.7	+24 03 12	B8 III	3.63	-0.08	0.02	-1.2	90
28 Tau	23862	3 49 11.1	+24 08 12	B8 IVe	5.06	-0.08	0.03	-0.7	29
-	23923	3 49 43.5	+23 42 42	B9 V	6.16	-0.05	0.02	0.2	160
-	24131	3 51 53.7	+34 21 33	B1 V	5.77	0.00	0.26	-3.5	550
44 ζ Per	24398	3 54 07.8	+31 53 01	B1 Ib	2.85	0.12	0.31	-5.7	340

STAR	HD	RA (2000)	DEC (2000)	Sp	V	B-V	E(B-V)	M_V	d(pc)
		h m s	o ' "						
-	24432	3 55 25.0	+49 02 28	B3 II	6.82	0.55	0.72	-3.9	530
X Per	24534	3 55 22.9	+31 02 45	O pe	6.10	0.29	0.62	-	-
45 ε Per	24760	3 57 51.1	+40 00 37	B0.5 V	2.89	-0.18	0.10	-4.0	40
46 ξ Per	24912	3 58 57.8	+35 47 28	O7.5 IIInf	4.04	0.01	0.33	-5.9	46
-	26571	4 12 51.2	+22 24 49	B8 II-III	6.20	0.19	0.29	-2.3	380
49 μ Tau	26912	4 15 32.0	+ 8 53 32	B3 V	4.29	-0.06	0.14	-1.7	140
53 Per	27396	4 21 33.1	+46 29 56	B3 V	4.85	-0.03	0.17	-1.7	170
55 Per	27777	4 24 29.1	+34 07 50	B7 V	5.60	-0.06	0.07	-0.6	160
DU Eri	28497	4 29 06.9	-13 02 55	B1 Vn	5.60	-0.23	0.03	-3.5	660
48 ν Eri	29248	4 36 19.1	- 3 21 09	B2 III	3.93	-0.21	0.03	-3.6	320
-	29309	4 38 15.2	+31 59 55	B3.5 V	7.12	0.33	0.53	-1.6	280
-	29647	4 41 07.9	+25 59 33	B6-7 IV	8.37	0.90	1.04	-1.5	170
-	29866	4 44 12.9	+40 47 13	B8 IVn	6.08	0.06	0.16	-0.6	210
9 α Cam	30614	4 54 03.0	+66 20 34	O9.5 Ia	4.29	0.03	0.30	-6.2	860
8 π^5 Ori	31237	4 54 15.0	+ 2 26 26	B2 III	3.72	-0.18	0.06	-3.6	290
AE Aur	34078	5 16 18.2	+34 18 43	O9.5 V	5.96	0.22	0.52	-4.4	630
-	34656	5 20 43.0	+37 26 18	O7 If	6.79	0.02	0.34	-6.5	2799
6 λ Lep	34816	5 19 34.4	-13 10 36	B0.5 IV	4.29	-0.26	0.02	-4.7	25

STAR	HD	RA (2000)	DEC (2000)	Sp	V	B-V	E(B-V)	M_V	d(pc)
		h m s	o ' "						
-	34989	5 21 43.5	+ 8 25 43	B1 V	5.80	-0.13	0.13	-3.5	670
22 Ori	35039	5 21 45.7	- 0 22 57	B2 IV	4.73	-0.17	0.07	-3.0	340
23 Ori	35149	5 22 49.9	+ 3 32 40	B1 V	5.00	-0.15	0.11	-3.5	470
-	35395	5 25 10.3	+20 35 02	B0.5 III	6.77	0.23	0.51	-5.1	1143
28 η Ori	35411	5 24 28.6	- 2 23 50	B1 V	3.36	-0.17	0.09	-3.5	230
25 Ori	35439	5 24 44.8	+ 1 50 47	B1 V	4.95	-0.20	0.06	-3.5	490
-	35600	5 27 08.3	+30 12 31	B9 Ib	5.74	0.16	0.18	-5.5	1400
30 ψ Ori	35715	5 26 50.2	+ 3 05 44	B2 IV	4.59	-0.21	0.03	-3.0	330
-	36166	5 29 54.7	+ 1 47 21	B1.5 V	5.78	-0.20	0.05	-3.0	560
25 χ Aur	36371	5 32 43.6	+32 11 31	B5 Iab	4.76	0.34	0.43	-6.3	930
34 δ Ori A	36486	5 32 00.3	- 0 17 57	O9.5 II	2.23	-0.22	0.08	-5.9	377
-	36665	5 34 39.1	+28 03 03	B1 e	8.03	0.39	0.64	-	-
37 ϕ^1 Ori	36822	5 34 49.2	+ 9 29 22	B0 IV	4.41	-0.16	0.14	-4.6	570
39 λ Ori A	36861	5 35 08.2	+ 9 56 02	O8 IIIf	3.39	-0.18	0.13	-5.8	571
-	36879	5 35 40.4	+21 24 12	O7.5 III	7.57	0.19	0.51	-5.8	2333
41 θ^1 Ori C	37022	5 35 16.4	- 5 23 23	O7 Vp	5.14	0.03	0.35	-5.2	709
44 ι Ori	37043	3 35 25.9	- 5 54 36	O9 III	2.76	-0.24	0.07	-6.0	570

STAR	HD	RA (2000)	DEC (2000)	Sp	V	B-V	E(B-V)	M_V	d(pc)
		h m s	o ' "						
46 ε Ori	37128	5 36 12.7	- 1 12 07	B0 Ia	1.70	-0.19	0.05	-6.2	370
123 ζ Tau	37202	5 37 38.6	+21 08 33	B2 IVp	3.00	-0.19	0.05	-3.0	150
-	37318	5 38 57.9	+28 27 37	B0.5 Ve	8.39	0.35	0.63	-4.2	1380
48 σ Ori	37468	5 38 44.7	- 2 36 00	O9.5 V	3.73	-0.24	0.06	-4.4	550
50 ζ Ori A	37742	5 40 45.5	- 1 56 34	O9.5 Ib	1.77	-0.21	0.06	-5.9	340
μ Col	38666	5 45 59.9	-32 18 23	O9.5 V	5.17	-0.28	0.02	-4.4	840
53 κ Ori	38771	5 47 45.3	- 9 40 11	B0.5 Ia	2.06	-0.17	0.05	-6.9	21
139 Tau	40111	5 57 59.6	+25 57 14	B1 Ib	4.82	-0.06	0.13	-5.7	1100
62 χ^2 Ori	41117	6 03 55.1	+20 08 18	B2 Ia	4.63	0.28	0.45	-6.8	1100
-	44506	6 20 36.2	-34 08 38	B2 Vn	5.53	-0.19	0.05	-2.5	400
2 β CMa	44743	6 22 41.9	-17 57 22	B1 II-III	1.98	-0.23	0.05	-4.8	220
-	46223	6 32 09.1	+ 4 49 23	O4 V	7.28	0.22	0.54	-5.9	2001
-	46883	6 36 09.6	+10 17 05	B2 Vn	7.79	0.40	0.64	-2.5	1000
-	47129	6 37 24.0	+ 6 08 07	O7.5 IIIf	6.06	0.05	0.36	-5.9	1476

STAR	HD	RA (2000)	DEC (2000)	Sp	V	B-V	E(B-V)	M_V	d(pc)
		h m s	o ' "						
15 Mon	47839	6 40 58.6	+ 9 53 45	O8 IIIf	4.66	-0.25	0.07	-5.8	22
-	48099	6 41 59.2	+ 6 20 42	O6.5 V	6.37	-0.05	0.27	-5.5	1611
-	50896	6 54 12.9	-23 55 42	WN5	6.86	-0.30	0.14	-	-
21 ε CMa	52089	6 58 37.5	-28 58 20	B2 II	1.50	-0.21	0.00	-4.4	150
19 Mon	52918	7 02 54.6	- 4 14 21	B1 V	4.99	-0.20	0.06	-3.5	500
24 o^2 CMa	53138	7 03 01.4	-23 50 00	B3 Ia	3.03	-0.09	0.04	-6.8	860
-	53975	7 06 35.8	-12 23 38	O7.5 V	6.48	-0.10	0.21	-5.2	1607
-	54662	7 09 20.2	-10 20 51	O6.5 V	6.21	0.03	0.35	-5.5	1333
-	55879	7 14 28.2	-10 19 00	BO IV	6.00	-0.18	0.12	-4.6	1200
29 CMa	57060	7 18 40.3	-24 33 32	O8.5 If	4.98	-0.15	0.16	-6.5	1574
30 τ Cma	57061	7 18 42.4	-24 57 15	O9 III	4.39	-0.16	0.15	-6.0	1100
-	57682	7 22 01.9	- 8 58 45	O9 V	6.43	-0.19	0.12	-4.8	1600
-	64740	7 53 03.7	-49 36 47	B2 III	4.63	-0.23	0.01	-3.6	440

STAR	HD	RA (2000)	DEC (2000)	Sp	V	B-V	E(B-V)	M_V	d(pc)
		h m s	o ' "						
	64760	7 53 18.2	-48 06 11	B3 Ib	4.24	-0.14	0.00	-5.7	970
χ Car	65575	7 56 46.7	-52 58 56	B2 IV	3.47	-0.18	0.06	-3.0	180
V Pup	65818	7 58 14.3	-49 14 42	B1.5 III	4.41	-0.17	0.08	-4.0	470
ζ Pup	66811	8 03 35.0	-40 00 12	O4 Inf	2.25	-0.26	0.06	-6.8	593
γ^2 Vel	68273	8 09 31.9	-47 20 12	O9 I + WC8	1.78	-0.22	0.05	-6.5	422
-	74375	8 40 37.0	-59 45 40	B2 III	4.33	-0.11	0.13	-3.6	350
α Pyx	74575	8 43 35.5	-33 11 11	B2 II	3.68	-0.18	0.03	-4.4	410
-	75149	8 46 30.6	-45 54 46	B2 II	5.46	0.27	0.48	-4.4	510
a Car	79351	9 10 57.9	-58 58 01	B2 IV	3.44	-0.19	0.05	-3.0	190
κ Vel	81188	9 22 06.8	-55 00 38	B2 IV	2.50	-0.18	0.06	-3.0	120
32 α Leo	87901	10 08 22.2	+11 58 02	B7 V	1.35	-0.11	0.02	-0.6	26
47 ρ Leo	91316	10 32 48.6	+ 9 18 24	B1 Ib	3.85	-0.14	0.05	-5.7	770
-	92693	10 40 52.8	-57 56 07	A2 Ia	6.99	1.07	1.02	-7.5	2100
-	92740	10 41 17.6	-59 40 37	WN7	6.42	0.08	0.33	-	-

STAR	HD	RA (2000)	DEC (2000)	Sp	V	B-V	E(B-V)	M_V	d(pc)
		h m s	o ' "						
θ Car	93030	10 42 57.4	-64 23 39	BO Vp	2.76	-0.23	0.07	-4.1	230
-	93521	10 48 23.4	+37 34 13	O9 Vp	7.06	-0.27	0.04	-4.8	2400
-	99171	11 24 22.0	-42 40 09	BO III	6.12	-0.18	0.12	-5.0	1500
o^2 Cen	100262	11 31 48.6	-59 30 56	A2 Ia	5.15	0.49	0.44	-7.5	2100
δ Cru	106490	12 15 08.6	-58 44 55	B2 IV	2.80	-0.23	0.01	-3.0	79
α^1 Cru	108248	12 26 35.9	-63 05 56	B1 IV	1.41	0.10	0.36	-3.9	110
-	112244	12 55 56.9	-56 50 09	O9 Ib	5.32	0.01	0.29	-6.1	1600
θ Mus	113904	13 08 07.0	-65 18 22	O9 II	5.51	-0.02	0.28	-5.9	1282
-	115842	13 20 48.2	-55 48 02	BO.5 Iab	6.02	0.29	0.53	-6.2	2100
67 α Vir	116658	13 25 11.5	-11 09 41	B1 V	0.98	-0.23	0.03	-3.5	79
ε Cen	118716	13 39 53.2	-53 27 58	B1 V	2.30	-0.22	0.04	-3.5	150
ν Cen	120307	13 49 30.2	-41 41 16	B2 V	3.41	-0.22	0.02	-2.5	150
85 η UMa	120315	13 47 32.3	+49 18 48	B3 V	1.86	-0.19	0.01	-1.7	33
μ Cen	120324	13 49 36.9	-42 28 25	B3 Ve	3.04	-0.17	0.03	-1.7	89
ζ Cen	121263	13 55 32.3	-47 17 17	B2 IV	2.55	-0.22	0.02	-3.0	110
φ Cen	121743	13 58 16.2	-42 06 02	B2 V	3.83	-0.21	0.03	-2.5	190

STAR	HD	RA (2000)	DEC (2000)	Sp	V	B-V	E(B-V)	M_V	d(pc)
		h m s	o ' "						
β Cen	122451	14 03 49.4	-60 22 22	B1 II	0.61	-0.24	0.00	-5.1	140
a Cen	125823	14 23 02.1	-39 30 44	B6 III	4.42	-0.18	0.00	-1.9	180
η Cen	127972	14 35 30.3	-42 09 28	B3 III	2.31	-0.19	0.01	-2.9	110
β Lup	132058	14 58 31.8	-43 08 02	B2 V	2.68	-0.22	0.02	-2.5	110
-	135591	15 18 48.8	-60 29 47	O9 Ib	5.46	-0.10	0.18	-6.1	1600
27 β Lib	135742	15 17 00.3	- 9 22 58	B8 V	2.61	-0.11	0.00	-0.2	37
δ Lup	136298	15 21 22.2	-40 38 51	B2 IV	3.22	-0.22	0.02	-3.0	180
γ Lup	138690	15 35 08.4	-41 10 00	B3 V	2.78	-0.20	0.00	-1.7	79
1 Sco	141637	15 50 58.6	-25 45 05	B3 V	4.64	-0.05	0.15	-1.7	170
6 π Sco	143018	15 58 51.0	-26 06 50	B1 V	2.89	-0.19	0.07	-3.5	190
η Lup	143118	16 00 07.1	-38 23 48	B2 V	3.41	-0.22	0.02	-2.5	150
7 δ Sco	143275	16 00 19.9	-22 37 18	B0 V	2.32	-0.12	0.18	-4.1	170
8 β^1 Sco	144217A	16 05 26.1	-19 48 19	B0.5 V	2.64	-0.07	0.21	-4.0	158
8 β^2 Sco	144218	16 05 26.4	-19 48 07	B2 V	4.92	-0.02	0.22	-2.5	250

STAR		HD	RA (2000)	DEC (2000)	Sp	V	B-V	E(B-V)	M_V	d(pc)
			h m s	o ' "						
9	ω^1 Sco	144470	16 06 48.3	-20 40 09	B1 V	3.96	-0.04	0.22	-3.5	250
14	ν Sco	145502	16 11 59.6	-19 27 38	B2 IV-V	4.00	0.05	0.29	-2.8	170
20	σ Sco	147165	16 21 11.2	-25 35 34	B1 III	2.89	0.13	0.39	-4.4	180
-		147343	16 22 19.8	-24 21 46	A1 V	9.36	0.66	0.64	0.9	197
-		147648	16 24 02.7	-25 24 52	B8 V	9.42	0.78	0.89	-0.1	225
-		147701	16 24 21.2	-24 01 29	B5 V	9.35	0.57	0.73	-0.9	395
-		147889	16 25 24.1	-24 27 57	B2 V	7.90	0.84	1.08	-2.5	320
5	ρ OphA	147933	16 25 34.9	-23 26 46	B2 V	4.59	0.24	0.48	-2.5	230
	ρ OphB	147934	16 25 35.0	-23 26 44	B2 V	5.00	0.24	0.48	-2.4	155
7	χ Oph	148184	16 27 01.3	-18 27 23	B2 V	4.42	0.28	0.52	-2.5	150
22	Sco	148605	16 30 12.4	-25 06 54	B2 V	4.79	-0.11	0.13	-2.5	260
-		148937	16 33 52.4	-48 06 40	O6 e	6.72	0.36	0.68	-	-
	μ Nor	149038	16 34 04.8	-44 02 43	B0 Ia	4.90	0.10	0.34	-6.2	1100
-		149404	16 36 22.4	-42 51 32	O9 I	5.47	0.40	0.68	-6.2	1500
23	τ Sco	149438	16 35 52.8	-28 12 58	B0 V	2.82	-0.25	0.05	-4.1	240

STAR	HD	RA (2000)	DEC (2000)	Sp	V	B-V	E(B-V)	M_V	d(pc)
		h m s	o ' "						
13 ζ Oph	149757	16 37 09.4	-10 34 02	O9.5 V	2.56	0.02	0.32	-4.4	170
-	149881	16 36 58.0	+14 28 31	B0.5 III	7.05	-0.18	0.10	-5.1	2333
-	150898	16 47 19.4	-58 20 29	B0 Iab	5.58	-0.08	0.16	-6.2	1900
-	151804	16 51 33.6	-41 13 50	O8 Iaf	5.22	0.07	0.38	-6.8	1472
μ^1 Sco	151890	16 51 52.1	-38 02 51	B1.5 V	3.04	-0.21	0.04	-3.0	160
μ^2 Sco	151985	16 52 20.0	-38 01 03	B2 IV	3.57	-0.21	0.03	-3.0	210
ζ^1 Sco	152236	16 53 59.6	-42 21 44	B1.5 Ia	4.73	0.49	0.67	-6.7	780
-	152408	16 54 58.2	-41 09 04	O8 Iaf	5.77	0.15	0.46	-6.8	1694
-	152424	16 55 03.1	-42 05 27	O9 I	6.28	0.38	0.66	-6.2	1900
-	154090	17 04 49.3	-34 07 22	B1 Iab	4.87	0.26	0.45	-6.2	890
-	154368	17 06 28.3	-35 27 04	O9.5 Iab	6.13	0.50	0.77	-6.2	1100
-	154445	17 05 32.1	- 0 53 32	B1 V	5.64	0.16	0.42	-3.5	410
-	155806	17 15 19.1	-33 32 54	O7.5 Vne	5.53	-0.01	0.30	-5.2	912
U Oph	156247	17 16 31.6	+ 1 12 38	B5 V	5.90	0.06	0.22	-1.1	200
42 θ Oph	157056	17 22 00.4	-24 59 58	B2 IV	3.27	-0.22	0.02	-3.0	180
γ Ara	157246	17 25 23.5	-56 22 39	B1 III	3.34	-0.13	0.13	-4.4	330
34 υ Sco	158408	17 30 45.6	-37 17 45	B3 Ib	2.69	-0.22	0.00	-5.7	480

STAR	HD	RA (2000)	DEC (2000)	Sp	V	B-V	E(B-V)	M_V	d(pc)
		h m s	o ' "						
35 λ Sco	158926	17 33 36.4	-37 06 14	B2 IV	1.63	-0.22	0.02	-3.0	84
57 μ Oph	159975	17 37 50.5	- 8 07 08	B8 V	4.62	0.11	0.22	-0.2	73
κ Sco	160578	17 42 29.0	-39 01 48	B2 IV	2.41	-0.22	0.02	-3.0	120
63 Oph	162978	17 54 53.8	-24 53 14	O8.5 IIIf	6.20	0.04	0.35	-5.8	1524
-	163472	17 56 18.2	+ 0 40 13	B2 V	5.82	0.09	0.33	-2.5	330
66 Oph	164284	18 00 15.5	+ 4 22 07	B2 Ve	4.64	-0.03	0.21	-2.5	250
67 Oph	164353	18 00 38.5	+ 2 55 53	B5 Ib	3.97	0.02	0.11	-5.7	740
-	164402	18 01 54.1	-22 46 50	B0 Ib	5.84	0.01	0.25	-5.8	1600
9 Sgr	164794	18 03 52.3	-24 21 38	O4 V	5.98	0.02	0.34	-5.9	1462
θ Ara	165024	18 06 37.6	-50 05 30	B1 II	3.66	-0.08	0.16	-5.1	480
v986 Oph	165174	18 04 37.1	+ 1 55 08	B0.5 III	6.14	0.00	0.28	-5.1	1186
13 μ Sgr	166937	18 13 45.6	-21 03 32	B8 Ia	3.86	0.23	0.24	-7.1	1200
16 Sgr	167263	18 15 12.7	-20 23 16	O9 II	5.98	0.04	0.35	-5.9	1442
15 Sgr	167264	18 15 12.7	-20 43 42	B0 Ia	5.38	0.07	0.31	-6.2	1400
-	169454	18 25 15.1	-13 58 41	B1 Ia	6.61	0.94	1.13	-6.6	950
-	169754	18 26 42.5	-11 21 24	B0.5 Ia	8.38	1.06	1.28	-6.9	1828
-	170740	18 31 25.5	-10 47 45	B2 V	5.72	0.24	0.48	-2.5	250

STAR	HD	RA (2000)	DEC (2000)	Sp	V	B-V	E(B-V)	M_V	d(pc)
		h m s	o ' "						
-	172028	18 37 56.6	- 0 23 10	B3 II	7.83	0.55	0.72	-3.9	870
CX Dra	174237	18 46 42.9	+52 59 17	B3 V	5.88	-0.09	0.11	-1.7	320
10 β^1 Lyr	174638	18 50 04.6	+33 21 46	B7 V	3.45	0.00	0.13	-0.6	92
34 σ Sgr	175191	18 55 15.7	-26 17 48	B3 IV-V	2.02	-0.22	0.00	-2.0	64
-	176162	18 59 23.6	-12 50 26	B5 V	5.90	0.00	0.16	-1.1	240
20 Aql	179406	19 12 40.5	- 7 56 23	B3 IV	5.34	0.13	0.33	-2.3	220
46 υ Sgr	181615	19 21 43.5	-15 57 18	B2 Vpe	4.61	0.10	0.34	-2.5	165
2 Cyg	182568	19 24 07.4	+29 37 17	B3 IV	4.97	-0.10	0.10	-2.3	260
-	183143	19 27 26.3	+18 17 45	B7 Ia	6.87	1.24	1.28	-7.1	1200
39 κ Aql	184915	19 36 53.3	- 7 01 39	B0.5 III	4.95	0.00	0.28	-5.1	685
18 δ Cyg	186882	19 44 58.4	+45 07 51	A0 III	2.87	-0.03	0.00	-0.6	49
-	186994	19 45 38.0	+44 57 51	B0 III	7.51	-0.12	0.18	-5.0	2800
53 α Aql	187642	19 50 46.8	+ 8 52 06	A7 IV-V	0.77	0.22	0.00	2.2	5.1
-	187982	19 52 01.4	+24 59 33	A2 Ia	5.57	0.71	0.66	-7.5	1800
-	188209	19 51 58.9	+47 01 38	O9.5 III	5.62	-0.07	0.23	-5.5	1300
-	188439	19 53 01.0	+47 48 27	B0.5 IIIp	6.29	-0.11	0.17	-5.1	1489

STAR	HD	RA (2000)	DEC (2000)	Sp	V	B-V	E(B-V)	M_V	d(pc)
		h m s	o ' "						
22 Cyg	188892	19 55 51.5	+38 29 12	B6 III	4.94	-0.08	0.06	-1.9	220
-	190066	20 02 22.0	+22 09 06	B1 Iab	6.48	0.18	0.37	-6.2	2100
-	190603	20 04 36.0	+32 13 07	B1.5 Ia	5.64	0.54	0.72	-6.7	1100
-	190967	20 06 09.9	+35 23 10	B1 Ib-II	8.04	0.41	0.65	-5.4	2200
-	191877	20 11 20.9	+21 52 32	B1 Ib	6.26	-0.02	0.17	-5.7	2000
-	192660	20 14 26.0	+40 19 46	B0 Ia	7.54	0.63	0.87	-6.2	1700
-	193007	20 16 31.2	+37 38 32	B1 II	8.01	0.36	0.60	-5.4	2042
34 P Cyg	193237	20 17 47.0	+38 01 59	B1 p	4.81	0.42	0.68	-	-
-	193322	20 18 06.8	+40 43 56	O8.5 III	5.84	0.10	0.41	-5.8	40
-	193426	20 18 39.5	+40 13 37	B9 Ia	7.73	1.23	1.23	-7.1	1800
-	193793	20 20 27.8	+43 51 16	WC6	6.85	0.40	0.72	-	--
α Pav	193924	20 25 38.7	-56 44 06	B3 IV	1.94	-0.20	0.00	-2.3	71
-	194279	20 23 18.0	+40 45 32	B1.5 Ia	7.02	1.02	1.20	-6.7	1000
-	195592	20 30 34.7	+44 18 54	O9.5 Ia	7.08	0.87	1.14	-6.2	970
50 α Cyg	197345	20 41 25.8	+45 16 49	A2 Ia	1.25	0.09	0.04	-7.5	560
55 Cyg	198478	20 48 56.2	+46 06 51	B3 Ia	4.84	0.41	0.54	-6.8	1000
-	199478	20 55 49.7	+47 25 04	B8 Ia	5.67	0.47	0.48	-7.1	2000
-	199579	20 56 34.6	+44 55 30	O6.5 III	5.96	0.05	0.37	-6.1	1524
59 Cyg	200120	20 59 49.3	+47 31 16	B1 IVe	4.74	-0.05	0.21	-3.9	480

STAR	HD	RA (2000)	DEC (2000)	Sp	V	B-V	E(B-V)	M_V	d(pc)
		h m s	o ' "						
-	202124	21 12 28.2	+44 31 56	O9.5 Ib	7.80	0.22	0.49	-5.9	2900
67 σ Cyg	202850	21 17 24.7	+39 23 41	B9 Ia	4.23	0.12	0.12	-7.1	1600
66 υ Cyg	202904	21 17 54.9	+34 53 48	B2 Ve	4.43	-0.11	0.13	-2.5	240
68 Cyg	203064	21 18 27.0	+43 56 46	O8 V	5.00	-0.01	0.30	-4.9	622
-	203938	21 23 49.9	+47 09 52	B0.5 IV	7.08	0.46	0.74	-4.7	789
69 Cyg	204172	21 25 46.9	+36 40 03	B0 Ib	5.94	-0.08	0.16	-5.8	1900
9 Cep	206165	21 37 55.0	+62 04 55	B2 Ib	4.73	0.30	0.46	-5.7	640
-	206267	21 38 57.5	+57 29 21	O6.5 V	5.62	0.21	0.53	-5.5	785
-	207198	21 44 53.1	+62 27 38	O9 II	5.95	0.31	0.62	-5.9	968
-	207538	21 47 39.5	+59 42 03	B0 V	7.31	0.33	0.63	-4.1	910
γ Gru	207971	21 53 55.6	-37 21 54	B8 III	3.01	-0.12	0.00	-1.2	70
13 Cep	208501	21 54 52.9	+56 36 41	B8 Ib	5.80	0.73	0.75	-5.6	710
α Gru	209952	22 08 13.8	-46 57 40	B5 V	1.74	-0.13	0.03	-1.1	21
19 Cep	209975	22 05 08.7	+62 16 48	O9.5 Ib	5.11	0.08	0.35	-5.9	1000
35 Aqr	210191	22 08 58.9	-18 31 11	B2 V	5.70	0.10	0.34	-2.5	430
22 λ Cep	210839	12 11 30.5	+59 24 53	O6 If	5.04	0.25	0.57	-6.5	42
31 Peg	212076	22 21 30.9	+12 12 19	B2 V	5.01	-0.13	0.11	-2.5	310

STAR	HD	RA (2000)	DEC (2000)	Sp	V	B-V	E(B-V)	M_V	d(pc)
		h m s	o ' "						
-	212978	22 27 26.3	+39 48 36	B2 V	6.14	-0.14	0.10	-2.5	520
26 Cep	213087	22 27 05.2	+65 07 57	B0.5 Ib	5.46	0.37	0.59	-6.1	883
6 Lac	213420	22 30 29.1	+43 07 25	B2 IV	4.51	-0.09	0.15	-3.0	280
-	214080	22 36 06.2	-16 23 16	B1 Ib	6.83	-0.13	0.06	-5.7	2900
10 Lac	214680	22 39 15.6	+39 03 01	O9 V	4.88	-0.20	0.11	-4.8	780
12 Lac	214993	22 41 28.5	+40 13 32	B2 III	5.25	-0.14	0.10	-3.6	560
-	217101	22 57 40.5	+39 18 32	B2 IV-V	6.18	-0.15	0.09	-2.8	590
1 o And	217675	23 01 55.1	+42 19 34	B6 IIIpe	3.60	0.10	0.24	-1.8	35
1 Cas	218376	23 06 36.7	+59 25 12	B1 III	4.85	-0.03	0.23	-4.4	570
-	219188	23 14 00.5	+ 4 59 49	B0.5 III	6.90	0.10	0.38	-5.1	1459
8 σ Cas	224572	23 59 00.4	+55 45 18	B1 V	4.88	-0.07	0.19	-3.5	400
VI Cyg 12	-	20 32	+41 18	B5 Ia-0	11.47	3.19	3.28	-8.4	1445
	BD No								
-	+30° 3639	19 34 45.2	+30 31 00	WC	10.2	-0.7	-	-	-
-	+31° 643	3 44 34.1	+32 09 46	B5 V	8.50	0.69	0.85	-0.9	225
-	+40° 4220	20 32 22.3	+41 18 19	O7 Ia	9.20	1.7	2.02	-6.8	887
-	+66° 1661	23 57 32.5	+67 33 16	O9 V	8.7	0.81	1.11	-4.5	895
-	+66° 1674	00 02 10.1	+67 25 46	O9.5 V	9.50	1.10	1.40	-4.2	794
-	+66° 1675	00 02 10.2	+67 24 33	O7	9.05	1.09	1.41	-	-
-	-14° 5037	18 25 06.0	-14 38 43	B1.5 Ia	8.24	1.39	1.57	-6.9	1135

Notes The equatorial co-ordinates RA and DEC, spectral type Sp, the star's visual magnitude V in the UBV photometric system, the colour index B-V, the absolute visual magnitude M_V and the star's distance d in parsecs, are taken in most cases from Sky Catalogue 2000.0, Vol 1 (Ref. 336), supplemented by data from other standard catalogues. In a few cases, coordinates for epoch 1950.0 from the Catalogue of Stellar Identifications have been precessed to 2000.0. The colour excess E(B-V) is calculated from B-V and the unreddened $(B-V)_o$ values given by FitzGerald (1970 : Ref. 136); small negative values due to observational error have been replaced by zero.

TABLE 27. COLUMN DENSITIES, IN LOG (N/cm^2). # = detected.

Star	CH	CH^+	$^{13}CH^+$	CO	^{13}CO	CN	C_2	C_3
886	-	<12.19 30 V	-	-	-	-	-	-
2905	12.91 30 V	12.66 30 V	-	-	-	<11.29 283 V	-	-
4180	-	# 10 V	-	-	-	-	-	-
5394	-	<12.22 30 V	-	-	-	-	-	-
10144	-	<11.09 405 V	-	-	-	-	-	-
10516	-	12.16 51 V	-	-	-	-	-	-
12953	-	13.23 59 V	-	15.68 151 R	-	12.62 59 V	-	-
14228	-	<11.69 405 V	-	<12.73 27UV	-	-	-	-
14489	-	# 59 V	-	-	-	-	-	-
14633	-	-	-	-	-	-	-	-
20041	-	13.06 59 V	-	<14.97 151 R	-	12.04 59 V	-	-
21278	-	12.66 30 V	-	>13.20 27 UV	-	-	-	-
21291	-	12.80 59 V	-	15.11 151 R	-	12.11 59 V	-	-
21389	-	-	-	<14.00 151 UV	-	-	-	-
21483	13.30 13 V	-	-	16.08 3 R	# 3 R	12.60 2 R	-	-
21856	13.00 13 V	13.02 13 V	-	-	-	-	-	-
22192	-	-	-	13.61 269 UV	-	-	-	-
22928	-	<12.23 30 V	-	-	-	-	-	-

Star	CH	CH^+	$^{13}CH^+$	CO	^{13}CO	CN	C_2	C_3
22951	-	# 10 V	-	-	-	<11.41 283 V	-	-
23180	13.11 30 V	12.76 30 V	-	14.18 14 UV	# 3 R	12.20 381 V	13.08 97 V	-
23288	<12.73 392 V	13.40 392 V	-	# 392 R	-	<12.10 392 V	-	-
23302	<12.38 392 V	<12.44 392 V	-	# 392 R	-	<11.91 392 V	-	-
23324	<12.68 392 V	<12.73 392 V	-	# 392 R	-	<12.25 392 V	-	-
23338	<12.69 392 V	12.67 392 V	-	# 392 R	-	<11.92 392 V	-	-
23408	12.18 30 V	13.47 392 V	<11.75 141 V	>13.23 27 UV	-	<11.67 392 V	# 164 V	-
23432	<12.99 392 V	13.36 392 V	-	# 392 R	-	<12.12 392 V	-	-
23441	<12.92 392 V	<13.02 392 V	-	# 392 R	-	<12.37 392 V	-	-
23480	<12.49 392 V	13.25 392 V	<12.01 141 V	# 392 R	-	<11.90 392 V	-	-
23512	13.50 392 V	<13.24 392 V	-	# 392 R	-	<12.91 392 V	-	-
23552	-	-	-	14.54 268 UV	13.93 268 UV	-	-	-
23568	<12.98 392 V	13.29 392 V	-	# 392 R	-	<12.31 392 V	-	-
23630	<12.53 392 V	12.64 392 V	-	<12.91 27 UV	-	<11.92 392 V	-	-
23753	<12.74 392 V	12.67 392 V	-	# 392 R	-	<12.10 392 V	-	<12.52 123 V
23850	<12.57 392 V	12.77 392 V	-	# 392 R	-	<11.97 392 V	-	-
23862	<12.62 392 V	<12.53 392 V	-	# 392 R	-	<12.07 392 V	-	-
23923	<12.79 392 V	<13.13 392 V	-	# 392 R	-	<12.42 392 V	-	-
24131	13.00 13 V	# 10 V	-	-	-	-	-	-

Star	CH	CH^+	$^{13}CH^+$	CO	^{13}CO	CN	C_2	C_3
24398	13.25 30 V	12.48 30 V	-	>13.56 27 UV	-	12.47 381 V	13.05 163 V	<12.57 123 V
24432	13.40 13 V	13.72 13 V	-	-	-	-	-	-
24534	13.78 330 V	13.12 13 V	-	# 3 R	-	13.19 4 V	13.48 393 UV	-
24760	<12.30 30 V	<12.01 30 V	-	12.95 27 UV	-	-	-	-
24912	13.04 30 V	13.32 30 V	<11.75 141 V	>13.45 27 UV	-	11.41 283 V	<12.30 53 UV	-
26571	13.21 256 V	-	-	15.50 151 UV	-	12.81 256 V	-	-
26912	# 10 V	# 10 V	-	-	-	-	-	-
27396	13.18 4 V	13.18 4 V	-	-	-	-	-	-
27777	-	# 44 V	-	-	-	-	-	-
28497	-	-	-	<12.67 27 UV	-	-	-	-
29248	-	-	-	-	-	-	-	-
29309	-	# 10 V	-	-	-	-	-	-
29647	14.23 326 V	<13.00 326 V	-	17.68 326 R	17.92 326 R	14.11 326 V	13.68 326 V	-
29866	-	-	-	13.72 268 UV	13.41 268 UV	-	-	-
30614	12.82 30 V	13.25 30 V	-	13.59 14 UV	-	-	-	-
31237	-	-	-	-	-	-	-	-
34078	<13.40 64 R	# 10 V	-	14.76 214 UV	-	12.32 4 V	-	-
34656	# 10 V	# 10 V	-	-	-	-	-	-
34816	-	-	-	-	-	-	-	-

Star	CH	CH^+	$^{13}CH^+$	CO	^{13}CO	CN	C_2	C_3
34989	-	-	-	-	-	-	-	-
35039	-	<11.79 405 V	-	-	-	-	-	-
35149	-	13.10 405 V	-	-	-	-	-	-
35395	-	# 10 V	-	-	-	-	-	-
35411	-	12.13 405 V	-	-	-	-	-	-
35439	-	-	-	-	-	-	-	-
35600	-	# 59 V	-	-	-	-	-	-
35715	-	-	-	-	-	-	-	-
36166	-	-	-	-	-	-	-	-
36371	13.18 4 V	13.02 4 V	-	-	-	-	-	-
36486	-	<12.25 30 V	-	<12.04 27 UV	-	-	-	-
36665	-	-	-	14.68 143 UV	-	-	-	-
36822	-	<11.99 405 V	-	-	-	-	-	-
36861	<13.52 64 R	<12.23 30 V	-	13.41 53 UV	-	-	-	-
36879	-	-	-	14.08 14 UV	-	-	-	-
37022	-	<12.61 30 V	-	-	-	-	-	-
37043	-	<12.15 30 V	-	12.43 27 UV	-	-	-	-
37128	-	<12.06 30 V	-	<12.30 27 UV	-	-	-	-
37202	-	<12.40 30 V	-	<12.32 27 UV	-	-	-	-

Star	CH	CH^+	$^{13}CH^+$	CO	^{13}CO	CN	C_2	C_3
37318	-	-	-	13.86 134 UV	-	-	-	-
37468	-	-	-	-	-	-	-	-
37742	-	<11.95 30 V	-	<12.72 27 UV	-	-	-	-
38666	-	-	-	-	-	-	-	-
38771	-	<12.25 30 V	-	-	-	-	-	-
40111	-	-	-	<13.00 27 UV	-	-	-	-
41117	13.23 4 V	13.41 51 V	-	14.10 34 UV	<13.16 34 UV	-	-	-
44506	-	-	-	-	-	-	-	-
44743	-	<12.15 30 V	-	-	-	-	-	-
46223	-	-	-	14.74 14 UV	-	-	-	-
46883	13.50 13 V	-	-	-	-	-	-	-
47129	12.94 152 V	# 10 V	-	14.30 34 UV	<13.56 34 UV	-	-	-
47839	-	<12.61 30 V	-	<12.81 27 UV	-	-	-	-
48099	12.56 152 V	-	-	-	-	-	-	-
50896	-	-	-	-	-	-	-	-
52089	-	<11.89 405 V	-	-	-	-	-	-
52918	-	-	-	-	-	-	-	-
53138	-	-	-	<12.97 27 UV	-	-	-	-
53975	-	-	-	-	-	-	-	-

Star	CH	CH^+	$^{13}CH^+$	CO	^{13}CO	CN	C_2	C_3
54662	13.04 152 V	13.07 405 V	-	-	-	-	-	-
55879	-	-	-	-	-	-	-	-
57060	<12.37 152 V	-	-	<12.67 27 UV	-	-	-	-
57061	<12.25 152 V	<11.69 405 V	-	<12.61 27 UV	-	-	-	-
57682	-	-	-	-	-	-	-	-
64740	-	-	-	-	-	-	-	-
64760	-	-	-	-	-	-	-	-
65575	-	-	-	-	-	-	-	-
65818	-	-	-	-	-	-	-	-
66811	<11.78 152 V	-	-	<12.11 27 UV	-	-	-	-
68273	-	-	-	<12.46 27 UV	-	-	-	-
74375	<11.90 152 V	-	-	-	-	-	-	-
74575	-	<11.39 405 V	-	-	-	-	-	-
75149	13.22 152 V	-	-	-	-	-	-	-
79351	-	-	-	-	-	-	-	-
81188	-	-	-	-	-	-	-	-
87901	-	<12.01 30 V	-	<12.28 27 UV	-	-	-	-
91316	-	<11.49 405 V	-	<12.78 27 UV	-	-	-	-
92693	-	-	-	-	-	-	12.78 408 V	-

Star	CH	CH^+	$^{13}CH^+$	CO	^{13}CO	CN	C_2	C_3
92740	12.67 152 V	-	-	-	-	-	-	-
93030	<11.78 152 V	<11.09 405 V	-	<11.95 27 UV	-	-	-	-
93521	-	-	-	-	-	-	-	-
99171	-	-	-	-	-	-	-	-
100262	-	12.88 405 V	-	-	-	-	-	-
106490	-	<11.79 405 V	-	-	-	-	-	-
108248	-	<11.39 405 V	-	-	-	-	-	-
112244	12.68 152 V	12.87 405 V	-	-	-	<11.50 283 V	-	-
113904	12.03 152 V	12.34 405 V	-	-	-	-	-	-
115842	13.25 152 V	-	-	-	-	-	-	-
116658	-	<11.95 30 V	-	-	-	-	-	-
118716	-	<11.39 405 V	-	-	-	-	-	-
120307	-	<11.39 405 V	-	-	-	-	-	-
120315	-	<11.90 30 V	-	-	-	-	-	-
120324	-	-	-	<13.07 268 UV	-	-	-	-
121263	-	<11.79 405 V	-	-	-	-	-	-
121743	-	<11.39 405 V	-	-	-	-	-	-
122451	-	-	-	-	-	-	-	-
125823	-	-	-	-	-	-	-	-

Star	CH	CH^+	$^{13}CH^+$	CO	^{13}CO	CN	C_2	C_3
127972	-	-	-	-	-	-	-	-
132058	-	<11.49 405 V	-	-	-	-	-	-
135591	-	-	-	-	-	-	-	-
135742	-	<11.19 405 V	-	<12.71 27 UV	-	-	-	-
136298	-	<11.39 405 V	-	-	-	-	-	-
138690	-	<11.19 405 V	-	-	-	-	-	-
141637	-	<12.09 405 V	-	-	-	-	-	-
143018	<11.70 152 V	11.75 405 V	-	11.95 27 UV	-	-	-	-
143118	-	<11.49 405 V	-	-	-	-	-	-
143275	12.33 152 V	12.50 405 V	-	12.95 48 UV	-	<11.11 283 V	-	-
144217A	12.27 152 V	12.73 405 V	-	13.08 48 UV	-	<11.11 283 V	-	-
144218	-	13.00 405 V	-	-	-	-	-	-
144470	12.50 152 V	12.80 405 V	-	13.60 48 UV	-	-	-	-
145502	12.76 152 V	12.81 405 V	-	13.60 48 UV	-	-	-	-
147165	12.48 152 V	12.76 405 V	-	13.15 48 UV	-	<11.11 283 V	-	-
147343	13.77 446 V	13.49 446 V	-	-	-	13.14 446 V	-	-
147648	13.87 446 V	-	-	-	-	<12.66 446 V	-	-
147701	13.81 446 V	13.47 446 V	-	-	-	13.33 446 V	-	-
147889	14.00 446 V	13.55 446 V	-	# 350 R	# 350 R	13.45 446 V	13.84 212 V	-

Star	CH	CH^+	$^{13}CH^+$	CO	^{13}CO	CN	C_2	C_3
147933	13.29 152 V	13.13 405 V	-	14.81 48 UV	-	12.30 283 V	13.18 195 V	-
147934	13.32 47 V	13.15 47 V	-	-	-	-	-	-
148184	13.44 152 V	13.11 405 V	-	15.25 55 UV	-	12.12 283 V	13.40 212 V	-
148605	13.34 64 R	12.09 405 V	-	-	-	-	-	-
148937	-	-	-	14.70 14 UV	-	-	-	-
149038	12.99 152 V	13.59 405 V	-	>13.49 27 UV	-	<11.29 283 V	-	-
149404	-	-	-	14.88 34 UV	14.06 34 UV	-	<12.30 212 V	-
149438	<13.25 64 R	<11.09 405 V	-	-	-	-	-	-
149757	13.31 152 V	13.52 405 V	<11.65 141 V	15.38 179 UV	13.64 179 UV	12.40 381 V	13.18 448 V	<12.18 123 V
149881	-	-	-	-	-	-	-	-
150898	-	-	-	-	-	-	-	-
151804	12.68 152 V	12.91 405 V	-	13.74 14 UV	-	-	-	-
151890	-	<11.69 405 V	-	-	-	-	-	-
151985	-	<11.39 405 V	-	-	-	-	-	-
152236	-	13.24 405 V	-	14.72 34 UV	13.65 34 UV	-	-	-
152408	12.72 152 V	-	-	-	-	-	-	-
152424	-	-	-	14.54 14 UV	-	-	-	-
154090	-	13.32 405 V	-	-	-	-	-	-
154368	14.41 25 V	13.78 25 V	-	>15.95 151 UV	-	13.63 25 V	13.53 212 V	-

Star	CH	CH^+	$^{13}CH^+$	CO	^{13}CO	CN	C_2	C_3
154445	13.43 4 V	13.50 4 V	-	-	-	-	-	-
155806	-	12.82 405 V	-	-	-	-	-	-
156247	13.30 4 V	13.50 4 V	-	-	-	-	-	-
157056	-	<11.99 405 V	-	-	-	-	-	-
157246	<11.78 152 V	11.90 405 V	-	12.66 277 UV	-	-	-	-
158408	-	<11.49 405 V	-	# 27 UV	-	-	-	-
158926	13.66 64 R	<11.39 405 V	-	-	-	-	-	-
159975	-	13.06 405 V	-	-	-	-	-	-
160578	-	<11.39 405 V	-	-	-	-	-	-
162978	-	# 10 V	-	-	-	-	-	-
163472	12.90 4 V	12.90 4 V	-	-	-	-	-	-
164284	-	-	-	-	-	-	-	-
164353	12.68 152 V	12.86 405 V	-	12.90 27 UV	-	<11.20 283 V	-	-
164402	-	-	-	-	-	-	-	-
164794	-	13.00 4 V	-	-	-	-	-	-
165024	-	<11.79 405 V	-	-	-	-	-	-
165174	-	# 10 V	-	-	-	-	-	-
166937	-	12.96 405 V	-	-	-	-	-	-
167263	12.71 152 V	12.77 405 V	-	-	-	-	-	-

Star	CH	CH^+	$^{13}CH^+$	CO	^{13}CO	CN	C_2	C_3
167264	12.68 152 V	12.90 405 V	-	13.99 34 UV	<13.16 34 UV	<11.41 283 V	-	-
169454	-	12.13 405 V	-	-	-	-	13.68 408 V	-
169754	13.20 13 V	13.61 13 V	-	-	-	-	-	-
170740	12.95 4 V	13.18 4 V	-	-	-	-	-	-
172028	13.20 13 V	13.41 13 V	-	-	-	-	-	-
174237	-	-	-	<12.86 268 UV	-	-	-	-
174638	-	12.90 51 V	-	-	-	-	-	-
175191	-	<11.19 405 V	-	<12.25 27 UV	-	-	-	-
176162	-	13.48 4 V	-	-	-	-	-	-
179406	13.57 4 V	-	-	15.28 3 R	-	13.59 4 V	-	-
181615	# 10 V	13.20 51 V	-	-	-	-	-	-
182568	13.20 4 V	-	-	-	-	-	-	-
183143	13.50 13 V	13.92 13 V	-	-	-	-	-	<12.64 123 V
184915	12.95 30 V	12.70 405 V	-	-	-	<11.35 283 V	-	-
186882	-	<12.46 51 V	-	-	-	-	-	-
186994	-	-	-	-	-	-	-	-
187642	-	<11.39 405 V	-	-	-	-	-	-
187982	-	-	-	-	-	-	-	-
188209	-	-	-	-	-	-	-	-

Star	CH	CH^+	$^{13}CH^+$	CO	^{13}CO	CN	C_2	C_3
188439	-	-	-	-	-	-	-	-
188892	-	# 10 V	-	-	-	-	-	-
190066	-	13.18 4 V	-	-	-	-	-	-
190603	# 10 V	13.67 4 V	-	-	-	-	-	-
190967	-	13.20 13 V	-	-	-	-	-	-
191877	-	# 10 V	-	-	-	-	-	-
192660	13.30 13 V	13.52 13 V	-	-	-	-	-	-
193007	# 10 V	# 10 V	-	-	-	-	-	-
193237	# 10 V	13.23 51 V	<12.01 141 V	# 3 R	-	-	-	-
193322	# 10 V	13.50 4 V	-	14.06 34 UV	13.12 34 UV	-	-	-
193426	# 13 V	# 13 V	-	-	-	-	-	-
193793	# 10 V	13.28 4 V	-	-	-	-	-	-
193924	-	<11.19 405 V	-	-	-	-	-	-
194279	-	# 10 V	-	-	-	-	-	-
195592	# 10 V	# 10 V	-	-	-	-	-	-
197345	-	<12.15 51 V	-	-	-	-	-	-
198478	<13.40 64 R	13.32 51 V	<11.95 141 V	15.18 3 R	-	12.38 4 V	-	<12.57 123 V
199478	13.15 4 V	13.95 4 V	-	-	-	-	-	-
199579	# 10 V	# 10 V	-	-	-	-	-	-

Star	CH	CH^+	$^{13}CH^+$	CO	^{13}CO	CN	C_2	C_3
200120	-	<12.59 30 V	-	12.73 27 UV	-	-	-	-
202124	-	-	-	-	-	# 57 V	-	-
202850	-	<12.15 51 V	-	-	-	-	-	-
202904	-	-	-	-	-	-	13.56 163 V	-
203064	12.91 30 V	12.69 30 V	-	14.18 34 UV	<12.92 34 UV	<11.29 283 V	-	-
203938	-	13.41 13 V	-	-	-	-	-	-
204172	-	-	-	-	-	-	-	-
206165	13.32 1 V	13.20 1 V	-	14.77 34 UV	13.77 34 UV	<11.82 1 V	-	-
206267	13.30 1 V	13.18 1 V	-	-	-	12.69 1 V	-	-
207198	13.49 1 V	13.11 1 V	-	15.34 3 R	-	12.52 1 V	-	-
207538	13.49 52 R	-	-	15.15 256 UV	-	-	-	-
207971	-	<11.39 405 V	-	-	-	-	-	-
208501	-	-	-	15.78 151 R	-	13.63 254 V	-	-
209952	-	<11.09 405 V	-	<12.23 27 UV	-	-	-	-
209975	-	-	-	14.08 14 UV	-	-	-	-
210191	-	<11.49 405 V	-	-	-	-	-	-
210839	13.25 1 V	13.01 1 V	-	14.68 34 UV	13.91 34 UV	12.20 1 V	-	-
212076	-	# 10 V	-	-	-	-	-	-
212978	# 10 V	# 10 V	-	-	-	-	-	-

Star	CH	CH^+	$^{13}CH^+$	CO	^{13}CO	CN	C_2	C_3
213087	-	-	-	14.87 14 UV	-	-	-	<12.64 123 V
213420	-	<12.32 51 V	-	-	-	-	-	-
214080	-	-	-	-	-	-	-	-
214680	-	<12.48 30 V	-	-	-	-	-	-
214993	-	-	-	-	-	-	-	-
217101	-	# 10 V	-	-	-	-	-	-
217675	<12.11 30 V	<11.95 30 V	-	<13.34 268 UV	-	-	13.89 163 V	-
218376	12.89 30 V	13.03 51 V	-	-	-	-	-	-
219188	-	-	-	-	-	-	-	-
224572	12.56 30 V	12.86 30 V	-	-	-	-	-	-
VI Cyg 12	-	-	-	-	-	-	14.35 146 V	-
+30°3639	-	-	-	<13.38 268 UV	-	-	-	-
+31°643	13.70 13 V	13.72 13 V	-	-	-	-	-	-
+40°4220	14.41 64 R	-	-	-	-	-	-	-
+66°1661	13.04 64 R	-	-	-	-	# 57 V	-	-
+66°1674	# 57 V	-	-	-	-	# 131 V	-	-
+66°1675	13.83 57 V	-	-	17.30 151 R	-	13.85 57 V	14.09 146 V	-
-14°5037	-	-	-	-	-	-	13.83 408 V	-

TABLE 27. COLUMN DENSITIES, IN LOG (N/cm^2). # = detected.

Star	H	H_2	HD	OH	H_2O	HCℓ	NH	N_2
886	20.26 361 UV	<14.20 70 UV	-	-	-	-	-	-
2905	21.26 361 UV	20.27 70 UV	-	-	-	-	-	-
4180	-	-	-	-	-	-	-	-
5394	20.30 361 UV	<17.50 70 UV	-	-	-	-	-	-
10144	-	<13.90 70 UV	-	-	-	-	-	-
10516	20.54 71 UV	19.08 70 UV	-	-	-	-	-	-
12953	-	-	-	-	-	-	-	-
14228	-	<17.00 70 UV	-	-	-	-	-	-
14489	-	-	-	-	-	-	-	-
14633	20.60 382 UV	<19.11 70 UV	-	-	-	-	-	-
20041	-	-	-	-	-	-	-	-
21278	-	19.48 70 UV	14.04 87 UV	-	-	-	-	-
21291	-	-	-	-	-	-	-	-
21389	-	-	-	-	-	-	-	-
21483	-	-	-	-	-	-	-	-
21856	21.04 71 UV	20.04 70 UV	-	-	-	-	-	-
22192	-	-	-	-	-	-	-	-
22928	-	19.30 70 UV	<13.34 107 UV	-	-	<12.04 117 UV	-	-

Star	H	H_2	HD	OH	H_2O	HCℓ	NH	N_2
22951	21.04 71 UV	20.46 70 UV	-	-	-	-	-	-
23180	20.85 361 UV	20.60 70 UV	15.87 8 UV	14.00 113 V	<12.91 8 UV	-	<11.84 74 V	<13.32 8 UV
23288	-	-	-	-	-	-	-	-
23302	-	-	-	-	-	-	-	-
23324	-	-	-	-	-	-	-	-
23338	-	-	-	-	-	-	-	-
23408	-	19.75 70 UV	<13.88 107 UV	-	-	-	-	-
23432	-	-	-	-	-	-	-	-
23441	-	-	-	-	-	-	-	-
23480	-	20.12 70 UV	-	-	-	-	-	-
23512	-	-	-	-	-	-	-	-
23552	-	-	-	-	-	-	-	-
23568	-	-	-	-	-	-	-	-
23630	-	19.54 70 UV	-	-	-	-	-	-
23753	-	-	-	-	-	-	-	-
23850	-	-	-	-	-	-	-	-
23862	-	-	-	-	-	-	-	-
23923	-	-	-	-	-	-	-	-
24131	-	-	-	-	-	-	-	-

Star	H	H_2	HD	OH	H_2O	HCℓ	NH	N_2
24398	20.81 71 UV	20.67 70 UV	15.71 56 UV	13.74 46 V	-	-	<11.76 46 V	-
24432	-	-	-	-	-	-	-	-
24534	20.70 382 UV	-	-	-	-	-	-	-
24760	20.47 361 UV	19.52 70 UV	13.81 107 UV	-	-	<11.70 117 UV	-	<12.64 119 UV
24912	21.04 382 UV	20.53 70 UV	14.30 107 UV	<14.12 53 UV	<13.15 53 UV	<12.08 117 UV	-	-
26571	-	-	-	-	-	-	-	-
26912	-	-	-	-	-	-	-	-
27396	-	-	-	-	-	-	-	-
27777	-	-	-	-	-	-	-	-
28497	20.30 361 UV	14.82 70 UV	-	-	-	-	-	-
29248	20.52 361 UV	<17.41 135 UV	-	-	-	-	-	-
29309	-	-	-	-	-	-	-	-
29647	-	21.54 326 V	-	-	-	-	-	-
29866	-	-	-	-	-	-	-	-
30614	21.08 382 UV	20.34 70 UV	14.88 107 UV	# 5 UV	<12.85 5 UV	<12.34 117 UV	-	-
31237	20.48 361 UV	<17.45 135 UV	-	-	-	-	-	-
34078	21.30 382 UV	21.08 214 V	-	-	-	-	-	-
34656	21.23 382 UV	-	-	-	-	-	-	-
34816	20.30 361 UV	<15.04 135 UV	-	-	-	-	-	-

Star	H	H_2	HD	OH	H_2O	HCℓ	NH	N_2
34989	21.11 71 UV	<18.45 70 UV	-	-	-	-	-	-
35039	-	-	-	-	-	-	-	-
35149	20.74 71 UV	<18.53 70 UV	-	-	-	-	-	-
35395	-	-	-	-	-	-	-	-
35411	-	-	-	-	-	-	-	-
35439	20.46 135 UV	<14.90 135 UV	-	-	-	-	-	-
35600	-	-	-	-	-	-	-	-
35715	20.57 361 UV	<14.90 135 UV	-	-	-	-	-	-
36166	20.32 135 UV	<15.00 135 UV	-	-	-	-	-	-
36371	-	-	-	-	-	-	-	-
36486	20.18 382 UV	14.68 70 UV	<12.80 107 UV	-	-	<11.48 117 UV	-	-
36665	21.43 361 UV	-	-	-	-	-	-	-
36822	20.81 361 UV	19.32 70 UV	-	-	-	-	-	-
36861	20.81 382 UV	19.11 70 UV	<13.34 107 UV	-	-	<11.90 117 UV	-	-
36879	21.36 382 UV	-	-	-	-	-	-	-
37022	21.52 382 UV	-	-	-	-	-	-	-
37043	20.04 382 UV	14.70 70 UV	<12.80 107 UV	-	-	<11.60 117 UV	-	-
37128	20.38 382 UV	16.57 70 UV	<12.80 107 UV	-	-	-	-	-
37202	20.04 71 UV	<17.67 70 UV	-	-	-	-	-	-

Star	H	H_2	HD	OH	H_2O	HCℓ	NH	N_2
37318	-	-	-	-	-	-	-	-
37468	20.56 361 UV	<18.30 135 UV	-	-	-	-	-	-
37742	20.41 382 UV	15.73 70 UV	12.81 107 UV	-	-	-	-	-
38666	20.04 361 UV	15.50 70 UV	<13.34 107 UV	-	-	-	-	-
38771	20.52 382 UV	15.68 70 UV	<12.80 107 UV	-	-	-	-	-
40111	21.08 361 UV	19.73 70 UV	13.91 107 UV	-	-	-	-	-
41117	21.40 361 UV	-	-	-	-	-	-	-
44506	20.30 135 UV	<14.84 135 UV	-	-	-	-	-	-
44743	<19.48 361 UV	<17.30 70 UV	-	-	-	-	-	-
46223	21.48 382 UV	-	-	-	-	-	-	-
46883	-	-	-	-	-	-	-	-
47129	21.18 382 UV	20.54 70 UV	-	-	-	-	-	-
47839	20.38 382 UV	15.54 70 UV	<13.34 107 UV	-	-	<11.95 117 UV	-	-
48099	21.11 382 UV	20.29 70 UV	-	-	-	-	-	-
50896	20.54 71 UV	19.30 70 UV	-	-	-	-	-	-
52089	<19.48 361 UV	<17.66 70 UV	-	-	-	-	-	-
52918	20.34 135 UV	<14.90 135 UV	-	-	-	-	-	-
53138	20.18 71 UV	-	-	-	-	-	-	-
53975	21.00 382 UV	19.23 70 UV	-	-	-	-	-	-

Star	H	H_2	HD	OH	H_2O	HCℓ	NH	N_2
54662	21.25 382 UV	20.00 70 UV	-	-	-	-	-	-
55879	20.85 361 UV	<18.90 70 UV	-	-	-	-	-	-
57060	20.70 382 UV	15.78 70 UV	<13.34 107 UV	-	-	-	-	-
57061	20.70 382 UV	15.46 70 UV	<13.34 107 UV	-	-	-	-	-
57682	20.84 382 UV	<18.95 70 UV	-	-	-	-	-	-
64740	20.35 361 UV	<14.95 135 UV	-	-	-	-	-	-
64760	20.26 361 UV	<14.60 135 UV	-	-	-	-	-	-
65575	<20.74 135 UV	<14.78 135 UV	-	-	-	-	-	-
65818	20.54 135 UV	15.08 135 UV	-	-	-	-	-	-
66811	20.00 382 UV	14.45 70 UV	<12.80 107 UV	-	-	-	-	-
68273	19.78 71 UV	14.23 70 UV	<12.80 107 UV	-	-	<11.48 117 UV	-	-
74375	20.82 71 UV	<18.34 70 UV	-	-	-	-	-	-
74575	20.60 361 UV	<15.04 135 UV	-	-	-	-	-	-
75149	-	-	-	-	-	-	-	-
79351	20.78 361 UV	<17.90 135 UV	-	-	-	-	-	-
81188	20.48 135 UV	<17.70 135 UV	-	-	-	-	-	-
87901	-	<14.98 70 UV	-	-	-	-	-	-
91316	20.36 382 UV	15.62 70 UV	<13.34 107 UV	-	-	-	-	-
92693	-	-	-	-	-	-	-	-

Star	H	H_2	HD	OH	H_2O	HCℓ	NH	N_2
92740	21.20 71 UV	19.97 70 UV	-	-	-	-	-	-
93030	20.28 71 UV	<17.65 70 UV	-	-	-	-	-	-
93521	20.04 382 UV	<18.54 70 UV	-	-	-	-	-	-
99171	20.65 71 UV	15.25 70 UV	-	-	-	-	-	-
100262	-	-	-	-	-	-	-	-
106490	20.04 135 UV	<14.08 135 UV	-	-	-	-	-	-
108248	19.84 135 UV	<14.18 135 UV	-	-	-	-	-	-
112244	21.11 361 UV	20.14 70 UV	-	-	-	-	-	-
113904	21.08 71 UV	19.83 70 UV	-	-	-	-	-	-
115842	-	-	-	-	-	-	-	-
116658	<19.44 361 UV	12.95 70 UV	-	-	-	-	-	-
118716	19.90 135 UV	<14.08 135 UV	-	-	-	-	-	-
120307	-	-	-	-	-	-	-	-
120315	20.90 451 UV	13.38 70 UV	-	-	-	-	-	-
120324	20.40 135 UV	<14.78 135 UV	-	-	-	-	-	-
121263	<20.02 71 UV	12.80 70 UV	-	-	-	-	-	-
121743	-	-	-	-	-	-	-	-
122451	19.63 361 UV	12.80 70 UV	-	-	-	-	-	-
125823	-	<17.99 70 UV	-	-	-	-	-	-

Star	H	H_2	HD	OH	H_2O	HCℓ	NH	N_2
127972	20.11 135 UV	<14.18 135 UV	-	-	-	-	-	-
132058	-	-	-	-	-	-	-	-
135591	21.04 382 UV	19.77 70 UV	-	-	-	-	-	-
135742	-	<14.34 70 UV	-	-	-	-	-	-
136298	20.18 135 UV	<14.25 135 UV	-	-	-	-	-	-
138690	20.23 135 UV	<14.25 135 UV	-	-	-	-	-	-
141637	21.19 71 UV	19.23 70 UV	-	-	-	-	-	-
143018	20.74 361 UV	19.32 70 UV	13.13 107 UV	-	-	-	-	-
143118	20.04 135 UV	<14.23 135 UV	-	-	-	-	-	-
143275	21.08 361 UV	19.41 70 UV	13.06 107 UV	-	-	-	-	<12.58 119 UV
144217A	21.08 361 UV	19.83 70 UV	-	-	-	-	-	-
144218	-	-	-	-	-	-	-	-
144470	21.18 71 UV	20.05 70 UV	-	-	-	-	-	-
145502	21.15 71 UV	19.89 70 UV	-	-	-	-	-	-
147165	21.28 361 UV	19.78 70 UV	13.45 107 UV	# 5 UV	<12.18 5 UV	-	-	-
147343	-	-	-	-	-	-	-	-
147648	-	-	-	-	-	-	-	-
147701	-	-	-	-	-	-	-	-
147889	-	-	-	-	-	-	-	-

Star	H	H_2	HD	OH	H_2O	HC ℓ	NH	N_2
147933	21.60 361 UV	20.57 70 UV	-	-	-	-	-	-
147934	-	-	-	-	-	-	-	-
148184	21.15 71 UV	20.63 70 UV	-	-	-	-	-	-
148605	20.95 71 UV	18.74 70 UV	-	-	-	-	-	-
148937	21.48 382 UV	-	-	-	-	-	-	-
149038	21.04 382 UV	20.45 70 UV	14.99 107 UV	-	-	-	-	-
149404	21.36 382 UV	-	-	-	-	-	-	-
149438	20.43 361 UV	14.50 70 UV	-	-	-	-	-	-
149757	20.78 382 UV	20.64 70 UV	14.20 107 UV	13.50 113 V	<12.72 120 UV	<11.86 194 UV	<12.87 54 V	-
149881	20.60 361 UV	<19.00 70 UV	-	-	-	-	-	-
150898	21.02 361 UV	19.81 70 UV	-	-	-	-	-	-
151804	21.15 382 UV	20.25 70 UV	-	-	-	-	-	-
151890	20.40 135 UV	<14.25 135 UV	-	-	-	-	-	-
151985	-	-	-	-	-	-	-	-
152236	21.74 361 UV	-	-	-	-	-	-	-
152408	21.18 382 UV	20.38 70 UV	-	-	-	-	-	-
152424	21.36 382 UV	-	-	-	-	-	-	-
154090	-	-	-	-	-	-	-	-
154368	-	-	-	-	-	-	-	-

Star	H	H_2	HD	OH	H_2O	HCℓ	NH	N_2
154445	-	-	-	-	-	-	-	-
155806	21.00 382 UV	19.92 70 UV	-	-	-	-	-	-
156247	-	-	-	-	-	-	-	-
157056	-	-	-	-	-	-	-	-
157246	20.65 382 UV	19.23 70 UV	13.41 107 UV	<14.20 277 UV	-	<11.84 117 UV	-	-
158408	<19.25 71 UV	<14.11 70 UV	-	-	-	-	-	-
158926	<19.85 361 UV	12.70 70 UV	-	-	-	-	-	-
159975	-	-	-	-	-	-	-	-
160578	20.36 135 UV	<14.23 135 UV	-	-	-	-	-	-
162978	21.20 382 UV	-	-	-	-	-	-	
163472	-	-	-	-	-	-	-	-
164284	20.82 135 UV	19.84 135 UV	-	-	-	-	-	-
164353	21.00 71 UV	20.26 70 UV	-	-	-	-	-	-
164402	21.11 71 UV	19.49 70 UV	-	-	-	-	-	-
164794	21.34 361 UV	-	-	-	-	-	-	-
165024	20.84 71 UV	<18.95 70 UV	-	-	-	-	-	-
165174	-	-	-	-	-	-	-	-
166937	-	-	-	-	-	-	-	-
167263	20.95 382 UV	20.18 70 UV	-	-	-	-	-	-

Star	H	H_2	HD	OH	H_2O	HCℓ	NH	N_2
167264	21.15 71 UV	20.28 70 UV	-	-	-	-	-	-
169454	-	-	-	-	-	-	-	-
169754	-	-	-	-	-	-	-	-
170740	-	-	-	-	-	-	-	-
172028	-	-	-	-	-	-	-	-
174237	20.65 361 UV	-	-	-	-	-	-	-
174638	-	-	-	-	-	-	-	-
175191	<19.48 71 UV	<14.00 70 UV	-	-	-	-	-	-
176162	-	-	-	-	-	-	-	-
179406	-	-	-	-	-	-	-	-
181615	-	-	-	-	-	-	-	-
182568	-	-	-	-	-	-	-	-
183143	-	-	-	-	-	-	-	-
184915	20.90 71 UV	20.30 70 UV	-	-	-	-	-	-
186882	-	-	-	-	-	-	-	-
186994	20.90 71 UV	<19.64 70 UV	-	-	-	-	-	-
187642	-	-	-	-	-	-	-	-
187982	-	-	-	-	-	-	-	-
188209	20.90 382 UV	20.01 70 UV	-	-	-	-	-	-

Star	H	H_2	HD	OH	H_2O	HCℓ	NH	N_2
188439	20.85 361 UV	19.95 70 UV	-	-	-	-	-	-
188892	-	-	-	-	-	-	-	-
190066	-	-	-	-	-	-	-	-
190603	-	-	-	-	-	-	-	-
190967	-	-	-	-	-	-	-	-
191877	-	-	-	-	-	-	-	-
192660	-	-	-	-	-	-	-	-
193007	-	-	-	-	-	-	-	-
193237	21.17 361 UV	-	-	-	-	-	-	-
193322	21.00 382 UV	20.08 70 UV	-	-	-	-	-	-
193426	-	-	-	-	-	-	-	-
193793	-	-	-	-	-	-	-	-
193924	<19.30 71 UV	<14.30 70 UV	-	-	-	-	-	-
194279	-	-	-	-	-	-	-	-
195592	-	-	-	-	-	-	-	-
197345	-	-	-	-	-	-	-	-
198478	-	-	-	-	-	-	-	-
199478	-	-	-	-	-	-	-	-
199579	21.08 382 UV	20.36 70 UV	-	-	-	-	-	-

Star	H	H_2	HD	OH	H_2O	HCℓ	NH	N_2
200120	20.30 361 UV	19.30 70 UV	13.81 107 UV	-	-	-	-	-
202124	-	-	-	-	-	-	-	-
202850	-	-	-	-	-	-	-	-
202904	20.68 135 UV	19.15 135 UV	-	-	-	-	-	-
203064	21.04 382 UV	20.30 70 UV	-	-	-	-	-	-
203938	-	-	-	-	-	-	-	-
204172	21.00 71 UV	19.60 70 UV	-	-	-	-	-	-
206165	-	-	-	-	-	-	-	-
206267	21.30 382 UV	-	-	-	-	-	-	-
207198	21.28 382 UV	-	-	-	-	-	-	-
207538	-	-	-	-	-	-	-	-
207971	-	-	-	-	-	-	-	-
208501	-	-	-	-	-	-	-	-
209952	-	<13.68 70 UV	-	-	-	-	-	-
209975	21.18 382 UV	20.08 70 UV	-	-	-	-	-	-
210191	20.70 361 UV	<18.60 70 UV	-	-	-	-	-	-
210839	21.20 382 UV	20.78 71 UV	-	-	-	-	-	-
212076	20.65 451 UV	-	-	-	-	-	-	-
212978	-	-	-	-	-	-	-	-

Star	H	H_2	HD	OH	H_2O	HCℓ	NH	N_2
213087	-	-	-	-	-	-	-	-
213420	-	-	-	-	-	-	-	-
214080	20.60 361 UV	<19.00 70 UV	-	-	-	-	-	-
214680	20.73 382 UV	19.22 70 UV	14.63 107 UV	-	-	-	-	-
214993	20.79 135 UV	19.63 135 UV	-	-	-	-	-	-
217101	-	-	-	-	-	-	-	-
217675	-	19.67 70 UV	-	-	-	-	-	-
218376	20.95 71 UV	20.15 70 UV	-	-	-	-	-	-
219188	20.74 361 UV	19.34 70 UV	-	-	-	-	-	-
224572	20.87 71 UV	20.23 70 UV	-	-	-	-	-	-
VI Cyg12	-	-	-	-	-	-	-	-
+30°3639	-	-	-	-	-	-	-	-
+31°643	-	-	-	-	-	-	-	-
+40°4220	-	-	-	-	-	-	-	-
+66°1661	-	-	-	-	-	-	-	-
+66°1674	-	-	-	-	-	-	-	-
+66°1675	-	-	-	-	-	-	-	-
-14°5037	-	-	-	-	-	-	-	-

TABLE 27

COLUMN DENSITIES IN LOG (N/cm^2) * = DETECTED

(MOLECULAR IONS OTHER THAN CH^+)

STAR	CS^+	CO^+	H_2O^+
23180	-	-	<12.30 211v
24398	<12.08 532v	-	<12.30 211v
24912	-	<15.11 53uv	-
29647	-	* 326v	-
143275	* 148v	-	-
149757	<11.28 532v	<13.36 54v	* 211v
187982	-	-	<12.48 211v

TABLE 28 - L.S.R. RADIAL VELOCITIES, in km/sec

STAR	CH	CH^+	CO	^{13}CO	CN	C_2	H_2	HD	OH
2905	-10.7 30V	-13.3 30V	-	-	-	-	-	-	-
4180	-	-1.9 10V	-	-	-	-	-	-	-
12953	-	-3.6 59V	-11.8 151R	-	-11.3 59V	-	-	-	-
14489	-	-1.7 59V	-	-	-	-	-	-	-
20041	-	-16.0 59V	-	-	-14.4 59V	-	-	-	-
21278	-	+3.4 30V	-	-	-	-	-	-	-
21291	-	-6.6,+6.4 59V	+0.9 151R	-	+1.0 59V	-	-	-	-
21389	-	-	-10.5 151R	-	-	-	-	-	-
21483	+0.6 13V	-	+5.9,+2.4 3R	+5.7,+1.8 3R	+1.8 2R	-	-	-	-
21856	+0.8 13V	+0.2 13V	-	-	-	-	-	-	-
23180	+7.7 30V	+5.5 30V	+7.5 8UV	+8.2 3R	+8.9 7V	-	-	+8.5 8UV	+6.5 8UV

STAR	CH	CH^+	CO	^{13}CO	CN	C_2	H_2	HD	OH
23288	–	+8.7 392V	+10.5 392R	–	–	–	–	–	–
23302	–	–	+10.5 392R	–	–	–	–	–	–
23324	–	–	+10.5 392R	–	–	–	–	–	–
23338	–	+8.0 392V	+10.5 392R	–	–	–	–	–	–
23408	+8.3 30V	+8.2 392V	+10.5 392R	–	–	–	–	–	–
23432	–	+9.2 392V	+10.5 392R	–	–	–	–	–	–
23441	–	–	+10.5 392R	–	–	–	–	–	–
23480	–	+9.6 392V	+10.5 392R	–	–	–	–	–	–
23512	–	–	+10.5 392R	–	–	–	–	–	–
23568	–	+7.8 392V	+10.5 392R	–	–	–	–	–	–
23630	–	+8.0 392V	+10.5 392R	–	–	–	–	–	–
23753	–	+8.4 392V	+10.5 392R	–	–	–	–	–	–

STAR	CH	CH^+	CO	^{13}CO	CN	C_2	H_2	HD	OH
23850	–	+6.7 392V	+10.5 392R	–	–	–	–	–	–
23862	–	–	+10.5 392R	–	–	–	–	–	–
23923	–	–	+10.5 392R	–	–	–	–	–	–
24131	+6.8 13V	–	–	–	–	–	–	–	–
24398	+8.1 30V	+7.1 30V	+7.0 56UV	–	+8.8 7V	+8.0 165V	–	+5.0 56UV	+5.0 56UV
24432	−10.9 13V	−11.5 13V	–	–	–	–	–	–	–
24534	+7.7 13V	+7.1 13V	+7.2 3R	–	–	–	–	–	–
24912	+0.3 30V	+1.4 30V	–	–	–	–	–	–	–
26571	+10.0 256V	–	+10.4 151R	–	+9.9 256V	–	–	–	–
26912	+10.6 10V	+11.2 10V	–	–	–	–	–	–	–
27396	+5.1 10V	+5.7 10V	–	–	–	–	–	–	–

STAR	CH	CH^+	CO	^{13}CO	CN	C_2	H_2	HD	OH
29647	+4.8 326V	+4.2 326V	+5.1,+6.5 326V	+5.1,+6.5 326V	+4.8 326V	+4.8 326V	–	–	–
30614	+1.3 30V	−0.7 30V	–	–	–	–	–	–	–
34078	+6.9 10V	+7.5 10V	+6.7,−4.3 214UV	–	–	–	–	–	–
35149	–	+6.4 405V	–	–	–	–	–	–	–
35395	–	+4.0 10V	–	–	–	–	–	–	–
34511	–	−8.6 405V	–	–	–	–	–	–	–
35600	–	+9.7 59V	–	–	–	–	–	–	–
36371	+1.6 10V	−2.0 10V	–	–	–	–	–	–	–
37043	–	–	–	–	–	–	−5.5,+15.4 107UV	–	–
37742	–	–	–	–	–	–	−18.5,+5.2 107UV	–	–
41117	+4.0 10V	+4.6 10V	–	–	–	–	–	–	–
46883	+2.9 13V	–	–	–	–	–	–	–	–

STAR	CH	CH^+	CO	^{13}CO	CN	C_2	H_2	HD	OH
47129	+10.2 152V	+10.7 10V	–	–	–	–	–	–	–
48099	+0.2 152V	–	–	–	–	–	–	–	–
54662	−0.1,+14.9 152V	+15.8 405V	–	–	–	–	–	–	–
75149	+4.8 152V	–	–	–	–	–	–	–	–
91316	–	–	–	–	–	–	−13.3,+13.7 107UV	–	–
92693	–	–	–	–	–	−24.3 408V	–	–	–
92740	−5.4 152V	–	–	–	–	–	–	–	–
93521	–	–	–	–	–	–	−10.6 252UV	–	–
100262	–	−34.3 405V	–	–	–	–	–	–	–
112244	−24.8,−0.2 152V	+1.9 405V	–	–	–	–	–	–	–
113904	−7.0 152V	−6.4 405V	–	–	–	–	–	–	–
143018	–	−8.2 405V	–	–	–	–	–	–	–

STAR	CH	CH^+	CO	^{13}CO	CN	C_2	H_2	HD	OH
143275	–	−3.2 405V	–	–	–	–	–	–	–
144217A	+1.9 30V	−0.5 405V	–	–	–	–	–	–	–
144218	–	−2.5 405V	–	–	–	–	–	–	–
144470	−0.6 152V	−1.0 405V	–	–	–	–	–	–	–
145502	+1.4 152V	+0.1 405V	–	–	–	–	–	–	–
147165	+3.8 30V	+3.5 405V	–	–	–	–	–	–	–
147701	+1.8 446V	+0.6 446V	–	–	+3.2 446V	–	–	–	–
147889	+1.3 446V	+0.1 446V	+3.2 350R	+3.7 350R	+1.7 446V	+2.7 212V	–	–	–
147933	+2.6 152V	+2.5 405V	+2.8,+11.3 3R	–	+3.1 332R	+3.0 195V	–	–	–
147934	+2.7 47V	+2.9 47V	–	–	–	–	–	–	–
148184	+0.6 152V	+1.5 405V	–	–	–	+0.7 212V	–	–	–
148605	+4.7 64R	+2.8 405V	–	–	–	–	–	–	–

STAR	CH	CH^+	CO	^{13}CO	CN	C_2	H_2	HD	OH
149038	+2.1 152V	+1.3 405V	–	–	–	–	–	–	–
149757	−0.5 152V	−0.8 405V	−0.5 11V	–	−1.1 144V	+0.3 195V	–	–	−0.6,+5.5 191R
151804	+9.3+11.9 152V	+1.1 405V	–	–	–	–	–	–	–
152236	–	−1.6,+7.3 405V	–	–	–	–	–	–	–
152408	+2.0,+7.4 152V	–	–	–	–	–	–	–	–
154090	–	+4.0 405V	–	–	–	–	–	–	–
154368	+5.7 58V	–	–	–	+3.8 58V	+5.5 212V	–	–	–
154445	+1.7 10V	+2.3 10V	–	–	–	–	–	–	–
155806	–	+6.7 405V	–	–	–	–	–	–	–
156247	+1.5 10V	+2.1 10V	–	–	–	–	–	–	–
157246	–	+2.5 405V	–	–	–	–	–	–	–
158926	+4.2 64R	–	–	–	–	–	–	–	–

STAR	CH	CH^+	CO	^{13}CO	CN	C_2	H_2	HD	OH
159975	–	+1.5 405V	–	–	–	–	–	–	–
163472	+2.4 10V	+3.0 10V	–	–	–	–	–	–	–
164353	+3.3 152V	+2.9,+9.2 405V	–	–	–	–	–	–	–
164794	–	+6.1 10V	–	–	–	–	–	–	–
166937	–	+6.3 405V	–	–	–	–	–	–	–
167263	+5.9 152V	+6.6 405V	–	–	–	–	–	–	–
167264	+6.6 152V	+4.7 405V	–	–	–	–	–	–	–
169454	–	+4.9 405V	–	–	–	+5.8 408V	–	–	–
169754	+30.9 13V	+30.3 13V	–	–	–	–	–	–	–
170740	+5.8 10V	+6.4 10V	–	–	–	–	–	–	–
172028	+6.1 13V	+5.5 13V	–	–	–	–	–	–	–
176162	–	+1.0 10V	–	–	–	–	–	–	–

STAR	CH	CH^+	CO	^{13}CO	CN	C_2	H_2	HD	OH
179406	+1.1 10V	–	+2.5,-3.3 3R	–	–	–	–	–	–
181615	+1.2 10V	+1.8 10V	–	–	–	–	–	–	–
182568	+8.3 10V	–	–	–	–	–	–	–	–
183143	+14.6 13V	+14.0 13V	–	–	–	–	–	–	–
184915	+1.3 30V	+1.2 405V	–	–	–	–	–	–	–
188892	–	+7.8 10V	–	–	–	–	–	–	–
190066	–	+13.3 10V	–	–	–	–	–	–	–
190603	+2.5 10V	+3.1 10V	–	–	–	–	–	–	–
190967	–	+4.5 13V	–	–	–	–	–	–	–
191877	–	+12.3 10V	–	–	–	–	–	–	–
192660	+11.7 13V	+11.1 13V	–	–	–	–	–	–	–
193007	+4.9 10V	+5.5 10V	–	–	–	–	–	–	–

STAR	CH	CH^+	CO	^{13}CO	CN	C_2	H_2	HD	OH
193237	+4.5 10V	+5.1 10V	+1.1 3R	–	–	–	–	–	–
193322	−5.0 10V	−4.4,+7.7 10V	–	–	–	–	–	–	–
193426	+3.6 13V	+3.0 13V	–	–	–	–	–	–	–
193793	+6.1 10V	+6.7 10V	–	–	–	–	–	–	–
198478	+2.4 10V	+3.0 10V	+1.1 3R	–	–	–	–	–	–
199478	−1.7 10V	−1.1 10V	–	–	–	–	–	–	–
199579	+5.3 10V	+5.9 10V	–	–	–	–	–	–	–
203064	+1.7 30V	+1.2 30V	–	–	–	–	–	–	–
203938	–	+2.5 13V	–	–	–	–	–	–	–
206165	+0.0 64R	–	−0.5,+6.0 3R	–	–	–	–	–	–
207198	–	–	−2.5,+4.0 3R	–	–	–	–	–	–
207538	−3.0 52R	–	−1.3,+2.3 3R	–	–	–	–	–	–

STAR	CH	CH^+	CO	^{13}CO	CN	C_2	H_2	HD	OH
208501	–	–	−1.6 151R	–	−1.9 254V	–	–	–	–
210839	–	–	+1.5 3R	–	–	–	–	–	–
212978	−0.7 10V	−0.1 10V	–	–	–	–	–	–	–
218376	+1.6 30V	−6.3,+3.4 30V,51V	–	–	–	–	–	–	–
224572	−8.4 30V	−9.5,−16.1 30V	–	–	–	–	–	–	–
VI CYG 12	–	–	–	–	–	+7.1 176V	–	–	–
+31°643	+5.5 13V	+4.9 13V	–	–	–	–	–	–	–
+40°4220	−20.1,−11.6, + 0.8,+ 6.9, +12.2 64R	–	–	–	–	–	–	–	–
+66°1661	−11.5 57V	–	–	–	−8.1 57V	–	–	–	–
+66°1674	−8.2 57V	–	–	–	−7.4 57V	–	–	–	–
+66°1675	−12.0 57V	–	−0.4,−6.2, −14.0 151R	–	−9.4 57V	–	–	–	–

TABLE 29. REFERENCES.

Star	CH	CH^+	$^{13}CH^+$	CO	^{13}CO	CN	C_2	C_3
886	-	30V	-	-	-	-	-	-
2905	30V,50R	30V	-	-	-	283V	-	-
4180	-	10V	-	-	-	-	-	-
5394	-	30V	-	-	-	-	-	-
10144	-	405V	-	-	-	-	-	-
10516	-	51V	-	-	-	-	-	-
12953	-	59V	-	151R	-	59V	-	-
14228	-	405V	-	27UV	-	-	-	-
14489	-	59V	-	-	-	-	-	-
14633	-	-	-	-	-	-	-	-
20041	-	59V	-	151R	-	59V	-	-
21278	-	30V	-	27UV	-	-	-	-
21291	-	59V	-	151R	-	59V	-	-
21389	-	-	-	151UV, R 247UV	-	-	-	-
21483	13V, 52R	-	-	3R	3R	2R, 184R	-	-
21856	13V, 52R,	13V	-	-	-	-	-	-
22192	-	-	-	269UV	-	-	-	-
22928	-	30V	-	-	-	-	-	-
22951	-	10V	-	-	-	283V	-	-
23180	10V, 13V, 30V, 105V, 7V, 52R 360V	13V, 30V, 105V, 7V, 10V	-	14UV, 27UV 8UV, 3R, 40R	3R, 40R	4V, 7V 381V	8UV, 97V	-
23288	392V	4V, 10V 392V	-	392R	-	392V	-	-

Star	CH	CH^+	$^{13}CH^+$	CO	^{13}CO	CN	C_2	C_3
23302	392V	44V, 10V 392V	-	392R	-	392V	-	-
23324	392V	392V	-	392R	-	392V	-	-
23338	392V	10V, 392V	-	392R	-	392V	-	-
23408	30V, 126V 64R, 392V	149V, 4V, 30V, 126V, 51V, 44V, 10V, 392V	141V, 149V	27UV 392R	-	392V	164V	-
23432	392V	10V, 392V	-	392R	-	392V	-	-
23441	392V	392V	-	392R	-	392V	-	-
23480	30V,126V, 64R,392V	30V,126V, 4V,51V,44V 392V, 10V	141V	392R	-	392V	-	-
23512	392V	392V	-	392R	-	392V	-	-
23552	-	-	-	268UV	268UV	-	-	-
23568	392V	392V	-	392R	-	392V	-	-
23630	30V,126V 392V	30V,126V, 10V,392V	-	27UV, 392R	-	392V	-	-
23753	392V	4V, 10V 392V	-	392R	-	392V	-	123V
23850	392V	10V, 392V	-	392R	-	392V	-	-
23862	392V	392V	-	392R	-	392V	-	-
23923	392V	392V	-	392R	-	392V	-	-
24131	13V, 52R	10V	-	-	-	-	-	-
24398	10V, 188R, 13V, 30V, 105V, 7V, 46V, 64R 360V	13V, 30V, 105V, 7V, 10V, 51V, 44V	-	27UV, 56UV	-	4V, 7V 381V	163V,164V 165V	123V

Star	CH	CH^+	$^{13}CH^+$	CO	^{13}CO	CN	C_2	C_3
24432	13V, 52R	13V	-	-	-	-	-	-
24534	4V, 10V, 13V, 64R, 330V, 52R	13V, 10V	-	3R	-	4V	393UV	-
24760	30V	30V	-	27UV	-	-	-	-
24912	52R,64R, 4V, 10V, 13V,30V, 105V, 7V	149V,4V, 13V, 51V, 30V, 7V 10V, 44V	141V,149V	27UV,53UV	-	7V,283V	53UV	-
26571	64R, 256V	-	-	151UV, R, 247 UV	-	131V, 256V	-	-
26912	10V	10V	-	-	-	-	-	-
27396	4V, 10V	4V, 10V	-	-	-	-	-	-
27777	-	44V	-	-	-	-	-	-
28497	-	-	-	27UV	-	-	-	-
29248	-	-	-	-	-	-	-	-
29309	-	10V	-	-	-	-	-	-
29647	326V	326V	-	326R	326R	326V	147V, 146V 326V	-
29866	-	-	-	268UV	268UV	-	-	-
30614	30V, 50R	30V	-	14UV, 53UV	-	-	-	-
31237	-	-	-	-	-	-	-	-
34078	64R, 10V	10V	-	214UV	-	4V	-	-
34656	10V	10V	-	-	-	-	-	-
34816	-	-	-	-	-	-	-	-
34989	-	-	-	-	-	-	-	-
35039	-	405V	-	-	-	-	-	-

Star	CH	CH^+	$^{13}CH^+$	CO	^{13}CO	CN	C_2	C_3
35149	-	4V, 30V, 10V 405V	-	-	-	-	-	-
35395	-	10V	-	-	-	-	-	-
35411	-	405V	-	-	-	-	-	-
35439	-	-	-	-	-	-	-	-
35600	-	59V	-	-	-	-	-	-
35715	-	-	-	-	-	-	-	-
36166	-	-	-	-	-	-	-	-
36371	4V, 10V	4V, 44V, 10V	-	-	-	-	-	-
36486	-	30V	-	27UV	-	-	-	-
36665	-	-	-	143UV	-	-	-	-
36822	-	405V	-	-	-	-	-	-
36861	64R	30V, 51V	-	53UV	-	-	-	-
36879	-	-	-	14UV	-	-	-	-
37022	-	30V	-	-	-	-	-	-
37043	-	30V	-	27UV	-	-	-	-
37128	-	30V, 51V	-	27UV	-	-	-	-
37202	-	30V	-	27UV	-	-	-	-
37318	-	-	-	134UV	-	-	-	-
37468	-	-	-	-	-	-	-	-
37742	-	30V	-	27UV	-	-	-	-
38666	-	-	-	-	-	-	-	-
38771	-	30V, 44V	-	-	-	-	-	-
40111	-	-	-	27UV	-	-	-	-

Star	CH	CH^+	$^{13}CH^+$	CO	^{13}CO	CN	C_2	C_3
41117	4V,10V, 64R	4V,51V, 44V,10V	-	14UV,34UV	34UV	-	-	-
44506	-	-	-	-	-	-	-	-
44743	-	30V	-	-	-	-	-	-
46223	-	-	-	14UV, 248UV	-	-	-	-
46883	13V	-	-	-	-	-	-	-
47129	152V,10V	10V	-	34UV	34UV	-	-	-
47839	-	30V	-	27UV	-	-	-	-
48099	152V	-	-	-	-	-	-	-
50896	-	-	-	-	-	-	-	-
52089	-	405V	-	-	-	-	-	-
52918	-	-	-	-	-	-	-	-
53138	-	-	-	27UV	-	-	-	-
53975	-	-	-	-	-	-	-	-
54662	152V	405V	-	-	-	-	-	-
55879	-	-	-	-	-	-	-	-
57060	152V	-	-	27UV	-	-	-	-
57061	152V	405V	-	27UV	-	-	-	-
57682	-	-	-	-	-	-	-	-
64740	-	-	-	-	-	-	-	-
64760	-	-	-	-	-	-	-	-
65575	-	-	-	-	-	-	-	-
65818	-	-	-	-	-	-	-	-
66811	152V	-	-	27UV	-	-	-	-
68273	-	-	-	27UV, 279UV	-	-	-	-

Star	CH	CH^+	$^{13}CH^+$	CO	^{13}CO	CN	C_2	C_3
74375	152V	-	-	-	-	-	-	-
74575	-	405V	-	-	-	-	-	-
75149	152V	-	-	-	-	-	-	-
79351	-	-	-	-	-	-	-	-
81188	-	-	-	-	-	-	-	-
87901	-	30V	-	27UV	-	-	-	-
91316	-	30V, 51V 405V	-	27UV	-	-	-	-
92693	-	-	-	-	-	-	408V	-
92740	152V	-	-	-	-	-	-	-
93030	152V	405V	-	27UV	-	-	-	-
93521	-	-	-	-	-	-	-	-
99171	-	-	-	-	-	-	-	-
100262	-	405V	-	-	-	-	-	-
106490	-	405V	-	-	-	-	-	-
108248	-	405V	-	-	-	-	-	-
112244	152V	405V	-	-	-	283V	-	-
113904	152V	405V	-	-	-	-	-	-
115842	152V	-	-	-	-	-	-	-
116658	-	30V	-	-	-	-	-	-
118716	-	405V	-	-	-	-	-	-
120307	-	405V	-	-	-	-	-	-
120315	-	30V	-	-	-	-	-	-
120324	-	-	-	268UV	-	-	-	-
121263	-	405V	-	-	-	-	-	-

Star	CH	CH^+	$^{13}CH^+$	CO	^{13}CO	CN	C_2	C_3
121743	-	405V	-	-	-	-	-	-
122451	-	-	-	-	-	-	-	-
125823	-	-	-	-	-	-	-	-
127972	-	-	-	-	-	-	-	-
132058	-	405V	-	-	-	-	-	-
135591	-	-	-	-	-	-	-	-
135742	-	30V, 405V	-	27UV	-	-	-	-
136298	-	405V	-	-	-	-	-	-
138690	-	405V	-	-	-	-	-	-
141637	-	405V	-	-	-	-	-	-
143018	152V	30V, 405V	-	27UV	-	-	-	-
143118	-	405V	-	-	-	-	-	-
143275	152V	30V, 51V, 405V	-	27UV, 48UV	-	283V	-	-
144217A	30V, 325V 152V	30V, 51V 325V, 405V	-	48UV	-	283V	-	-
144218	-	405V	-	-	-	-	-	-
144470	13V, 30V 152V,325V	13V, 30V 325V,405V	-	27UV, 48UV	-	-	-	-
145502	30V, 152V,325V	30V, 51V 325V, 405V	-	27UV, 48UV	-	-	-	-
147165	30V, 152V,325V	13V, 30V, 51V 325V, 405V	-	48UV	-	283V	-	-
147343	446V	446V	-	-	-	446V	-	-
147648	446V	-	-	-	-	446V	-	-
147701	13V, 213V,52R 446V	13V, 446V	-	-	-	446V	-	-

Star	CH	CH^+	$^{13}CH^+$	CO	^{13}CO	CN	C_2	C_3
147889	13V, 213V,52R 188R, 348V 446V	13V, 348V 446V	-	350R	350R	213V, 348V 446V	212V	-
147933	52R,64R, 13V, 4V, 10V, 47V, 152V, 213V	13V,10V,4V, 47V,405V	-	3R, 14UV, 27UV, 48UV	-	283V, 332R 184R	195V	-
147934	213V,4V, 47V, 10V	4V, 47V, 10V	-	-	-	-	-	-
148184	64R,47V, 10V,4V, 23V,152V	47V,51V, 4V,23V, 10V,405V	-	55UV, 151R	-	23V, 283V	195V, 212V	-
148605	64R	405V	-	-	-	-	-	-
148937	-	-	-	14UV	-	-	-	-
149038	152V	405V	-	27UV	-	283V	-	-
149404	-	-	-	14UV, 34UV	34UV	-	212V	-
149438	64R	106V, 405V	-	-	-	-	-	-
149757	10V,152V, 4V,47V, 54V,144V, 131V,52R 360V	149V,22V,4V, 24V,144V, 10V,51V, 140V,47V, 54V,131V, 362V, 405V	22V,24V 141V, 144V, 149V	179UV 11UV, 21UV, 27UV,3R, 53UV,43UV, 40R	179UV, 11UV, 43UV, 40R	4V,54V, 144V, 281V, 283V, 131V, 296V 381V,10V 511V	104V,166V 183UV,175UV 163V,11UV 175UV,178V, 195V,448V	123V
149881	-	-	-	-	-	-	-	-
150898	-	-	-	-	-	-	-	-
151804	152V	405V	-	14UV	-	-	-	-
151890	-	405V	-	-	-	-	-	-
151985	-	405V	-	-	-	-	-	-
152236	-	405V	-	34UV	34UV	-	-	-

Star	CH	CH^+	$^{13}CH^+$	CO	^{13}CO	CN	C_2	C_3
152408	152V	-	-	-	-	-	-	-
152424	-	-	-	14UV	-	-	-	-
154090	-	405V	-	-	-	-	-	-
154368	25V,58V, 6V	25V,58V 6V	-	151UV,247UV 184R	-	25V,58V,6V 2R	212V	-
154445	4V,10V	4V,10V	-	-	-	-	-	-
155806	-	405V	-	-	-	-	-	-
156247	4V,10V, 64R	4V,10V	-	-	-	-	-	-
157056	-	405V	-	-	-	-	-	-
157246	152V	405V	-	277UV	-	-	-	-
158408	-	405V	-	27UV	-	-	-	-
158926	64R	405V	-	-	-	-	-	-
159975	-	4V,51V,10V 405V	-	-	-	-	-	-
160578	-	405V	-	-	-	-	-	-
162978	-	10V	-	-	-	-	-	-
163472	4V,10V	4V,10V	-	-	-	-	-	-
164284	-	-	-	-	-	-	-	-
164353	64R,30V, 152V	30V,405V	-	27UV	-	283V	-	-
164402	-	-	-	-	-	-	-	-
164794	-	4V,10V	-	-	-	-	-	-
165024	-	405V	-	-	-	-	-	-
165174	-	10V	-	-	-	-	-	-
166937	-	4V,51V,10V 405V	-	-	-	-	-	-
167263	152V	10V,405V	-	-	-	-	-	-

Star	CH	CH^+	$^{13}CH^+$	CO	^{13}CO	CN	C_2	C_3
167264	152V	30V,10V,405V	-	34UV	34UV	283V	-	-
169454	-	405V	-	-	-	-	408V	-
169754	13V,52R	13V	-	-	-	-	-	-
170740	4V,10V	4V,10V	-	-	-	-	-	-
172028	13V,52R	13V	-	-	-	-	-	-
174237	-	-	-	268UV	-	-	-	-
174638	-	51V	-	-	-	-	-	-
175191	-	30V,405V	-	27UV	-	-	-	-
176162	-	4V,10V	-	-	-	-	-	-
179406	4V,10V	-	-	3R	-	4V	-	-
181615	10V	51V,10V	-	-	-	-	-	-
182568	4V,10V	-	-	-	-	-	-	-
183143	10V,13V 52R	13V,10V	-	-	-	-	-	123V
184915	30V	30V,405V	-	-	-	283V	-	-
186882	-	51V	-	-	-	-	-	-
186994	-	-	-	-	-	-	-	-
187642	-	405V	-	-	-	-	-	-
187982	-	-	-	-	-	-	-	-
188209	-	-	-	-	-	-	-	-
188439	-	-	-	-	-	-	-	-
188892	-	10V	-	-	-	-	-	-
190066	-	4V, 10V	-	-	-	-	-	-
190603	10V	4V, 10V	-	-	-	-	-	-
190967	-	13V	-	-	-	-	-	-
191877	-	10V	-	-	-	-	-	-

Star	CH	CH^+	$^{13}CH^+$	CO	^{13}CO	CN	C_2	C_3
192660	13V, 52R	13V	-	-	-	-	-	-
193007	10V	10V	-	-	-	-	-	-
193237	10V	4V, 51V 10V	141V	3R	-	-	-	-
193322	10V	10V, 4V	-	34UV	34UV	-	-	-
193426	13V	13V	-	-	-	-	-	-
193793	10V	4V, 10V	-	-	-	-	-	-
193924	-	405V	-	-	-	-	-	-
194279	-	10V	-	-	-	-	-	-
195592	10V	10V	-	-	-	-	-	-
197345	-	51V	-	-	-	-	-	-
198478	64R,10V	10V,51V	141V	3R	-	4V	-	123V
199478	4V,10V	4V,10V	-	-	-	-	-	-
199579	10V	10V	-	-	-	-	-	-
200120	-	30V	-	27UV	-	-	-	-
202124	-	-	-	-	-	57V	-	-
202850	-	51V	-	-	-	-	-	-
202904	-	-	-	-	-	-	147V,163V	-
203064	30V	30V	-	34UV	34UV	283V	-	-
203938	-	13V	-	-	-	-	-	-
204172	-	-	-	-	-	-	-	-
206165	1V,64R	1V,51V	-	34UV,41UV, 3R	34UV	1V	-	-
206267	1V	1V	-	-	-	1V	-	-
207198	1V	1V	-	3R	-	1V	-	-
207538	52R	-	-	3R,256UV	-	-	-	-
207971	-	405V	-	-	-	-	-	-

Star	CH	CH^+	$^{13}CH^+$	CO	^{13}CO	CN	C_2	C_3
208501	-	-	-	151R	-	131V,254V	-	-
209952	-	405V	-	27UV	-	-	-	-
209975	-	-	-	14UV	-	-	-	-
210191	-	405V	-	-	-	-	-	-
210839	1V	1V	-	3R,34UV 256UV	34UV	1V	-	-
212076	-	10V	-	-	-	-	-	-
212978	10V	10V	-	-	-	-	-	-
213087	-	-	-	14UV	-	-	-	123V
213420	-	51V	-	-	-	-	-	-
214080	-	-	-	-	-	-	-	-
214680	-	30V	-	-	-	-	-	-
214993	-	-	-	-	-	-	-	-
217101	-	10V	-	-	-	-	-	-
217675	30V	30V,51V	-	27UV,268UV	-	-	147V,163V	-
218376	30V	30V,51V	-	-	-	-	-	-
219188	-	-	-	-	-	-	-	-
224572	30V	30V	-	-	-	-	-	-
VI Cyg 12	-	-	-	-	-	-	146V,163V 176V	-
+30°3639	-	-	-	268UV	-	-	-	-
+31°643	13V,64R, 188R	13V	-	-	-	-	-	-
+40°4220	64R	-	-	-	-	-	-	-
+66°1661	64R,57V	-	-	-	-	57V	-	-
+66°1674	57V	-	-	-	-	131V,57V	-	-
+66°1675	57V,64R	-	-	151R	-	57V	146V	-
-14°5037	-	-	-	-	-	-	408V	-

TABLE 29. REFERENCES.

Star	H	H_2	HD	OH	H_2O	HCl	NH	N_2
886	71UV 361UV	70UV 87UV	-	-	-	-	-	-
2905	71UV 361UV	70UV	-	-	-	-	-	-
4180	-	-	-	-	-	-	-	-
5394	71UV 361UV	70UV	-	-	-	-	-	-
10144	-	70UV, 87UV	-	-	-	-	-	-
10516	71UV	70UV	-	-	-	-	-	-
12953	-	-	-	-	-	-	-	-
14228	-	70UV	-	-	-	-	-	-
14489	-	-	-	-	-	-	-	-
14633	71UV 361UV 382UV	70UV	-	-	-	-	-	-
20041	-	-	-	-	-	-	-	-
21278	-	70UV, 87UV	87UV	-	-	-	-	-
21291	-	-	-	-	-	-	-	-
21389	-	-	-	-	-	-	-	-
21483	-	-	-	-	-	-	-	-
21856	71UV	70UV	-	-	-	-	-	-
22192	-	-	-	-	-	-	-	-
22928	-	70UV 89UV	107UV	-	-	117UV	-	-
22951	71UV	70UV	-	-	-	-	-	-
23180	71UV 361UV	70UV, 8UV	8UV	183UV,8UV 113V,40R	8UV 182UV	-	74V	8UV

Star	H	H_2	HD	OH	H_2O	HCl	NH	N_2
23288	-	-	-	-	-	-	-	-
23302	-	-	-	-	-	-	-	-
23324	-	-	-	-	-	-	-	-
23338	-	-	-	-	-	-	-	-
23408	-	70 UV	107 UV	-	-	-	-	-
23432	-	-	-	-	-	-	-	-
23441	-	-	-	-	-	-	-	-
23480	-	70 UV	-	-	-	-	-	-
23512	-	-	-	-	-	-	-	-
23552	-	-	-	-	-	-	-	-
23568	-	-	-	-	-	-	-	-
23630	-	70 UV	-	-	-	-	-	-
23753	-	-	-	-	-	-	-	-
23850	-	-	-	-	-	-	-	-
23862	-	-	-	-	-	-	-	-
23923	-	-	-	-	-	-	-	-
24131	-	-	-	-	-	-	-	-
24398	71 UV	70UV,56UV 87UV	56UV 87UV	5UV,56UV 46V	-	-	46V	-
24432	-	-	-	-	-	-	-	-
24534	382 UV	-	-	-	-	-	-	-
24760	71 UV 72 UV 361 UV	70 UV 87 UV	87 UV 107 UV	-	-	117 UV	-	119 UV
24912	71 UV 72 UV 361 UV 382 UV	70UV,72UV 87UV	87 UV 107UV	53 UV	53 UV	117 UV	-	-
26571	-	-	-	-	-	-	-	-

Star	H	H_2	HD	OH	H_2O	HCl	NH	N_2
26912	-	-	-	-	-	-	-	-
27396	-	-	-	-	-	-	-	-
27777	-	-	-	-	-	-	-	-
28497	71 UV 361 UV 506 UV	70 UV	-	-	-	-	-	-
29248	79 UV 135 UV 361 UV	79 UV 135 UV	-	-	-	-	-	-
29309	-	-	-	-	-	-	-	-
29647	-	326 V	-	-	-	-	-	-
29866	-	-	-	-	-	-	-	-
30614	71 UV 361 UV 382 UV	70 UV 87 UV	107 UV 87 UV	5 UV	5 UV	117 UV	-	-
31237	79 UV 135 UV 361 UV	79 UV 135 UV	-	-	-	-	-	-
34078	214 UV 361 UV 382 UV	214 UV	-	-	-	-	-	-
34656	382 UV	-	-	-	-	-	-	-
34816	79 UV 135 UV 361 UV	79 UV 135 UV	-	-	-	-	-	-
34989	71 UV	70 UV	-	-	-	-	-	-
35039	-	-	-	-	-	-	-	-
35149	71 UV	70 UV	-	-	-	-	-	-
35395	-	-	-	-	-	-	-	-
35411	-	-	-	-	-	-	-	-
35439	79 UV 135 UV	79 UV 135 UV	-	-	-	-	-	-
35600	-	-	-	-	-	-	-	-

Star	H	H_2	HD	OH	H_2O	HCl	NH	N_2
35715	79 UV 135 UV 361 UV	79 UV 135 UV	-	-	-	-	-	-
36166	79 UV 135 UV	79 UV 135 UV	-	-	-	-	-	-
36371	-	-	-	-	-	-	-	-
36486	71 UV 361 UV 382 UV	87 UV 70 UV 107 UV	107 UV	-	-	117 UV	-	-
36665	361 UV	-	-	-	-	-	-	-
36822	71 UV 361 UV	70 UV	-	-	-	-	-	-
36861	71 UV 361 UV 382 UV	87 UV 70 UV	107 UV	-	-	117 UV	-	-
36879	361 UV 382 UV	-	-	-	-	-	-	-
37022	382 UV	-	-	-	-	-	-	-
37043	71 UV 361 UV 382 UV	70 UV 107 UV	107 UV	-	-	117 UV	-	-
37128	71 UV 361 UV 382 UV	70 UV 107 UV	107 UV	-	-	-	-	-
37202	71 UV	70 UV	-	-	-	-	-	-
37318	-	-	-	-	-	-	-	-
37468	79 UV 135 UV 361 UV	79 UV 135 UV	-	-	-	-	-	-
37742	71 UV 361 UV 382 UV	87 UV 70 UV 107 UV	107 UV	-	-	-	-	-
38666	71 UV 361 UV 506 UV	70 UV 107 UV	107 UV	-	-	-	-	-

Star	H	H_2	HD	OH	H_2O	HCl	NH	N_2
38771	71 UV 361 UV 382 UV	70 UV 107 UV	107 UV	-	-	-	-	-
40111	71 UV 361 UV	70 UV 87 UV	87 UV 107 UV	-	-	-	-	-
41117	361 UV	-	-	-	-	-	-	-
44506	79 UV 135 UV	79 UV 135 UV	-	-	-	-	-	-
44743	71 UV 361 UV	70 UV	-	-	-	-	-	-
46223	361 UV 382 UV	-	-	-	-	-	-	-
46883	-	-	-	-	-	-	-	-
47129	71 UV 361 UV 382 UV	70 UV	-	-	-	-	-	-
47839	71 UV 361 UV 382 UV	70 UV 107 UV	107UV	-	117 UV	-	-	
48099	71 UV 361 UV 382 UV	70 UV	-	-	-	-	-	-
50896	71 UV	70 UV	-	-	-	-	-	-
52089	71 UV 361 UV	70 UV	-	-	-	-	-	-
52918	79 UV 135 UV	79 UV 135 UV	-	-	-	-	-	-
53138	71 UV	-	-	-	-	-	-	-
53975	71 UV 361 UV 382 UV	70 UV	-	-	-	-	-	-
54662	71 UV 361 UV 382 UV	70 UV	-	-	-	-	-	-

Star	H	H_2	HD	OH	H_2O	HCl	NH	N_2
55879	71 UV 361 UV	70 UV	-	-	-	-	-	-
57060	71 UV 361 UV 382 UV	70UV, 107UV	107 UV	-	-	-	-	-
57061	71 UV 361 UV 382 UV	70UV, 107UV	107 UV	-	-	-	-	-
57682	71 UV 361 UV 382 UV	70 UV	-	-	-	-	-	-
64740	79 UV 135 UV 361 UV	79 UV 135 UV	-	-	-	-	-	-
64760	79 UV 135 UV 361 UV	79 UV 135 UV	-	-	-	-	-	-
65575	79 UV 135 UV	79 UV 135 UV	-	-	-	-	-	-
65818	79 UV 135 UV	79 UV 135 UV	-	-	-	-	-	-
66811	71 UV 361 UV 382 UV	70 UV 107 UV	107 UV	-	-	-	-	-
68273	71 UV	70 UV 107 UV	107 UV	-	-	117 UV	-	-
74375	71 UV	70 UV	-	-	-	-	-	-
74575	79 UV 135 UV 361 UV	79 UV 135 UV	-	-	-	-	-	-
75149	-	-	-	-	-	-	-	-
79351	79 UV 135 UV 361 UV	79 UV 135 UV	-	-	-	-	-	-
81188	79 UV 135 UV	79 UV 135 UV	-	-	-	-	-	-
87901	-	70 UV	-	-	-	-	-	-

Star	H	H_2	HD	OH	H_2O	HCl	NH	N_2
91316	71 UV 506 UV 361 UV 382 UV	70 UV 107 UV	107 UV	–	–	–	–	–
92693	–	–	–	–	–	–	–	–
92740	71 UV	70 UV	–	–	–	–	–	–
93030	71 UV	70 UV	–	–	–	–	–	–
93521	71 UV 252 UV 361 UV 382 UV 506 UV	70 UV 252 UV	–	–	–	–	–	–
99171	71 UV	70 UV	–	–	–	–	–	–
100262	–	–	–	–	–	–	–	–
106490	79 UV 135 UV	79 UV 135 UV	–	–	–	–	–	–
108248	79 UV 135 UV	79 UV 135 UV	–	–	–	–	–	–
112244	71 UV 361 UV	70 UV	–	–	–	–	–	–
113904	71 UV	70 UV	–	–	–	–	–	–
115842	–	–	–	–	–	–	–	–
116658	71 UV 361 UV	70 UV	–	–	–	–	–	–
118716	79 UV 135 UV	79 UV 135 UV	–	–	–	–	–	–
120307	–	–	–	–	–	–	–	–
120315	451 UV	70 UV	–	–	–	–	–	–
120324	79 UV 135 UV	79 UV 135 UV	–	–	–	–	–	–
121263	71 UV	70 UV	–	–	–	–	–	–
121743	–	–	–	–	–	–	–	–

Star	H	H_2	HD	OH	H_2O	HCl	NH	N_2
122451	71 UV 361 UV	70 UV	-	-	-	-	-	-
125823	-	70 UV	-	-	-	-	-	-
127972	79 UV 135 UV	79 UV 135 UV	-	-	-	-	-	-
132058	-	-	-	-	-	-	-	-
135591	71 UV 361 UV 382 UV	70 UV	-	-	-	-	-	-
135742	-	70 UV	-	-	-	-	-	-
136298	79 UV 135 UV	79 UV 135 UV	-	-	-	-	-	-
138690	79 UV 135 UV	79 UV 135 UV	-	-	-	-	-	-
141637	71 UV	70 UV	-	-	-	-	-	-
143018	71 UV 361 UV	70 UV	107 UV	-	-	-	-	-
143118	79 UV 135 UV	79 UV 135 UV	-	-	-	-	-	-
143275	71 UV 100 UV 361 UV	70 UV 100 UV	107 UV	-	-	-	-	119 UV
144217A	71 UV 361 UV	70 UV	-	-	-	-	-	-
144218	-	-	-	-	-	-	-	-
144470	71 UV	70 UV	-	-	-	-	-	-
145502	71 UV	70 UV	-	-	-	-	-	-
147165	71 UV 361 UV	70 UV	107 UV	5 UV	5 UV	-	-	-
147343	-	-	-	-	-	-	-	-
147648	-	-	-	-	-	-	-	-
147701	-	-	-	-	-	-	-	-

Star	H	H_2	HD	OH	H_2O	HCl	NH	N_2
147889	-	-	-	-	-	-	-	-
147933	71 UV 361 UV	70 UV	-	-	-	-	-	-
147934	-	-	-	-	-	-	-	-
148184	71 UV	70 UV	-	-	-	-	-	-
148605	71 UV	70 UV	-	-	-	-	-	-
148937	382 UV	-	-	-	-	-	-	-
149038	71 UV 361 UV 382 UV	70 UV	107 UV	-	-	-	-	-
149404	361 UV 382 UV	-	-	-	-	-	-	-
149438	71 UV 361 UV	70UV, 87UV 107 UV	-	-	-	-	-	-
149757	71 UV 361 UV 382 UV	70 UV 87 UV	87 UV 107 UV	5UV, 183UV 54V, 113V 11UV, 191R	182UV 183UV 5UV, 120UV 11UV	194 UV 11 UV	54 V	-
149881	71 UV 361 UV 506 UV	70 UV	-	-	-	-	-	-
150898	71 UV 361 UV	70 UV	-	-	-	-	-	-
151804	71 UV 361 UV 382 UV	70 UV	-	-	-	-	-	-
151890	79 UV 135 UV	79 UV 135 UV	-	-	-	-	-	-
151985	-	-	-	-	-	-	-	-
152236	361 UV	-	-	-	-	-	-	-
152408	71 UV 361 UV 382 UV	70 UV	-	-	-	-	-	-
152424	382 UV	-	-	-	-	-	-	-

Star	H	H_2	HD	OH	H_2O	HCl	NH	N_2
154090	-	-	-	-	-	-	-	-
154368	-	-	-	-	-	-	-	-
154445	-	-	-	-	-	-	-	-
155806	71 UV 361 UV 382 UV	70 UV	-	-	-	-	-	-
156247	-	-	-	-	-	-	-	-
157056	-	-	-	-	-	-	-	-
157246	71 UV 361 UV 382 UV	70UV, 87UV	107 UV	277 UV	-	117 UV	-	-
158408	71 UV	70UV, 87UV	-	-	-	-	-	-
158926	71 UV 361 UV	70UV, 87UV	-	-	-	-	-	-
159975	-	-	-	-	-	-	-	-
160578	79 UV 135 UV	79 UV 135 UV	-	-	-	-	-	-
162978	382 UV	-	-	-	-	-	-	-
163472	-	-	-	-	-	-	-	-
164284	79 UV 135 UV	79 UV 135 UV	-	-	-	-	-	-
164353	71 UV	70UV, 87UV	-	-	-	-	-	-
164402	71 UV	70 UV	-	-	-	-	-	-
164794	361 UV	-	-	-	-	-	-	-
165024	71 UV	70 UV	-	-	-	-	-	-
165174	-	-	-	-	-	-	-	-
166937	-	-	-	-	-	-	-	-
167263	71 UV 361 UV 382 UV	70 UV	-	-	-	-	-	-

Star	H	H_2	HD	OH	H_2O	HCl	NH	N_2
167264	71 UV	70 UV	-	-	-	-	-	-
169454	-	-	-	-	-	-	-	-
169754	-	-	-	-	-	-	-	-
170740	-	-	-	-	-	-	-	-
172028	-	-	-	-	-	-	-	-
174237	361 UV	-	-	-	-	-	-	-
174638	-	-	-	-	-	-	-	-
175191	71 UV	70UV, 87UV	-	-	-	-	-	-
176162	-	-	-	-	-	-	-	-
179406	-	-	-	-	-	-	-	-
181615	-	-	-	-	-	-	-	-
182568	-	-	-	-	-	-	-	-
183143	-	-	-	-	-	-	-	-
184915	71 UV	70 UV	-	-	-	-	-	-
186882	-	-	-	-	-	-	-	-
186994	71 UV	70 UV	-	-	-	-	-	-
187642	-	-	-	-	-	-	-	-
187982	-	-	-	-	-	-	-	-
188209	71 UV 361 UV 382 UV	70 UV	-	-	-	-	-	-
188439	71 UV 361 UV	70 UV	-	-	-	-	-	-
188892	-	-	-	-	-	-	-	-
190066	-	-	-	-	-	-	-	-
190603	-	-	-	-	-	-	-	-
190967	-	-	-	-	-	-	-	-

Star	H	H_2	HD	OH	H_2O	HCl	NH	N_2
191877	-	-	-	-	-	-	-	-
192660	-	-	-	-	-	-	-	-
193007	-	-	-	-	-	-	-	-
193237	361 UV	-	-	-	-	-	-	-
193322	71 UV 361 UV 382 UV	70 UV	-	-	-	-	-	-
193426	-	-	-	-	-	-	-	-
193793	-	-	-	-	-	-	-	-
193924	71 UV	70UV,87UV	-	-	-	-	-	-
194279	-	-	-	-	-	-	-	-
195592	-	-	-	-	-	-	-	-
197345	-	-	-	-	-	-	-	-
198478	-	-	-	-	-	-	-	-
199478	-	-	-	-	-	-	-	-
199579	71 UV 361 UV 382 UV	70 UV	-	-	-	-	-	-
200120	71 UV 361 UV	87 UV 70 UV	87 UV 107 UV	-	-	-	-	-
202124	-	-	-	-	-	-	-	-
202850	-	-	-	-	-	-	-	-
202904	79 UV 135 UV	79 UV 135 UV	-	-	-	-	-	-
203064	71 UV 361 UV 382 UV	70 UV	-	-	-	-	-	-
203938	-	-	-	-	-	-	-	-
204172	71 UV	70 UV	-	-	-	-	-	-
206165	-	-	-	-	-	-	-	-

Star	H	H_2	HD	OH	H_2O	HCl	NH	N_2
206267	382 UV	-	-	-	-	-	-	-
207198	361 UV 382 UV	-	-	-	-	-	-	-
207538	-	-	-	-	-	-	-	-
207971	-	-	-	-	-	-	-	-
208501	-	-	-	-	-	-	-	-
209952	-	70UV, 87UV	-	-	-	-	-	-
209975	71 UV 361 UV 382 UV	70 UV	-	-	-	-	-	-
210191	71 UV 361 UV 506 UV	70 UV	-	-	-	-	-	-
210839	71 UV 361 UV 382 UV	71 UV	-	-	-	-	-	-
212076	361 UV 451 UV	-	-	-	-	-	-	-
212978	-	-	-	-	-	-	-	-
213087	-	-	-	-	-	-	-	-
213420	-	-	-	-	-	-	-	-
214080	71 UV 361 UV 506 UV	70 UV	-	-	-	-	-	-
214680	71 UV 361 UV 382 UV	70 UV 87 UV	87 UV 107 UV	-	-	-	-	-
214993	79 UV 135 UV	79 UV 135 UV	-	-	-	-	-	-
217101	-	-	-	-	-	-	-	-
217675	-	70 UV	-	-	-	-	-	-
218376	71 UV	70 UV	-	-	-	-	-	-

Star	H	H_2	HD	OH	H_2O	HCl	NH	N_2
219188	71 UV 361 UV 506 UV	70 UV	-	-	-	-	-	-
224572	71 UV	70 UV	-	-	-	-	-	-
VI Cyg 12	-	-	-	-	-	-	-	-
+30°3639	-	-	-	-	-	-	-	-
+31°643	-	-	-	-	-	-	-	-
+40°4220	-	-	-	-	-	-	-	-
+60°1661	-	-	-	-	-	-	-	-
+66°1674	-	-	-	-	-	-	-	-
+66°1675	-	-	-	-	-	-	-	-
-14°5037	-	-	-	-	-	-	-	-

2. CORRELATION DIAGRAMS

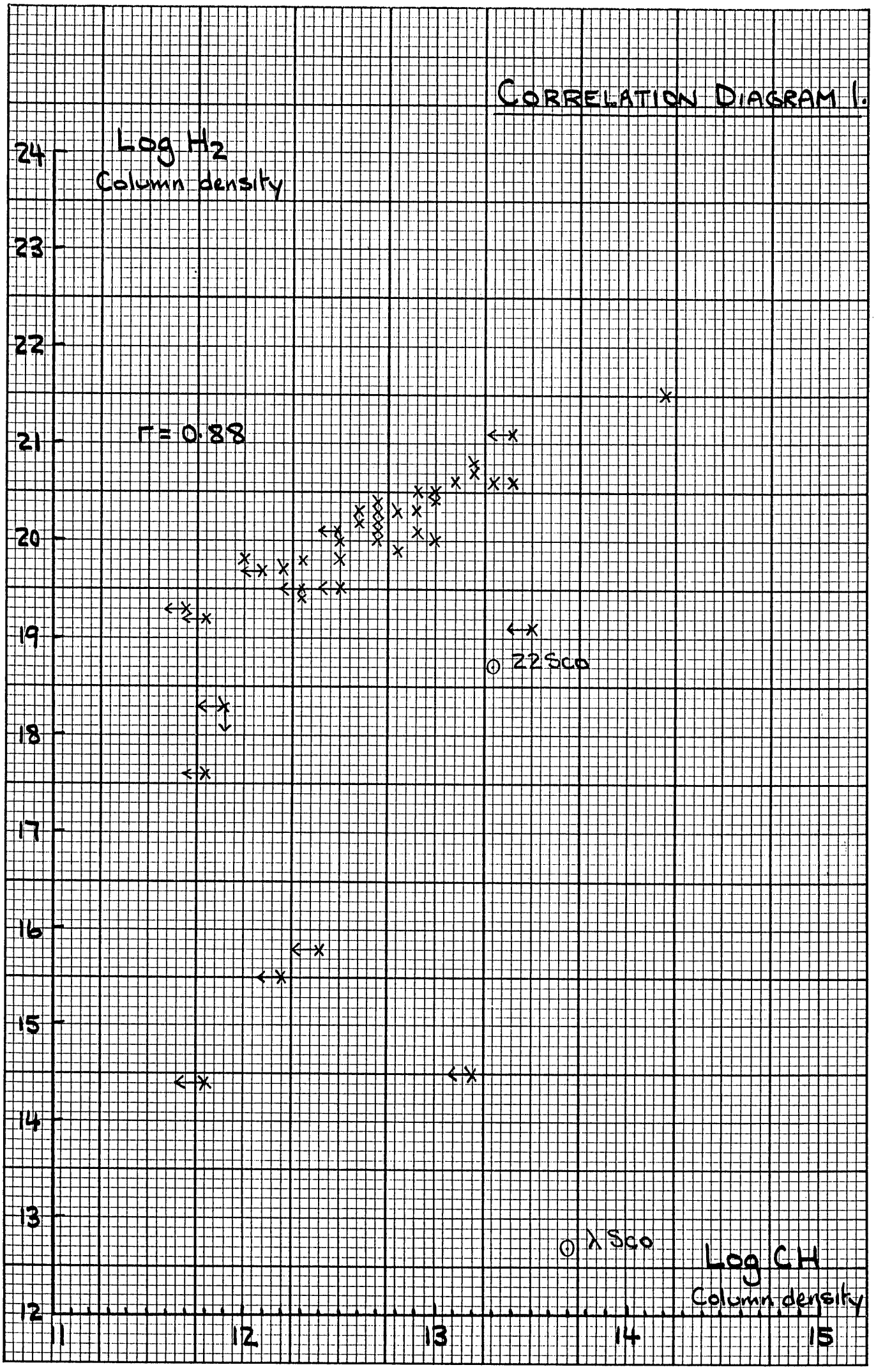
CORRELATION DIAGRAM I.
Log H_2
Column density
r = 0.88
24
23
22
21
20
19
18
17
16
15
14
13
12
11
12
13
14
15
22 Sco
λ Sco
Log CH
Column density

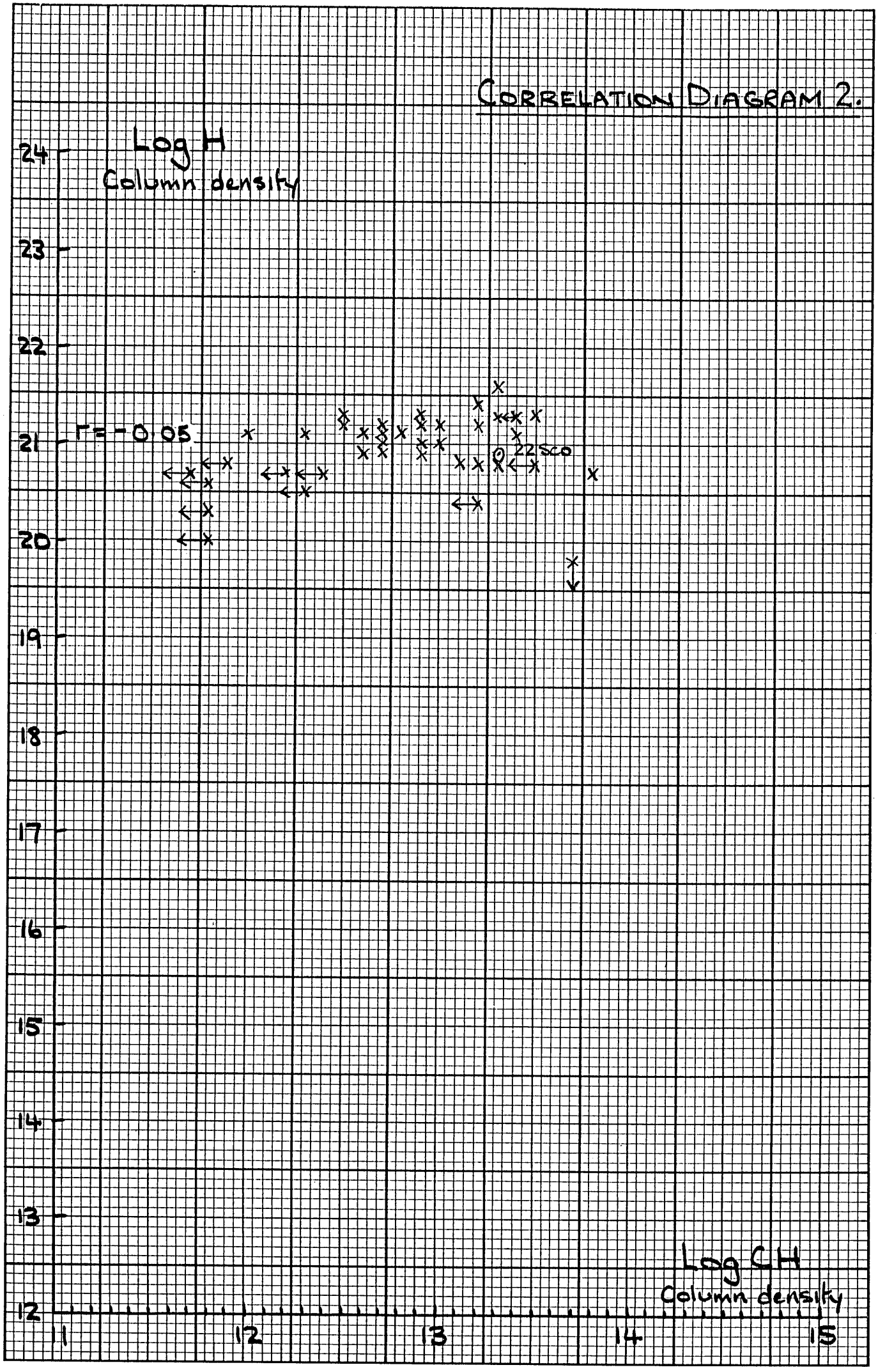
CORRELATION DIAGRAM 2.
Log H
Column density
24
23
22
21
20
19
18
17
16
15
14
13
12
r = -0.05
22SCO
Log CH
Column density
11
12
13
14
15

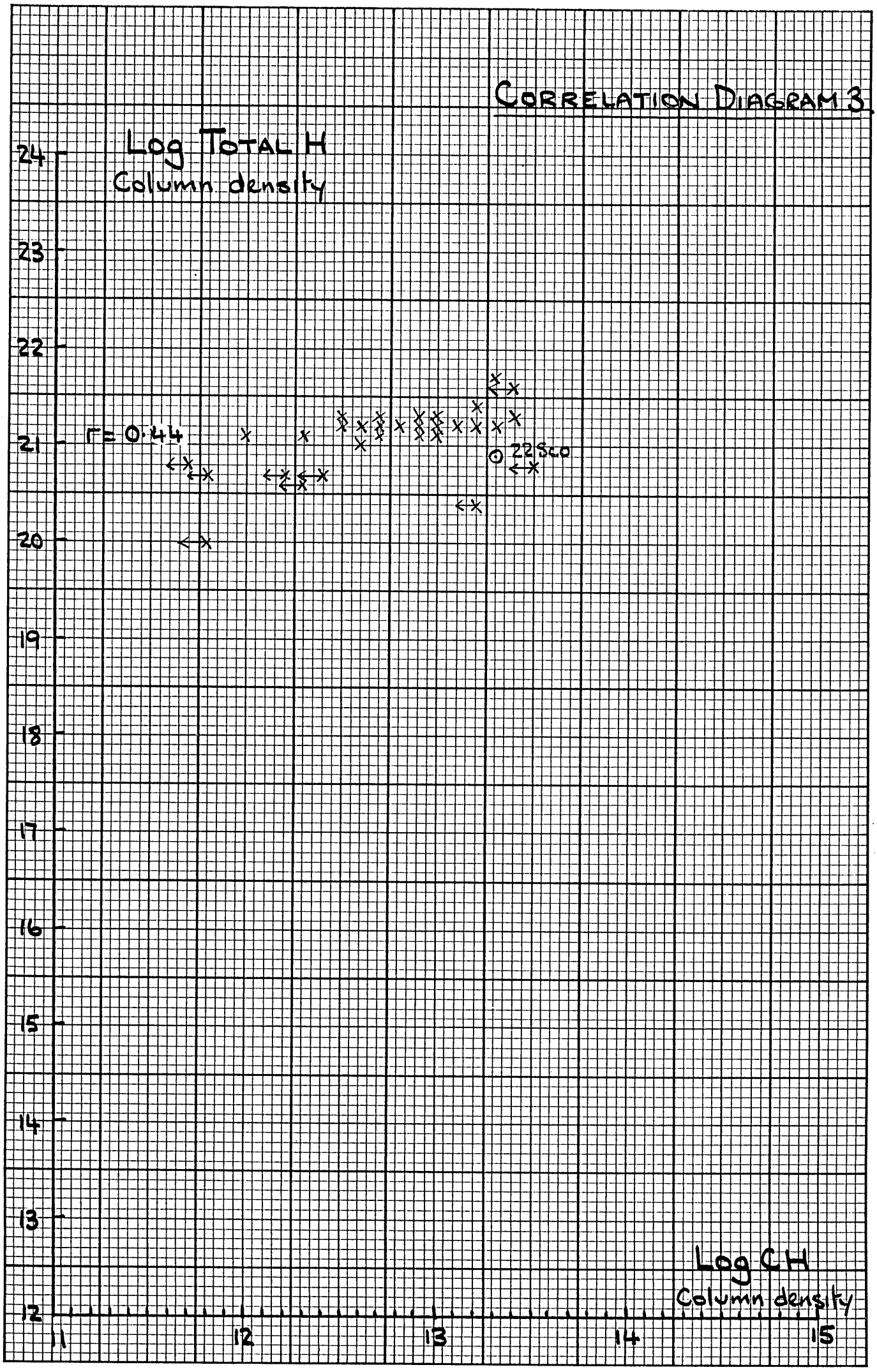
CORRELATION DIAGRAM 3
Log TOTAL H
Column density
r = 0.44
22 Sco
24
23
22
21
20
19
18
17
16
15
14
13
12
11
12
13
14
15
Log CH
Column density

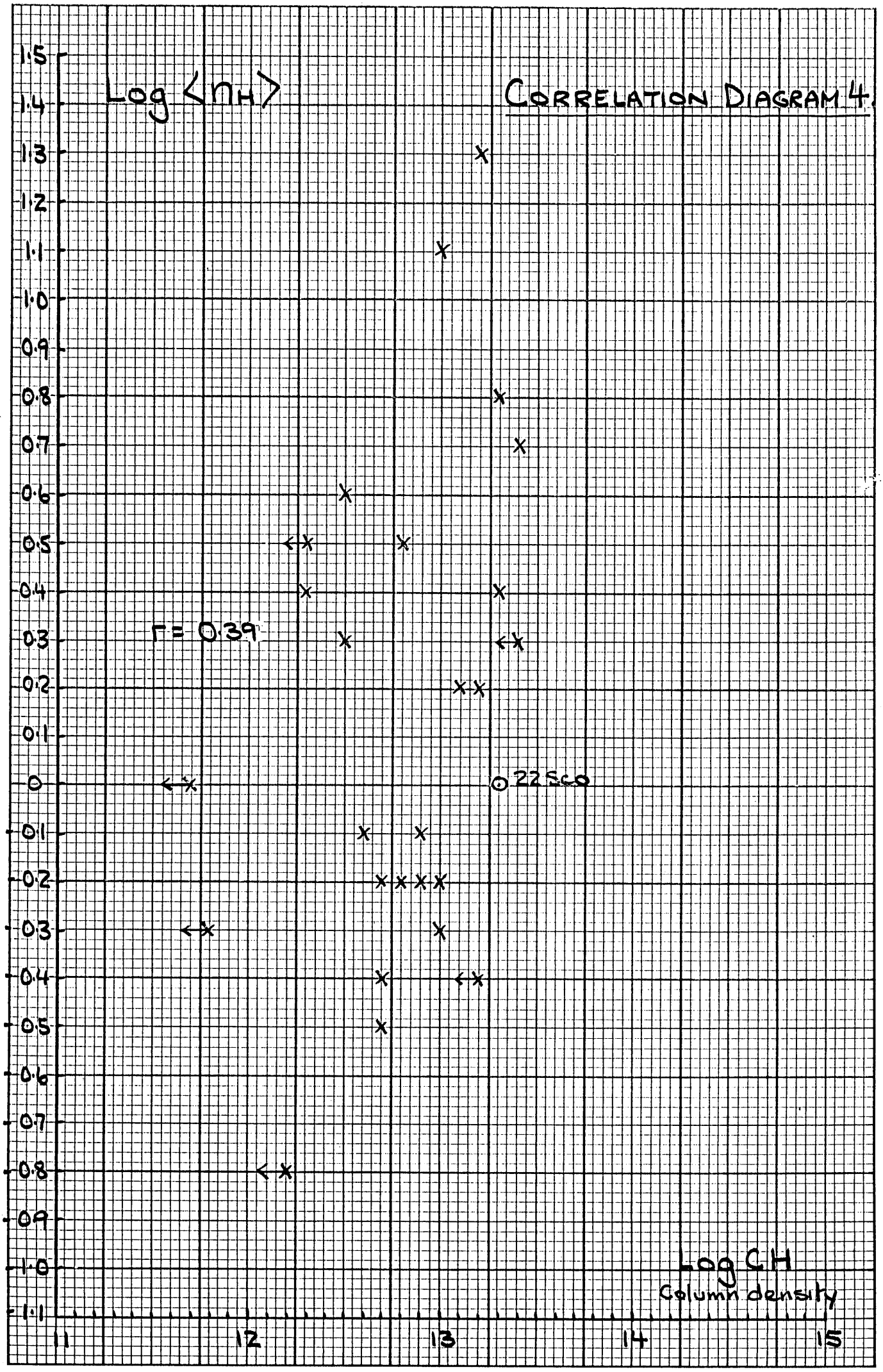
Log ⟨nH⟩
CORRELATION DIAGRAM 4
1.5
1.4
1.3
1.2
1.1
1.0
0.9
0.8
0.7
0.6
0.5
0.4
0.3
0.2
0.1
0
0.1
0.2
0.3
0.4
0.5
0.6
0.7
0.8
0.9
1.0
1.1
Γ = 0.39
22 Sgr
11
12
13
14
15
Log CH
Column density

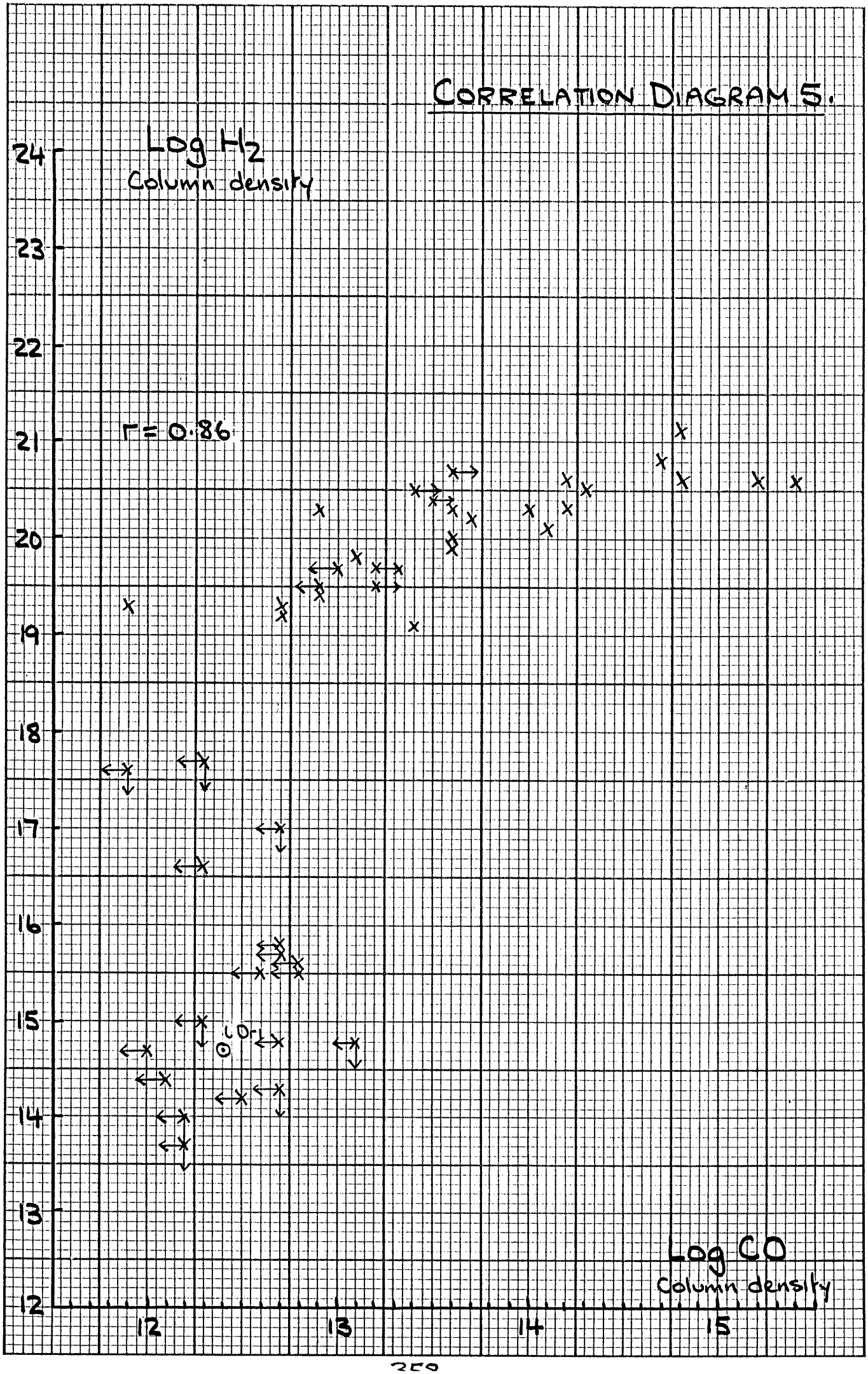
CORRELATION DIAGRAM 5.
Log H_2
Column density
r = 0·86
Log CO
Column density
24
23
22
21
20
19
18
17
16
15
14
13
12
12
13
14
15

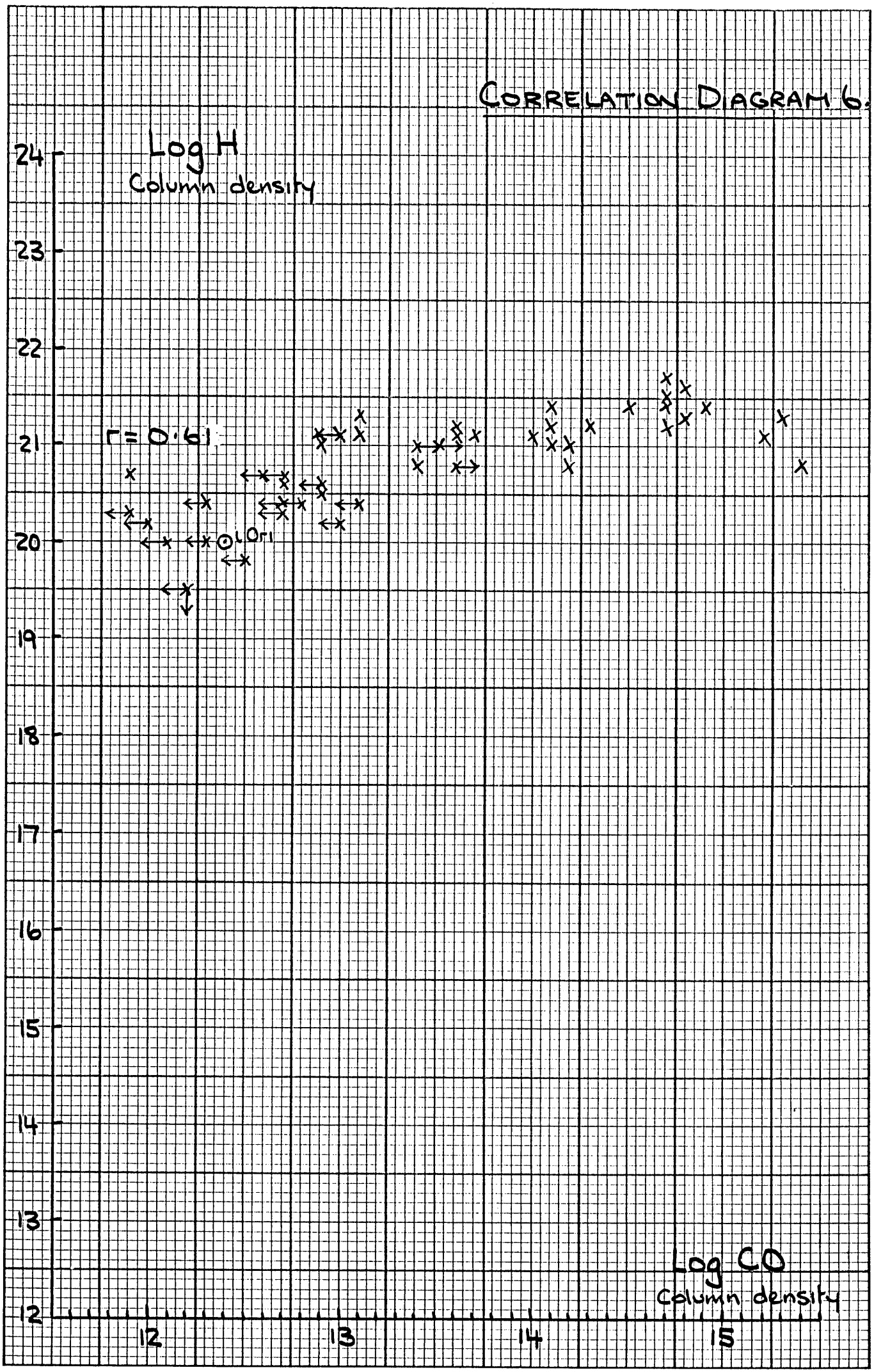
CORRELATION DIAGRAM 6.
Log H
Column density
r = 0·61
Log CO
Column density
24
23
22
21
20
19
18
17
16
15
14
13
12
12
13
14
15

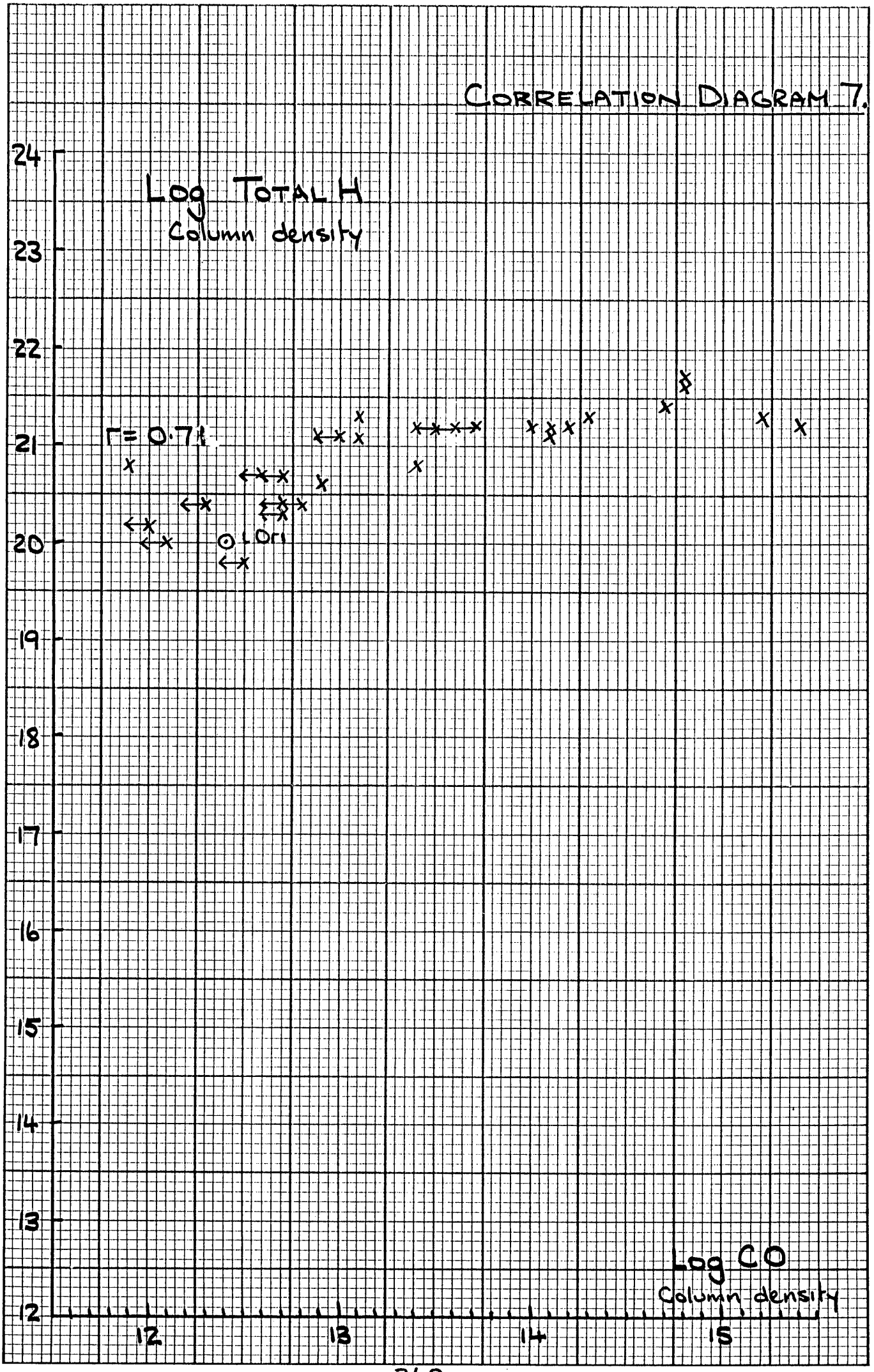
CORRELATION DIAGRAM 7.
Log TOTAL H
Column density
r = 0.7
ζ Ori
24
23
22
21
20
19
18
17
16
15
14
13
12
12
13
14
15
Log CO
Column density

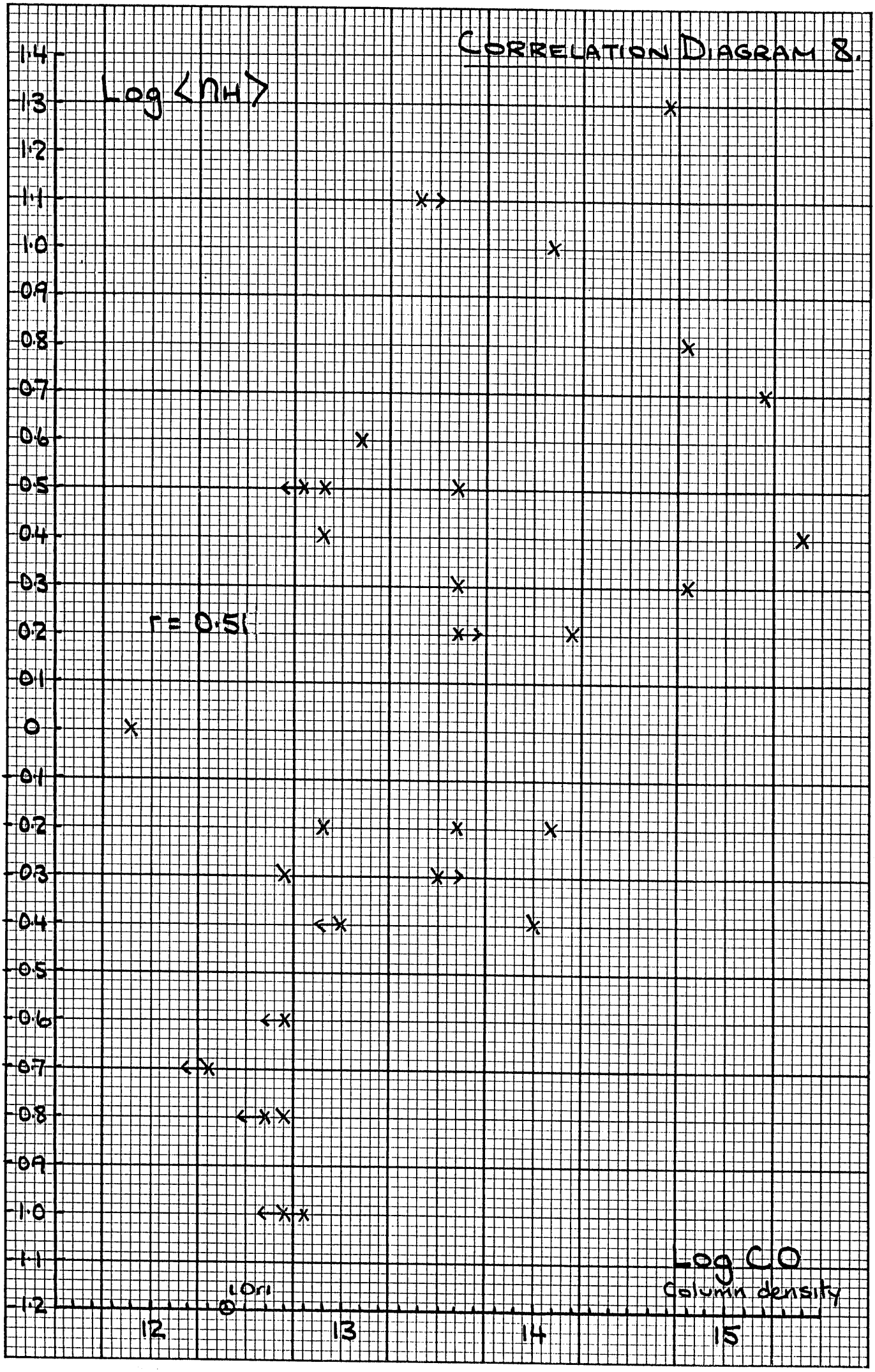
CORRELATION DIAGRAM 8.
Log ⟨nH⟩
r = 0.51
Log CO
Column density
Ori
1·4
1·3
1·2
1·1
1·0
0·9
0·8
0·7
0·6
0·5
0·4
0·3
0·2
0·1
0
-0·1
-0·2
-0·3
-0·4
-0·5
-0·6
-0·7
-0·8
-0·9
-1·0
-1·1
-1·2
12
13
14
15

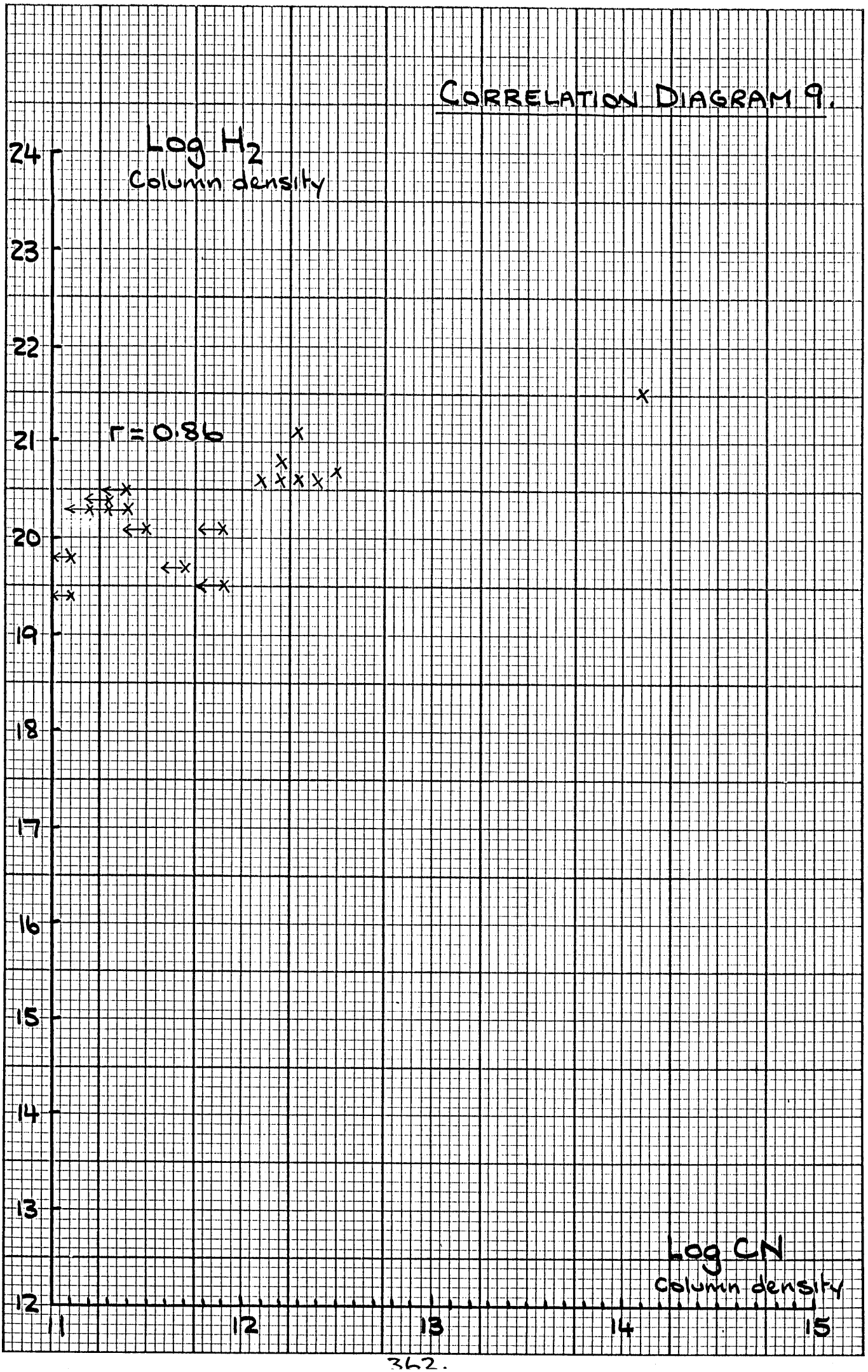
CORRELATION DIAGRAM 9.
Log H_2
Column density
r = 0·86
24
23
22
21
20
19
18
17
16
15
14
13
12
11
12
13
14
15
Log CN
Column density

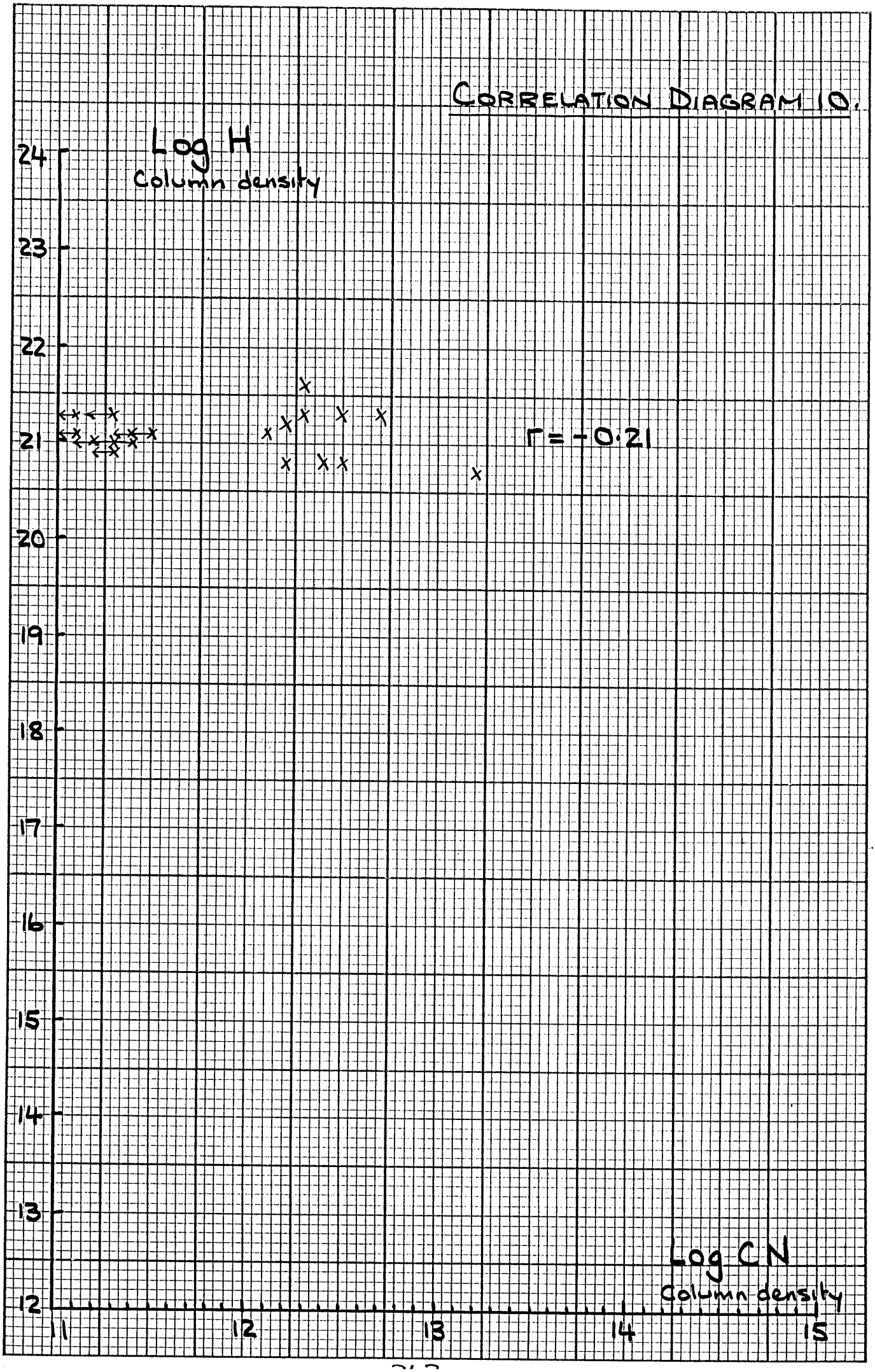
CORRELATION DIAGRAM 10.
Log H
Column density
24
23
22
21
20
19
18
17
16
15
14
13
12
r = -0·21
Log CN
Column density
11
12
13
14
15

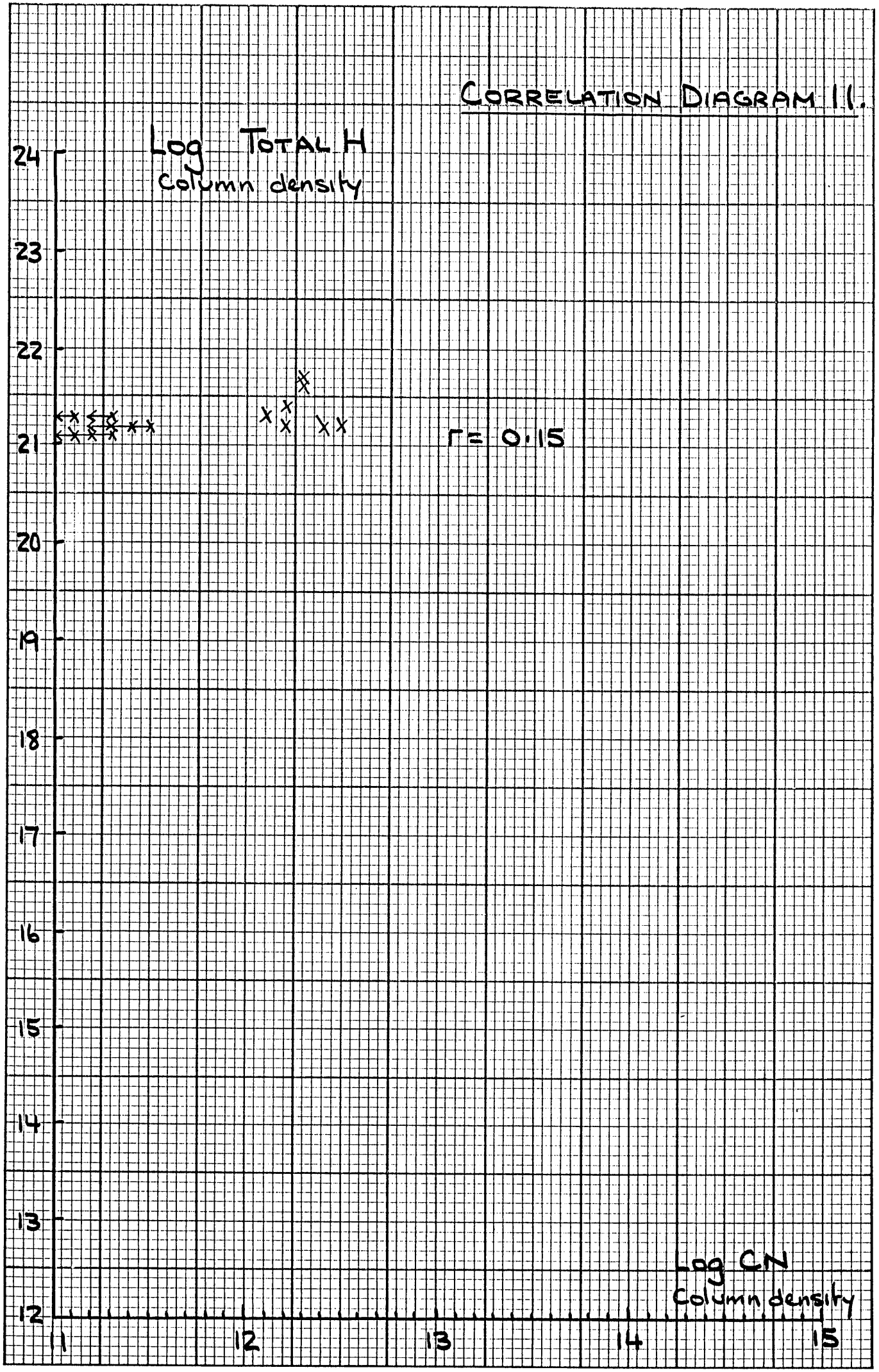
CORRELATION DIAGRAM 11.
Log TOTAL H
Column density
r = 0·15
Log CN
Column density
24
23
22
21
20
19
18
17
16
15
14
13
12
11
12
13
14
15

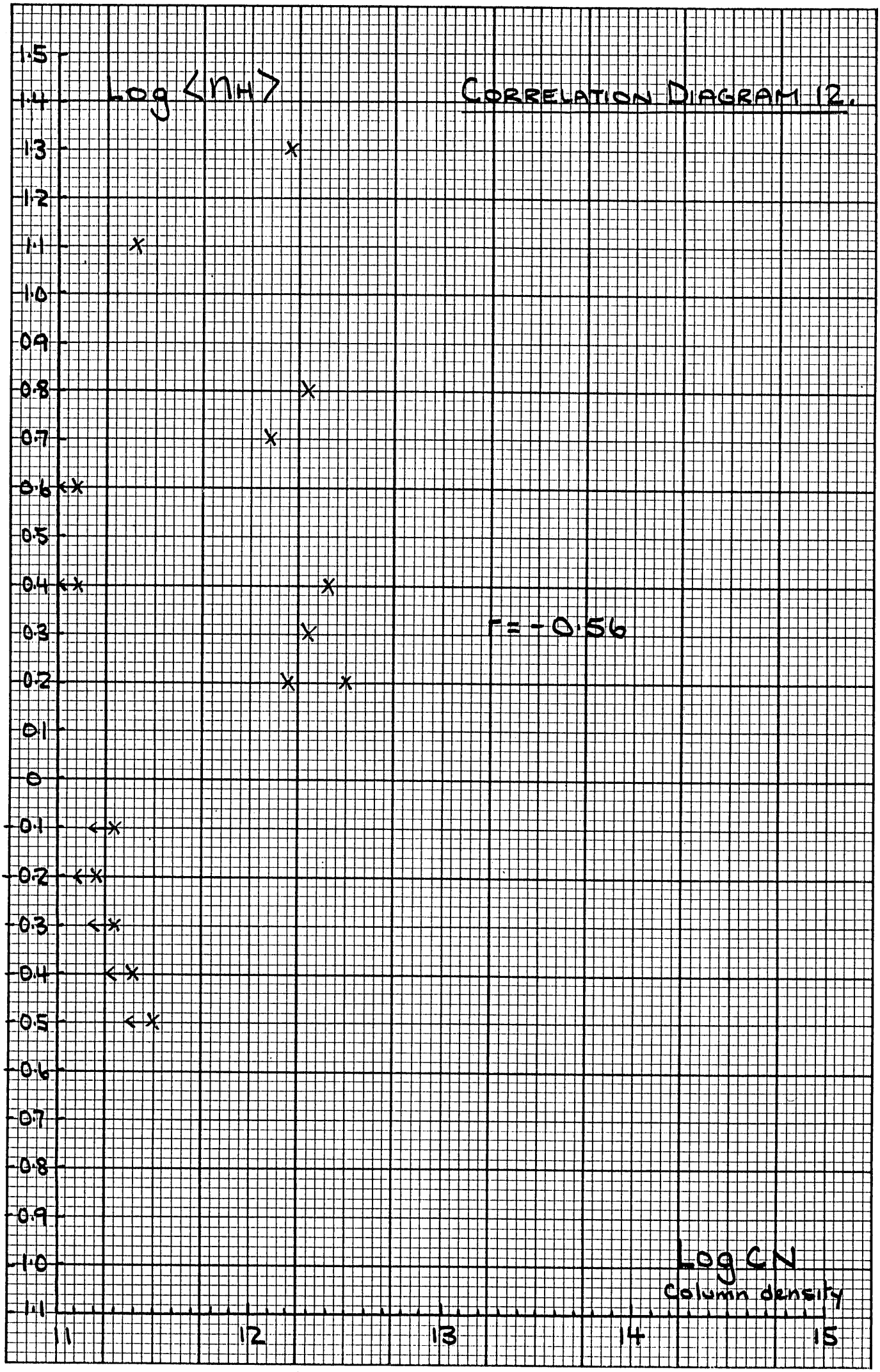
Log ⟨nH⟩
CORRELATION DIAGRAM 12.
r = -0.56
Log CN
Column density
1.5
1.4
1.3
1.2
1.1
1.0
0.9
0.8
0.7
0.6
0.5
0.4
0.3
0.2
0.1
0
-0.1
-0.2
-0.3
-0.4
-0.5
-0.6
-0.7
-0.8
-0.9
-1.0
-1.1
11
12
13
14
15

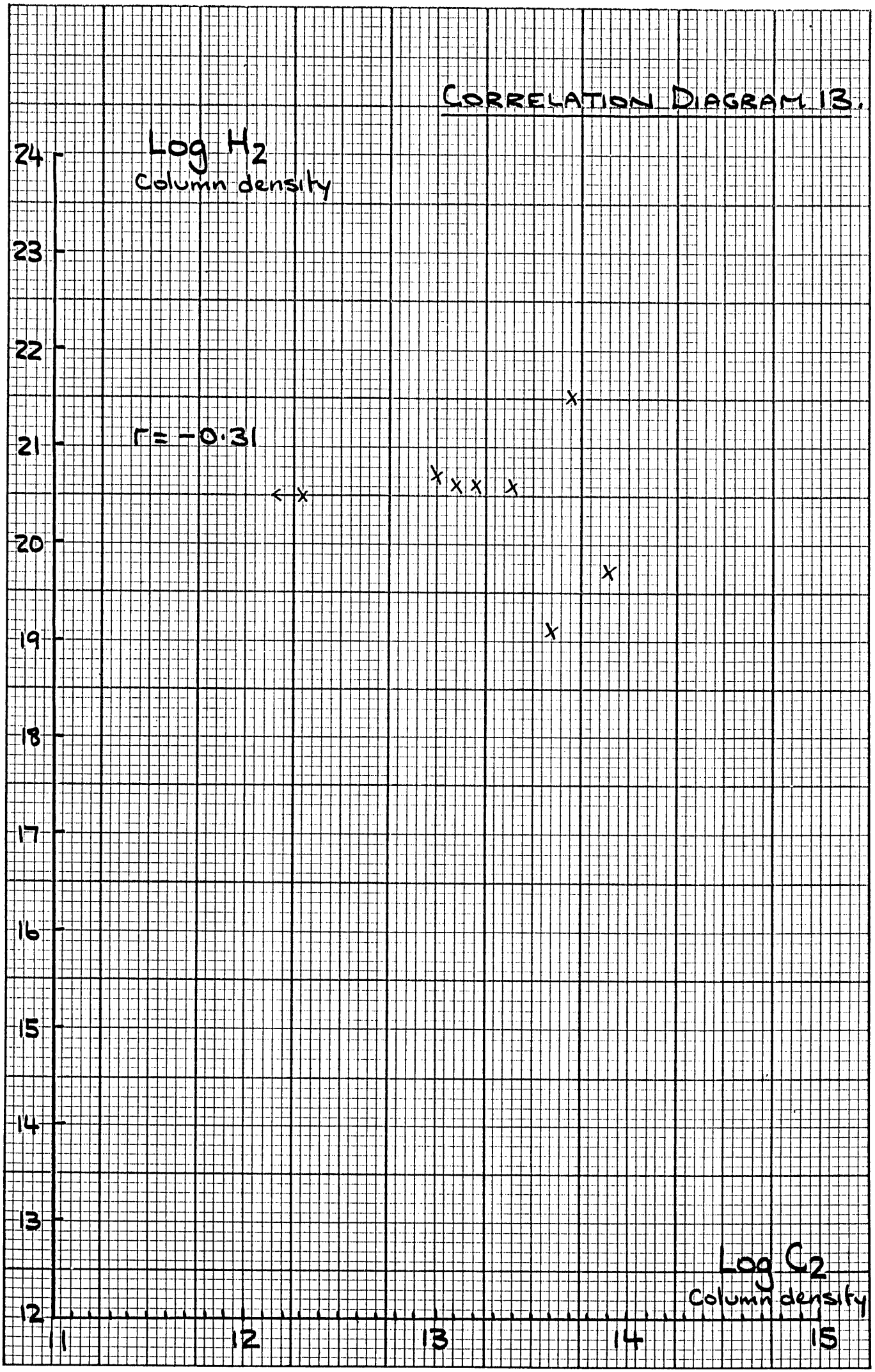
CORRELATION DIAGRAM 13.
Log H_2
Column density
$r = -0.31$
24
23
22
21
20
19
18
17
16
15
14
13
12
11
12
13
14
15
Log C_2
Column density

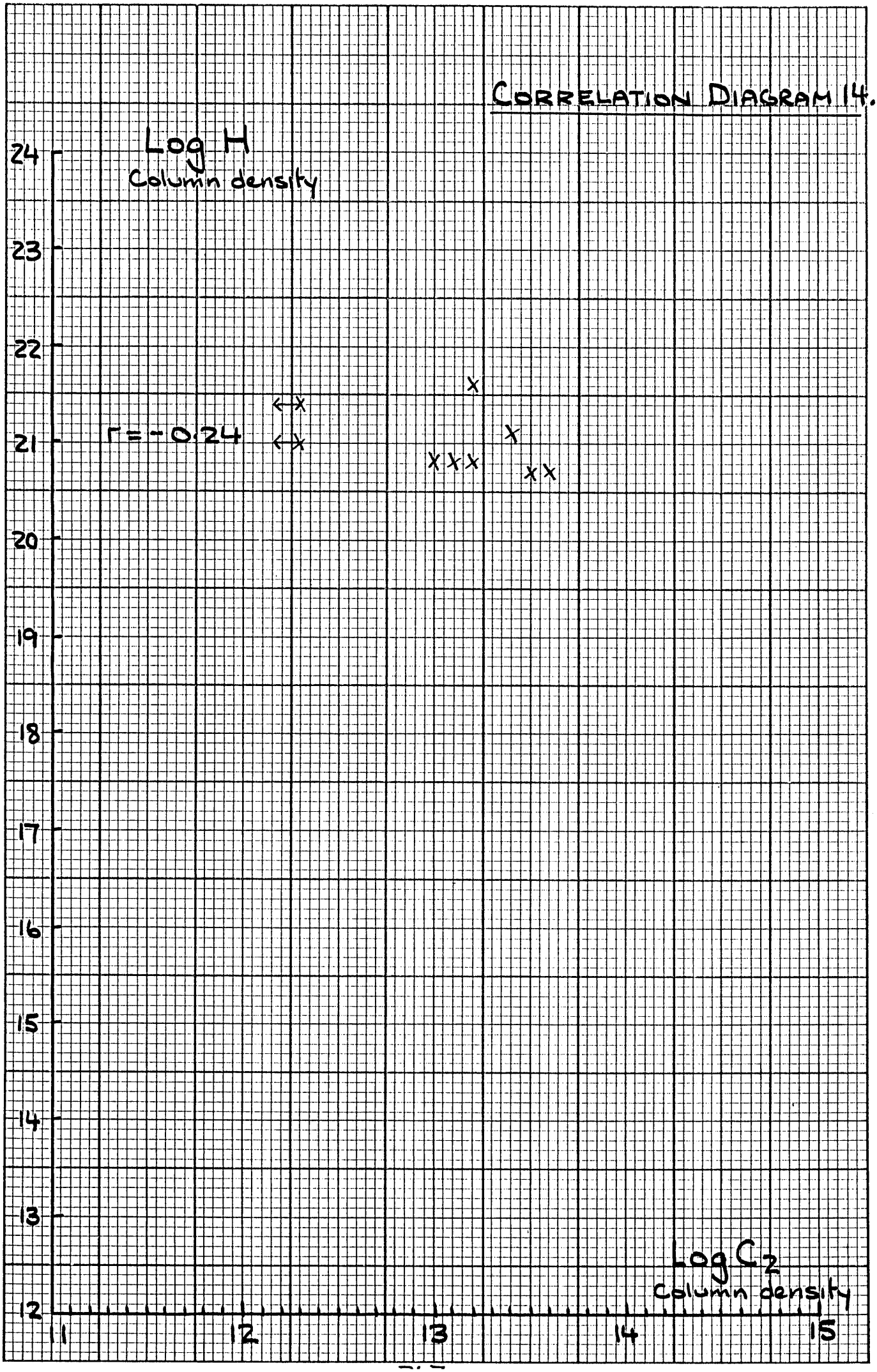
CORRELATION DIAGRAM 14.
Log H
Column density
24
23
22
21
20
19
18
17
16
15
14
13
12
r = -0.24
Log C_2
Column density
11
12
13
14
15

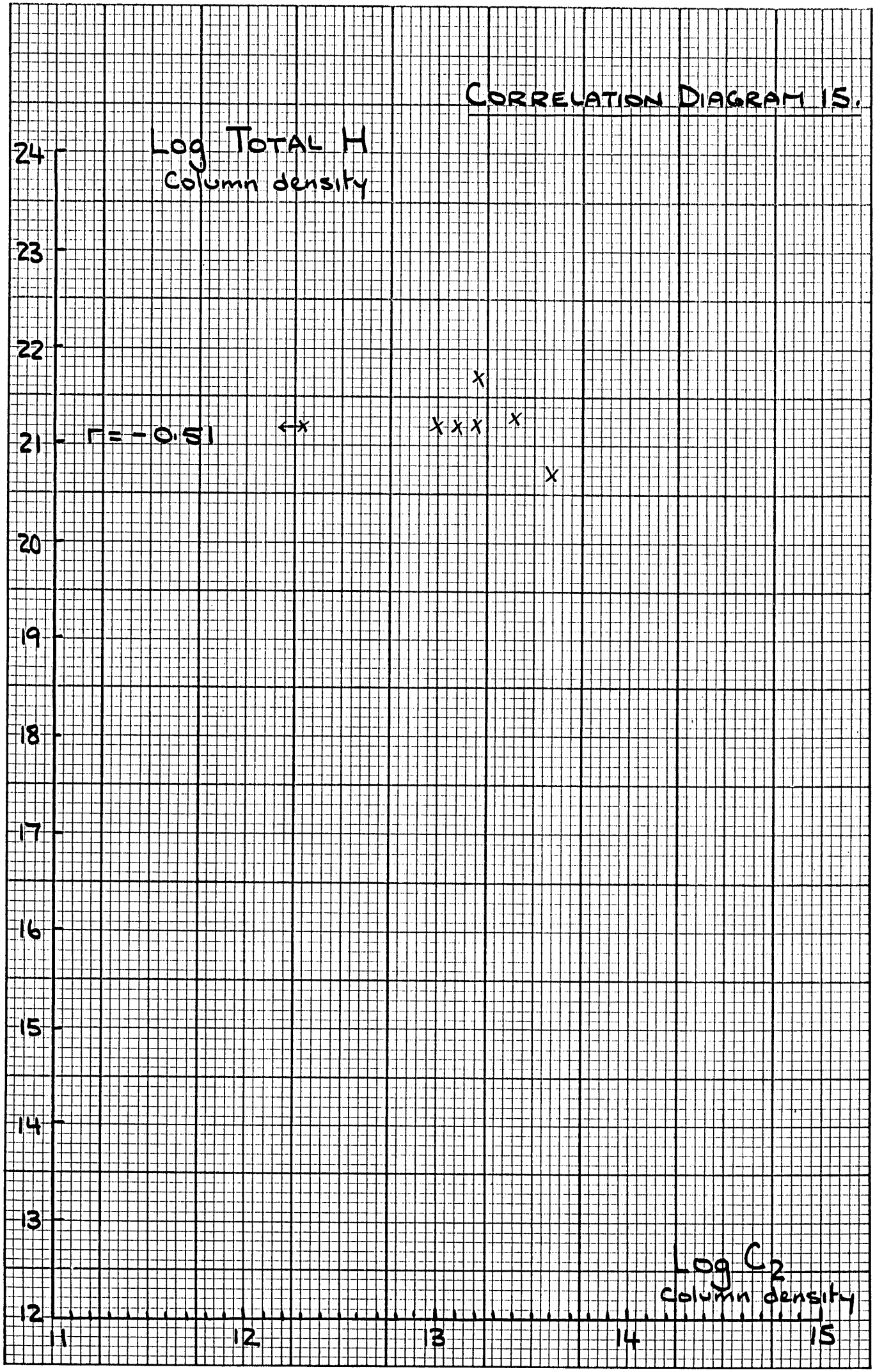
CORRELATION DIAGRAM 15.
Log TOTAL H
Column density
24
23
22
21
20
19
18
17
16
15
14
13
12
r = -0.51
Log C2
Column density
11
12
13
14
15

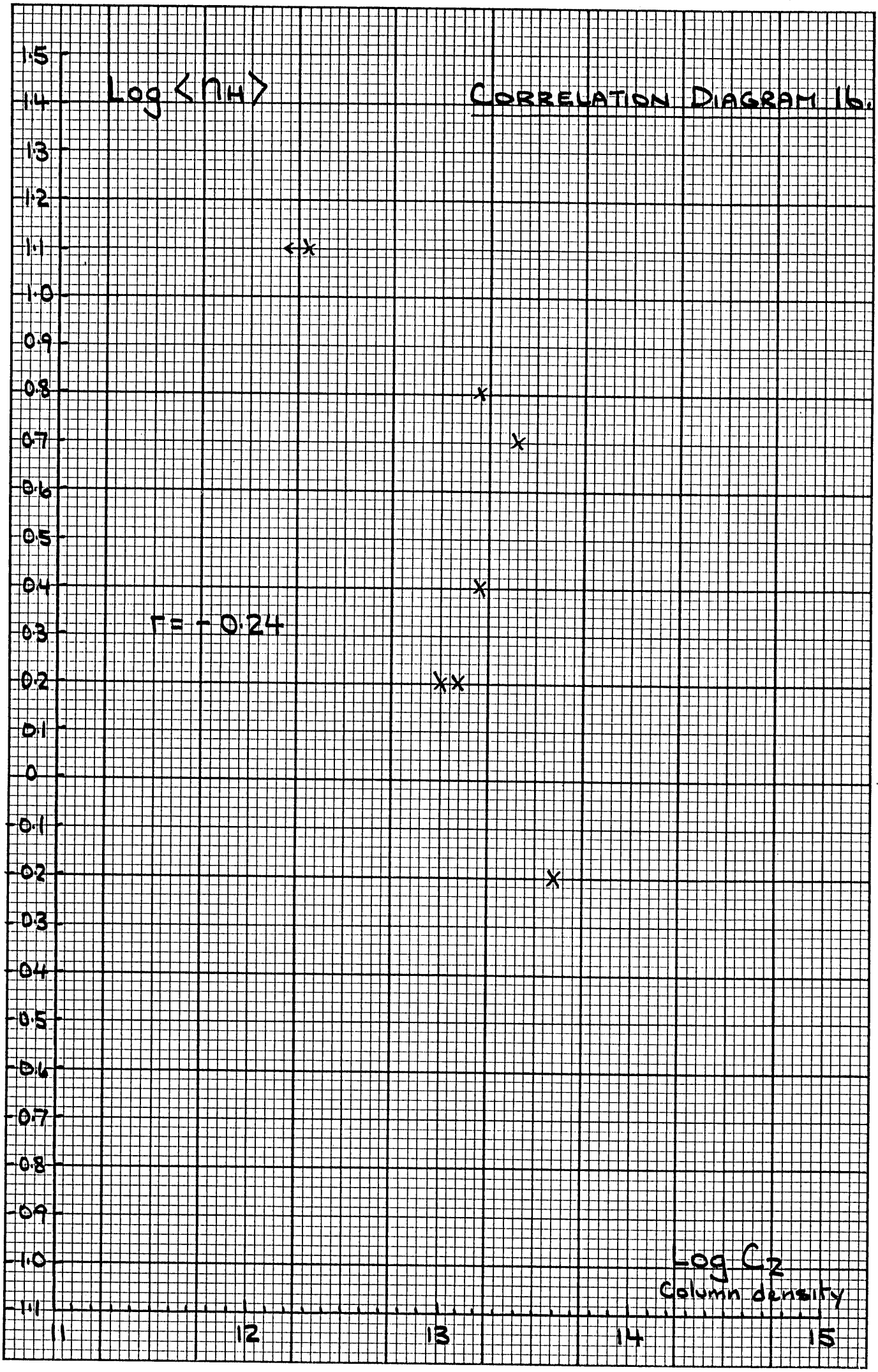
Log ⟨nH⟩
CORRELATION DIAGRAM 16.
r = - 0.24
Log C2
Column density
1.5
1.4
1.3
1.2
1.1
1.0
0.9
0.8
0.7
0.6
0.5
0.4
0.3
0.2
0.1
0
-0.1
-0.2
-0.3
-0.4
-0.5
-0.6
-0.7
-0.8
-0.9
-1.0
-1.1
11
12
13
14
15

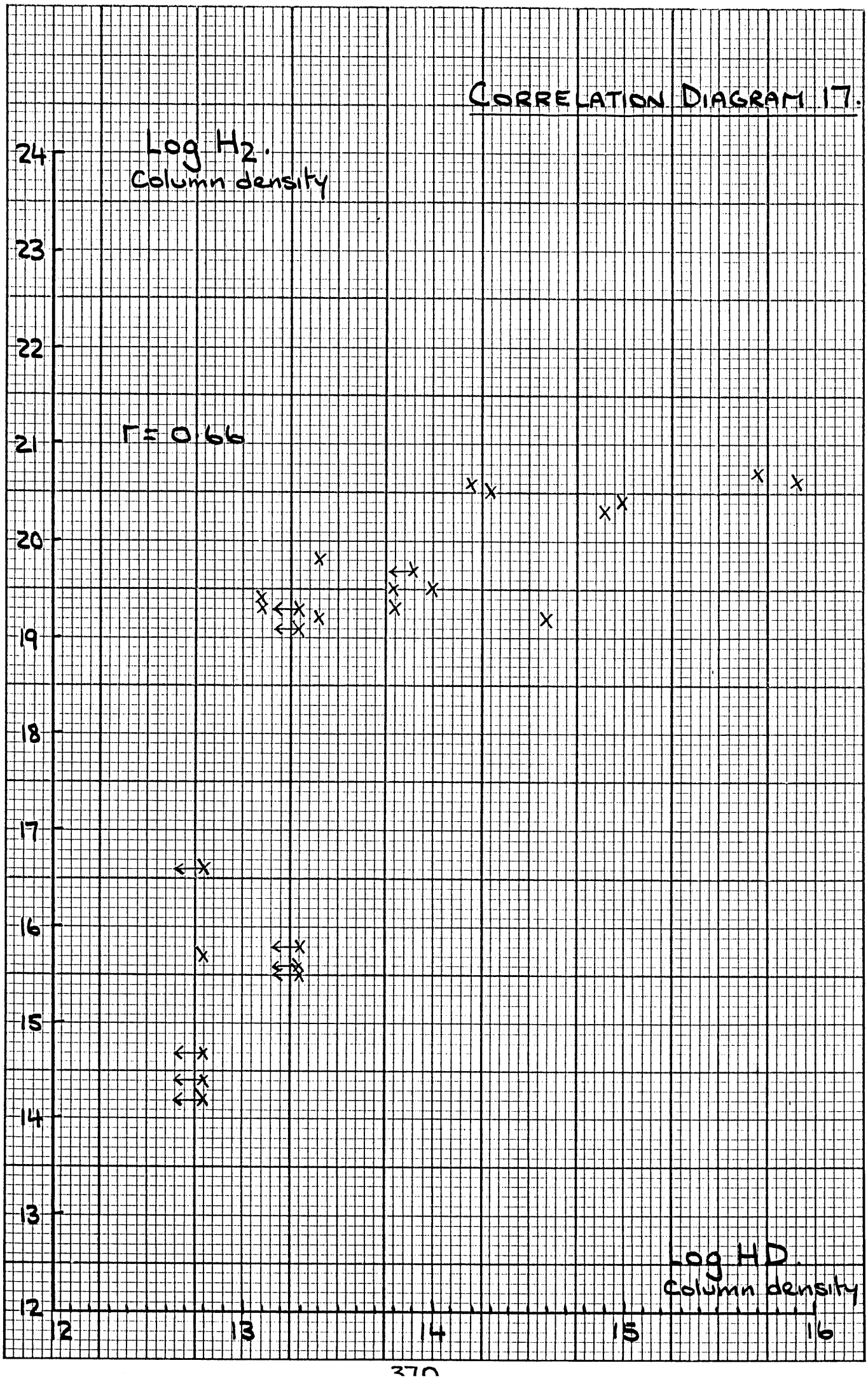
CORRELATION DIAGRAM 17.
Log H_2.
Column density
r = 0.66
24
23
22
21
20
19
18
17
16
15
14
13
12
12
13
14
15
16
Log HD
Column density

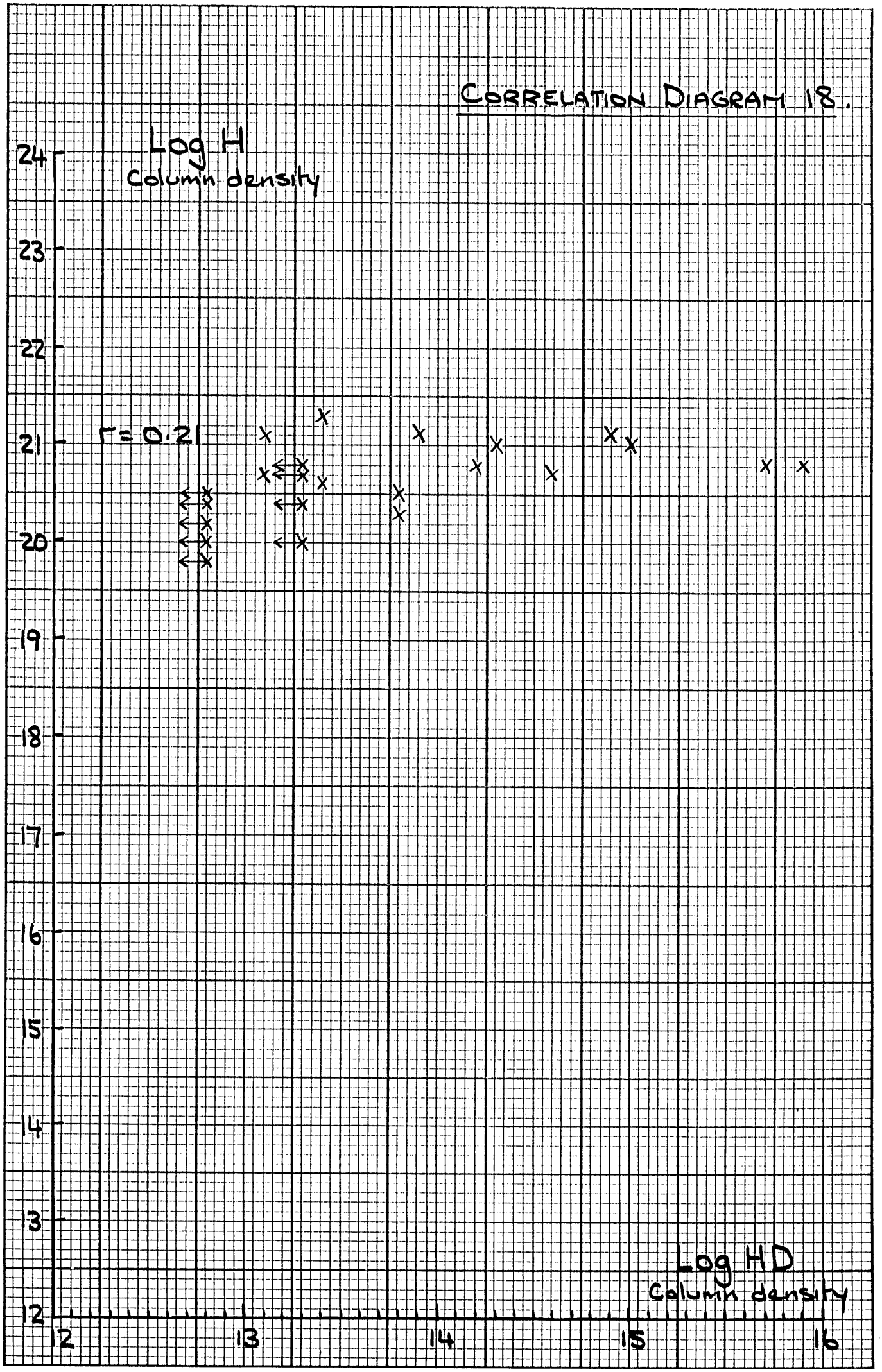
CORRELATION DIAGRAM 18.
Log H
Column density
r = 0·21
24
23
22
21
20
19
18
17
16
15
14
13
12
12
13
14
15
16
Log HD
Column density

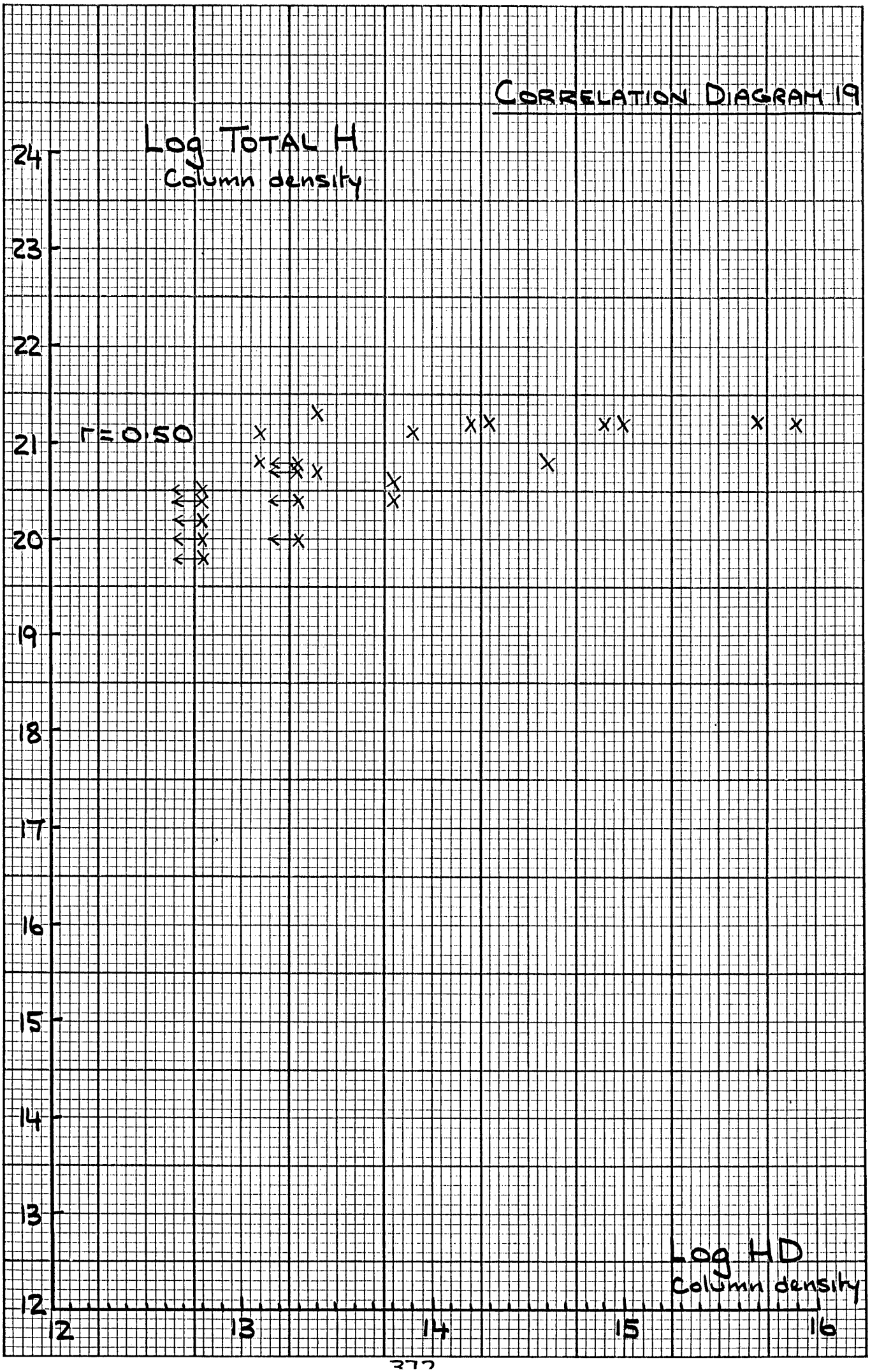
CORRELATION DIAGRAM 19
LOG TOTAL H
Column density
r=0.50
LOG HD
Column density
24
23
22
21
20
19
18
17
16
15
14
13
12
12
13
14
15
16

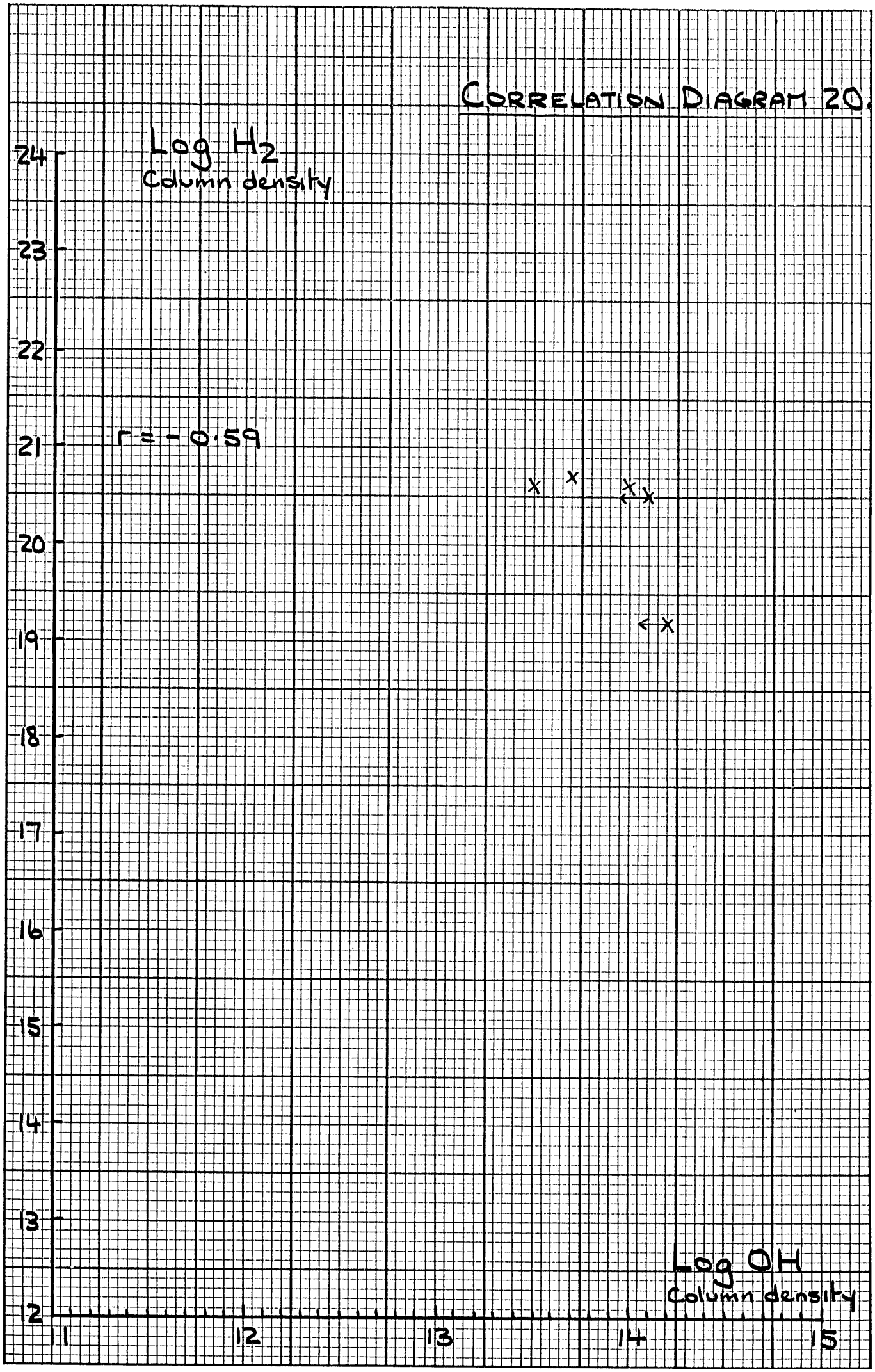
CORRELATION DIAGRAM 20.
Log H_2
Column density
r = -0·59
24
23
22
21
20
19
18
17
16
15
14
13
2
11
12
13
14
15
Log OH
Column density

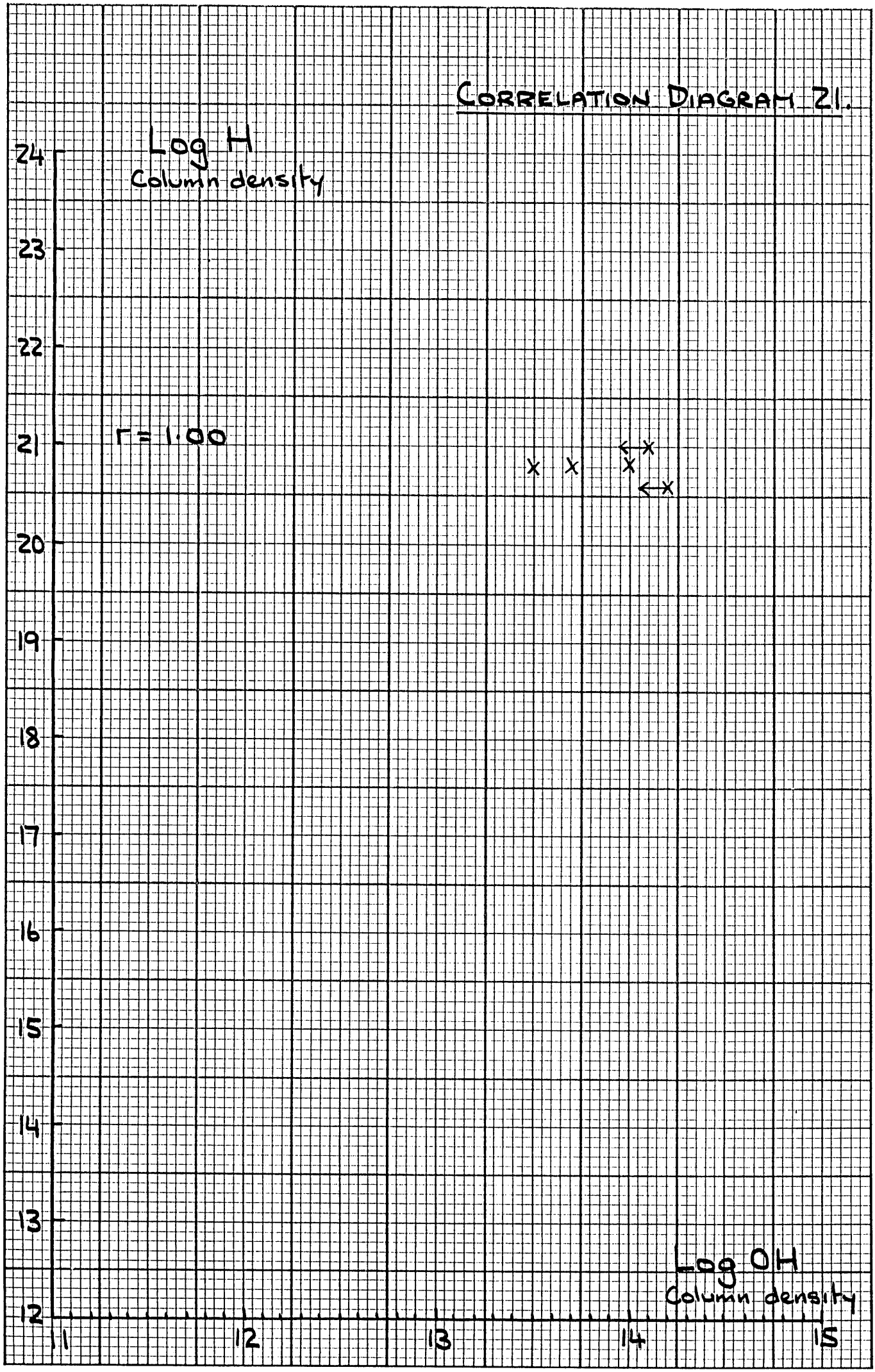
CORRELATION DIAGRAM 21.
Log H
Column density
r = 1.00
24
23
22
21
20
19
18
17
16
15
14
13
12
11
12
13
14
15
Log OH
Column density

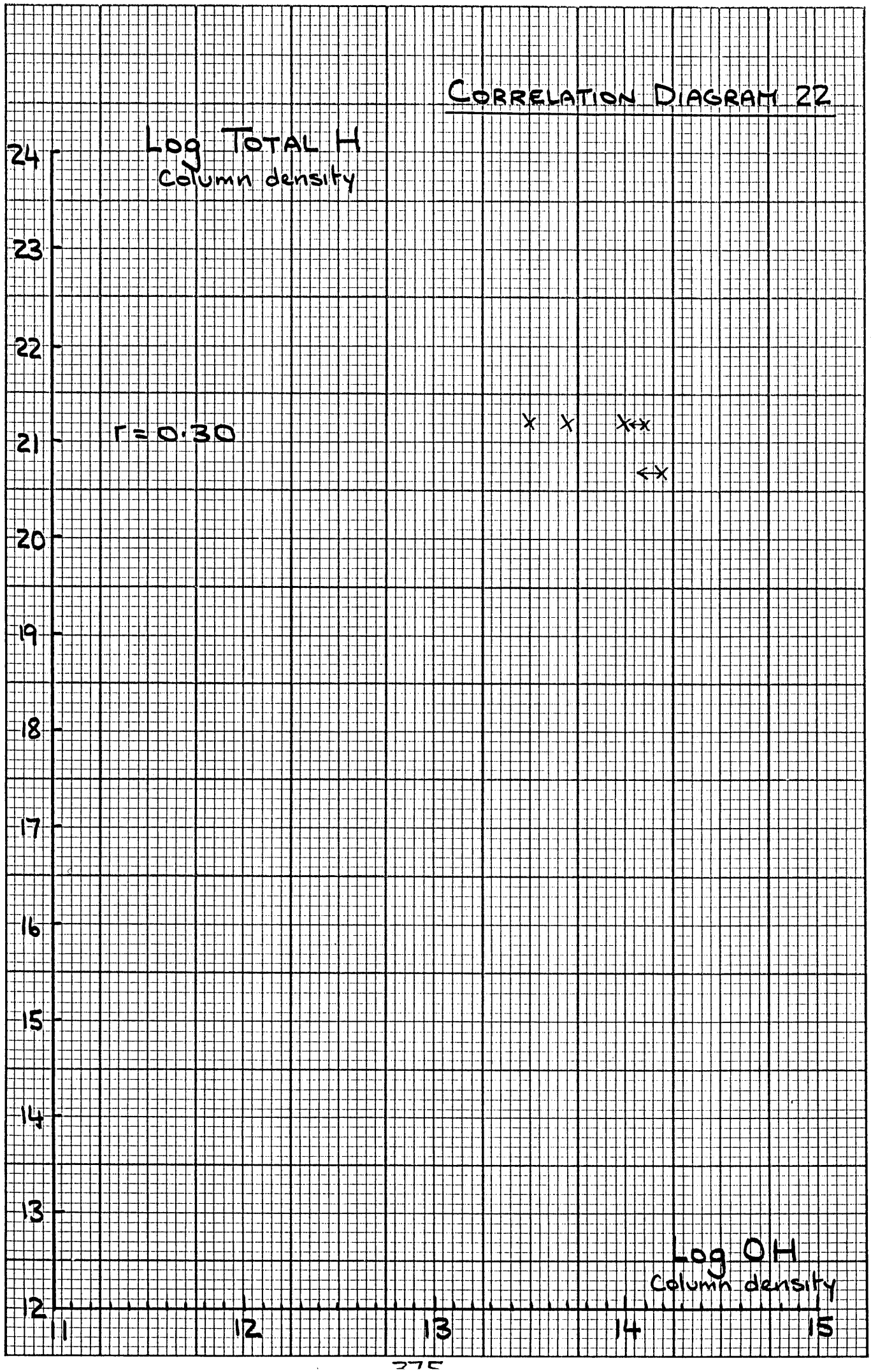
CORRELATION DIAGRAM 22
Log TOTAL H
Column density
r = 0·30
24
23
22
21
20
19
18
17
16
15
14
13
12
11
12
13
14
15
Log OH
Column density

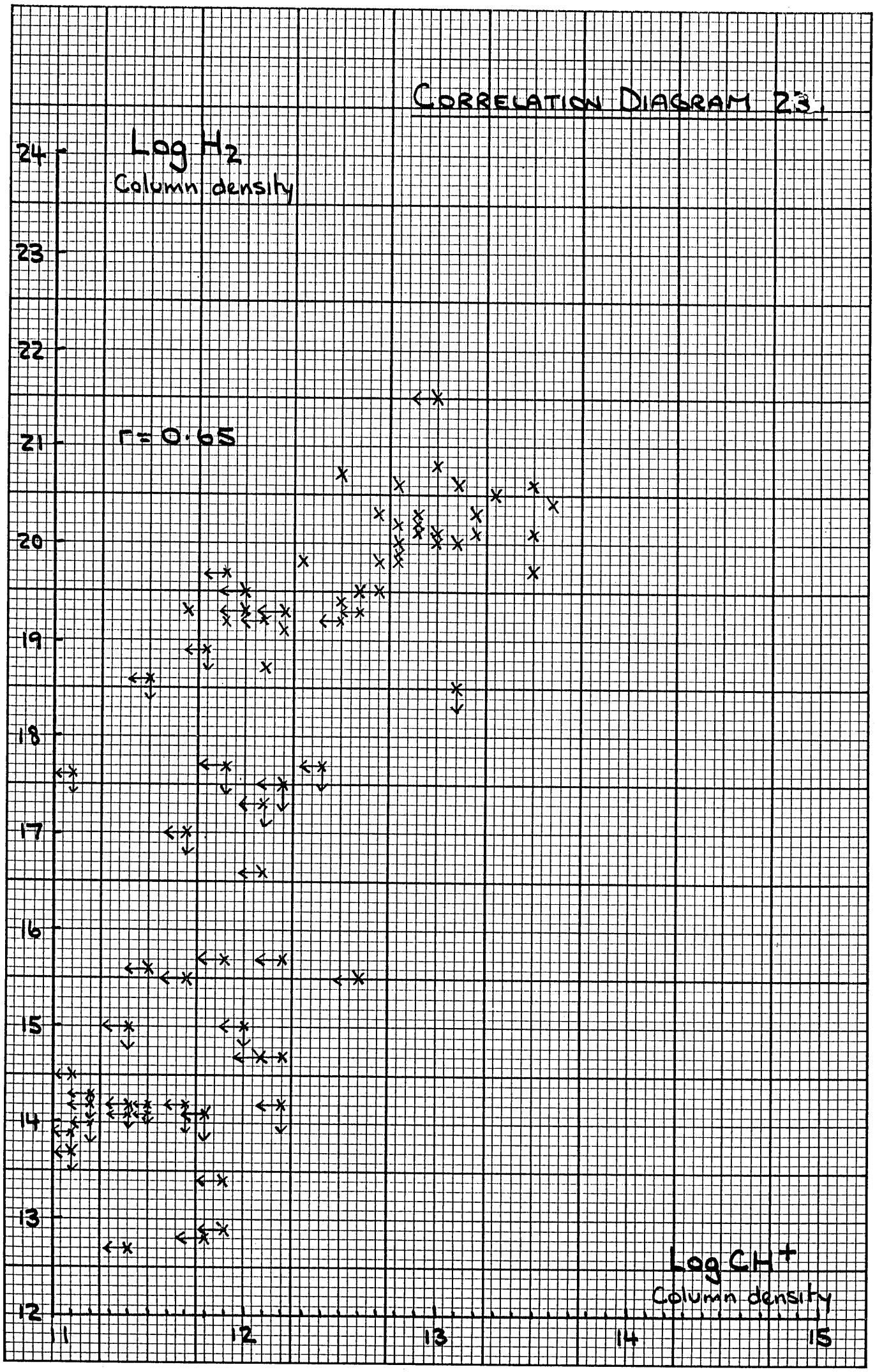
CORRELATION DIAGRAM 23.
Log H_2
Column density
r = 0·65
24
23
22
21
20
19
18
17
16
15
14
13
12
11
12
13
14
15
Log CH^+
Column density

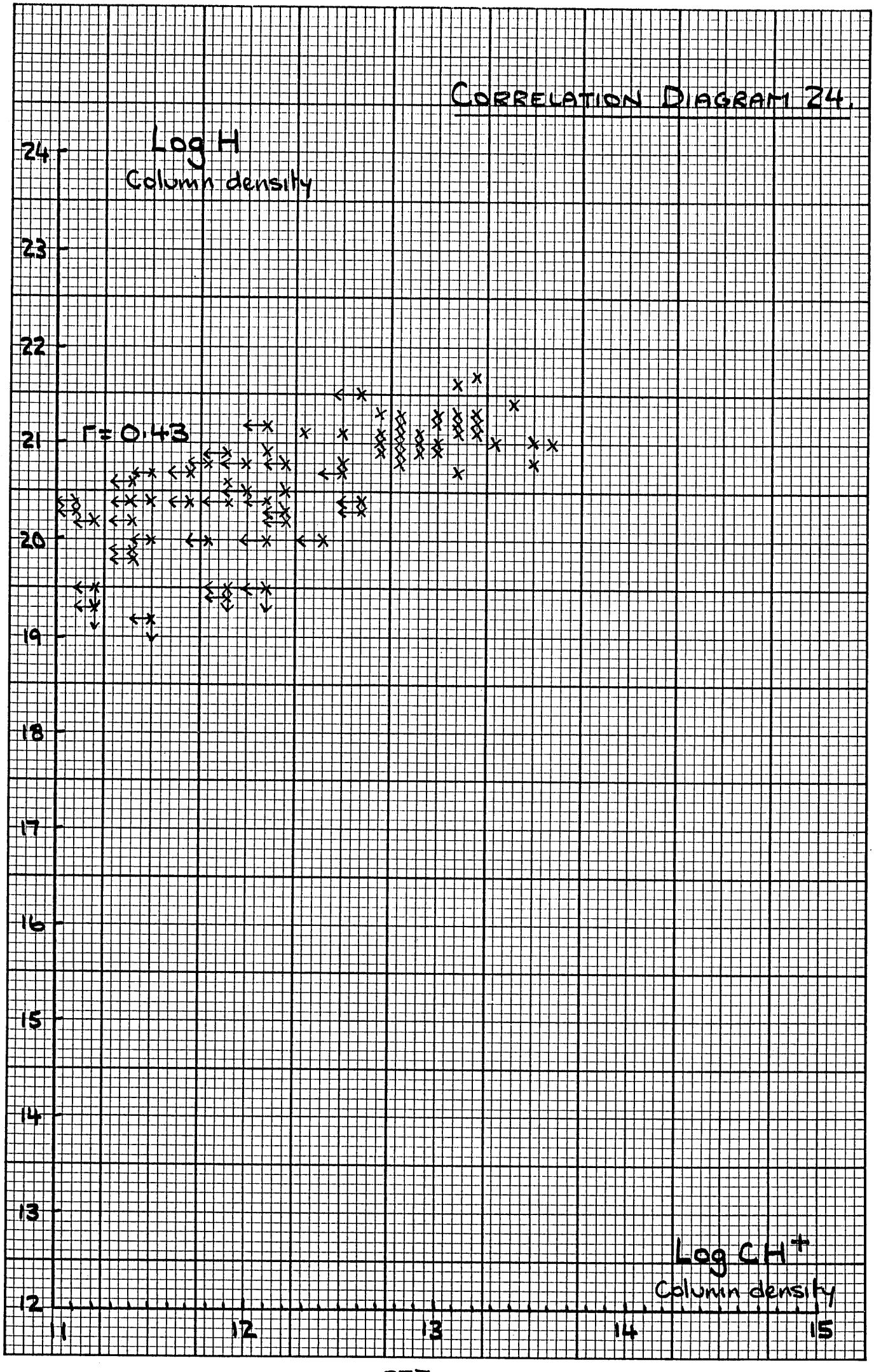
CORRELATION DIAGRAM 24.
Log H
Column density
r = 0·43
24
23
22
21
20
19
18
17
16
15
14
13
12
11
12
13
14
15
Log CH+
Column density

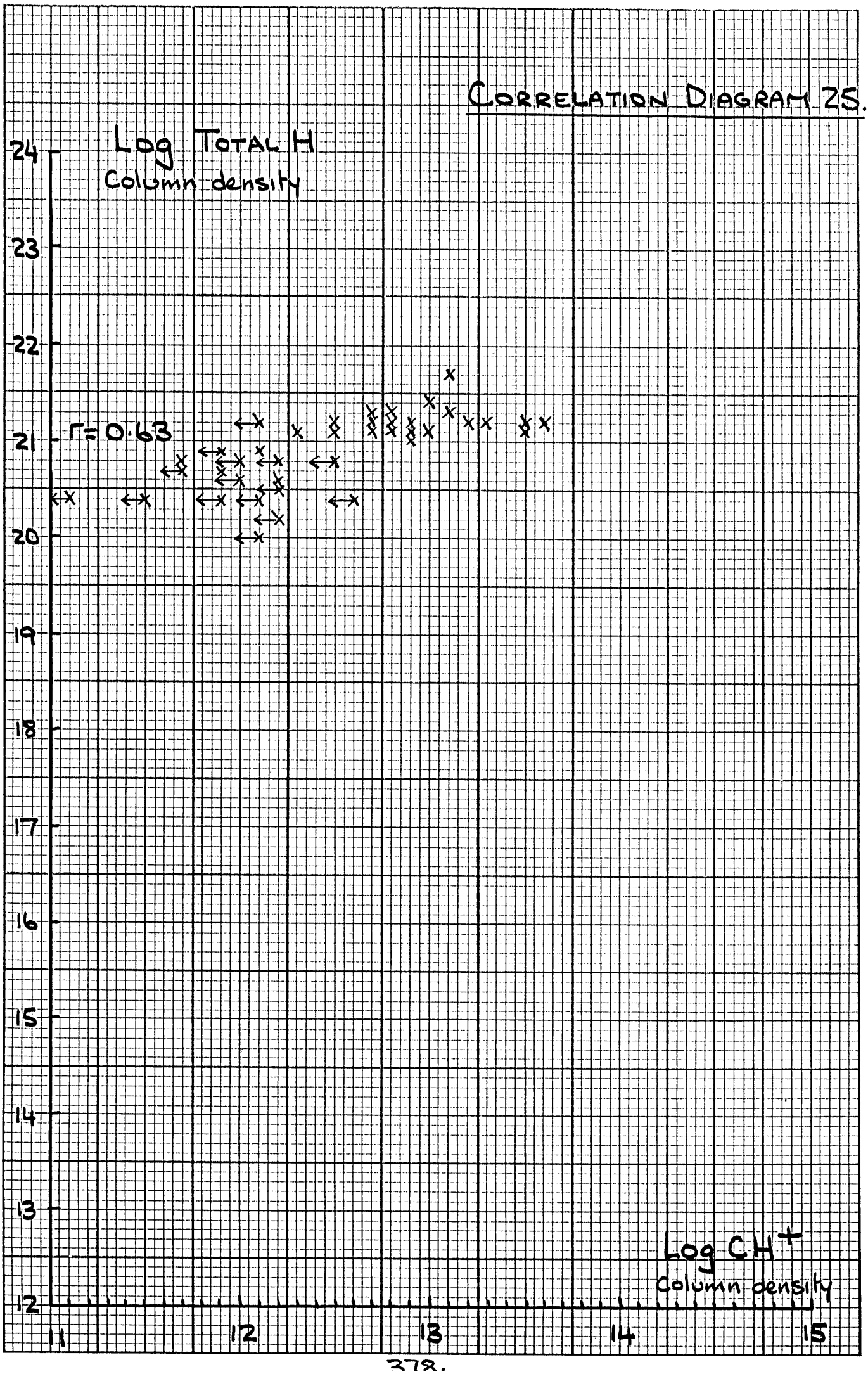
CORRELATION DIAGRAM 25.
Log TOTAL H
Column density
r = 0.63
Log CH+
Column density
24
23
22
21
20
19
18
17
16
15
14
13
12
11
12
13
14
15

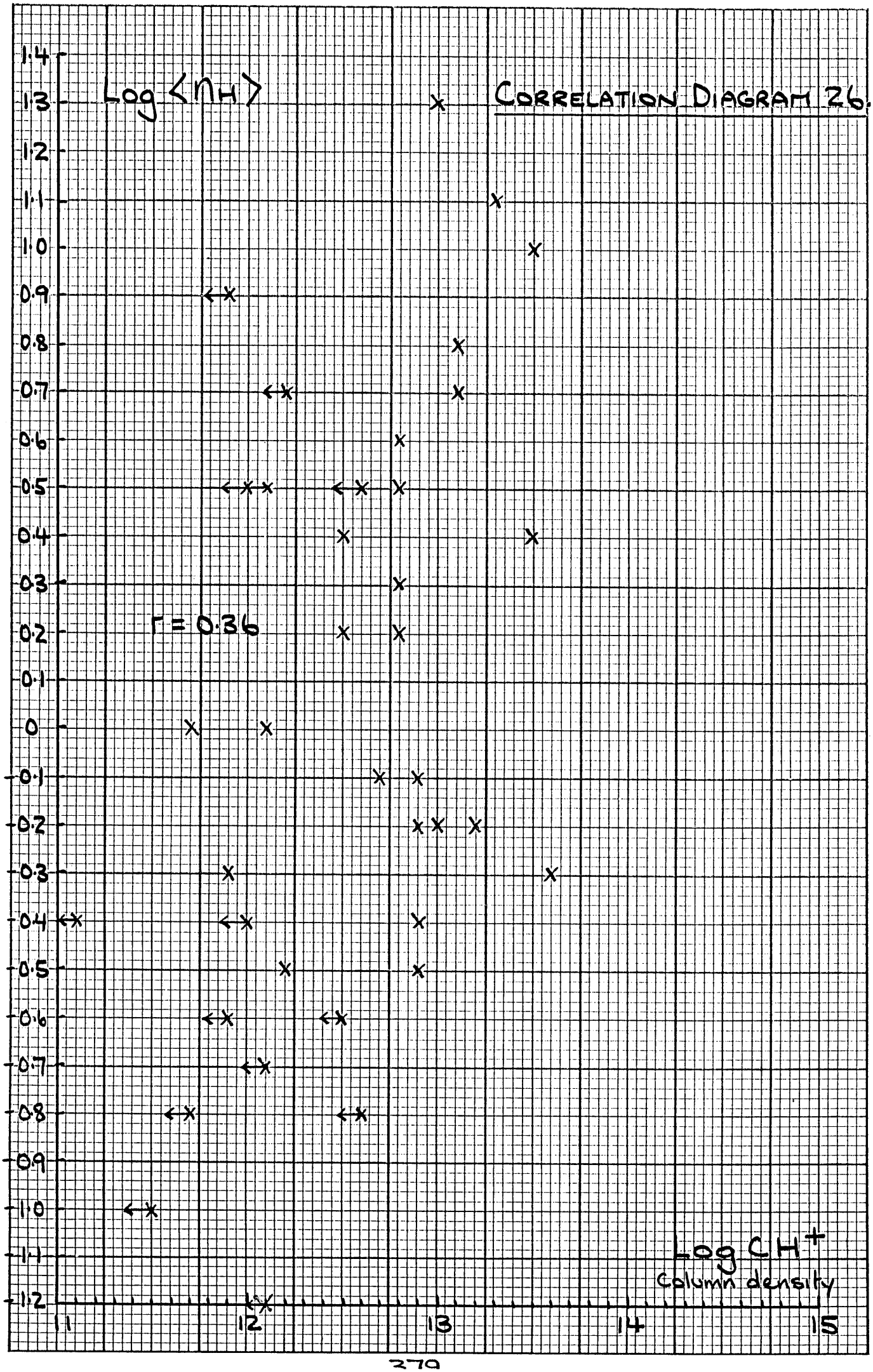
Log ⟨nH⟩
CORRELATION DIAGRAM 26.
r = 0.36
1·4
1·3
1·2
1·1
1·0
0·9
0·8
0·7
0·6
0·5
0·4
0·3
0·2
0·1
0
-0·1
-0·2
-0·3
-0·4
-0·5
-0·6
-0·7
-0·8
-0·9
-1·0
-1·1
-1·2
11
12
13
14
15
Log CH+
column density

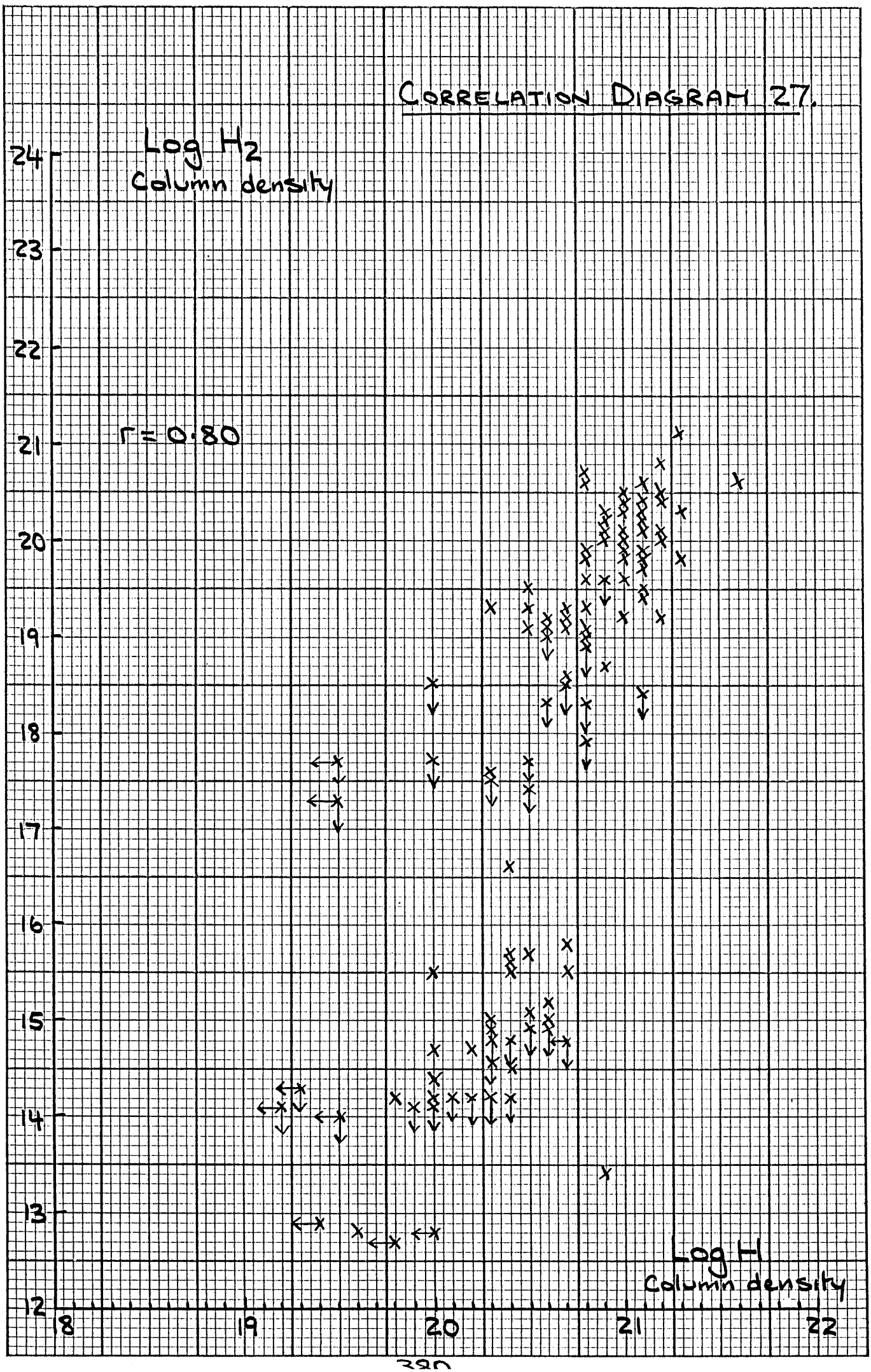
CORRELATION DIAGRAM 27.
Log H_2
Column density
r = 0·80
24
23
22
21
20
19
18
17
16
15
14
13
12
18
19
20
21
22
Log H
Column density

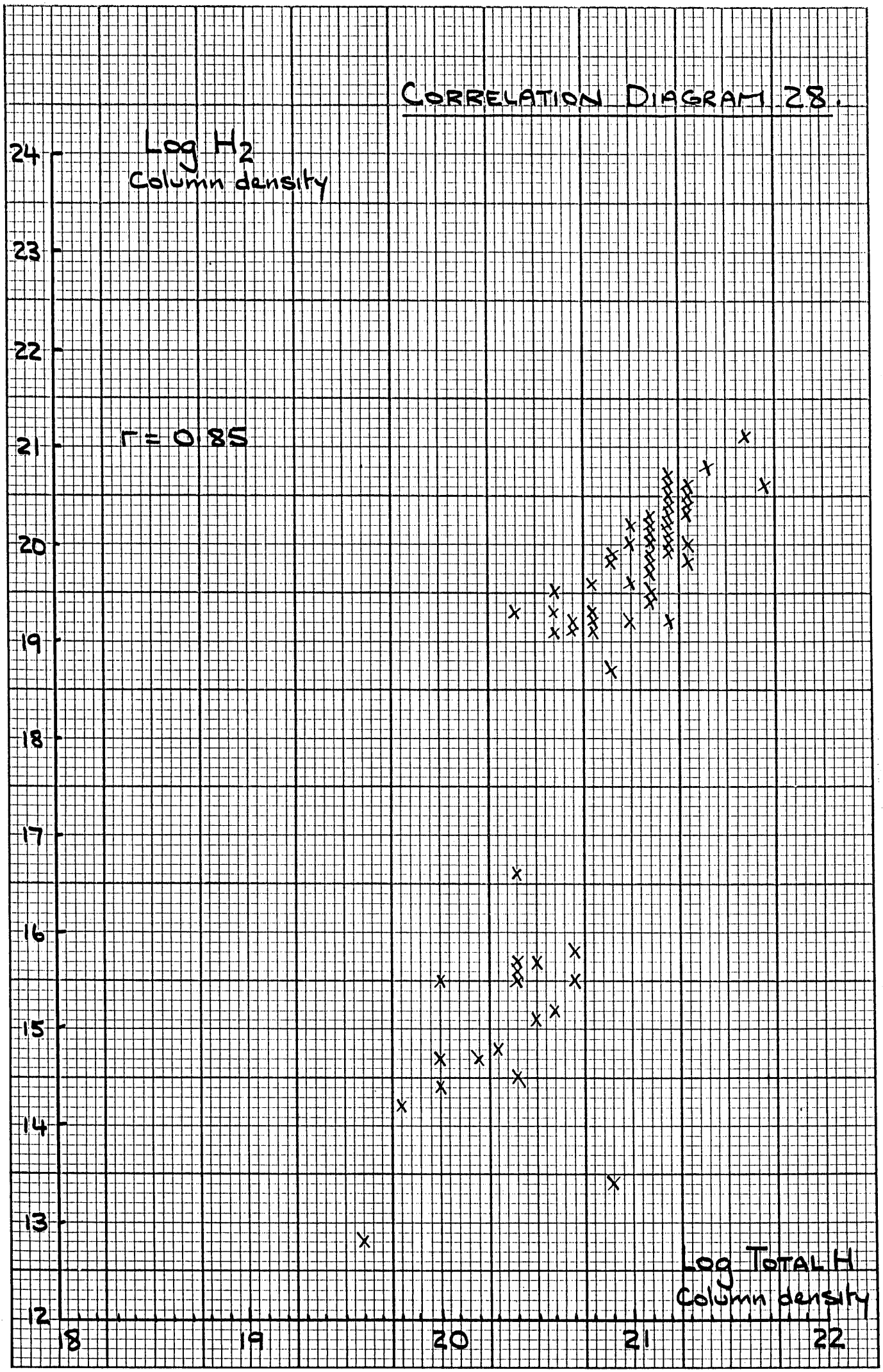
CORRELATION DIAGRAM 28.
Log H_2
Column density
r = 0.85
Log TOTAL H
Column density
24
23
22
21
20
19
18
17
16
15
14
13
12
18
19
20
21
22

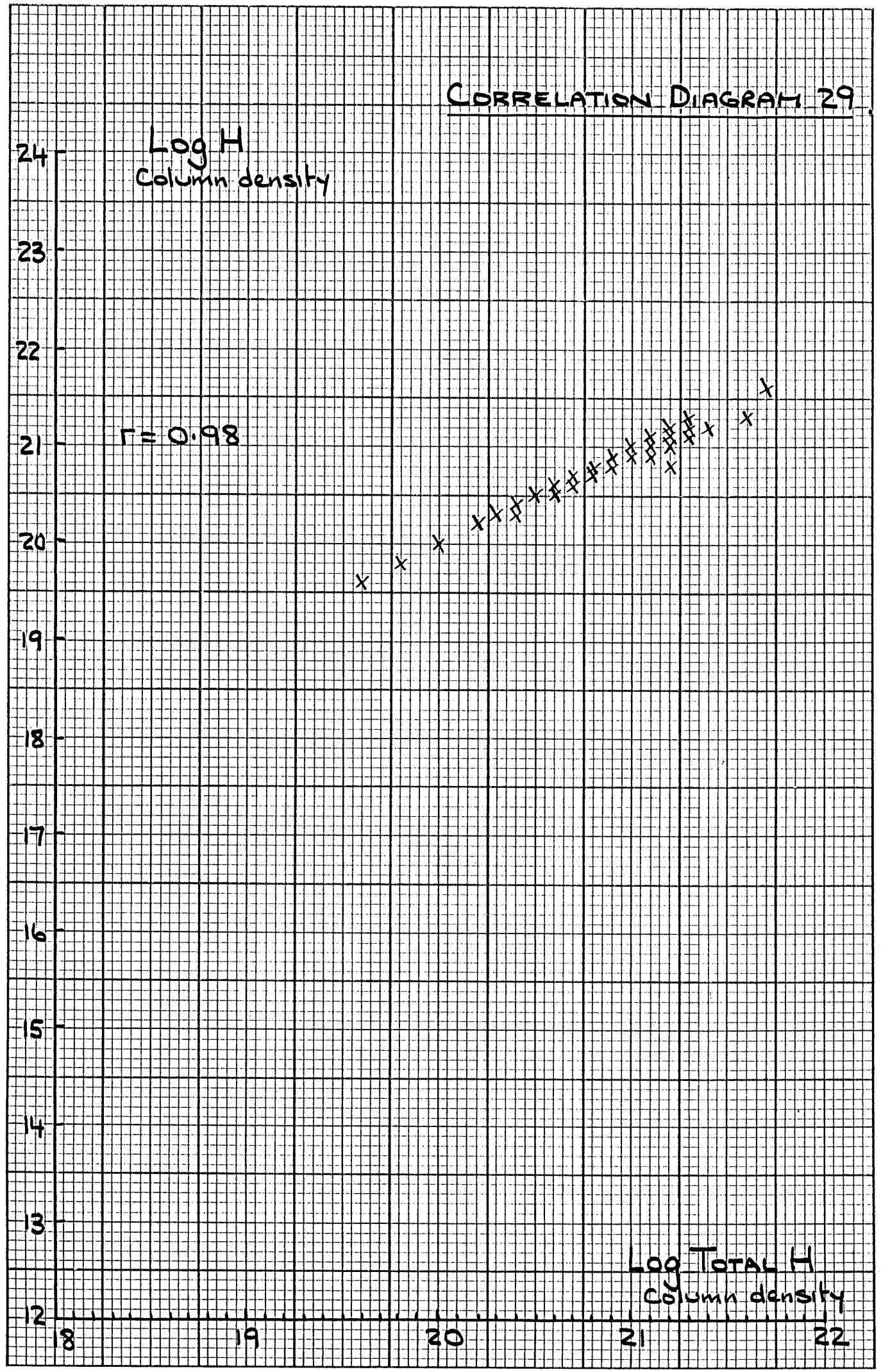
CORRELATION DIAGRAM 29.
Log H
Column density
r = 0.98
24
23
22
21
20
19
18
17
16
15
14
13
12
18
19
20
21
22
LOG TOTAL H
Column density

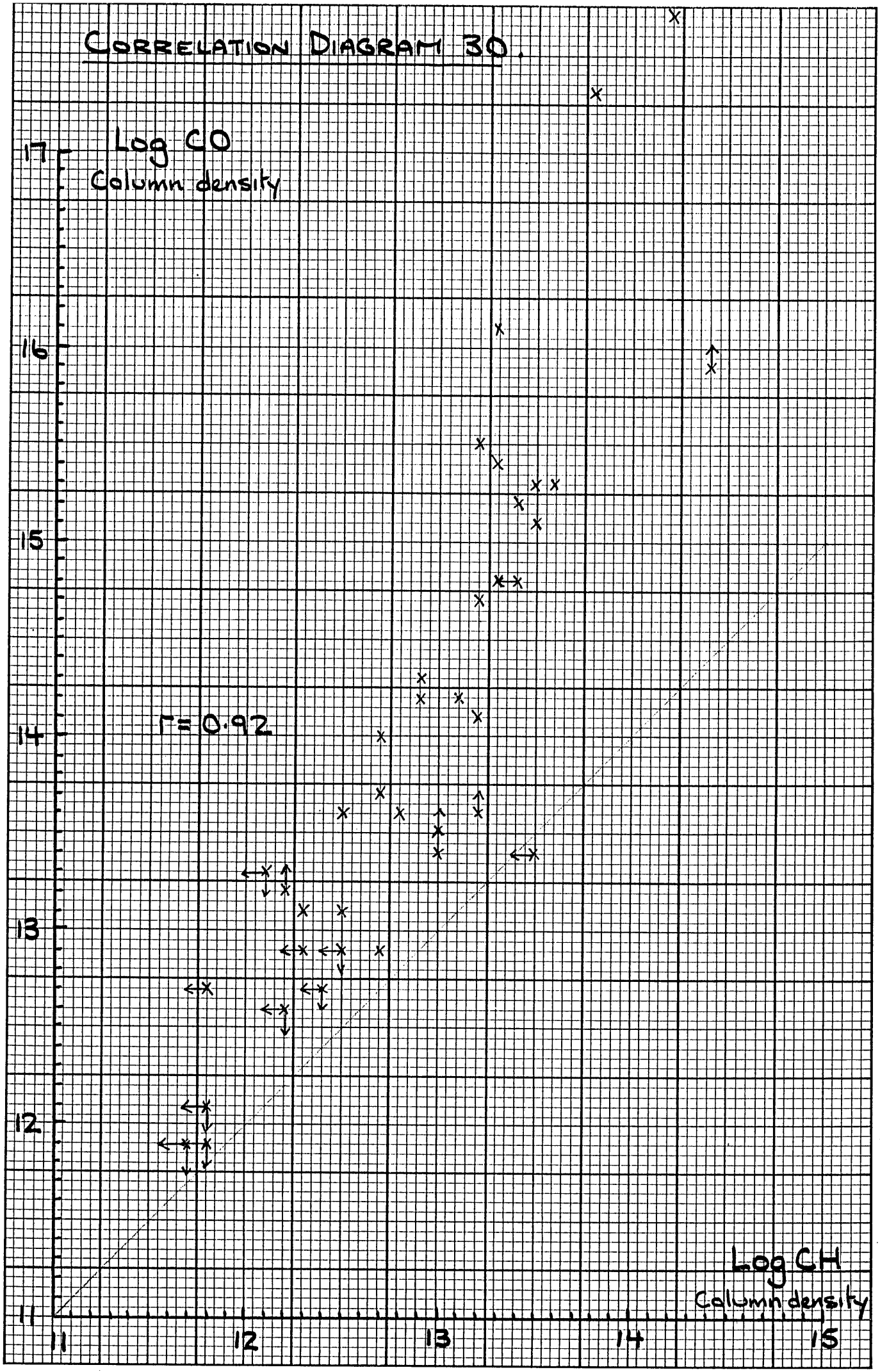
CORRELATION DIAGRAM 30.
Log CO
Column density
17
16
15
14
13
12
11
r = 0.92
Log CH
Column density
11
12
13
14
15

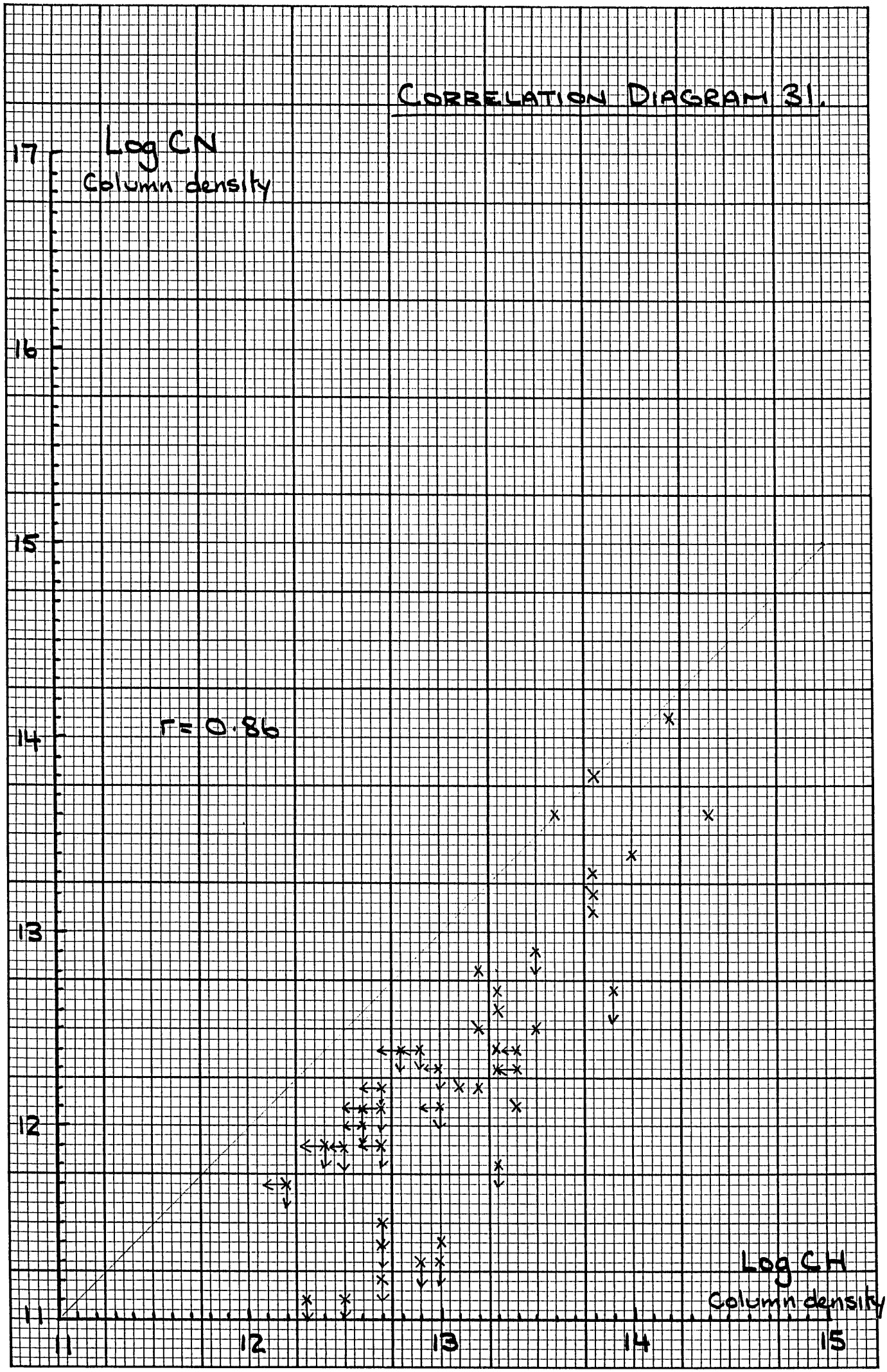
CORRELATION DIAGRAM 31.
Log CN
Column density
17
16
15
14
13
12
11
r = 0.86
Log CH
Column density
11
12
13
14
15

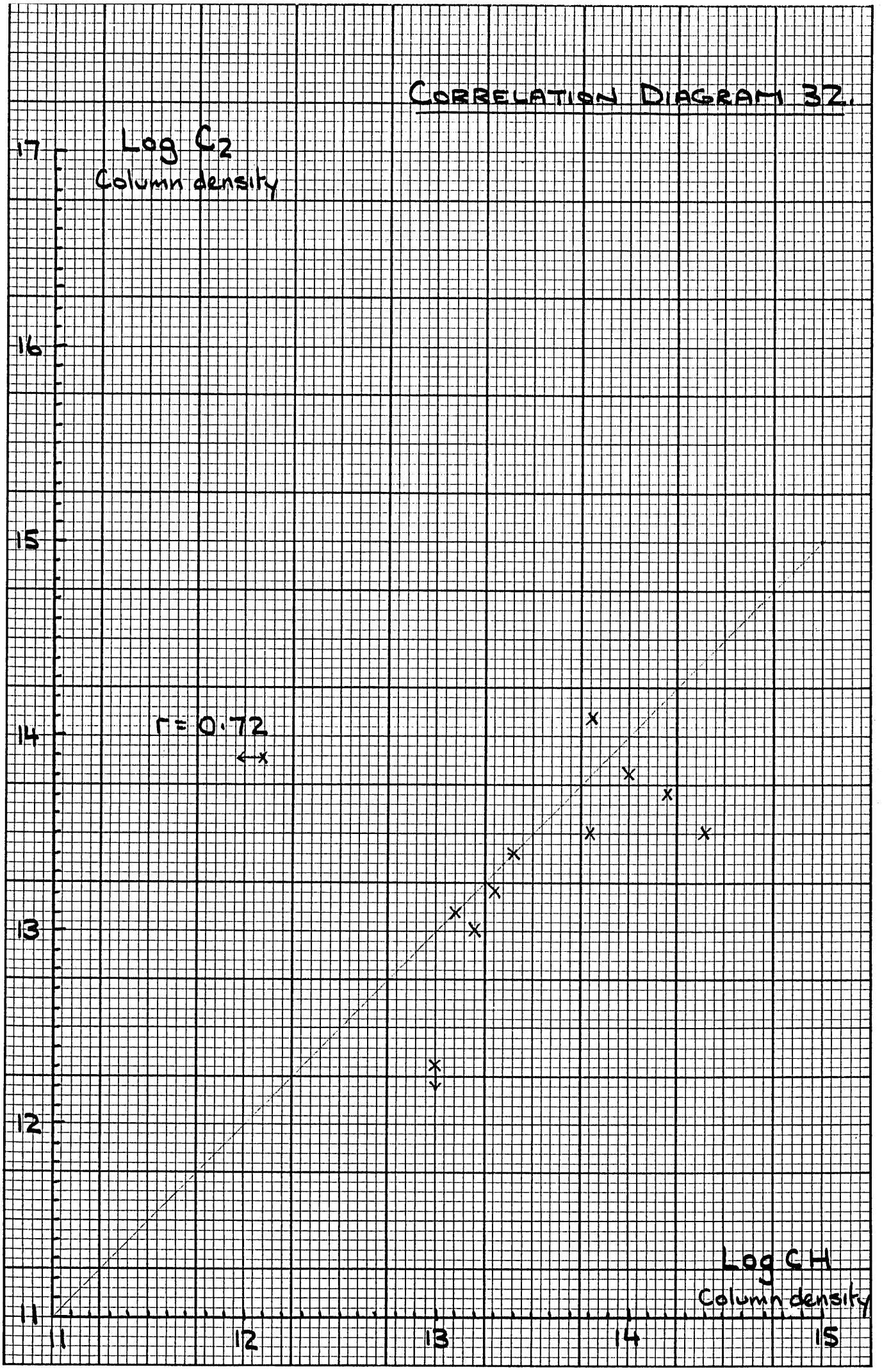
CORRELATION DIAGRAM 32.
Log C_2
Column density
17
16
15
14
13
12
11
r = 0·72
Log C H
Column density
11
12
13
14
15

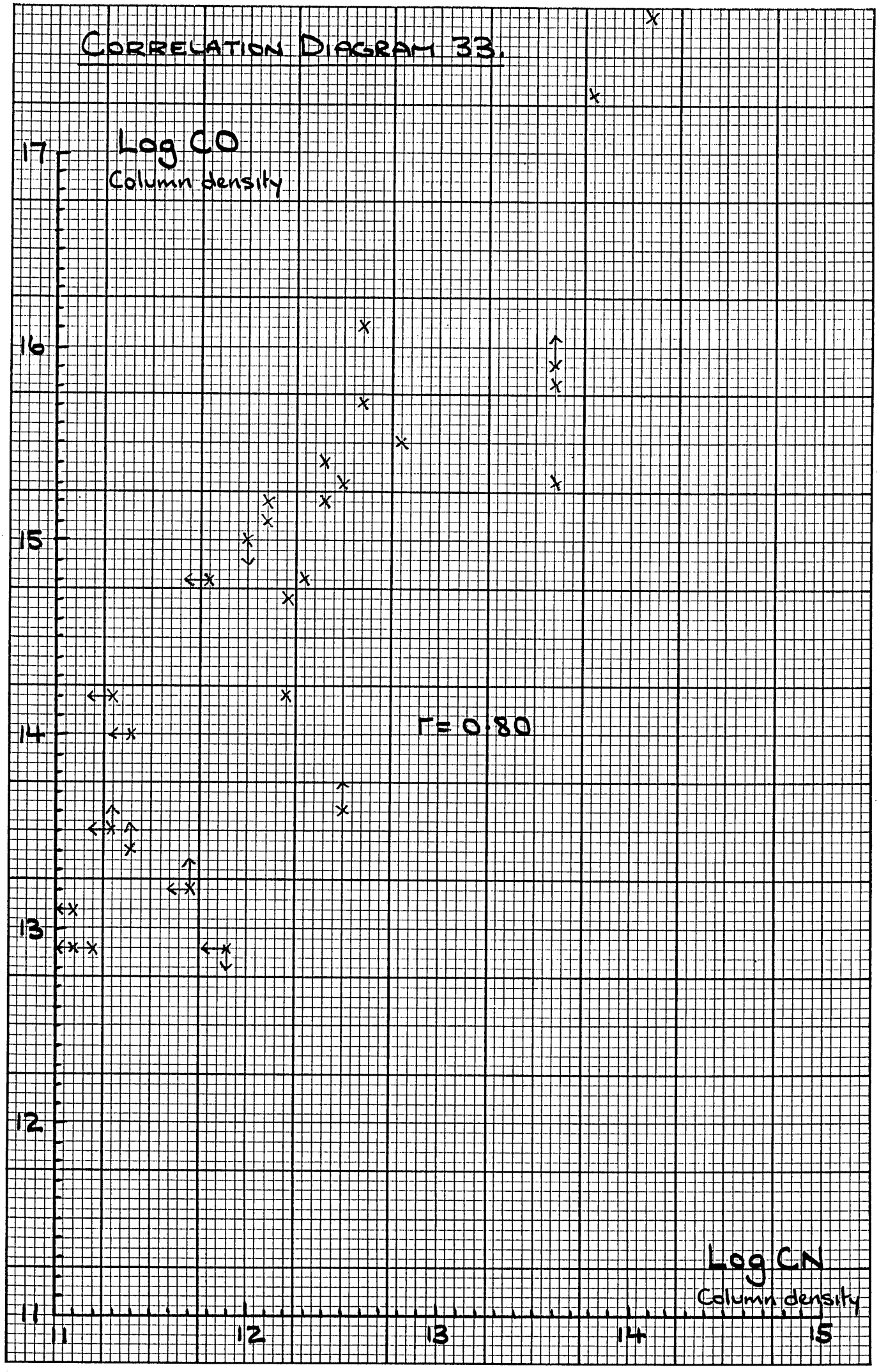
CORRELATION DIAGRAM 33.
Log CO
Column density
17
16
15
14
13
12
11
r = 0·80
Log CN
Column density
11
12
13
14
15

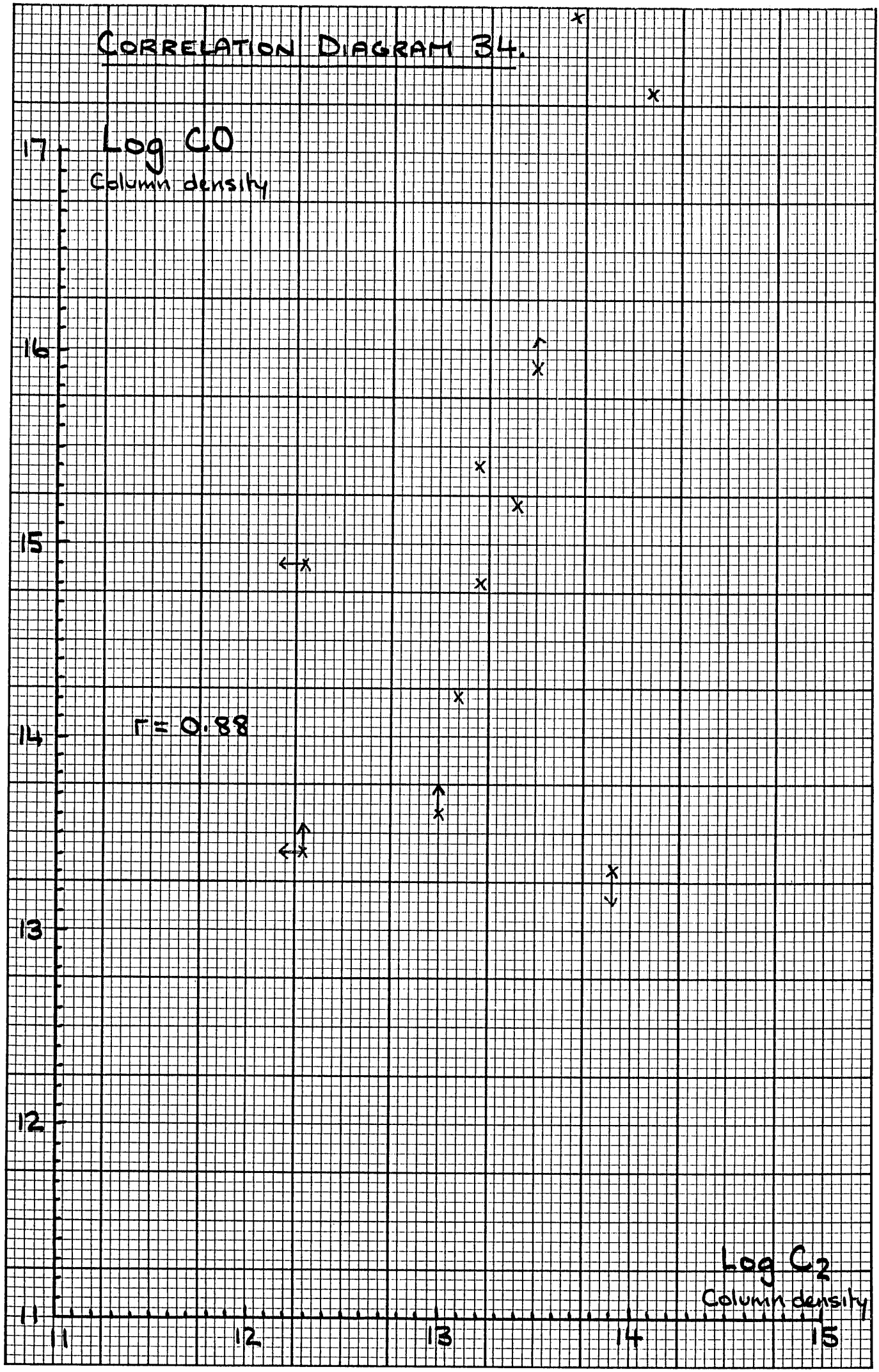
CORRELATION DIAGRAM 34.
Log CO
Column density
17
16
15
14
13
12
11
r = 0.88
Log C_2
Column density
11
12
13
14
15

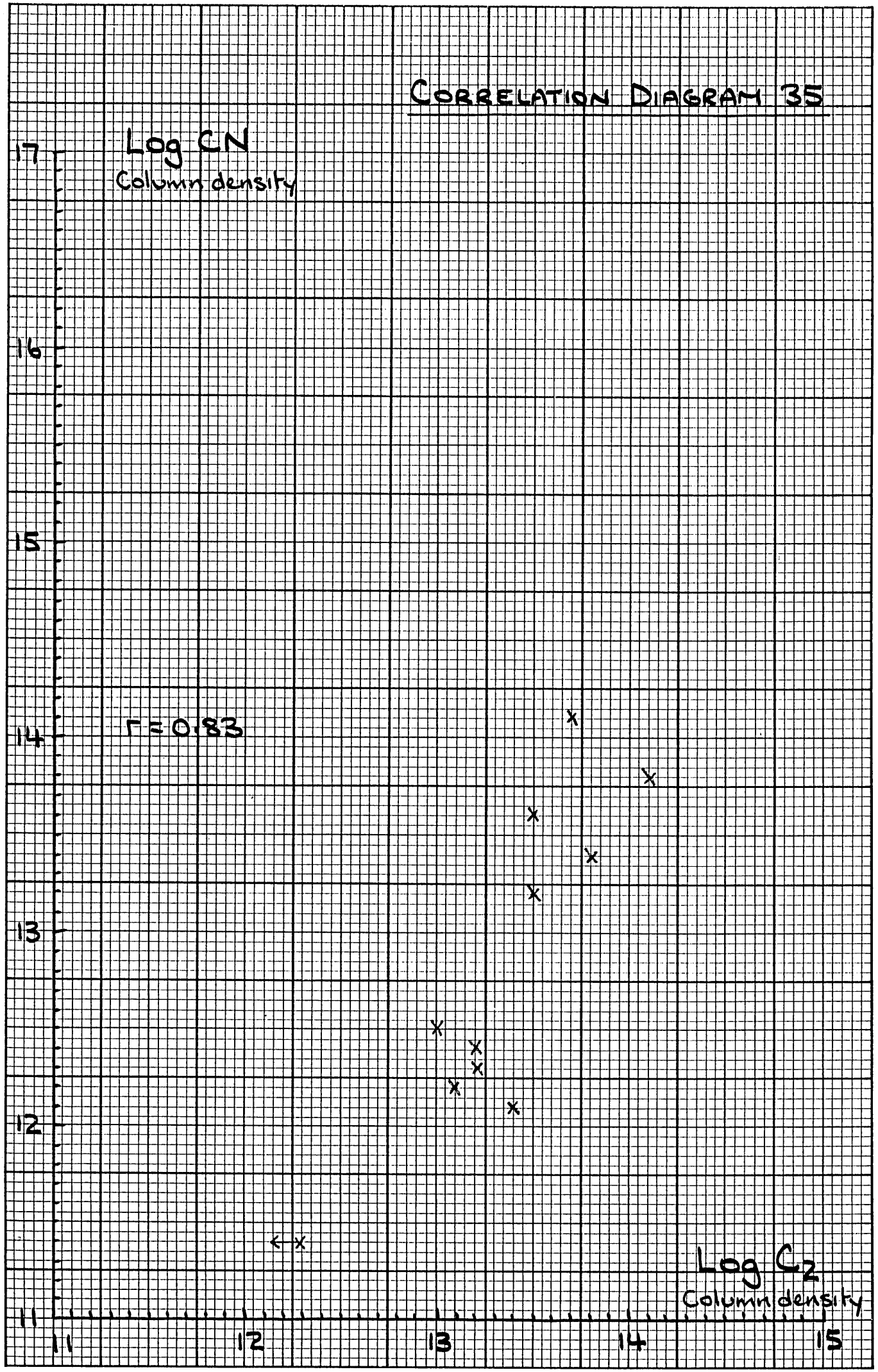
CORRELATION DIAGRAM 35
Log CN
Column density
17
16
15
14
13
12
11
r = 0.83
Log C2
Column density
11
12
13
14
15

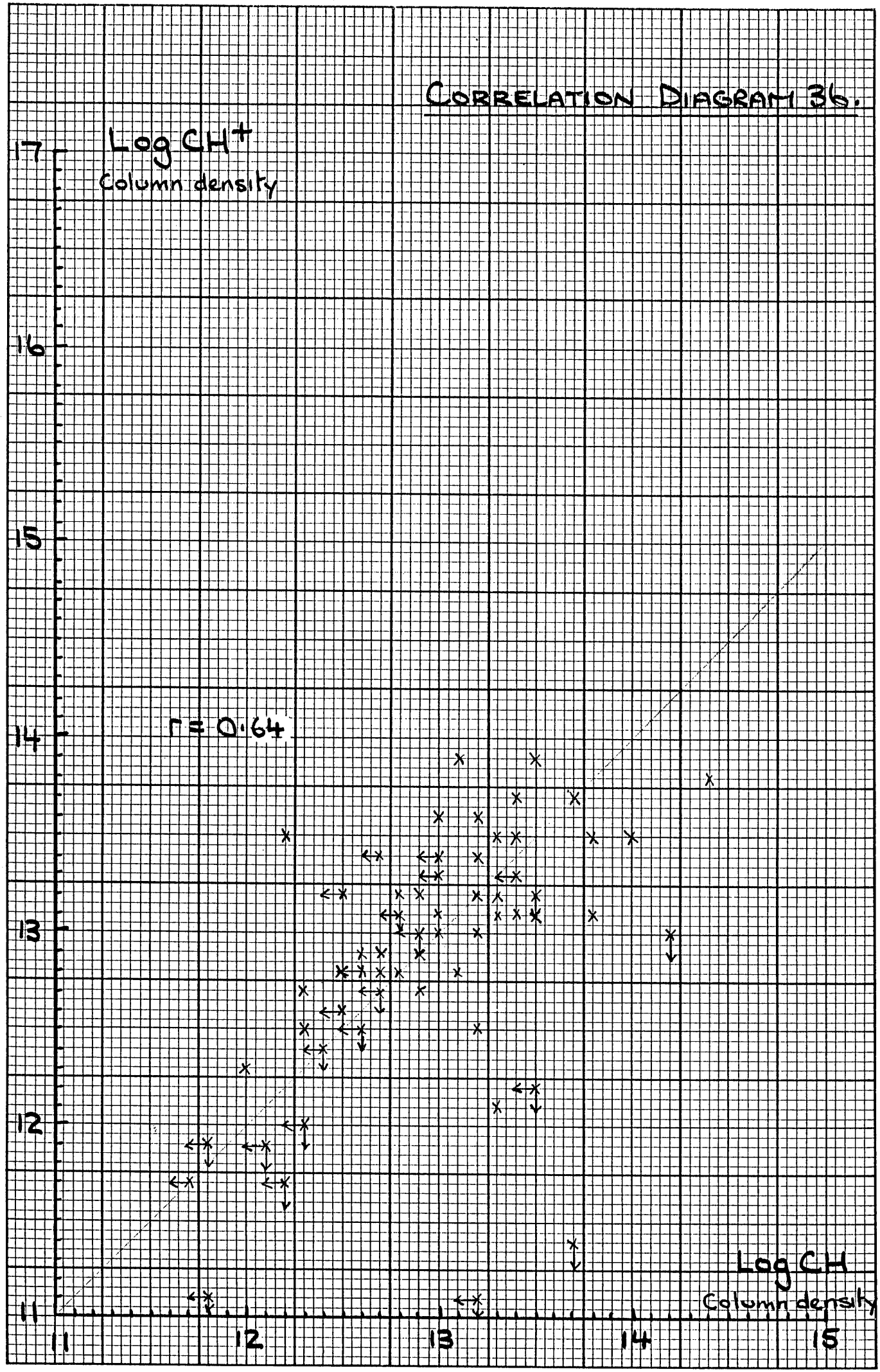
CORRELATION DIAGRAM 36.
Log CH+
Column density
17
16
15
14
13
12
11
r = 0·64
Log CH
Column density
11
12
13
14
15

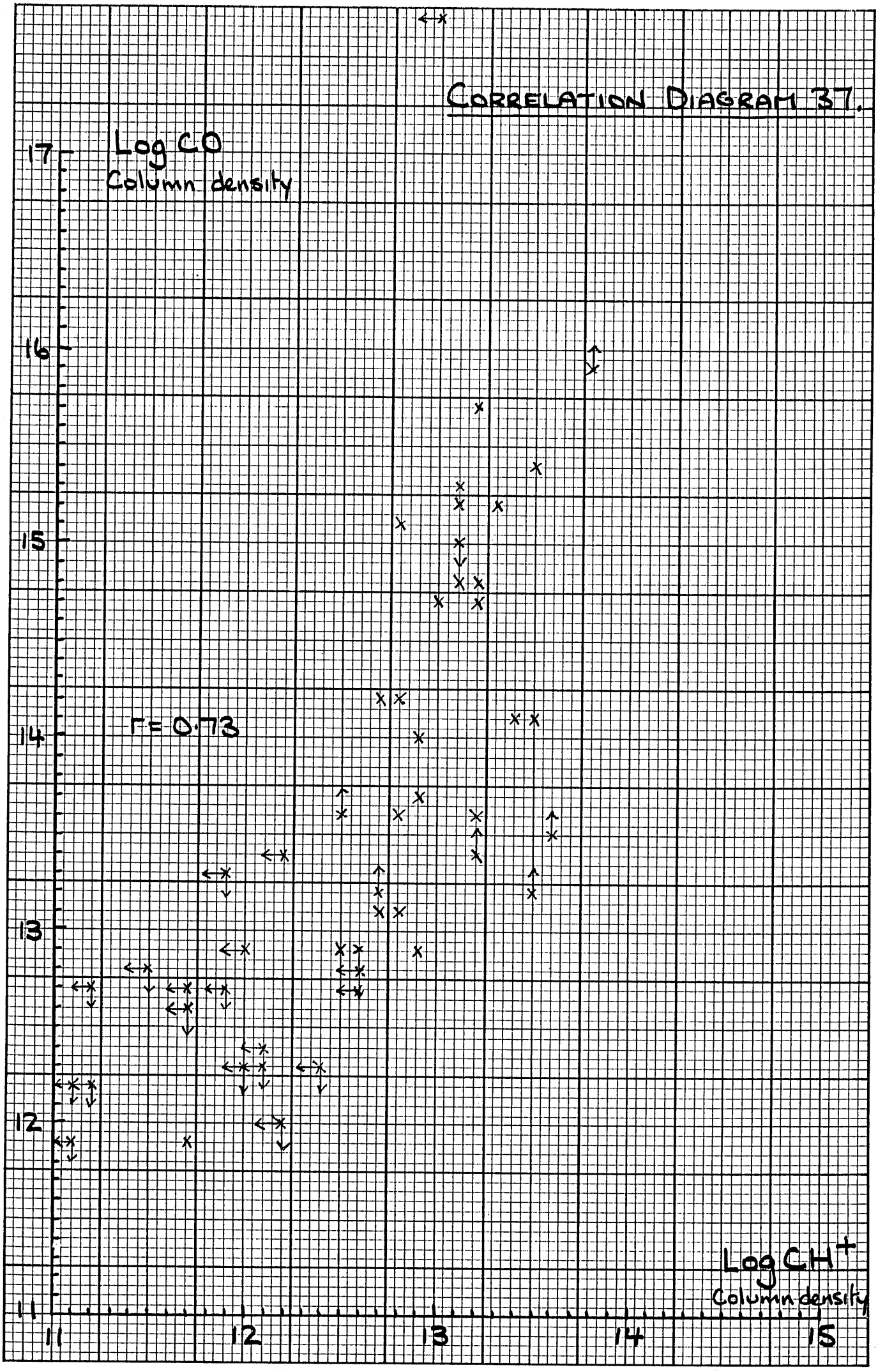
CORRELATION DIAGRAM 37.
Log CO
Column density
17
16
15
14
13
12
11
r = 0·73
Log CH+
Column density
11
12
13
14
15

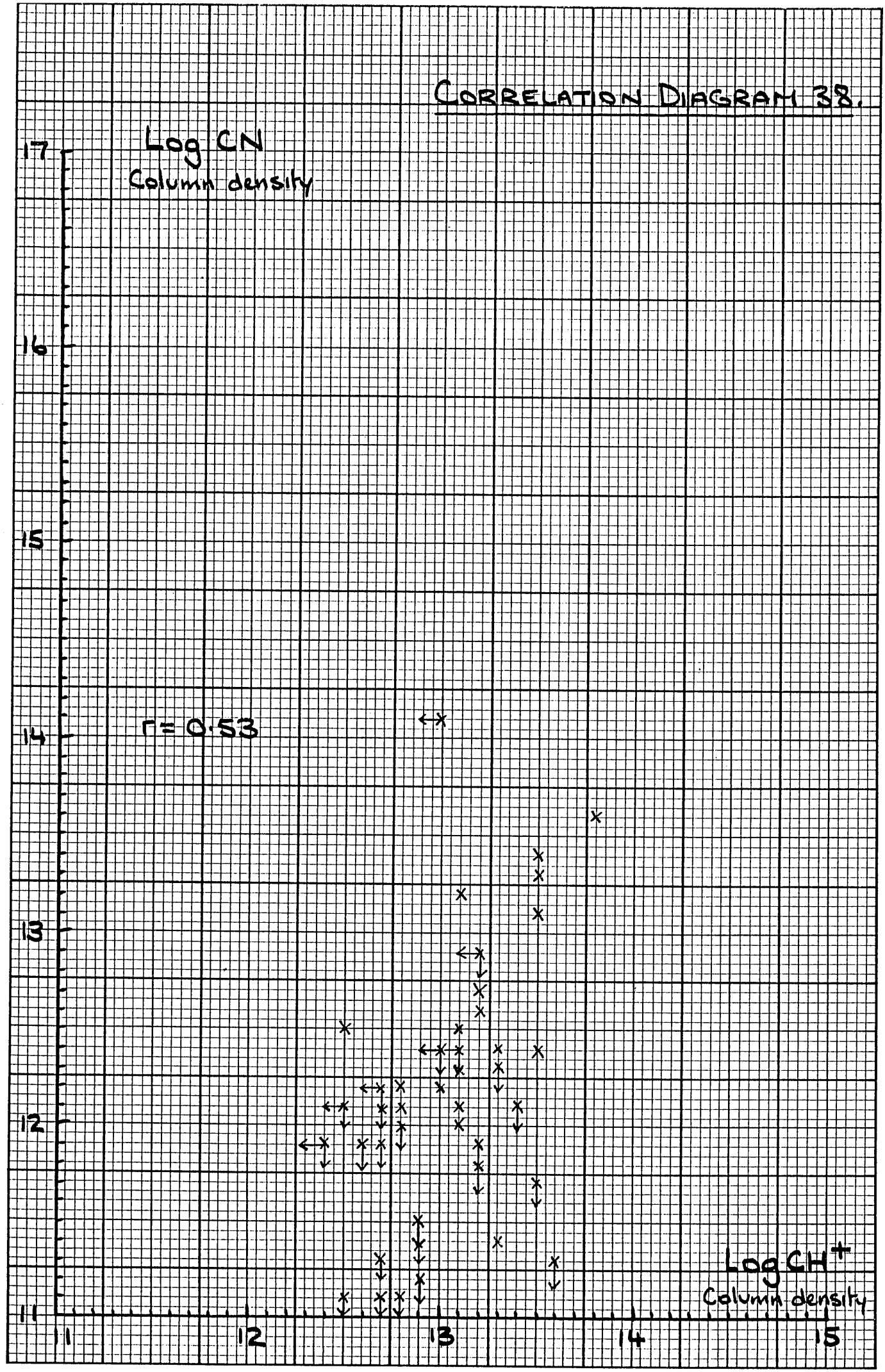
CORRELATION DIAGRAM 38.
Log CN
Column density
17
16
15
14
13
12
11
r = 0·53
11
12
13
14
15
Log CH+
Column density

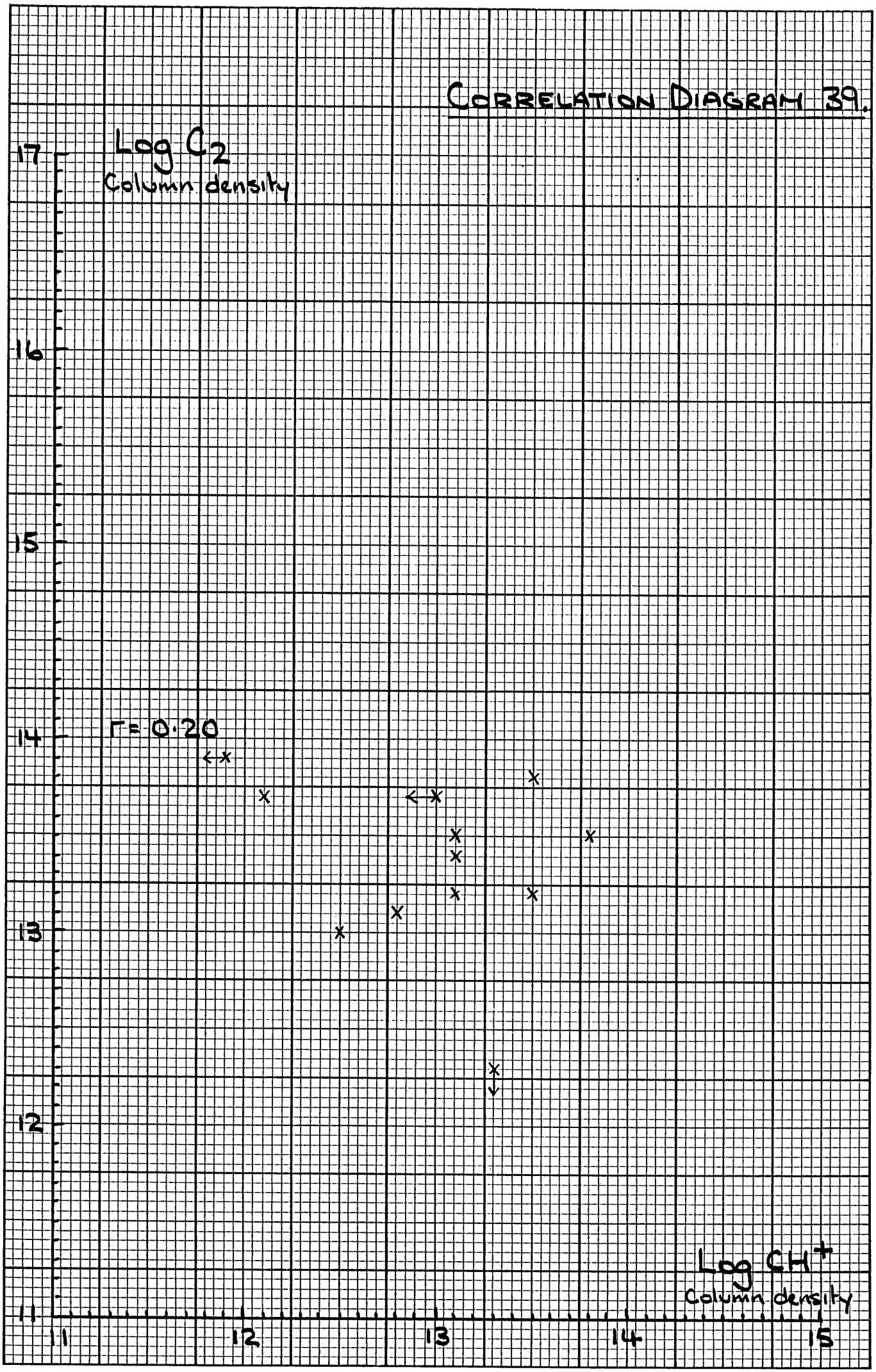
CORRELATION DIAGRAM 39.
Log C_2
Column density
17
16
15
14
13
12
11
r = 0·20
Log CH^+
Column density
11
12
13
14
15

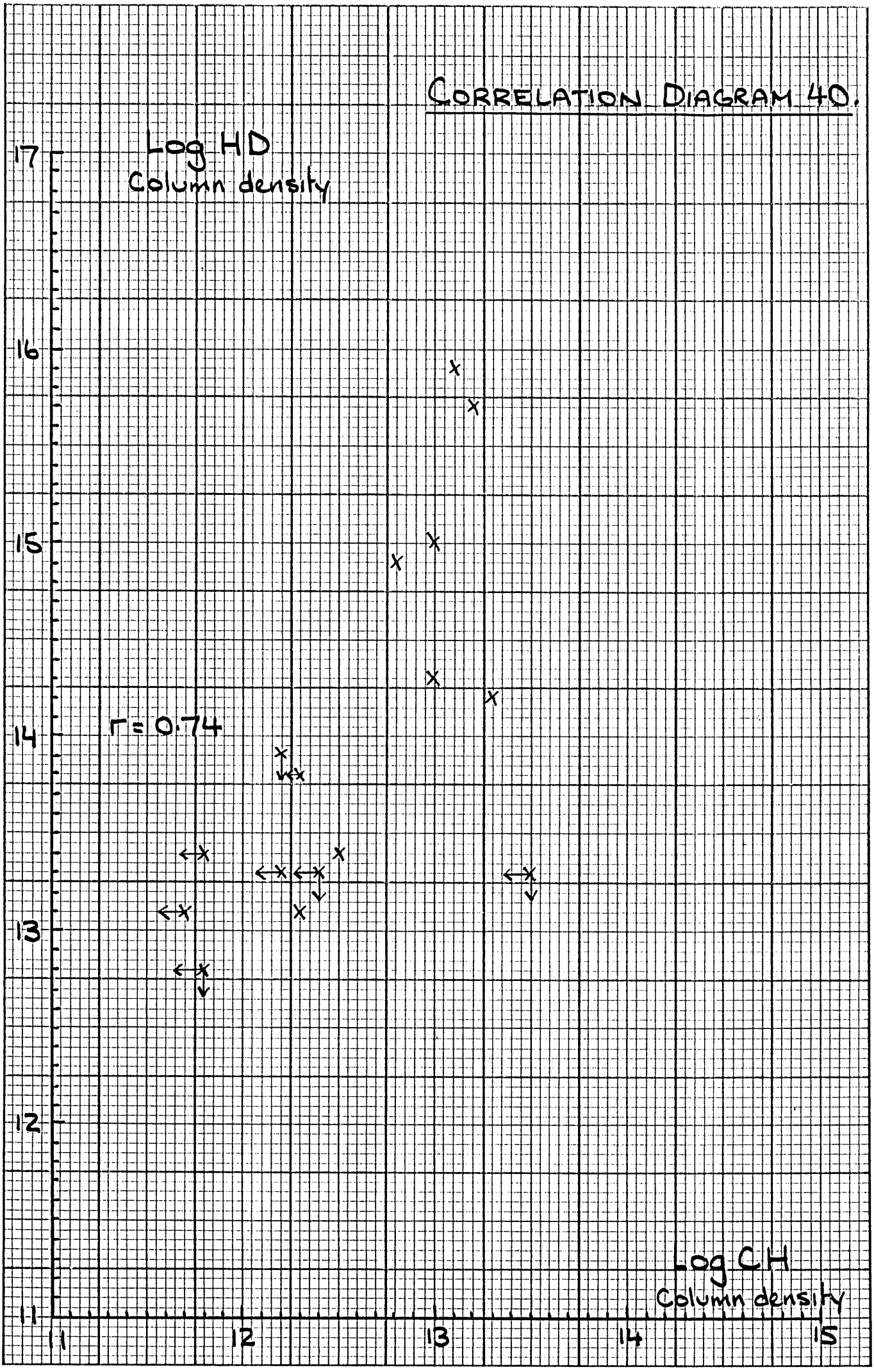
CORRELATION DIAGRAM 40.
Log HD
Column density
17
16
15
14
13
12
11
r = 0.74
Log CH
Column density
11
12
13
14
15

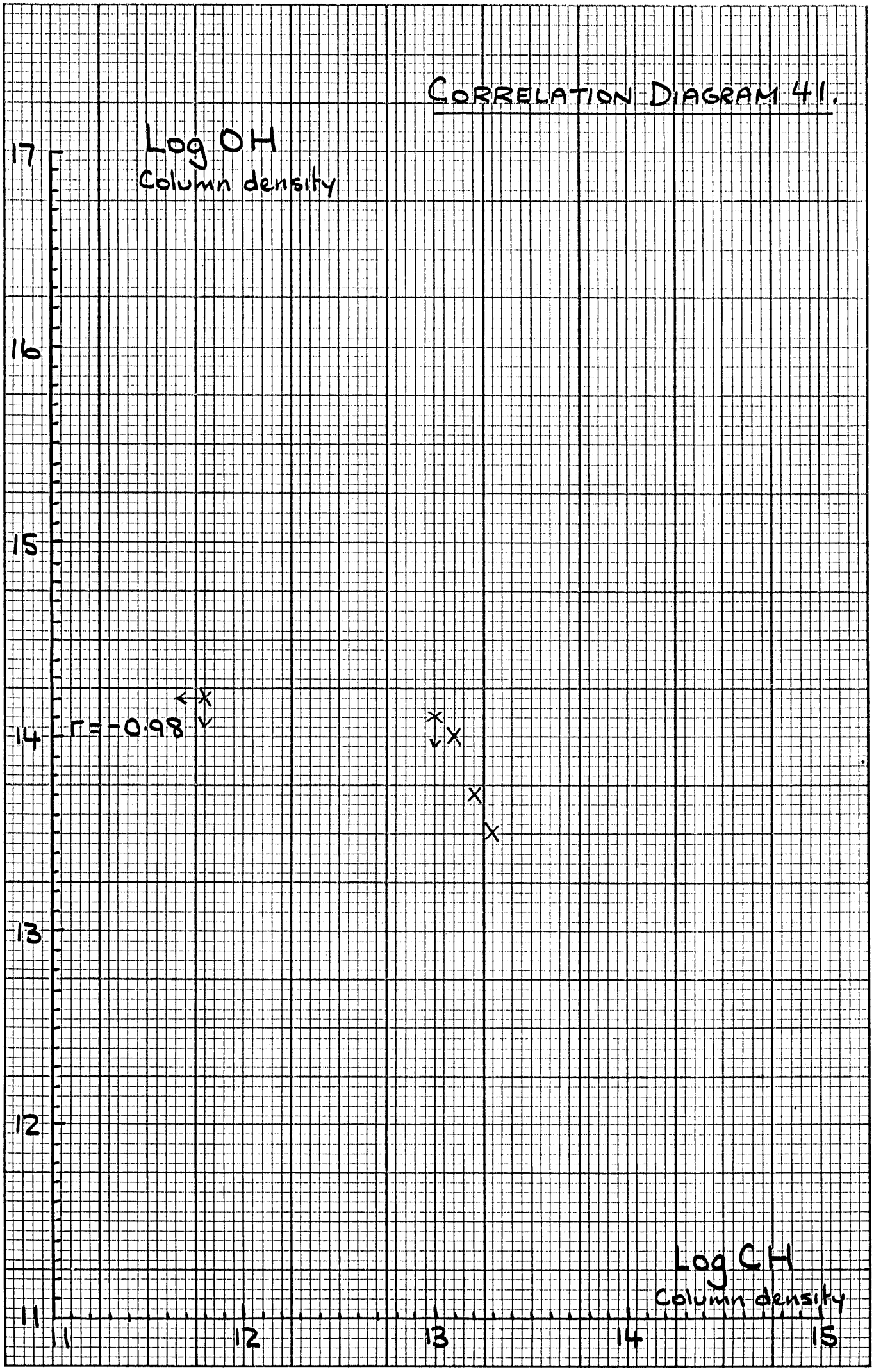
CORRELATION DIAGRAM 41.
Log OH
Column density
17
16
15
14
13
12
11
r=-0.98
Log CH
Column density
11
12
13
14
15

CORRELATION DIAGRAM 42.

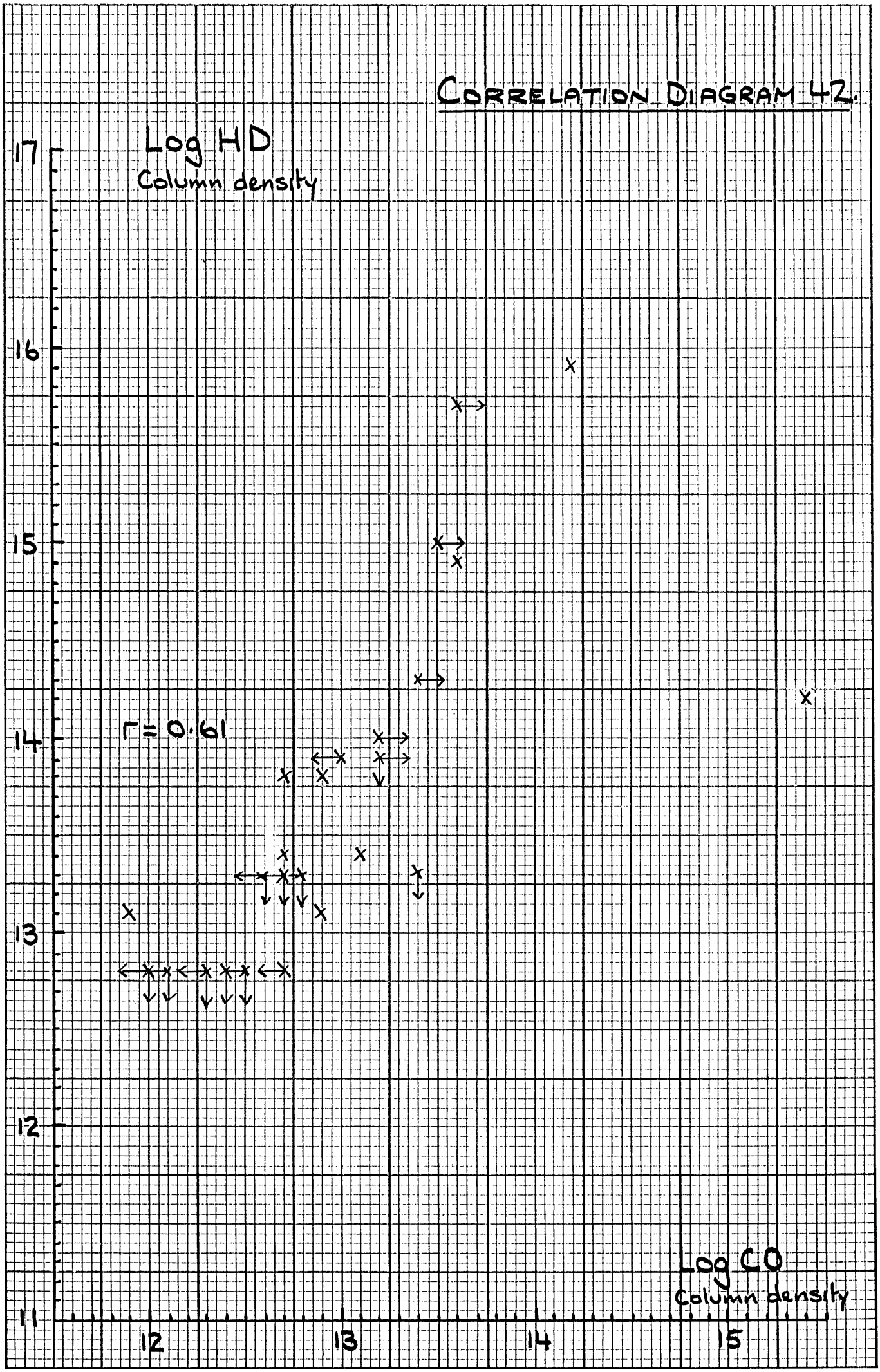

CORRELATION DIAGRAM 43.

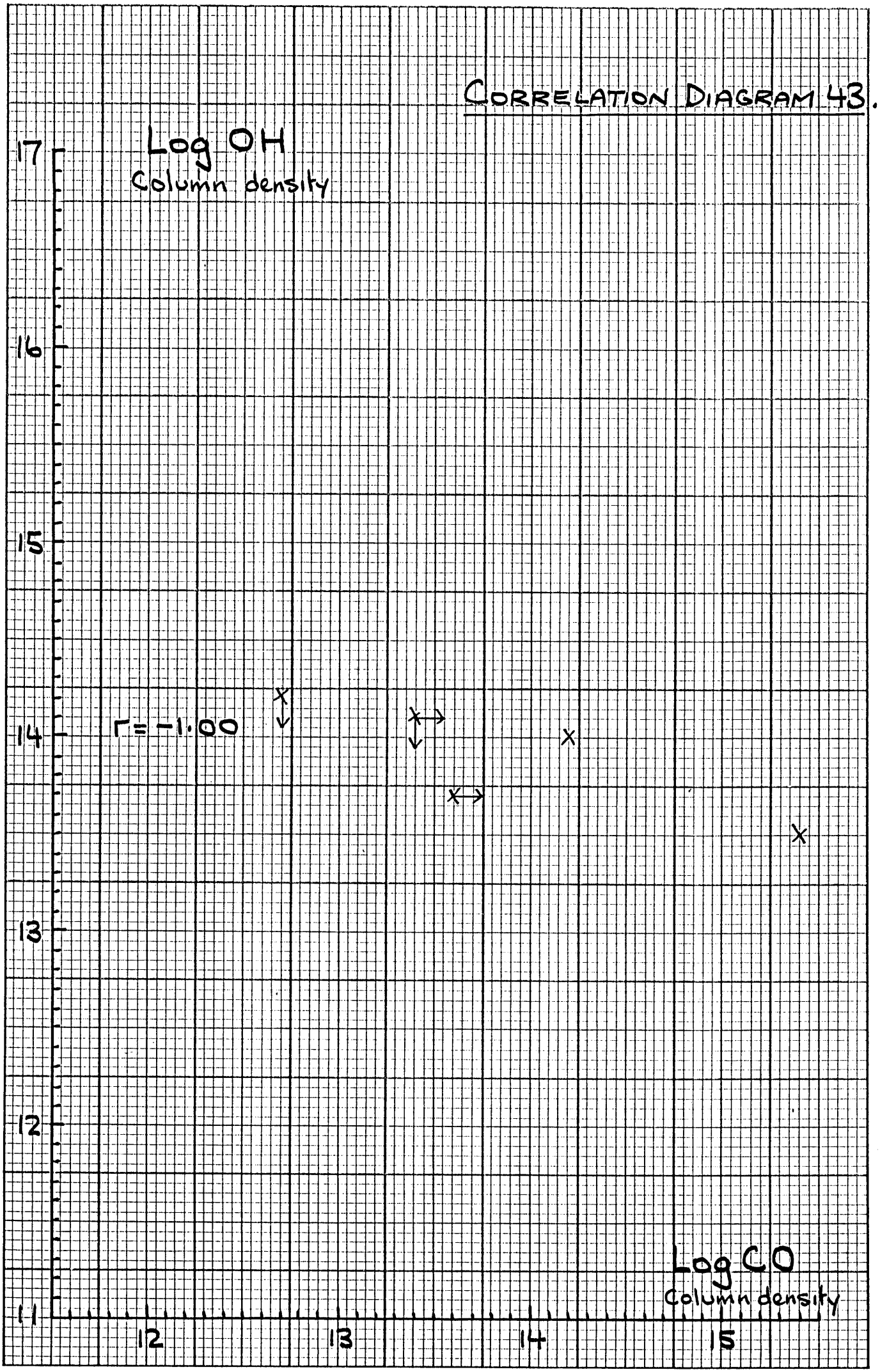

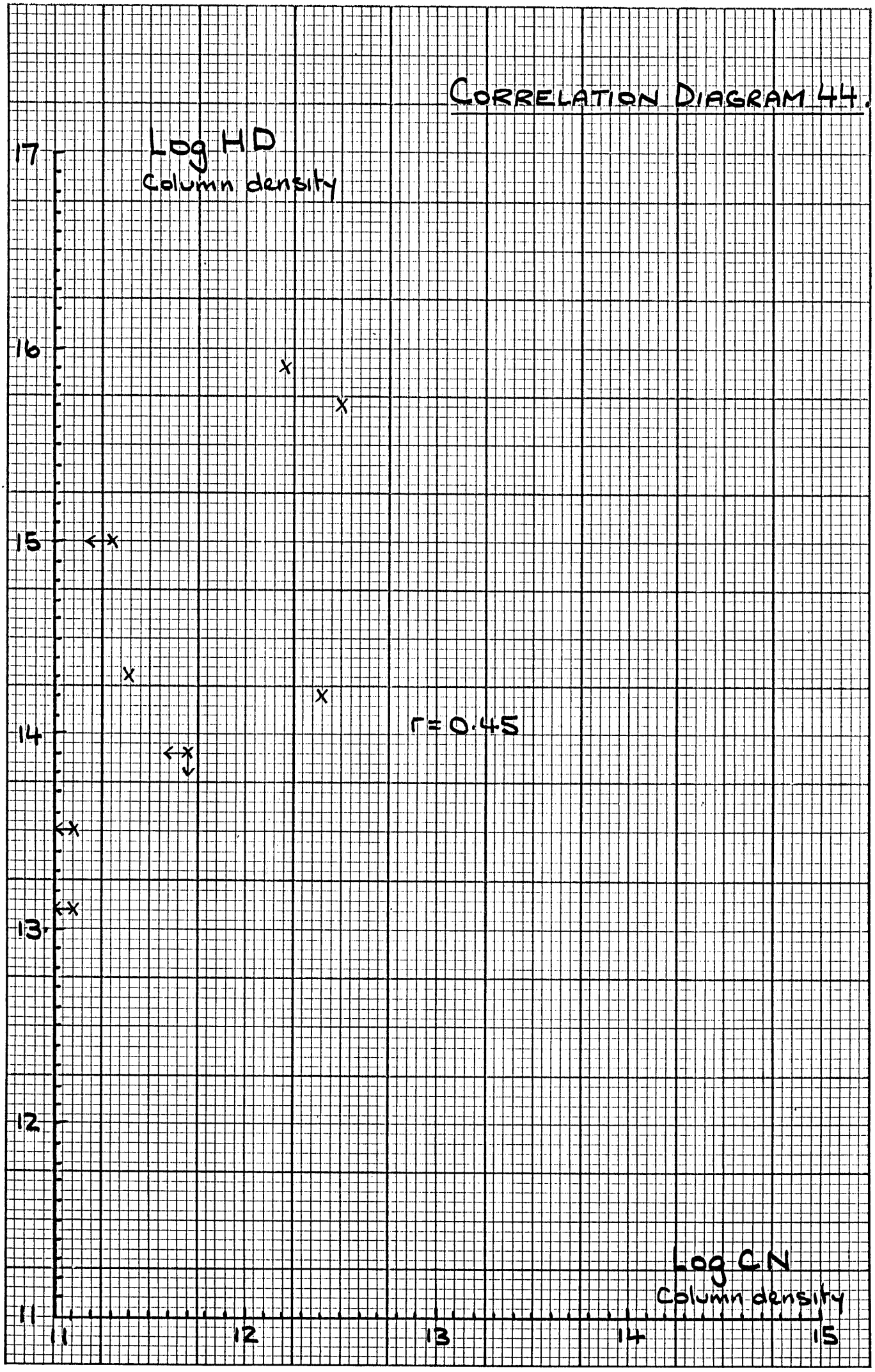
CORRELATION DIAGRAM 44.
Log HD
Column density
17
16
15
14
13
12
11
r = 0.45
Log CN
Column density
11
12
13
14
15

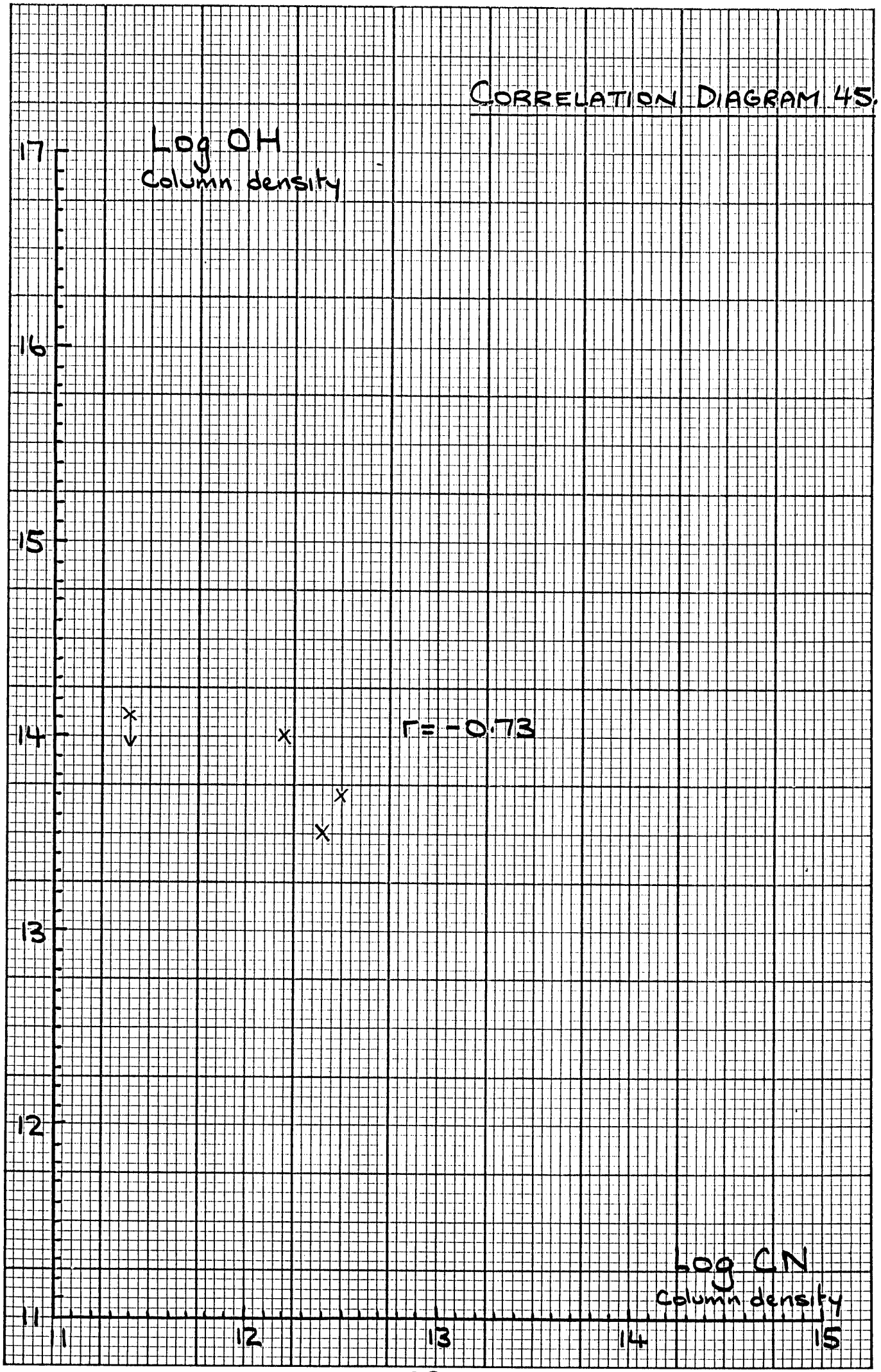
CORRELATION DIAGRAM 45.
Log OH
Column density
17
16
15
14
13
12
11
r = -0.73
Log CN
Column density
11
12
13
14
15

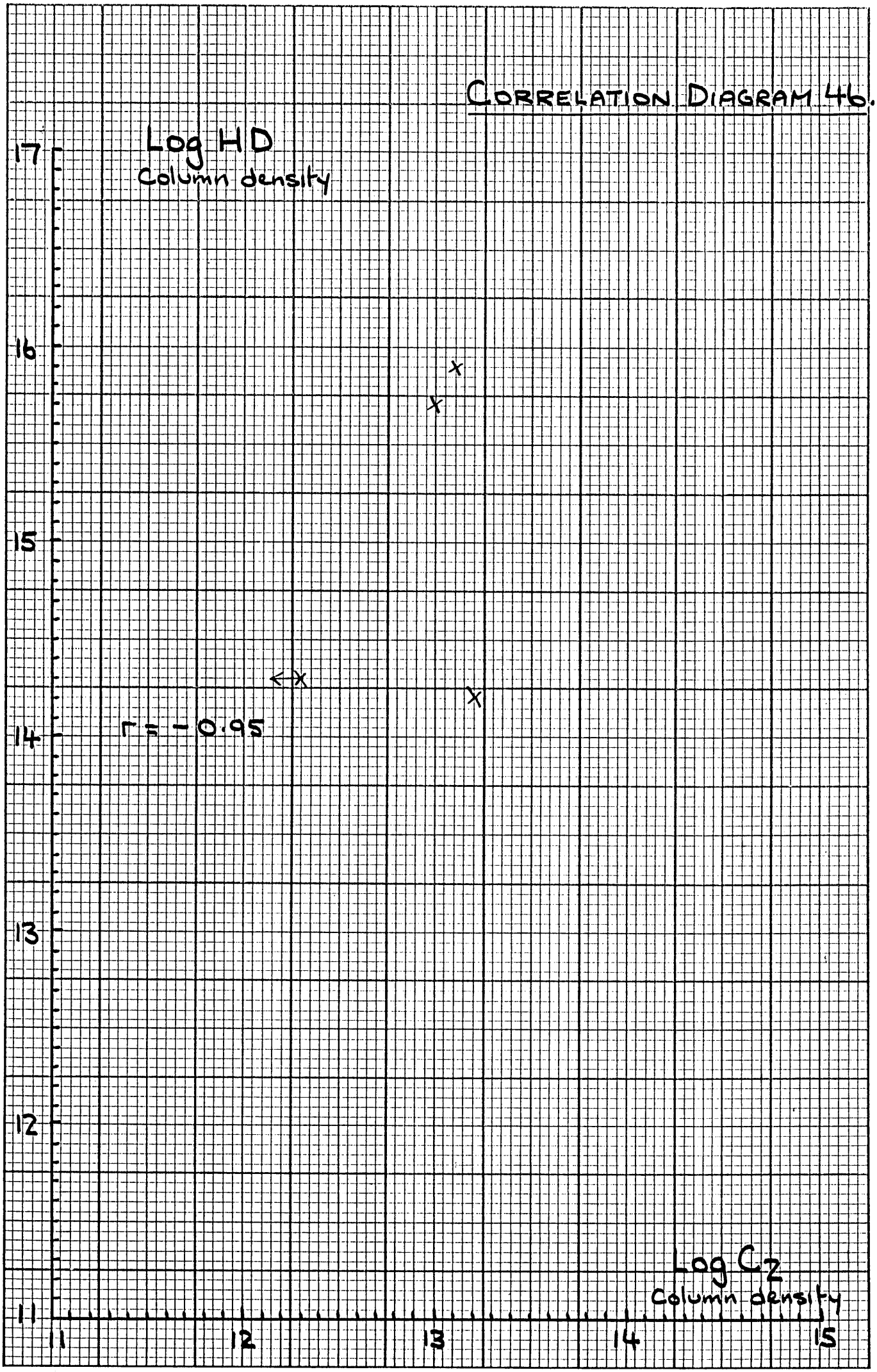
CORRELATION DIAGRAM 46.
Log HD
column density
17
16
15
14
13
12
11
r = -0.95
Log C2
column density
11
12
13
14
15

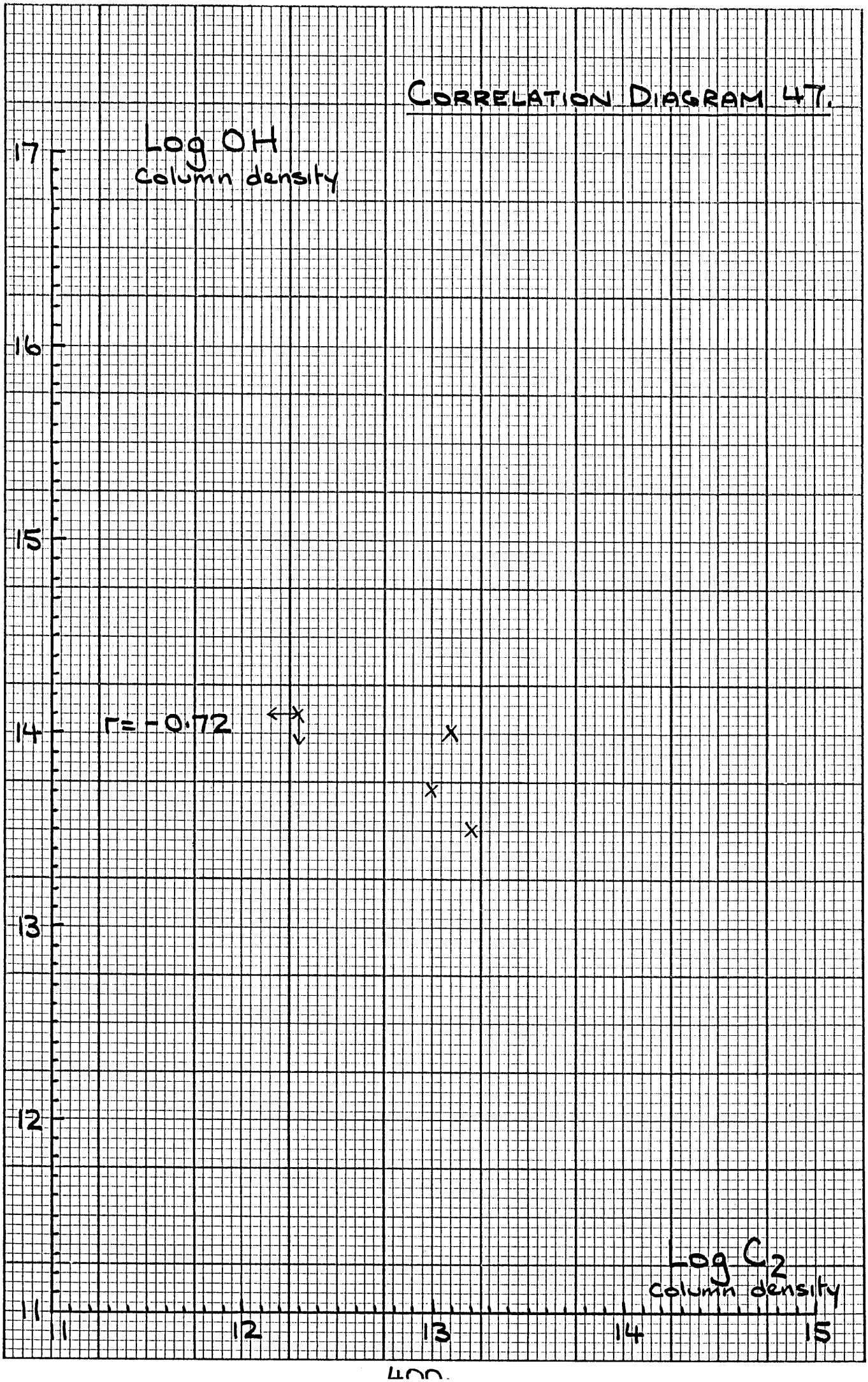
CORRELATION DIAGRAM 47.
Log OH
column density
17
16
15
14
13
12
11
r = -0.72
Log C_2
column density
11
12
13
14
15

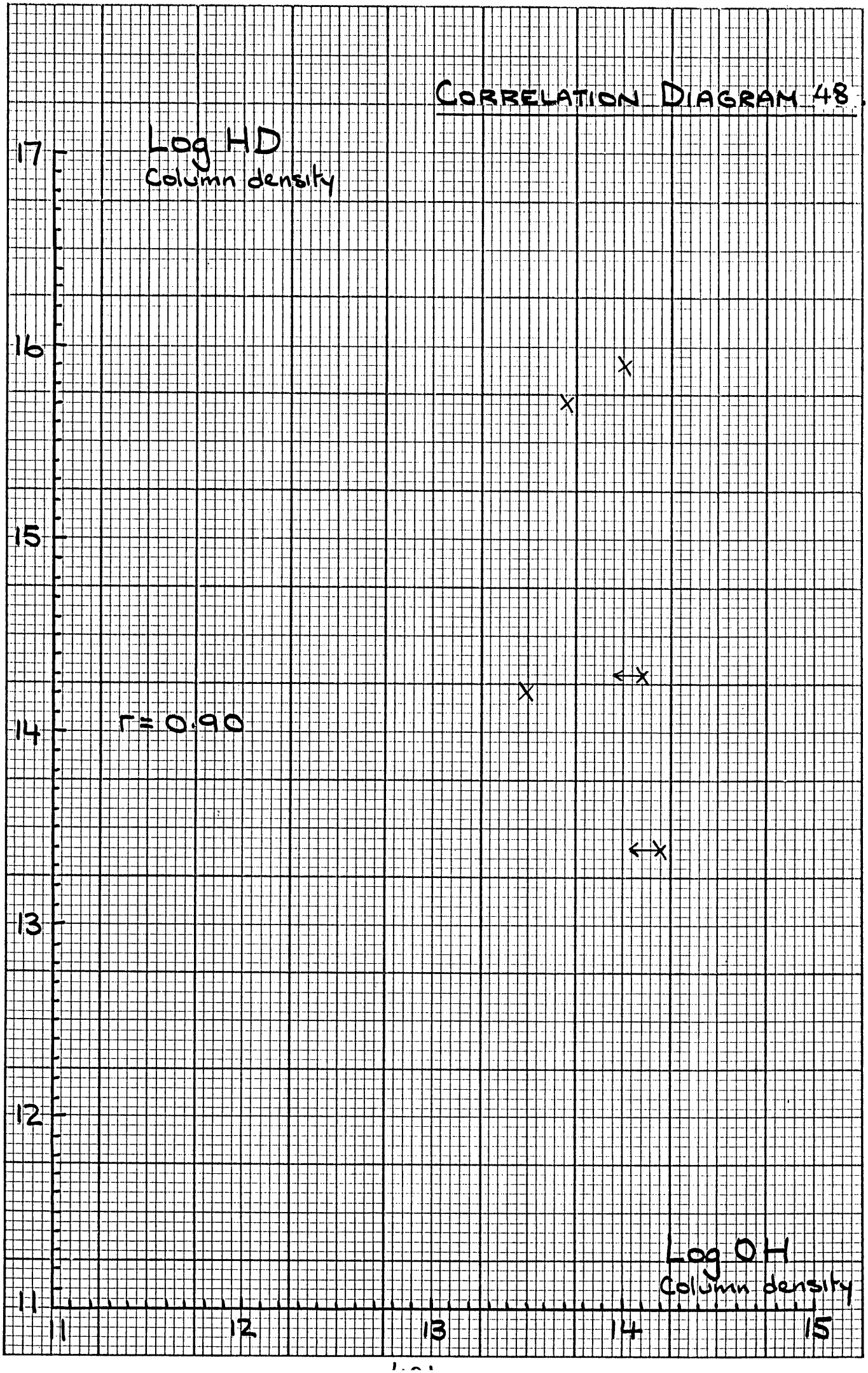
CORRELATION DIAGRAM 48.
Log HD
Column density
17
16
15
14
13
12
11
r = 0.90
Log OH
Column density
11
12
13
14
15

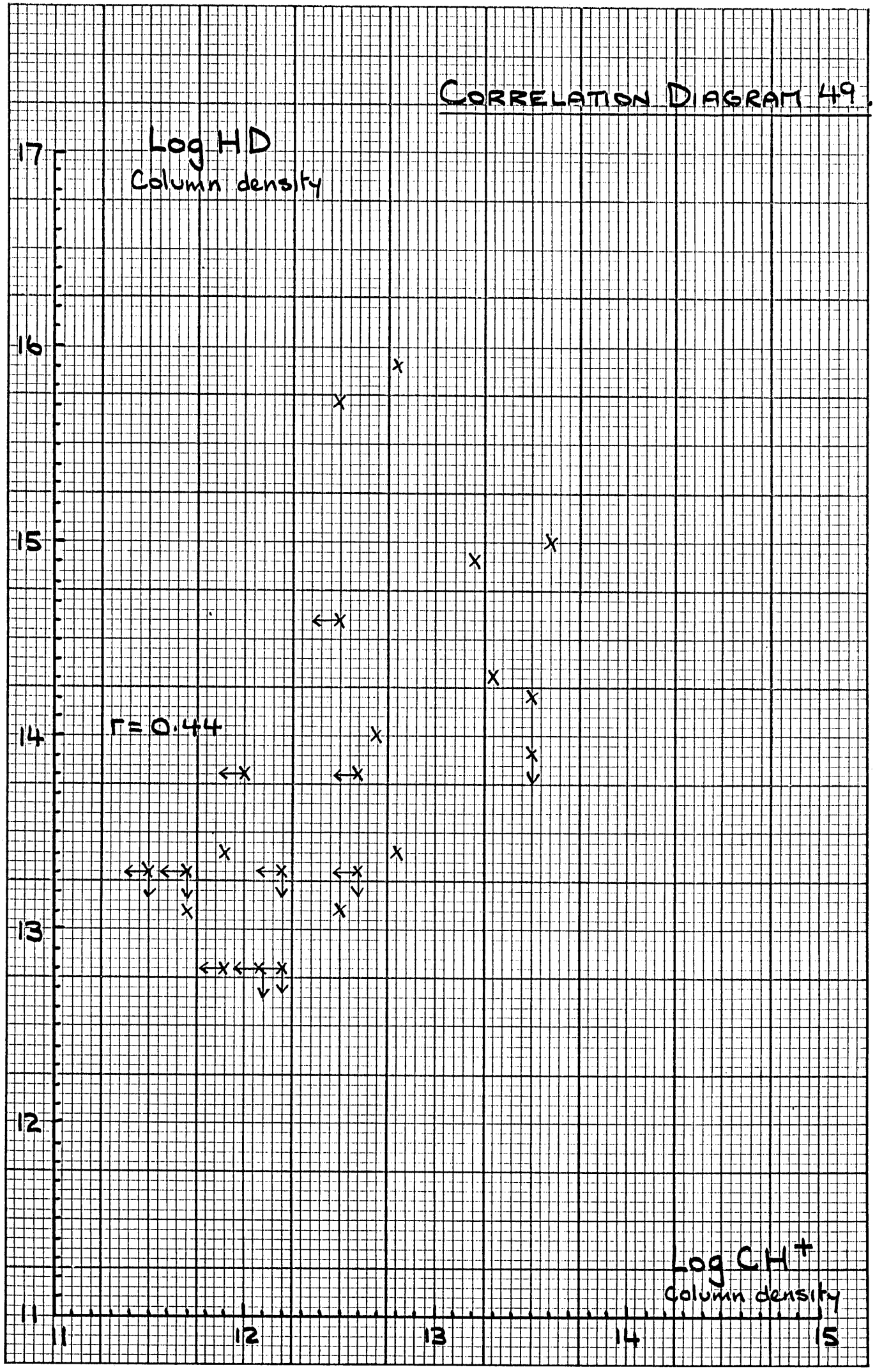
CORRELATION DIAGRAM 49.
Log HD
Column density
17
16
15
14
13
12
11
r = 0.44
Log CH+
Column density
11
12
13
14
15

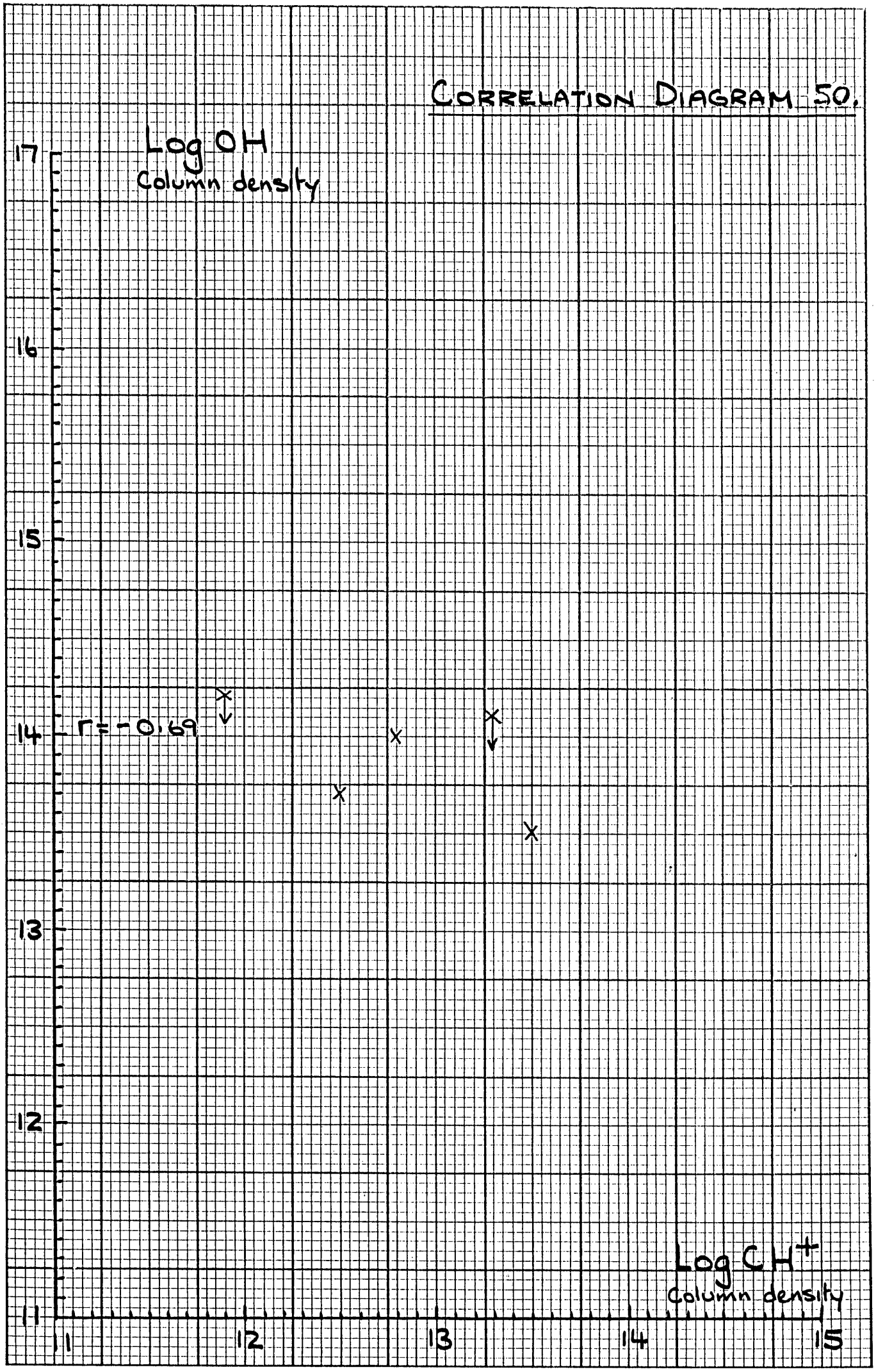
CORRELATION DIAGRAM 50.
Log OH
Column density
17
16
15
14
13
12
11
r = -0.69
Log C_{H^+}
Column density
11
12
13
14
15

3. CORRELATIONS BETWEEN MOLECULES

3. CORRELATIONS BETWEEN MOLECULES

3.1 THE SAMPLE CORRELATION COEFFICIENT

The purpose of this evaluation is to determine how two variables x and y are related linearly. In this case the variables are the logarithms of the various molecular column densities given in the tables. A correlation diagram in which x is plotted against y, for example Log N(CH) vs Log $N(CH^+)$, gives an idea of how the two variables are related. However it is not always clear from such diagrams if there is a linear relationship or not. A numerical measure of the linear relationship between x and y is given by the Sample Correlation Coefficient r. This is given by

$$r = \frac{\Sigma(x-\bar{x})(y-\bar{y})}{\sqrt{[\Sigma(x-\bar{x})^2][\Sigma(y-\bar{y})^2]}} \qquad (3.1)$$

where $\bar{x}$ and $\bar{y}$ are the mean of x and y respectively.

or we can write,

$$r = m\frac{\sigma_x}{\sigma_y} \qquad (3.2)$$

where m = slope of the line of best fit.

σ_x = Standard deviation of x.

σ_y = Standard deviation of y.

The sample correlation coefficient is an estimate of a theoretical quantity known as the population correlation coefficient ρ. The value of ρ, and r, is always between -1 and +1. A value of r equal to -1 indicates a perfect linear relationship between x and y, with the value of y decreasing as the value of x increases. A value of r equal to +1 also indicates a perfect linear relationship between x and y, but one in which the value of y increases as the value of x increases. If there is no linear relationship between x and y then r will have a value near to zero.

Sample correlation coefficients have been calculated for the eight molecules positively detected, atomic hydrogen and the total hydrogen column density N(H TOTAL) = $N(H) + 2N(H_2)$. These are

given in table 30, along with the number of pairs of points used to derive each correlation coefficient. Unless stated otherwise optical, UV and radio results have been used. (Although observations at optical and UV wavelengths have been given preference to radio observations when available). This is in order to keep the number of points as large as possible. Observations of molecules that are clearly in error, the radio results for CH toward 22 Sco and λ Sco and the Copernicus UV result for CO toward ι Ori, have been culled for the purpose of calculating the correlation coefficients. These points are clearly marked on the correlation diagrams. The other radio measurements for CH, CO and CN, appear not to be in error, most of the emission comes from molecules that lie in the line of sight to the star, and have therefore been included.

TABLE 30

NUMBERS OF AVAILABLE PAIRS AND SAMPLE CORRELATION COEFFICIENTS FOR MOLECULES

Column Density, Log N(X)

Column Density, Log N(X)	CH	CH^+	CO	CN	C_2	H_2	H	Htot	HD	OH
CH		$^{\Delta}$0.64	0.92	0.86	0.72	*0.88	$^{\Delta}$-0.05	$^{\Delta}$0.44	0.74	-0.98
CH^+	51		0.73	0.53	0.20	0.65	0.43	0.63	0.44	-0.69
CO	25	25		0.80	0.88	†0.86	†0.61	†0.71	0.61	-1.00
CN	19	18	16		0.83	0.86	-0.21	0.15	0.45	-0.73
C_2	10	9	6	10		-0.31	-0.24	-0.51	-0.95	-0.72
H_2	33	37	25	9	8		0.80	0.85	0.66	-0.59
H	35	41	33	11	7	78		0.98	0.21	1.00
Htot	31	33	24	8	6	78	78		0.50	0.30
HD	8	11	9	4	3	16	15	15		0.90
OH	3	3	2	3	3	3	3	3	3	

NOTES:

$^{\Delta}$ The point for 22Sco has been culled.

* The points for 22 Sco and λ Sco have been culled.

† The point for i Ori has been culled.

3.2 CORRELATIONS WITH THE AVERAGE TOTAL HYDROGEN DENSITY $\langle n_H \rangle$

Studies of the interstellar medium along lines of sight to several stars have shown some correlations between atomic column densities and the average total hydrogen density $\langle n_H \rangle$ where,

$$\langle n_H \rangle = \frac{N(H) + 2N(H_2)}{d} = \frac{N(H\ TOTAL)}{d} \qquad (3.3)$$

$N(H) + 2N(H_2)$ is the total hydrogen column density N(HTOTAL) and d is the stellar distance.

Jenkins, Savage and Spitzer 1986 (431) have found marked anti-correlations of A(X) with Log $\langle n_H \rangle$ for Fe, P, Cl , Mn and Mg, where A(X) is the logarithmic abundance ratio

$$A(X) = \text{Log}\left[\frac{N(X)}{N(HTOTAL)}\right] = \text{Log } N(X) - \text{Log } N(HTOTAL) \qquad (3.4)$$

i.e. the abundance of element X relative to the total hydrogen column density. N(X) is the column density of element X, (table 31). See also the work of Snow 1975 (513), Harris & Bromage 1984 (509), 1984 (542) on Cl , Savage & Bohlin 1979 (510) on Fe, Murray et al 1984 (512) on Mg, Keenan et al 1986 (522) on N, O and Mg, and Harris et al 1984 (543).

The results are interpreted in terms of a recent idealised theory by Spitzer 1985 (365). Spitzer's theory gives a relationship between $\langle n_H \rangle$ and the types of cloud that provide most of the material along a line of sight. The gas in the interstellar medium is represented by three constituents, a warm relatively uniform low density gas and two types of cold clouds. The diffuse clouds, and the larger highly clumped, more heavily obscuring clouds. For lines of sight where $\langle n_H \rangle < 0.2 cm^{-3}$ the warm gas predominates. For large values, $\langle n_H \rangle > 3.0 cm^{-3}$, the darker clouds contribute most of the HI gas, and for intermediate values of $\langle n_H \rangle = 0.7 cm^{-3}$, the contribution from the diffuse clouds tends to dominate.

TABLE 31

CORRELATIONS OF ATOMIC ABUNDANCES WITH THE AVERAGE TOTAL HYDROGEN DENSITY $\langle n_H \rangle$

	LOG $\langle n_H \rangle$
A(Fe)	-0.81 (40)
A(P)	-0.64 (44)
A(Cl)	-0.50 (30)
A(Mn)	-0.52 (57)
A(Mg)	-0.62 (58)

Sample correlation coefficients from Jenkins, Savage and Spitzer 1986 (431).

Numbers of available pairs are given in brackets.

With increasing $\langle n_H \rangle$ the relative contributions of the three types of cloud to the total hydrogen column density along a line of sight changes. Any correlations of physical properties with $\langle n_H \rangle$ may therefore be attributed in part to changes in cloud type. The observational evidence is consistent with the assumption that for each element the depletion (given by the logarithmic depletion defined as D(X) = A(X) - A(X) cosmic, where A(X) cosmic is the cosmic logarithmic abundance ratio) has one value in the warm neutral gas and a different enhanced value in the cold gas which includes both diffuse clouds and the more heavily obscuring clouds. Many workers have found a clear increase of D with increasing $\langle n_H \rangle$ See Spitzer 1985 (365) and references therein.

An attempt to correlate molecular abundances with Log $\langle n_H \rangle$ has been made. Sample correlation coefficients have been calculated for Log N(X) against Log $\langle n_H \rangle$, where X is CH, CH^+, CO, CN or C_2.

The results are given in table 32.

3.3 THE GRADIENT OF THE SLOPE OF A CORRELATION DIAGRAM

The correlation diagrams are log-log plots of two variables x and y, in this case molecular column densities. If the log-log plot is a straight line then the two variables follow an equation of the form,

$$\text{Log } y = m \text{ Log } x + \text{Log } A, \quad \therefore \quad y \propto x^m \tag{3.5}$$

where A = Constant

m = Gradient of the slope of the points on the log-log plot.

A straight line with a 45° slope has a gradient of 1, and equation 3.5 above reduces to

$$y \propto x \tag{3.6}$$

There is a direct proportionality between x and y.

TABLE 32

CORRELATIONS OF MOLECULAR ABUNDANCES WITH THE AVERAGE TOTAL HYDROGEN DENSITY $\langle n_H \rangle$

	LOG $\langle n_H \rangle$
Log N(CH)	0.39 (20) *
Log N(CH^+)	0.36 (25)
Log N(CO)	0.51 (19) †
Log N(CN)	-0.56 (8)
Log N(C_2)	-0.24 (6)

Numbers of available pairs are given in brackets.

* Point for 22Sco culled.

† Point for i Ori culled.

In this case the two molecules are closely related, since they have the same ratio in different clouds, independent of properties such as density or cloud size. Their chemistry must be simply related. If the log log plot has a slope with a gradient not equal to 1 then the ratio is different from one cloud to another, the chemistry relating the two molecules depends on cloud properties such as density or size.

Also, Federman 1987 (406) notes that molecules formed after several steps of gas phase reactions involving neutral molecules are expected to vary more and more steeply with the H_2 density in diffuse clouds, as the number of intermediate neutral species increases. With each stage of the chemistry for neutral molecules another factor of density and optical depth enter into the chemical rate equation. CH is the first neutral molecule formed in a reaction sequence starting with $C^+ + H_2 \longrightarrow CH_2^+ + h\nu$ and is called a first stage molecule. However the reaction scheme leading to CN also involves CH and C_2. CN is therefore a third stage molecule.

3.4 CONCLUSIONS

1. CORRELATIONS WITH HYDROGEN

1.1 NEUTRAL MOLECULES

CH vs H_2

There is good correlation between CH and H_2. In calculating the CH vs H_2 correlation coefficient r = 0.88, two results have been omitted. These are the CH measurements for 22 Sco and λ Sco. Both stars appear to have exceptionally high CH column densities in their lines of sight for the amount of H_2 present. The CH column densities are derived from the measurement of CH emission at radio wavelengths and appear to include material that lies behind the star. Including

these two results gives rise to an extremely low and misleading value for r. The points are clearly marked on correlation diagram 1 by a circle in place of a cross. The correlation coefficient r = 0.88, agrees with the results of Danks et al 1984 (152), r = 0.8 and those of Federman 1982 (30), r = 0.9.

The log-log plot of N(CH) vs $N(H_2)$, (correlation diagram 1) has a slope with a gradient of 0.81

$$\text{Log } N(H_2) = 0.81 \text{ Log } N(CH) + \text{Log } A,$$

$$N(H_2)^{1.2} \propto N(CH)$$

This shows that N(CH) varies linearly with $N(H_2)$ and that the ratio of CH to H_2 does not change with cloud density or size.

The CH molecule is the first neutral carbon molecule formed in the chemical scheme that begins with the reaction of molecular hydrogen and ionised atomic carbon. CH is a first stage molecule. The reaction network describing the formation of CH is given below,

$$C^+ + H_2 \longrightarrow CH_2^+ + h\nu \qquad (2)$$

followed by

$$CH_2^+ + H_2 \longrightarrow CH_3^+ + H \qquad (3)$$

Dissociative recombination of the CH_2^+ and CH_3^+ ions gives CH.

$$CH_2^+ + e^- \longrightarrow CH + H \qquad (4)$$

$$CH_3^+ + e^- \longrightarrow CH + H_2 \qquad (5)$$

CH is destroyed by photodissociation and reaction with C^+. The equilibrium density of this scheme depends on the local cloud density and the ultraviolet radiation field. The reaction network predicts that $N(CH) \propto N(H_2)$.

CH vs H, Htotal & $\langle n_H \rangle$

The correlation of CH with H and Htotal (correlation diagrams 2 and 3) is poor (in agreement with Federman 1982 (30)), the

CH column density is independent of the atomic hydrogen column density. This lends support to the idea that CH is produced in regions where molecular hydrogen is present and not in HI regions. The correlation coefficient for CH vs Htotal tends to be an average of the values for CH vs H_2 and CH vs H. The correlation diagram for CH vs $\langle n_H \rangle$ (number 4) also shows that the CH column density is virtually independent of the average total hydrogen density.

CO vs H_2

Correlation of CO with H_2 is also good, r = 0.86. To calculate this result one point, that for i Ori, has been omitted. This point has been discussed in detail by Federman 1980 (27) and is now thought to be in error. (Somerville 1986 (549)). New IUE observations of the line of sight toward i Ori have been made, but have not been published.

The log-log plot of N(CO) vs N(H_2), (correlation diagram 5) has a slope with a gradient of 0.45 The CO column density increases with the second power of the H_2 column density.

$$\text{Log } N(H_2) = 0.45 \text{ Log } N(CO) + \text{Log } A.$$

$$N(H_2)^{2.2} \propto N(CO)$$

This result agrees with Federman et al 1980 (27) who examined the relationship between CO and H_2. Since the relative abundance of CO increases rapidly with the amount of material in the line of sight the abundance of CO must be greater in denser and more extensive clouds. The quadratic variation of CO with H_2 indicates that CO is a second stage molecule.

CO is formed via reactions involving the neutral molecule OH. The important route for the synthesis of CO is a two step process known as oxygen charge exchange. The name refers

to the reaction producing the O^+ ion.

$$H^+ + O \longrightarrow H + O^+ \qquad (6)$$

OH is then formed from several reactions including

$$O^+ + H_2 \longrightarrow OH^+ + H \qquad (7)$$

$$OH^+ + H + e^- \longrightarrow OH + H \qquad (8)$$

OH then reacts with C^+ to form CO.

$$C^+ + OH \longrightarrow CO^+ + H \qquad (9)$$

$$CO^+ + H \longrightarrow CO + H^+ \qquad (10)$$

Alternatively

$$CO^+ + H_2 \longrightarrow HCO^+ + H \qquad (11)$$

$$HCO^+ + e^- \longrightarrow CO + H \qquad (12)$$

CO vs H, Htotal & $\langle n_H \rangle$

CO correlates fairly well with atomic hydrogen, r = 0.61 (correlation diagram 6). This may be due to its ability to withstand photodissociation in HI regions. Correlation with Htotal (correlation diagram 7) mirrors the H result. The CO concentration appears to show some increase with $\langle n_H \rangle$ (correlation diagram 8).

CN vs H_2

CN correlates very well with H_2, r = 0.86, despite the few points available. The abundance of CN is very dependent on the ultraviolet optical depth of the cloud since photodissociation is a major destruction mechanism for CN. The result is that CN is associated with the darker molecular hydrogen clouds. The slope of the points on the log-log plot of N(CN) vs $N(H_2)$ (correlation diagram 9) has a gradient of 0.39. The CN column density increases with the third power of the H_2 column density.

$$\text{Log } N(H_2) = 0.39 \text{ Log } N(CN) + \text{Log } A$$

$$N(H_2)^{2.6} \propto N(CN).$$

The steep dependence of CN on H_2 contrasts with the case of CH vs H_2 which shows a linear relationship. Molecules formed after several steps of gas phase reactions involving neutral molecules are expected to vary more steeply with the H_2 density in diffuse clouds.

CN is a third stage molecule.

The initiating steps for the formation of CN are the ion molecule reactions,

$$C^+ + NH \longrightarrow CN^+ + H \qquad (13)$$

$$CH^+ + N \longrightarrow CN^+ + H \qquad (14)$$

and the neutral neutral reactions

$$CH + N \longrightarrow CN + H \qquad (15)$$

$$C_2 + N \longrightarrow CN + C \qquad (16)$$

The important reaction is 16. To produce the steep dependence of CN on H_2, this must dominate as described by Federman 1984 (283). If reaction 15 dominated, the relationship would be $N(H_2)^2 \propto N(CN)$, which is not the case.

CN is formed by the sequence

$$CH \longrightarrow C_2 \longrightarrow CN \qquad (17)$$

The CH and C_2 molecules are produced from C^+ and H_2 through a series of ion molecule reactions. Photodissociation of CH, C_2 and CN results in a strong dependence of N(CN) on gas density and optical depth, leading to rapid variation between CN and H_2.

CN vs H, Htotal & $\langle n_H \rangle$

CN correlates poorly with H and Htotal (correlation diagrams 10 and 11) in agreement with Federman 1984 (283). The CN column density is independent of the atomic hydrogen column density and the average total hydrogen density $\langle n_H \rangle$ (correlation diagram 12).

C_2 vs H_2

There are very few C_2 vs H_2 points, which makes the results susceptible to error. Theory suggests a quadratic variation of C_2 with H_2, (correlation diagram 13)

$$N(H_2)^2 \propto N(C_2)$$

C_2 vs H, Htotal & $\langle n_H \rangle$

Too few points available to make any firm conclusions. (correlation diagrams 14, 15 and 16).

HD vs H_2

Correlation between H_2 and HD is not as good as might be expected, r = 0.66. However the slope of the points on the log-log plot of N(HD) vs $N(H_2)$ has a gradient of 0.86, (correlation diagram 17)

$$\text{Log } N(H_2) = 0.86 \text{ Log } N(HD) + \text{Log } A$$

$$N(H_2)^{1.1} \propto N(HD)$$

The linear relationship between H_2 and HD means that the chemistry is independent of cloud conditions. HD is produced by the gas phase reaction.

$$D^+ + H_2 \longrightarrow HD + H^+ \qquad (18)$$

In diffuse clouds HD is destroyed by photodissociation. Since the HD abundance is always low, self shielding of HD never occurs as it does for H_2 so that reaction 18 must be fast to account for the observed abundance of HD.

HD vs H and Htotal

The plots of HD vs H, and HD vs Htotal, show HD to be independent of the atomic and total hydrogen column density. (correlation diagrams 18 and 19).

OH vs H_2

There are too few points for OH to determine any statistically significant correlation between OH and H_2 (correlation diagram 20)

. . .

OH vs H, & Htotal

Too few points. (correlation diagrams 21 and 22).

1.2 MOLECULAR IONS

CH^+ vs H_2

Correlation of CH^+ with H_2 is fair, r = 0.65. This is better than the result r = 0.30, given by Federman 1982 (30). The slope of the points on the log-log plot of $N(CH^+)$ vs $N(H_2)$ has a gradient of 0.73, (correlation diagram 23).

$$\text{Log } N(H_2) = 0.73 \text{ Log } N(CH^+) + \text{Log A.}$$

$$N(H_2)^{1.4} \propto N(CH^+)$$

This indicates an almost linear variation of CH^+ with H_2. H_2 is only a minor constituent of the shocked gas where CH^+ is formed, and it may be that the CH^+ molecules lie in the outer lower density portion of the cloud when observed in the same line of sight as H_2. Molecular hydrogen is necessary for the production of CH^+ in shocks through the endothermic reaction

$$C^+ + H_2 \longrightarrow CH^+ + H \qquad (19)$$

CH^+ is destroyed by slow photochemical reactions and ion molecule reactions. CH^+ has a large cross section with H_2, H and electrons, and is destroyed rapidly in all environments. The level of CH^+ in diffuse clouds can only be achieved through a fast production rate for reaction 19 which requires CH^+ to be produced in the hot conditions behind shock fronts. Models based on equilibrium chemistry in cool HI and H_2 clouds give CH^+ abundances 100X less than those actually observed.

Lambert and Danks 1986 (405) have shown that $N(CH^+)$ correlates strongly with the column density of the upper rotational (excited) levels of H_2 This correlation is strong evidence that CH^+ is formed in the hot gas behind a shock front.

H_2 is formed from atomic hydrogen gas as the shock passes through the interstellar medium.

CH^+ vs H, Htotal & $\langle n_H \rangle$

Correlation of CH^+ with H is poorer than it is with H_2 (correlation diagram 24) indicating that H_2 is more important for the formation of CH^+. This agrees with Federman 1982 (30). Correlation with the total hydrogen column density is fair (correlation diagram 25). The CH^+ column density is independent of the average total hydrogen density. (correlation diagram 26).

1.3 ATOMIC HYDROGEN

H vs H_2

Molecular hydrogen is formed on interstellar grains by a surface reaction between hydrogen atoms. There is good correlation between H and H_2, r = 0.80. The correlation diagram for H vs H_2 (number 27) shows two distinct groupings that arise from a discontinuity in the H_2 column density. At this point the H_2 column density increases rapidly. In regions that are not opaque to ultraviolet radiation the dominant destruction process is photodissociation. However molecular hydrogen is self shielding so that the molecules in the cloud interior are protected from the ultraviolet radiation and the H_2 column density increases rapidly. The lower H_2 results are representative of the surfaces of clouds, whose denser interiors contain much more molecular hydrogen giving rise to the larger H_2 column densities in the second grouping.

H total vs H_2

Correlation between total hydrogen and H_2 is good, r = 0.85. The correlation diagram (number 28) shows the two distinct groupings found for the H vs H_2 diagram. This is to be

expected since the major part of the total hydrogen column density in diffuse clouds is due to atomic hydrogen.

H vs Htotal

There is almost perfect correlation between H and Htotal, r = 0.98. This is because the total hydrogen column density in diffuse clouds consists mainly of atomic hydrogen (correlation diagram 29).

2. CORRELATIONS BETWEEN CARBON BEARING MOLECULES

2.1. NEUTRAL MOLECULES

CH vs CO

The correlation between CH and CO is very good, r = 0.92. This is better than the result given by Dickman et al 1983 (151) who give r = 0.33 but using fewer points. The slope of the log-log plot of N(CH) vs N(CO) has a gradient of 2.41 (correlation diagram 30).

$$\text{Log } N(CO) = 2.41 \text{ Log } N(CH) + \text{Log } A.$$

$$N(CO) \propto N(CH)^{2.4}$$

CH and CO are clearly related but their chemistry depends on cloud properties such as density. The ratio $^{CO}/_{CH}$ will increase in denser and more extensive clouds. The ζ Oph cloud is an example of a typical diffuse cloud with a density $n = 10^2$ to 10^3 cm^{-3} where $n = n(H) + 2n(H_2)$, (Cohen 1973 (13) estimates a density of 10^3 cm^{-3} for the ζ Oph cloud). In clouds whose density is greater than ζ Oph the ratio $^{CO}/_{CH}$ should be larger. Theoretical plot 1 based on the steady state model taken from Mitchell Ginsburg & Kuntz 1978 (215) and the time dependent model of Prasad & Huntress 1980 (551) which gives the molecular abundances at 10^7 years, predicts this behaviour. However the actual CO/CH abundances toward ζ Oph and the denser ρ Oph A cloud are closest to the values predicted by Prasad & Huntress.

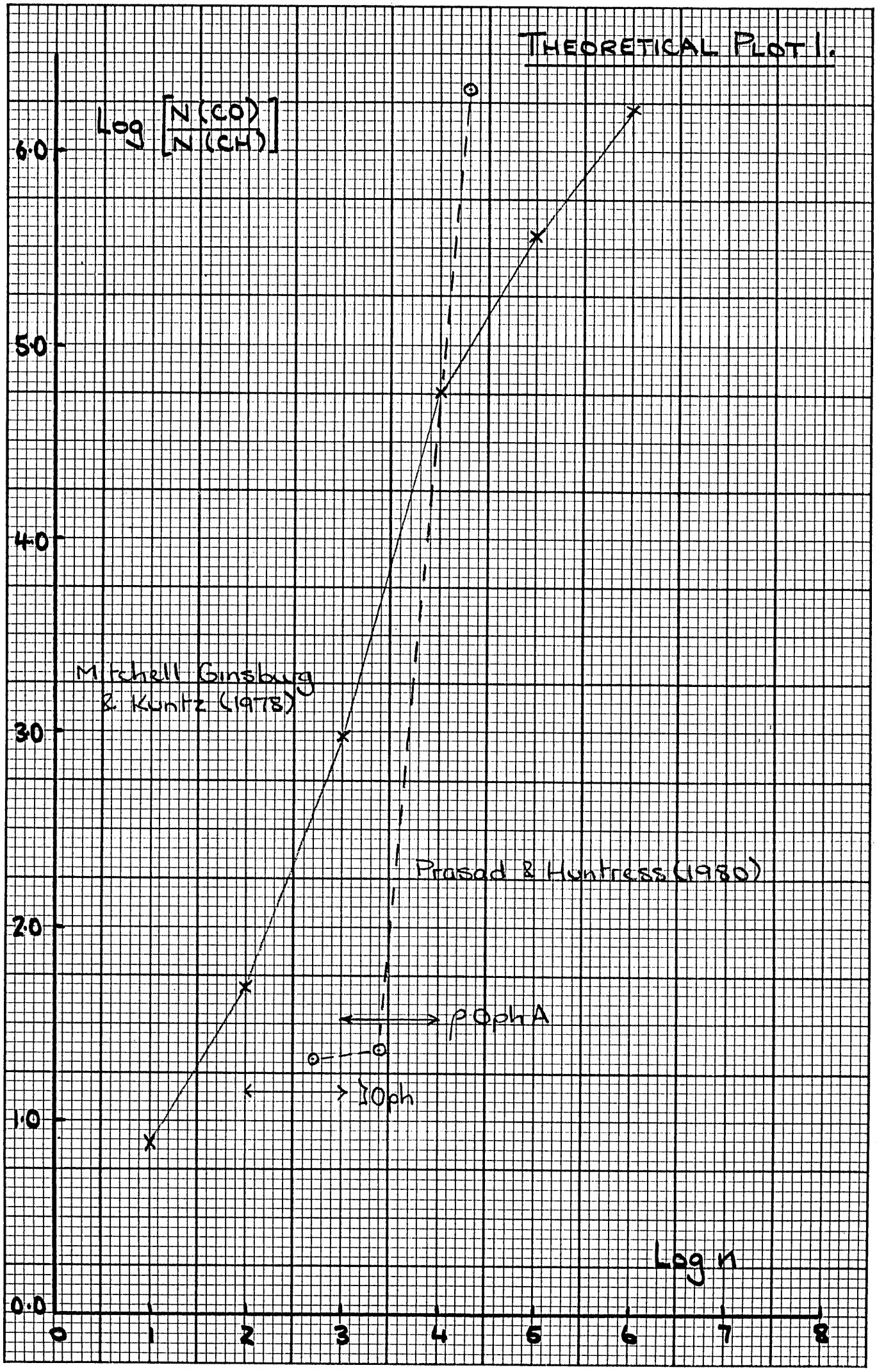
THEORETICAL PLOT I.
Log [N(CO) / N(CH)]
6·0
5·0
4·0
3·0
2·0
1·0
0·0
0
1
2
3
4
5
6
7
8
Log n
Mitchell Ginsburg & Kuntz (1978)
Prasad & Huntress (1980)
ρ Oph A
10 pk

CH vs CN

Correlation between CH and CN is also good, r = 0.86. Dickman et al 1983 (151) give r = 0.54. The slope of the log-log plot of N(CH) vs N(CN) has a gradient of 1.56 (correlation diagram 31)

$$\text{Log } N(CN) = 1.56 \text{ Log } N(CH) + \text{Log } A$$

$$N(CN) \propto N(CH)^{1.6}$$

The ratio CN/CH should increase with cloud density. Theoretical plot 2 based on the steady state model of Mitchell, Ginsburg & Kuntz 1978 (215) and the time dependent model of Prasad & Huntress 1980 (551) predicts this behaviour; CN/CH increasing with density. The more diffuse cloud toward ζ Oph is well represented by the Mitchell Ginsburg & Kuntz model, whereas the denser cloud toward ρ Oph A is better represented by the Prasad & Huntress model. The time dependent chemical model may be more accurate because in dense clouds molecules have longer lifetimes and the model predicts densities at 10^7 years.

CH vs C_2

Correlation of CH with C_2 is good, r = 0.72. The slope of the log-log plot of N(CH) vs $N(C_2)$ has a gradient of 0.55 (correlation diagram 32)

$$\text{Log } N(C_2) = 0.55 \text{ Log } N(CH) + \text{Log } A$$

$$N(C_2) \propto N(CH)^{0.5}$$

This result indicates that the ratio C_2/CH should decrease with an increase in cloud density. Theoretical plot 3 based on the steady state model of Mitchell Ginsburg & Kuntz 1978 (215) and the time dependent model of Prasad & Huntress 1980 (551) shows a decrease in C_2/CH at densities greater than $n = 10^3$ to 10^4 cm^{-3}.

CN vs CO

Correlation of CN with CO is also good r = 0.80, in

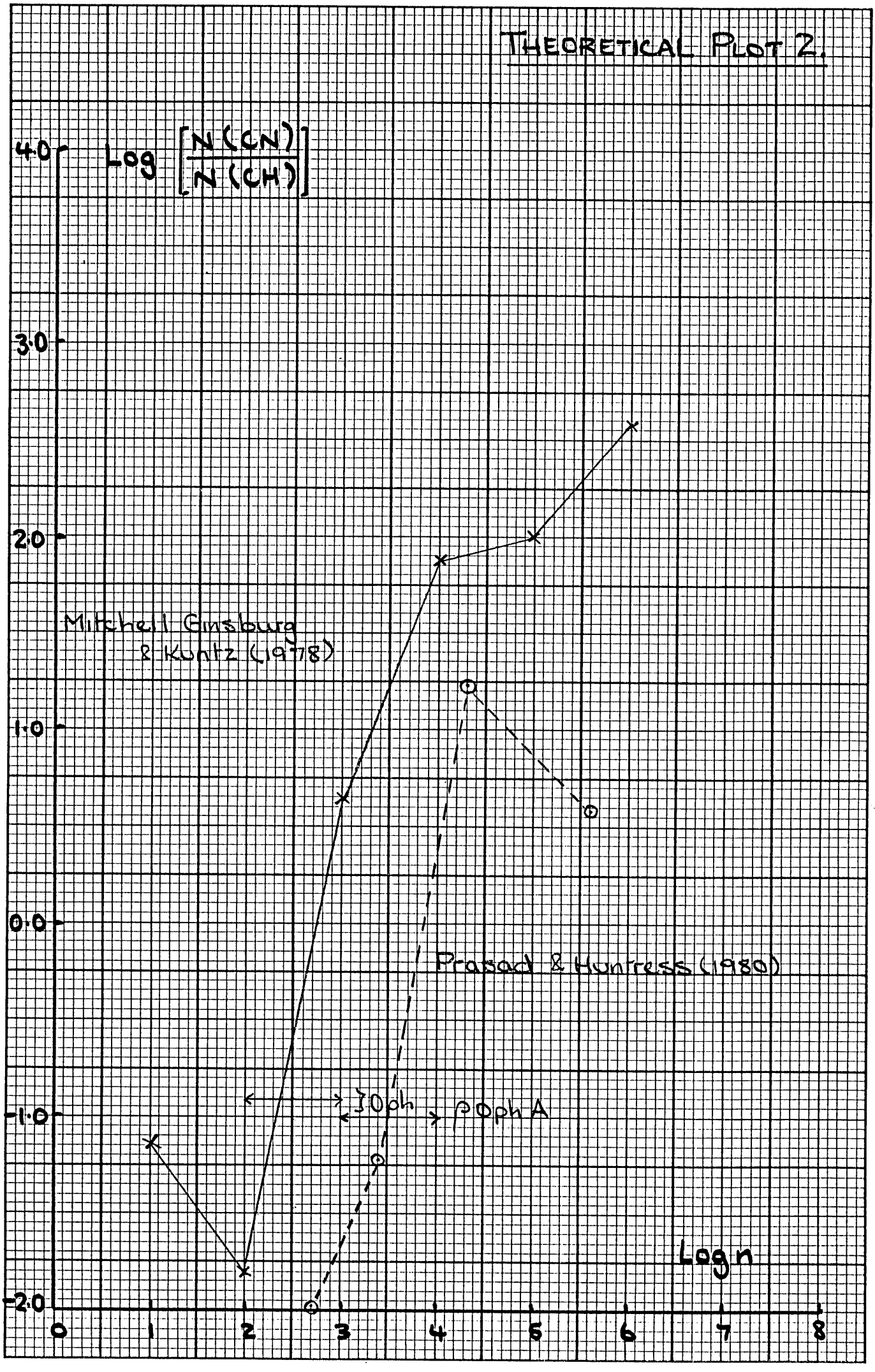
THEORETICAL PLOT 2.
Log [N(CN) / N(CH)]
4·0
3·0
2·0
1·0
0·0
-1·0
-2·0
0
1
2
3
4
5
6
7
8
Log n
Mitchell Ginsburg & Kuntz (1978)
Prasad & Huntress (1980)
30ph
POPH A

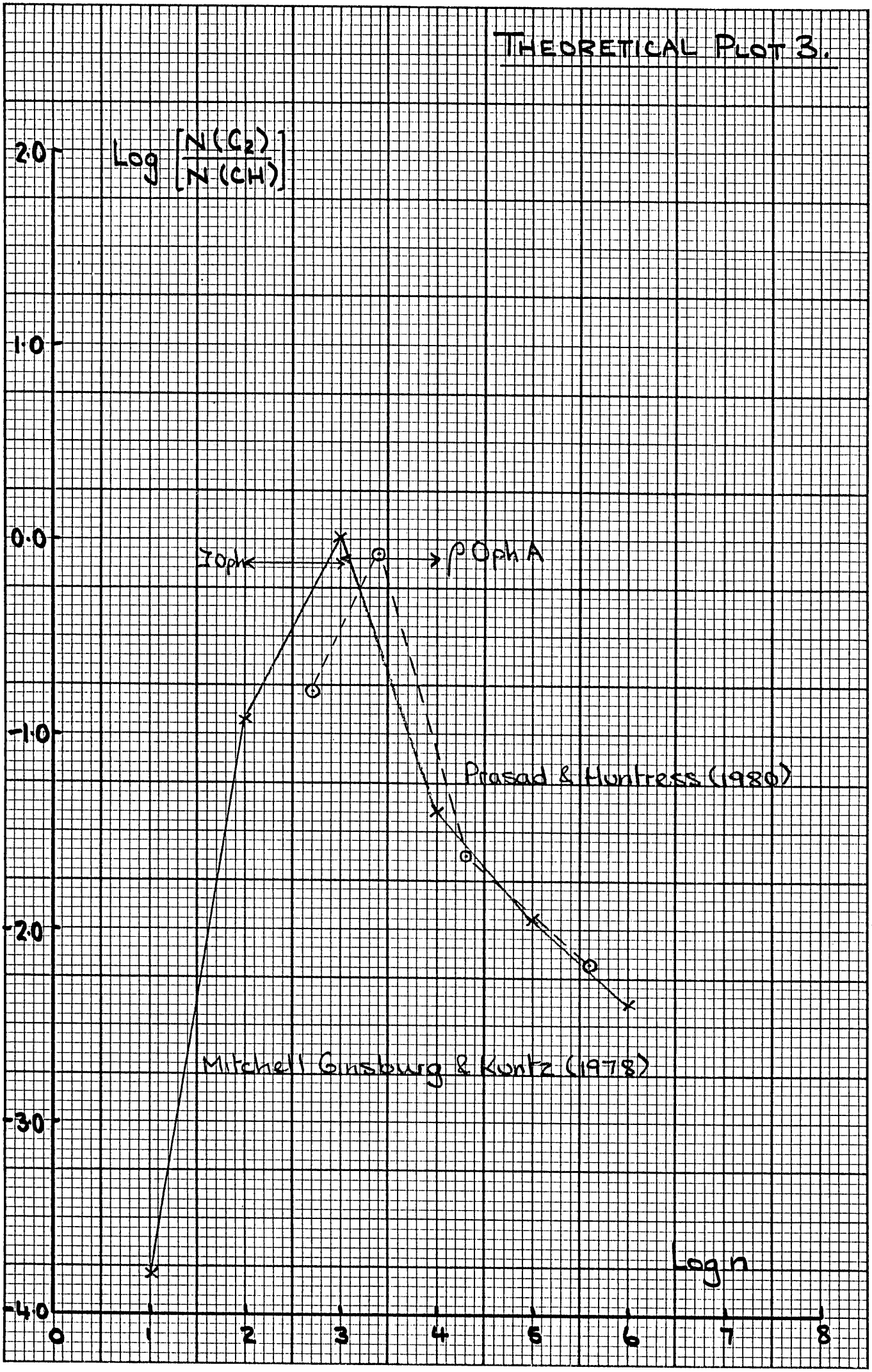
THEORETICAL PLOT 3.
Log [N(C2) / N(CH)]
2·0
1·0
0·0
-1·0
-2·0
-3·0
-4·0
0
1
2
3
4
5
6
7
8
Log n
ζ Oph
ρ Oph A
Prasad & Huntress (1980)
Mitchell Ginsburg & Kuntz (1978)

agreement with Dickman et al 1983 (151) who give r = 0.82. The slope of the log-log plot of N(CN) vs N(CO) has a gradient of 1.09 (correlation diagram 33)

$$\text{Log } N(CO) = 1.09 \text{ Log } N(CN) + \text{Log } A$$

$$N(CO) \propto N(CN)^{1.1}$$

The linear relationship between CO and CN indicates that their chemistry is independent of cloud density.

The CN/CO ratio is a sensitive parameter for testing theories of cloud chemistry. The ratio remaining constant over the range of column densities for diffuse clouds. The steady state gas phase chemical model of Mitchell Ginsburg & Kuntz 1978 (215) achieves an adequate match to the diffuse cloud data for the line of sight toward ζ Oph. It also matches the CN/CO ratio for the slightly denser clouds, with n = 10^3 to 10^4 cm^{-3}, toward ρ Oph A. An earlier CN/CO ratio for the line of sight toward ρ Oph based on the radio observations of Allen & Knapp 1978 (184) could only be represented by the model due to Prasad & Huntress 1980 (551). This model deviates sharply from that of Mitchell Ginsburg & Kuntz at densities $> 10^4$ cm^{-3}. (see theoretical plot 4).

C_2 vs CO

Correlation between C_2 and CO is good, r = 0.88. The slope of the log-log plot of $N(C_2)$ vs N(CO) has a gradient of 3.21 (correlation diagram 34).

$$\text{Log } N(CO) = 3.21 \text{ Log } N(C_2) + \text{Log } A$$

$$N(CO)^{0.3} \propto N(C_2)$$

The ratio C_2/CO will decrease with cloud density. This agrees with the predictions of the steady state model of Mitchell Ginsburg & Kuntz 1978 (215) and the time dependent model of Prasad & Huntress 1980 (551). Theoretical plot 5

THEORETICAL PLOT 4.

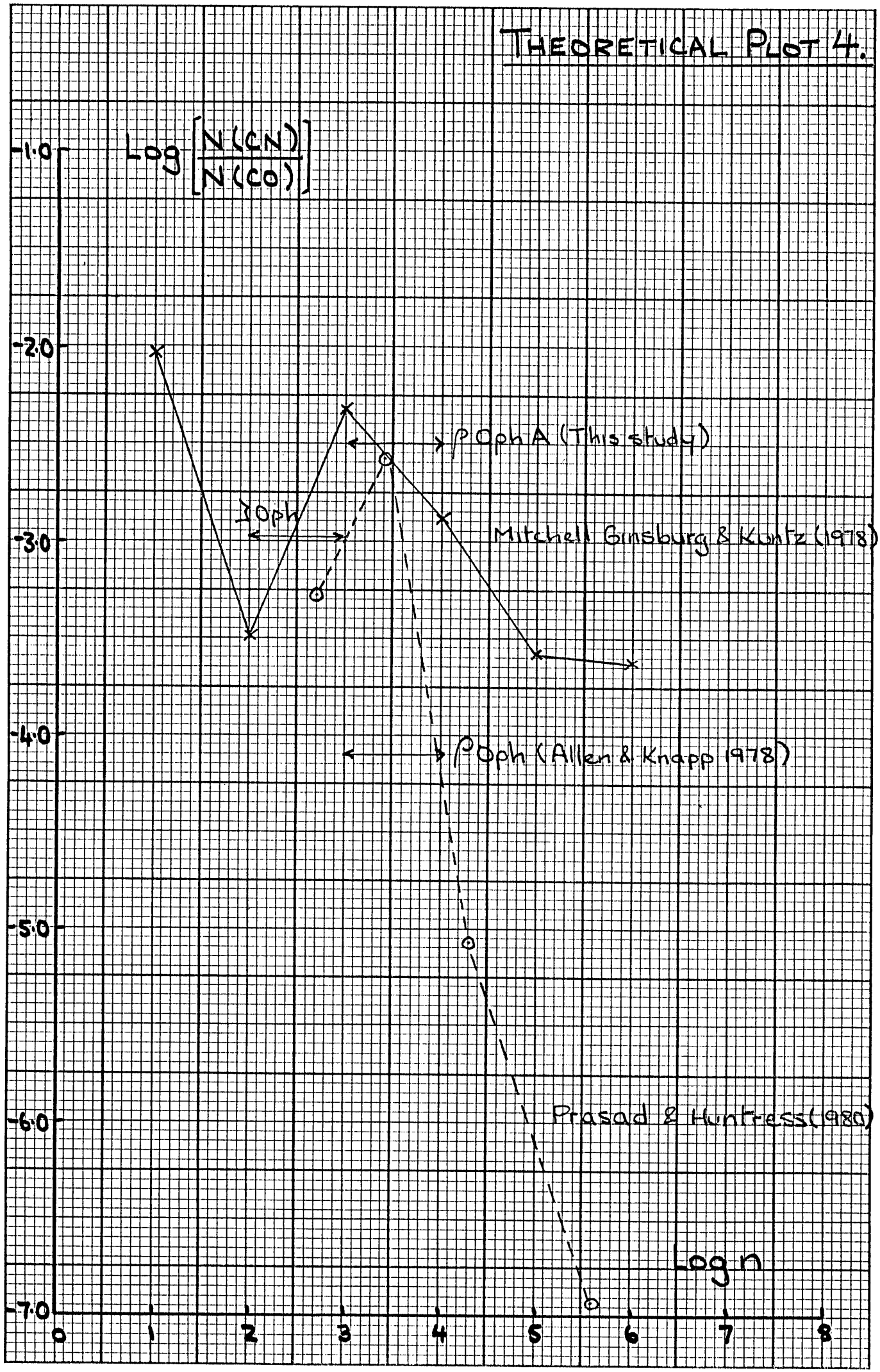

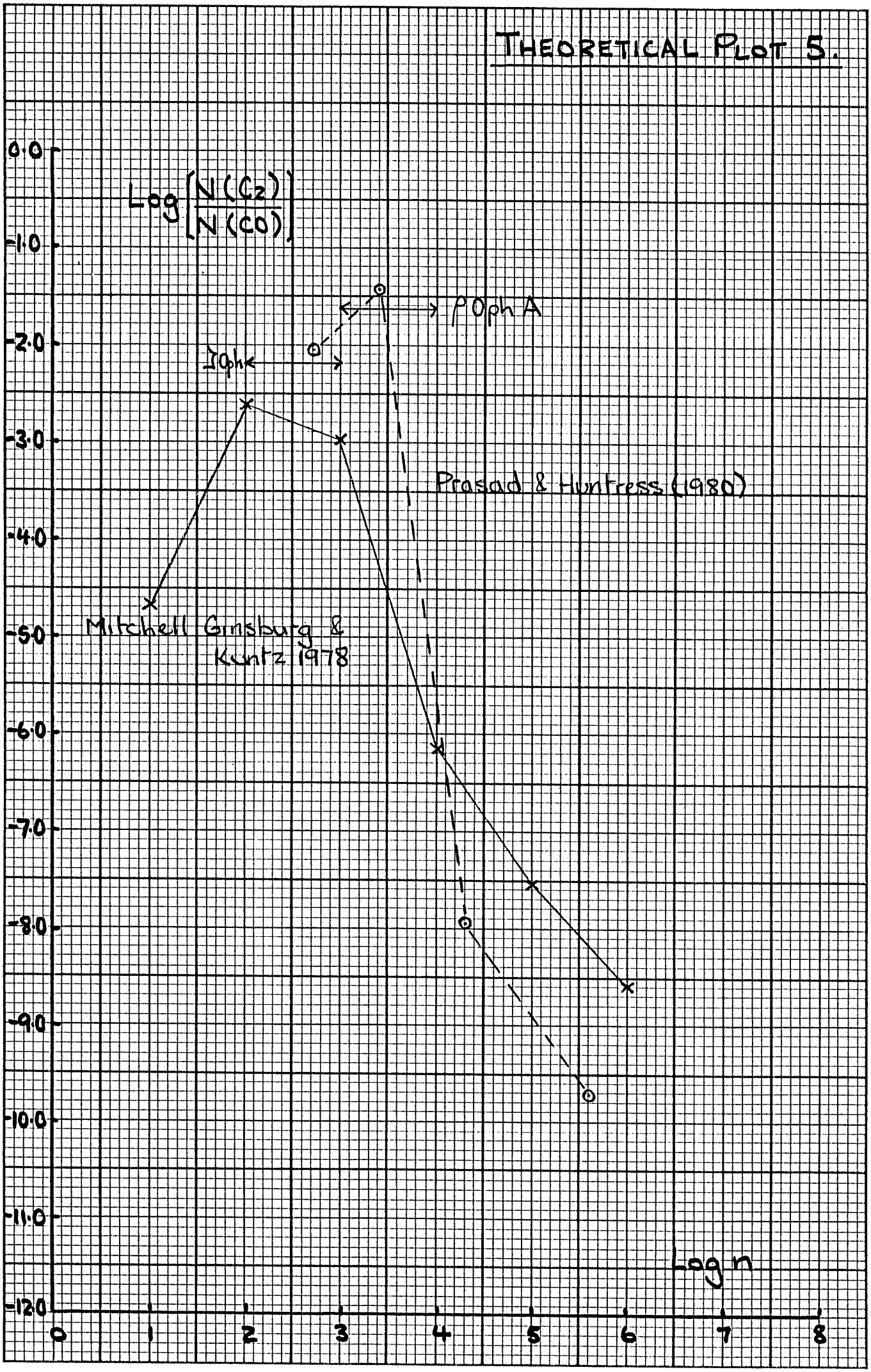
THEORETICAL PLOT 5.
Log [N(C2) / N(CO)]
0·0
-1·0
-2·0
-3·0
-4·0
-5·0
-6·0
-7·0
-8·0
-9·0
-10·0
-11·0
-12·0
0
1
2
3
4
5
6
7
8
Log n
ρ0ph A
I0ph
Prasad & Huntress (1980)
Mitchell Ginsburg & Kuntz 1978

shows a decrease in C_2/CO with density. The time dependent model shows a better fit to the C_2/CO ratio in the denser clouds toward ρ Oph A.

C_2 vs CN

C_2 and CN are also well correlated, r = 0.83. The log-log plot of $N(C_2)$ vs N(CN) (correlation diagram 35) has a slope with a gradient of 1.81.

$$\text{Log } N(CN) = 1.81 \text{ Log } N(C_2) + \text{Log A}$$

$$N(CN)^{0.5} \propto N(C_2)$$

The ratio C_2/CN should decrease with cloud density. Theoretical plot 6 shows this variation based on the steady state model of Mitchell Ginsburg & Kuntz 1978 (215) and the time dependent model of Prasad & Huntress 1980 (551).

C_2 and CN are related through the neutral neutral reaction

$$C_2 + N \longrightarrow CN + C \qquad (20)$$

which is important for the formation of CN (Federman et al 1984 (283)).

2.2. MOLECULAR IONS

CH^+ vs CH

In calculating the CH^+ vs CH correlation coefficient, the CH result for 22Sco has been omitted. Using the greater number of points available the correlation coefficient, r = 0.64 is much better than the result reported by Federman 1982 (30). He gives r = 0.20, and suggests that there is a random variation between CH^+ and CH (Dickman et al 1983 (151) give r = 0.28) The log-log plot of N(CH) vs $N(CH^+)$ shows considerable scatter consistent with this. The general tendency for the two molecules to increase together may be a general trend of all interstellar column densities to increase with distance which produces apparent correlations between totally unrelated species. The slope has a gradient of 0.53 (correlation

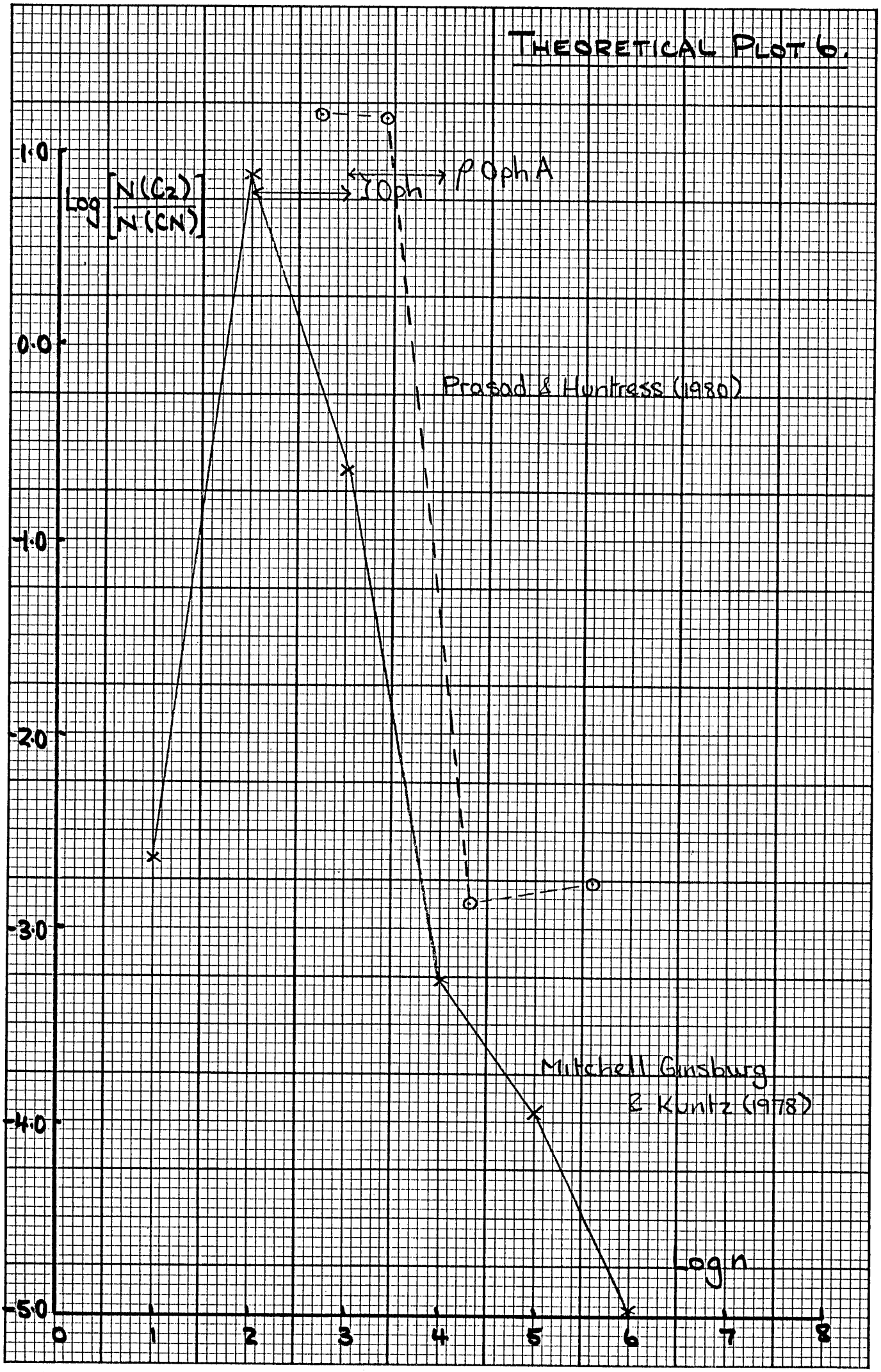
THEORETICAL PLOT 6.
1·0
0·0
-1·0
-2·0
-3·0
-4·0
-5·0
Log [N(C2)] / [N(CN)]
10ph
ρ 0ph A
Prasad & Huntress (1980)
Mitchell Ginsburg & Kuntz (1978)
Log n
0
1
2
3
4
5
6
7
8

diagram 36).

$$\text{Log } N(CH^+) = 0.53 \text{ Log } N(CH) + \text{Log } A$$

$$N(CH^+)^{1.9} \propto N(CH)$$

The steady state theory of Mitchell, Ginsburg & Kuntz 1978 (215) and the time dependent model of Prasad & Huntress 1980 (551) predict that the ratio CH^+/CH will decrease with cloud density, in line with the observational results. However the actual ratio of CH^+/CH toward ζ Oph is much greater than either theory predicts. This problem is overcome by the shock model of Mitchell & Watt 1985 (377). Theoretical plot 7 shows the CH^+/CH ratio in diffuse clouds after a 10Km s^{-1} shock has passed, with increasing initial cloud density. The plot shows a decrease in CH^+/CH with an increase in density but this time the calculated CH^+/CH abundance ratio toward ζ Oph is nearer to the observed value. This is evidence in favour of the theory that CH^+ is produced in the hotter conditions of a shock and not through steady state chemistry. However the fit to the theoretical model is still not good enough to be conclusive.

<u>CH^+ vs CO</u>

CH^+ correlates very well with CO, r = 0.73 (Dickman et al 1983 (151) give r = 0.21). According to the model of Mitchell and Deveau 1983 (161) CO increases in abundance in a shock (where CH^+ is produced) due to the reaction.

$$C^+ + OH \longrightarrow CO + H^+ \qquad (21)$$

which occurs in the hot post shock phase. It seems that the abundance of CH^+ is paralleled by the abundance of CO. CO owes its enhanced production in shocks to increases in the production of H_2O, HCO^+ and CN as well as OH. The slope of the log-log plot of $N(CH^+)$ vs N(CO) has a gradient of 1.69,

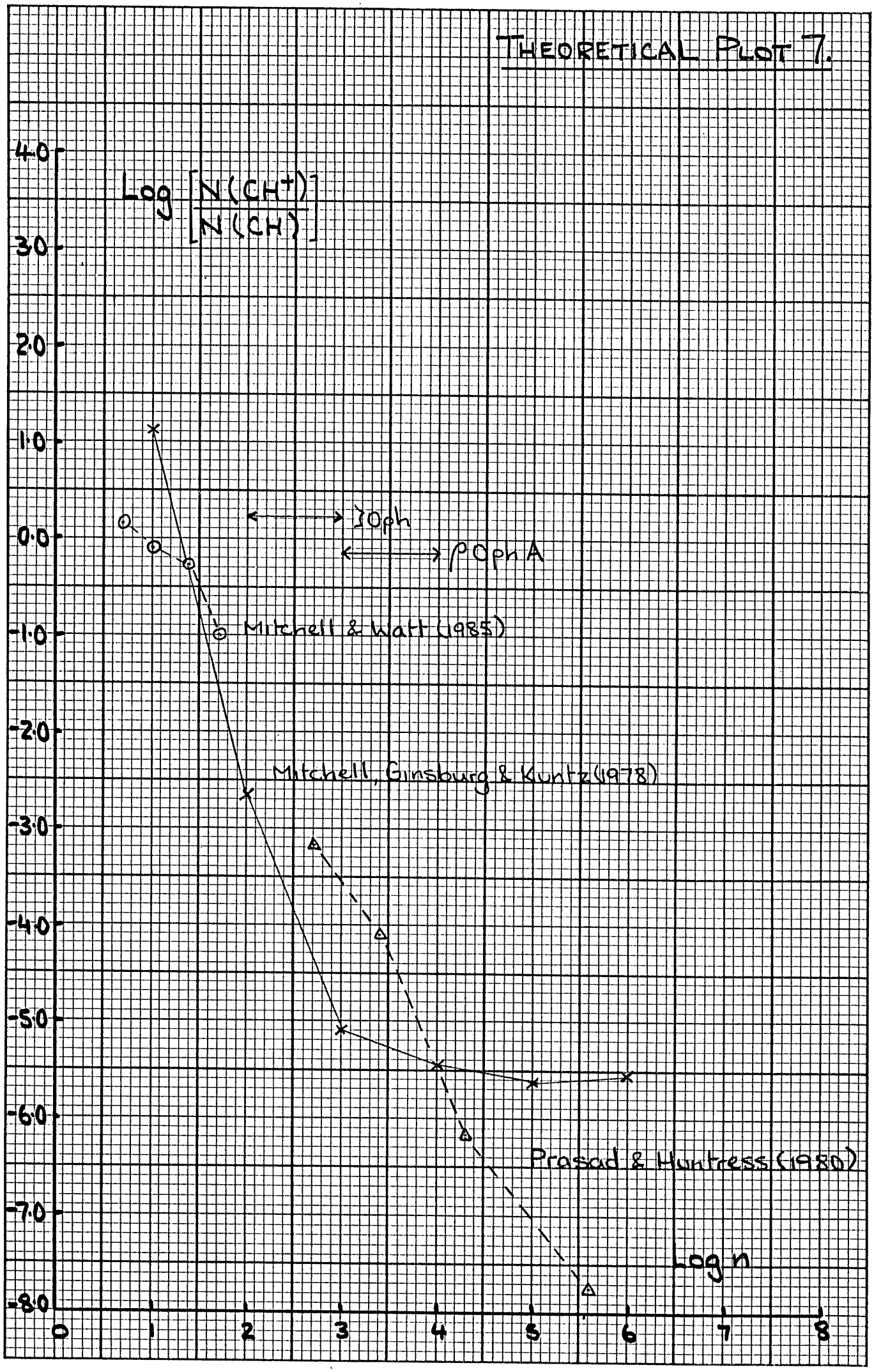
THEORETICAL PLOT 7.
$\log \left[\frac{N(CH^+)}{N(CH)}\right]$
4·0
3·0
2·0
1·0
0·0
-1·0
-2·0
-3·0
-4·0
-5·0
-6·0
-7·0
-8·0
0
1
2
3
4
5
6
7
8
log n
10ph
10phA
Mitchell & Watt (1985)
Mitchell, Ginsburg & Kuntz (1978)
Prasad & Huntress (1980)

(Correlation diagram 37).

$$\text{Log } N(CO) = 1.69 \text{ Log } N(CH^+) + \text{Log } A,$$

$$N(CO) \propto N(CH^+)^{1.7}$$

The theories of Mitchell, Ginsburg & Kuntz 1978 (215) and Prasad & Huntress 1980 (551) predict that the ratio CH^+/CO will decrease with density. However the actual abundance ratio CH^+/CO toward ζ Oph is much greater than predicted by the steady state and time dependent models. The shock model of Mitchell and Watt 1985 (377) also shows a decrease in CH^+/CO with cloud density, (Theoretical Plot 8), but the calculated ratio is nearer to the actual ratio for ζ Oph.

CH^+ vs CN

CN attains a high abundance behind the shock front, remaining high in shielded regions. The log-log plot of $N(CH^+)$ vs N(CN) has a slope with a gradient of 0.97. (Correlation diagram 38)

$$\text{Log } N(CN) = 0.97 \text{ Log } N(CH^+) + \text{Log } A$$

$$N(CN) \propto N(CH^+)^{1.0}$$

This suggests a linear relationship between the two molecules independent of cloud properties. However the correlation coefficient r = 0.53 does not support this (Dickman et al 1983 (151) give r = 0.68). The slope of 0.97 is probably indicative of a tendency for the column density of both molecules to increase with distance.

The steady state time dependent and shock models all predict a decrease in CH^+/CN with cloud density. However for the diffuse cloud toward ζ Oph the actual CH^+/CN ratio is much greater than the steady state model of Mitchell Ginsburg & Kuntz 1978 (215) and the time dependent model of Prasad & Huntress 1980 (551) predict. The observed value is nearer to that predicted by the shock model of Mitchell & Watt 1985 (377), (theoretical plot 9).

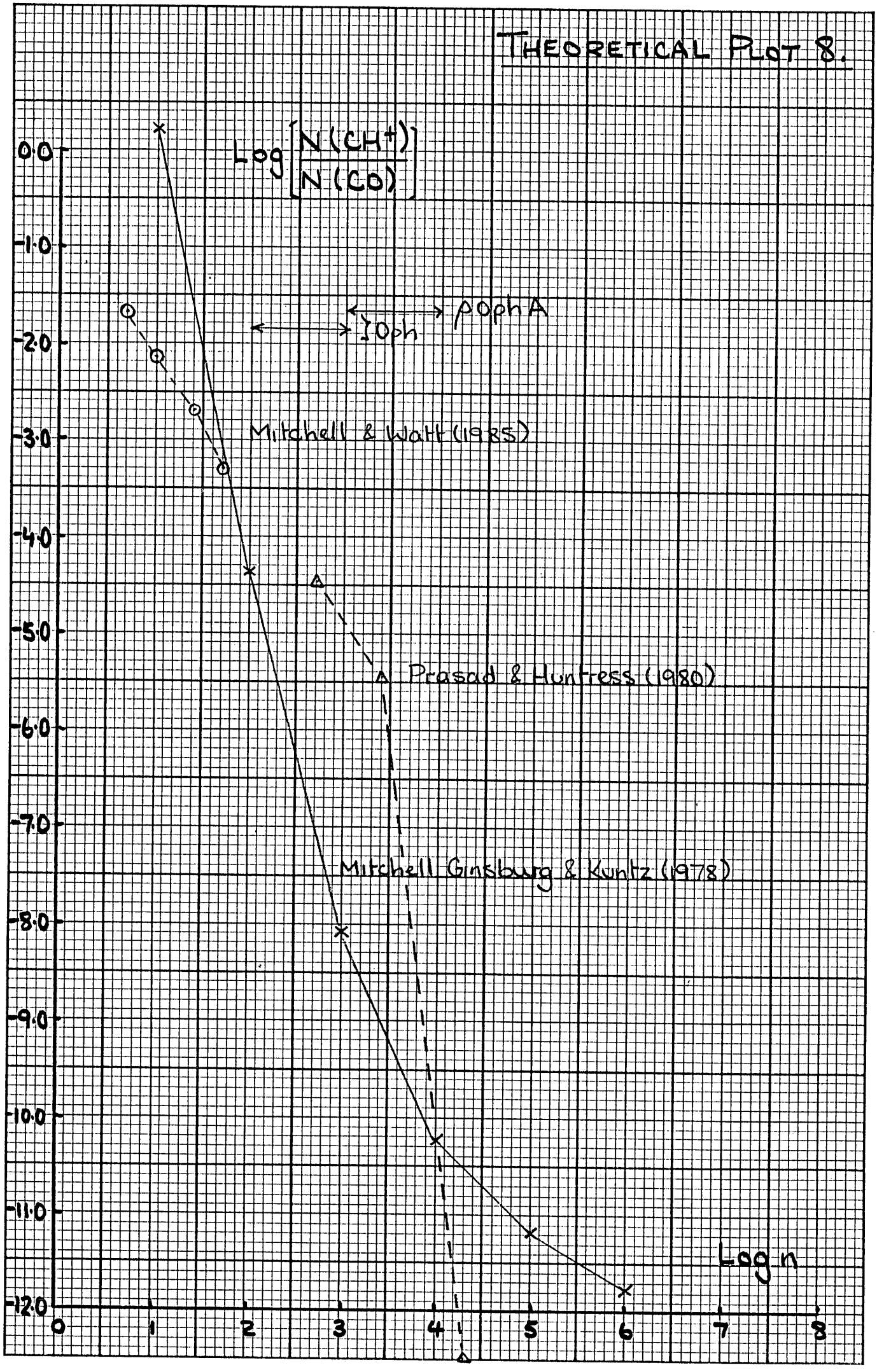
THEORETICAL PLOT 8.
$\log\left[\frac{N(CH^+)}{N(CO)}\right]$
0·0
-1·0
-2·0
-3·0
-4·0
-5·0
-6·0
-7·0
-8·0
-9·0
-10·0
-11·0
-12·0
0
1
2
3
4
5
6
7
8
log n
ρ0phA
τ0ph
Mitchell & Watt (1985)
Prasad & Huntress (1980)
Mitchell Ginsburg & Kuntz (1978)

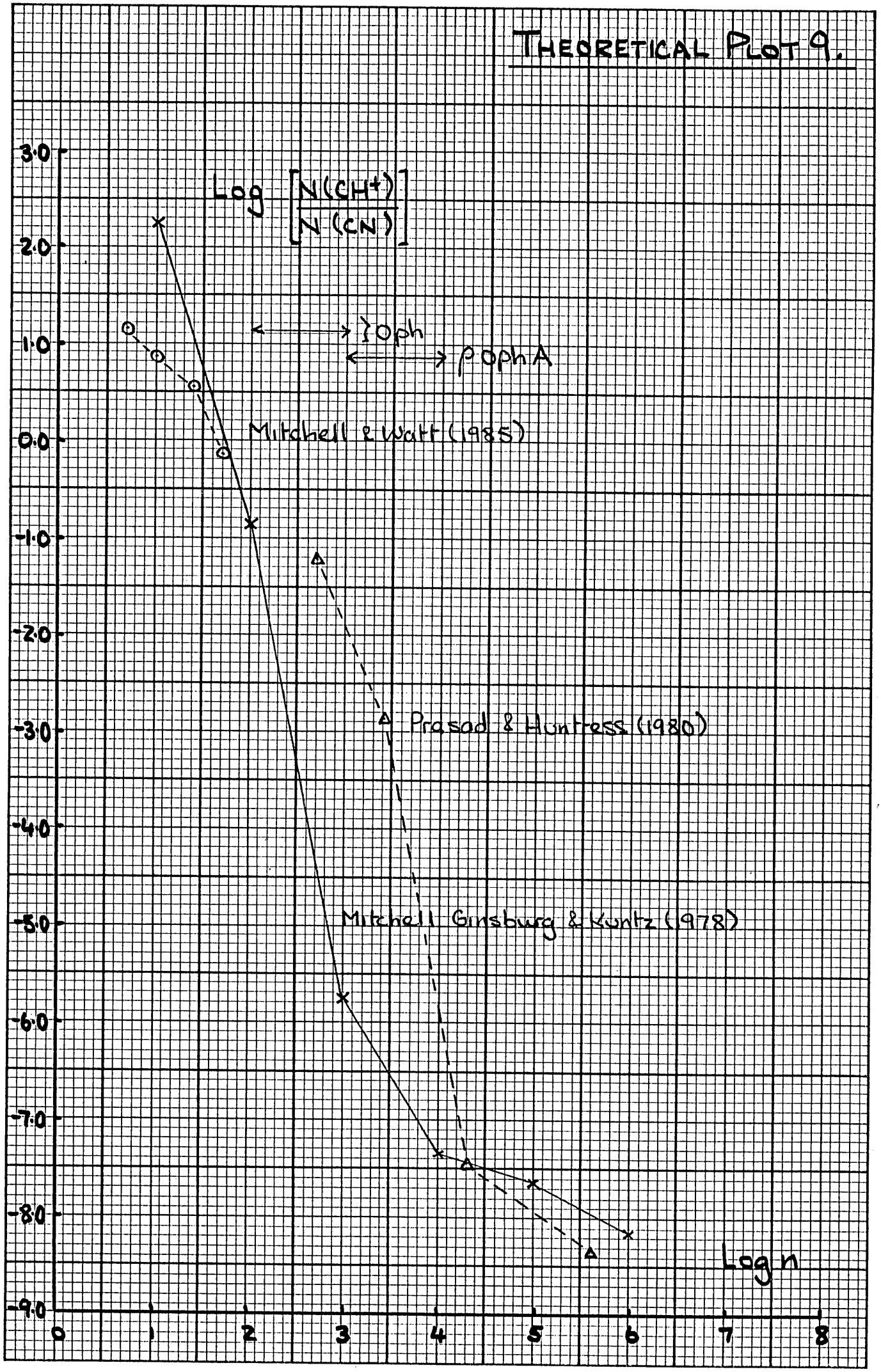
THEORETICAL PLOT 9.
Log [N(CH+) / N(CN)]
3·0
2·0
1·0
0·0
-1·0
-2·0
-3·0
-4·0
-5·0
-6·0
-7·0
-8·0
-9·0
0
1
2
3
4
5
6
7
8
Log n
Mitchell & Watt (1985)
Prasad & Huntress (1980)
Mitchell Ginsburg & Kuntz (1978)

CH^+ vs C_2

The results for CH^+ vs C_2 are hampered by the lack of C_2 data with which to derive a statistically valid conclusion (correlation diagram 39)

3. CORRELATIONS BETWEEN OTHER MOLECULES

3.1. NEUTRAL MOLECULES

CH vs HD

Correlation of CH with HD is good, r = 0.74. The slope of the log-log plot of N(CH) vs N(HD) has a gradient of 2.11. (correlation diagram 40)

$$\text{Log } N(HD) = 2.11 \text{ Log } N(CH) + \text{Log } A,$$

$$N(HD) \propto N(CH)^{2.1}$$

Clearly cloud properties are important to the chemistry in this case, and should be contrasted with the case of CH vs H_2 which shows a linear relationship between the two molecules

CH vs OH

There are too few points for OH to give a significant result (correlation diagram 41)

CO vs HD

Correlation of CO with HD is fair, r= 0.61. The slope of the log-log plot of N(CO) vs N(HD) has a gradient of 0.55. (correlation diagram 42).

$$\text{Log } N(HD) = 0.55 \text{ Log } N(CO) + \text{Log } A,$$

$$N(HD) \propto N(CO)^{0.5}$$

This is a similar relationship to that found for CO and H_2.

CO vs OH

Too few OH points to give a significant result. (correlation diagram 43).

CN vs HD

Correlation between CN and HD is not good r = 0.45, but this result is based on too few points to draw any firm conclusions. (Correlation diagram 44).

CN vs OH

To few points to give a significant result. (Correlation diagram 45).

C_2 vs HD

Too few points. (Correlation diagram 46).

C_2 vs OH

Too few points. (Correlation diagram 47).

OH vs HD

Too few points. (Correlation diagram 48).

3.2 MOLECULAR IONS

CH^+ vs HD

Correlation between CH^+ and HD is poor $r = 0.44$ (Correlation diagram 49)

CH^+ vs OH

Too few points (Correlation diagram 50).

APPENDICES

APPENDICES

1. SPECTRAL TYPE AND LUMINOSITY CLASS

The spectral classification of stars is based on work carried out at the Harvard College Observatory by E.C. Pickering, A.J. Cannon and others, culminating in the Henry Draper (HD) Catalogue of Stellar Spectra which was published between 1918 and 1924. This catalogue used a spectral classification of stars that had evolved from the original Harvard catalogue of 1890. The sequence of spectral types is arranged according to the prominence or absence of certain lines in the spectra of stars. Spectral lines of the elements and simple molecules have widely differing strengths in stars of different temperatures. The present sequence is arranged so that the spectral types are in order of decreasing stellar surface temperature.

The majority of stars can be divided into seven spectral types, O, B, A, F, G, K and M. Stars belonging to the first three groups are often referred to as early type stars. The cooler stars are called late stars. (For a list of the major spectral types and their properties see table 33.) Since temperature and colour are linked the Harvard classification is also a sequence of colour from the hot blue O stars to the cool red M stars. In fact the spectral type is often replaced by the B-V colour index. The HD spectral types R, N and S are also sometimes used. These refer to cool giant stars with molecular absorption lines other than the TiO lines typical of K and M stars. The R and N type stars show lines of neutral metals, C_2, CN and CH bands and the S type stars show lines of neutral metals and ZrO and TiO bands. Wolf Rayet stars have spectra characterised by broad emission lines from ejected matter (mostly H and He). They are designated by the letters WC for stars showing carbon and oxygen emission, WN for stars showing nitrogen emission and WR for all other cases.

TABLE 33

SPECTRAL TYPES

SPECTRAL TYPE	TEMPERATURE AND COLOUR	SPECTRUM	EXAMPLE
O	HOT BLUE	Ionised & neutral He, ionised metals, weak H	} Ori 09.5
B	HOT BLUE	Neutral He, ionised metals, stronger H.	Spica (α Vir) B1
A	BLUE WHITE	H dominant singly ionised, metals	Sirius (α CMa) A1
F	WHITE	H weaker neutral & singly ionised metals	Canopus (α Car) F0
G	YELLOW	CaII prominent, H weaker, neutral metals	The Sun G2
K	ORANGE RED	Neutral metals, some molecular bands	Aldebaran (α Tau) K5
M	COOL RED	Neutral metals, TiO bands dominant	Antares (α Sco) M1

NON STANDARD SPECTRAL FEATURES

e	Emission lines	m	Metallic lines
n	Nebulous lines	p	Peculiar spectrum
s	Sharp lines	v	Variable
k	Interstellar lines		

The spectral classes are subdivided into ten subclasses denoted by the digits 0 to 9 placed after the letter, for example A0, B2.... These subdivisions are based on a variety of complex empirical criteria, mainly the ratios of certain sets of lines in a spectrum. Other spectral characteristics such as the presence of emission lines are indicated by a small letter. For example B8Ipe indicates emission lines are present and that the spectrum is unusual.

Stars of a particular spectral type may have widely different luminosities and several luminosity classes are used to account for this. Luminosity L is defined as the intrinsic or absolute brightness of a star. It is related to the stars surface area, radius and effective temperature by a form of Stefan's Law.

$$L = 4 \pi r^2 \sigma Te^4 \qquad (4.1)$$

where σ = Stefans Constant

r = Stellar radius

Te = Effective temperature (the surface temperature of a star expressed as the temperature of a black body having the same radius and radiating the same total energy).

Thus two stars with the same effective temperature (and spectral type) but different luminosities mustdiffer in size. The currently used luminosity classes were developed by W.W. Morgan, P.C. Keenan and E.Kellman at Yerkes Observatory in the 1930s and 1940s. The classification is called the MKK or MK system, (see Keenan 1985 (537)). Stars of a given spectral type are divided into one of six luminosity classes denoted by Roman numerals. (See table 34). Stars falling between adjacent luminosity classes are assigned an intermediate brightness. For example, Altair (αAql) is A7 IV - V.

Stars of different luminosity, but with the same effective temperature also differ in surface gravity, and atmospheric density. These produce the spectral effects used to differentiate between luminosity classes.

TABLE 34

LUMINOSITY CLASSES

LUMINOSITY CLASS	STAR
Ia	Bright supergiant
Ib	Supergiant
II	Bright giant
III	Giant
IV	Subgiant
V	Main sequence (Dwarf)
VI	Sub dwarf
VII	White dwarf

One effect is the pressure boadening of spectral lines, which increases as the atmospheric density and the pressure increases (and the stellar radius decreases). Thus the spectral lines of a bright supergiant, in which the outer atmosphere is more rarified, are much narrower than those of a main sequence star of the same spectral type.

Stellar luminosity is usually expressed in terms of the absolute magnitude M defined by,

$$M = -2.5 \text{ Log } L + \text{Constant} \qquad (4.2)$$

Mv is the stars absolute visual magnitude, the stars brightness if it were located 10pc from the Sun. Mv is related to the apparent visual magnitude V in the UBV photometric system by

$$V = Mv + 5 \text{ Log } d - 5 + 3.1 \, E(B-V) \qquad (4.3)$$

where d = Distance in parsecs.

E(B-V)= Colour excess.

The majority of the spectral types and luminosity classes, absolute & apparent visual magnitudes, and distances in table 26 details of the stars toward which molecules have been searched for, are taken from Sky Catalogue 2000 Vol. 1 (336). Values of Mv not in this Catalogue are taken from Grenier et al 1985 (538) or Landolt - Börnstein 1982 (548) and the distance d calculated from equation 4.3.

2. COLOUR AND COLOUR EXCESS

Since stellar magnitudes are logarithmic, the ratio of light intensities in two wavebands transforms to a difference in stellar magnitudes in the two wavebands. This difference in magnitude is called the colour index of the star because it is a numerical measurement of the colour.

In practice the difference between the apparent magnitude of a star at one standard wavelength and the apparent magnitude at another longer standard wavelength is measured. In the UBV system the colour index is usually expressed as the difference B-V where B and V are the broad band magnitudes measured with blue starlight centred on 4400Å and greenish yellow (visual) starlight centred on 5500Å. The colour index U-B is also used where U is the apparent magnitude measured with ultraviolet radiation centred on 3600Å. Stars are classified into spectral types each of which has an intrinsic colour index $(B - V)_o$ and $(U-B)_o$ defined as zero for AO main sequence stars. They are therefore negative for hotter O and B stars, (see figure 37).

The colour excess of a star is the difference between the observed colour index and the intrinsic colour index and is denoted by E(B-V) or E(U-B) where,

$$E(B-V) = (B-V) - (B-V)_o \qquad (4.4)$$

$$E(U-B) = (U-B) - (U-B)_o \qquad (4.5)$$

Any colour excess indicates reddening of starlight due to the extinction of blue light by interstellar dust. The extinction decreases with increasing wavelength of starlight. Most of the stars in this catalogue are reddened by a few tenths of a magnitude although values of up to two magnitudes are not uncommon. There are many more heavily reddened stars, in fact most stars in the Galaxy are totally obscured. The result is that heavily reddened stars are much fainter. E(B-V) is always greater or equal to zero.

The values of E(B-V) given in this study were calculated from the B-V values given in Sky Catalogue 2000, Vol. 1 (336) and the $(B-V)_o$ values

Figure 37

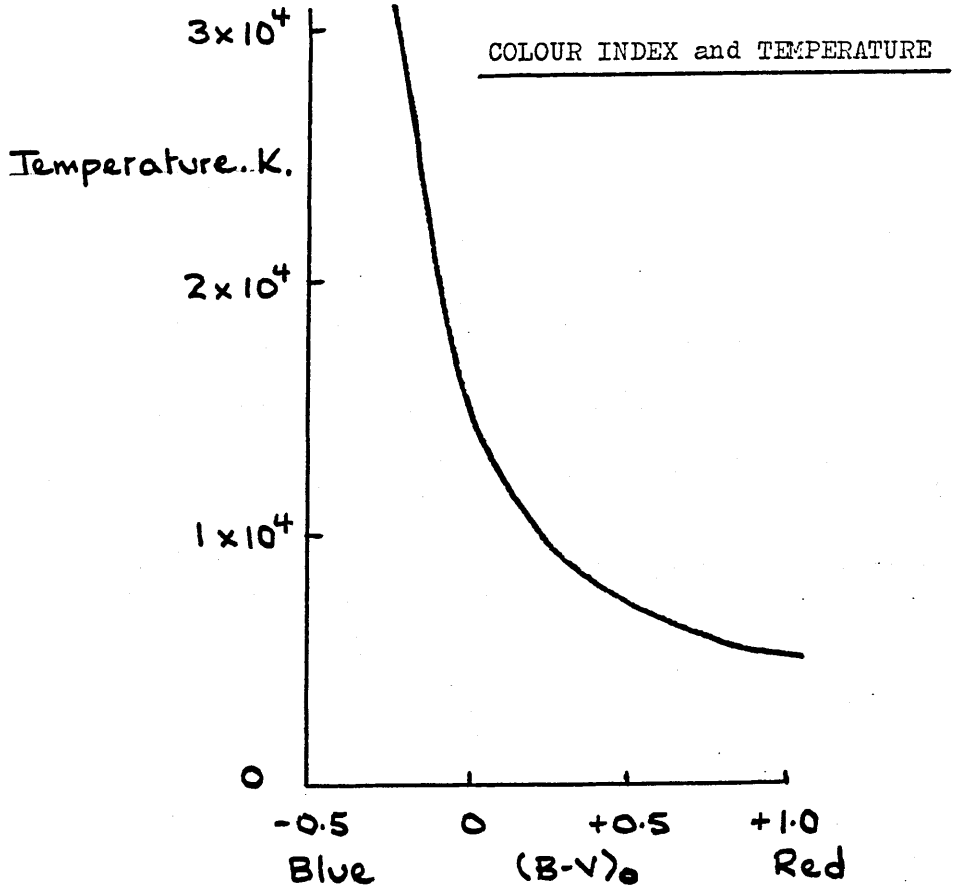

Figure 38

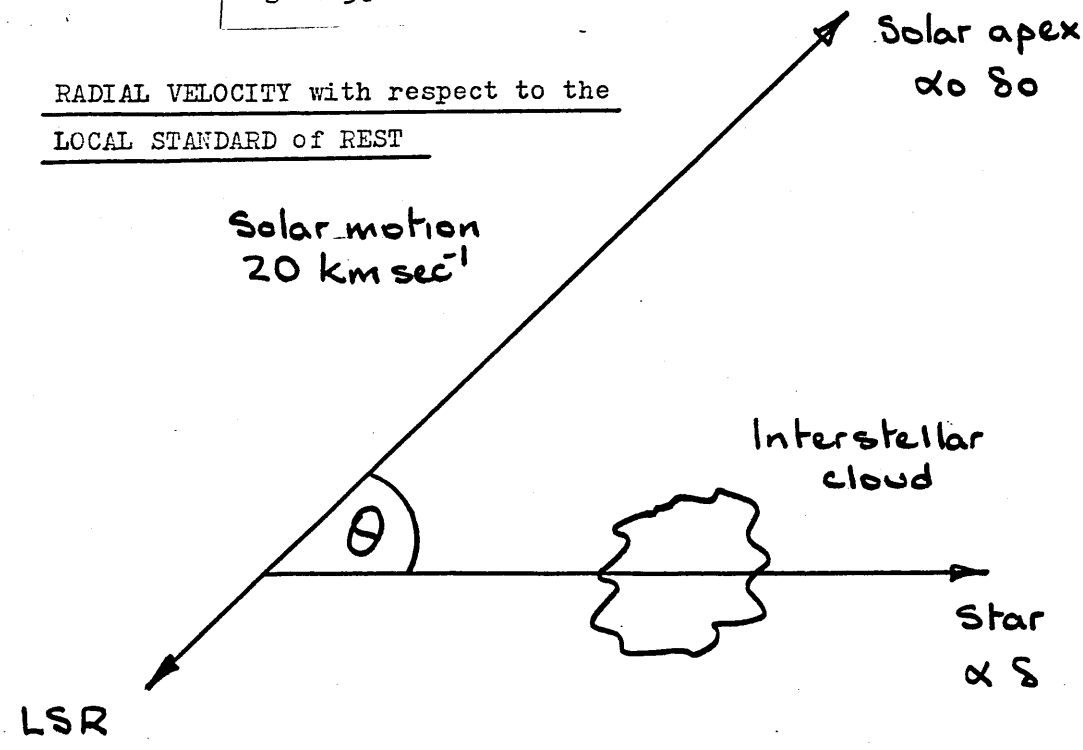

given by FitzGerald 1970 (136).

3. RADIAL VELOCITY

The parameter used to describe the position of a molecule in a given interstellar cloud is its radial velocity which is derived from the wavelength of a given spectral line relative to its wavelength for the same molecule at rest.

The frequency of radiation from a moving source (such as the molecules in an interstellar gas cloud) depends on the velocity of the source relative to the observer. The observed frequency increases if the motion is towards the observer and decreases if the motion is away from the observer. This is the well known Doppler effect, so that only for a stationary cloud will the frequency observed be the natural frequency. Spectral lines are also broadened due to the same effect by the random motion of the molecules that make up the gas. In this case however let us consider the gas as a whole moving through space. From the Doppler principle it follows that if a source of radiation of wavelength λ_o is moving in the line of sight with velocity V away from the observer then the apparent wavelength λ measured by the observer will be,

$$\lambda = \lambda_o\left(1 + \frac{V}{C}\right) \tag{4.6}$$

where C = Velocity of light.

Motion away from the observer produces a shift to longer wavelengths (a red shift) and such motion is taken as being positive. From equation 4.6 it follows that

$$\frac{\lambda - \lambda_o}{\lambda_o} = \frac{V}{C} \tag{4.7}$$

$$\frac{\Delta\lambda}{\lambda_o} = \frac{V}{C}$$

$$V = \frac{C\,\Delta\lambda}{\lambda_o} \tag{4.8}$$

Hence V may be determined from observational data. The line of sight or radial velocities of interstellar clouds are thus determined from the displacement of spectral lines due to the Doppler effect.

Radial velocities are usually given in terms of the Sun's position so that the Earths orbital motion has no effect. A radial velocity with respect to the Sun in which the orbital motion of the Earth around the Sun, about 30 Km s^{-1}, is corrected for is called a Heliocentric radial velocity. The average velocity of all the stars in the solar neighbourhood defines the Local Standard of Rest (LSR). This is a frame of reference centred on the Sun in which the space velocities (the velocity in space of a star relative to the Sun) of all the stars averages to zero. The LSR moves in a circular orbit around the Galactic centre so that all neighbouring stars are essentially at rest. The velocity of any star in the solar neighbourhood with respectto the LSR is called the peculiar velocity of the star. The Sun is also moving relative to the LSR in the direction of the Solar Apex at 20 Km s^{-1}. This lies in the constellation Hercules at RA $18^h\ 08^m$, Dec + 30^o (2000). The Suns peculiar velocity is called the Solar Motion. The relationship between Heliocentric and LSR radial velocities is given by

$$V_{LSR} = V_{Heliocentric} + 20 \cos\theta \qquad (4.9)$$

where $\cos\theta = \sin\delta.\sin\delta_o + \cos\delta.\cos\delta_o.\cos(\alpha-\alpha_o)$

and α_o = R A of the Solar Apex

δ_o = Dec of the Solar Apex

α = R A of the star in the line of sight

δ = Dec of the star in the line of sight

This is illustrated in figure 38.

All radial velocities in this study are given with respect to the Local Standard of Rest.

Some scaling of radial velocities has been necessary because of the use of different values for the rest wavelength λ_o. Adams 1949 (10) used 4300.338 Å as the rest wavelength for the $A^2\Delta - X^2\pi$ (00) $R_2(1)$ transition of CH. The accepted value of λ_o for the A-X line of CH is now 4300.321Å so that Adam's radial velocities have been increased by 1.2 Km Sec^{-1} to account

for this.

For the CH^+ molecular ion the latest value of λ_o for the $A^1\Pi$-$X^1\Sigma^+$ (00)R(0) transition is 4232.548Å given by Carrington & Ramsay 1982 (407). Adams 1949 (10) used 4232.573Å so that his values have been increased by 1.8 Km sec^{-1}. In the past a majority of workers have used 4232.539Å, and in these cases the radial velocities have been decreased by 0.6 Km sec^{-1}. The use of 4232.548Å as the rest wavelength for the A-X transition of CH^+, to calculate radial velocities, is in line with the latest survey of CH^+ in diffuse clouds by Lambert and Danks 1986 (405).

. . .

REFERENCES AND BIBLIOGRAPHY

LIST OF REFERENCES AND BIBLIOGRAPHY

1. Chaffe F.H. & Dunham T. 1979
   Astrophys J. Vol. 233 pp 568.
2. Turner B.E. & Gammon R.H. 1975
   Astrophys J. Vol 198 pp 71.
3. Knapp G.R. & Jura M. 1976
   Astrophys J. Vol 209 pp 782.
4. Frisch P.C. 1972
   Astrophys J. Vol 173 pp 301.
5. Smith W.H. & Snow T.P. 1979
   Astrophys J. Vol 228 pp 435
6. Blades J.C. & Bennewith P.D. 1973
   MNRAS Vol 161 pp 213
7. Chaffee F.H. 1974
   Astrophys J. Vol 189 pp 427.
8. Snow T.P. 1975
   Astrophys J. (Lett) Vol 201 L 21.
9. Dickman R.L., Somerville W.B. et al 1981
   Preprint.
10. Adams W.S. 1949
    Astrophys J. Vol 109 pp 354.
11. Morton D.C. 1975
    Astrophys J. Vol 197 pp 85.
12. Mann A.P.C. & Williams D.A. 1980
    Nature Vol 283 pp 721.
13. Cohen J.G. 1973
    Astrophys J. Vol 186 pp 149.

14. Black J.H. 1980
Interstellar Molecules.
IAU Symposium No. 87. pp 257.

15. Dalgarno A. 1980
Interstellar Molecules
IAU Symposium No. 87. pp 273.

16. Winnewisser G. 1981
Topics in Current Chemistry Vol 99 pp 39.

17. Somerville W.B. Jacobs L.A. et al 1982
Proc. 3rd European IUE Conference ESA SP 176 pp 399.

18. Dalgarno A & Black J.H. 1976
Rep. Prog. Phys. Vol 39 pp 573.

19. Dalgarno A. 1976
Chemistry of the Interstellar Medium. Chapter 8 in
Frontiers of Astrophysics.
Ed. E.H. Avrett. pp 352. Harvard University Press.

20. Huntress W.T. 1977
Chem. Soc. Rev. Vol 6 pp 295.

21. Smith A.M., Krishna Swamy K.S. et al 1978.
Astrophys J. Vol 220 pp 138.

22. Vanden Bout P.A. 1972
Astrophys J. (Lett) Vol 176, L127.

23. Frisch P.C. 1979
Astrophys J. Vol 227 pp 474.

24. Bortolot V.J., Thaddeus P. 1969
Astrophys J (Lett) Vol 155, L17.

25. Blades J.C. 1978
MNRAS Vol 185 pp 451.

26. Mitchell G.F. Ginsburg J.L. Kuntz P.J. 1977
Astrophys J. Vol 212 pp 71.

27. Federman S.R., Glassgold A.E. et al 1980.
Astrophys J. Vol 242 p 545.

28. Townes C.H. 1977.
Observatory Vol 97 pp 52.

29. Black J.H. Dalgarno A. 1973
AstrophysLett Vol 15 p 79.

30. Federman S.R. 1982.
Astrophys J. Vol 257 p 125.

31. Shull J.M. 1980.
Appl Optics Vol 19 pp 4002.

32. Delsemme A.H. 1980.
Appl Optics Vol 19 pp 4007.

33. Somerville W.B. 1977
Rep Prog Phys. Vol 40 p 483.

34. Tarafdar S.P., Krishna Swamy K.S. 1982
MNRAS Vol 200 pp 431.

35. Stecher T.P. Williams D.A. 1974
MNRAS Vol 168 pp 51P.

36. Stecher T.P., Williams D.A. 1974.
MNRAS Vol 168 pp 23P.

37. Anders E. Hayatsu R. & Studier M.H. 1974
Astrophys J. (Lett) Vol 192 L101.

38. Bates D.R. & Spitzer L. 1951.
Astrophys J. Vol 113 pp 441.

39. Cook A.H. 1975
Q.J. R.A.S. Vol 16 pp 21.

40. Crutcher R.M. 1976
Astrophys J. (Lett) Vol 206 L171

41. Tarafdar S.P., Krishna Swamy K.S. & Vardya M.S. 1980
MNRAS Vol 192 pp 417.

42. Douglas A.E. & Herzberg G. 1941
Astrophys J. Vol 94 pp 381.

43. Smith A.M. & Stecher T.P. 1971
Astrophys J. (Lett) Vol 164 L43.

44. Rogerson J.B, Spitzer L. & Bahng J.D. 1959
Astrophys J. Vol 130, pp 991.

45. Nicholls R.W. 1977
Ann Rev Astron Astrophys Vol 15 pp 197.

46. Chaffee F.H. & Lutz B.L. 1977
Astrophys J. Vol 213 pp 394.

47 Chaffee F.H. 1975
Astrophys J. Vol 199 pp 379.

48. Snow T.P. & Jenkins E.B. 1980
Astrophys J. Vol 241 pp 161.

49. Brooks N.H. & Smith W.H. 1975
Astrophys J. Vol 196 pp 307.

50. Federman S.R. & Willson R.F. 1982
Astrophys J. Vol 260 pp 124.

51. Hobbs L.M. 1973
Astrophys J. Vol 181 pp 79.

52. Lang K.R. & Willson R.F. 1978
Astrophys J. Vol 224 pp 125.

53. Jenkins E.B. Drake J.F., Morton D.C., Rogerson J.B.,
Spitzer L. & York D.G. 1973
Astrophys J (Lett) Vol 181 L122.

54. Herbig G.H. 1968
Z. Ap. Vol 68 pp 243.

55. Frisch P.C. 1980
Astrophys J. Vol 241 pp 697.

56. Snow T.P. 1977

Astrophys J Vol 216 pp 724.

57. Munch G. 1964

Astrophys J. Vol 140 pp 107.

58. Blades J.C. 1975

Spectroscopic Studies of the Interstellar Gas.

PhD. Thesis. University of London.

59. Peimbert M. 1968

Bol Obs Tonanzintla y Tacubaya

Vol 4 pp 233.

60. Elitzur M. & Watson W.D. 1980

Astrophys J. Vol 236 pp 172.

61 Yoshimine M., Green S., Thaddeus P., 1973

Astrophys J. Vol 183 pp 899.

62. Mahan B.H. & O'Keefe A. 1981

Astrophys J. Vol 248 pp 1209.

63. Erman P. 1977

Astrophys J (Lett) Vol 213 L89.

64. Willson R.F. 1981

Astrophys J. Vol 247 pp 116.

65. Solomon P.M. & Klemperer W. 1972

Astrophys J. Vol 178 pp 389.

66. McNally D. 1971

Highlights of Astronomy. p 339

IAU 1971

67. Pickles J.B. & Williams D.A. 1981

MNRAS. Vol 197 pp 429.

68. Dalgarno A. 1976

The Interstellar Molecules CH and CH^+

Chapter 5 in Atomic Processes and Applications.

Ed. P.G. Burke & B.L. Moiseiwitsch

pp 109 North Holland.

69. McKellar A. 1940
Pub Astron Soc Pac. Vol 52 pp 187.

70. Savage B.D., Bohlin R.C., Drake J.F. & Budich W. 1977
Astrophys J. Vol 216 pp 291.

71. Bohlin R.C., Savage B.D. & Drake J.F. 1978
Astrophys J. Vol 224 pp 132

72. Carruthers G.R. 1970
Astrophys J. (Lett) Vol 161, L81.

73. Dunham T. 1937
Pub. Astron. Soc. Pac Vol 49, pp 26.

74. Crutcher R.M. & Watson W.D. 1976.
Astrophys J. Vol 209, pp 778.

75. Black J.H., Hartquist T.W. & Dalgarno A. 1978
Astrophys J. Vol 224 pp 448.

76. Kirby K. & Dalgarno A. 1978
Astrophys J. Vol 224 pp 444.

77. Black J.H. & Dalgarno A. 1973
Astrophys J. (Lett) Vol 184, L101.

78. Black J.H. & Dalgarno A. 1977
Astrophys J. (Supp) Vol 34 pp 405.

79. Bohlin R.C., Hill J.K., Jenkins E.B., et al 1982
Wisconsin Astrophysics No. 156

80. Salpeter E.E. & Watson W.D. 1973
Interstellar Dust & Related Topics.
IAU Symposium No. 52. pp 363.

81. Snyder L.E. 1973
Interstellar Dust & Related Topics
IAU Symposium No. 52. pp 351.

82. Harteck P., Beaudoin A. & Reeves R. 1973
Interstellar Dust & Related Topics.
IAU Symposium No. 52. pp 395.

83. Breuer H.D. 1973
Interstellar Dust & Related Topics
IAU Symposium No. 52. pp 399.

84. Shimizu M. 1973
Interstellar Dust & Related Topics.
IAU Symposium No. 52. pp 405.

85. Stecher T.P. & Williams D.A. 1972
Astrophys J. (Lett). Vol 177, L141.

86. Brown R.D. 1974
Galactic Radio Astronomy
IAU Symposium No. 60 pp 129.

87. Spitzer L., Drake J.F., Jenkins E.B., Morton D.C.,
Rogerson J.B. & York D.G. 1973
Astrophys J. (Lett) Vol. 181 L116.

88 Watson W.D. 1973
Astrophys J. (Lett) Vol. 182 L73.

89. Watson W.D. 1973
Astrophys J. (Lett) Vol. 183 L17.

90. Dalgarno A., Oppenheimer M. & Berry R.S. 1973
Astrophys J. (Lett) Vol 183. L21.

91. Krauss M. & Julienne P.S. 1973
Astrophys J. (Lett) Vol. 183 L139.

92. Williams D.A. 1971
Astrophys Lett Vol. 10 pp 17.

93. Snyder L.E. & Buhl D. 1970
Sky & Telescope Vol. 40 No. 5 pp 267.

94. Snyder L.E. & Buhl D. 1970
Sky & Telescope Vol. 40 No. 6 pp 345.

95. Brzozowski J., Bunker P., Elander N., Erman P., 1976
Astrophys J. Vol. 207 pp 414.

96. Frisch P.C. & Jura M 1980.
Astrophys J. Vol. 242 pp 560.

97. Hobbs L.M. 1981
Astrophys J. Vol. 243 pp 485.

98. Watson W.D. 1974
Astrophys J. Vol. 189 pp 221.

99. Adams W.S. 1941
Astrophys J. Vol. 93 pp 11.

100. Smith A.M. 1973
Astrophys J. (Lett) Vol. 179 L 11

101. Hollenbach D.J., Werner M.W. & Salpeter E.E. 1971
Astrophys J. Vol. 163 pp 165.

102. Wilson R.W., Jefferts K.B. & Penzias A.A. 1970
Astrophys J. (Lett) Vol. 161 L 43.

103. Jefferts K.B., Penzias A.A. & Wilson R.W. 1970
Astrophys J. (Lett) Vol. 161 L 87.

104. Chaffee F.H. & Lutz B.L. 1978
Astrophys J. (Lett) Vol. 221 L 91.

105. Federman S.R. 1980
Astrophys J. (Lett) Vol. 241 L109.

106. Jura M. & Smith W.H. 1977
Astrophys J. Vol. 215 pp 517.

107. Spitzer L. Cochran W.D. & Hirshfeld A. 1974
Astrophys J. (Supp) Vol. 28 pp 373.

108. Swings P. & Rosenfeld L. 1937
Astrophys J. Vol 86 pp 483.

109. Adams W.S. 1943
Astrophys J. Vol 97 pp 105

110. Stromgren B. 1948

Astrophys J. Vol. 108 pp 242.

111. Schadee A. 1967

J. Quant Spec. & Rad. Trans. Vol 7 pp 169.

112. Bennett R.G. & Dolby F.W. 1960

J. Chem. Phys. Vol. 32 pp 1716.

113. Crutcher R.M. & Watson W.D. 1976

Astrophys J. (Lett) Vol. 203 L123.

114. Dalgarno A. et al 1973

Astrophys Lett Vol. 14 pp 77.

115. Elitzur M. & Watson W.D. 1978

Astrophys J (Lett) Vol. 222 L141.

116. Jura M. 1974.

Astrophys J. (Lett) Vol. 190 L33.

117. Jura M. & York D.G. 1978

Astrophys J. Vol. 219 pp 861.

118. Kirby K., Saxon R.P. & Liu B. 1979

Astrophys J. Vol. 231 pp 637.

119. Lutz B., Owen. T. & Snow T.P. 1979

Astrophys J. Vol. 227 pp 159.

120. Snow T.P. & Smith W.H. 1981.

Astrophys J. Vol 250 pp 163.

121. Allison A. & Dalgarno A. 1970.

Atomic Data Vol. 1 pp 289.

122. Green S. Hornstein S. & Bender C.F. 1973.

Astrophys J. Vol. 179 pp 671

123. Clegg R.E.S. & Lambert D.L. 1982

MNRAS Vol. 201 pp 723.

124. Juhenne P.S. & Krauss M. 1973

Molecules in the Galactic Environment

Ed. M.A. Gordon & L.E. Snyder

pp 354. Wiley-Interscience

125. Prasad S.S. & Huntress W.T. 1980.
Astrophys J. (Supp) Vol. 43 pp 1.

126. Federman S.R. 1982
Astrophys J. Vol. 253 pp 601.

127. Smith W.H. 1978
Phys. Scripta Vol. 17 pp 513.

128. Lassettre E.N. & Skerbele A. 1971.
J. Chem. Phys. Vol. 54 pp 1597

129. Fink. E.H. & Welge K.H. 1967
J. Chem. Phys. Vol. 46 pp 4315.

130. Golden D.M., Del Greco F.P. & Kaufman F. 1963
J.Chem. Phys. Vol. 39 pp 3034.

131. Thaddeus P. 1972
Ann Rev. Astron. Astrophys. Vol. 10 p 305.

132. de Loore C., Burger M. et al 1981.
Astron. Astrophys. Vol. 104 p 150.

133. Sitko M.L. 1983.
Astrophys J. Vol. 265 pp 848.

134. Phillips A.P. & Gondhalekar P.M. 1983
MNRAS Vol. 202. pp 483.

135. Bohlin R.C. Hill J.K. et. al 1983.
Astrophys. J. (Supp) Vol. 51 pp 277.

136. Fitzgerald M.P. 1970.
Astron. Astrophys. Vol. 4 pp 234.

137. Beals C.S. 1936
MNRAS Vol. 96 pp 661.

138. Hartmann J. 1904.
Astrophys J. Vol. 19 pp 268.

139. Hegar M.L. 1919
Lick Obser Bull Vol. 10 pp 59.

140. Hobbs L.M. 1973

Astrophys. J. (Lett) Vol. 180 L 79.

141. Hobbs L.M. 1972.

Astrophys. J. (Lett) Vol. 175 L 39.

142. Field G.B. Somerville W.B. & Dressler K. 1966

Ann Rev. Astron. Astrophys. Vol4 p 207.

143. Gondhalekar P.M. & Phillips A.P. 1980

MNRAS Vol. 191, pp 13P.

144. Bortolot V.J., Clauser J.F. & Thaddeus 1969.

Phys. Rev. Lett Vol. 22, p 307.

145. Brzozowski J., Elander N., et al 1974

Astrophys J. Vol. 193 pp 741.

146. Lutz B.L. & Crutcher R.M. 1983

Astrophys J. (Lett) Vol. 271 L101.

147. Hobbs L.M., Black J.H. & Van Dishoeck E.F. 1983

Astrophys. J. (Lett) Vol. 271 L95

148. Ferlet R., Roueff. E. et al 1983.

Astron. Astrophys. Vol. 125, L5

149. Vanden Bout P.A. & Snell R.L. 1980

Astrophys. J. Vol. 236 pp 460.

150. Heger M.L. 1921

Lick Observatory Bull, Vol. 10 pp 141.

151. Dickman R.L., Somerville W.B., et al 1983.

Astrophys. J. (Supp) Vol. 53 pp 55.

152. Danks A.C., Federman S.R. & Lambert D.L. 1984

Astron Astrophys Vol. 130 pp 62.

153. Russell H.N. 1935

MNRAS Vol. 95 pp 610

154. Hesser J.E. & Lutz B.L. 1970

Astrophys. J. Vol 159 pp 703

155. Aannestad P.A. 1973

Astrophys. J. (Supp) Vol. 25 pp 205.

156 McCrea W.H. & McNally D. 1960

MNRAS Vol. 121 pp 238

157. Brooks N.H. & Smith W.H. 1974

Astrophys. J. Vol 194 pp 513.

158. Plaskett J.S. & Pearce J.A. 1933

Pub. Dom. Astrophys. Obs. Vol. 5 pp 167

159. Quarta M.L. & Singh P.D. 1981

Astron. Astrophys. Vol. 98 pp 384.

160. Barlow M.J. & Silk J. 1976

Astrophys. J. Vol. 207 pp 131.

161. Mitchell G.F. & Deveau T.J. 1983

Astrophys. J. Vol. 266 pp 646.

162. Erman P. et al 1982

Astrophys J. Vol. 253 pp 983.

163. Cosmovici C.B. & Strafella F. 1981

Astron. Astrophys. Vol. 98 pp 408

164. Hobbs L.M. 1979

Astrophys J. (Lett) Vol. 232 L175

165. Chaffee F.H., Lutz B.L. et al 1980.

Astrophys. J. Vol. 236 pp 474.

166. Hobbs L.M. & Campbell B. 1982.

Astrophys J. Vol. 254 pp 108.

167. Reis V.H. 1965

J. Quant Spec. & Rad. Trans. Vol. 5 pp 585.

168. Smith W.H. 1971

J. Chem. Phys. Vol. 54 pp 1384.

169. Pouilly B. 1983

J. Phys. B. Vol. 16 pp 437

170. van Dishoeck E.F. & Dalgarno A. 1983
J.Chem. Phys. Vol. 79 pp. 873.

171. Brazier C.R. & Brown J.M. 1983
J. Chem. Phys. Vol 78 pp 1608.

172. Lambert D.L. 1978
MNRAS Vol. 182 pp 249.

173. Jenkins E.B. 1971
Astrophys J. Vol. 169 pp 25.

174. Merrill P.W. 1934
Pub. Astron. Soc. Pac. Vol. 46 pp 206.

175. Snow T.P. 1978
Astrophys. J. (Lett) Vol. 220 L93

176. Souza S.P. & Lutz B.L. 1977
Astrophys J. (Lett) Vol. 216. L49

177. Roux F., Cerny D. & d'Incan J. 1976
Astrophys. J. Vol. 204, pp 940.

178. Lutz B.L. & Souza S.P. 1977
Astrophys. J. (Lett) Vol. 213, L129.

179. Wannier P.G., Penzias A.A. & Jenkins E.B. 1982.
Astrophys. J. Vol 254. pp 100.

180. Smith P.L. et al 1981
Astrophys. J. Vol 250 pp 166.

181. Smith P.L. et al 1980
Astrophys J. Vol. 238 pp 874.

182. Smith P.L. & Parkinson W.H. 1978
Astrophys. J. (Lett) Vol. 223 L127

183. Snow T.P. 1976
Astrophys. J. (Lett) Vol. 204 L127

184. Allen M. & Knapp G.R. 1978
Astrophys J. Vol. 225 pp 843

185. Liszt H.S. 1979
Astrophys. J. (Lett) Vol. 233 L147

186. Rydbeck O.E.H., Elldér J. et al 1974
Astron. Astrophys. Vo. 33 pp 315

187. Turner B.E. & Zuckerman B. 1974
Astrophys. J. (Lett) Vol. 187 L59.

188. Zuckerman B. & Turner B.E. 1975
Astrophys J. Vol. 197 pp 123.

189. Hjalmarson A., Sume A. et al 1977
Astrophys. J. (Supp) Vol. 35 pp 263.

190. Herbst E. 1978
Astrophys J. Vol. 222 pp 508.

191. Crutcher R.M. 1979
Astrophys J. (Lett) Vol. 231 L151

192. Smith W.H. & Zweibel E.G. 1976
Astrophys. J. Vol. 207 pp 758

193. Ray S. & Kelly H.P. 1975
Astrophys J. (Lett) Vol. 202 L57

194. Wright E.L. & Morton D.C. 1979
Astrophys J. Vol. 227 pp 483.

195. Danks A.C. & Lambert D.L. 1983
Astron. Astrophys. Vol 124 pp 188.

196. Smith W.H. 1969
Astrophys J. Vol 156 pp 791

197. Watson W.D. 1978
Ann Rev. Astron. Astrophys. Vol 16 pp 585.

198. Shull J.M. & Beckwith S. 1982
Ann Rev. Astron. Astrophys. Vol. 20 pp 163.

199. Johns J.W.C. 1963
Can. J. Phys. Vol. 41 pp 209.

200. Cooper D.M. & Nicholls R.W. 1975
J.Quant Spec. & Rad. Trans. Vol. 15 pp 139

201. Watson W.D. 1976

Rev. Mod Phys. Vol. 48 pp 513

202. Connerade J.P., Baig M.A. et al 1980

J. Phys. B. Vol. 13 L705

203. Hirota E. 1983

J. Phys. Chem. Vol 87 pp 3375

204. Bogey M. Demuynck C. et al 1983

Chem. Phys. Lett Vol 100 pp 105.

205. Herbst E. & Klemperer W. 1976

Phys. Today. Vol. 29 pp 32.

206. Dalgarno A. & McCray R.A. 1973

Astrophys J. Vol. 181 pp 95.

207. Jeunehomme M. & Duncan A.B.F. 1964

J. Chem.Phys. Vol. 41 pp 1692

208. Schadee A. 1978

J. Quant Spec. & Rad. Trans. Vol. 19, pp 451

209. Curtis L. Engman B. & Erman P. 1976

Phys. Scripta. Vol. 13 pp 270

210. Fehsenfeld F.C. et al 1974

Astrophys J. Vol. 188 pp 43.

211. Smith W.H., Schempp W.V. & Federman S.R. 1984

Astrophys J. Vol. 277 pp 196

212. van Dishoeck E.F. & de Zeeuw T. 1984

MNRAS. Vol. 206 pp 383.

213. Cohen J.G. & Wallerstein G. 1974

Astrophys J. Vol. 189, pp 259.

214. McLachlan A. & Nandy K. 1984

MNRAS Vol. 207 pp 355.

215. Mitchell G.F., Ginsburg J.L. & Kuntz P.J. 1978

Astrophys J. (Supp) Vol. 38 pp 39.

216. Zuckerman B. & Palmer P. 1974
Ann Rev. Astron. Astrophys Vol. 12 pp 279.

217. De Noyer L.K. &Frerking M.A. 1981
Astrophys J. (Lett) Vol. 246 L37

218. Meerts W.L. & Dymanus A. 1975
Can. J. Phys. Vol. 53. pp 2123

219. Brault J.W. et al 1982
Astron. Astrophys Vol. 108 pp 201

220. Brown J.M. & Evenson K.M. 1983
Astrophys J. (Lett) Vol. 268 L51

221. Ziurys L.M., Henkel C. & Saykally R.J. 1983
Astrophys J. Vol. 275 pp 175.

222. Cartwright D.C. & Hay P.J. 1982
Astrophys J. Vol. 257 pp 383.

223. Sancisi et al 1974
Astron. Astrophys. Vol. 35 pp 445.

224. Mitchell G.F. 1983
MNRAS Vol 205 pp 765

225. Turner J.L. & Dalgarno A. 1977
Astrophys J. Vol. 213 pp 386

226. Black J.H. et al 1974
Astrophys J. (Lett) Vol. 191 L 45.

227. A'Hearn M.F., Feldman P.D. & Schleicher D.G. 1983
Astrophys. J. (Lett) Vol. 274 L99

228. Larsson M., Siegbahn P.E.M. & Agren H. 1983
Astrophys. J. Vol. 272 pp 369

229. Morgan W.W., Johnson H.L. & Roman N. 1954
Pub. Astron. Soc. Pac. Vol. 66 p 85

230. Danks A.C., Federman S.R. & Lambert D.L. 1983
Preprint

231. Bouloy D. Nguyen Q-Rieu & Field D. 1984
Astron. Astrophys. Vol. 130 pp 380.

232. Somerville W.B. 1978
Advances in Atomic & Mol. Phys. Vol. 13 pp 383.

233. Van Dishoeck E.F. 1983
Chem. Phys. Vol. 77 pp 277

234. Macchetto F. & Penston M.V.
ESA Bulletin No. 13 pp 9.

235. Evenson K.M., Radford H.E. & Moran M.M. 1971
App. Phys. Lett Vol. 18 pp 426

236. Barlow S.E., Dunn G.H. & Schauer 1984
Phys. Rev. Lett Vol. 52 pp 902.

237. Kirchner N.J. et al 1984
Phys. Rev. Lett Vol. 52 pp 26.

238. Mitchell J.B.A. et al 1983
Phys. Rev. Lett Vol. 51 pp 885

239. Golton E. & Dunford E. 1979
J.Brit Interplanetary Soc. Vol 32 pp 47

240. Herzberg G. 1950
Molecular Spectra and Molecular Structure.
Vol. 1 Spectra of Diatomic Molecules.
Van Nostrand Reinhold Company.

241. Herzberg G. 1983
In : Molecular Ions, Spectroscopy, Structure and Chemistry pp 1.
Ed. T.A. Miller & V.E. Bondybey. North Holland.

242. Woods R.C. 1983
In : Molecular Ions, Spectroscopy, Structure and Chemistry pp 11
Ed. T.A. Miller & V.E. Bondybey. North Holland.

243. Oka T. 1983
In : Molecular Ions Spectroscopy, Structure and Chemistry pp 79
Ed. T.A. Miller & V.E. Bondybey. North Holland.

244. Herzberg G. & Johns J.W.C. 1969

Astrophys J. Vol. 158 pp 399.

245. Herbst E. Adams N.G. & Smith D. 1983

Astrophys J. Vol. 269 pp 329.

246. Bates D.R. 1983

Astrophys J. (Lett) Vol. 267 L121

247. Whittet D.C.B., McNally D. & Dickman R. 1979

The First Year of IUE. Symposium held at University College London, 4-6 April 1979. pp.31

248. Black J.H. et al 1979

The First Year of IUE. Symposium held at University College London, 4-6 April 1979. pp 11.

249. Boggess A. et al 1978

Nature Vol. 275 pp 2.

250. Boggess A. et al 1978

Nature Vol. 275 pp 7.

251. Dalgarno A. 1975

Phil. Trans Royal Soc. Lond. A Vol 279 pp 323.

252. Grewing M. et al 1978

Nature Vol. 275 pp 24.

253. Coxon J.A. et al 1979

Can. J. Phys. Vol. 57 pp. 619

254. Somerville W.B., Whittet D.C.B. & Baines D.W.T.

"In Preparation"

255. Henderson C. 1972

Contemp. Phys. Vol. 13 pp 479.

256. Herbig G.H. 1978

Private Communication.

257. Spitzer L. 1982

Searching between the Stars, Yale University Press.

258. Mulliken R.S. 1931

Rev. Mod. Phys. Vol. 3 pp 89

259. Mulliken R.S. 1927.

Phys. Rev. Vol. 30 pp 785

260. Allen C.W. 1973

Astrophysical Quantities.

3rd Edition

Athlone Press.

261. Heiles C. 1974

Galactic Radio Astronomy

IAU Symposium No.60 pp 13.

262. Halmann M. & Laulicht I 1966

Astrophys. J. (Supp) Vol. 12 pp 307

263. Erickson N.R., Snell R.L. et al 1981

Astrophys J. (Lett) Vol. 245 L83.

264. White R.E. 1973

Astrophys J. Vol. 183 pp 81

265. Routly P.M. & Spitzer L. 1952

Astrophys J. Vol. 115 pp 227

266. Jones A.P. & Williams D.A. 1984

MNRAS Vol. 209 pp 955.

267. Mann A.P.C. & Williams D.A. 1984

MNRAS Vol. 209 pp 33.

268. Tarafdar S.P. 1983

MNRAS. Vol 204 pp 1081

269. Tarafdar S.P. & Krishna Swamy K.S. 1981

MNRAS Vol. 196 pp 67

270. Smith W.H. 1969

J. Quant Spec. & Rad. Trans. Vol. 9 pp 1191

271. Erman P. 1975

Phys. Scripta Vol. 11 pp 65.

272. Liszt H.S. & Smith W.H. 1972

J. Quant Spec. & Rad. Trans. Vol. 12 pp 947

273. Lawrence G.M., Mickey D.L. & Dressler K. 1968
J.Chem. Phys. Vol. 48 pp 1989.

274. Danylewych L.L. & Nicholls R.W. 1978
Proc. Royal Soc. Lond. A. Vol 360 pp 557

275. Hesser J.E. 1968
J. Chem. Phys. Vol. 48 pp 2518

276. Field G.B. & Hitchcock J.L. 1966
Astrophys J. Vol 146 pp 1

277. Morton D.C. & Hu E.M. 1975
Astrophys J. Vol. 202 pp 638

278. Hinze J., Lie, G.C. & Liu B. 1975
Astrophys J. Vol. 196 pp 621

279. Morton D.C. & Bhavsar S.P. 1979
Astrophys J. Vol. 228 pp 147.

280. Crutcher R.M. & Watson W.D. 1981
Astrophys J. Vol. 244 pp 855.

281. Meyer D.M. & Jura M. 1984
Astrophys J. (Lett) Vol. 276 L 1.

282. Federman S.R. & Willson R.F. 1984
Astrophys. J. Vol. 283 pp 626

283. Federman S.R., Danks A.C. & Lambert D.L. 1984.
Astrophys. J. Vol 287 pp 219

284. Dieke G.H. & Crosswhite H.M. 1962
J. Quant Spec. & Rad. Trans. Vol. 2 pp 97

285. Weaver H., Williams D.R.W., Dieter N.H. & Lum W.T. 1965
Nature Vol. 208 pp 29.

286. Weinreb S. et al 1963
Nature Vol. 200 pp 829

287. Becker K.H. et al 1979
Chem. Phys. Lett Vol. 60 pp 502

288. Duric N., Erman P., & Larsson M. 1978

Phys. Scripta Vol. 18 pp 39.

289. Mumma M.J. and Donn B.D. 1973

Molecules in the Galactic Environment

Ed. M.A. Gordon & L.E. Snyder pp 296

Wiley

290. Donn B.D. 1973

Molecules in the Galactic Environment

Ed. M.A. Gordon & L.E. Snyder pp 306

Wiley

291. Stief L.J. 1973

Molecules in the Galactic Environment

Ed. M.A. Gordon & L.E. Snyder pp 314

Wiley

292. Spitzer L. 1978

Radiative Processes

Chapter 3 in Physical Processes in the Interstellar Medium, pp 32

Wiley

293. Blades J.C., Wynne Jones L and Wayte R.C. 1980

MNRAS Vol 193 pp 849.

294. Rich J.C. 1968

Astrophys J. Vol. 153 pp 327

295. Clavel J. & Flower D. 1980

Proc. 2nd Euro. IUE Conf. pp 197, March 1980

ESA SP 157.

296. Hegyi D.J., Traub W.A. & Carleton N.P. 1972

Phys. Rev. Lett Vol 28 pp 1541

297. Linevsky M.J. 1967

J. Chem. Phys. Vol. 47 pp 3485.

298. Jackson W.M. 1974

J. Chem. Phys. Vol. 61 pp 4177

299. Larsson M. 1983

Astron. Astrophys. Vol. 128 pp 291.

300. Viggiano A.A. et al 1980
Astrophys. J. Vol. 236 pp 492

301. Jenkins E.B. & Shaya E.J. 1979
Astrophys J. Vol. 231 pp 55.

302. Jenkins E.B., Jura M. & Loewenstein M. 1983
Astrophys J. Vol. 270 pp 88.

303. Blitz L. 1982
Scientific American Vol. 246 (April) pp 72.

304. Solomon P.M. & Sanders D.B. 1980
Giant Molecular Clouds in the Galaxy
Ed P.M. Solomon & M.G. Edmunds, pp 41
Pergamon Press

305. Mack J.E. et al 1963
Appl. Optics Vol. 2 pp 873.

306. Webster A.S. & Longair M.S. 1984
Contemp. Phys. Vol. 25 pp 519.

307. Churchwell E. 1980
Astrophys. J. Vol. 240 pp 811

308. Cook. A.H. 1977
Celestial Masers
Cambridge University Press

309. Winnewisser G. et al 1974
Interstellar Molecules, ppl
Cosmochemistry
Topics in Current Chemistry No. 44

310. Arnold J.O. & Nicholls R.W 1973
J. Quant Spec. & Rad. Trans. Vol. 13 pp 115.

311. Pilling M.J., Bass A.M. & Braun W. 1971.
J. Quant Spec. & Rad. Trans. Vol. 11 pp 1593.

312. Tsang W., Bauer S.H. & Cowperthwaite M. 1962
J.Chem. Phys. Vol. 36 pp 1768

313. Cook. T.J. & Levy D.H. 1972

J. Chem. Phys. Vol. 57 pp 5059.

314. Mumma M.J., Stone E.J. & Zipf. E.C. 1971

J. Chem. Phys. Vol. 54 pp 2627.

315. Peric´ Radic´ J. et al 1977

Chem. Phys. Lett Vol. 50 pp 344.

316. Bennett R.G. & Dalby F.W. 1962

J. Chem. Phys. Vol. 36 pp 399.

317. Moore J.H. & Robinson D.W. 1968

J.Chem. Phys. Vol. 48 pp 4870.

318. Luk C.K. & Bersohn R. 1973

J. Chem. Phys. Vol. 58 pp 2153

319. Liszt H.S. & Hesser J.E. 1970

Astrophys J. Vol. 159 pp 1101.

320. Liszt H.S. & Turner B.E. 1978

Astrophys J. (Lett) Vol. 224 L 73.

321. Simonson C. 1976

Astron. Astrophys. Vol. 46 pp 261.

322. Dwivedi P.H. et al 1978

Astrophys J. (Supp) Vol. 36 pp 573

323. Levitt B.P. & Parsons A.B. 1969

Trans. Faraday Soc. Vol. 65 pp 1199.

324. Matter in the Universe S256

Open University 1985

325. Meyers K.A., Snow T.P., Federman S.R. & Breger M.I. 1985

Astrophys J. Vol. 288 pp 148

326. Crutcher R.M. 1985

Astrophys J. Vol. 288 pp 604

327. Croswell K. & Dalgarno A. 1985

Astrophys J. Vol. 289 pp 618

328. Tarafdar S.P., Prasad S.S. et al 1985
Astrophys. J. Vol. 289 pp 220.

329. Michels H.H. & Hobb R.H. 1984
Astrophys. J. (Lett) Vol. 286 L 27

330. Lien D.J. 1984
Astrophys J. Vol 284 pp 578

331. White R.E. 1984
Astrophys J. Vol. 284 pp 695

332. Crutcher R.M., Churchwell E. & Ziurys L.M. 1984
Astrophys J. Vol. 283 pp 668.

333. Sciama D.W. 1975
The detection of Cosmic Microwave Radiation
Chapter 14 in Modern Cosmology
Cambridge University Press.

334. Carozza J. & Anderson R. 1977
J. Opt. Soc. Amer. Vol. 67 pp 118

335. Black J.H. & Smith P.L. 1980
Interstellar Molecules. IAU Symposium No. 87
pp 271.

336. Hirshfeld A. & Sinnott R.W. 1982
Sky Catalogue 2000
Vol. 1 Stars to Magnitude 8.0.
Cambridge University Press

337. Millar T. & Williams D. 1985
New Scientist, 11th April, pp 12

338. Meyer V.D., Skerbele A. & Lassettre E.N. 1965
J. Chem. Phys. Vol. 43 pp 805

339. Spindler R.J. 1965
J. Quant Spec. & Rad. Trans Vol. 5 pp 165

340. Smith W.H. 1969
J. Chem. Phys. Vol. 51 pp 520

341. Smith W.H. 1970

J. Chem. Phys. Vol. 53 pp 792.

342. Notes for Applicants to the 5th year of the I.U.E. Guest Investigator Programme

June 1981 S.E.R.C.

343. Tatum J.B. 1967

Astophys. J. (Supp) Vol. 14 pp 21

344. Davis S.P., Smith W.H. et al 1984

AstrophysJ. Vol. 287 pp 455.

345. Chesnavich W.J., Akin V.E. & Webb D.A. 1984

Astrophys J. Vol. 287 pp 676

346. Dalgarno A. & Lepp S. 1984

Astrophys J (Lett) Vol. 287 L47

347. Schadee A. 1975

Astron. Astrophys. Vol. 41 pp 203.

348. Crutcher R.M. & Chu Y.H. 1985

Astrophys J. Vol 290 pp 251

349. Federman S.R., Danks A.C. & Lambert D.L. 1984

Preprint.

350. Myers P.C., Ho P.T.P. et al 1978

Astrophys J. Vol. 220 pp 864

351. Duley W.W. & Williams D.A. 1984

Interstellar Chemistry

Academic Press

352. Farhoomand J. Blake G.A. & Pickett H.M. 1985

Astrophys J. (Lett) Vol. 291 L19

353. Mann A.P.C. & Williams D.A. 1985

MNRAS Vol. 214 pp 279

354 Van Dishoeck E.F. & Black J.H. 1982

Astrophys J. Vol. 258 pp 533

355. Smith D., Adams N.G. & Alge E. 1982
Astrophys J. Vol. 263 pp 123

356. Brown J.M., Curl R.F. & Evenson K.M. 1985
Astrophys J. Vol. 292 pp 188

357. Ziurys L.M. & Turner B.E. 1985
Astrophys J. (Lett) Vol. 292 L25.

358. Green S. 1981
Ann Rev. Phys. Chem. Vol. 32 pp 103.

359. Chabalowski C.F. et al 1983
Chem. Phys. Vol. 81 pp 57

360. Jura M. & Meyer D.M. 1985
Astrophys J. Vol. 294 pp 238

361. Shull J.M. & Van Steenberg M.E. 1985
Astrophys J. Vol. 294 pp 599

362. Hawkins I., Jura M. & Meyer D.M. 1985
Astrophys J. (Lett) Vol. 294 L 131

363. Lovas F.J. 1974
Astrophys J. Vol. 193 pp 265

364. Augason G.C. & Herbig G.H. 1967
Astrophys J. Vol. 150 pp 729

365. Spitzer L. 1985
Astrophys J. (Lett) Vol. 290 L21

366. Spectroscopy Volume 3.
Ed. B.P. Straughan & S. Walker
Chapman & Hall 1976

367. Dixon R.N. 1959
Can. J. Phys. Vol. 37 pp 1171

368. Carre M. 1969
Physica Vol. 41 pp 63

369. Spectroscopic Constants for Selected Homonuclear Diatomic Molecules
Volume1, A through I.
Suchard S.N. & Melzer J.E.
Aerospace Corporation 1976.

370. Banwell C.N. 1972
Electronic Spectroscopy of Molecules.
Chapter 6 in Fundamentals of Molecular Spectroscopy pp 205
McGraw Hill.

371. Dyson J.E. & Williams D.A. 1980
The Physics of the Interstellar Medium
Manchester University Press.

372. Bauer W., Becker K.H. et al 1985
Astrophys J. Vol 296 pp 578

373. Adams N.G., Smith D. & Clary D.C. 1985
Astrophys J. (Lett) Vol. 296, L31

374. Flower D.R., Pineau des Forets G. & Hartquist T.W. 1985
MNRAS Vol. 216 pp 775

375. Viscuso P.J., Stacey G.J. et al 1985
Astrophys J. Vol 296 pp 149

376. Viscuso P.J., Stacey G.J. et al 1985
Astrophys J. Vol 296 pp 142.

377. Mitchell G.F. & Watt G.D. 1985
Astron Astrophys Vol 151 pp 121

378. Watson W.D. & Walmsley C.M. 1982
Regions of Recent Star Formation.
Ed. R.S. Roger & P.E. Dewdney, pp 357.
D. Reidel.

379. Whipple F.L. & Huebner W.F. 1976
Ann Rev. Astron. Astrophys. Vol. 14 pp 143

380. Arpigny C. 1965

Ann Rev. Astron. Astrophys. Vol. 3 pp 351.

381. Meyer D.M. & Jura M. 1985

Astrophys J. Vol. 297 pp 119.

382. Prinja R.K. 1985

Ph.D. Thesis.

University of London

383. Lambert D.L. & Mallia E.A. 1974

Bull Astron. Inst. Czech. Vol. 25 pp 216.

384. Clementi E. 1960

Astrophys J. Vol 132 pp 898

385. Hartquist T.W., Oppenheimer M. & Dalgarno A. 1980

Astrophys J. Vol. 236 pp 182

386. Mitchell G.F. 1984

Astrophys J.(Supp)Vol. 54 pp 81

387. Somerville W.B. 1987

Astrochemistry

IAU Symposium No. 120 pp 133.

388. Watt G.D. 1983

MNRAS Vol. 205 pp 321

389. McCray R. & Snow T.P. 1979

Ann Rev. Astron. Astrophys Vol. 17 pp 213

390. Swings P. 1937

MNRAS Vol. 97 pp 212

391. Interstellar Matter.

IAU Reports on Astronomy 1985, pp 437.

392. White R.E. 1984

Astrophys J. Vol. 284 pp 685

393. Lien D.J. 1984

Astrophys J. (Lett) Vol. 287 L95

394. Smith P.L. 1987

Astrochemistry

IAU Symposium No. 120. pp95

395. Kurucz R.L. 1976

The Fourth Positive System of Carbon Monoxide

Smithsonian Astrophysical Observatory

Special Report No. 374.

396. Smith P.L. Griesinger H.E. et al 1984

Astrophys J. Vol 277 pp 569

397. Ferlet R., Vidal-Madjar A. & Gry C. 1985

Astrophys J. Vol 298 pp 838.

398. Smith D. & Adams N.G. 1985

Astrophys J. Vol 298 pp 827

399. Williams D.A. 1985

Q.J. RAS. Vol. 26 pp 463

400. Johansson L.E.B. 1985

The Milky Way Galaxy

IAU Symposium No. 106 pp 211

401. Pottasch S.R. 1985

The Milky Way Galaxy

IAU Symposium No. 106 pp 575

402. Richard L.J. & Palmer P. 1985

The Milky Way Galaxy

IAU Symposium No. 106 pp 193

403. Leitch-Devlin M.A. & Williams D.A. 1985

MNRAS Vol. 213 pp 295

404. Ingham M.F. 1962

MNRAS Vol. 124 pp 505

405. Lambert D.L. & Danks A.C. 1986

Astrophys J. Vol. 303 pp 401

406. Federman S.R. 1987
Astrochemistry
IAU Symposium No. 120 pp 123

407. Carrington A. & Ramsay D.A. 1982
Phys. Scripta Vol. 25 pp 272

408. Gredel R. & Munch G. 1986
Astron. Astrophys. Vol. 154 pp 336

409. Garland N.L. & Crosley D.R. 1985
J. Quant Spec. & Rad. Trans. Vol 33 pp 591.

410. Larsson M. & Siegbahn E.M. 1983
Chem. Phys. Vol 76 pp 175.

411. Mohlmann G.R., Bhutani K.K. et al 1978
Chem. Phys. Vol. 31 pp 273

412. Field R.W., Benoist d'Azy.O. et al 1983
J. Chem. Phys. Vol. 78 pp 2838

413. Cooper D.M. & Langhoff S.R. 1981
J. Chem. Phys. Vol. 74 pp 1200.

414. Diffenderfer R.N. Yarkony D.R. & Dagdigian P.J. 1983
J. Quant Spec. & Rad. Trans. Vol 29 pp 329

415. Fairchild P.W., Smith G.P. et al 1984
Chem. Phys. Lett Vol. 107 pp 181.

416. Larsson M. & Siegbahn E.M. 1983
J. Chem. Phys. Vol. 79 pp 2270

417. Van Dishoeck E.F., Van Hemert M.C. & Dalgarno A. 1982
J. Chem. Phys. Vol. 77 pp 3693

418. Wang C.C. & Huang C.M. 1980
Phys. Rev. A. Vol. 21 pp 1235

419. Holland R.F. & Maier W.B. 1972
J. Chem. Phys. Vol. 56 pp 5229

420. Smith G.P. & Crosley D.R. 1981
Eighteenth Symposium (International)
on Combustion pp 1511
The Combustion Institute, Pittsburgh

421. Goldanskii V.I. 1986
Scientific American(February) pp 38

422. Curtis L.J. & Erman P. 1977
J. Opt. Soc. Amer. Vol. 67 pp 1218

423. Hsu D.K. & Smith W.H. 1977
Spectroscopy Lett Vol. 10 pp 181.

424. Dimpfl W.L. & Kinsey J.L. 1979
J. Quant Spec. & Rad. Trans. Vol 21 pp 233

425. Saxon R.P., Kirby K. & Liu B. 1980
J. Chem. Phys. Vol 73 pp 1873

426. Becker K.H. Brenig H.H. & Tatarczyk T. 1980
Chem. Phys. Lett Vol. 71 pp 242

427. Lew H. 1976
Can. J. Phys. Vol. 54 pp 2028

428. Lew H. & Heiber I. 1973
J. Chem. Phys. Vol. 58 pp 1246

429. Chauville J. Maillard J.P. & Mantz A.W. 1977
J. Mol. Spect. Vol 68 pp 399.

430. Norris R. 1986
Sky & Telescope. March pp 248

431. Jenkins E.B., Savage B.D. & Spitzer L. 1986
Astrophys. J. Vol. 301 pp 355

432. Blake G.A., Anicich V.G. & Huntress W.T. 1986
Astrophys J. Vol 300 pp 415

433. Herbst E. 1985
Astron. Astrophys. Vol 153 pp 151

434. Phillips T.G. et al 1985

Astrophys J. (Lett) Vol. 294 L 45

435. Steimle T.C., Woodward D.R. & Brown J.M. 1985

Astrophys J. (Lett) Vol. 294 L59

436. Festou M.C. et al 1986

Astron. Astrophys. Vol. 155 L17

437. Williams D.A. 1986

Q.J. RAS. Vol 27 pp 64.

438. Hartquist T.W. 1986

Q.J. RAS. Vol. 27 pp 71

439. Dalgarno A. 1986

Q.J. RAS. Vol. 27 pp 83

440. Urch D.S. 1970

Orbitals and Symmetry

Penguin

441. Cotton F.A. 1971

Chemical Applications of Group Theory

2nd Edition

Wiley

442. de Boer K.S. & Savage B.D. 1982

Scientific American (August) pp 52

443. Hey. J.S. 1983

Chapter 7 in The Radio Universe

3rd Edition

Pergamon Press.

444. Mulliken R.S. 1933

Phys. Rev. Vol. 43 pp 279

445. Walsh A.D. 1953

J. Chem. Soc. pp 2260

446. Cardelli J.A. & Wallerstein G. 1986
Astrophys J. Vol 302 pp 492

447. Black J.H. & Van Dishoeck E.F. 1986
Preprint of The Steward Observatory No. 629
University of Arizona

448. Van Dishoeck E.F. & Black J.H. 1986
Astrophys. J. Vol 307 pp 332.

449. Black J.H. et al 1986
Preprint of The Steward Observatory No. 631
University of Arizona

450. Van Dishoeck E.F. & Black J.H, 1986
Preprint of The Steward Observatory No. 641
University of Arizona

451. Lockman F.J., Hobbs L.M. & Shull J.M. 1986
Astrophys J. Vol. 301 pp 380

452. Grevesse N. & Sauval A.J. 1973
Astron. Astrophys. Vol 27 pp 29.

453. Elander N. Oddershede J. & Beebe N.H.F. 1977
Astrophys J. Vol 216 pp 165

454. Elmergreen B.G. & Smith W.H. 1972
Astrophys J. Vol 178 pp 557

455. Vanderslice J.T., Tilford S.G. & Wilkinson P.G. 1965
Astrophys J. Vol. 141 pp 395

456. Tilford S.G., Wilkinson P.G. & Vanderslice J.T. 1965
Astrophys J. Vol. 141 pp 427

457. Marshall A., de Zafra R.L. & Metcalf H. 1969
Phys. Rev. Lett Vol. 22 pp 445.

458. German K.R. & Zare R.N. 1969
Phys. Rev. Lett Vol. 23 pp 1207

459. German K.R. & Zare R.N. 1969
Phys. Rev. Vol. 186 pp 9

460. de Zafra R.L., Marshall A. & Metcalf H. 1971
Phys. Rev. A. Vol. 3 pp 1557

461. Henneker W.H. & Popkie H.E. 1971
J. Chem. Phys. Vol 54 pp 1763

462. Huo W.M. 1968
J. Chem. Phys. Vol 49. pp 1482

463. Smith W.H. 1969
J. Chem. Phys. Vol. 51 pp 520.

464. Anketell J. & Pery-Thorne A. 1967
Proc. Royal Soc. A. Vol 301 pp 343

465. Herzberg G. 1967
Molecular Spectra and Molecular Structure Vol. 3
Electronic spectra and electronic structure of polyatomic molecules.
Van Nostrand. Reinhold Company.

466. Ballik E.A. & Ramsay D.A. 1963
Astrophys. J. Vol. 137 pp 61.

467. Krishna Swamy K.S. & O'Dell C.R. 1979
Astrophys J. Vol. 231 pp 624

468. Lambert D.L.& Danks A.C. 1986
Preprint

469. Cardelli J.A. & Wallerstein G. 1986
Preprint

470. Bel N., Viala Y.P. & Guidi I. 1986
Astron. Astrophys. Vol 160 pp 301

471. Mattila K. 1986
Astron. Astrophys. Vol. 160 pp 157

472. Seaquist E.R. & Bell M.B. 1986
Astrophys J. (Lett) Vol. 303 L 67

473. Davis S.P. et al 1986
Astrophys J. Vol. 303 pp 892

474. Greisen E.W. & Liszt H.S. 1986

Astrophys J. Vol 303 pp 702

475. Fairbairn A.R. 1964

AIAA Journal. Vol. 2 pp 1004

476. Dwyer R.J. & Oldenberg O. 1944

J. Chem. Phys. Vol 12 pp 351.

477. Mulliken R.S. 1940

J. Chem. Phys. Vol. 8 pp 382

478. White J.U. 1940

J. Chem Phys. Vol 8 pp 459

479. White J.U. 1940

J. Chem. Phys. Vol 8. pp 79

480. Carrington T. 1959

J. Chem. Phys. Vol 31 pp 1243

481. Bennett R.G. & Dalby F.W. 1964

J. Chem. Phys. Vol 40 pp 1414

482. Dyne P.J. 1958

J. Chem. Phys. Vol 28 pp 999

483. Sawada T. & Kamada H. 1970

Bull. Chem. Soc. Jap. Vol. 43 pp 331

484. Smith W.H. & Liszt H.S. 1971

J. Quant Spec. & Rad. Trans. Vol 11 pp 45

485. Harrington J.A. Modica A.P. & Libby D.R. 1966

J. Quant Spec. & Rad. Trans. Vol 6 pp 799

486. Lapp M. 1961

J. Quant Spec. & Rad. Trans. Vol 1 pp 30

487. Watson R. & Ferguson W.R. 1965

J. Quant Spec. & Rad. Trans Vol. 5 pp 595

488. Bird P.F. & Schott G.L. 1965

J. Quant Spec. & Rad. Trans. Vol 5 pp 783

489. Lyddane R.H. & Rogers F.T. 1941

Phys. Rev. Vol 60 pp 281

490. Hurley A.C. 1959

Proc. Royal Soc. Lond. A. Vol. 249 pp 402

491. Le Calvé et al 1969

Le Journal de Physique Vol. 30 pp 807

492. Stephenson G. 1951

Proc. Royal Soc. Lond. A. Vol. 64 pp 666

493. Douglas A.E. 1963

Disc. Faraday Soc. Vol. 35 pp 158

494. Gausset L. Herzberg G. Lagerqvist A. & Rosen B. 1965

Astrophys J. Vol. 142 pp 45

495. Douglas A.E. & Routly P.M. 1955

Astrophys J. (Supp) Vol. 1 pp 295

496. Matthews H.E. & Irvine W M. 1985

Astrophys J. (Lett) Vol. 298 L 61

497. Thaddeus P., Vrtilek J.M. & Gottlieb C.A. 1985

Astrophys J. (Lett) Vol. 299 L 63

498. Schadee A. 1971

Astron. Astrophys. Vol. 14 pp 401

499. Grevesse N. & Sauval A.J. 1970

Astron. Astrophys. Vol. 9 pp 232

500. Grevesse N. & Sauval A.J. 1971

J. Quant Spec. & Rad. Trans. Vol. 11 pp 65

501. Douglas A.E. & Morton J.R. 1960

Astrophys J. Vol. 131 pp 1

502. Grevesse N. & Sauval A.J. 1971

Astron. Astrophys. Vol. 14 pp 477

503. Huber M.C.E. & Sandeman R.J. 1980

Phys. Scripta. Vol. 22 pp 373.

504. Hofzumahaus A. & Stuhl. F. 1985

J. Chem. Phys. Vol 82 pp 3152

505. Foster. E.W. 1964

Rep. Prog. Phys. Vol. 27 pp 469

506. Hobbs L.M., Morgan W.W., Albert C.E. & Lockman F.J. 1982

Astrophys J. Vol. 263 pp 690

507. Douglas A.E. & Herzberg G. 1942

Can J. Res. Vol. A20 pp 71

508. Van Wijngaarden W.A. et al 1986

Phys. Rev. Lett. Vol. 56 pp 2024

509. Harris A.W. & Bromage G.E. 1984

MNRAS Vol. 208 pp 941

510. Savage B.D. & Bohlin R.C. 1979

Astrophys. J. Vol. 229 pp 136

511. Crane P., Hegyi D.J., Mandolesi N. & Danks A.C. 1986

Astrophys J. Vol. 309 pp 822

512. Murray M.J., Dufton P.L., Hibbert A. & York D.G. 1984

Astrophys J. Vol. 282 pp 481

513. Snow T.P. 1975

Astrophys J. (Lett) Vol 202 L87

514. Mann A.P.C. & Williams D.A. 1986

Astrophys.Space Sci. Vol. 121 pp 387

515. Pwa T.H. & Pottasch S.R. 1986

Astron. Astrophys Vol 164 pp 116

516. Van Disoeck E.F. & Black J.H. 1986

Preprint of the Steward Observatory No. 630.

University of Arizona

517. Brown J.M. et al 1986

Astrophys J. Vol 307 pp 410

518. Duvert G., Cernicharo J. & Baudry A. 1986

Astron. Astrophys Vol. 164 pp 349

519. Krishnakumar E. & Srivastava S.K. 1986

Astrophys J. Vol 307 pp 795

520. Draine B.T. & Katz N. 1986
Astrophys J. Vol 306 pp 655

521. Shuter W.L.H. et al 1986
Astrophys J. Vol 306 pp 255

522. Keenan F.P. et al 1986
MNRAS Vol. 222 pp 143

523. Millar T.J. et al 1986
MNRAS Vol. 221 pp 673

524. Duley W.W. 1986
Q.J. RAS. Vol. 27 pp 403

525. Whittet D.C.B. 1981
Q.J. RAS. Vol. 22 pp 3

526. Disney M.J. & Wallace P.T. 1982
Q.J. RAS. Vol. 23 pp 485

527. Greenberg J.M. 1984
Scientific American(May) pp 96

528. Van Dishoeck E.F. & Black J.H. 1986
Center for Astrophysics. Preprint No. 2396
Cambridge. Mass. USA.

529. Duley W.W. & Williams D.A. 1986
MNRAS Vol. 223 pp 177

530. Anicich V.G. & Huntress W.T. 1986
Astrophys J. (Supp) Vol. 62 pp 553

531. Sharpless S. 1957
Pub. Astron. Soc. Pac. Vol. 69 pp 239

532. Ferlet R., Roueff E., Czarny J. & Felenbok P 1986
Astron. Astrophys Vol. 168 pp 259

533. Pineau des Forets, Roueff E. & Flower D.R. 1986
MNRAS Vol. 223 pp 743

534. Millar T.J., Williams D.A., Jones A.P. & Freeman A. 1984
Nearby Molecular Clouds. Ed. G. Serra
Lecture Notes in Physics No. 237. Springer Verlag.

535. Walmsley C.M. & Wilson T.L. 1984
Nearby Molecular Clouds. Ed. G. Serra.
Lecture Notes in Physics No. 237
Springer Verlag.

536. Millward C.G. & Walker G.A.H. 1985
Astrophys J. (Supp) Vol. 57 pp 63

537. Keenan P.C. 1985
Calibration of Fundamental Stellar Quantities
IAU Symposium No. 111 pp 121

538. Grenier S., Gomez A.E., Jaschek C., Jaschek M. & Heck A 1985
Astron. Astrophys Vol. 145 pp 331

539. Norton A.P. 1986
Norton's Star Atlas (17th Edition)
Longman

540. Larsson M. 1985
Chem. Phys. Lett Vol. 117 pp 331

541. Gauyacq D. & Horani M. 1978
Can. J. Phys. Vol. 56 pp 587

542. Harris A.W. & Bromage G.E. 1984
Proc. 4th European IUE Conference
ESA SP 218 pp 157

543. Harris A.W., Bromage G.E. & Gry C. 1984
Proc. 4th European IUE Conference
ESA SP 218 pp 151

544. Pwa T.H. & Pottasch S.R. 1984
Proc. 4th European IUE Conference
ESA SP 218 pp 167

545. Blades J.C. 1984
Proc. 4th European IUE Conference
ESA SP 218 pp 11

546. Crane P., Hegyi D.J., Mandolesi N. & Danks A.C. 1986
European Southern Observatory
Preprint No. 447

547. Basic Astronomical Data
Ed K. Aa. Strand
University of Chicago Press 1963

548. Landolt - Börnstein
Group VI.Astronomy, Astrophysics & Space Research
Vol. 2. Astronomy & Astrophysics.
Sub volume b. Stars & Star Clusters
Ed. K.H. Hellwege.
Springer Verlag 1982

549. Somerville W.B. 1986
Private Communication to S.R. Federman

550. Turner B.E.
Interstellar Molecules.
In New Frontiers in Astronomy
Readings from Scientific American
W.H. Freeman 1975

551. Prasad S.S. & Huntress W.T. 1980
Astrophys J. Vol. 239 pp 151

552. Heiles C. 1971
Ann Rev. Astron. Astrophys. Vol. 9 pp 293

553. Jacq T., Baudry A., Despois D., Gerard E. & Johansson L.E.B. 1987
Astron. Astrophys Vol. 173 pp 347

554. White G.J., Rainey R., Hayashi S.S. & Kaifu N. 1987
Astron. Astrophys. Vol. 173 pp 337

555. Crane P. 1986
The Messenger No. 45. September
European Southern Observatory

556. Van de Kamp P. 1971

Ann Rev. Astron. Astrophys Vol. 9 pp 103

557. Watson W.D. 1975

Atomic and Molecular Physics and the Interstellar Matter

Les Houches, Session XXVI 1st July - 23rd August 1974

Ed. R. Balian et al

North Holland

558. Brown R.D. & Rice E.H.N. 1986

MNRAS Vol. 223 pp 405

559. Brown R.D. & Rice E.H.N. 1986

MNRAS Vol 223 pp 429

560. Dalgarno A. 1975

Atomic and Molecular Processes in Astrophysics.

Swiss Society of Astronomy and Astrophysics.

5th Advanced Course.

Ed. M.C.E. Huber & H. Nussbaumer.

Geneva Observatory.

561. Hartquist T.W. & Dalgarno A. 1982

Proc. 16th ESLAB Symposium on Galactic & Extragalactic

Infrared Spectroscopy 6-8 December 1982. Toledo, Spain.

ESA SP 192. pp 29

562. Kitchin C.R. 1987

Stars, Nebulae and the Interstellar Medium.

Adam Hilger.